SOVIET PHYSICS

JETP

A translation of the Journal of Experimental and Theoretical Physics of the USSR.

SOVIET PHYSICS JETP VOL. 35 (8), NO. 6, pp. 923-1135 JUNE, 1959

ACADEMICIAN VLADIMIR ALEKSANDROVICH FOCK

(on his sixtieth birthday).

J. Exptl. Theoret. Phys. (U.S.S.R.) **35**, 1321-1324 (December, 1958)

ACADEMICIAN Vladimir Aleksandrovich Fock, one of our greatest theoretical physicists, completed his sixtieth year on December 22, 1958.

Fock's scientific work began in his student days (his first published work appeared in 1923) and continued without interruption and with inexhaustible energy until the present time. It has dealt with a wide range of problems, and here we can mention only the main directions of Fock's scientific achievements, those which are best known and have brought him world-wide renown.

His first interest was quantum mechanics and quantum field theory. His first work in this field,[1-4] some of which was carried out during his stay abroad in 1927, immediately made Fock well known as a theoretical physicist. Some papers were devoted to the basic principles of quantum theory. Fock's work on the many-electron problem in quantum mechanics[5-7] led to the formulation of the method of the self-consistent field with exchange, the so-called Hartree-Fock method, and to the discovery of other approximate methods for constructing wave-functions. This made it possible to calculate precisely the electronic shells of various atoms. A review of the basic results is given in reference 8.

Fock's book "Principles of Quantum Mechanics" appeared in 1932. It was the first Soviet book on quantum mechanics and contained much original work.

Fock's papers on quantum field theory, written from 1928 to 1937 and recently collected into a book,[9-14,15] were not only of fundamental importance for the development of quantum electrodynamics, but are also still useful today. The mathematical ideas and methods which Fock introduced in these papers were applied and generalized in the development of quantum field theory in the last few years. One remarkable paper on the hydrogen atom[16] occupies a special position in this field. In it he established an unexpected connection between the so-called "accidental" degeneracy of the hydrogen levels and a four-dimensional rotational symmetry.

The second main direction in Fock's scientific work is the theory of gravitation. The starting point was a paper of 1939,[17] in which the equations of motion of extended masses with spherical symmetry were derived from Einstein's field equations. The final result was a book "Theory of Space, Time and Gravitation,"[18] which appeared in 1955 and excited much interest and lively discussions among physicists. The book included solutions of many important problems of gravitation theory, and in particular a very complete discussion of the motion of a system of bodies taking account of their rotation and internal structure. Fock also derived a number of general results which allowed him to survey the theory of gravitation as a whole.

Fock worked intensively during the war and postwar years in a third field, the theory of diffraction. The importance of this subject arose originally from the rapid development of modern radio technology. He studied the propagation of radio waves around the earth as a problem in diffraction. He also studied the diffraction of electromagnetic waves by large conducting bodies having dimensions and radii of curvature much greater than the wavelength. These investigations were distinguished by the novelty of the mathematical methods and by the generality of the results. They have set a standard for all modern work in the theory of diffraction.

The monograph "Diffraction of Radio Waves around the Surface of the Earth"[19] was awarded a Stalin Prize, first class. It gave a complete solution to the problem of the field of an elementary dipole on the surface of a spherical earth. Later the results were generalized to the case of elevated sources of radiation,[20] and detailed tables of the propagation of radio waves were computed under Fock's guidance.

Fock's work[21,22] on diffractive propagation in a non-uniform atmosphere, whose refractive index is a function of altitude, led him to an elegant solution of the difficult problem of the range of radio waves under conditions of anomalous propagation. In the course of this work he made a very exact study of the classical analog of the tunnel-effect, the leakage of waves through the boundary of an inversion layer.

In three papers[24-26] Fock calculated the diffractive field produced by a plane wave incident upon the surface of a conducting convex body. In another paper[27] he investigated the field at great distances from the body. He showed that the field arising from diffraction by a convex body can be expressed in terms of the same functions (defined by contour integrals) which he had introduced in his theory of wave propagation over a spherical earth. This opens the possibility of a solution of diffraction problems for large bodies of arbitrary shape.

Fock loves to find practical problems which lead him to investigations requiring original mathematical techniques and the development of new methods. In such cases he usually provides not only a solution in principle, but a reduction of the solution to practical formulae and tables. Many researches of this kind, devoted to quite diverse problems, reveal Fock in the role of a specialist in mathematical methods. One should also mention one paper[28] in which he found an elegant solution to the complicated problem of the skin-effect in a ring.

The best known of Fock's works in pure mathematics are papers[29,30] on the theory of integral equations with a kernel that depends only on the difference between the variables. This work has become a standard tool in theoretical physics and has led to exact solutions of many interesting problems.

Fock takes an active interest in all questions relating to the healthy development of Soviet physics. Sometimes, in the course of scientific research, scientific truth is in danger of being distorted, and sometimes scientists do not observe the normal ethical standards of scientific and creative work. In such cases, if the questions at issue concern him, he invariably speaks out and expresses his opinion with the same directness and exactitude with which he formulates the results of his scientific research. The honesty and the directness of the "Fockian" character are well known not only here but also among scientists abroad. This honesty is especially clear when he is concerned with philosophy or with the fundamental problems of modern physics. Fock reacts hotly against incorrect and unscientific papers, either in the theory of relativity or in quantum theory, when they occasionally appear in our journals, and he always defends modern physical theory. He considers this activity, in distinction to his purely scientific work, as a part of his public duty.

Fock is an alumnus of Leningrad University, in which his scientific and teaching career began in 1922. In Leningrad he continues his fundamental scientific work still. In Leningrad University he holds a chair and gives much time to the education of the young people. Many are the pupils of Fock's school who are working successfully in various branches of theoretical and mathematical physics.

Having a sociable character, Fock is an entertaining companion, widely read in the most diverse fields of human culture and knowledge. His participation at congresses, meetings and other scientific gatherings is always desired both here and abroad.

The editors of JETP, in the name of all Soviet physicists, heartily congratulate dear Vladimir Aleksandrovich Fock on his sixtieth birthday, and wish him health and many more years of fruitful activity.

Bibliography of V. A. Fock

[1] Schrödinger's Wave Mechanics. Z. Physik **38**, 242 (1926).

[2] An Invariant Form of the Wave Equation and the Equation of Motion of a Charged Particle. Z. Physik **39**, 226 (1926).

[3] The Relation Between the Schrödinger Equation and the Integrals of Quantum-Mechanical Equations of Motion. Z. Physik **49**, 323 (1928).

[4] Generalization and Solution of the Statistical Equation of Dirac. Z. Physik **49**, 339 (1928).

[5] An Approximate Method for Solving Quantum-Mechanical Many-Body Problems. Z. Physik **61**, 126 (1930).

[6] Self-Consistent Field with Exchange for Sodium. Z. Physik **62**, 795 (1930).

[7] Quantum Exchange Energy. Z. Physik **81**, 195 (1933); J. Exptl. Theoret. Phys. (U.S.S.R.) **4**, 1 (1934).

[8] The Many-Electron Problem in Quantum Mechanics and the Structure of the Atom. Anniversary Volumes Celebrating Thirty Years of the Great October Socialist Revolution, Vol. 1, Moscow-Leningrad, Academy of Sciences Press, 1947, p. 255.

[9] Configuration Space and Second Quantization. Z. Physik **75**, 622 (1932); **76**, 352 (1932).

[10] Dirac's Quantum Electrodynamics (With B. Podol'skii), Sow. Phys. **1**, 798 (1932).

[11] Quantization of Electromagnetic Waves and Interaction of Charges in Dirac's Theory (with B. Podol'skii), Sow. Phys. **1**, 801 (1932).

[12] Quantum Electrodynamics (with P. A. Dirac and B. Podol'skii), Sow. Phys. **2**, 468 (1932).

[13] Quantum Electrodynamics. Sow. Phys. **6**, 425 (1934).

[14] Proper Time in Classical and Quantum Field Theory. Izv. Akad. Nauk, SSSR, Ser. Fiz. **4-5**, 551 (1937); Sow. Phys. **12**, 404 (1937).

[15] Papers in Quantum Field Theory. Leningrad State University Press, 1957.

[16] The Theory of the Hydrogen Atom. Z. Physik **98**, 145 (1935).

[17] The Motion of Finite Masses in General Relativity. J. Exptl. Theoret. Phys. (U.S.S.R.) **9**, 375 (1939).

[18] Теория пространства, времени и тяготения (Theory of Space, Time and Gravitation) Moscow, GITTL, 1955.

[19] Диффракция радиоволн вокруг земной поверхности (Diffraction of Radio Waves around the Surface of the Earth) Moscow-Leningrad. Academy of Sciences Press, 1946.

[20] The Field of a Vertical and a Horizontal Dipole above the Surface of the Earth. J. Exptl. Theoret. Phys. (U.S.S.R.) **19**, 916 (1946).

[21] Propagation of a Plane wave around the Earth Taking Account of Diffraction and Refraction. Izv. Akad. Nauk, SSSR, Ser. Fiz. **12**, 81 (1948); Сб. Исследования по распространению радиоволн (Investigations on the Propagation of Radio Waves) Vol. 2, edited by B. A. Vvedenskii, Moscow-Leningrad, Academy of Sciences Press, 1948.

[22] Theory of Propagation of Radio Waves from an Elevated Source in an Inhomogeneous Atmosphere. Izv. Akad. Nauk, SSSR, Ser. Fiz. **14**, 70 (1951).

[23] Approximate Formula for the Distance of the Horizon with Anomalous Propagation. Радиотехника и электроника (Radio Engineering and Electronics) **1**, 560 (1956).

[24] Distribution of Current Induced by a Plane Wave on the Surface of a Conductor. J. Exptl. Theoret. Phys. (U.S.S.R.) **15**, 693 (1945).

[25] The Field of a Plane Wave Near the Surface of a Conducting Body. Izv. Akad. Nauk, SSSR, Ser. Fiz. **10**, 171 (1946).

[26] The Laws of Fresnel Reflection and Diffraction, Usp. Fiz. Nauk **36**, 308 (1948).

[27] Fresnel Diffraction by Convex Bodies. Usp. Fiz. Nauk **43**, 587 (1951).

[28] Skin Effect in a Ring. Sow. Phys. **1**, 215 (1932).

[29] A Class of Integral Equations. Math. Z. **21**, 161 (1924).

[30] Some Integral Equations of Mathematical Physics. Матем. сб. (Math. Collection) **14**, 3 (1944).

Translated by F. J. Dyson
288

SOVIET PHYSICS JETP VOLUME 35 (8), NUMBER 6 JUNE, 1959

COULOMB EXCITATION OF HIGH-ENERGY NUCLEAR LEVELS IN EVEN ISOTOPES OF TUNGSTEN

D. G. ALKHAZOV, A. P. GRINBERG, G. M. GUSINSKII, K. I. EROKHINA, and I. Kh. LEMBERG

Leningrad Physico-Technical Institute, Academy of Sciences, U.S.S.R.

Submitted to JETP editor May 26, 1958

J. Exptl. Theoret. Phys. (U.S.S.R.) **35**, 1325-1334 (December, 1958)

Natural tungsten and samples enriched in W^{182}, W^{184}, and W^{186} were irradiated with α particles having energies from 8.3 to 14.5 Mev. The existence of the following excited states was established: 1.22 Mev in W^{182}, 0.90 Mev in W^{184}, and 0.73 Mev in W^{186}. The reduced probabilities B(E2) of transition to the ground state computed for these levels are 0.051, 0.038, and 0.040, respectively (in units of $e^2 \times 10^{-48}$ cm^4). The assumption that these levels are vibrational levels is discussed.

1. INTRODUCTION

COULOMB excitation of nuclear levels of even isotopes of tungsten has been studied in several papers.[1-3] These authors observed the excitation of the first rotational levels (with quantum numbers 2^+), determined the energies of these levels and the reduced probability for electric quadrupole transition from the ground state to the first rotational state.

Coulomb excitation of the second rotational levels (with quantum numbers 4^+) in even-even nuclei is much more difficult since this process requires the occurrence of an E4 transition. For this reason Coulomb excitation of the second rotational level has as yet not been observed in any even-even nuclei.

But on the basis of the uniform model of the nucleus one should expect that among the excited states of deformed nuclei there should be 2^+ levels located above the first few lowest levels of the first rotational band which is associated with the ground state of the nucleus. The new levels to which we refer are vibrational levels. In addition the quantum numbers 2^+ can occur for some levels of the rotational bands associated with single particle or "pair" excitation (where the latter refers to the simultaneous transition of two nucleons to excited states). Because of the collective character of the vibrational level, the magnitude of the reduced transition probability B(E2) to such a level is larger than the value of B(E2) for a single particle transition, so that the cross section for Coulomb excitation to a vibrational level should be greater than that for excitation of a single particle level.

We have shown in previous papers[4,5] that by using α particles with energy ~ 15 Mev for Coulomb excitation, one can excite levels in various even-even nuclei up to 1.5 Mev excitation. One may expect to excite such levels in the tungsten isotopes if the level energies do not exceed 1.5 Mev. Their excitation is much more probable than excitation of the second level of the lowest rotational band.

Highly excited levels of the tungsten isotopes were not observed in references 1 to 3 because the bombarding particles used in these experiments had low energies, while the cross section for Coulomb excitation of high energy levels depends strongly on the energy of the bombarding particles. Recently,[6] using 5-Mev protons, a level with $\Delta E = 730$ kev in W^{186} was excited.

Experiments in which the level scheme is studied by investigating artificial radioactivity of the corresponding nuclei are of interest in settling the question of the existence of excited levels up to 1.5 Mev in the even tungsten isotopes. Among such experiments we should especially mention reference 7 in which the decay of Ta^{182} was studied. As a result of parallel study of the β and conversion electron spectrum using a β spectrometer, and of the γ spectrum using a bent-crystal spectrometer, these authors succeeded in setting up a complex scheme of levels and transitions in W^{182} and assigning quantum numbers to the levels. The superior resolution of the γ-spectrometer (0.1% for low energy γ rays and approximately 1.5% in the high energy region) enabled them to determine very accurately the relative intensities of individual γ lines, despite the fact that there were a large number of lines

(~30). According to the level scheme of W^{182} proposed in reference 7, this isotope has an excited 2^+ level at $\Delta E = 1222$ kev. The authors note that though the 2^+ assignment seems most likely from the analysis of various facts, it cannot be regarded as confirmed by a direct experiment since the conversion coefficients for transition from this level have not been measured accurately enough. It has been shown[8] using the ratio of the γ intensities emitted in transitions to the ground level and the first and second excited rotational levels, that the 1222-kev level in W^{182} is a γ-vibrational level. The authors of references 9 and 10 used a scintillation spectrometer to determine the energies and relative intensities of the γ rays emitted in the β decay of Ta^{184} and Ta^{186} to W^{184} and W^{186}, respectively. They did not propose level schemes for these nuclei and did not consider the possible quantum assignments of the levels.

On the basis of the uniform model and data on nuclear level systematics, Peker[11] used the information about energies and relative intensities of γ-rays given in references 9 and 10 to construct level schemes for W^{184} and W^{186}. In these level schemes the level at $\Delta E = 900$ kev in W^{184} and the level at $\Delta E = 730$ kev in W^{186} are assigned as γ vibrational levels, i.e., as levels with quantum numbers 2^+.

Our experiments on Coulomb excitation of high energy levels in the even isotopes of tungsten had the following purposes:

(1) To check whether the energy levels mentioned above are excited, and thus to show the existence of these levels directly. The presence of the corresponding γ rays in Coulomb excitation would serve both as a proof that the previously observed γ lines correspond to transtions from these levels to the ground level and not to transitions between higher levels, and as an independent confirmation of the 2^+ assignment for these levels.

(2) To measure the relative intensities of γ rays emitted in transitions from highly excited states to the levels of the lowest rotational band.

(3) To determine the reduced probability for excitation of these levels from the ground state.

2. EXPERIMENTAL METHOD AND TREATMENT OF RESULTS

We used α particles accelerated in a cyclotron for Coulomb excitation of levels of the even isotopes of tungsten. Altogether we used four fixed energies for the α particles: 8.3, 10.2, 13.1, and 14.5 Mev. The targets were 0.25 mm thick foils of natural tungsten and samples enriched in various tungsten isotopes, in metallic powder form, a layer of which was pressed onto a lead backing $50\,\mu$ thick. In all cases the target thickness was enough to slow the α particles down to an energy at which the Coulomb excitation cross section was very small.

The beam of α particles extracted from the cyclotron was focused on the target by a system of two magnetic quadrupole lenses. The target was located on the bottom of an insulated metallic container which served as a Faraday cup. An electronic current integrator was connected to the cup. The γ radiation emitted in the de-excitation of the excited nuclear states was studied by means of a scintillation spectrometer. The detecting system consisted of a NaI (Tl) crystal 40 mm in diameter and 40 mm high and a FEU-S photomultiplier; the recording system was a 50-channel pulse-height analyzer.

To prevent loading of the amplifier by the large number of pulses resulting from Coulomb excitation of the first rotational level of the tungsten nuclei and from the characteristic tungsten radiation emitted under the action of the α particles, a 1.8 mm lead absorber was placed between the scintillator and the target.

More detailed information concerning the experimental arrangement is given in reference 4. It also describes the procedure for processing the experimental results. The computations are complicated somewhat by the following fact. As the data to be presented in Sec. 3 show, the de-excitation of highly excited levels in tungsten occurs via two parallel transitions (a $2' \to 0$ transition to the ground state and a $2' \to 2$ transition to the first rotational level). Thus the value of the reduced probability $B(E2)_{0\to 2'}$ for transition from the ground state to the excited state must be computed from the sum of the yields of the γ rays in the $2' \to 0$ and $2' \to 2$ transitions. According to the principle of detailed balancing, the quantities $B(E2)_{2'\to 0}$ and $B(E2)_{0\to 2'}$ are related by the formula

$$(2I_f + 1)\,B(E2)_{2'\to 0} = (2I_0 + 1)\,B(E2)_{0\to 2'}.$$

In our case, $I_0 = 0$ and $I_f = 2$, so that

$$B(E2)_{2'\to 0} = {}^1/_5\,B(E2)_{0\to 2'}.$$

In Sec. 4 we shall give arguments in favor of the assumption that the $2' \to 2$ transition is mainly electric quadrupole. Making this assumption, we can calculate the value of $B(E2)_{2'\to 2}$ using the formula

$$N_{2'\to 2}/N_{2'\to 0} = (B(E2)_{2'\to 2}/B(E2)_{2'\to 0})\,(\Delta E_{2'\to 2}/\Delta E_{2'\to 0})^5,$$

where N is the intensity of the γ radiation emitted in the corresponding transition and ΔE is the energy of the γ quanta.

The mean life τ of the $2'$ state was computed from the formula

$$1/\tau = 1/\tau_{2'\to 0} + 1/\tau_{2'\to 2}.$$

The values of the partial lifetimes ($\tau_{2'\to 0}$ and $\tau_{2'\to 2}$) were calculated from the values of $B(E2)_{2'\to 0}$ and $B(E2)_{2'\to 2}$ found earlier.

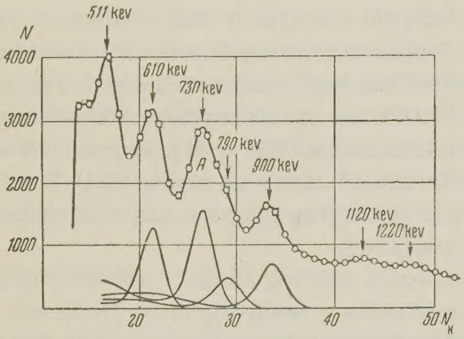

FIG. 1. Instrumental spectrum of γ rays emitted in Coulomb excitation of natural tungsten; E_α = 14.5 Mev.

3. RESULTS OF THE MEASUREMENTS

Figure 1 shows the instrumental spectrum of γ lines emitted after Coulomb excitation of natural tungsten.* The lines at 1120 and 1220 kev must be assigned as radiation in W^{182}, emitted in the $2'\to 2$ and $2'\to 0$ transitions. The maxima in the spectrum are shown more clearly in Fig. 2, which gives the instrumental spectrum taken when the lower limit of the circuit transmitting the pulses to the input of the 50-channel analyzer was set so that pulses of relatively low amplitude did not reach the analyzer. The difference in energy of the two γ lines corresponds to the energy of the first rotational level of W^{182}, which is 100.1 kev, according to the data of reference 3.

The line at 900 kev should be assigned to the $2'\to 0$ transition in W^{184}. Since the energy of the first rotational level[3] of W^{184} is 111 kev, the energy of the $2'\to 2$ transition to the first rotational level of W^{184} should be 900 − 111 = 789 kev. Actually we see from Fig. 1 that peak A is composite — on its right edge there is an indication of a peak with ΔE = 790 kev.

The lines at 730 and 610 kev should be assigned to the radiation emitted in the $2'\to 0$ and $2'\to 2$ transitions in W^{186}. The difference in energy of these lines corresponds to the energy of the first rotational level of W^{186}, which is 122.5 kev according to the data of reference 3.

The 511 kev line is apparently annihilation radiation. Positron emitters can be formed in (α, n) reactions on light element impurities in the tungsten.

The theoretical line shapes are shown for the 900, 790, 730, and 610 kev lines in the lower part of Fig. 1; these curves were drawn on the basis of data given in reference 12. The fact that peak A is composite and consists of two peaks with the energies given above is confirmed as usual: when we add the individual peaks with ΔE = 730 and 790 kev shown at the bottom of Fig. 1, we get a composite peak of the same shape as that found in the experiment.

Figures 3 and 4 show the instrumental γ spectra found after Coulomb excitation of targets enriched in W^{184} and W^{186} respectively. The results obtained with these targets give additional proof of the correctness of the identification of the γ lines found in the spectrum of natural tungsten. In fact, when we irradiate a target enriched in W^{184}, only the 790 and 900 kev lines appear, and we see only the 610 and 730 kev lines from a target enriched in W^{186}. Unfortunately the amount of impurities in the enriched samples proved to be considerably greater than in natural tungsten. One can judge the relative amounts of impurities in various targets from the relative intensity of the 511-kev line in Figs. 1 and 4. The increased content of impurities caused the peak-to-background ratio for the enriched samples to be almost a tenth of that for natural tungsten. The values of $B(E2)$ found from the experiments with W^{184} and W^{186} differ little from the results obtained with natural tungsten. In view of our previous remarks concerning

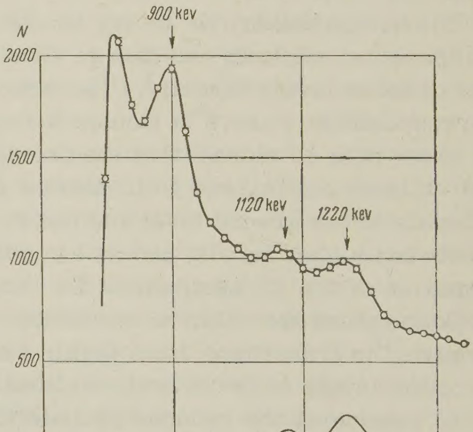

FIG. 2. Expanded spectrum of γ rays emitted in Coulomb excitation of natural tungsten; E_α = 14.5 Mev.

---

*We shall use N_k for the channel number and N for the total number of counts in a channel per microcoulomb in the bombarding beam.

the ratio of effect to background, we used only the data obtained from measurements on natural tungsten targets in calculating the averaged values of $B(E2)_{2'\to 0}$ given in Table I.

The yield of γ quanta from Coulomb excitation of a level drops markedly with increasing excitation energy of the level. Thus in using a sample enriched in W^{182} but containing all sorts of impurities the intensity of the peaks corresponding to deexcitation of the excited level at $\Delta E = 1222$ kev in W^{182} was so small compared to background that the energy of the corresponding γ rays could not be measured reliably.

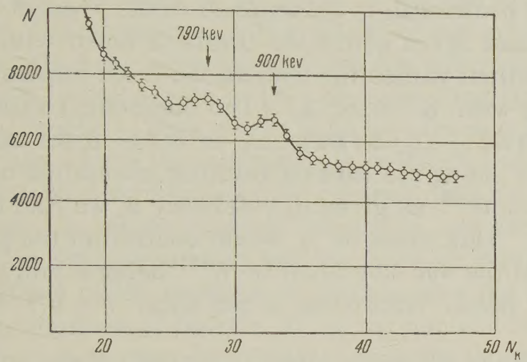

FIG. 3. Instrumental spectrum of γ rays emitted in Coulomb excitation of W^{184}; $E_\alpha = 13.1$ Mev.

The data obtained from Coulomb excitation of natural tungsten are presented in Table I. The values of $B(E2)_{2'\to 0}$ and $B(E2)_{2'\to 2}$ are the averages of data of ten experiments at four different values of E_α in the case of W^{184} and W^{186}, and of the data of four experiments at $E_\alpha = 14.5$ Mev in the case of W^{182}.

The table also gives the ratios $\eta = B(E2)_{2'\to 0}/B(E2)_{2'\to 2}$, the lifetimes of the excited states and, finally, the values of F which is the ratio of the experimental value of $B(E2)_{2'\to 0}$ to the value computed from the formula for single particle transitions on the assumption that the nuclear radius is $R_0 = 1.2\,A^{1/3} \times 10^{-13}$ cm. The standard deviation of the values of $B(E2)_{2'\to 0}$ and $B(E2)_{2'\to 2}$ was less than 10%. The overall error in these quantities due to the arbitrariness in drawing the background curve and to statistical errors amounts to 25% according to our estimates. The error in the ratio η is 15% for W^{186}, 20% for W^{184}, and 30% for W^{182}. The error in the value of η for W^{184} and W^{186} is smaller than the error in the individual values of $B(E2)_{2'\to 2}$ and $B(E2)_{2'\to 0}$ because η is affected less by the inaccuracy in drawing the background curve. On the other hand, the overall error in the values of $B(E2)_{2'\to 2}$ and $B(E2)_{2'\to 0}$ for W^{182} is determined to a large extent by statistical errors, so in this case the error in the ratio η will be greater than the errors in the individual values of $B(E2)$.

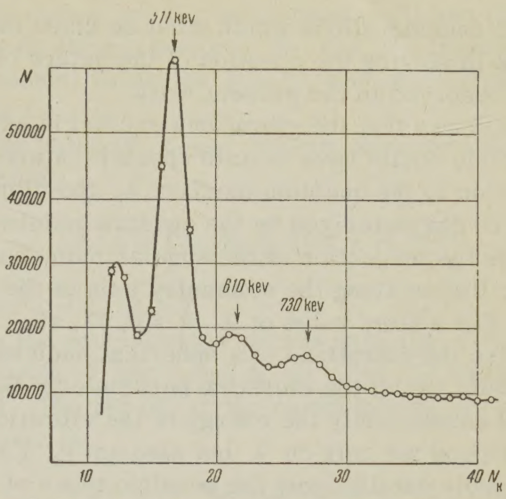

FIG. 4. Instrumental spectrum of γ rays emitted in Coulomb excitation of W^{186}; $E_\alpha = 14.5$ Mev.

4. DISCUSSION OF RESULTS

As already mentioned, in the spectrum of γ rays emitted in Coulomb excitation of tungsten nuclei we observed γ rays corresponding to excitation of a level in W^{182} at 1220 kev, a level at 900 kev in W^{184}, and a level at 730 kev in W^{186}. These results show that the 1220, 900, and 730-kev γ lines correspond to transitions to the ground states (and are not emitted in transitions between higher levels), and that these levels can be assigned as 2^+ states. We have thus obtained experimental confirmation of the assumptions made in reference 11 regarding the levels of W^{184} and W^{186} and have found independent additional evidence for the 2^+ assignment of the level with $\Delta E = 1220$ kev in W^{182}.

In Coulomb excitation of nuclei, one can excite single particle and "pair" levels in addition to rotational and vibrational levels. We next discuss

TABLE I

Isotope	$\Delta E_{0\to 2'}$, Mev	$\frac{B(E2)_{2'\to 0}}{e^2}$, 10^{-48} cm^4	$\delta\left(\frac{B(E2)_{2'\to 0}}{e^2}\right)$, %	$\frac{B(E2)_{2'\to 2}}{e^2}$, 10^{-48} cm^4	$\frac{B(E2)_{2'\to 0}}{B(E2)_{2'\to 2}}$	$\delta\left(\frac{B(E2)_{2'\to 0}}{B(E2)_{2'\to 2}}\right)$, %	τ, 10^{-12} sec	F
W^{182}	0.22	0.051	25	0.043	1.2	30	0.38	8
W^{184}	3.90	0.038	25	0.055	0.69	20	2.2	6
W^{186}		0.040	25	0.076	0.53	15	5.6	6

various considerations which must be taken into account in solving the question of the nature of the levels observed in the present work.

It is known that the vibrations excited in axially symmetric nuclei have certain special features.[13] In addition to the quantum number λ, the vibrations are characterized by the quantum number ν which is the projection of the angular momentum of the oscillation along the symmetry axis of the nucleus. For a fixed value of λ, $\nu = 0, \pm 1, \pm 2, \ldots \pm \lambda$.

Unlike the vibrations of a spherical nucleus, for spheroidal nuclei the vibration parameters B_2 and C_2 and consequently the energy of the vibrational state depend not only on λ but also on ν. For $\lambda = 2$ (quadrupole oscillations) the possible types of oscillation of a spheroidal nucleus correspond only to the values $\nu = 0$ and $\nu = \pm 2$, since vibrations with $\nu = \pm 1$ are equivalent to a rotation of the nucleus. Vibrational levels corresponding to $\nu = 0$ are called β vibrations and those with $\nu = \pm 2$ are called γ vibrations.

For rotational bands associated with single phonon excitation, the projection K of the total angular momentum on the nuclear symmetry axis is equal to $|K_0 \pm \nu|$, where K_0 is the value of K in the ground state of the nucleus. For even-even nuclei $K_0 = 0$, so that K = 2 for γ-vibrational levels and K = 0 for β-vibrational levels. Figure 5 shows the spins and parities of the levels of the rotational bands.

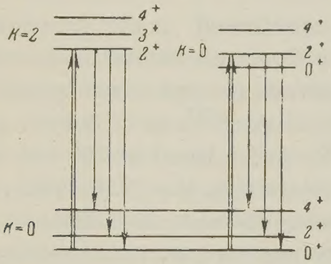

FIG. 5. Level sequence in rotational bands. The lowest band is associated with the nuclear ground state. On the left are excited γ-vibrational states, on the right excited β-vibrational states.

Since the most probable transitions resulting from Coulomb excitation are E_2 transitions, it follows from Fig. 5 that in Coulomb excitation of vibrational levels in even-even nuclei either the second level of the rotational band associated with β vibration or the first level of the band associated with excitation of γ vibration will be excited. Both levels have the same spin value (I = 2) and they have the same parity as the ground state, but their K values are different.

It was shown in reference 8 that the ratios of the reduced probabilities for transitions of a given multipolarity from any level to the levels of a rotational band can be expressed in terms of Clebsch-Gordan coefficients for whose calculation we need to know only the values of I and K and the multipolarities of the transitions between the various states. For the case of electric quadrupole transition from a level with I = 2′, K = 2 to levels with I = 0, 2, and 4, and K = 0 (which form the rotational band associated with the ground state), these ratios are 0.7 : 1 : 0.05 respectively. If the same levels are reached by transitions from a level with I = 2′, K = 1 or I = 2′, K = 0, the ratios are 2.8 : 1 : 2.3 and 0.7 : 1 : 1.8, respectively.

From Table I we see that the ratios of the reduced probabilities determined in the present experiment agree within the limits of error with the theoretical values for transitions from vibrational levels with K = 0 or 2. (The theoretical value of $\eta = B(E2)_{2' \to 0}/B(E2)_{2' \to 2}$ is 0.7). If we calculate η using the data on relative intensities of γ rays in W^{184} as given in reference 9, we find that $\eta \approx 3$. This value of η would contradict the picture of the 900-kev level in W^{184} being a vibrational level. According to our data, $\eta \approx 0.7$ for W^{184}.

The closeness of the experimental values of η to the values computed theoretically for vibrational levels is a necessary but not a sufficient condition for identifying the tungsten levels which we are treating as vibrational levels. If we assume that these levels are single particle or "pair" levels, then since they are excited as a result of Coulomb interaction their spin must be 2 and their parity the same as that of the tungsten ground state. If in addition the quantum number K is 0 or 2 for these levels, the value of η will be the same as for transitions from β-vibrational or γ-vibrational levels, respectively.

From the data of reference 7 on the relative intensities of radiations emitted by W^{182} in transitions from the 1222-kev level to lower-lying levels of the rotational band based on the ground state of the W^{182} nucleus, it follows that this level has K = 2. Thus the 1222-kev level is not excited as the result of a pair transition (since we would then have to get a level with K = 0).

The energies of the excited levels of W^{184} and W^{186} considered in the present work are much lower than the level in W^{182}. It is known that in a heavy nucleus the energy of a level formed by a pair transition always exceeds 1 Mev. We should thus assume that the levels with $\Delta E = 900$ kev in W^{184} and 730 kev in W^{186} are also not "pair" levels.

For Coulomb excitation of a single particle level in an even-even nucleus, the value of K for the level must be 2 since the level has I = 2 and K = I for single particle excitation. In this case the value of η will be the same as for γ-vibrational levels. Thus our experimental data on the ratio of the values of B(E2) generally speaking do not exclude the possibility that the highly excited levels of the tungsten isotopes which we are considering are the result of single particle transitions, and that these levels have K = 2, I = 2 and parity the same as that of the ground state.*

However there are arguments in favor of the assumption that these levels are γ-vibrational levels. The value J′ of the moment of inertia of the W^{182} nucleus in the excited state (ΔE = 1222 kev) is close to the value J for the ground state of this nucleus. (The values of the moments of inertia were determined from the energies of the two lowest levels in the corresponding rotational bands.) This result is to be expected for the case where the excitation is collective and the internal structure of the nucleus does not change. In single-particle excitation, the particle outside the closed shell has the familiar distorting effect on the nucleus, so in this case the value of the moment of inertia J′ of the nucleus in the excited state should be greater than the value J for the ground state.

Excitation of a single particle level in even-even nuclei must occur as a result of breaking up a pair of nucleons. In the nuclei we are considering, the pairing energy exceeds 1 Mev. Since the energies of the states excited in W^{184} (ΔE = 900 kev) and W^{186} (ΔE = 730 kev) are less than the energy of the state excited in W^{182} and also less than 1 Mev, if we assume that the level at ΔE = 1220 kev in W^{182} is not a single particle level we can also make the same assertion for these levels in W^{184} and W^{186}.

Reference 14 gives formulas for calculating the parameters B_2 and C_2 for γ-vibrational states:

$$\frac{B(E2)_{2'\to 0}}{e^2} = \frac{1}{5}\left(\frac{3}{4\pi} Z R_0^2 \beta\right)^2 \frac{\hbar}{\sqrt{B_2 C_2}}, \tag{1}$$

$$E_{\mathbf{vibr.}} = \hbar \sqrt{C_2 / B_2}. \tag{2}$$

Here Z is the atomic number of the nucleus, R_0 its radius, $E_{\text{vibr.}}$ the energy of the vibrational transition, and β the nuclear deformation parameter.

If on the basis of the arguments presented above we assume that these excited states are γ-vibrational states, we can use formulas (1) and (2) to compute the parameters B_2 and C_2 from the experimental values of B(E2) and $E_{2'\to 0}$ given in Table I.

The value of $E_{\text{vibr.}}$ was determined from the equation

$$E_{2'\to 0} = E_{\mathbf{vibr.}} + \frac{\hbar^2}{2J}[I(I+1) - K^2],$$

where I = 2, K = 2.

In the computations we assumed that the moment of inertia J was equal to its value J_0 in the ground state. The results of the computations are shown in Table II.

TABLE II

Isotope	C_2, Mev	$\hbar^2/B_2$, Mev
W^{182}	21	0.023
W^{184}	18	0.042
W^{186}	14	0.10

In reference 14 the values of C_2 for vibrations in W^{182} and W^{186} were calculated using the eigenfunctions found by Nilsson.[15] These values are 24.5 and 27 Mev, respectively. In view of the experimental error in determining B(E2), the agreement between the values of C_2 given in Table II and the theoretical values must be considered to be satisfactory.

It is known that the energy of a rotational level with spin I is decreased by an amount ΔE_I as a result of interaction between rotational and vibrational excitation. Knowing the energies of the first and second rotational levels enables us to determine ΔE_I from the experiment. If we disregard the decrease in energy of rotational levels due to interaction with β vibrations, i.e., if we assume that ΔE_I is completely determined by the interaction between rotational and γ-vibrational excitations, we find from reference 14 that

$$\Delta E_I = -\frac{1}{6C_2}\left(\frac{\hbar^2}{J}\right)^2 I^2 (I+1)^2,$$

Then using the values of ΔE_I and $\hbar^2/J$ found from experiment, we can determine C_2. For W^{182}, C_2 = 12.5 Mev. This calculation gives a lower limit for C_2.

Lack of precise data for the energy of the second rotational level of W^{184} and W^{186} prevents us from making similar calculations for these nuclei.

It is known that

$$B(E2)_{2'\to 0} = B(E2)_{2\to 0} E_{\mathbf{vibr.}} / C_2. \tag{3}$$

For the tungsten isotopes $E_{\text{vibr}}/C_2 \approx 1/20$, while

---

*If the 2′ level has K = 2, the transition 2′ → 2 occurs with a change in K of two units. According to the selection rules given in reference 8, the M1 transition is forbidden in this case (K-forbiddenness), so that the 2′ → 2 transition will be mainly electric quadrupole.

$B(E2)_{2\rightarrow 0}$ is approximately 140 times as great as the reduced probability for a single particle transition. It follows from formula (3) that the ratio $F = B(E2)_{2'\rightarrow 0}/B(E2)_{s.p.}$ should be ~7. As we see from the values of F given in Table I, the value of F found from experiment actually is in this range.

We are very grateful to B. L. Birbair, L. K. Peker, and L. A. Sliv for discussion of the results presented here.

---

[1] McClelland, Mark, and Goodman, Phys. Rev. **97**, 1191 (1955).

[2] Huus, Bjerregaard, and Elbek, Kgl. Danske Videnskab. Selskab Mat.-fys. Medd. **30**, No. 17 (1956).

[3] Chupp, Clark, Du Mond, Gordon, and Mark, Phys. Rev. **107**, 745 (1957).

[4] Alkhazov, Andreev, Erokhina, and Lemberg, J. Exptl. Theoret. Phys. (U.S.S.R.) **33**, 1347 (1957); Soviet Phys. JETP **6**, 1036 (1958).

[5] Alkhazov, Andreev, Gal'perin, Grinberg, Gusinskii, Erokhina, and Lemberg, Тезисы докладов на Всесоюзной конференции по ядерным реакциям при малых и средних энергиях (Reports of the All-Union Conference on Low and Medium Energy Nuclear Reactions) Acad. Sci. Press, Moscow, 1957, p. 42.

[6] P. Leman, Reports of the All-Union Conference on Low and Medium Energy Nuclear Reactions, Moscow, 1957.

[7] Murray, Boehm, Marmier, and Du Mond, Phys. Rev. **97**, 1007 (1955).

[8] Alaga, Alder, Bohr and Mottelson, Kgl. Danske Videnskab. Selskab Mat.-fys. Medd. **29**, No. 9 (1955).

[9] F. D. S. Butement and A. J. Poë, Phil. Mag. **46**, 482 (1955).

[10] A. J. Poë, Phil. Mag. **46**, 1165 (1955).

[11] L. K. Peker, Report to the 8'th Annual Conference on Nuclear Spectroscopy, Leningrad, 1958.

[12] Maeder, Müller, and Wintersteiger, Helv. Phys. Acta **27**, 3 (1954).

[13] Alder, Bohr, Huus, Mottelson and Winther, Revs. Modern Phys. **28**, 432 (1956).

[14] Birbrair, Sliv, and Peker, J. Exptl. Theoret. Phys. (U.S.S.R.), in press.

[15] S. G. Nilsson, Kgl. Danske Videnskab. Selskab Mat.-fys. Medd. **29**, No. 16 (1955).

Translated by M. Hamermesh
289

SOVIET PHYSICS JETP VOLUME 35(8), NUMBER 6 JUNE, 1959

ENERGY SPECTRA AND NUCLEAR INTERACTIONS OF COSMIC-RAY PARTICLES

N. M. KOCHARIAN, G. S. SAAKIAN, and Z. A. KIRAKOSIAN

Physics Institute, Academy of Sciences, Armenian S.S.R.

Submitted to JETP editor June 7, 1958

J. Exptl. Theoret. Phys. (U.S.S.R.) 35, 1335-1349 (December, 1958)

Results are presented of an investigation carried out at 3200 m above sea level at the Aragats high-altitude laboratory during 1953 to 1956. The energy distributions of protons and μ mesons were measured in the range up to 100 Bev. The proton and μ-meson spectra can be approximated by the expressions $3.2 \times 10^{-3}(2+E)^{-2.8}dE$ ($E > 3$ Bev) and $0.5(5+E)^{-3}dE$ ($E > 4$ Bev) respectively. Data are given on the cross sections for inelastic nuclear interactions of high-energy π mesons and protons in graphite, copper, and lead. The inelastic nuclear interaction cross sections for protons and π mesons (σ_a) were found to be equal. The following values were found for graphite, copper, and lead respectively: $\sigma_a = 0.65\,\sigma_0$, $0.75\,\sigma_0$, and $0.9\,\sigma_0$, where $\sigma_0 = \pi(1.4 \times 10^{-13} A^{1/3})^2$ is the geometrical nuclear cross-section.

1. ENERGY SPECTRUM OF μ MESONS AT 3200 m ABOVE SEA LEVEL

THE energy spectrum of the μ mesons was determined with the magnetic spectrometer shown in Fig. 1. The accuracy of momentum measurements was higher than in the previous experiments.[1,2] The standard deviation amounted to 3, 10, 22, and 66% for 1, 5, 10, and 30 Bev/c respectively.

Protons and π mesons were distinguished from μ mesons by the nuclear interactions which they underwent in graphite absorbers A_1 to A_5 placed below the gap. The energy distribution of the μ mesons was calculated subtracting the background of nuclear active particles. The results are given in Table I.

Nuclear interactions in the absorbers placed below the gap were identified by scanning the tracks of separate particles on special diagrams, which consisted of scaled vertical cross-sections of the apparatus, parallel and perpendicular to the lines of forces (cf. Fig. 1). It was not possible to determine the particle sign for particles with 33 Bev/c momentum. For the particles of this momentum range we give therefore the total number of particles of both signs. The number 7 represents the total number of nuclear interactions of protons and π mesons with momentum > 33 Bev/c in absorbers A_1 to A_5.

The total number of μ mesons (Table I, column 8) was obtained by subtracting the number of the nuclear-active particles present in the μ-meson flux from the sum of positive and negative particles; the number of nuclear active particles was obtained in turn by dividing the number of interacting particles by the interaction probability for protons and π mesons in absorbers A_1 to A_5. The latter is given by the expression $W = 1 - \exp(-x/\lambda)$ where $x = 43$ g.cm^{-2} is the total absorber thickness, and λ is the mean free path for inelastic nuclear interactions in graphite. For protons and π mesons in the energy range $E \leq 10$ Bev, $\lambda = 95$ g-cm^{-2} (cf. Sec. 4). Accordingly, it was assumed for all momentum intervals that $W = 0.365$.

The distribution of μ mesons with respect to their deviation in the magnetic field was determined and momentum distribution was then calculated. The following relation between the particle momentum p and the deviation δ was used: $p = 5.09/\delta$. Absolute values of the differential spectrum were obtained by comparing the momentum distribution with the differential spectrum of μ mesons with $p < 14$ Bev/c found in reference 2. It was found that the ordinates of the observed momentum distribution have to be multiplied by 5.47×10^{-7} to obtain absolute values. Within the limits of the statistical errors of both experiments, the above factor is constant in the range $p < 14$ Bev/c. The ordinates of the differential energy spectrum of μ mesons are given in the last column of Table I.

The energy distribution of μ mesons was measured later again. The same array was used (cf. Fig. 1) but the graphite absorbers A_1 to A_5 were replaced by 86.2, 28.6, 47.8, 77.5 and 57 g/cm^2 of lead respectively. Accounting for the thickness of counter walls, the total amount of

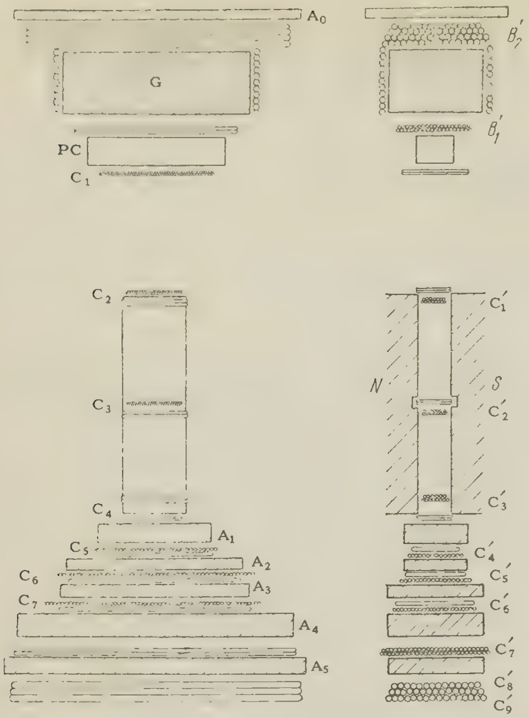

FIG. 1. Vertical cross-sections of the magnetic spectrometer, parallel and perpendicular to the magnetic lines of force. A_0) lead 32 g/cm² thick for absorption of the electron-photon component; $A_1 - A_5$ graphite, copper, or lead absorbers. $C_1 - C_4$) coordinate counter trays; G) graphite absorber; PC) proportional counter; C and B (with indices and dashes) – Geiger counter trays.

matter below the gap was equal to 300 g/cm². The results of the measurements are given in Table II. As in the first experiment, it was necessary to subtract the flux of nuclear active particles from the total flux to determine the flux of μ mesons. It was possible to find the number of nuclear interactions during the total time of observation by analyzing the particle trajectories. In this series of measurements we considered the interactions in the three first absorbers A_1 to A_5 only, the total thickness of which was 156 g/cm². In the measurements of the μ-meson spectrum, misses occurred sometimes in the last tray of counters C_9 and C_9' (counters did not fire) and we decided therefore to exclude absorbers A_4 and A_5 from consideration in order to avoid possible errors. It follows from our data (cf. Sec. 4) that, in the measured momentum range, the mean free path for inelastic nuclear interactions of protons and π mesons in lead is approximately equal to $\lambda = 195$ g/cm². The probability of an inelastic nuclear interaction in absorbers A_1 to A_3 is $W = 1 - \exp(-156/195) = 0.551$. Consequently, the actual number of protons and π mesons is equal to the ratio of the number of observed interactions to the value of the probability $W = 0.551$. The numbers of positive and negative μ mesons obtained by subtracting the background of protons and π mesons, are given in columns 8 and 9, and their total number in column 10 of Table II. The momentum distribution of the particles was calculated from the deviation distribution:

$$N(p) = N(\delta)\,d\delta / dp = \delta^2 N(\delta) / 5.09.$$

Furthermore, the ordinates of the obtained distribution were multiplied by 3.0×10^{-7} to obtain absolute values. This factor was found by comparing the measured momentum distribution with that given in reference 2. Corresponding ordinates of the differential μ mesons distribution are given in column 11 of Table II. The obtained spectrum is

TABLE I. Energy distribution of μ mesons (first experiment)

Deviation range δ, cm	Momentum range, Bev/c	Mean momentum, Bev/c	Total number of particles		Number of interacting particles		Total number of μ mesons	Ordinates of the differential μ meson spectrum cm^{-2} sec^{-1} sterad^{-1} Bev^{-1}
			positive	negative	positive	negative		
1	2	3	4	5	6	7	8	9
2.47—2.30	2.06—2.20	2.12	416	285	21	1	641	$(2.47 \pm 0.09) \cdot 10^{-3}$
2.30—2.14	2.20—2.38	2.30	434	325	23	0	702	$(2.30 \pm 0.09) \cdot 10^{-3}$
2.14—1.97	2.38—2.58	2.48	456	306	18	1	710	$(1.98 + 0.07) \cdot 10^{-3}$
1.97—1.81	2.58—2.82	2.70	443	322	14	2	721	$(1.70 + 0.06) \cdot 10^{-3}$
1.81—1.64	2.82—3.09	2.95	476	360	12	2	798	$(1.53 \pm 0.05) \cdot 10^{-3}$
1.64—1.48	3.09—3.45	3.27	525	366	17	2	839	$(1.35 \pm 0,05) \cdot 10^{-3}$
1.48—1.31	3.45—3.88	3.65	527	362	20	1	832	$(1.07 \pm 0.03) \cdot 10^{-3}$
1.31—1.14	3.88—4,44	4.10	530	375	18	2	848	$(8.42 \pm 0.30) \cdot 10^{-4}$
1.14—0.980	4.44—5.20	4.8	574	370	15	1	900	$(6.61 \pm 0.20) \cdot 10^{-4}$
0.980—0.815	5.20—6.25	5.7	537	367	17	1	855	$(4.50 \pm 0.15) \cdot 10^{-4}$
0.815—0.649	6.25—7.80	7.0	528	376	12	1	869	$(2.97 \pm 0.09) \cdot 10^{-4}$
0.649—0.484	7.8—10.4	9.0	559	327	10	2	853	$(1.76 \pm 0.06) \cdot 10^{-4}$
0.484—0.319	10.4—16	12.7	474	293	8	2	740	$(7.60 \pm 0.30) \cdot 10^{-5}$
0.319—0.153	16—33.2	21.5	363	203	6	2	545	$(1.94 \pm 0.11) \cdot 10^{-5}$
0.153—0.000	33.2—∞	66.5	407		7		388	$(1.59 \pm 0.11) \cdot 10^{-6}$

TABLE II. Energy distribution of μ mesons (second experiment)

Deviation range δ, cm	Mean momentum, Bev/c	Total number of particles		Total number of interactions		Nuclear interaction probability	Number of μ^+ mesons	Number of μ^- mesons	Total number of μ mesons	Ordinates of the differential μ meson spectrum cm^{-2} sec^{-1} sterad^{-1} (Bev/c)$^{-1}$
		positive	negative	positive $(p+\pi^+)$	negative (π^-)					
1	2	3	4	5	6	7	8	9	10	11
2.47—2.30	2.12	793	560	54	1	0.551	695	558	1253	$(2.56\pm0.07)\cdot10^{-3}$
2.30—2.14	2.39	780	539	49	2	0.551	692	536	1228	$(2.17\pm0.06)\cdot10^{-3}$
2.14—1.97	2.48	816	577	48	1	0.551	760	575	1335	$(2.03\pm0.06)\cdot10^{-3}$
1.97—1.81	2.70	837	623	49	3	0.551	747	618	1365	$(1.75\pm0.05)\cdot10^{-3}$
1.81—1.64	2.95	866	636	39	5	0.551	796	627	1423	$(1.52\pm0.04)\cdot10^{-3}$
1.64—1.48	3.27	913	668	34	3	0.551	852	663	1515	$(1.33\pm0.03)\cdot10^{-3}$
1.48—1.31	3.65	971	722	33	4	0.551	911	715	1626	$(1.13\mp0.03)\cdot10^{-3}$
1.31—1.14	4.10	983	709	30	5	0.551	931	700	1631	$(8.76\pm0.22)\cdot10^{-4}$
1.14—0.980	4.80	1017	705	29	3	0.551	965	700	1665	$(6.75\pm0.17)\cdot10^{-4}$
0.980—0.815	5.70	999	647	29	3	0.551	947	642	1589	$(4.6\pm0.12)\cdot10^{-4}$
0.815—0.649	7.0	944	642	25	5	0.551	900	633	1533	$(2.95\pm0.07)\cdot10^{-4}$
0.649—0.484	9.0	839	602	23	4	0.551	798	595	1393	$(1.65\pm0.05)\cdot10^{-4}$
0.484—0.319	12.7	707	561	20	3	0.551	670	556	1226	$(7.14\mp0.2)\cdot10^{-5}$
0.319—0.153	21.5	555	458	12	2	0.551	533	454	987	$(1.98\pm0.06)\cdot10^{-5}$
0.153—0.0	66.5	720		7		0.551	709		709	$(1.64\mp0.06)\cdot10^{-6}$

in a good agreement with that measured in the first series of measurements. The energy distribution of the μ mesons is shown in Fig. 2. The top curve represents the integral distribution, and the lower one the differential distribution. A portion of the curve, for $E < 2$ Bev, is taken from reference 2. In the range $E > 4$ Bev the obtained energy spectrum can be accurately described by the power

$$n_{\mu}(E)\,dE = 0.5\,(E+5)^{-3}dE. \qquad (1)$$

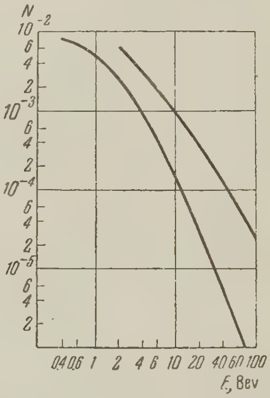

FIG. 2. Differential (lower curve) and integral (upper curve) energy spectrum of μ mesons at 3200 m above sea level. The y-axis represents the intensity N in units of cm^{-2} sec^{-1} sterad^{-1} Bev^{-1} for the differential, and cm^{-2} sec^{-1} sterad^{-1} for the integral spectrum.

2. ENERGY SPECTRUM OF PROTONS AT 3200 m ABOVE SEA LEVEL

The energy distribution of the protons was determined in four independent experiments.

Experiment 1. Three ordinates of the differential proton spectrum were obtained from the experimental data on the μ-meson energy distribution given in reference 2, where the experimental setup is described. In these experiments there were no absorbers above the gap, with exception of a light cover 7 g/cm^2 thick made of wood and iron. Six absorbers A_1 to A_6 were placed below the gap. The absorber A_1 was made of lead 45.2 g/cm^2 thick, the remaining ones were made of copper, 8.9, 37.4, 16, 53.4, and 17.8 g/cm^2 respectively. The relation between the particle momentum in Bev/c and their deviation in the magnetic field was $p = 7/\delta$. The projections of the trajectories of all particles were plotted on diagrams and carefully analyzed. This procedure made it possible to establish whether a particle underwent an inelastic nuclear interaction in absorbers A_1 to A_6, or traversed them without interacting. Stars, particles stopping without a visible effect, and large-angle (> 10°) scattering events were counted as interactions. Interacting particles were assumed to be protons and π^+ mesons if positive and π^- mesons if negative. The measurements were carried out during 267 hours. The number of positive particles recorded in the ranges $2.33 < p < 3.5$, $3.5 < p < 7$, and $7 < p < \infty$ Bev/c was 1650, 1715, and 1448 respectively. It was found in scanning that 160, 111, and 57 of these particles, respectively, underwent inelastic nuclear interactions. In the corresponding momentum ranges, the number of particles was 1086, 1212, and 768 respectively, of which 5, 9, and 6 underwent inelastic nuclear interactions. It is reasonable to assume that, at mountain altitudes, the number of π mesons of both signs in air is equal. The difference between the numbers of positive and negative interacting particles represents therefore the number

TABLE III. Energy distribution of protons

Deviation range δ, cm	Momentum range, Bev/c	Energy range, Bev	Mean energy, Bev	Number of particles observed	Aperture	Stopping probability	Ordinates of differential spectrum	
							Momentum cm^{-2} sec^{-1} $sterad^{-1}$ $(Bev/c)^{-1}$	Energy cm^{-2} sec^{-1} $sterad^{-1}$ Bev^{-1}
1	2	3	4	5	6	7	8	9
26—21	0.245—0.303	0.03—0.05	0.04	105	0.732	1.00	42±4.1	150±15
21—17	0.303—0.376	0.05—0.07	0.06	228	0.815	1.00	65.4±4.3	193±13
17—14	0.376—0.455	0.07—0.10	0.08	369	0.875	1.00	93.2±4.9	221±11
14—12	0.455—0.531	0.10—0.14	0.12	436	0.905	1.00	108±5	234±11
12—11	0.531—0.579	0.14—0.16	0.15	284	0.92	1.00	110±6	220±13
11—10	0.579—0.636	0.16—0.19	0.18	398	0.93	1.00	128±6	252±13
10—9	0.636—0.707	0.19—0.24	0.21	506	0.94	1.00	129±6	208±9
9—8	0.707—0.795	0.24—0.29	0.26	617	0.95	1.00	126±5	209±8
8—7	0.795—0.91	0.29—0.37	0.34	731	0.96	1.00	114±6	162±9
7—6	0.91—1.06	0.37—0.47	0.44	827	0.97	1.00	99.7±6.3	145±9
6—5	1.06—1.27	0.47—0.64	0.60	772	0.98	0.91±0.04	70.2±6.2	87±6
5—4	1.27—1.60	0.64—0.91	0.80	562	0.99	0.66±0.06	44.6±3.8	54.5±5.0
4—3	1.60—2.10	0.91—1.38	1.20	503	1.0	0.46±0.05	37.3±3.5	39.5±4.4
3—2	2.10—3.20	1.38—2.38	1.9	386	1.0	0.33±0.04	18.6±2.9	20.5±2.5
2—1	3.20—6.36	2.38—5.50	3.9	108	1.0	0.23±0.04	2.53±0.46	2.56±0.44
1—0	6.36—∞	5.50—∞	14	13	1.0	0.14±0.04	0.055±0.023	0.055±0.023

of protons which underwent an interaction in absorbers A_1 to A_6. According to the results of Sec. 4, the cross section for inelastic interaction of nucleons in heavy elements, in the energy range studied, amounts to ~ 75% of the geometrical cross-section. Consequently, the probability that the nucleons will interact in absorbers A_1 to A_6 is approximately equal to $1 - \exp(-x/\lambda) = 0.68$ where $x = 45.2$ g/cm^{-2} Pb + 133.5 g/cm^2 Cu = $1.52\lambda_0$ is the total absorber thickness (λ_0 is the mean free path corresponding to the geometrical cross-section of the nucleus; $\lambda = \lambda_0/0.75$ is the mean free path of inelastic interaction). The ratio of interacting protons to the interaction probability 0.68 yields the number of protons in the μ-meson flux. For the ratio of protons to μ mesons we obtained the following expressions:

$$\frac{N_p(p)}{N_\mu(p)} = \begin{cases} 0.0354 \pm 0.0041 & \text{for } \bar{p} = 14 \text{ Bev/c} \\ 0.0546 \pm 0.0045 & \text{for } \bar{p} = 4.66 \text{ Bev/c} \\ 0.0917 \pm 0.0061 & \text{for } \bar{p} = 2.8 \text{ Bev/c} \end{cases} \tag{2}$$

For particles with these momenta we find for the ordinates of the differential μ-meson spectrum $N_\mu(p)$ the values 4.7×10^{-4} and 1.74×10^{-3} respectively. Accounting for Eq. (2) we thus obtain for the ordinates of the differential energy spectrum:

$$N_p(E) = \begin{cases} (1.66 \pm 0.23) \cdot 10^{-6} & \text{for } \bar{E} = 13 \text{ Bev} \\ (3.57 \pm 0.36) \cdot 10^{-5} & \text{for } \bar{E} = 3.9 \text{ Bev} \\ (1.68 \pm 0.14) \cdot 10^{-4} & \text{for } \bar{E} = 2 \text{ Bev} \end{cases} \tag{3}$$

Experiment 2. Six copper absorbers, A_1 to A_6, with total thickness 178 g/cm^2 = $1.65\lambda_0$ were placed under the gap in this series of measurements, and 6852 protons with energy > 30 Mev stopping in the absorbers were recorded during the time of operation ($t = 1.77 \times 10^6$ sec). The energy distribution of these particles is given in Table III, column 5. Protons with $p < 1$ Bev/c stopped in the absorbers as a result of ionization losses, and those with $p > 1$ Bev/c were stopped by inelastic nuclear interactions. The last tray of counters, placed under absorber A_6, was connected in anticoincidence and only the particles which did not reach that tray, i.e., which stopped in absorbers A_1 to A_6, were recorded. Thus, from the observed number of protons with $p < 1$ Bev/c, we can construct directly the spectrum of these particles, while for the region $p > 1$ Bev/c it is necessary to know the stopping probability of the protons in absorbers A_1 to A_6 as a function of energy. This probability was found in the course of the first experiment, in which the conditions were similar with exception of an immaterial difference, namely that in the first experiment absorber P_1 was made of lead, and in the second of copper. The total thickness of absorbers A_1 to A_6, measured in units of mean free path λ_0 corresponding to the geometrical nuclear cross-section, was equal to 1.52 in the first experiment and to 1.65 in the second. As far as nuclear interactions and the stopping of particles were concerned, the physical conditions were therefore almost identical. The area of the absorbers and of the counter trays placed between them are also important, but in that respect the conditions were identical.

It was found in the first experiment that, during a total observation time, 84, 163, and 235 protons with momenta in the ranges $7 < p < \infty$, $3.5 < p < 7$, and $2.33 < p < 3.5$ Bev/c, respectively, traversed

TABLE IV. Energy distribution of protons

Momentum range, Bev/c	Mean momentum, Bev/c	Number of interactions		Mean kinetic energy of protons	Interaction probability	Number of protons		Ratio of protons to μ mesons in air	Ordinates of the differential proton energy spectrum $cm^{-2}\,sec^{-1}\,sterad^{-1}\,Bev^{-1}$
		positive particles	negative particles			Interacting	Total		
1	2	3	4	5	6	7	8	9	10
2.06—2.82	2.38	76	4	1.62	0.365	72 ± 7	197 ± 19	0.071 ± 0.007	$(1.58\pm0.15)\cdot10^{-4}$
2.82—3.88	3.25	49	5	2.45	0.365	44 ± 6	121 ± 16	0.049 ± 0.006	$(6.72\pm0.82)\cdot10^{-5}$
3.88—5.20	4.45	33	3	3.6	0.365	30 ± 5	82 ± 14	0.047 ± 0.008	$(3.76\pm0.64)\cdot10^{-5}$
5.20—7.8	6.3	29	2	5.4	0.365	27 ± 4	74 ± 11	0.043 ± 0.006	$(1.68\pm0.23)\cdot10^{-5}$
7.8—16	10.5	18	4	9.6	0.365	14 ± 4	38 ± 11	0.024 ± 0.007	$(3.12\pm0.91)\cdot10^{-6}$
16—∞	32	15	(3)	31	0.48	12 ± 3	25 ± 6	0.027 ± 0.006	$(2.7\pm0.7)\cdot10^{-7}$
33.2—∞	66	7		65	0.48			0.032 ± 0.012	$(4.5\pm1.7)\cdot10^{-8}$

the array. It was found in scanning the track diagrams of interacting particles that in 12, 37, and 71 cases respectively the protons were stopped in the absorbers together with their secondary products. We find thus that the stopping probability is equal to 0.143 ± 0.044, 0.227 ± 0.041, and 0.302 ± 0.041 for $\overline{p} = 14$, 4.7, and 2.8 Bev/c respectively. The dependence of the stopping probability on momentum was plotted using these points and the point $W = 1$ for $p = 1$ Bev/c. The resulting curve was used to determine the proton stopping probability in the given experiment (cf. Table III, column 7). To calculate the ordinates of the differential energy spectrum of protons, it is necessary to divide the number of stopping protons (Table III, col. 5) by

$$S\omega t\sigma fW(E)\,\Delta E = 5.88\sigma W(E)\,\Delta E\cdot10^6, \qquad (4)$$

where ΔE is the width of the energy interval, $t = 1.77 \times 10^6$ sec is the period of observation, S is the area of the lowest counter tray, ω is the acceptance angle of the array, σ is its aperture, $f = 0.78$ is the particle detection efficiency[3] and $W(E)$ is the proton stopping probability in absorbers A_1 to A_6. In these measurements, $S\omega = 4.26$ cm^2-sterad. The ordinates of the differential momentum and energy spectra of protons are given in Table III, columns 8 and 9 respectively.

Experiment 3. The experimental data on the energy spectrum of μ mesons given in Table I contain as well all the material necessary to determine the proton energy distribution (cf. Table IV). It should be noted (cf. Fig. 1) that there is 32 g/cm^2 of lead above the array to absorb the electron-photon component. Five graphite absorbers A_1 to A_5 with total thickness equal to 43 g/cm^2 were placed under the gap. Nuclear interactions in the absorbers were identified by a careful scanning of the trajectory projections of all particles in the diagrams. The proton interaction probability in absorbers A_1 to A_5 is given in Table IV, column 6. The interaction probability is $W = 1 - \exp(-x/\lambda)$, where $x = 43$ g/cm^2 and λ is the inelastic interactive mean free path for protons. According to the data of Sec. 4, it was assumed for the first five momentum intervals that $\lambda = 95$ g/cm^2 and $W = 0.365$. For the two remaining ones ($E > 16$ Bev) it was assumed that the cross section for inelastic nuclear interactions of protons in graphite is equal to the geometrical cross section of the nucleus and, accordingly, $\lambda = 67$ g/cm^2 and $W = 0.48$. The difference between the numbers of positive (column 3) and negative (column 4) interacting particles are given in column 7 (Table IV). The total numbers of protons present in the μ-meson beam are given in column 8. These were obtained dividing the values of column 7 by the probability W. The ratio of protons to μ mesons is given in column 9. Multiplying these figures by the corresponding coordinates of the μ-meson energy spectrum,[2] we obtain the ordinates of the differential energy spectrum of the protons (column 10). For momenta ≥ 33 Bev/c it was not possible to determine the sign of the charge. A total of 388 particles, seven of which underwent an interaction, was observed in this range. We find thus, accounting for the interaction probability, that the ratio of protons and π mesons to μ mesons in the atmosphere is 0.038 ± 0.012. The relative number of π mesons at the altitude of Aragats was calculated from the production spectrum of the π mesons.[4] It was found that, at 66 Bev, the ratio of π to μ mesons at that altitude is approximately equal to 0.007. Consequently, the ratio of protons to μ mesons for $p = 66$ Bev/c is equal to 0.031 ± 0.012.

Experiment 4. Table II contains data which can be used to find the proton energy spectrum. The total number of protons and π^+ mesons $N(p + \pi^+)$ is given in column 5, and the number of π^- mesons $N(\pi^-)$ which underwent inelastic nuclear interactions in absorbers A_1 to A_3 is

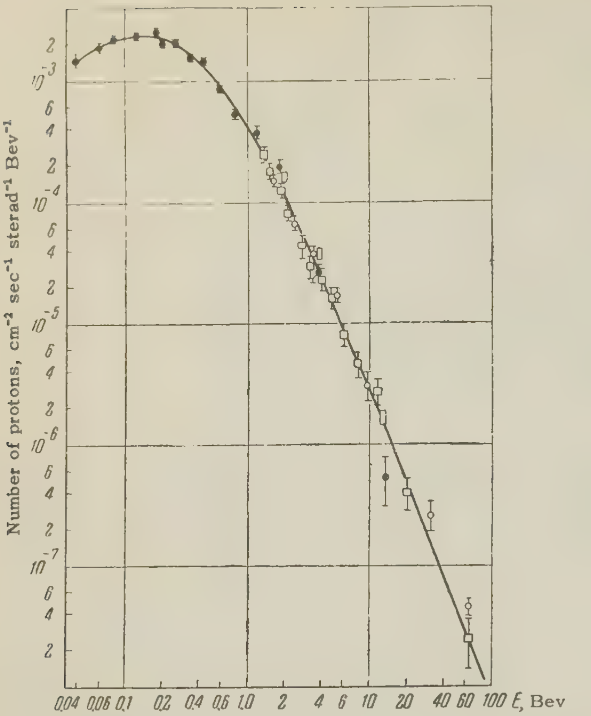

FIG. 3. Differential energy spectrum of protons at 3200 m above sea level.

listed in column 6. It was assumed, as in the previous experiment, that the number of interacting protons is equal to the difference $N(p+\pi^+) - N(\pi^-)$. To obtain the absolute number of protons which traversed the array during its operation, it was necessary to divide the number of interacting protons by the stopping probability $W = 0.551$. Further reduction of data was carried out according to the method explained in the preceding experiment. The final results are shown in Fig. 3. The ordinates of the differential proton spectrum, corresponding to experiments 1, 2, 3, and 4 are denoted by rectangles, black and white circles, and squares respectively. The energy distribution may be approximated, for $E > 3$ Bev, by the expression

$$3.2 \cdot 10^{-3} (2+E)^{-2.8}, \qquad (5)$$

where E is the kinetic energy of the protons in Bev.

3. ABSORPTION OF THE NUCLEONIC COMPONENT IN THE ATMOSPHERE

We shall calculate now, on the basis of the data given in the preceding section, the absorption mean free path of a vertical flux of nucleons in the atmosphere. We shall compare our data with those on the primary intensity. The geomagnetic latitude of the Aragats laboratory is 35°. The primary particle spectrum is cut off at that latitude at approximately 6.7 Bev/c. It is evident that the geomagnetic cut-off will not influence nucleon intensities for $E > 3$ Bev at mountain altitudes. One can assume that the intensities of protons and neutrons are equal in this energy range at mountain altitudes. Such an assumption is confirmed by the fact that for $E > 3$ Bev the number of proton and neutron stars in emulsions is equal within the limits of statistical error.[5-7]

The integral spectrum of primary nucleons can be approximated with a good accuracy by the formula[8]

$$N(0) = 6.1 \cdot (6.34 + E)^{-1.8}.$$

According to Eq. (5), the corresponding nucleon intensity at the altitude of Aragats (pressure equal to 710 g/cm^2, accounting for the small amount of matter above the array) is $N(710) = 3.56 \times 10^{-3}(2+E)^{-1.8}$. Consequently, the absorption mean-free-path of a vertical flux of nucleons with energy $> E$ is

$$l = 710 / \ln[N(0)/N(710)]$$
$$= 394 / \{4.13 + \ln[(E+2)/(E+6.34)]\}.$$

It follows that for nucleon energies E = 3, 5, 10, 30, 50, and 100 Bev we obtain l = 112, 108, 103, 99, 97, and 96 g/cm^2 of air, respectively. The results are in disagreement with those of references 9 to 12, where it was found that for nucleons with energy of the order of 1000 Bev, $l = 112 \pm 6$; 116 ± 9 g/cm^2 [9,12] and $l = 120$ g/cm^2.[10,11] To explain the discrepancy, one has to assume that either the nucleon intensity is too low by a factor of two or that the intensity in the primary flux is too high by the same factor, or that the errors of the spectra are such that their ratio may be wrong by a factor of two. Such an error, however, seems to us improbable. Apparently, the discrepancy is due mainly to the following reason: in the cited litera-

TABLE V. Cross sections for inelastic nuclear interactions of π^- mesons in graphite

Total energy range, Bev 1	Mean energy, Bev 2	Absorber thickness, g/cm^2 3	Total number of π^- mesons 4	Number of interacting π^- mesons 5	Cross section σ_a, mbn 6
0.36—0.55	0.43	43	201	72	206^{+22}_{-25}
0.55—0.79	0.65	43	107	38	202^{+32}_{-33}
0.79—1.15	0.94	43	53	22	248^{+54}_{-57}
1.15—2.00	1.5	43	39	14	206^{+52}_{-60}
2.00—4.00	2.8	43	33	12	210^{+59}_{-68}
4.00—66.0	15	43	11	4	208^{+97}_{-120}

ture, the actual mean free path of the nuclear-active component was determined while we measured the nucleonic component. The difference may be considerable when a large amount of dense substances is present in the array.

4. CROSS-SECTIONS FOR NUCLEAR INTERACTIONS OF π MESONS AND PROTONS IN COPPER, GRAPHITE, AND LEAD

Under certain conditions, a magnetic spectrometer may be used for measurement of the total cross section for inelastic nuclear interactions of π mesons and protons with matter. For that purpose it is necessary to place an absorber over the array and, by means of Geiger-Müller counters, to detect and study the charged particles produced by neutrons in the absorber. The negative particles are π^- mesons only, and the positive ones are π^+ mesons and protons. We assume that heavy mesons do not constitute an important fraction of the number of particles. The cross section for inelastic nuclear interactions of π mesons and protons in the absorber substance can be determined by studying the nuclear interactions in the absorbers placed below the magnetic gap.

For the study of the trajectories and their interactions in the absorbers, we used scaled diagrams representing the array in two perpendicular cross sections (cf. Fig. 1). The projections of the trajectories were plotted in these planes. If a particle did not undergo a nuclear interaction, the projection of its trajectory on the plane parallel to the magnetic lines of force is a straight line passing throughout the array. The projection of the trajectory of such a particle on the plane perpendicular to the lines of force consists of a circular arc within the magnetic field, and in the absorbers outside the field — of a straight line tangential to the circle at the point where the particle left the field. When a particle undergoes a nuclear interaction in the absorbers, the following effects may be observed: (1) visible star production, (2) nuclear scattering, and (3) stopping.

Stars were defined as events in which multiple discharges were observed in counter trays placed between the absorbers. Such a criterion, however, would have been too weak, since multiple discharges could be caused by δ electrons and chance coincidences due to stray particles. Events involving δ electrons may be recognized by the fact that discharges occur always in two adjoining counters, close to the trajectory of the particle, which is then a straight line traversing all absorbers. In the majority of stars, a deviation from a straight line may be observed in at least one projection of the trajectory. In addition, for stars it is possible to construct rays intersecting in one point, and roughly the same number of rays is emitted into the upper and lower hemispheres. It is also characteristic for stars that the prongs directed backwards are generally shorter than those directed forwards, which penetrate the next absorbers, and sometimes traverse all of them. The number of chance coincidences is in general small. In addition, tracks due to these do not intersect in one point, i.e., do not form a star. In spite of the above characteristics of stars, it is sometimes difficult to decide in which absorber the interaction has occurred.

We define as nuclear scattering a deviation of one or both trajectory projections by an angle $\theta \gtrsim 10°$. At the meson energies studied, the angle of multiple Coulomb scattering is small. The above criterion is therefore sufficient for the detection of nuclear scattering events. Some of the cases assumed by us to represent nuclear scattering of mesons, could have been stars, the products of which but one were absorbed in the absorbers and did not reach the counters placed above and below the absorber in which the star was produced.

Finally, we define as particle stopping events in which the particle emerging from the magnetic field disappears in one of the absorbers. Up to that point, the particle should not undergo any interactions. A part of these events represents charge-exchange phenomena and large angle scattering events in which the particle left the apparatus. It is also possible that a star consisting of slow particles only is produced and the secondaries in the same absorber in which they were emitted. Evidently, the number of such cases tends to zero with increasing meson energy.

The cross section for nuclear interactions of π^- mesons was determined directly, since the flux of negative particles consists of π^- mesons only. The cross-section was calculated according to the formula

$$\sigma_a^{(p)} = (N_+\sigma_a^+ - N_\pi\sigma_a^{(\pi)}) / (N_+ - N_\pi), \qquad (6)$$

where N_+ is the number of positive particles, N_π is the number of π^+ mesons assumed to be equal to the number of π^- mesons,[13] $\sigma_a^{(+)}$ and $\sigma_a^{(\pi)}$ are the cross sections for inelastic nuclear interactions of positive particles (π^+, p) and of π^- mesons respectively. It was assumed that $\sigma_a^{(\pi^+)} = \sigma_a^{(\pi^-)}$. This method was used for determination of the inelastic nuclear interaction cross-section of π^- mesons and protons in graphite, copper, and lead.

TABLE VI. Nuclear interactions of positive particles produced in graphite

Momentum range, Bev/c	Mean momentum, Bev/c	Absorber thickness g/cm²	Total number of particles	Number of interacting particles	Cross section σ_a, mbn
1	2	3	4	5	6
2—4	2.7	43	161	58	205 ± 27
3—4	3.3	43	59	20	191^{+41}_{-45}
4—16	6.7	43	30	11	212^{+60}_{-70}

TABLE VII. Cross sections for inelastic interactions of π^- mesons in copper

Total energy range, Bev	Mean energy, Bev	Absorber thickness, g/cm²	Total number of particles	Number of interacting particles	Cross section σ_a, mbn
0.51—0.71	0.60	29	134	33	1030^{+170}_{-157}
0.71—0.91	0.81	52	80	31	996^{+174}_{-171}
0.91—1.07	1.00	52	44	13	712^{+230}_{-269}
1.07—1.28	1.12	88.6	54	29	917^{+193}_{-163}
1.28—1.60	1.50	88.6	46	25	934^{+216}_{-176}
1.60—2.12	1.85	88.6	51	23	712^{+161}_{-139}
2.12—3.18	2.6	141.3	50	30	685^{+139}_{-121}
3.18—6.36	4.2	141.3	31	20	775^{+201}_{-165}
6.36—∞	12	141.3	35	22	742^{+183}_{-150}

(a) Cross sections for inelastic nuclear interactions of π mesons and protons in graphite. In this series of measurements five graphite absorbers A_1 to A_5, 10.1, 5.6, 7.1, 11.7, and 8.5 g/cm² respectively, were placed below the gap. The thickness given include the walls of the counters placed between the absorbers. The total thickness of walls was equal to 3 g/cm² of copper which, for nuclear interactions, is equivalent to 2 g/cm² of graphite. The π^- mesons and protons were produced by neutrons in a graphite absorber (cf. Fig. 1) 32 g/cm² thick.

Data one nuclear interactions of the negative particles (π^- mesons) are given in Table V. Standard deviations of the cross sections for inelastic nuclear interactions of π^- mesons with graphite nuclei, calculated according to the formula $\sqrt{NW(1-W)}$, where N is the number of particles and W is the interaction probability, are given in the table.

The angle of diffraction scattering in graphite is of the order of $\theta = c\hbar/Rp \sim (3.5/p)°$, where $R = 3.2 \times 10^{-13}$ cm is the radius of the graphite nucleus and p is the particle momentum in Bev/c. Large angle ($\theta \gtrsim 10°$) scattering events were also regarded as nuclear interactions. The diffraction scattering angle amounts to 8, 5, and 4° for the first three momentum ranges respectively. The measured cross-sections for these ranges, given in Table V, column 6, include therefore a certain fraction of the cross section for elastic scattering of π^- mesons. For the remaining three energy ranges the angles of diffraction scattering are sufficiently small and the given cross sections refer to inelastic interactions only. It can be seen that, for mean energies equal to 1.5, 2.8, and 15 Bev the cross section σ in graphite is constant within the limits of statistical errors, and approximately equal to $0.65\,\sigma_0$, where $\sigma_0 = 3.22 \times 10^{-25}$ cm² is the geometrical cross-section of the graphite nucleus.

Data necessary for calculating the cross-section for nuclear interactions of positive particles are given in Table VI. From a comparison of the numbers of π^- mesons and of positive particles we can conclude that protons constitute the majority of produced positive particles. The resulting cross sections given in Table VI, represent σ_a of graphite for a mixture of π^+ and p. This cross section, within experimental errors, is equal to that for π^-

TABLE VIII. Total cross sections for inelastic interactions of protons in copper

Momentum range, Bev/c	Absorber thickness g/cm²	Total number of positive particles	Number of interacting particles	Total cross section for positive particles σ_a^+, mbn	Kinetic energy range of protons, Bev	Cross section for protons σ_a, mbn
1	2	3	4	5	6	7
0.91—1.06	29	352	75	872^{+114}_{-91}	0.37—0.47	893^{+134}_{-110}
1.06—1.27	29	329	70	872^{+114}_{-108}	0.47—0.64	867^{+141}_{-133}
1.27—1.59	52	305	102	825^{+92}_{-83}	0.64—0.91	807^{+111}_{-102}
1.59—2.12	52	240	76	764^{+101}_{-84}	0.91—1.38	778^{+135}_{-113}
2.12—3.18	88.6	191	86	712^{+80}_{-73}	1.38—2.38	718^{+118}_{-107}
3.18—6.36	141.3	111	69	727 ± 90	2.38—5.5	711^{+147}_{-143}
6.36—∞	141.3	67	42	737^{+128}_{-113}	5.5—∞	738^{+334}_{-288}

TABLE IX. Cross sections for inelastic interactions of π^- mesons in lead

Total energy range, Bev	Mean energy, Bev	Absorber thickness, g/cm²	Total number of particles	Number of interacting particles	Cross section σ_a, mbn
1	2	3	4	5	6
2.65—3.98	3.18	242	37	29	1835±197
3.19—5.30	3.93	242	40	31	1960±180
3.98—7.95	5.30	242	34	26	1840±139
5.30—15.9	7.95	242	27	20	1815±197
7.95—∞	34.4	242	29	24	1810±215

mesons. One may conclude therefore that, for $p = 2.7$, 3.3, and 6.7 Bev/c, $\sigma_a^{(\pi)} \approx \sigma_a^{(p)} \approx 0.65\,\sigma_0$.

The graphite nucleus is therefore semi-transparent to protons and π mesons at proton energies $E \lesssim 6$ Bev.

(b) Cross sections for inelastic nuclear interactions of π mesons and protons in copper. For the determination of σ_a in copper, absorbers made of that material, 10, 18.3, 23.1, 36.4, 52.9, and 35.6 g/cm² thick, were placed below the gap. The conditions of particle selection were similar to those in the experiments with graphite. The diffraction scattering angle in copper is less than in graphite and is $\theta = (2/p)°$. The data on nuclear interactions of π^- mesons in copper are given in Table VII. It follows from these that, in the energy range above 1 Bev, the cross section for inelastic nuclear interaction is constant within the limits of experimental errors and equals $0.75\,\sigma_0$. Data necessary to determine $\sigma_a^{(p)}$ from Eq. (6) are given in Table VIII.

(c) Cross sections for inelastic nuclear interactions of π mesons and protons in lead. In these experiments interactions were studied in lead absorbers A_1 to A_5, 86.2, 28.6, 47.8, 77.5, and 57.0 g/cm² in thickness. The diffraction scattering angle for lead is $\theta = (1.4/p)°$, and the angle of multiple Coulomb scattering for the first four absorbers taken together in which the interactions were studied is approximately equal to $(5/p)°$. To exclude the contribution of Coulomb scattering we have limited our study to particles with $p \gtrsim 3$ Bev/c. All the data on nuclear interactions of π^- mesons and protons in lead are given in Tables IX and X.

Let us compare our results with the data of other workers. Lindenbaum and Yuan[14] obtained for 0.59-Bev π mesons in graphite $\sigma_a = (186 \pm 22)$ millibarns which, within the limits of experimental errors, is in a good agreement with our results. For 5-Bev π^- mesons in aluminum it was found[15] that $\sigma_a = 0.40$ barns, which amounts to ~72% of the geometrical cross section. In reference 16 it was found that $\sigma_a = 0.218$ barns in graphite at $E_\pi = 4.2$ Bev, which is close to the value obtained by us for that energy range. Our result for graphite in the high-energy range does not contradict the data of reference 16.

Data on the cross sections for inelastic interactions of protons in graphite are available in the literature for low energies only. It was found[17] that $\sigma_a = 0.25$ barns for $E = 0.87$ Bev. In references 18 and 19 it was found respectively that the cross section for 1.4-Bev neutrons in graphite is 0.200 and 0.231. Our results are in agreement with the cited works.

For copper it was found[14] that $\sigma_a = (0.73 \pm 0.11)$ barns at a total π^- meson energy of 0.59 Bev. In reference 20 it was found that $\sigma_a = 0.7$ barns at 3 Bev. For 4.2 Bev π^- mesons produced in an accelerator, it was found that $\sigma_a = 0.794$ barns.[16] The agreement is satisfactory within the limits of experimental accuracy.

Our results are not in disagreement with the

TABLE X. Cross section for inelastic interactions of protons in lead

Momentum range, Bev/c	Absorber thickness g/cm²	Total number of positive particles	Number of interacting particles	Cross section for positive particles, mbn	Kinetic energy of protons, Bev	Cross section for protons σ_a, mbn
1	2	3	4	5	6	7
3.19—5.30	242.2	157	113	1780±170	3.6	1791±220
3.98—7.95	242.2	111	84	1860±208	5.16	1850±260
5.30—15.9	242.2	64	46	1780±230	7.46	1711±300
7.95—∞	242.2	51	39	1830±280	24.6	1770±360

available data on the cross section for inelastic interactions of nucleons in copper.[17-19,21] Cross sections in lead were measured up to 970 Mev. At that energy it was found that $\sigma_a = (1828 \pm 100)$ millibarns.[22] It was found, using the Brookhaven cosmotron, that $\sigma_a = 1730$ millibarns $(\mp 5\%)$ for 1.4 Bev neutrons. In another work[23] it was obtained for 860 Mev protons that $\sigma_a = (1690 \pm 900)$ millibarns. For the low-energy range we have no data to compare with the literature. It should be noted, however, that the cross sections given in Table IX and X for $E > 3$ Bev are, within the limits of statistical errors, identical with the cited values.

On the basis of the data obtained one can draw the following conclusions:

1. The cross sections for inelastic nuclear interactions of π mesons and protons in the energy range $\gtrsim 1$ Bev are, within the limits of experimental errors, equal and independent of energy.

2. If we assume that the geometrical cross section of the nucleus is $\sigma_0 = \pi(1.4 \times 10^{-13} A^{1/3})^2$, the nuclei are partially transparent for π meson and protons with $E > 1$ Bev. The transparency decreases with increasing atomic number. For graphite, copper, and lead we have $\sigma_a = 0.65\,\sigma_0$, $0.75\,\sigma_0$, and $0.9\,\sigma_0$ respectively.

---

[1] N. M. Kocharian, J. Exptl. Theoret. Phys. (U.S.S.R.) 28, 160 (1955), Soviet Phys. JETP 1, 128 (1955).

[2] Kocharian, Aivazian, Kirakosian, and Aleksanian, J. Exptl. Theoret. Phys. (U.S.S.R.) 30, 243 (1956), Soviet Phys. JETP 3, 350 (1956).

[3] N. M. Kocharian, Doctorate Dissertation, Phys. Inst. Acad. Sci., Moscow 1954.

[4] G. S. Saakian, Dokl. Akad. Nauk ArmSSR 24, 3 (1957).

[5] Brown, Camerini, Fowler, Heitler, King, and Powell, Phil. Mag. **40**, 307 (1949).

[6] Camerini, Davies, Fowler, Franzinetti, Muirhead, Lock, Perkins, and Yekutieli, Phil. Mag. **42**, 1241 (1951).

[7] M. Teucher, Helv. Phys. Acta **26**, 434 (1953).

[8] P. Budini and G. Moliere, Das Zusammenspiel der Komponenten. Vortraege ueber kosmische Strahlung. Ed. by W. Heisenberg, 1953, Berlin, p. 365.

[9] K. P. Ryzhkova and L. I. Sarycheva, J. Exptl. Theoret. Phys. (U.S.S.R.) 28, 618 (1955), Soviet Phys. JETP 1, 572 (1955).

[10] Kaplong, Klose, Ritson, and Walker, Phys. Rev. **91**, 1573 (1953).

[11] Klose, Kaplong, Ritson, and Walker, Phys. Rev. **92**, 855 (1953).

[12] G. T. Zatsepin, Doctoral Dissertation, Phys. Inst. Acad. Sci., Moscow 1954.

[13] A. V. Khrimian, Izv. Akad. Nauk SSSR, Ser. Fiz. **19**, 700 (1955) [Columbia Tech. Transl. **19**, 638 (1955)].

[14] S. J. Lindenbaum and L. C. L. Yuan, Phys. Rev. **92**, 1578 (1953).

[15] Ilse Jr., Lagarrigue, and Pyle, Phys. Rev. **100**, 1799 (1955).

[16] Winker, Bostick, and Mayer, Bull. Am. Phys. Soc. **1**, 252 (1956).

[17] Chew, Leavitt, and Shapiro, Bull. Am. Phys. Soc. **29**, 47 (1954).

[18] Coor, Hill, Hornyak, Smith, and Snow, Phys. Rev. **98**, 1369 (1955).

[19] Snow, Coor, Hill, Hornyak, and Smith, Bull. Am. Phys. Soc. **29**, 54 (1954).

[20] Schein, Haskin, and Glasser, Nuovo cimento **1**, 131 (1956).

[21] W. O. Lock and P. V. March, Proc. Roy. Soc. **230A**, 222 (1955).

[22] Abashian, Coll, and Cronin, Bull. Am. Phys. Soc. **7**, 350 (1956).

[23] Chew, Leavitt, and Shapiro, Phys. Rev. **99**, 857 (1955).

Translated by H. Kasha
290

SOVIET PHYSICS JETP VOLUME 35(8), NUMBER 6 JUNE, 1959

OBSERVATIONS OF THE λ-TRANSITION IN HELIUM IN THE PRESENCE OF A THERMAL CURRENT THROUGH THE PHASE BOUNDARY

V. P. PESHKOV

Institute of Physical Problems, Academy of Sciences, U.S.S.R.

Submitted to JETP editor June 14, 1958

J. Exptl. Theoret. Phys. (U.S.S.R.) **35**, 1350-1354 (December, 1958)

Experiments involving the observation of density and temperature discontinuities at the boundary between superfluid and non-superfluid helium in the presence of a thermal current are described. The reasons for the stability of the boundary are explained, and examples of disturbance of this stability at high thermal current densities are presented.

As has been previously communicated,[1] a clearly visible boundary appears in the presence of a thermal flux from non-superfluid in superfluid helium, and discontinuities in the temperature and density are developed at the boundary. Experiments on the observation of this phenomenon were set up in the following manner. In the Dewar vessel 1 of liquid helium illustrated in Fig. 1 there was placed a chamber 3 attached to the tube 2. The chamber formed an optical wedge, bounded on the sides and rear by the glass aperture 4 and made up of two plane-parallel glass flats 5. A flat heater wound of constantan wire was placed on the rear wall to generate a thermal current along the chamber. The forward end of the chamber was sealed hermetically by a platinum foil 6 using BF-4 polymerizing cement. A pressure of one atmosphere measured by means of the manometer 9, was maintained in the liquid helium within the chamber through the tubes 7 and 8. Two chambers, 1.5 and 3 mm in depth, were used for the experiments. Both chambers were 4 mm wide and 16 mm long. With the aid of the telescope 10 and the optical system illustrated in the figure, fringes of equal optical thickness were observed in the chamber in the light of a low-pressure mercury lamp 11. Since the index of refraction for liquid helium differs but little from unity ($n = 1.027$), the variation in the helium density can be obtained from the simple formula $\Delta\rho = Ak$, where k is the number of fringes passing across a given section of the chamber, $\Delta\rho$ is the density variation, and A is a constant of the apparatus. Inasmuch as the most reliable thermometer is a density thermometer, the temperature of the liquid helium was determined from the density. When sufficient power was supplied to the heater, with the temperature of the external bath somewhat below the λ points, the temperature within the chamber began to rise, and, as it passed the λ-point, a visible boundary appeared within the chamber near the heater and moved toward the cold end. It could be maintained at any point in the chamber by suitable adjustment of the power or of the temperature of the external bath.

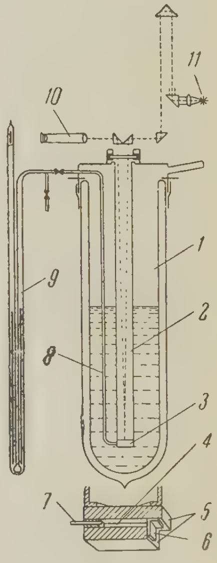

FIG. 1. Apparatus for visual observation of the boundary between superfluid and non-superfluid helium.

In row 1 of Fig. 2 are shown photographs of fringes of equal thickness in the 1.5-mm chamber, containing superfluid helium at a temperature very close to the λ-point, in the absence of a thermal current along the chamber; the photographs in rows 2, 3 and 4 in column a show the interference patterns, respectively, for 0.06, 0.11, and 0.19 w/cm^2. The remaining photos will be discussed in more detail later. The visible boundary shows that in the presence of a thermal current a discontinuity in the density exists at the interface between superfluid and non-superfluid helium. As the thermal flux is reduced the density discontinuity decreases, and the boundary becomes less well-defined and

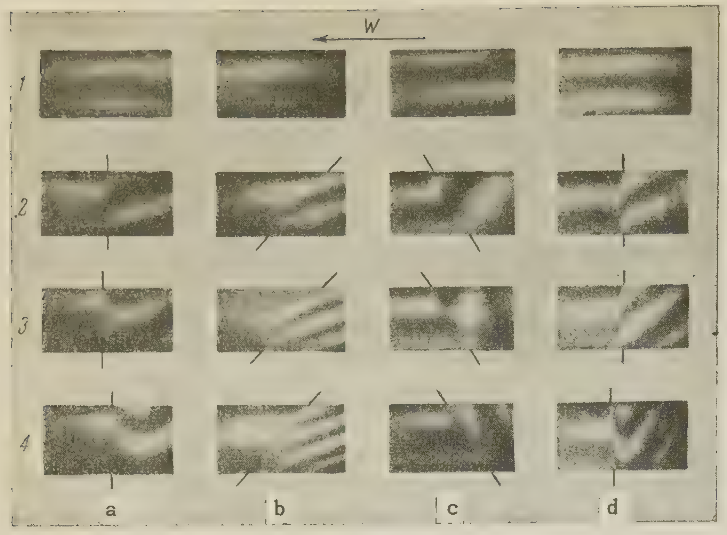

FIG. 2. Fringes of equal optical thickness. Column a) chamber horizontal; columns b and c) chamber inclined laterally by 7° to one side and to the other; column d) chamber inclined by 4.5° with the heater end elevated. Rows correspond, from top to bottom, to thermal fluxes of of 0, 0.06, 0.11 and 0.19 w/cm².

finally becomes invisible. From the corresponding displacement of the interference fringes it is possible to determine the dependence of the magnitude of the density discontinuity upon the intensity of the thermal current.

When the temperature of the external bath was raised and the thermal current was simultaneously reduced in such a way that the boundary remained in one place, no visible displacement of the fringes in the superfluid helium region, and consequently no variation in the temperature, were observed. In the non-superfluid region, however, a gradual procession of the interference fringes took place as the thermal current was decreased. In the 3-mm chamber the pattern was displaced by 2.5 fringes at the boundary as the current density was varied from 0.16 to 0.04 w/cm^2. The results of these measurements are presented in Fig. 3.

As has already been communicated,[1] the discontinuity in the density is proportional to the square of the thermal current density; at 0.16 w/cm^2 the density of the non-superfluid helium at the boundary is less than the superfluid helium density by 1.3×10^{-3} g/cm^3, or approximately 1%, which is equivalent to a temperature rise of 0.3°. Thus, in the presence of a thermal flux through the boundary, equilibrium between the superfluid and non-superfluid helium is established with discontinuities existing in density and temperature.

If the chamber is tilted by 7° to the right (column b) or to the left (column c), then, since the superfluid helium is heavier than the non-superfluid, the boundary is turned obliquely, through an angle of approximately 45°. If the density or temperature discontinuities are now referred to the thermal current passing through unit area of the increased surface, the magnitude of the discontinuity remains the same, to within the experimental error (20%), as for the horizontal chamber. Tilting of the chamber by 4.5° with the heater upward (column d) leads to the same result. For a more detailed investigation of this phenomenon, a resistance thermometer of 40 μ phosphor bronze was placed in one of the chambers, permitting the temperature of the liquid to be measured as the boundary passed through. With this arrangement it was found that the temperature of the superfluid helium at the boundary falls with increasing thermal flux. The fall is approximately linear, and amounts to 0.0009° at 1 w/cm^2. Moreover, a temperature gradient $dT/dx = 1.5 \times 10^{-3}$ deg/cm was observed in the superfluid helium for $W = 0.08$ w/cm^2. In the non-superfluid helium, for inputs in excess of 0.06 w/cm^2, a phenomenon is observed which is at first glance completely incomprehensible. For a thermal flux of 0.08 w/cm^2 the temperature rises by 0.03° in a 0.5 mm interval just beyond the boundary; in the next 0.5 mm it falls by 0.02° and there then follows a sharp increase with a gradient of

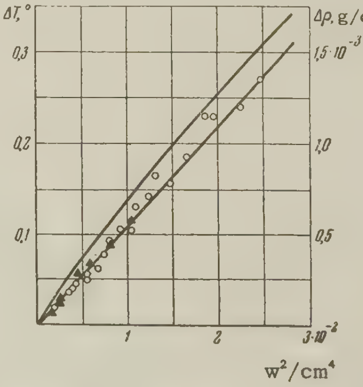

FIG. 3. Dependence of the density discontinuity Δρ (lower curve), and the temperature discontinuity ΔT computed from the change in density (upper curve), upon the square of the thermal current density. o) measurements in the 3-mm chamber; ▲) measurements in the 1.5-mm chamber.

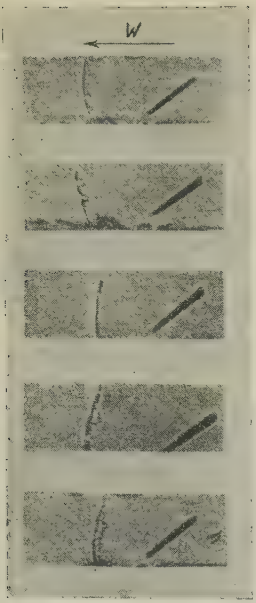

FIG. 4. Vortices extracted by turbulence from the superfluid helium.

10 deg/cm. This phenomenon can also be detected in the photographs of Fig. 2, from the break in the interference fringes in the non-superfluid region at the boundary. In apparent violation of the laws of thermodynamics, a transfer of heat takes place from cold to hot. With lower inputs this phenomenon is not observed.

In order to gain an understanding of what this contradiction involves, the boundary was photographed with flashbulb illumination, under conditions of high thermal flux; the photographs are presented in Fig. 4. As can be seen, vortices of superfluid helium are formed, situated on a thin line at the boundary. The diameter of the vortices is on the order of 0.3 mm. These vortices do not remain in one place, but move from the center of the boundary toward its edges, or, if the chamber is inclined laterally, run toward the lower side. Since both the thermometer and the interference process average the temperature, it is natural that the apparent temperature should be lower in the region of the centers of the vortices than at their origin; no violation of the laws of thermodynamics actually occurs.

It seems strange that a sharp boundary should be able to exist at all. Non-superfluid helium has an extremely small thermal conductivity (6×10^{-5} cal/deg-cm-sec), and in it heat transfer takes place by vigorous convection. Following Prandtl,[2] we shall estimate the effectiveness of convective heat transfer using the formula

$$W = \rho C_p l v \, \partial T / \partial x$$

where W is the thermal current density, ρ is the density of liquid helium, C_p is the specific heat, l is the scale of the turbulence, and v is the pulsation velocity.

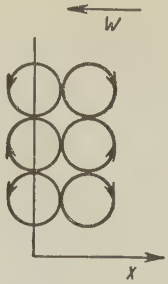

FIG. 5

The crudest model of turbulent transfer is represented by the diagram shown in Fig. 5. By the pulsation velocity v we may here understand the linear velocity of rotation of the helium at the vortex periphery, and the scale l of the turbulence is determined if we compute the heat transfer for such a model to be

$$W = \frac{1}{2r} \int_{-r}^{+r} \rho C_p \omega r \frac{\partial T}{\partial x} \, r dr = \rho C_p \frac{\omega r^2}{3} \frac{\partial T}{\partial x} = \rho C_p v \frac{r}{3} \frac{\partial T}{\partial x},$$

i.e., $l = r/3$.

For $W = 0.11$ w/cm^2 the temperature gradient in the non-superfluid helium is 0.8 deg/cm, and from the photograph in Fig. 4 the scale of the turbulence 1 may be estimated from the radius of the vortices as 0.005 cm. Then

$$v = W / \rho C_p l \frac{\partial T}{\partial x} = 80 \text{ cm/sec.}$$

It is clear that at the boundary there can be no forces capable of preventing the penetration of such turbulence into the superfluid helium. Estimation of the velocity with which the superfluid helium moves through the thin vortex line in the photographs of Fig. 4, under the assumption that the thermal current density is the same at the surface of the vortices as at the boundary, leads to values on the order of 30 cm/sec. Estimation of the critical velocity for superfluid motion at the boundary using the formula $v_{sc} = W/\rho_s Q$, where Q is taken from the measurements of Kapitza and ρ_s is determined from the $\rho_s(T)$ curve at the measured $\Delta T = T_\lambda - T$, leads to values on the order of 80 cm/sec. Moreover, the critical velocity is to a first approximation constant, since

$$\rho_s = \frac{d\rho_s}{dT} \Delta T = \frac{d\rho_s}{dT} \frac{dT}{dW} W = \text{const} \cdot W.$$

Inasmuch as estimates of the critical velocity, the flow velocity in the vortices, and the pulsation velocity yield quantities of the same order, the removal of the vortices from the superfluid and destruction of the sharp boundary at still higher inputs seem natural, since under this condition the velocity of turbulent motion begins to exceed the critical velocity for the motion of the superfluid.

It should be noted that mechanical forces can play no significant part in the processes associated with the displacement of the boundary. If the boundary is displaced by δ, in fact, a thermal energy of order $\epsilon_t = \rho C_p \Delta T \delta$ per unit displaced area must be absorbed or emitted, where ΔT is the temperature discontinuity and C_p is the specific heat of the non-superfluid helium. At the same time, the kinetic energy stored in the volume is $\epsilon_k = \rho v^2 \delta/2$. Thus, the ratio of the energies $\epsilon_k/\epsilon_t = v^2/2C_p\Delta T$; i.e., if we take $C_p \approx 0.6$ cal/g-deg, and, with $W = 0.6$ w/cm^2, $v \approx 50$ cm/sec, and $\Delta T \sim 0.1°$, then $\epsilon_k/\epsilon_t = 5 \times 10^{-5}$. Thus the conditions governing the motion of the boundary must be the thermal relations.

The sharpness of the boundary in this case may be explained on the assumption that, up to some limit at which the turbulent motion begins to remove the vortices from the superfluid helium, heat transfer from the non-superfluid to the superfluid helium for a given temperature discontinuity remains constant, and that any projection on the boundary tends to straighten itself, and the boundary therefore remains even. Since the boundary cannot withstand the penetration of turbulence from the non-superfluid into the superfluid helium and vice-versa, the heat-transfer process may be represented in the following way. Let the boundary move as shown in Fig. 5. The temperature to the left of the boundary is T_λ, while that on the right is T_1 and may in the first approximation be regarded as constant within a distance r from the boundary. The volume taking part in the motion of a vortex centered on the boundary remains for a time $t = \pi r/v = \pi/\omega$ in the superfluid helium region. If we take the relaxation time for the establishment of thermal equilibrium in the superfluid helium to be τ, the temperature of the volume flowing out of it will be $T_2 = T_\lambda + (T_1 - T_\lambda)e^{-t/\tau}$. The thermal flux through the boundary will therefore be written in the form

$$W = \frac{1}{2r}\int_0^r \rho C_p \omega r T_1\, dr + \frac{1}{2r}\int_{-r}^0 \rho C_p \omega r T_2\, dr = \rho C_p \frac{\omega r}{4}(T_1 - T_2);$$

$$W = \rho C_p \frac{v}{4}(T_1 - T_\lambda)(1 - e^{-\pi r/v\tau}).$$

On the basis of this formula it is possible to estimate the relaxation time, which turns out to be of order $\tau \sim 5 \times 10^{-3}$ sec, while the survival time in the superfluid helium $t \sim 10^{-3}$ sec; the formula may therefore be simplified:

$$W \approx \rho C_p \pi r \Delta T / 4\tau.$$

Since from the experiment $\Delta T \propto W^2$, we have in this case $r \sim 1/W$. Although the ideas presented above indicate a pattern for heat transfer through the boundary between superfluid and non-superfluid helium, the question of why the temperature discontinuity is proportional to the square of the thermal flux remains as yet open. It seems to me that an investigation of the phenomena occurring at the boundary between superfluid and non-superfluid helium is of particular interest, since we have here a case in which superfluid helium — a system of strongly-interacting particles particularly subject to quantum-mechanical conditions — interacts with a system which, from its properties, is similar to ordinary liquids for which the classical approximations are completely valid.

I take this opportunity to express my gratitude to Academician P. L. Kapitza for his constant interest and concern with this work, and also to A. I. Filimonov and I. A. Uriutov for their aid in performing the experiments.

---

[1] V. P. Peshkov, J. Exptl. Theoret. Phys. (U.S.S.R.) **30**, 581 (1956); Soviet Physics JETP **3**, 628 (1956).

[2] L. Prandtl, Hydroaeromechanics, IIL, 1949, pp. 149-50.

[3] P. L. Kapitza, J. Exptl. Theoret. Phys. (U.S.S.R.) **11**, 581 (1941).

Translated by S. D. Elliott
291

SOVIET PHYSICS JETP VOLUME 35 (8), NUMBER 6 JUNE, 1959

RATIO OF ISOMERIC AND GROUND STATE YIELDS OF Zn^{69} PRODUCED IN VARIOUS NUCLEAR REACTIONS

K. I. ZHEREBTSOVA, T. P. MAKAROVA, Iu. A. NEMILOV, and B. L. FUNSHTEIN

Radium Institute, Academy of Sciences, U.S.S.R.

Submitted to JETP editor June 16, 1958

J. Exptl. Theoret. Phys. (U.S.S.R.) 35, 1355-1357 (December, 1958)

The ratio of the amounts of Zn^{69} produced in the isomeric and ground states in the $Zn^{68}(dp)Zn^{69}$, $Ga^{69}(np)Zn^{69}$, and $Ga^{71}(d\alpha)Zn^{69}$ reactions was studied. In the first reaction the relative yield of the isomeric state initially increases with increasing deuteron energy, and then remains constant (at about half the ground-state yield). In the second reaction, the ratio is 1.4 for 14-Mev neutrons; in the third reaction it is about 0.5 for 6 to 8 Mev deuterons. The results are discussed on the basis of various reaction mechanisms (direct interactions like stripping, and compound nucleus formation).

IT was shown in various papers[1,2] that when thermal neutron capture can result in formation of the isomeric and ground states of the final nucleus, there is preferential formation of the final state whose spin is closer to that of the initial nucleus.

The suggestion has been made that in reactions with faster particles the probabilities of formation of the isomeric and ground states should be proportional to the statistical weights of these states,[2,3] but this hypothesis is not always in agreement with the experimental data.[3] The apparent explanation is that the probabilities of formation of the final nucleus in various states depend to a considerable extent on the reaction mechanism. If the reaction proceeds via formation of a compound nucleus, then for low energies of the initial particles there should be preferential formation of those states of the final nucleus whose spin differs least from that of the initial nucleus, since the influence of the centrifugal barrier will lead to preferential formation of states of both the compound and final nucleus whose spins are close to that of the target nucleus. With increasing energy of the primary particles, the influence of the centrifugal barrier decreases, and there is an increase in the number of competing cascade transitions and the number of possible excited states in which the final nucleus is formed. This should make the populations of the isomeric and ground states of the final nucleus proportional to the statistical weights of the states. In reactions which proceed via direct interaction, the most probable process may lead to final states with all sorts of spin values, so that the ratio of the populations of the isomeric and ground states should be characteristic for the particular reaction and have entirely different numerical values for different reactions.

In order to determine the relative importance of direct interactions and compound nucleus formation, we undertook an experiment to find the ratio σ^*/σ of the yields in the isomeric and ground states of Zn^{69} formed in various nuclear reactions. Zn^{69} is a β^- emitter with a half life of 57 min, and has an isomeric state which decays to the ground state with a half life of 13.8 hr. Since these periods are markedly different, one can find the ratio σ^*/σ by analysis of the decay curve obtained by counting β particles in a Geiger counter which is not sensitive to γ-rays. Previous to this, measurements have been made of ratios of isomeric to ground state of Zn^{69} formed from thermal neutron capture[1] in Zn^{68} ($\sigma^*/\sigma = 0.29$), and of Zn^{69} produced in the $Ge^{72}(n, \alpha)Zn^{69}$ reaction with 14-Mev neutrons[4] ($\sigma^*/\sigma = 1.1$).

We have studied the $Zn^{68}(d, p)Zn^{69}$, $Ga^{69}(n, p)Zn^{69}$, and $Ga^{71}(d, \alpha)Zn^{69}$ reactions. The deuteron irradiations were done inside the cyclotron chamber. The energy spread of the deuterons in the cyclotron and the effect of target thickness gave an overall energy spread of the order of 0.5 Mev. We should therefore expect several excited states of the compound nucleus to be produced. The targets were irradiated with neutrons in a neutron generator with a tritium target. In both the neutron and deuteron irradiations several interfering activities are produced, so it was necessary to separate the zinc by radiochemical methods.

The ratios σ^*/σ found for Zn^{69} from the $Zn^{68}(d, p)Zn^{69}$ reaction for various deuteron en-

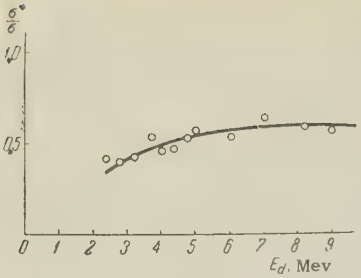

FIG. 1. Ratio σ^*/σ of probabilities of formation of Zn^{69} in isomeric and ground states from the Zn^{68} (d, p) Zn^{69} reaction, as a function of deuteron energy.

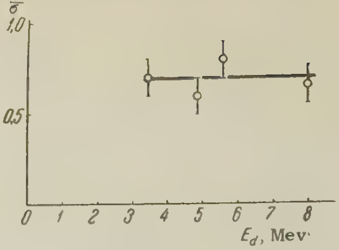

FIG. 2. Ratio σ^*/σ of probabilities of formation of Zn^{69} in isomeric and ground states from the Ga^{71} (d, α) Zn^{69} reaction, as a function of deuteron energy.

ergies are shown in Fig. 1. From the curve of Fig. 1 we see that with increasing deuteron energy the ratio σ^*/σ tends toward a constant value of ~ 0.5, and that there is a relative drop of the probability of formation of Zn^{69} in the isomeric state only at low energies. Such a dependence is completely understandable. The target nucleus has spin 0, and in Zn^{69} the ground state has spin $^1\!/_2$ while the isomeric state has spin $^9\!/_2$. Reactions like (d, p) should proceed with high probability via the stripping mechanism; for low deuteron energies the entry of the neutron into the nucleus into a $^9\!/_2$ level is hindered by the centrifugal barrier, so this naturally results in a relative decrease in the yield of Zn^{69} in the isomeric state.

For the $Ga^{69}(n, p)Zn^{69}$ reaction we found the ratio σ^*/σ only for 14-Mev neutrons. It was 1.4, so in this case formation of the isomeric state is more probable. In the $Zn^{68}(d, p)Zn^{69}$ reaction, at the highest deuteron energies the same compound nucleus Ga^{70} is formed with approximately the same excitation as in the second reaction. The marked difference in the ratio σ^*/σ for the two cases shows that in these processes, or in any case in one of them (probably the first) the principal reaction mechanism is not related to formation of a compound nucleus.

The values of σ^*/σ found for the $Ga^{71}(d, \alpha)Zn^{69}$ reaction at various deuteron energies are shown in Fig. 2; they are all equal to ~ 0.5 within the limits of accuracy of the measurements. A different reaction, $Ge^{72}(n, \alpha)Zn^{69}$, which leads to formation of Zn^{69} via the compound nucleus Ge^{73}, was studied by Levkovskii.[4] For 14-Mev neutrons he found $\sigma^*/\sigma = 1.1$. The energies of excitation of the compound nucleus are the same in the $Ga^{71}(d, \alpha)Zn^{69}$ reaction with 6-Mev deuterons and in the $Ge^{72}(n, \alpha)Zn^{69}$ reaction with 14-Mev neutrons, while the values of σ^*/σ differ by more than a factor of two. From this we must conclude that at least one of these reactions proceeds mainly via a mechanism which is not related to compound nucleus formation.

In the reactions $Zn^{68}(d, p)Zn^{69}$ and $Ga^{71}(d, \alpha)Zn^{69}$, for which we have measured σ^*/σ as a function of energy of the incident particles, this ratio remained almost constant. It therefore seems most reasonable to assume that the processes we have studied proceed mainly via direct interactions, where for each type of primary particle and target nucleus there are certain processes which have high probability and which lead to formation of definite final states which are characteristic for the particular reaction and depend very little on the energy of the incident particles.

---

[1] E. Segré and A. C. Helmholz, Revs. Modern Phys. 21, 271 (1949).

[2] E. der Mateosian and M. Goldhaber, Phys. Rev. 108, 766 (1957).

[3] Meadows, Diamond and Sharp, Phys. Rev. 102, 190 (1956).

[4] V. N. Levkovskii, Тезисы доклада на конференции по ядерным процессам при средних и низких энергиях, ноябрь 1957 г. (Reports of the Conference on Medium and Low Energy Nuclear Processes, Nov. 1957) Acad. Sci. Press.

Translated by M. Hamermesh
292

MULTI-CHARGED PARTICLES EMITTED IN DISINTEGRATION OF CARBON NUCLEI BY 660-Mev PROTONS

V. I. OSTROUMOV and Iu. P. IAKOVLEV

Polytechnic Institute of Leningrad

Submitted to JETP editor June 16, 1958

J. Exptl. Theoret. Phys. (U.S.S.R.) 35, 1358-1363 (December, 1958)

Multi-charged particles ejected from a thin polystyrene film bombarded with 660-Mev protons and possessing ranges larger than $20\,\mu$ were investigated by means of nuclear emulsions. The effective cross section for production of these particles and their angular and energy distribution have been obtained. Measurements of the thickness of tracks produced by the fragments were used to determine the charge of particles with ranges above $40\,\mu$ in the emulsion.

RECENT experiments[1,2] on the disintegration of various nuclei by high energy particles have shown that multi-charged particles called fragments (Li, Be, B and other nuclei) are emitted in such processes with a cross section of the order of several millibarns. Experiments making use of photographic plates and magnetic and radiochemical analyses have yielded some understanding of this process. Unfortunately very little experimental data is presently available and it is difficult to interpret it in terms of a single hypothesis. Photoemulsion techniques may yield valuable information on the process of fragmentation as it permits one to observe the elementary interaction of a fast nucleon with a nucleus. However, nuclear emulsion targets suffer from the disadvantage that the disintegration of heavy (Ag and Br) as well as light nuclei (C, O, N) are registered in the emulsion stack, and it may not always be possible to decide with sufficient certainty whether an observed event belongs to one or the other nuclear group. Various criteria are used to identify the nuclear target (in the above sense). Lazhkin and Perfilov,[1] for example, assume that a star containing fragments and produced by a high-energy proton is due to the disintegration of Ag and Br nuclei if it contains a nuclear recoil track (the maximum length of which is 9 or $10\,\mu$) or if the sum of the observed charges in the star exceeds 8e. In reference 3 this criterion is supplemented by the requirement that a star without nuclear recoil track contain at least one α particle or a proton track of low energy (less than 8 and 4 Mev respectively) to be classified as a disintegration of a light emulsion nucleus. It is evident that this method of selection is not quite exact and it is desirable to carry out some controlled experiment in order to check the reliability of the assumed criteria and to refine earlier experimental results.

In our work we studied multi-charged particles ejected by carbon nuclei bombarded by 660-Mev protons. A $20\,\mu$ polystyrene film mounted on a photographic plate served as target. Fragments emitted from the film were registered in an emulsion stack. Such a method definitely guarantees an exact identification of the disintegrated nucleus but it does not allow observation of the complete picture of the inelastic interaction of a proton with a nucleus leading to the ejection of a fragment. Nonetheless it is possible to obtain valuable data on this process and thus supplement available facts.

We used an emulsion of type P-9, which is sensitive to protons of energy up to 30 Mev; it is very fine grained and permits one to separate easily the tracks of fragments (charge > 3) from those of α particles over a range of approximately $10\,\mu$.[1]

Irradiation by the external proton beam of the synchrocyclotron of the Joint Institute for Nuclear Research was carried out in darkness without protective black paper, in order to minimize background tracks from particles not originating in the polystyrene film. The bombarding beam was passed through a collimating system, and its direction was defined to within $\sim 2°$. The distance between the back edge of the last collimator and the plates was over 2 m. The plates were singly exposed every time. Irradiation took place for three positions of the emulsion plane with respect to the beam direction: (1) parallel, (2) perpendicular, (3) at an angle of 30°. Such a choice of geometry was dictated by the need for minimizing the uncertainty in the measurement of the range of multi-charged par-

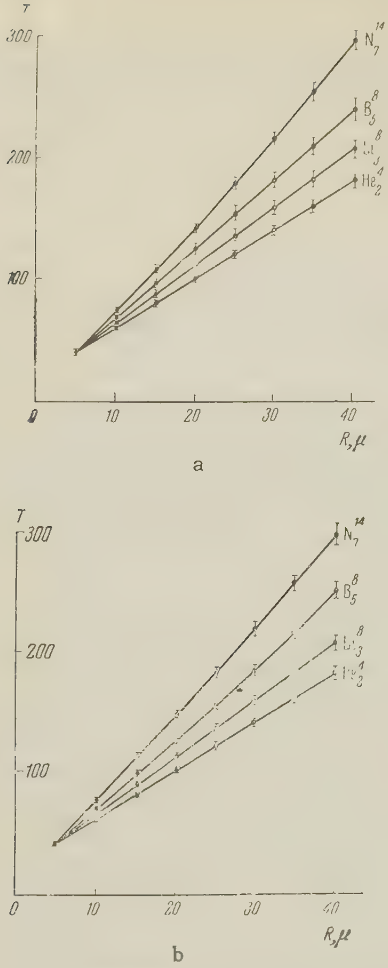

FIG. 1. a) Dependence of the interval thickness of the track upon the range of particles of various charges inclined at 30° to the emulsion. The statistical spread of individual events is indicated; b) same as in (a) for an inclination of 30 to 60°.

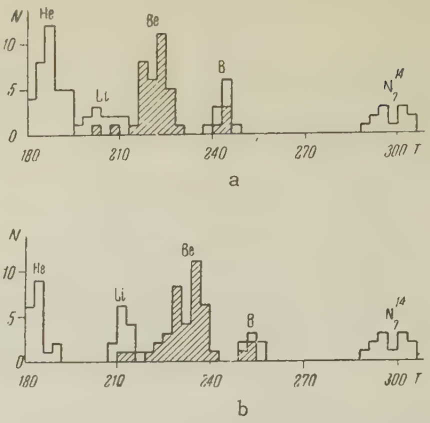

FIG. 2. a) Distribution of tracks belonging to particles of different charges over the integral thickness for a range of 40 μ. Angle of inclination up to 30°. The shaded distribution was obtained from measurements of tracks coming from the film; b) same as in (a) for an inclination of 30 to 60°.

ticles, arising from the finite width of the film.

In examining the plates, we recorded the dense tracks formed by heavy particles which entered the surface of the emulsion at an angle no greater than 60° (for undeveloped emulsion) and stopped within the sensitive layer. The angular distribution of these particles with respect to the beam was obtained in the usual manner, i.e., from measurements of the vertical and horizontal components and angles projected on the emulsion surface. The shrinkage factor of the emulsion was taken as 2.6 ± 0.1. In computing the range, account was taken of particle retardation in the film and it was assumed that the point of departure of the particles lie in the middle plane of the film. The stopping power of polystyrene was computed from the atomic stopping power of carbon and hydrogen.

The charge of the particles was obtained as follows: the track thickness was measured with an eyepiece micrometer at intervals equally spaced along the track length, starting from the end.[4] The integrated thickness (i.e., the sum of the thicknesses up to that point) was then plotted as a function of track length. These curves were found to differ considerably for particles of different charges. To construct an absolute independent calibration, we have used α-particle tracks and hammer tracks of Li_3^8 and B_5^8 found in the same emulsion. In addition, we used plates of the same type of emulsion* irradiated by a current of N_7^{14} ions. To minimize errors due to different inclinations of the tracks with respect to the emulsion surface, measurements were compared only for tracks having approximately the same inclination. Figure 1 presents the results of measurements of control tracks of two groups: one includes tracks at an angle of inclination of no more than 30° (in the undeveloped emulsion), and the other from 30° to 60°.† Figure 2 shows the distribution of individual cases according to interval thickness at a range of 40 μ. In particular, it is seen from this figure that the hammer tracks are sharply divided into two groups which we have identified as Li_3^8 and B_5^8.

Of the total number of 302 tracks found for multi-charged particles coming from the film, 204 were used in the final measurements. The rest were rejected because their inclination exceeded 60°. In addition to these, there were also observed 8 cases of emission into one direction of two α particles of about equal energy which may be considered as due to the decay-in-flight

---

*These plates were kindly obtained for us by O. V. Lozhkin.

†The tracks of the nitrogen ions were inclined at 30°.

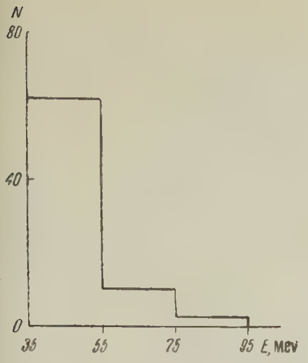

FIG. 3. Energy spectrum of fragments having a range > 40.

FIG. 4. Angular distribution of fragments relative to the proton beam (per unit solid angle). The dotted lines correspond to the distribution obtained in reference 1.

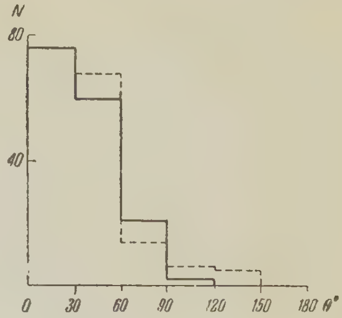

of the B_4^8 nucleus. These cases are not included in our experimental results.

The charge was determined for 80 tracks of length greater than $40\,\mu$. The results of this measurement are shown as the shaded portion of Fig. 2. The energy of every fragment identified by its track was determined from the energy-range relation for multi-charged ion introduced in reference 5. Figure 3 presents the energy spectrum of fragments having range greater than $40\,\mu$, and consisting mainly of Be nuclei (69 of 80 tracks are due to fragments having $Z = 40$). The angular distribution of multi-charged particles with respect to the direction of bombarding protons is given in Fig. 4. It does not vary noticeably for different kinetic energies of the emitted fragments. The angular distribution and energy spectrum were computed taking proper account of slowing down and absorption of particles in the polystyrene film. The method for computing corrections in track losses is given in the appendix.

The effective cross section for fragmentation of carbon nuclei by 660 Mev protons was also estimated. A repeated search for multi-charged particles in the same plate was carried out to verify scanning effectiveness and revealed that about 5% of the tracks are lost during scanning. This scanning effectiveness remained practically the same for plates exposed to different intensity flux. Background of isolated fragment tracks not formed in the carbon carrying film was measured by scanning control plates exposed under identical conditions though without the film. The background accounted for less than 10%. The proton flux was determined from the number of stars formed with emulsion nuclei in the same plate. The cross section for star formation was taken as equal to 1060 millibarns.[6] In so doing, account was taken of the lesser effectiveness of star counting for stars with small number of rays. The computation of omissions of stars with few rays was carried out according to the data of Bernardini et al.[7] The cross section for fragmentation of carbon nuclei was found to be 1.4 ± 0.5 millibarns. The uncertainty includes statistical error and uncertainty in flux measurement. This cross section corresponds to ejection of multi-charged particles having range greater than $20\,\mu$ and charge greater than 3. The effective cross section for emission of Li_3^8 nuclei (for $E > 10$ Mev) equals $(5 \pm 2) \times 10^{-29}$ cm^2.

The present experimental results are in satisfactory agreement with the results of Lozhkin and Perfilov.[1] We can therefore assert that the identification of stars with fragments by the presence of nuclear recoil tracks assumed in reference 1 is a good approximation and does not lead to serious errors, at least for disintegration of nuclei by protons of 600 to 700 Mev energy.

To obtain the total yield curve for all the particles emitted from light nuclei during the cascade stage of a disintegration process, we have made use of the data of Serebrennikov[8] who analyzed stars produced by 660-Mev protons in C, O, N nuclei in a gelatin emulsion. Figure 5 shows, on a semi-logarithmic scale, points calculated from the data of reference 8 and of the present investi-

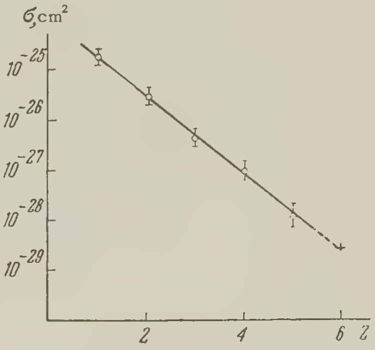

FIG. 5. Cross section for ejection of cascade particles from carbon nuclei for an incident-proton energy of 660 Mev. The particle charge is plotted along the abscissa; the effective cross section is plotted along the ordinate on a semi-logarithmic scale. The points for $Z = 1$ to 3 were obtained from reference 8. The cross indicates the value of the cross section for ejection of carbon nuclei, obtained by extrapolation of the experimental straight line.

gation. It is interesting tc extend the straight line going through these points to a value of $Z = 6$. Such an extrapolation yields a cross section for the ejection of carbon nuclei with range greater than $40\,\mu$, equal to $\sim 3 \times 10^{-30}$ cm^2/sterad, and which may be considered as the elastic (or quasi-elastic) scattering cross section for protons against carbon nuclei in an angular interval of 60 to 180° in the laboratory system.* This value is not in disagreement with the results of reference 9, which gives $\sim 10^{-33}$ cm^2/sterad as the upper limit of the elastic scattering cross section of 660-Mev protons at an angle of $\sim 180°$.

The total cross section for ejection from C nuclei of multi-charged particles having $Z \geq 3$ and range $> 20\,\mu$ (which corresponds to a kinetic energy > 1 or 2 Mev per nucleon) is close to 4 mbn.

The authors are deeply grateful to O. V. Lozhkin, Iu. I. Serebrennikov, and P. A. Filov who have helped greatly in carrying out the experiment and taken part in the interpretation of the results, and to N. A. Perfilov for his interest in this work.

APPENDIX

The transition from experimentally obtained values of angular or energetic distribution of fragments ejected from a layer of thickness a can be carried out as follows.

Assume that the particles are uniformly created throughout the film and are characterized by a distribution $N(\theta, R)$, where R is their range and θ the angle which their track froms with the bombarding beam (which is perpendicular to the surface of the emulsion). Then the number of fragments emitted into a unit solid angle, created within the layer $(t, t+dt)$ and having a range from ρ to $\rho+d\rho$ in emulsion at an ejection angle θ, will be

$$N\left(\theta, \rho + \frac{t}{\cos\theta}\right)\frac{dt}{a}\,d\rho, \qquad (1)$$

where we assume for simplicity that the stopping powers of the emulsion and the film are the same. (This limitation is easily removed by introducing into ρ a coefficient that accounts for the different stopping powers of polystyrene and the emulsion.) Integrating (1) with respect to t, we get

$$\frac{1}{a}\left[\int_0^a N\left(\theta, \rho + \frac{t}{\cos\theta}\right)dt\right]d\rho = n(\theta, \rho)\,d\rho; \qquad (2)$$

$n(\theta, \rho)$ is known from experiments on the angle and range distribution of particles in emulsion. The integral equation (2) may be solved by differentiation with respect to ρ:

$$\frac{\cos\theta}{a}\left[N\left(\theta, \rho + \frac{a}{\cos\theta}\right) - N(\theta, \rho)\right] = \frac{\partial n(\theta, \rho)}{\partial\rho}. \qquad (3)$$

We impose an obvious physical condition on the function $N(\theta, R)$: at sufficiently large values of R the function must reduce to zero.

Adding to (3) the system of equations

$$\frac{\cos\theta}{a}\left[N(\theta, \rho_{k+1}) - N(\theta, \rho_k)\right] = \frac{\partial n(\theta; \rho_k)}{\partial\rho}, \qquad (4)$$

where $\rho_k = \rho + ka/\cos\theta$ $(k = 0, 1, 2, \ldots)$, we obtain

$$N(\theta, \rho) = -\frac{a}{\cos\theta}\sum_{k=0}^{\infty}\frac{\partial n(\theta, \rho_k)}{\partial\rho}. \qquad (5)$$

The angular distribution of particles will have the following form

$$N(\theta) = \int_{R_{\min}}^{R_{\max}} N(\theta, R)\,dR = \frac{a}{\cos\theta}\sum_{k=0}^{\infty} n\left(\theta, \rho_{\min} + k\frac{a}{\cos\theta}\right). \qquad (6)$$

$R_{\min}$ is here the minimum particle range that can be recorded within the photo emulsion, and $R_{\max}$ is the maximum range.

The energy spectrum of the particles is easily obtained from the range distribution of particles of a given charge. The latter in turn may be obtained from (5) by integrating over all angles θ from 0 to π. In practice the right-hand sides of (5) and (6) include only a finite number of terms based on the chosen condition at infinity (in R) for the function $N(\theta, R)$.

---

*Not a single case of ejection of a sextuply-charged ion was recorded in our experiment.

[1] O. V. Lozhkin and N. A. Perfilov, J. Exptl. Theoret. Phys. (U.S.S.R.) **31**, 913 (1956), Soviet Phys. JETP **4**, 790 (1957).

[2] V. M. Sidorov and E. L. Grigor'ev, J. Exptl. Theoret. Phys. (U.S.S.R.) **33**, 1179 (1957); Soviet Phys. JETP **6**, 906 (1958).

[3] Ostroumov, Perfilov, and Filov, J. Exptl. Theoret. Phys. (U.S.S.R.) **36**, 367 (1959); Soviet Phys. JETP **9** (in press).

[4] Nakagawa, Tamai, Huzita, and Okudaira, J. Phys. Soc. Japan **11**, 191 (1956).

[5] J. P. Lonchamp, J. Phys. Rad. **14**, 433 (1953).

[6] E. L. Grigor'ev and L. P. Solov'eva, J. Exptl. Theoret. Phys. (U.S.S.R.) **31**, 934 (1956), Soviet Phys. JETP **4**, 801 (1957).

[7] Bernardini, Booth, and Lindenbaum, Phys. Rev. **88**, 1017 (1952).

[8] Iu. I. Serebriannikov, Научно-техн. информ. бюлл. (Sci.-Tech. Info. Bull. Leningrad Polytech. Inst.) No. 12, 75 (1957).

[9] G. A. Leksin and Iu. P. Kumekin, J. Exptl. Theoret. Phys. (U.S.S.R.) **33**, 1147 (1957), Soviet Phys. JETP **6**, 883 (1958).

Translated by M. A. Melkanoff
293

SOVIET PHYSICS JETP VOLUME 35(8), NUMBER 6 JUNE, 1959

GROWTH AND DISSOLUTION OF PORES IN CRYSTALS

R. I. GARBER, V. S. KOGAN, and L. M. POLIAKOV

Physico-Technical Institute, Academy of Sciences, Ukrainian S.S.R.

Submitted to JETP editor June 17, 1958

J. Exptl. Theoret. Phys. (U.S.S.R.) 35, 1364-1368 (December, 1958)

The time dependence of the diffusion processes of sintering and coalescence of pores in rock salt has been determined experimentally. The results agree satisfactorily with the theoretical equations of Lifshitz and Slezov.[1] Numerical values have been determined for the parameters characterizing diffusion in rock salt. It is shown that sintering results not only from the dissolution of pores and direct emergence of vacancies on the free surface, but also via an intermediate stage wherein vacancies accumulate on macrodefects with subsequent formation of large "negative crystals" of the latter. Coalescence of pores has been observed in annealed single crystals of metallic samples, the method of preparation of which (distillation in vacuum, iodide method etc.) caused the initial fine porosity.

In crystals with high concentrations of vacancies the number of vacancies is reduced by processes which occur during annealing, such as (1) sintering by the escape of excess vacancies to the outside surfaces of samples, and (2) coalescence of excess vacancies to form macroscopic pores.

Lifshitz and Slezov[1] have studied the kinetics of grain growth in substances precipitated from supersaturated solid solutions, a special case of this being the kinetics of pore growth in a crystal containing excess vacancies. It was shown that during the annealing of such crystals the following two competing processes take place:

1. Far from the crystal boundary, pore growth obeys the law

$$\overline{R}^3 = {}^4/_9 D_v \alpha \tau. \qquad (1)$$

2. Near the boundary, pores dissolve in a zone whose width ξ depends on time according to the equation

$$\xi(\tau) = 2\,(D_v \alpha \tau)^{1/3} / Q_0^{1/2}. \qquad (2)$$

These are asymptotic equations, being applicable only to sufficiently long times, when the pores have become relatively large, when there is small supersaturation, and coalescence occurs (large pores "devouring" small pores). The following notation has been used: D_V is the coefficient of vacancy diffusion, τ is the annealing time, Q_0 is the total initial supersaturation (vacancies plus voids),

$$\alpha = \sigma V c_0 / kT, \qquad (3)$$

σ is the surface tension, V is the volume of a single vacancy and c_0 is the (equilibrium) vacancy concentration.

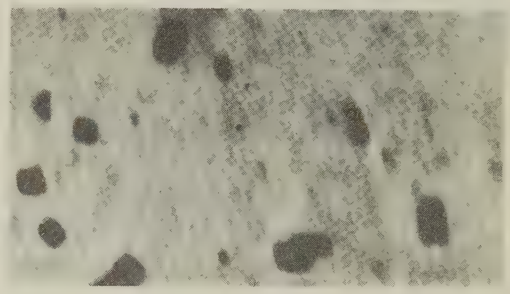

FIG. 1. Cleavage plane of initial rock salt sample. Magnification 25000×.

It should be noted that, unlike the usual equations of the type $\xi(\tau) \sim \tau^{1/2}$ that describe diffusion processes, in the present case the time dependence of the characteristic linear size is given by $\xi(\tau) \sim \tau^{1/3}$.

Pore formation in the body of a crystal during annealing and the growth of a pore-free zone near the surface were previously observed in rock salt.[2] It was of interest to determine the quantitative laws of these processes experimentally, for comparison with the theoretical equations (1) and (2).

As in reference 2, our samples were transparent rock salt crystals without apparent internal defects but with a fine mosaic pattern and ~0.1 μ pores which could be observed with an electron microscope but not optically. These pores were a source of vacancies for the growth of the larger pores which clouded the sample. Large pores were formed on the boundaries of mosaic blocks. In the electron-microscope photograph (Fig. 1) of a cleavage plane of an initial sample in microscopic pores are squares or rectangles with rounded corners.

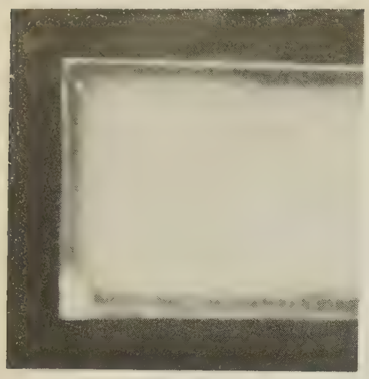

Fig. 2. Transmission photograph of rock salt crystal after annealing at 500°C for 43 hr. Magnification 8×.

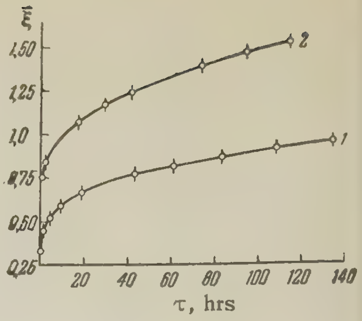

FIG. 4. Thickness of sintered zone as a function of time. Annealing temperature: 1) 500 °C; 2) 650 °C.

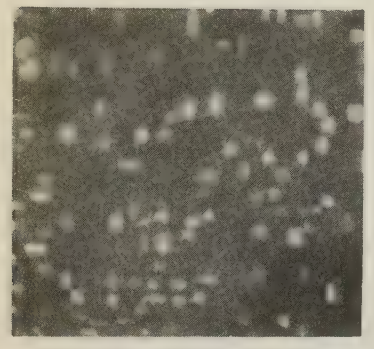

FIG. 3. Pores created on the surface of a mosaic block in the middle of a sample after annealing at 500 °C for 43 hr. Magnification 600×.

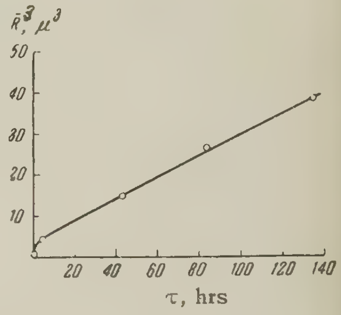

FIG. 5. Pore size as a function of annealing time. Annealing temperature t = 500 °C.

Our samples permitted microscopic observation and measurement of pore sizes in the interior and of the thickness of the sintered zone on the surface. The pore-free sintered region is clearly revealed by transmitted light because of its transparency, in contrast with the interior of the crystal, which scatters light because of the formation of pores whose dimensions are greater than the wavelengths of visible light (Fig. 2).

The samples were 8×10×25 mm parallelopipeds, annealed in a muffle furnace at 420, 500, 650 and 750°C. The crystals were placed in a thick-walled ceramic tube where equilibrium vapor pressure of the salt was maintained during the anneal. At definite time intervals samples were removed from the furnace together with the tube, thus insuring slow cooling, and microscope measurements were made of the thickness ξ of the transparent surface region in different cross sections. The samples were also split along a cleavage plane, and a metallographic microscope with ocular micrometer was used to measure pore dimensions within the crystals (Fig. 3). Eight to ten values of the sintered zone thickness ξ_i in different cross sections and several pore sizes R_i were averaged to give the plots of $\xi(\tau)$ and $\bar{R}^3(\tau)$ in Figs. 4 and 5.

The curves of $\xi(\tau)$ for individual cross sections of a sample are parallel to the curve of average values within the limits indicated in Fig. 4. Whenever macrodefects in the form of cracks appeared close to the surface the character of the time dependence of transparent zone growth changed since vacancies accumulated at the defects. The average value $\bar{\xi}$ was determined without including values for the transparent zone in cross sections passing through these defects.

Assuming that the width $\bar{\xi}$ of the transparent zone is a power function of time, the exponent n of τ was determined from the experimental curves and compared with the theoretical formula (2). The latter is valid only for sufficiently large τ; it was therefore impossible to use absolute values of the experimental coordinates on the curves. The power exponent was determined from the relation

$$\Delta\bar{\xi}/\Delta\tau = nA\tau^{n-1}. \tag{4}$$

Figure 6 shows straight lines representing the function $\ln(\Delta\bar{\xi}/\Delta\tau) = f(\ln\tau)$ plotted from the curves of Fig. 4 for 420, 500, 650, and 750°C (Curves 1, 2, 3, and 4). The slope of these curves gives $n = 0.31 \pm 0.02$,* which is in good agreement with the theoretical value 0.33.

The curve of $\bar{R}^3(\tau)$ in Fig. 5 also agrees with the theoretical relation (1). By means of Eq. (1), derived for spherical pores, the slope of the straight portion of this curve can be utilized to determine $D_V\alpha = D_V c_0\,\sigma V/kT$ and thus to estimate the atomic diffusion coefficient

$$D = D_v c_0.$$

The mean volume of vacancies in the rock salt lat-

---

*The range of values of n is determined from the spread of experimental points, taking into account the error in measuring the width of the transparent zone ($\delta\bar{\xi}(\tau) = \pm 0.02$ mm).

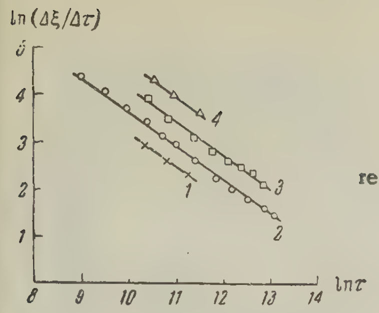

FIG. 6. Graphs of the relation $\ln(\Delta\overline{\xi}/\Delta\tau) = f(\ln\tau)$.

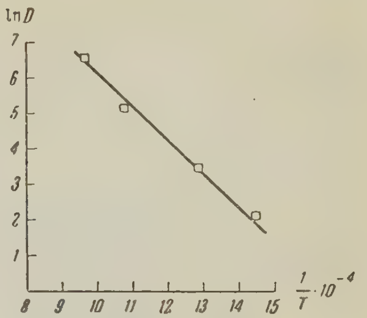

FIG. 7. Graph of $\ln D = f(1/T)$.

tice is $V = 1.15 \times 10^{-23}$ cm³. For mosaic crystals of rock salt we can assume $\sigma = 10^3$ erg/cm².[3] With these values of V and σ, $D = 3.1 \times 10^{-9}$ cm²/sec for 500°C.

Since the experimental relation for $\overline{\xi}(\tau)$ agreed with the theoretical relation (2), we have $A = 2(D\alpha)^{1/3}/Q_0^{1/2}$ in Eq. (4). By using the value of A obtained from the line intersecting the $\ln(\Delta\xi/\Delta\tau)$ axis in Fig. 6 (Curve 2) and the value of D for the same temperature (500°C), we obtain the total initial supersaturation $Q_0 = 2.2 \times 10^{-4}$. This is the relative volume of voids in the crystal after annealing. Figure 3 provides an independent means of determining the volume of pores per unit of mosaic block surface. The volume of pores on the surface of a block (of linear size $\sim 10^{-2}$ cm) divided by its total volume agrees with the calculated value of Q_0.

Pore size in the zone next to the transparent region at the free surface is the critical value at which pore dissolution begins. From the knowledge of this value we can use the expression for critical pore size,[4]

$$R^* = c_0 2\sigma V / \Delta c\, kT, \qquad (5)$$

to determine the degree of supersaturation in the crystal.

Assuming $R^* = 3 \times 10^{-4}$ cm and $V = 1.15 \times 10^{-23}$ cm³, we obtain

$$\Delta c / c_0 = 0.7 \cdot 10^{-3},$$

which agrees with the values given in other papers.[4]

By combining data on the relation between transparent zone thickness and annealing time at 420, 650, and 750°C (Curves 1, 3, and 4 of Fig. 6) with the value of D at 500°C (Curve 2 of Fig. 6) we obtained the diffusion coefficients at all of these temperatures (see the table).

Temperature, °K	Diffusion coefficient, cm²/sec
693	$7.9 \cdot 10^{-10}$
773	$3.1 \cdot 10^{-9}$
923	$1.6 \cdot 10^{-8}$
1023	$0.7 \cdot 10^{-7}$

The data in the table and the graph of $\ln D = f(1/T)$ plotted therefrom (Fig. 7) were used to determine the activation energy of diffusion in rock salt, $E = 19{,}000$ cal/g-atom and the exponential coefficient $D_0 = 6.8 \times 10^{-4}$ cm²/sec. Since in the given rock salt crystals the pores were located on the boundaries of mosaic blocks and the diffusion processes which cause coalescence and sintering also occur on the boundaries of these blocks, the diffusion coefficients and activation energies obtained above apply to boundary diffusion.

Annealing at high temperatures (750°C and above) induces a rapid growth of pores inside the crystal, which produces local transparency and the growth of the transparent zone on the surface. Local transparency in the interior occurs principally around separate defects, where pores are formed through the accumulation of vacancies.

Under prolonged annealing the transparent regions merge, and the entire crystal becomes transparent. In that event some pores may remain within the crystal and continue to grow because of defects. Such pore growth has been observed in an annealed rock salt crystal containing a macrocrack. Figure 8 is a transmission photograph of pores formed on a crack after 18-hour annealing at 760°C. These pores are spherical cavities into which the crack was divided through surface tension.

Annealing for 75 hours induces some increase of pore size; the pores acquire crystallographic

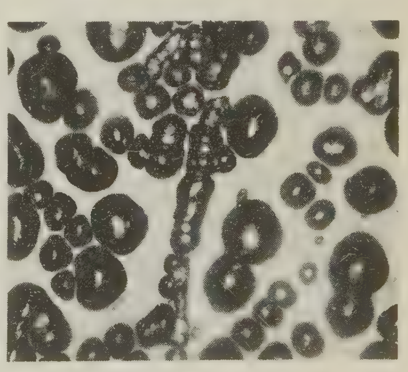

FIG. 8. Crack in rock salt after annealing at 760°C for 18 hr.

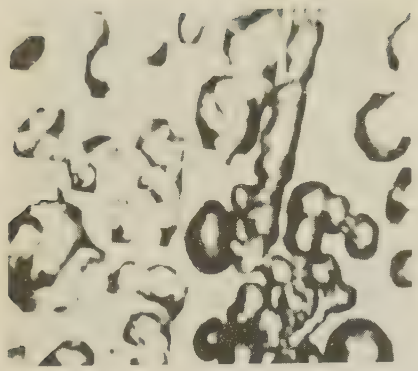

FIG. 9 The same crack as in Fig. 8, but after annealing at 760°C for 75 hr. Magnification 37×.

FIG. 10. "Negative crystal" in rock salt after annealing at 760-790°C for 200 hr. Magnification 21×.

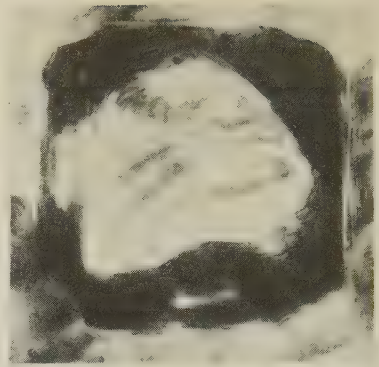

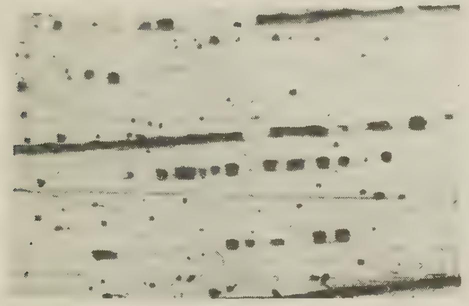

FIG. 11. Iron single crystal after annealing in vacuum at 1000°C for 42 hr. Magnification 315×.

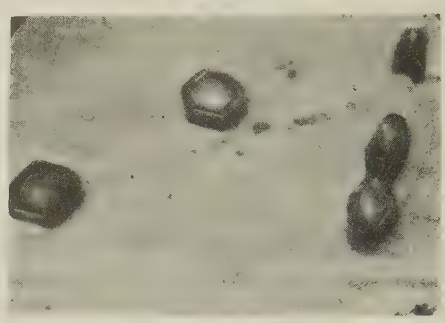

FIG. 12. Magnesium single crystal after annealing at 400 to 420°C for 60 hr. Magnification 420×.

faces and neighboring pores coalesce (Fig. 9). At this stage internal defects serve as sites for vacancy accumulation, competing with the free surface. These defects grow into large "negative crystals". Figure 10 shows such a "crystal" (~ 2 mm) with clearly preceptible faces in the (100) and (110) planes which resulted from annealing for 200 hours at 760 to 780°C.

Coalescence of pores is also observed in metal crystals with high vacancy concentration or high initial porosity. Such crystals are produced, for example, from the gases of some metals in vacuum distillation or from the decomposition of their iodides.

Figures 11 and 12 show pores formed in single crystals of iron and magnesium that were produced by vacuum distillation and subsequently annealed. The iron was annealed in vacuum for 42 hours at 1000°C; the magnesium was annealed for 60 hours at 400 to 420°C. The original samples had small pores (3 to 5 μ) without clearly defined crystallographic faces. The annealed samples were ground down 1 to 1.5 mm and the surfaces were used for the sections shown in the photographs.

The section of the iron crystal in Fig. 11 reveals well-defined rectangular pores arranged in lines that coincide with the directions of single-crystal growth during precipitation. Single-crystal iron needles apparently grow in the form of blocks parallel to the needle axis. Large pores form on the surfaces of these blocks. Magnesium sections (Fig. 12) clearly show large pores with six faces (20 to 25 μ) on block surfaces. The pore faces possess a stepped fine structure that is clearly visible in the photograph. Zirconium produced by the iodide method also contains six-sided pores. Rectangular pores on block surfaces have also been observed in a nickel single crystal produced by vacuum distillation.

Pores appear during the annealing of crystals which, depending on the method of production, possess excess vacancies or initial fine porosity. Pores have not been observed in compact metal castings subjected to annealing.

The authors wish to thank Professor I. M. Lifshitz and V. V. Slezov for discussions of the results, and V. K. Sklyarov for experimental assistance.

---

[1] I. M. Lifshitz and V. V. Slezov, J. Exptl. Theoret. Phys. (U.S.S.R.) 35, 479 (1958), Soviet Phys. JETP 8, 331 (1959).

[2] Garber, Kogan, and Poliakov, Физика металлов и металловедение (Physics of Metals and Metal Research) 4, 89 (1957).

[3] V. D. Kuznetsov, Поверхностная энергия твердых тел (Surface Energy of Solids), GITTL, 1954.

[4] Ia. E. Geguzin, Usp. Fiz. Nauk. 61, 217 (1957).

Translated by I. Emin
294

SOVIET PHYSICS JETP VOLUME 35(8), NUMBER 6 JUNE, 1959

HARD GAMMA RADIATION FROM As^{76}

THE As^{76} *DECAY SCHEME*

L. V. GUSTOVA and O. V. CHUBINSKII

Leningrad State University

Submitted to JETP editor, June 17, 1958

J. Exptl. Theoret. Phys. (U.S.S.R.) **35**, 1369-1379 (December, 1958)

Measurements were made of the hard γ radiation emitted by As^{76}. Six γ lines were found with energies of 1.21, 1.43, 1.76, 2.08, 2.42, and 2.65 Mev. Their relative intensities were found to be ~ 500, ~ 54, 37, 100, 5.7, and 4.6 respectively. The decay scheme of As^{76} is discussed. It is suggested that the following excited states of Se^{76} exist: 0.56 Mev (2^+), 1.21 Mev (2^+), 1.76 Mev (1.2^+), 2.07 Mev (1.2^+), 2.42 Mev (2.3^+), and 2.64 Mev (3^+). It is also suggested that there may exist states with energies ~ 1.02 Mev and ~ 1.26 Mev (0^+ or 4^+).

1. INTRODUCTION

THE radioactive isotope $_{33}As^{76}_{43}$ ($T = 26.5$ hr) is located between the two stable isobars $_{32}Ge^{76}_{44}$ and $_{34}Se^{76}_{42}$. The decay of As^{76} to Ge^{76} has not been observed: $\epsilon/\beta^- < 2\cdot 10^{-4}$; $\beta^+/\beta^- < 10^{-6}$.[1,2]

The decay scheme depicted in Fig. 1 summarizes the results of numerous studies of the β^- and γ emission of As^{76} carried out from 1946 through 1956.[3-13] This scheme agrees satisfactorily with all measurements of β^-, e^-, and γ spectra of As^{76},[3-9,11,13] and of β-γ and γ-γ coincidences and correlations[10-13] that had been reported in publications up to 1956. However, the scheme does not include the 1.76-Mev γ transition observed by some[4-6] but not by others.[9,13]

A comparison of the experimental data obtained by various authors, as well as a discussion of the As^{76} decay scheme, can be found in the final section of this article.

Our aim in studying the hard γ radiation from As^{76} was to determine (1) whether a γ line with $h\nu = 1.76$ Mev exists, and (2) whether γ transitions with energy greater than 2.1 Mev exist.

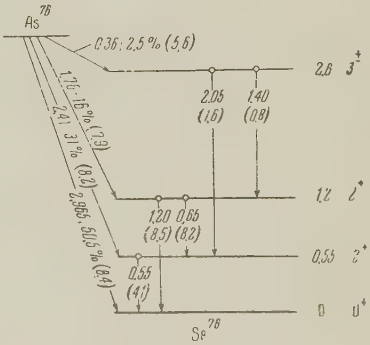

FIG. 1. The As^{76} decay scheme according to data by J. J. Kraushaar and M. Goldhaber[11] and by Kurbatov et al.[13]

2. EXPERIMENTAL ARRANGEMENT AND METHOD

Hard γ radiation from As^{76} was studied by observing recoil electrons in a magnetic spectrometer (γ hodoscope). The construction of the instrument and its spectral properties have been described by B. S. Dzhelepov[14] and O. V. Chubinskii.[15] The energy of a γ ray is determined from the strength of the magnetic field H, the radius ρ of the projected trajectory of the recoil electron (onto a plane perpendicular to H), and from the angle φ between the direction taken by the γ ray and that taken by the emitted recoil electron. The measurements were made under standard conditions: the celluloid target was 150 μ thick, the instrument was filled with a mixture of helium (87%) and methane (13%) to an overall pressure of 30 cm Hg, and the windows of the rectangular Geiger-Müller counters were not covered with film. To minimize the experimental distortion caused by electrons scattered over wide angles in the target, in the counter walls, etc., only those recoil trajectories with small Compton angles φ were included in the results.

For a given magnetic field H, the instrument registers a determined energy interval whose width varies roughly with H (from ~ 1 Mev when $H = 500$ oersteds to ~ 2 Mev when $H = 1000$ oersteds). To include all of the spectral region of interest, the γ radiation was measured for different fields with overlapping energy intervals.

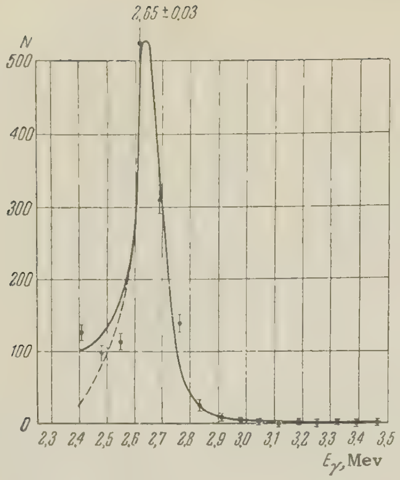

FIG. 2. Measurements of γ radiation emitted by As^{76} when H = 1050 oersteds (As_2O_3 source).

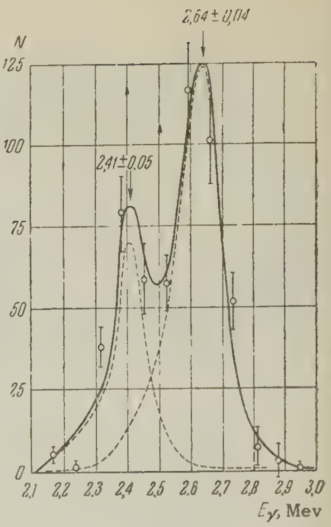

FIG. 3. Measurements of γ radiation emitted by As^{76} when H = 970 oersteds (metallic arsenic source).

3. EXPERIMENTAL RESULTS

Different sources were used to complete several series of measurements. The source for the first experiments was arsenic oxide activated by neutrons. Several γ lines were observed, including some with energies of 2.42 and 2.65 Mev.[2] Control experiments revealed that the As_2O_3 compound used in these measurements was contaminated with Sb^{124} (T = 60 days) and, possibly, with traces of more long-lived activity. The Sb^{124} impurity caused quite a distortion of the As^{76} spectrum in the 1.3 to 2.0 Mev energy region. In the hard part of the γ spectrum ($h\nu > 2$ Mev) the Sb^{124} contribution was considerably less than 1%.

Figure 2 shows the measurements of the γ radiation emitted by As^{76} when H = 1050 oersteds. The line at $h\nu = 2.65$ Mev is quite clearly visible. The counting rate for this line decreased with the corresponding half-life of As^{76} (~ 26 hr).

Pure metallic arsenic was separated from the two contaminated As_2O_3 compounds. The method and complete procedure for the isolation and purification of the arsenic was worked out by M. K. Nikitin. The purity of the metallic arsenic was checked by measuring the γ rays emitted by the radioactive impurities. The contaminant activity of the purified compound was less than 10^{-4} times that of the original compound. Thus, two sources were prepared, each a sealed quartz ampoule containing powdered metallic arsenic (~ 0.4 and ~ 0.7 g) irradiated by slow neutrons. The control measurements showed that these sources did not contain any substantial quantity of long-lived radioactive impurities. Measurements of the γ radiation emitted by the two sources were in agreement. A preliminary report has already been published.[16] Here we discuss the final results.

The quartz ampoule containing 0.72 g of metallic arsenic was 45 mm long and 7 mm in diameter and had an initial activity of ~ 750 mC. During the experiment the magnetic field H was set at 970, 900, 810, 713, 630, 607, and 550 oersteds. The same line was observed at the different values of H, which made it possible to determine more exactly the energies and relative intensities of the γ rays. Figures 3 to 7 show the results of some of the measurements (with the background activity subtracted).

The γ-spectra components were calculated with allowance for the dependence of the instrumental form of the line on $h\nu$ and H. There was good agreement among the γ-ray energies determined from the line maxima for the different values of H. For $h\nu > 1$ Mev we observed six γ lines with the following energies: 2.65 ± 0.04, 2.42 ± 0.05, 2.08 ± 0.03, 1.76 ± 0.04, 1.43 ± 0.05, and 1.21 ± 0.04 Mev.

After the subtraction of the individual lines from the experimental curves, there remained excesses of recoil electrons in the 1.5 to 1.6 and 1.8 to 1.9 Mev regions. Since the statistical errors were rather considerable and the resolving power of the instrument was not great, it may be that these excesses were due to an inaccurate resolution of the spectra into the components.

The relative intensities of the γ lines were determined as follows. The intensity I (in arbitrary units) was computed for each γ line at the different values of H by the formula

$$I = S / W \sum_i A_i t_i,$$

where S is the area beneath the line, W is the probability of registering a γ line for a given H as obtained from the spectral sensitivity curve,

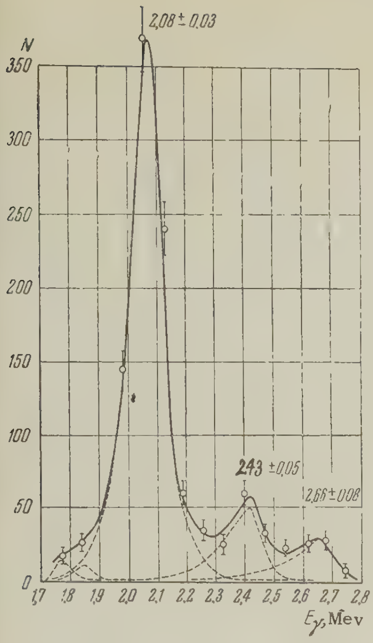

FIG. 4. The same as in Fig. 3, but with H = 810 oersteds.

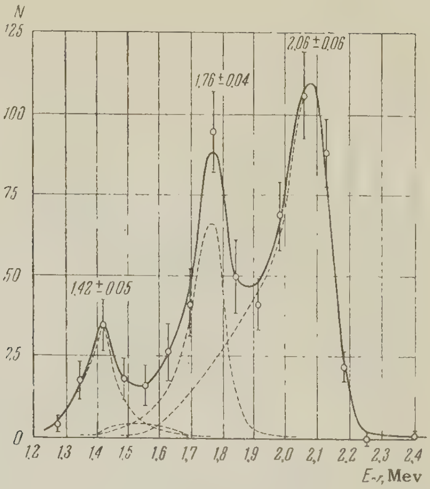

FIG. 6. The same as in Fig. 3, but with H = 607 oersteds.

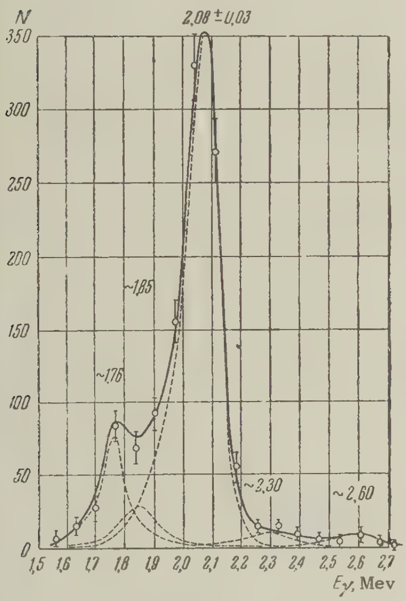

FIG. 5. The same as in Fig. 3, but with H = 713 oersteds.

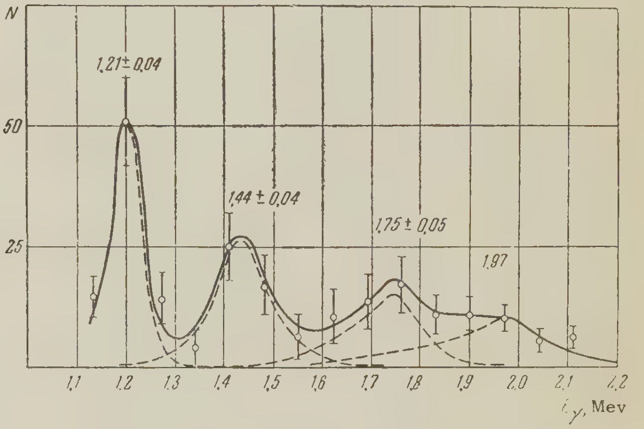

FIG. 7. The same as in Fig. 3, but with H = 550 oersteds.

$\sum_i A_i t_i$ is the so-called effective measurement time for a given H, and A_i is the average activity of the source during the time interval t_i. The intensity unit chosen was that of the 2.08-Mev line, since this line showed good agreement for the different values of H. Table I (column 12) shows the average values of the relative intensities $I/I_{2.08}$ of the γ lines.

The relative intensities of soft γ lines (especially the 1.21 Mev line) are in the nature of approximate evaluations. The probable error in the determination of the relative intensities of the hard γ rays (1.76, 2.08, 2.42, and 2.65 Mev) does not exceed 30%. The fall-off of the 2.65 line on the high-energy side (Fig. 2, 3) permits us to conclude that the γ spectrum of As^{76} apparently has no harder γ lines. If, nevertheless, such γ transitions do exist, their intensity cannot exceed 10% (hν = 2.7 to 2.8 Mev) and 1% (hν = 2.8 Mev) of the intensity of the 2.65 Mev line.

4. DISCUSSION OF THE MEASUREMENTS AND DECAY SCHEME OF As^{76}

Recent new experiments have broadened and improved our knowledge of the β and γ radiation emitted by As^{76}. Table I summarizes the data on the energies, relative intensities, and multipolarities of γ transitions and on γ-γ coincidences.

Substantially new data on γ radiation from As^{76} is to be found in the 1956 article by Dzhelepov et al.[17] So far this is the only paper reporting the discovery of five new, very weak γ lines in the 0.7 to 1.9 Mev region. To facilitate comparison between the data given in the above article and our data, we have shown in Table I (column 10)

TABLE I

Bair et al.[6] (scintillation spectrometer)	P. Hubert[9] (lens spectrometer)		Kurbatov et al.[13] (scintillation and lens spectrometer)		Grifor'ev, et al.[2,16] (β spectrometer)		Dzhelepov, et al.[17] (riton)			Present data (γ hodoscope)		$\gamma-\gamma$ coincidences, $h\nu$ (Mev)	Multipolarity of the γ transitions
$h\nu$ (Mev)	$h\nu$ (Mev)	$I/I_{0.56}$	$h\nu$ (Mev)	$I/I_{0.56}$	$h\nu$ (Mev)	$I/I_{0.56}$	$h\nu$ (Mev)	$I/I_{0.56}$	$I/I_{2.08}$	$h\nu$ (Mev)	$I/I_{2.08}$		
1	2	3	4	5	6	7	8	9	10	11	12	13	14
0.58	0.555+0.002	100	0.549±0,004	100	0.553±0.003	100	0.562	100	5130	—	—	1.2[9]; 0.65, 1.4, 2,1[13]; 0.65, 1,2[11]; 2,06[22]	$E2$[7,8,12,16]
—	0,648±0,002	9.5±1	0.643±0,006	20	0,646±0.004	19	0.660	14,3	733	—	—	0,56[10,11,13,22]	$E2(M1<<1\%)$[22] 98% $E2+$ +2% $M1$[27]
—	—	—	—	—	—	—	(0,730)	0.5	26	—	—	—	—
—	—	—	—	—	—	—	(0,870)	0,5	26	—	—	—	—
1,20	1,210±0.005	25±2	1.200±0.006	21	1,206±0,005	18	1.222	12,7	651	1.21±0.04	~500	1.4[13,22,25]; 1,2?[13] 0.56[9]	—
—	—	—	—	—	—	—	(1.400)	0.17	8.7	—	—	—	—
—	1,410±0.006	1,6±0,4	1,402±0,015	2	—	—	1,43	0.8	41	1.43±0.05	~54	0.56, 1.2[13]; 1,2[22,25]	$M1$[22]
—	—	—	—	—	—	—	(1,51)	0.1	5,1			—	—
—	—	—	—	—	—	—	(1,62)	0,04	2	1.5—1.6	10	—	—
1,76	—	—	—	—	—	—	1.765	0,72	37	1,76±0.04	37	—	—
—	—	—	—	—	—	—	(1.85)	0,05	2,6	1,8—1.9	10	—	—
2,02	2,06±0,01	5.5±1	2,053±0,018	4	—	—	2,085	1,95	100	2.08±0.03	100	0,56[13,22]	95% $E2+$ +5% $M1$[22]
—	—	—	—	—	—	—	2.5	0,16	8,2	2.42±0,05	5.7	—	—
—	—	—	—	—	—	—	2,75			2.65±0.04	4,6	—	—

TABLE II

Tomlinson et al.[7,28]		P. Hubert[9]			Kurbatov et al.[13]			Grigor'ev et al.[16]			Pohm et al.[21]	$\beta-\gamma$ coincidences, $h\nu$ (Mev)	Type of β transition
E_{r} (Mev)	%	E_{r} (Mev)	%	log ft	E_{r} (Mev)	%	log ft	E_{r} (Mev)	%	log ft	E_{r} (Mev)		
2.98±0,01	52	2,96±0.01	52.5	8.4	2,965	50.5	8,4	2.96±0.02	58	8.3	2.97±0.01	No $\beta-\gamma$ coincidences[9,13]	$\Delta I=2$, yes [7,9 16,21]
2.40±0,03	33	2,40	31.5	8,2	2,41	31.0	8,2	2,41±0,03	28	8.2	2,42±0.01	0.55[13,21]	$\Delta I=0$, yes [21]
1,76	12	1,75	6.5	8.5	1.76	16.0	7,9	1,76±0,04	7	8.3	1.77±0.02	1,2[13]; >0,5[21]	—
—	—	1,20	6	7.5	—	—	—	—	—	—	—	—	—
—	—	—	—	—	—	—	—	0,88±0,1	3	7.5	—	—	—
0.48	3	—	—	—	—	—	—	—	—	—	—	—	—
—	—	0.35	2,5	5.9	0.36	2.5	5,6	0,35±0.03	4	5.9	—	—	—

their γ-line intensities referred to the 2.08-Mev line as unity.

Our data on the energies and relative intensities of the 1.76 and 2.08 Mev γ lines are in good agreement with the data given by Dzhelepov et al.,[17] but there is considerable discrepancy in the energies determined for the two hardest γ lines. This portion of the γ spectrum was studied with a "Ritron" (for a description of this instrument see Dzhelepov et al.[18]) operated under conditions of increased transmission when the half-width of the experimental lines for $h\nu = 1.76$ to 2.65 Mev amounted to 13.5%. An excess of recoil electrons was observed in the 2.2 to 2.8 Mev region and it was possible to break this excess down into its components in different ways. In particular, the excess was attributed to the existence of two lines with energies of 2.5 and 2.75 Mev.

The conditions of measurement with the γ hodoscope were a good deal more favorable. The half-width of the experimental lines in this energy region amounted to ~ 6.5%, and the 2.42 and 2.65 Mev γ lines stood out quite distinctly (Figs. 2 to 4).

With the new data, the decay scheme for As^{76} has been supplemented as shown in Fig. 8.

Energies and Quantum Characteristics of the Levels

1. The ground state of Se^{76} is of the 0^+ type (even-even nucleus).

2. The ground state of As^{76} is of the 2^- type. This follows from direct measurements of the spin of As^{76},[19,20] as well as from an analysis of the form of the hardest component of the β spectrum ($\Delta I = 2$; yes).[7,9,16,21]

3. The sequence of the first excited levels of Se^{76}, 0 – 0.55 – 1.2 Mev, and their quantum characteristics (0^+, 2^+, 2^+) as represented in our decay scheme of As^{76} (Fig. 1), have been confirmed anew by E. G. Funk Jr. and M. L. Wiedenbeck.[22] Precise measurements[23] indicate that the energy of the first excited level of Se^{76} is 0.5605 ± 0.0003 Mev. The energy of the second excited level is not so accurately known (~ 1.21 Mev).

The first two excited states of Se^{76} possess all the characteristic properties of quadrupole vibration levels of even-even nuclei (the energy ratios, spins and parity, E 2 multipolarity of the $2^+ \rightarrow 2^+$ transition, and the large cross section for Coulomb excitation in the first excited state).[24] In all known cases the intensity of a direct γ transition between a 2^+ two-phonon vibrational level and a 0^+ ground state (for example $h\nu = 1.21$ Mev) is less by a factor of 1.5 to 3 or more than the intensity of a $2^+ \rightarrow 2^+$ transition (for example, $h\nu = 0.65$ Mev). As is known, this experimental fact can be explained within the framework of the generalized nuclear model (the prohibition of a direct transition with a vibrational quantum number change $\Delta n = 2$). So far the only exception to this rule in the region where $A = 58$ to 90 has been Se^{76}; the intensities of the 0.65 and 1.21 Mev γ lines are approximately equal. As will be shown below, it is quite probable that a portion of the γ rays with $h\nu = 1.21$ Mev (~ 30%) originate in transitions between other levels of Se^{76} (see Fig. 8). The mentioned discrepancy can thus be explained.

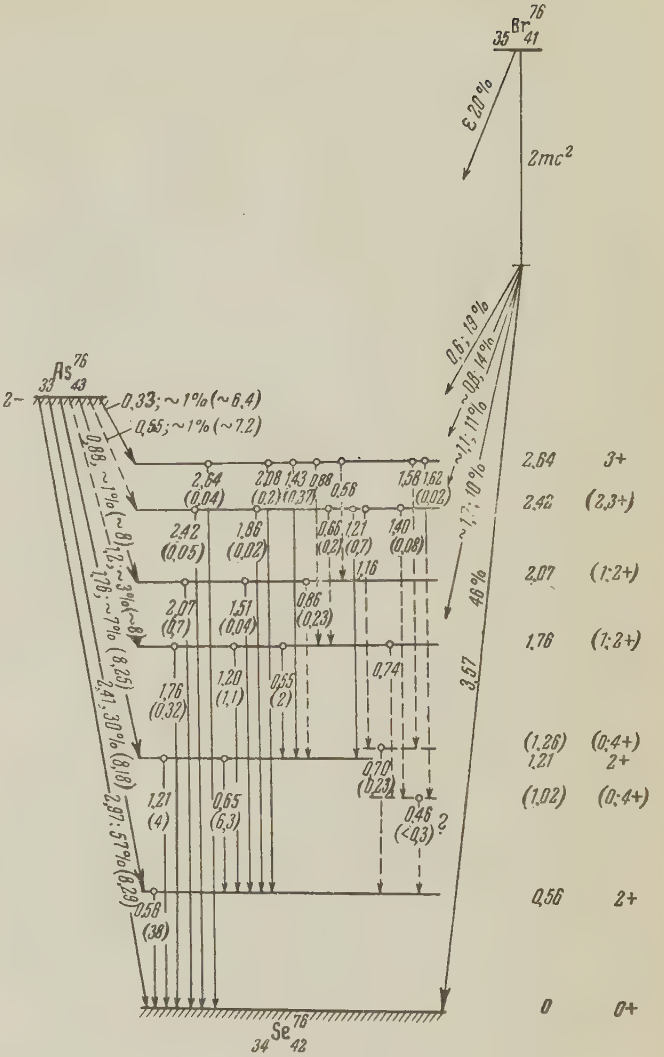

FIG. 8. Proposed As^{76} decay scheme. The energy of the transition from the 2.64 level to the (1.26) level is 1.38 Mev.

4. We have included the 1.76 Mev level to explain transitions with $h\nu = 1.76$ and 0.87 Mev. The presence of a relatively intense transition from the 1.76 Mev level to the ground state of Se^{76} indicates the possibility of spin values of 1 or 2 for this level. There should have been transitions with $h\nu = 0.55$ and 1.2 Mev from the 1.76-Mev level to lower ex-

cited levels. This is experimentally confirmed, albeit by not very accurate data. Thus, P. Hubert[9] bases his conclusion as to the presence of a 1.2 — 0.56 Mev cascade on measurements of γ-γ coincidences. J. J. Kraushaar and M. Goldhaber[11] have observed coincidences involving 1.2-Mev γ rays and the softer γ rays. The counting rate at the single peak as compared with the counting rate at the coincidences for the 1.2 Mev line was considerably greater than might have been expected had the 1.2-Mev line been in a direct cascade with the prominent soft lines. For this reason the authors ascribe the coincidences observed by them to γ rays with $h\nu = 1.4$ Mev and with $h\nu = 0.56$ Mev. However, another explanation of this same experimental fact may be that only some of the γ rays with $h\nu = 1.2$ Mev coincide with those with $h\nu = 0.56$ Mev.

We suggest that there actually exist transitions with $h\nu = 0.55$ Mev and $h\nu = 1.20$ Mev from the 1.76-Mev level. The intensity balance indicates that, apparently, the most intense transition from this level is one with $h\nu = 0.55$ Mev (~ 0.02 quanta per decay), that a less intense transition is one with $h\nu = 1.20$ Mev, and that the weakest transition is one with $h\nu = 1.76$ Mev (~ 0.003 quanta per decay). This intensity ratio for the γ transitions conflicts with the suggestion that the 1.76-Mev level is of a single-particle nature, but the ratio can be satisfactorily explained if this level is assumed to be a three-phonon quadrupole vibrational one with a 2^+ spin. Further evidence in favor of this latter suggestion is the approximate equidistance of the 0.56, 1.21, and 1.76 Mev levels.

5. If a β transition with $E_\gamma \approx 0.88$ Mev exists,[16] a level with an energy of ~ 2.07 Mev and with possible quantum characteristics of 0^+, 1^+, 2^+, 3^+, or 4^+ must be included. In the γ spectrum of As^{76} lines are observed with $h\nu = 2.08$, 1.51, and 0.87 Mev and with a total intensity of $\sim 1.2 \times 10^{-2}$ quanta per decay.[17] These lines can be ascribed to transitions from the 2.07-Mev level. However, the existence of a level at ~ 2.07 Mev cannot be considered proved, because (a) the data on the end-point energy and intensity of the β transition ($E_\gamma \approx 0.88$ Mev) are very inexact, and (b) γ transitions with $h\nu = 2.08$ and 0.87 Mev may occur in other ways (see Fig. 8).

It is known that γ rays with $h\nu = 2.08$ Mev coincide with γ rays with $h\nu = 0.56$ Mev. Heretofore these coincidences have been ascribed entirely to a 2.08 — 0.56 cascade (transitions between the levels $2.6 \rightarrow 0.56 \rightarrow 0$ Mev). Now, however, another possibility cannot be overlooked, i.e., a 0.56 — 2.08 Mev cascade (transitions between the levels $2.6 \rightarrow 2.07 \rightarrow 0$ Mev). At the present time it is impossible to settle definitely on either of these two possibilities. If a β transition with $E_\gamma \approx 0.88$ Mev exists and its intensity is on the order of 1%, we are presented with the following logical consequences: (a) the main portion of the γ rays with $h\nu = 2.08$ Mev must be attributable to a $2.07 \rightarrow 0$ Mev transition, (b) the intensity of the γ transition between the levels 2.64 and 2.07 Mev ($h\nu = 0.57$ Mev) must be $\leq 1\%$, and (c) the most probable spin and parity values of the 2.07 Mev level are 1^+

6. The 2.42 Mev level was included because of two experimental facts: (a) the presence of γ transitions with $h\nu = 2.42$ and 1.85 Mev; (b) the observation of coincidences for γ rays with $h\nu = 1.2$ Mev and $h\nu = 1.2$ Mev.[13] The latter argument cannot be considered to be very rigorously supported, because the accuracy with which the γ-γ coincidences were measured was insufficient for an unequivocal interpretation of the results.

The intensity balance (see below) indicates that some of the 1.21 Mev γ rays are produced, apparently, by transitions between the 2.42 and 1.21 Mev levels. At the present time there are no definite experimental data on the quantum characteristics of the 2.42-Mev level. E. G. Funk and M. L. Wiedenbeck[22] have studied the angular γ-γ correlation between γ rays with $h\nu \geq 1.20$ Mev. These authors attribute their findings to a 1.4 — 1.2 Mev cascade ($2.64 \rightarrow 1.21 \rightarrow 0$ Mev transitions). The only interpretation not in conflict with the experimental results is that a transition with $h\nu = 1.4$ Mev is purely M1 and that the level ~ 2.6 Mev is of the 3^+ type. If a 1.2 — 1.2 Mev cascade transition exists, this conclusion could obviously be extended to apply also to the 2.42 Mev level. However, it is difficult to reconcile the spin value 3 with the comparatively great probability of a direct $3^+ \rightarrow 0^+$ transition ($h\nu = 2.42$ Mev). According to the Weisskopf formula, this transition should be 10^7 times weaker than transitions to the 2^+ levels. If we take this point of view and assume a transition to the 2.42 Mev level to be first forbidden, it appears probable that the 2.42 Mev level is of the 2^+ type.

7. The existence of a level at ~ 2.6 Mev is proved by many measurements of β spectra emitted by As^{76} and of γ-γ coincidences, as well as by the γ transition with $h\nu = 2.65$ Mev reported here. The energy ratios of the γ transitions indicate that the energy for this level is 2.64 to 2.62 Mev. Correlation measurements[22,25] have shown that this level is of the 3^+ type. This fact, as in the case of the 2.42-Mev level, is difficult to reconcile with the presence of a relatively intense direct γ transition to the ground level of

Se^{76}. The hypothesis advanced by Funk and Wiedenbeck[22] that the level at ~2.6 Mev is due to a coupling of a single-particle excitation of the ground state configuration with a two-phonon vibrational excitation provides an explanation for the high probability of a transition with $h\nu = 1.43$ Mev as against the probability of other γ transitions, but this hypothesis makes it even harder to understand why the direct transition with $h\nu = 2.64$ Mev is so intense. It may be that near 2.6 Mev there are two close levels with different quantum characteristics.

8. To find a place in the As^{76} decay scheme for weak γ transitions with energies of 0.73, 1.40, and 1.62 Mev,[17] it must be assumed that still one or two more excited levels of Se^{76} exist. The dotted lines on the right side of Fig. 8 represent two of the possible variants. Inclusion of the 1.02-Mev level makes it possible to explain all three γ transitions. If the 1.02-Mev level is of the 0^+ or 4^+ type and the β transition to it is second forbidden ($\log ft \approx 10$), then practically the only way in which this level can decay would be by the emission of a γ quanta with an energy of ~0.46 Mev with an intensity of 3×10^{-3} quanta per decay (the total intensity of γ rays with $h\nu = 0.7$, 1.4, and 1.6 Mev). If part of the γ transitions pass through the 1.26 Mev level, the intensity of the 0.46 Mev line will be even less. A line at $h\nu = 0.46$ Mev is at least 130 times weaker than the neighboring one at $h\nu = 0.56$ Mev. It may be that this weak line has thus far escaped notice.

The question of the existence of type 0^+ and 4^+ levels near the 1.21-Mev level is very interesting from the standpoint of verifying the theories behind the generalized nuclear model. According to this model, a two-phonon vibrational level (1.21 Mev, 2^+) should, because of nucleonic interaction, split into close sublevels of the 0^+, 2^+, and 4^+ types. Unfortunately, so far there are too little experimental data to settle this question once and for all.

9. Measurements[26] of the β^+ spectrum of Br^{76} lend some support to the Se^{76} levels presented here. The Br^{76} data make possible at least a qualitative conclusion that Se^{76} has excited levels in the 1.7 to 2, 2.4 to 5, and 2.7 to 3 Mev regions.

Intensity Balance

When the intensity balance condition is considered, discrepancies appear between the data on the relative intensities of the partial β spectra, on the one hand, and the data on the relative intensities of the γ lines on the other. These discrepancies are attributable first of all to inadequate accuracy in the measurements. An intensity balance is made even more difficult because the intense γ lines 0.56, 0.65, 1.21, and 2.08 Mev can be placed differently in the scheme. Let us examine these problems in greater detail.

1. From Table II it is evident that there are some discrepancies among the relative intensities determined for hard β spectra and important discrepancies among the end-point energies and relative intensities of soft β spectra with $E_\gamma \leq 1.76$ Mev. However, all the reports are in agreement that the sum of all the β spectra with $E_\gamma \leq 1.76$ Mev is no less than 14% of the total number of β transitions.

The article by Grigor'ev et al.[16] differs from the other references in reporting that the authors used a Kurie plot to analyze the spectrum into its components without reference to any decay scheme. Apparently, these are the most objective data available at the present time.

2. The data given by Dzhelepov et al.[17] differ from those given by Chubinskii et al.[2] and by Kurbatov et al.[13] with regard to the values found for the relative intensities of 0.56, 0.65, and 1.21-Mev γ rays.

We used several different assumptions in order to compute the relative intensities of the β spectra and obtained the following results.

(a) If the data on relative γ-ray intensities supplied by Dzhelepov et al.[17] are used, if the intensity of the hardest β spectrum is assumed to range from 52 to 58%, and if the 0.56, 1.21, and 2.08-Mev γ transitions are assumed to occur only at $0.56 \rightarrow 0$ Mev, $1.21 \rightarrow 0$ Mev, and $2.64 \rightarrow 0.56$ Mev respectively, then the sum of the intensities of the β spectra with $E_\gamma \leq 1.76$ Mev is 3 to 4 times less than that reported by Grigor'ev et al.[16]

(b) If the same assumptions concerning γ rays are retained and it is further assumed that the sum of the intensities of all the β spectra with $E_\gamma \leq 1.76$ Mev amounts to 14%, we obtain for the β-spectrum intensities the following values: I (2.97 Mev) = 47%, I (2.41 Mev) = 39%, I (1.76 Mev) = 11.9%, and $\Sigma I = 2.1\%$ for all the soft β spectra with $E_\gamma < 1.7$ Mev. This is clearly in conflict with the results of Grigor'ev et al.[16]

(c) The discrepancy between the computed and experimental values for the intensities of the two hardest β spectra is reduced if one assumes the 0.56-Mev γ line as found by Dzhelepov et al.[17] to be somewhat more intense than the other γ lines.

(d) The computed and experimental values for β-spectrum intensities are brought into satisfactory agreement if it is further assumed that a small portion (~5%) of the 0.56-Mev γ rays are produced by $1.76 \rightarrow 1.21$ Mev transitions and that about 30% of the 1.21-Mev γ rays are due to $1.76 \rightarrow 0.56$ Mev and $2.42 \rightarrow 1.21$ Mev transitions.

Figure 8 shows approximate values for the intensities of β and γ transitions computed on the basis of the assumptions in (c) and (d) above. The intensity of the hard β transitions and the total intensity of all the soft β transitions with $E_\gamma <$ 1.7 Mev are in good agreement with the experimental data. However, the intensities of individual β components with $E_\gamma < 1.7$ Mev do not coincide with the results obtained by analyzing the β spectrum.

The suggested decay scheme for As^{76} is basically in agreement with the experimental data available at present, but it is not free of all discrepancies. We have attempted to point out the weaknesses in the scheme. It must be stressed that the quantity and, above all, the quality of experimental research have been far from adequate to lead to an unequivocal decay scheme for As^{76}.

The authors express their deep gratitude to L. P. Popovaia and T. V. Poleshchuk for their assistance with the measurements and to M. K. Nitkitin for preparing the sources. We are obliged to B. S. Dzhelepov for his interest in our work and for discussions of the results and to P. P. Zarubin for his opinions on this article.

---

[1] J. Scobie, Nucl. Phys. **3**, 465 (1957).

[2] Chubinskii, Grigor'ev, Gustova, Zolotavin, Kratsik, Kraft, Poleshchuk, and Iushkevich, Тезисы докладов на VII совещании по ядерной спектроскопии (Reports of the VII Conference on Nuclear Spectroscopy) Acad. Sci. Press, Moscow-Leningrad (1957), p. 24.

[3] L. C. Miller and L. F. Curtiss, Phys. Rev. **70**, 983 (1956).

[4] K. Siegbahn, Arkiv Mat. Astron. Fysik., **A34**, No. 7 (1947).

[5] Wu, Havens, and Rainwater, Phys. Rev. **74**, 1248 (1948).

[6] J. K. Bair and F. Maienschein, Phys. Rev. **81**, 463 (1951).

[7] E. P. Tomlinson and S. L. Ridgway, Phys. Rev. **88**, 170(A) (1952).

[8] F. R. Metzger, Phys. Rev. **86**, 435 (1952).

[9] P. Hubert, Thesis, Paris (1953); Ann. Phys., **8**, 662 (1953).

[10] F. R. Metzger and W. B. Todd, J. Franklin Inst. **227**, 256 (1953).

[11] J. J. Kraushaar and M. Goldhaber, Phys. Rev. **89**, 1081 (1953).

[12] Hamilton, Lemonick, and Pipkin, Phys. Rev. **92**, 1191 (1953).

[13] Kurbatov, Murray, and Sakai, Phys. Rev. **98**, 674 (1955).

[14] B. S. Dzhelepov, Izv. Akad. Nauk. SSSR, Ser. Fiz. **21**, 1580 (1957). [Columbia Techn. Transl. **21**, 1569 (1957)].

[15] O. V. Chubinskii, Izv. Akad. Naul. SSSR, Ser. Fiz. **21**, 1583 (1957). [Columbia Techn. Transl. **21**, 0000 (1957)].

[16] Grigor'ev, Gustova, Zolotavin, Kratsik, Poleshchuk and Chubinskii, Вестник ЛГУ (Bulletin, Leningrad State University), Phys. and Chem. Series, **10**, 37 (1957).

[17] Dzhelepov, Prikhodtseva, Feoktistov and Khol'nov, Izv. Akad. Nauk. SSSR, Ser. Fiz. **20**, 1351 (1956). [Columbia Techn. Transl. **20**, 1245 (1956)].

[18] Dzhelepov, Zhukovskii, and Khol'nov, Izv. Akad. Nauk SSSR, Ser. Fiz. **18**, 599 (1954) [Columbia Techn. Transl. **18**, 285 (1954)].

[19] F. M. Pipkin and J. W. Culvahouse, Phys. Rev. **106**, 1102 (1957).

[20] Christensen, Bennewitz, Hamilton, Reynolds, and Stroke, Phys. Rev. **107**, 633 (1957).

[21] Pohm, Waddell, and Jensen, Phys. Rev. **101**, 1315 (1956).

[22] E. G. Funk Jr. and M. L. Wiedenbeck, Phys. Rev. **109**, 922 (1958).

[23] N. Ryde and B. Andersson, Proc. Phys. Soc., **B68**, 1117 (1955).

[24] Alder, Bohr, Huus, Mottelson, and Winther, Revs. Modern Phys. **28**, 432 (1956).

[25] Tor Wiedling, Nucl. Sci. Abstr. **11**, 333 (1957).

[26] S. C. Fultz and M. L. Pool, Phys. Rev. **86**, 347 (1952).

[27] T. Lindqist and I. Marklund, Nucl. Phys. **4**, 189 (1957).

[28] Way, King, McGinnis, and van Lieshout, Nuclear Level Schemes ($40 \leq A \leq 92$), U. S. Atomic Energy Commission, Washington (1955).

Translated by A. Skumanich

SOVIET PHYSICS JETP VOLUME 35(8), NUMBER 6 JUNE, 1959

COMPARISON OF THE DECAY RATES OF PLASMA IN HYDROGEN AND DEUTERIUM

G. I. GLOTOVA, V. L. GRANOVSKII, and V. I. SAVOSKIN

All-Union Electrotechnical Institute, Moscow

Submitted to JETP editor June 24, 1958

J. Exptl. Theoret. Phys. (U.S.S.R.) 35, 1380-1385 (December, 1958)

The deionization rate in hydrogen and deuterium at pressures $p = 15$ to 600μ Hg, tube diameters $d = 3.2$ to 6.5 cm and values of the preceding current $I_0 = 60$ to 1500 ma was studied by means of oscillographic observation of the ion current in a negative probe. Under the conditions employed the relative deionization rate in H and D decreased with time. The dependence of the rate of the process on the pressure is a non-monotonic function and goes through a maximum at $pd \sim 10^{-1}$ to 1 mm Hg·cm. The ratio of the deionization "time constants" (initial as well as final) in deuterium and hydrogen, τ_D/τ_H, is close to 1.4, i.e., $\approx (m_D/m_H)^{1/2}$ at all pressures both in the diffusion regime $(p < p_m)$, and also in the recombination mode $(p > p_m)$. The latter indicates that volume recombination under these conditions takes place primarily by means of triple collisions with neutral molecules $(M^+ + e + M)$.

1. STATEMENT OF THE PROBLEM

In decaying plasmas in different gases the rates of their deionization, all other conditions being the same (equal degrees of rarefaction and ionization, the same configurations of boundary surfaces, etc.), depend on a number of properties of the molecules of these gases: effective cross sections, masses, ionization and excitation potentials. In different isotopes of the same element the relative rates of deionization $\left(-\frac{1}{n}\frac{dn}{dt}\right)$ may differ only as a result of the difference in their atomic weights A. Different elementary processes in a gas are affected by the atomic weight in a different manner. Therefore, by means of studying the dependence of the rate of deionization upon A, we can judge as to which elementary processes play the main role in the deionization of the gas under given conditions. The object of our work was (1) to compare the rates of deionization of the hydrogen isotopes H and D (which have the most pronounced difference of atomic weights of all the stable gaseous isotopes), and (2) to compare their ratio with the ratio of the atomic weights of the two gases and to deduce from such a comparison possible conclusions with respect to processes that lead to the deionization of the gas.

2. METHOD AND APPARATUS

We measured the rate of deionization of the plasma that remains after the passage of $\frac{1}{4}$ cycle of 50 cps sinusoidal current, interrupted at the maximum. The investigation was carried out by oscillographic observation of the ion current in a negative probe introduced into the plasma. This method, used in a number of investigations,[1-3] enables us to observe deionization, i.e., the decrease in the concentration of positive ions, while high-frequency methods (references 4, 5, and others) indicate the rate of de-electronization, i.e., the decrease in concentration of free electrons.

An analysis of the conditions under which the probe operated, according to the theory of Langmuir and Mott-Smith,[6] showed that in our experiments, with $E_p = 140$ v, $(i_p)_0 = 0.1$ to 6 ma, the probe operated in the orbitally-limited current mode ($r_{layer}/r_{probe} = 2.7$ to 15). Under these conditions the current to the probe, after the velocity distribution of the positive ions and of the neutral molecules has been equalized, is proportional to the concentration of positive ions n_p. Therefore, from the shape of the curves $i_p = F(t)$, we can directly determine the rate of deionization and the quantity reciprocal to it

$$\tau = -\frac{dt}{d[\ln(n/n_0)]} = -\frac{dt}{d[\ln(i_p/i_{p0})]}.$$

The experiments were carried out in straight cylindrical experimental tubes of diameter 32 and 65 mm, of length 220 and 400 mm, with an oxide cathode. Cylindrical probes (diameter 0.8 mm, length 11 mm) were situated along the axis of the tube; the inactive parts of the probes were

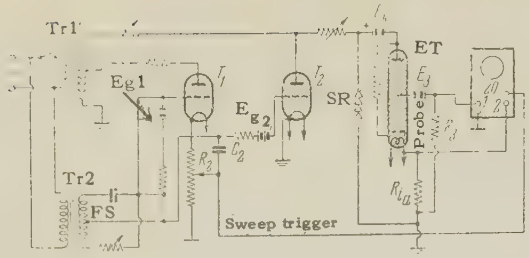

FIG. 1. Circuit for the measurement of the rate of deionization in hydrogen.

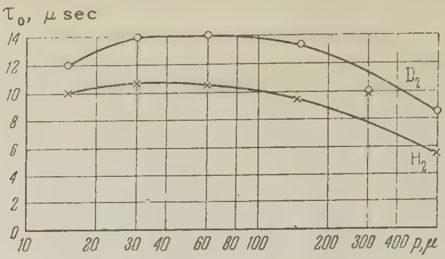

FIG. 3. The initial deionization "time-constant" τ_0 in D_2 and in H_2 as a function of the pressure; $I_0 = 0.5$ amp, d = 65 mm.

insulated from the plasma by a capillary of 1.0 mm diameter. The gases to be investigated (H_2 and D_2) were obtained by means of electrolysis H_2O or D_2O; they were first purified by means of silica gel, then by heated copper filings and, finally, by freezing in a liquid-nitrogen trap.

Mass-spectrometric analyses of the gas taken from the tube when the cathode was heated showed that D_2 contained a certain amount of H_2 and traces of other gases. This could not have significantly affected the results of the experiments. The pressure of H_2 and D_2 was varied in the course of the experiments within the range 0.015 to 0.6 mm Hg.

The electric circuit used in the experiments is given in Fig. 1. The current in the experimental tube ET was interrupted at its maximum by means of a shunting thyratron T_2. The reversed voltage was picked off ET by selenium rectifier SR connected in parallel to ET. The delayed sweep of the oscillograph (marked 20 in the diagram) was triggered by a pulse from the thyratron T_1, which through a delay circuit (C_2, R_2) also triggered the shunting thyratron T_2. To calibrate the sweep, timing markers were produced on the oscillogram every 1.2 or 5μ sec. The vertical deflection was calibrated by a sinusoidal current (not shown in the circuit diagram), but this calibration played no role in the determination of the relative rate of deionization.

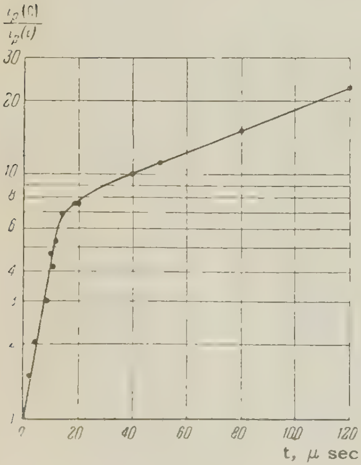

FIG. 2. The ratio $i_p(0)/i_p(t)$ shown as a function of the time. The vertical axis has a logarithmic scale.

3. EXPERIMENTAL RESULTS

(a) The shape of the probe current vs. time curve, i.e., the time dependence of the decrease in the concentration of the positive ions $n_p(t)$ for both isotopes, could be observed already 2 to 4μ sec* after the cessation of current. As had already been shown by previous observations in Hg[2] and in H_2^3, this falling-off in H_2 and in D_2 takes place in a nonexponential manner. As an example, Fig. 2 shows the shape of the curve $i_p(0)/i_p(t) = f(t)$ in a tube of 65 mm diameter filled with D_2 at $p = 600\mu$ Hg and $I_0 = 0.9$ amp. It is clearly seen that the shape of the curve is on the whole nonexponential, but that its beginning,† and particularly its end, can be represented by exponentials with different "time-constants" τ_0 and τ_c, with $\tau_c > \tau_0$. Wherever possible we tried to determine both quantities (τ_0 and τ_c). But in contrast to the microwave method the quantity τ_0, which characterizes the rate at the beginning of the process, is determined from the probe oscillograms more reliably than τ_c, which refers to the conclusion of the process, since the initial deflections on the screen are considerably greater than those near the end.

(b) The dependence of the rate of deionization on the degree of rarefaction of the gas and on the extent of the ionized region is similar in both isotopes (H and D). This refers both to the initial rate of deionization characterized by the quantity reciprocal to τ_0, and to the rate of the process in the latest stage, i.e., to τ_c. The dependence of τ_0 on the gas pressure p can be seen in Fig. 3.

---

*This is one of the advantages of the probe method over the microwave method, which usually discloses the later stages of the process (after 30 to 50 μsec).

†With the exception of the first few microseconds during which the ionization of the gas ceases and the plasma starts to decay.

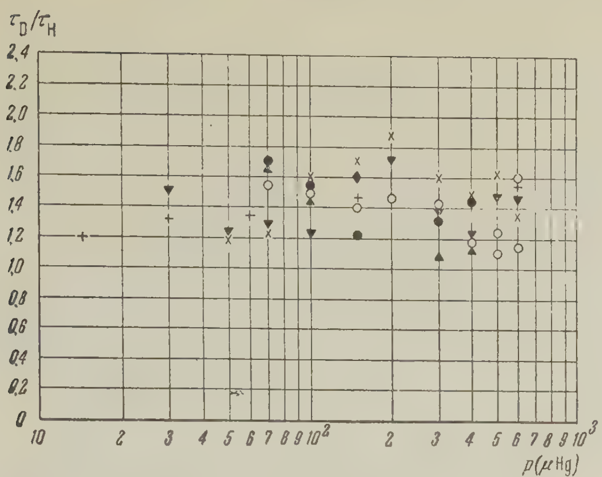

FIG. 4. The ratio of the deionization time constants in deuterium and in hydrogen τ_D/τ_H as a function of the pressure for τ_0 (initial) corresponding to ○) d= 36 mm, I_0 = 500 ma; ●) d = 65 mm; I_0 = 500 ma; +) d = 65 mm, I_0 = 60 ma; for τ_c (final) corresponding to ▲) d = 36 mm, I_0 = 1500 ma; ▼) d = 65 mm, I_0 = 1500 ma; ×) d = 65 mm, I_0 = 60 ma.

It turns out to be non-monotonic both in H_2 and in D_2, in agreement with Gavrilov's data[3] on H_2: there exists a pressure p_m for which τ_0 has a maximum value and, consequently, the deionization proceeds at the slowest rate. A similar dependence on the pressure is observed also in the latest stage of the processes.

As the diameter of the positive column is increased, the rate of deionization is considerably slowed down in the pressure range investigated by us. The minimum rate of deionization occurs at pd ~ 10^{-1} to 1 mm Hg • cm.

(c) A comparison of the rates of deionization in both isotopes (H and D) shows that both τ_0 and τ_c are larger in deuterium than in hydrogen, under all the conditions investigated by us. The ratio of the time-constants of deionization in both gases τ_D/τ_H measured with all other conditions being equal (the same d, p and I_0, and at the same stages of the process) may be taken as a characteristic quantity in this case. Figure 4 shows values of this ratio found in six series of measurements.

In spite of the considerable scatter of points (the average error of a single measurement is 0.19), they are all grouped about one mean value, 1.4 ± 0.03. It is the same both in the initial and in the final stages of the process. Also, it does not depend (at least in the first approximation) on the gas pressure within the range investigated by us. If the data referring to $p < 100\,\mu$ Hg and to $p > 300\,\mu$ Hg are treated separately, it turns out that in the latter region the average value of τ_D/τ_H is somewhat smaller and is equal to 1.3_1; however we cannot assert that this difference lies outside the experimental error.

4. DISCUSSION OF RESULTS

I. The difference in the rate of deionization at the beginning and at the end of the process, i.e., the gradual slowing down of the process with time ($\tau_c > \tau_0$) is associated, as was shown earlier, with the gradual "cooling down" of the electron gas and with the transition of the plasma from the initial nonequilibrium state (at $t = 0$, $T_e \gg T_g$) to thermal equilibrium (at $t \to \infty$, $T_e \to T_g$).[2] A decrease in T_e during the deionization stage was observed in references 7 and 8.

II. The non-monotonic dependence of τ_0 and τ_c on the gas pressure is due to the fact that as the pressure changes the relative role played by the various elementary deionization processes is altered. For $p < p_m$ [the increasing branch of the curve $\tau = f(p)$] the charge carriers primarily diffuse from the gas towards the walls where they recombine (the diffusion mode). For $p > p_m$ the volume recombination in the gas itself begins to play the principal role (the recombination mode,[2,3] cf. also reference 7). As the diameter of the column is increased the diffusion proceeds more slowly and volume recombination begins to play a greater role. Therefore for large diameters the curve $\tau = f(p)$ passes through a maximum earlier (at lower pressures).

III. Both in the diffusion and in the recombination modes, we have $\tau_D/\tau_H = 1.41$, i.e., within experimental error $\tau_D/\tau_H = (A_D/A_H)^{1/2} = (m_D/m_H)^{1/2}$ (A is the atomic weight). In the diffusion mode ($p < p_m$) we have $\tau = \Lambda^2/D_a$, where Λ is the so-called diffusion length; in the present case $\Lambda = d/2\mu$ ($\mu \leq 2.405$ is the eigenvalue of the diffusion boundary-value problem); D_a is the coefficient of bipolar diffusion,

$$D_a = b_p\,[T_e(\mathrm{V}) + T_g(\mathrm{V})],$$

where $T_e(V)$ and $T_g(V)$ are the temperatures of the electron and the neutral gas expressed in volts.[2] At the beginning of the process $T_e(0) \gg T_g$ and $D_a \approx b_p T_e(0)$; at the end of the process $T_e \approx T_g$ and $D_a \approx 2 b_p T_g(V)$. Further

$$b_p \approx e_0 \lambda_p / m_p \bar{c}_p = e_0^{1/2} \lambda_p / (2 T_g m_p)^{1/2},$$

since in the deionization stage $T_p \approx T_g$ almost from the start. The quantities T_g, λ_p, and T_e may differ somewhat in H and in D. Thus, because of the lower rate of diffusion in D_2 the mean ionization frequency z ($\sec^{-1}$) (and consequently also the value of $T_e(0)$ in D_2) must be somewhat lower than in H_2 (cf. also references 9 and 10). Further, since the average fraction of the kinetic energy transferred by elastic collisions between electrons and molecules, $\kappa = 2m_e/m_g$, is smaller in D_2 than in H_2, the gas temperature T_g can also be less in D_2 than in H_2. However, all these differences are small compared with the difference in the mobilities of the D and H ions; therefore in the first approximation we should expect that in the diffusion mode

$$\tau_D / \tau_H = (D_a)_H / (D_a)_D$$

$$= (b_p)_H / (b_p)_D = (m_D / m_H)^{1/2} = \sqrt{2} = 1.41,$$

which is indeed observed experimentally.

A more complicated state of affairs exists in the recombination mode $(p > p_m)$. Here various types of elementary recombination processes can occur: (1) those involving radiation $(M^+ + e \rightarrow M + h\nu)$, (2) triple collisions involving two electrons $(M^+ + 2e \rightarrow M + e)$, (3) triple collisions involving neutral molecules $(M^+ + e + M \rightarrow 2M)$, (4) electron capture by a neutral molecule and the subsequent recombination of the ions $(e + M \rightarrow M^-;\ M^- + M^+ \rightarrow 2M)$, and (5) dissociative recombination $(M_2 + e \rightarrow M^* + M)$. The recombination coefficients in cases (1), (2) and (5) depend only on the average velocities of the electrons (i.e., on T_e) and on the effective cross sections and the statistical weights of the ions, which are also determined by T_e (cf., for example, reference 11). Consequently in the first approximation* the rate of recombination in these two cases should not depend appreciably on the atomic weight of the gas. And since experiment shows that in the recombination mode deionization occurs more slowly in D_2 than in H_2, therefore under our experimental conditions recombination plays no significant role in either double collisions [cases (1) and (5)] or triple collisions with two electrons. Conversely, the third and the fourth processes enumerated above both lead to the required result. The recombination coefficient β in the third case is proportional to the average velocity of the gas molecules; in the fourth case it is proportional to the average velocity of the ions. In both cases $\beta \sim (m_g)^{1/2}$ and, consequently, one can expect that $\tau \sim A^{1/2}$. The choice between the third and the fourth process under our experimental conditions is facilitated by estimating the mean time for the capture of electrons by molecules:

$$\tau_{\text{capt}} = (s_{\text{capt}} \bar{c}_e \cdot n_g)^{-1}.$$

The literature contains data on the calculated values of s_{capt} for H atoms:[12] $s_{\text{capt}} \sim 10^{-22}$ cm^2. To obtain an upper limit for the estimate of the capture cross section for the H_2 and D_2 molecules, we take a value greater by an order of magnitude: 10^{-21} cm^2. Further we set $\bar{c}_e = 10^8$ cm/sec; at the highest pressure investigated by us (p = 0.6 mm Hg) $n_g = 2 \times 10^{16}$ cm^{-3}; then $\tau_{\text{capt}} \sim (10^{-21} \times 10^8 \times 2 \times 10^{16})^{-1} = 0.5 \times 10^{-3}$ sec $= 500\,\mu$ sec. Since the deionization process in our experiments occurred mainly during a time ≤ 30 to $50\,\mu$ sec, the formation of negative ions could not have played any significant role in this case. Consequently the principal recombination process under the above conditions is recombination in a triple collision involving a neutral molecule.

5. CONCLUSIONS

1. The process of plasma deionization occurs in deuterium at a rate which is 1.4 times slower than in hydrogen over the whole range of conditions investigated by us (pressures from 15 to 600 μ Hg, tube diameters 3.2 and 6.5 cm, preceding current from 60 to 1500 ma). This ratio is equal to the square root of the ratio of the molecular weights of the two gases.

2. For $pd \leq 10^{-1}$ mm Hg·cm deionization occurs primarily by means of the diffusion of charged particles to the walls where they recombine.

3. For $pd \geq 1$ mm Hg·cm volume electronic recombination is predominant in the process of deionization of hydrogen and deuterium. The principal elementary process is now recombination in triple collisions involving a neutral molecule.

---

*Neglecting the small difference of T_e in H_2 and D_2, which has been already noted above.

[1] W. Koch, Z. Techn. Physik **16**, 484 (1935).

[2] V. L. Granovskii, Izv. Akad. Nauk SSSR, Ser. Fiz. **4**, 449 (1938); J. Tech. Phys. (U.S.S.R.) **13**, 123 (1943).

[3] S. N. Gavrilov, Dokl. Akad. Nauk SSSR **71**, 265 (1950).

[4] M. Biondi and S. C. Brown, Phys. Rev. **75**, 1700 (1949).

[5] M. Biondi, Rev. Sci. Instr. **22**, 500 (1941).

[6] I. Langmuir and H. M. Mott-Smith, Phys. Rev. **28**, 127 (1926).

[7] F. Mohler, Nat. Bur. Stand. J. Res. **19**, 447, 559 (1937).

[8] G. Mierdel, Z. Physik **118**, 574 (1943).

[9] D. J. Rose, Phys. Rev. **104**, 273 (1956).

[10] A. Güntherschultze and H. Schultger, Z. Physik **94**, 395 (1937).

[11] V. L. Granovskii, Электрический ток в газе (Electric Currents in Gasses) **1**, §63, Moscow, 1953.

[12] H. S. W. Massey and E. H. S. Burhop, Electronic and Ionic Impact Phenomena, Oxford, 1952, p. 335.

Translated by G. Volkoff
296

SOVIET PHYSICS JETP VOLUME 35(8), NUMBER 6 JUNE, 1959

POLARIZATION OF PROTONS ELASTICALLY SCATTERED FROM Si^{28} NUCLEI

P. V. SOROKIN, A. K. VAL'TER, I. Ia. MALAKHOV, and A. Ia. TARANOV

Physico-Technical Institute, Academy of Sciences, Ukrainian S.S.R.

Submitted to JETP editor July 5, 1958

J. Exptl. Theoret. Phys. (U.S.S.R.) 35, 1386-1390 (December, 1958)

The degree of polarization of protons scattered through angles of 60, 90, 125 and 150° in the center-of-mass system in the energy interval 1.6 to 2.2 Mev has been calculated on the basis of a phase-shift analysis of elastic scattering data. The polarization was measured at 60 and 90° with He^4 as the analyzer. The calculated and measured results are in agreement within the experimental accuracy.

INTRODUCTION

OLNESS, Haeberli, and Lewis point out in a short communication[1] the existence of resonances in the cross section for p-Si^{28} scattering at E_p = 1.65 and 2.09 Mev with widths of 60 and 25 kev respectively, as well as a broad resonance at 2.9 Mev apparently due to a number of levels.

The results of measurements of the p-Si^{28} elastic scattering cross section for 1.5 to 3.1 Mev protons and their phase shift analysis are contained in the work of Val'ter et al.[2] The information on the levels of the P^{29} nucleus, corresponding to the 1.65 and 2.08 Mev resonances, obtained from this analysis is given in Table I.

The experimental values for level widths determined in reference 2 differ significantly from the corresponding quantities as given in reference 1. However the results of Val'ter et al.[2] are in good agreement with the data on the width of the corresponding levels obtained in the study of the $Si^{28}(p\gamma)$ reaction.[3] The information on the spin and parity of the 4.31-Mev level given in this review[3] is in agreement with the results obtained in reference 2.

The great width of the 4.31-Mev level and the $^3/_2{}^-$ spin value lead one to believe that the scattered proton beam will be polarized to a significant extent in a large energy interval.

It follows from reference 2 that the experimental results can be satisfactorily reproduced theoretically using the characteristics of the levels given in Table I. Therefore these characteristics apparently form a hopeful basis for the calculation of proton polarization.

In this note we report results of calculations and of an experimental study of the energy dependence of proton polarization at various angles for p-Si^{28} scattering.

COMPUTATION OF THE POLARIZATION

The polarization resulting from proton scattering is described by the vector

$$\mathbf{P} = P(\theta, E)\,\mathbf{n},$$

where $\mathbf{n} = (\mathbf{k} \times \mathbf{k}_0)/|\mathbf{k} \times \mathbf{k}_0|$ is a unit vector perpendicular to the scattering plane.

The function $P(\theta, E)$, in the case of elastic scattering by a spin 0 nucleus (in particular p-Si^{28} scattering), can be expressed as follows[4] in terms of the phase shifts $\delta_l^{\pm}$ corresponding to scattering in a state of total angular momentum $l + \frac{1}{2}$ and $l - \frac{1}{2}$:

$$P(\theta, E) = \frac{AB^* + BA^*}{|A|^2 + |B|^2}, \tag{1}$$

TABLE I

E_p, Mev	Level energy, Mev	Level width Γ, kev, c.m.s.	Level spin and parity	Reduced width γ_λ^2, Mev cm	The ratio* $\gamma_\lambda^2 \Big/ \frac{3}{2}\frac{\hbar^2}{ma}$
1.65	4.31	48	$^3/_2{}^-$	$2.23 \cdot 10^{-13}$	0.2
2.08	4.73	13	$^1/_2{}^+$	$0.13 \cdot 10^{-13}$	0.01

*$a = 5.86 \times 10^{-13}$ cm

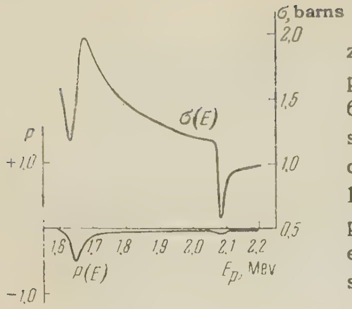

FIG. 1. The proton polarization P(E) resulting from p – Si^{28} elastic scattering at 60° in the center-of-mass system and the corresponding cross section σ(E), calculated on the basis of the phase-shift analysis of the experimental data on the scattering cross section.

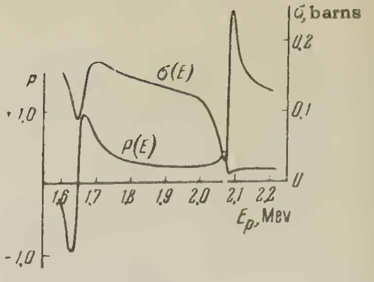

FIG. 3. Same as Fig. 1 but at 125°.

where

$$A(\theta) = -\frac{\eta}{2k}\operatorname{cosec}^2\frac{\theta}{2}\exp\left(i\eta\ln\operatorname{cosec}^2\frac{\theta}{2}\right)$$
$$+\frac{1}{k}\sum_{l=0}^{\infty}\left[(l+1)e^{i\delta_l^+}\sin\delta_l^+ + le^{i\delta_l^-}\sin\delta_l^-\right]e^{i\alpha_l}P_l(\cos\theta);$$
$$B(\theta) = \frac{i}{k}\frac{d}{d\theta}\sum_{l=1}^{\infty}\left(e^{i\delta_l^+}\sin\delta_l^+ - e^{i\delta_l^-}\sin\delta_l^-\right)e^{i\alpha_l}P_l(\cos\theta), \tag{2}$$

where $\eta = (Ze^2)/(\hbar v)$; $k = \mu v/\hbar$; $\alpha_l = 2\sum_{S=1}^{l}\tan^{-1}\frac{\eta}{S}$ is the Coulomb phase shift. The phase shifts $\delta_l^{\pm}$ necessary for the computation were obtained from the expression:[5]

$$\delta_l^{\pm} = \left[-\tan^{-1}\frac{F_l}{G_l} + \tan^{-1}\frac{k\gamma_\lambda^2 / A_l^2}{E_\lambda + \Delta_\lambda - E}\right]_{r=a};$$
$$\Delta_\lambda = \left[-\frac{k\gamma_\lambda^2}{\rho}\left(\frac{\rho}{A_l}\frac{dA_l}{d\rho} + l\right)\right]_{\rho=ka}; \tag{3}$$
$$A_l^2 = F_l^2 + G_l^2.$$

Here F_l and G_l are Coulomb wave functions, while E_λ and γ_λ^2 are the characteristic energy and reduced level width of the compound nucleus and $\rho = kr$.

The values of γ_λ^2 were taken from Table I. The calculations were carried out for scattering through angles of 60, 90, 125 and 150° in the center-of-mass system for protons with energies in the interval from 1.6 to 2.2 Mev. The results are shown in Figs. 1 to 4 together with the corresponding curves for the scattering cross section $\sigma(E) = (|A|^2 + |B|^2)k^2$.

MEASUREMENT OF THE POLARIZATION P(E)

For elastic scattering of spin ½ particles by spin zero nuclei the polarization is more sensitive than the cross section to the choice of the characteristics of the levels. Therefore even comparatively crude measurements of the polarization yield valuable information for checking results obtained from an analysis of scattering cross section data. For this reason we performed experiments to determine the proton polarization.

The proton polarization was determined from double scattering experiments. Si^{28} was used as the first, and He^4 as the second scatterer. The apparatus and experimental procedure have previously been described in detail.[6,7] A free film was used as the first target, obtained by evaporating silicon of natural isotopic composition 1 mg/cm^2 thick in vacuum. The experiments were performed with the electrostatic generator of the Physico-Technical Institute of the Academy of Sciences, Ukrainian S.S.R. The results are shown in Table II. Column 1 gives the scattering angle at which the polarization P(E) was measured, column 2 gives the energy of the incident protons, and column 3 gives the value of the asymmetry R in the secondary scattering from He^4. Column four gives the polarization determined from the expression

$$P_{\exp} = \frac{1-R}{P_{\text{eff.}}(1+R)},$$

where P_{eff} is the effective polarization of the

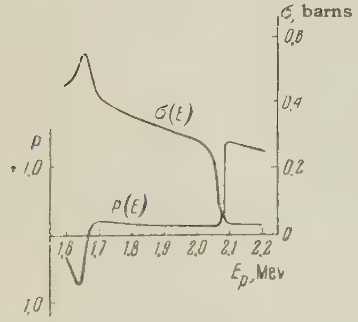

FIG. 2. Same as Fig. 1 but at 90°.

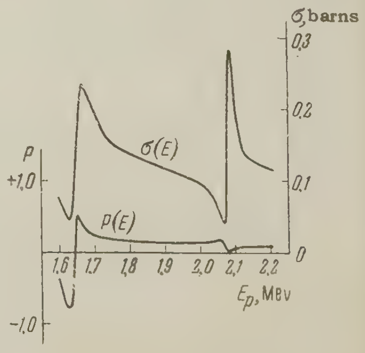

FIG. 4. Same as Fig. 1 but at 150°.

TABLE II

θ, c.m.s.	E_p, Mev	R	P_{exp}	P_{calc}
	1.7	0.86±0.04	−0.34±0.08	−0.26
	1,75	0.90±0.04	−0.18±0,05	−0.19
	1.8	0,90±0.04	−0.14±0.05	−0,07
60°	1,85	0.96±0.04	−0.05±0.04	−0.03
	2,0	0,96±0.04	−0.04±0.04	−0.02
	2,05	0,97±0.04	−0.02±0,03	−0.03
	2.10	0.97±0.04	−0.02±0.03	−0,04
90°	2.15	1,28±0.05	+0,16±0.03	+0.15

helium analyzer determined from the calibration curve published previously.[6,7]

Since a target of considerable thickness was used the values P_{exp} correspond to an average over the energy interval resulting from the energy losses in the target. Therefore, to compare experimental and calculated results, the latter were averaged over energy according to the formula

$$P_{calc} = \int_{E}^{E-\Delta E} P(E)\,\sigma(E)\,dE \Big/ \int_{E}^{E-\Delta E} \sigma(E)\,dE,$$

where ΔE is the energy loss of the protons in the silicon target; $P(E)$, $\sigma(E)$ are shown in Figs. 1 and 2. It was assumed that the stopping power dE/dx is constant in the interval ΔE and that the distribution of the protons as they traverse the foil is energy independent.

The integration was performed graphically. No errors were included in the determination of P_{calc} since they are much smaller than the experimental errors in P_{exp}. The results of the calculation, P_{calc}, are given in the last column of Table II.

DISCUSSION OF RESULTS

It can be seen from Table II that the experimental and calculated values for the polarization are in agreement within the experimental accuracy. Since the errors in the determination of P_{exp} are rather large we cannot discuss this agreement quantitatively. However it is possible, on the basis of the results obtained, to draw definite conclusions about the spin and parity of the levels near which the polarization was measured.

It follows from Eqs. (1) and (2) that the near vanishing of the polarization for 2.08-Mev protons is a convincing proof that the spin and parity of the 4.73-Mev level of P^{29} is $\frac{1}{2}^{+}$. If one assumes that the spin of the 4.31-Mev level is $\frac{1}{2}$, then the value of the function $B(\theta)$ in Eq. (2) would have the opposite sign to that which it has for spin $^3/_2$, and the polarization would, correspondingly, have the opposite sign to what is experimentally observed. (It follows uniquely from a qualitative analysis of the experimental data on the p-Si^{28} scattering cross section[2] that the 4.31-Mev level is due to the capture of an $l = 1$ proton and has odd parity.)

Thus the present investigation provides new confirmation of the validity of the phase shift analysis of the experimental data on the scattering cross section.[2] The results indicate that p-Si^{28} elastic scattering at energies close to 1.65 Mev can be used for manufacturing proton beams of a given polarization, as well as for analyzing of polarized protons, in addition to the presently known (pp) processes on He^4 and C^{12}.

---

[1] Olness, Haeberli and Lewis, Bull. Amer. Phys. Soc. **2**, 34 (1957).

[2] Val'ter, Malakhov, Sorokin, and Taranov, Report at All-Union Conference on Nuclear Spectroscopy 1958; Izv. Akad. Nauk SSSR, Ser. Fiz. **22**, 871 (1958).

[3] P. M. Endt and C. M. Braams, Revs. Modern Phys. **29**, 683 (1957).

[4] J. V. Lepore, Phys. Rev. **79**, 137 (1950).

[5] E. P. Wigner and L. Eisenbud, Phys. Rev. **72**, 29 (1947).

[6] Sorokin, Val'ter and Taranov, Тр. Харьковского гос. ун-та (Reports, Khar'kov State University) **7**, 119 (1958).

[7] P. V. Sorokin and A. Ia. Taranov, Dokl. Akad. Nauk SSSR **111**, 82 (1956), Soviet Phys. "Doklady" **1**, 637 (1956).

Translated by A. M. Bincer
297

SOVIET PHYSICS JETP VOLUME 35(8), NUMBER 6 JUNE, 1959

MAGNETIC ANISOTROPY OF SINGLE-CRYSTAL $CuSO_4$ *IN THE ANTIFERROMAGNETIC STATE*

N. M. KREINES

Institute of Physics Problems, Academy of Sciences, U.S.S.R.; All Union Institute for Physico-Technical and Electronic Measurements

Submitted to JETP editor July 8, 1958

J. Exptl. Theoret. Phys. (U.S.S.R.) **35**, 1391-1397 (December, 1958)

The magnetic anisotropy of a single crystal of anhydrous copper sulfate has been measured between 1.5° and 300°K. The transition to the antiferromagnetic state has been found to be accompanied by an anomalous growth of $\chi_\perp$, while the parallel susceptibility varied in the usual way. A quadratic temperature dependence has been established for $\chi_{\parallel}$. A possible magnetic structure of $CuSO_4$ is discussed.

1. INTRODUCTION

THE magnetic susceptibility of anhydrous copper sulfate was first measured, down to hydrogen temperatures, by Gorter and de Haas in 1931.[1] They performed the measurements on a polycrystalline specimen at nitrogen and hydrogen bath temperatures. They found that at nitrogen temperatures and above, the Curie-Weiss law $\chi = c/(T - \Theta)$ holds, with $\Theta = -77.5°$. At hydrogen temperatures, the value of the susceptibility is considerably greater than that calculated by the Curie-Weiss law and is independent of the temperature. In 1941 Stout[2] observed in anhydrous copper sulfate at $T = 34.8°K$, a heat-capacity anomaly characteristic of a second-order phase transition. The data indicated above, together with our magnetic investigations[3] of a group of anhydrous sulfates of Ni^{++}, Cl^{++}, Fe^{++}, and Cu^{++}, suggest that the anhydrous copper sulfate, like the other foregoing compounds, is antiferromagnetic.

The temperature dependence of the magnetic susceptibility of a polycrystalline specimen of $CuSO_4$, which we have obtained in a previous investigation,[4] show that at $T = 34.5°K$ this substance experiences a transition and apparently becomes antiferromagnetic below this temperature. The transition itself is unusual and is distinguished by an anomalously rapid growth of the susceptibility near $T = 34.5°K$. To explain the character of the observed anomaly and to investigate in greater detail the behavior of the susceptibility below the temperature of this anomaly, we have undertaken to measure of the temperature dependence of the susceptibility in a single crystal $CuSO_4$. The results are reported in this paper.

2. APPARATUS AND SPECIMENS

The magnetic susceptibility was measured by the Faraday method with apparatus analogous to that previously described.[5] This apparatus made it possible to cover without a broad continuous band of temperatures from 1.3 to 300°K. The temperature was measured in the 1.3 to 4.2°K range by determining the vapor pressure of a helium bath, from 4.2 to 20°K by determining the resistance of a carbon thermometer, and from 20 to 300°K by determining the resistance of a copper thermometer calibrated with a standard platinum resistance thermometer.[6] The carbon thermometer was calibrated by the Clement and Quinnell method.[7]

The susceptibility was measured at several magnetic field intensities between 12.5 and 13.5 kilooersteds. The susceptibility was measured in various directions in a plane perpendicular to the line of suspension of the specimen. The error in the absolute value of the susceptibility did not exceed $\pm 1 \times 10^{-4}$ per mole; the relative error did not exceed 2 to 6% in the various temperature ranges. The relative errors were somewhat higher than in previous investigations, owing to the smallness of the specimens. A correction was introduced for the diamagnetism of the SO_4^{--} ion.[8] Single-crystal specimens of anhydrous copper sulfate were used in the investigations. These specimens were obtained* from a solution of cuprous oxide in molten ammonia sulfate.[9] The $(NH_4)_2SO_4$ decomposes, above 360°C and the anhydrous copper sulfate drops out as a crystalline precipitate. Preliminary investigations have shown that the size and quality of the resultant crystals depend, firstly, on the rate of decomposition of the $(NH_4)_2SO_4$ and, secondly, on the value and constancy of the temperature during the entire process. If the process is carried out at ~ 390 or 400°C, an intermediate compound of the type $[Cu(MH_3)_4]SO_4 \cdot H_2O$ is first formed and is then transformed into $CuSO_4$, but not in form of crystals but in the form of a powder. If a higher temperature, approximately 500°C, is maintained during the entire process, the $CuSO_4$ may decompose after the removal of the decomposition products of $(NH_4)_2SO_4$. We therefore chose an intermediate temperature of 430°C, which was maintained accurate to 2 or 3°. At this temperature, the entire process was completed in 20 hours. The optimum initial proportion was one part $CuSO_4$ four parts of $(NH_4)_2SO_4$ (by weight).

---

*The author is very grateful to N. N. Mikhailov for permitting him to grow crystals in his laboratory and for constant interest in this work.

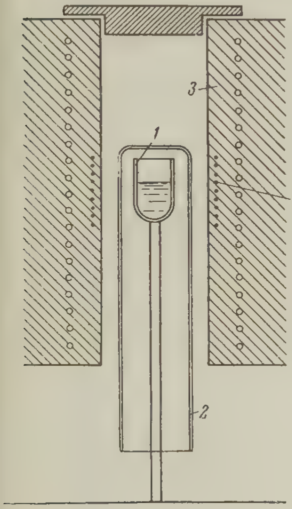

FIG. 1. Diagram of the equipment used to grow single crystals of $CuSO_4$.

Figure 1 shows the diagram of the equipment used to grow single crystals of $CuSO_4$. Approximately 10 g of a mixture of $CuSO_4$ and $(NH_4)_2SO_4$ were placed in cup 1. The decomposition products were removed through test tube 2. A feature of this equipment is that the optimum rate of decomposition can be chosen for any specified temperature. Smooth variation of the mounting height of test tube 2 regulates the gap between the bottom of test tube 2 and cup 1, thus regulating the speed of removal of the decomposition products.

The temperature of the oven 3 was regulated with a platinum resistance thermometer 4, connected in a dc bridge circuit. The null device of the bridge was a type MRShchPr-54 regulating millivoltmeter which controlled the operation of the oven. This circuit maintained the oven temperature accurate to 2 or 3°. The platinum resistance thermometer served only to regulate the temperature. The oven temperature was measured with a copper-constantan thermocuple attached to the upper part of test tube 2. The thermocouple readings were recorded by an automatic millivoltmeter.

The foregoing procedure has yielded single crystals of anhydrous copper sulfate measuring 3×1×0.2 mm and weighing 1 to 2 mg (see reference 4). These crystals are transparent and have a weak gray color. Unlike the polycrystalline $CuSO_4$, obtained by roasting in vacuum, they can be exposed to air for a sufficiently long time (approximately 15 days) without absorbing any moisture. Most crystals are elongated prisms with rhombic cross section, terminating in most cases with quadrilateral pyramids. The angles between

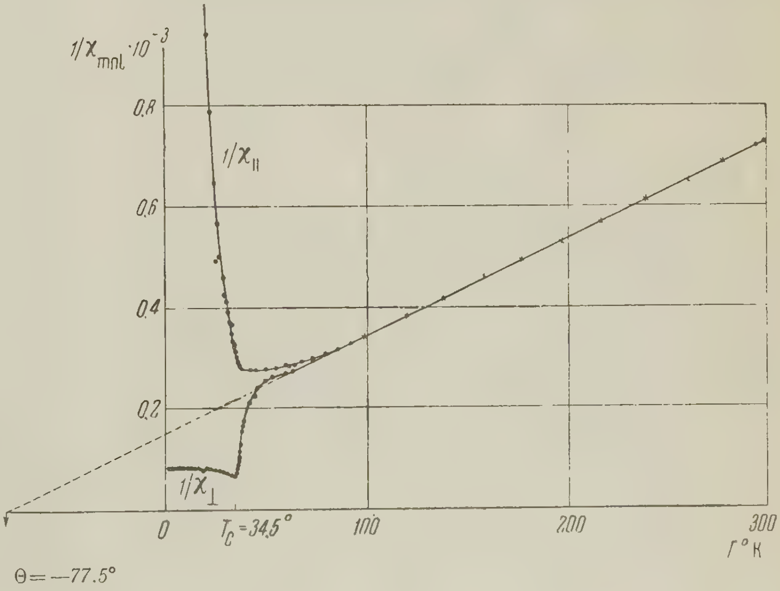

FIG. 2. Temperature dependence of the reciprocal molar susceptibility $1/\chi_{mol}$ of single-crystal $CuSO_4$. ●) data of present work, ×) data of reference 4.

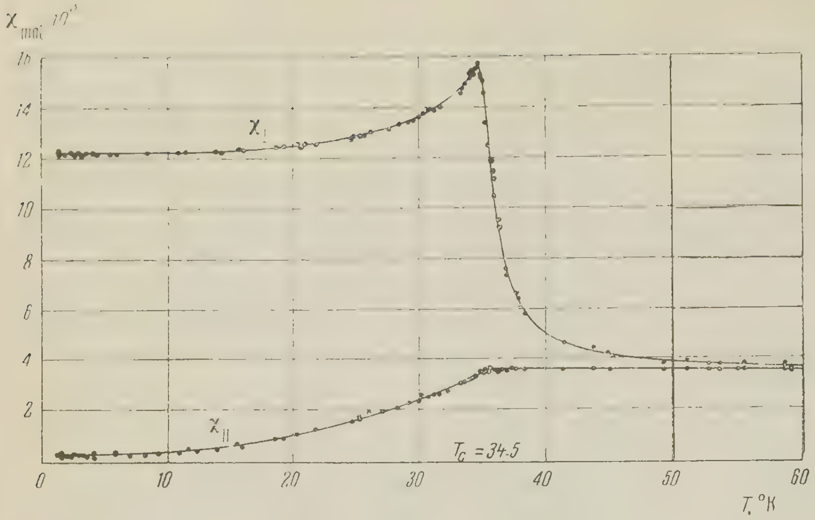

FIG. 3. Temperature dependence of the molar magnetic susceptibility χ_{mol} of single-crystal $CuSO_4$.

the prism faces are approximately 66 and 114° respectively.

The structure of anhydrous copper sulfate has not yet been thoroughly studied. Hammel[10] has obtained x-ray diffraction patterns of anhydrous sulfates of transition metals by the powder method. He has established that the lattice of these compounds is apparently rhombic with four molecules in each elementary cell. For $CuSO_4$ he obtained the following lattice parameters: $a = 4.88$ A, $b = 6.66$ A, and $c = 9.32$ A.

Preliminary x-ray structural investigations, made by Porai-Koshitz* with single crystals of $CuSO_4$ produced by us, have confirmed Hammel's data. Hammel has found later that the principal plane forming the prism is $\{120\}$ and that the c axis coincides with the long edge of the prism, while axes a and b lie along the long and short diagonals of the rhombic section of the prisms, respectively. According to these data, the angles between the faces of the prism should be 60°30′ and 111°30′ respectively, which is in good agreement with our data.

3. MEASUREMENT RESULTS

The susceptibility was measured with two single-crystal $CuSO_4$ specimens weighing 0.95 and 1.1 mg. The susceptibility was measured in the first specimen in the ab plane (c axis directed along the suspension line), and in the second specimen in the planes ab (c axis along the suspension line) and ac (b axis along the suspension line). In the entire investigated temperature range, the susceptibility component χ_c in the c direction coincides with the component χ_b along the b axis. We denote henceforth $\chi_\perp = \chi_b = \chi_c$ and $\chi_{||} = \chi_a$.

Figure 2 shows the temperature dependence of the reciprocal of the molar susceptibility of $CuSO_4$. In the temperature range from 300 to 85°K, within the limits of experimental accuracy, $\chi_\perp$ coincides with $\chi_{||}$ and with the susceptibility values obtained by us with polycrystalline $CuSO_4$.[4] Figure 2 shows therefore, for this range of temperatures, the data obtained for a polycrystalline specimen, which are more accurate. The diagram shows that the Curie-Weiss law holds in the temperature interval form 300 to 85°K. The constants are $C = 0.517$ and $\Theta = -77.5°$. The value of the g factor, calculated from these data, is 2.38.

Figure 3 shows the results of the measurement of the magnetic susceptibility below 60°K, plotted in coordinates χ_{mol} and T°. When $T \approx 35°K$, $\chi_\perp$ increases sharply, almost tripling in value within approximately 2.5°, reaching a maximum at $T = 34.5°K$. It then drops to three quarters of its maximum. From 12 or 14°K down to 1.5°K $\chi_\perp$ does not change with temperature. Below 60°K $\chi_{||}$ is almost constant down to 36°K, below which it diminshes practically to zero. The small remanent value of $\chi_{||}$, observed at $T = 1.3°K$, may be due to an imperfectly accurate mounting of the crystal and corresponds to a 1° deviation from the crystallographic direction. The maximum value of $\chi_{||}$ corresponds to approximately one quarter of the maximum value of $\chi_\perp$. A dependence of $\chi_\perp$ on the magnetic field is observed in the transition region. Qualitatively this dependence is similar to that observed in polycrystalline specimens,[4] in that the susceptibility decreases with increasing magnetic field, and its maximum shifts towards the lower temperatures.

Quantitatively this dependence is difficult to

---

*The author is deeply grateful to M. A. Porai-Koshitz for supplying him with data on the structure of $CuSO_4$ and for much valuable advice.

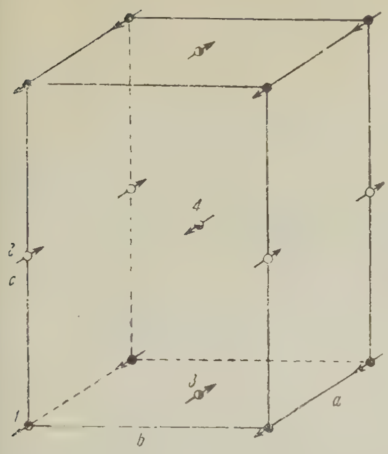

FIG. 4. Assumed magnetic structure of $CuSO_4$. a = 4.88 A, b = 6.66 A, c = 9.32 A.

estimate for a single-crystal specimen, since the susceptibility can be measured only in strong magnetic fields, owing to the smallness of the specimen. No field dependence was observed at all for $\chi_{||}$. We did not find within the limits of the measurement accuracy, the dependence of the susceptibility on the field, observed by de Haas and Wiersma[11] at hydrogen temperatures, or the residual moment observed by Schultz et al.[12] at the same temperatures in a polycrystalline specimen.

4. DISCUSSION OF RESULTS

Our measurements of the temperature dependence of the magnetic susceptibility of anhydrous copper sulfate in a single-crystal specimen show that at 34.5°K the substance experiences a transition, below which it becomes antiferromagnetic. While it was difficult to conclude the character of the observed transition (whether it is a first-order or second-order transition), from the data for the polycrystalline specimen of $CuSO_4$, the behavior of $\chi_{||}(T)$ in a single-crystal specimen is unequivocal evidence of a second-order transition. This conclusion is also confirmed by Stout's[2] data on the heat capacity of $CuSO_4$.

According to the observed temperature dependences for χ_a, χ_b, and χ_c in the antiferromagnetic state, the $CuSO_4$ in the antiferromagnetic state is uniaxial in the magnetic sense. The direction of least magnetization coincides with the a axis.

As indicated above, we still do not know the exact crystalline structure of $CuSO_4$. However, from data on the crystalline structure of $NiSO_4$[13] and from preliminary results on the x-ray structural investigation of $CuSO_4$ made by Porai-Koshitz, we may assume that the arrangement of the Cu^{++} ions in the elementary cell of $CuSO_4$ is as shown in Fig. 4.

Let us attempt to ascertain what type of ordering of the magnetic moments is the most likely for the structure we are investigating. Following the theory of the molecular field,[14,15] we divide the initial lattice into four simple sublattices, as indicated in Fig. 4. Let M_i be the mean magnetization per unit volume of the i-th sublattice. We consider only interactions between ions that are 4.0 to 5.0 A apart, and introduce the following symbols: A — interaction constant between ions inside each sublattice, Γ_1 — constant of the interaction between ions of sublattices I and II and sublattices III and IV, Γ_2 — constant of interaction between ions of sublattices I and III and sublattices II and IV. For the mean moments of the four sublattices we can write the following equations:

$$\begin{aligned} M_1 &= \frac{C}{4T}[H - 2AM_1 - 2\Gamma_1 M_2 - 4\Gamma_2 M_3]; \\ M_2 &= \frac{C}{4T}[H - 2\Gamma_1 M_1 - 2AM_2 - 4\Gamma_2 M_4]; \\ M_3 &= \frac{C}{4T}[H - 4\Gamma_2 M_1 - 2AM_3 - 2\Gamma_1 M_4]; \\ M_4 &= \frac{C}{4T}[H - 4\Gamma_2 M_2 - 2\Gamma_1 M_3 - 2AM_4]. \end{aligned} \tag{1}$$

Using these equations, we determine the Curie temperature T_C in the following cases:

$$\begin{aligned} &1. \quad M_2 = -M_1;\ M_3 = -M_1;\ M_4 = M_1; \\ &\qquad T_{C_1} = \frac{C}{2}(\Gamma_1 + 2\Gamma_2 - A); \\ &2. \quad M_2 = -M_1;\ M_3 = M_1;\ M_4 = -M_1; \\ &\qquad T_{C_2} = \frac{C}{2}(\Gamma_1 - 2\Gamma_2 - A); \\ &3. \quad M_2 = M_1;\ M_3 = -M_1;\ M_4 = -M_1; \\ &\qquad T_{C_3} = \frac{C}{2}(2\Gamma_2 - \Gamma_1 - A). \end{aligned} \tag{2}$$

It is obvious that the most probable order corresponds to the maximum T_C. To estimate T_C we first estimate the magnitudes of the interactions A, Γ_1, and Γ_2. Assuming that the exchange interaction between the magnetic ions increases with diminishing distance between them, we obtain

$$\Gamma_2 > \Gamma_1 > A. \tag{3}$$

Using (3) to estimate T_C in (2) we find that the most likely type of ordering is the first one, i.e., $M_2 = -M_1$, $M_3 = -M_1$, $M_4 = M_1$ (see Fig. 4).

From the data obtained for the susceptibility of a single-crystal of $CuSO_4$ we can draw certain conclusions regarding the temperature dependences for $\chi_{||}$ and $\chi_{\perp}$ below the Curie point. It is seen from Fig. 5, which is plotted in coordinates $\chi_{||}$ and T^2, that $\chi_{||} = a + b(T/T_C)^2$ from ~15 to 34°K. This result agrees with the general deductions of the theory of spin waves.[16-19] The presence of the constant a may be due to an incorrect allowance for the diamagnetic correction for the SO_4^{--} ion. No

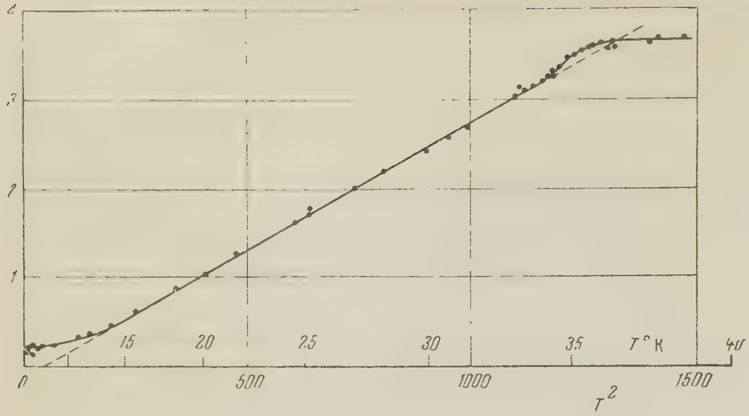

FIG. 5. Temperature dependence of the parallel magnetic susceptibility of a single crystal of $CuSO_4$ below the Curie point.

simple power-law approximation could be found for $\chi_\perp$.

The most interesting is the anomalous increase in anisotropy, which we observed in the narrow region of the transition point. Since the exchange interaction is isotropic, we must assume that the establishment of antiferromagnetic ordering is accompanied by a change in the spin-orbit interaction. Attention should be called to the fact that the value of the g factor in $CuSO_4$ is considerably greater than 2. This is evidence that in the splitting of the orbital levels by the crystal field, the distance between the lower levels becomes relatively small. One can assume that the exchange interaction leads to a further change in the splitting picture. We made no numerical calculations, but qualitatively such a scheme could explain the anomalous increase in the anisotropy.

The author expresses deep gratitude to A. S. Borovik-Romanov for continuous attention and for guiding the project. The author is thankful to Academician P. L. Kapitza for continuous attention to the work and also to Professor P. G. Strelkov for much valuable advice. In addition, the author is indebted to V. I. Kolokol'nikov for aid in the measurements.

---

[1] W. J. De Haas and C. J. Gorter, Leid. Commun. **215a** (1931).

[2] J. W. Stout, J. Chem. Phys. **9**, 285 (1941).

[3] Borovik-Romanov, Karasik, and Kreines, J. Exptl. Theoret. Phys. (U.S.S.R.) **31**, 19 (1956), Soviet Phys. JETP **4**, 109 (1957).

[4] A. S. Borovik-Romanov and N. M. Kreines, J. Exptl. Theoret. Phys. (U.S.S.R.) **33**, 1119 (1957). Soviet Phys. JETP **6**, 862 (1958).

[5] A. S. Borovik-Romanov and N. M. Kreines, J. Exptl. Theoret. Phys. (U.S.S.R.) **29**, 790 (1955), Soviet Phys. JETP **2**, 657 (1956).

[6] Borovik-Romanov, Orlova, and Strelkov, Установление шкалы низких температур между 90 и 10° K. (Establishment of a Low-Temperature Scale between 90° and 10°K) Moscow, 1954.

[7] J. R. Clement and E. H. Quinnell, Rev. Sci. Instr. **23**, 213 (1952).

[8] Ia. G. Dorfman, **Магнитные свойства и строение вещества.** (Magnetic Properties and the Structure of Matter), GITTL, Moscow, 1955, p. 164.

[9] M. P. Klobb, Compt. rend. **114**, 836 (1892).

[10] F. Hammel, Ann. Chim. **11**, 247 (1939).

[11] W. J. De Haas and E. C. Wiersma, Leiden Commun. Suppl. **74**, 36-70 (1932).

[12] De Haas, Schultz, and Koolhaas, Physica **7**, 57 (1940).

[13] P. J. Dimaras, Acta Crystallogr. **10**, 313 (1957).

[14] L. Neel, Ann. phys. **5**, 232 (1936).

[15] J. H. Van Vleck, J. Chem. Phys. **9**, 85 (1941).

[16] P. W. Anderson, Phys. Rev. **79**, 350, 705 (1950).

[17] R. Kubo, Phys. Rev. **87**, 568 (1952).

[18] M. I. Kaganov and V. M. Tsukernik, J. Exptl. Theoret. Phys. (U.S.S.R.) **34**, 106 (1958).

[19] E. A. Turov and V. G. Sharov, **Тр. Ин-та физики металлов, УФИАН.** (Trans. Inst. of Metal Physics, Ural Branch, Acad. Sci.) 1957.

Translated by J. G. Adashko
298

SOVIET PHYSICS JETP VOLUME 35(8), NUMBER 6 JUNE, 1959

TRIPLE SCATTERING OF 660-Mev PROTONS

*I. MEASUREMENT OF THE DEPOLARIZATION PARAMETER D(90°)**

Iu. P. KUMEKIN, M. G. MESHCHERIAKOV, S. B. NURUSHEV, and G. D. STOLETOV

Joint Institute for Nuclear Research

Submitted to JETP editor July 15, 1958

J. Exptl. Theoret. Phys. (U.S.S.R.) **35**, 1398-1401 (December, 1958)

Experiments on triple scattering of 660-Mev protons are described. The depolarization parameter D(90°) is found to be equal to 0.93 ± 0.17. This result indicates that p-p scattering through 90° is mainly due to the $C(\sigma_1 + \sigma_2) \cdot \mathbf{n}$ term in the scattering matrix.

1. INTRODUCTION

THE parameter D, introduced by Wolfenstein,[1] serves as a measure of the change in the normal component of the polarization vector in the second scattering. It follows from his formulas that for p-p scattering the depolarization parameter is determined by the expression

$$\sigma_0 (1 - D) = {}^1/_4 \, | G - N - B |^2 + | H |^2,$$

where $\sigma_0 = \frac{1}{4} | B |^2 + 2 | C |^2 + \frac{1}{4} | G - N |^2 + \frac{1}{2} | N |^2 + \frac{1}{2} | H |^2$ is the cross section for the scattering of an unpolarized proton beam by hydrogen, and B, C, G, H and N are five complex amplitudes of the p-p scattering matrix in the same notation as used in reference 1. The amplitudes B, C, G, H, and N are functions of the scattering angle and energy. The measurement of the parameter D is of considerable interest from the point of view of obtaining full information about p-p scattering, in particular if the measurement is performed at angles smaller and larger than 90° in the center of mass sytem (c.m.s.) where singlet-triplet interference might appear.

In this communication we report the results of a measurement of the depolarization parameter in p-p scattering at 90° in c.m.s. at 640 Mev. The experiment was performed on the six-meter synchrocyclotron of the Joint Institute for Nuclear Research.

2. EXPERIMENTAL PROCEDURE

660-Mev protons underwent first scattering inside the synchrocyclotron chamber from a beryllium target-polarizer 4 cm thick. A proton beam with polarization[2] $P_1 = 0.58 \pm 0.03$ and energy 640 ± 12 Mev was obtained, predominantly by diffraction scattering to the left at an angle of 9°. The flux density of the beam in the experimental area, after passage through a collimator 3 cm in diameter, was 7×10^5 protons/cm²sec. The location of the second and third scatterers and the detection apparatus in the plane of the first scattering (which produces the polarized beam) are shown in the figure.

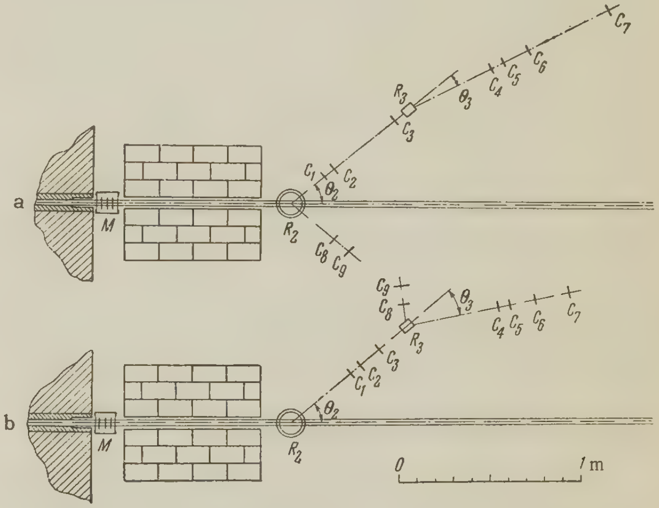

Schematic diagram of the location of the scatterers and detection apparatus in the scattering plane. M – monitor; R_2 – second target (vessel with liquid hydrogen); R_3 – third target: a – 5 × 8 × 6 cm graphite block, b – polyethylene block of the same dimensions; C_1 through C_9 – scintillation counters.

The second scattering took place in a glass vessel 12 cm in diameter filled with liquid hydrogen. The average energy of the protons was 635 Mev in the center of the second target. Three counters C_1, C_2 and C_3 selected the beam of twice-scattered protons. The profile of this beam was, for all practical purposes, symmetric with respect to the axis of the telescope $C_1C_2C_3$. In the second target, scattering of protons by protons took place at an angle $\theta_2 = 41 \pm 2.5°$ ($90 \pm 5°$ in the c.m.s.). The energy of the twice-scattered protons was 315 Mev with a spread of ±40 Mev.

---

*Reported on May 22, 1958 at the IV Session of the Scientific Council of the Joint Institute for Nuclear Research.

The normal component of the polarization vector of doubly scattered protons was determined in two ways. In one method (Fig. 1a) the asymmetry ϵ_{3n} after a third scattering, through an angle $\theta_3 = 12°$, in a carbon target-analyzer was measured with the help of counters C_4, C_5, C_6 and C_7. The use of carbon as analyzer has definite advantages at large second scattering angles, when formation of π mesons in the third target is either negligible or absent altogether. The contribution from π mesons and secondary protons from the reactions $pp \rightarrow pn\pi^+$ and $pp \rightarrow pp\pi^0$ to the count of the protons elastically scattered from the second target was substantially reduced by detecting both elastically scattered protons with the conjugate telescopes $C_1C_2C_3$ and C_8C_9 whose opening angle corresponded to the kinematics of elastic p-p collisions. The counters were connected in groups of three to standard triple coincidence circuits ($\tau \approx 2 \times 10^{-8}$ sec), whose signals were in turn in coincidence. The plastic scintillators of counters C_1 through C_9 measured, in the horizontal and vertical directions respectively, 6.5×6.5, 6×7, 6×7, 6×6, 6×6.5, 6.5×7, 6.5×6.5, 7.5×12, and 8.5×13 cm and were 6 mm thick. The background of accidental coincidences did not exceed 3% of the hydrogen effect.

The second method (Fig. 1b) for the determination of the normal component of the proton polarization vector after the second scattering consisted of measuring the asymmetry ϵ_{3n} at an angle $\theta_3 = 30°$ after p-p scattering in the third target made of polyethylene. The scattering of 315-Mev protons by protons in the third target was differentiated from inelastic processes by registering both the scattered and recoil protons with the conjugate telescopes $C_4C_5C_6C_7$ and C_8C_9 placed first symmetrically to the right and then to the left of the beam which passed through the telescope $C_1C_2C_3$. The coincidence signals from the conjugate telescopes were picked up in coincidence with the signal from the telescope $C_1C_2C_3$. The background from accidental nine-fold coincidences with the same scintillators did not exceed 1% of the hydrogen effect. This method for determining the normal component of the polarization vector of doubly-scattered protons can be used when the second scattering is through amall angles and it becomes impossible to distinguish elastic p-p scatterings by means of conjugate telescopes.

The value of the depolarization parameter, when the second scattering is through 90° in the c.m.s., is given by

$$D(90°) = \varepsilon_{3n} / \varepsilon_3,$$

where ϵ_3 is the asymmetry obtained in scattering by the third target analyzer of a proton beam with polarization P_1 and energy equal to the energy of the protons in the doubly-scattered beam. The reduction in energy from 640 to 315 Mev of the once-scattered polarized beam was accomplished by a set of polyethylene and lead absorbers placed in the path of the protons before and after the purifying magnet in such a way that the angular spread of the slowed down protons was approximately the same as that of the proton beam which underwent a second scattering in the hydrogen target. Control experiments indicated that the slowing down of the protons did not depolarize the beam.

The measurement of the asymmetry ϵ_3 (calibration of the analyzer) was performed under the same geometrical conditions and with the same detection apparatus as the measurement of ϵ_{3n}. The counters C_1, C_2 and C_3 and the target analyzer were placed in the path of the slowed-down proton beam and the second hydrogen target was removed. In the calibration of the carbon analyzer, the asymmetry was determined by means of coincidences between the telescope $C_1C_2C_3$ (which selected the symmetric proton beam), and the telescope $C_4C_5C_6C_7$ (which registered the scattered protons). It should be emphasized that all measurements with the carbon analyzer were performed without a filter between the counters in the telescope $C_4C_5C_6C_7$, so that the observed asymmetries ϵ_3 and ϵ_{3n} were proportional to the polarization of the incident proton beam and to the analyzing power of the carbon as determined by the proton polarization from diffraction as well as from inelastic scattering. In the calibration of the polyethylene analyzer, p-p scattering was selected by means of conjugate telescopes in the same manner as in the measurement of the asymmetry ϵ_{3n} after p-p scattering in the third target.

In the processing of the experimental data, corrections were included for the background of accidental coincidences, for the effect of the empty liquid hydrogen vessel, and for the effect of the scintillator C_3, placed close to the third carbon target.

3. RESULTS

On the basis of data from nine separate series of measurements, we find that protons which are previously doubly scattered have, after scattering by the carbon target, an asymmetry

$$\varepsilon_{3n} = 0.200 \pm 0.032.$$

On the other hand, the calibration measurements of the asymmetry in the scattering by a carbon target of the primary polarized proton beam, whose energy was reduced to 315 Mev, gave the value

$$\varepsilon_3 = 0.216 \pm 0.012.$$

We indicate only statistical errors; they predominate over the systematic errors due to uncertainties in the estimates of various geometric factors. In a great majority of measurements values for ϵ_{3n} and ϵ_3 were obtained coinciding, within the error, with the average values of the corresponding quantities.

It follows from the values of the asymmetries ϵ_{3n} and ϵ_3 that

$$D(90^\circ) = 0.93 \pm 0.17.$$

The same result, but with smaller precision, was also obtained when the experiment was performed by the second method.

This value for D (90°) is noticeably larger than the values found at 310 (reference 3) and 415 Mev (reference 4), and is close to the upper limit of the −1 to +1 interval to which the values of D(90°) are confined. This fact indicates that the change in the normal component of the polarization vector in p-p scattering is small. In that case the amplitudes G and N of the scattering matrix vanish and the following relation results

$$D(90^\circ) = \frac{2|C|^2 - {}^1/_2|H|^2}{{}^1/_4|B|^2 + 2|C|^2 + {}^1/_2|H|^2}.$$

The proximity of D(90°) to +1 indicates that of all the terms entering into the p-p scattering matrix only the $C(\sigma_1 + \sigma_2)\cdot\mathbf{n}$ term is important for scattering through 90°. Judging from the average value of D(90°) the contribution to scattering through 90° of the $C(\sigma_1 + \sigma_2)\cdot\mathbf{n}$ term is not less than ~ 90%, the contribution of the tensor term $H[(\sigma_1\cdot\mathbf{k})(\sigma_2\cdot\mathbf{p}) - (\sigma_1\cdot\mathbf{p})(\sigma_2\cdot\mathbf{k})]$ may reach ~ 4%; thus the contribution of scattering in the singlet state is not more than ~ 7%. In Born approximation the $C(\sigma_1 + \sigma_2)\cdot\mathbf{n}$ term corresponds to a simple spin-orbit coupling.[5]

It should be noted that if D(90°) = 1 exactly, and consequently the scattering amplitudes are determined solely by the function C, all the polarization properties are determined uniquely once $\sigma_0(90^\circ)$ and D(90°) are measured. In that case all three tensors (correlation polarization P_{ik}, depolarization D_{ik}, and recoil polarization K_{ik}) are equal to each other and have only normal components:

$$P_{ik}(90^\circ) = D_{ik}(90^\circ) = K_{ik}(90^\circ) = n_i n_k$$

(n_i are the components of the normal $\mathbf{n}$)

The authors are obliged to Ia. A. Smorodinskii and R. M. Ryndin for useful discussions.

---

[1] L. Wolfenstein, Phys. Rev. **96**, 1654 (1954).

[2] Meshcheriakov, Nurushev and Stoletov, J. Exptl. Theoret. Phys. (U.S.S.R.) **31**, 361 (1956), Soviet Phys. JETP **4**, 337 (1957).

[3] Ypsilantis, Wiegand, Tripp, Segrè, and Chamberlain, Phys. Rev. **98**, 840 (1955).

[4] Kane, Stallwood, Sutton, and Fox, Bull. Am. Phys. Soc. **1**, 9 (1956).

[5] L. Wolfenstein, Bull. Am. Phys. Soc. **1**, 36 (1956).

Translated by A. M. Bincer
299

SOVIET PHYSICS JETP VOLUME 35(8), NUMBER 6 JUNE, 1959

PHYSICAL PHENOMENA THAT OCCUR WHEN BODIES COMPRESSED BY STRONG SHOCK WAVES EXPAND IN VACUO

Ia. B. ZEL' DOVICH and Iu. P. RAIZER

Submitted to JETP editor July 11, 1958

J. Exptl. Theoret. Phys. (U.S.S.R.) 35, 1402-1406 (December, 1958)

The glow of an initially solid opaque body that appears after its compression by strong shock wave with subsequent expansion into a vacuum is studied. Condensation of the vapor of the substance and recombination of ions and electrons under these conditions are also considered.

EXPLOSIVES can be used to produce very strong shock waves in solids. Pressures of the order of ten million atmospheres are achieved, with temperatures behind the shock front of the order of tens or hundreds of thousands of degrees.[1-3] It is natural to inquire whether the radiation from a shock-compressed body can be used for the measurement of its temperature.* Such measurements have recently been performed for a transparent body (Plexiglass),[2] but transparent substances are, of course, exceptions. It would be most interesting to investigate compressed metals, even very thin layers of which ($\sim 10^{-5}$ cm) are opaque to visible light. A fundamental difficulty is presented by the fact that before the shock wave reaches the surface the compressed material is covered with an undisturbed opaque layer. Expansion begins immediately after the shock wave reaches the surface; between the compressed material and the observer there is a layer of material which undergoes compression followed by expansion. Therefore the radiation observed when the wave emerges at the surface of an opaque body cannot be used to measure the temperature reached during compression. However, the study of this radiation is of independent interest. Experiments performed by Kormer, Sinitsyn, and Kuriapin have shown that the optically measured temperatures of opaque bodies are much lower than the calculated compressional temperatures. The measured temperature falls off considerably in the time interval, from 0.1 to 2 or 3 microseconds, when measurements can be obtained. The lower limit, 0.1 microsecond, is set by the resolving power of the apparatus. These experiments have led to the theoretical study of optical and other physical phenomena that should occur on the surfaces of expanding bodies following shock compression.

1. THE HYDRODYNAMICS OF EXPANSION

When a shock wave reaches the interface between the solid and air or a vacuum the material begins to expand from the surface. The hydrodynamic solution for a rarefaction wave is well known (see references 7 and 8, for example). This is the self-similar solution, in which all hydrodynamic quantities depend only on the ratio x/t, where x is distance from the initial position of the boundary and t is time computed from the instant when the shock wave reaches the boundary. The motion is isentropic and each particle of matter expands adiabatically.

When a relatively weak shock wave reaches the surface with energy that is insufficient to cause evaporation of the solid the velocity of the matter while being unloaded to atmospheric pressure (or zero pressure when bounded by a vacuum) becomes $2u_0$, which is double the velocity u_0 acquired in the shock wave. The material, which is heated irreversibly by the shock wave, remains in a final solid phase.

The unloading process is entirely different when a solid body is heated by a strong shock wave to a temperature of the order of tens of thousands of degrees so that its thermal energy is considerably above the heat of vaporization. The adiabatically expanding and cooling material in the unloading region is then in its gaseous phase. The adiabatic curve passes above the critical point, and the material density at the leading edge of the unloading wave falls to practically zero together with the temperature and pressure when the substance unloads into a vacuum.

In first approximation we find, when the material is assumed to be a gas with the adiabatic exponent γ, that the velocity of particles on the surface of the body during expansion into a vacuum is $[1+\sqrt{2\gamma/(\gamma-1)}]u_0$ where u_0 is again the velocity of the shock-compressed material. Taking the effective value $\gamma \approx 1.3$ (with account of ionization), we obtain approximately $4u_0$ for the velocity of the boundary.

---

*The glow of gases, particularly air, in shock waves has been considered theoretically in references 4 and 5. For further bibliography see the review article, reference 6.

In the unloading zone the density passes continuously through a very wide range of values from zero to the density of the shock-compressed solid. The density of an individual particle obeys the law $\rho \sim t^{-2/(\gamma+1)}$. A number of interesting phenomena occur in the unloading zone.

2. GLOW DURING UNLOADING

The surface of the unloading wave glows brightly. The radiation is the typical emission from a gas with a steep temperature distribution. The absorption and emission of visible light in the case of a monatomic gas, such as a metallic vapor, are due principally to photoelectric transitions from highly excited atomic levels and to the reverse process of photorecombination. The absorption coefficient is sharply reduced with decreasing temperature following the Boltzmann law* and is proportional to the density:

$$\varkappa_\nu \sim \rho \exp[-(I-h\nu)/kT],$$

where I is the ionization potential, which may be somewhat reduced through the strong Coulomb interaction of the plasma in regions of high density.

At sufficiently low temperatures, where the range of light is greater than the characteristic distance u_0t, the gas is transparent; on the other hand, at sufficiently high temperatures the gas becomes absolutely opaque. Therefore the radiating layer corresponds to temperatures at which $l_\nu(T) \sim u_0t$.

More precisely, the effective (visual) temperature is given by the condition

$$\int \varkappa_\nu dx = 1,$$

where the integral is taken from the gas-to-vacuum interface up to the radiating layer with a temperature approximately equal to the effective temperature T_{eff}.

Making use of the equation of the adiabate, $\rho \sim T^{1/(\gamma-1)}$, and the hydrodynamic solution $\rho = \rho(x/t)$, we go over to the new independent variable, the temperature

$$T = T(x/t), \quad x = tf(T), \quad dx = tf'(T)\,dT.$$

We obtain our condition in the form

$$\text{const}\cdot t \int_0^{T_{\text{eff}}} \exp[-(I-h\nu)/kT]\,T^\alpha dT = 1,$$

where α is a constant on the order of a few units. The behavior of the integral is determined principally by the exponential function. Approximate integration leads to the transcendental equation

$$T_{\text{eff}} = (I-h\nu)/k \ln(tT_{\text{eff}}^{\beta}\cdot\text{const})$$

where β, which is a constant of the order of a few units, depends on the adiabatic exponent γ.

A numerical estimate shows that the effective temperatures of metals with $I \sim 5$ to 8 ev, range from 3000 to 7000°, beginning already with very small times, $\sim 10^{-10}$ sec.

The screening of radiation in the unloading region fundamentally limits the possibility of observing temperatures of hundreds or thousands of degrees in the region not yet reached by the rarefaction wave. This region becomes invisible when the unloading region becomes of the order of the range of light, i.e., $u_0t \sim 10^{-6}$ cm, which at velocities $u_0 \sim 10^6$ corresponds to $t \sim 10^{-12}$ sec. Thus it is impossible to follow the frequently-advanced suggestion that the temperature in a shock wave be measured from the brightness of the glow when the wave reaches a vacuum-bounded surface. (Even if an instrument with time resolution $\sim 10^{-12}$ sec is constructed, it is practically impossible to make the wave front parallel to the surface of the body with accuracy $\sim 10^{-6}$ cm.) Therefore at present the temperature of the wave front can be measured from the brightness of the glow only in the case of transparent bodies, as was suggested in reference 2.

However in a more detailed study of the optical properties of a gas the curve of $T_{\text{eff}}(t)$ may yield some information regarding the gas density in the emitting region, where the temperature $\approx T_{\text{eff}}$, i.e., it may be possible to estimate the entropy of the gas, which in virtue of the isentropic motion equals the entropy in the shock wave.

It must be noted that the measured mechanical parameters of a shock wave do not indicate directly the entropy and temperature in the wave.[9]

3. CONDENSATION DURING UNLOADING

Under certain conditions the brightness of the unloading wave may be affected by vapor condensation at the low temperatures that exist on the leading edge. Condensation is of interest independently of the wave brightness. The adiabate of the vapor during expansion must intersect the curve of equilibrium between the condensed material and saturated vapor since in the adiabate T and ρ are related by the power law $T \sim \rho^{\gamma-1}$ and in the phase equilibrium curve by the exponential law $\rho \sim \exp\{-q/kT\}$, where q is the heat of vaporization. The number of condensation nuclei is determined by the adiabatic vapor cooling rate; the degree of supersaturation at which strong condensation begins, thus preventing further supersaturation, increases with the adiabatic cooling rate, i.e., with the shock wave amplitude.

---

*In accordance with the number of atoms whose excitation energy is high enough so that a light quantum of frequency ν can induce ionization.

Vapor condenses on nuclei which are formed at the initial moment when maximum supersaturation is reached; new drops are then no longer formed. A kind of quasi-stationary state is established in which the degree of condensation "follows" the further expansion of the material. Calculation shows that the number of condensed drops is so large that even with total condensation of the vapor the drops are considerably smaller than visible light wavelengths. This indicates that the drops absorb light volumetrically, i.e., only in proportion to the total quantity of condensed vapor, which increases with time. After sufficient time this absorption can screen the glow completely.

It would be very interesting to investigate how small drops of a condensate diffusely scatter light from an outside source illuminating the unloading wave. The scattering of light by small droplets is proportional to the square of their volume, unlike the case for absorption. Therefore such an experiment would enable us to investigate both the total quantity of condensate and the droplet size.

It should be noted that diffuse scattering of light depends strongly on the existence of condensed drops, since a gas scatters very weakly. Therefore the method of recording the scattered light is a very sensitive means of detecting condensation.

4. CONDITIONS AT THE LEADING EDGE DURING UNLOADING INTO A VACUUM

A small quantity of matter at the leading edge of the unloading wave is subjected to nonadiabatic conditions, since it absorbs light that proceeds from deeper layers. This nonmechanical transfer of energy from deep layers to outside layers increases the velocity of the leading edge compared with the velocity of adiabatic unloading. The conditions at the leading edge approximate those in an isothermal rarefaction wave, where the velocity of the leading edge is known to be infinite as the density drops exponentially. It would be of great interest to investigate electrical conduction in a rarefaction wave just as the electrical conductivity of a plasma is studied in a shock tube.

As a result of the rapid drop in density, recombination processes, which require triple collisions, do not reach equilibrium at the leading edge. The kinetic equation of these processes is

$$dc/dt = f(c)\rho^2; \quad \int dc/f(c) = \int \rho^2\,dt,$$

where c is the specific concentration of atoms, electrons or ions, and $f(c) \sim c^2$ or $\sim c$, depending upon whether we are considering pair-wise recombination or adherence to inert molecules. When the density drop obeys the law $\rho \sim t^{-2/(\gamma+1)}$ the integral on the right converged, approaching a finite limit in infinite time. However the equation for radiative recombination contains the first power rather than the second power of the density. The integral (with the cross section $\sim 1/T$) diverges for any $\gamma > 1$. Consequently, $c \to 0$, the decrease of c being determined by photorecombination.

Even a brief enumeration of the phenomena that occur in unloading waves of solids heated by strong shock waves shows the broad possibilities of this method, which can be used to investigate diversified physical processes in the vapors of metals and other solids at high temperatures and in the broad range of densities which cannot be achieved by other laboratory methods.

We take this opportunity to thank L. V. Al'tshuler and S. B. Kormer for valuable discussions.

---

[1] Al'tshuler, Krupnikov, and Brazhnik, J. Exptl. Theoret. Phys. (U.S.S.R.) **34**, 886 (1958), Soviet Phys. JETP **7**, 614 (1958); Al'tshuler, Krupnikov, Ledenev, Zhuchikhin, and Brazhnik, J. Exptl. Theoret. Phys. (U.S.S.R.) **34**, 874 (1958), Soviet Phys. JETP **7**, 606 (1958).

[2] Zel'dovich, Kormer, Sinitsyn, and Kuriapin, Dokl. Akad. Nauk SSSR **122**, 48 (1958), Soviet Phys. "Doklady" **4**, 000 (1958).

[3] Walsh, Rice, McQueen, and Yarger, Phys. Rev. **108**, 196 (1957).

[4] Ia. B. Zel'dovich, J. Exptl. Theoret. Phys. (U.S.S.R.) **32**, 1126 (1957), Soviet Phys. JETP **5**, 919 (1957).

[5] Iu. P. Raizer, J. Exptl. Theoret. Phys. (U.S.S.R.) **33**, 101 (1957) and **34**, 483 (1958), Soviet Phys. JETP **6**, 77 (1958) and **7**, 331 (1958).

[6] Ia. B. Zel'dovich and Iu. P. Raizer, Usp. Fiz. Nauk **63**, 613 (1957).

[7] Ia. B. Zel'dovich, **Введение в газодинамику и теория ударных волн** (Introduction to Gas Dynamics and Shock Wave Theory), Acad. Sci. Press, 1946.

[8] L. D. Landau and E. M. Lifshitz, **Механика сплошных сред** (Mechanics of Continuous Media), Gostekhizdat, M., 1948.

[9] Ia. B. Zel'dovich, J. Exptl. Theoret. Phys. (U.S.S.R.) **33**, 700 (1957), Soviet Phys. JETP **6**, 537 (1957).

Translated by I. Emin
300

SOVIET PHYSICS JETP VOLUME 35(8), NUMBER 6 JUNE, 1959

INTERACTION BETWEEN A MEDIUM AND A RING CURRENT INCIDENT ON IT

V. N. TSYTOVICH

Moscow State University

Submitted to JETP editor March 10, 1958

J. Exptl. Theoret. Phys. (U.S.S.R.) 35, 1407-1416 (December, 1958)

An analysis is given of the spectral distribution of the current in a turn that impinges with a constant nonrelativistic velocity on a medium possessing arbitrary $\epsilon(\omega)$ and μ. Derivations are given of the criterion for reflection at nonrelativistic velocities, and of the expression for the acting forces.

1. FORMULATION OF THE PROBLEM

In an earlier paper[1] the author has calculated the interaction between a semi-infinite medium and a constant rectilinear current incident on it with a constant velocity $\beta = v/c$. If the current is incident on plasma (or on metal), the force of repulsion does not depend on the electron density or on other characteristics of the plasma, and as $\beta \rightarrow 1$ the force increases as $1/(1-\beta^2)^{1/2}$, provided the velocity exceeds a certain critical value $\beta \gg \beta_{cr} = c\gamma_0/\omega_0^2 r$ (cf. reference 1). When $\beta \ll \beta_{cr}$ the force decreases, practically linearly with decreasing β (if the logarithmic term is not taken into account). These results are not applicable to a ring current even if the distances to the plasma are sufficiently small so that the curvature of the current is negligible, since the change in the magnetic flux through the current circuit as it approaches the plasma will change significantly the magntidue of the current, and therefore also the magnitude of the forces, unless we assume that such a change in current is compensated by some additional electromotive forces. Consequently the restuls of the earlier paper[1] are applicable to a ring current only under the assumption that the magnitude of the incident current is at its limit.

In the present paper we consider the field of a ring current of radius a, which is incident with a constant velocity v on a medium occupying the semi-infinite space $z \leq 0$. The medium is described by arbitrary μ and $\epsilon = \epsilon(\omega)$. It is assumed that the plane of the ring current is parallel to the plane surface of the medium. Further, we assume that the ring is characterized by infinite conductivity, so that the total flux of the magnetic field linked with the current circuit is a constant of the motion. When the distance from the circuit to the medium is infinite, $z \rightarrow \infty$ (cf. Fig. 1), the magnitude of the current I_∞ is considered to be given, and its subsequent variation is determined by the motion of the circuit. It is assumed that the radius of the ring does not change in the course of the motion. Thus, the current density can be written

$$j_z = j_\rho = 0, \quad j_\varphi = I(t)\,\delta(z + vt)\,D(\rho, a), \tag{1}$$

where a is the radius of the ring, $I(-\infty) = I_\infty$.

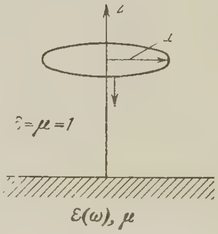

FIG. 1

A change in the current in the course of the motion of the ring means that of definite frequencies are excited in the ring. Without solving the problem it is possible to make a number of qualitative statements with respect to the frequency distribution of the excited currents from the uncertainty relation $\Delta\omega\Delta t \sim 1$ in the same way as is done in the case of radiation in accelerators. The order of magnitude of the maximum excited frequency can be estimated as $\omega_{max} \sim 1/\tau_{col}$, where τ_{col} is the characteristic time for the collision of the ring with the wall. At speeds $v \sim c$, as a result of relativistic contraction, this time is of order of magnitude $a(1-\beta^2)^{1/2}/c$, i.e., $\omega_{max} \sim c/a(1-\beta^2)^{1/2}$. Thus, as $\beta \rightarrow 1$ successively higher harmonics will be excited in the ring. The object of the present work is a quantitative investigation of this effect.

To analyze the frequency distribution we expand all the quantities in Fourier integrals. In particular,

$$I(t) = \int I_\omega e^{-i\omega t} d\omega, \tag{2}$$

$$I(t)\,\delta(z + vt) = \frac{1}{2\pi}\int I_{\omega+\varkappa v} e^{-i\omega t + i\varkappa z} d\omega\, d\varkappa. \tag{3}$$

In view of the cylindrical symmetry of the problem it is convenient to expand the radial function $D(\rho, a)$ in terms of Bessel functions:

$$D(\rho, a) = a\int_0^\infty g(k)\, kJ_1(k\rho)\, J_1(ka)\, dk. \tag{4}$$

A linear ring current corresponds to $g(k) = 1$ and $D(\rho, a) = \delta(\rho - a)$. The quantity $g(k)$ has the meaning of a form factor that characterizes the "smearing" of the current and which must cut off values of k greater than $1/\delta$, where δ is a dimension that characterizes the current cross section. Since the specific form of $g(k)$ is not important in the case of thin rings, which will be discussed from now on, it is convenient in specific calculations to take $g(k) = \exp\{-k\delta\}$. In accordance with Eqs. (1) to (4), the potential of the field of the ring current can be written in the form*

$$A^0 = \frac{2a}{c}\int \frac{I_{\omega+\varkappa v}}{k^2 + \varkappa^2 - \omega^2/c^2} e^{i(\varkappa z - \omega t)} kJ_1(k\rho) J_1(ka)\, g(k)\, dk d\varkappa\, d\omega. \tag{5}$$

Generally speaking, it is necessary to add to the expression $1/(k^2 + \kappa^2 - \omega^2/c^2)$ a δ-function term that leads to retarded potentials, and to interpret the integral containing $1/(k^2 + \kappa^2 - \omega^2/c^2)$ in the sense of its principal value (cf., for example, Bolotovskii[2]). This operation is equivalent to specifying a definite method of going around the poles by means of infinitesimally small imaginary (or, in general, complex) additions to the denominator. We assume that the rules of going around the poles are specified by prescribing a complex ϵ which differs from unity by an arbitrarily small amount, while the sign of the imaginary term in the complex expression for ϵ must correspond to dissipative processes for a given choice of the sign of the frequency (cf. Bolotovskii[2]). This requirement leads in an unambiguous way to the displacement of the poles into the upper half-plane of complex ω, which is equivalent to adding to the principal value of $P(1/(k^2 + \kappa^2 - \omega^2/c^2))$ the δ-function term $(\pi i\omega/|\omega|)\,\delta(k^2 + \kappa^2 - \omega^2/c^2)$. Expressions containing such denominators will be interpreted henceforth in this sense.

2. THE METHOD OF IMAGES

Let the medium be described by certain $\epsilon(\omega)$ and μ. We assume that the field for $z \geq 0$ consists of the field A^0 in the absence of the medium and the field of the "reflected" current, the potential $A^{(1)}$ due to the latter being obtainable from A^0 by letting $z \to -z$ and by multiplying the Fourier components of the current by $\Phi_1(\omega, \kappa)$:

$$A|_{z\geqslant 0} = A^0 + A^{(1)}, \tag{6}$$

$$A^{(1)} = \frac{2a}{c}\int \Phi_1(\omega, \varkappa) \times \frac{I_{\omega+\varkappa v}}{k^2 + \varkappa^2 - \omega^2/c^2} e^{-i(\varkappa z + \omega t)}\, dk\, d\varkappa\, d\omega\, kJ_1(k\rho)\, J_1(ka)\, g(k). \tag{7}$$

The field for $z \leq 0$ is the field whose potential $A^{(2)}$ can be obtained from A^0 by letting $z \to \zeta z$, where $\zeta = \zeta(\omega, \kappa)$, by multiplying the Fourier component of the current by $\Phi_2(\omega, \kappa)$, and by replacing c by $c/\sqrt{\epsilon\mu}$:

$$A|_{z\leqslant 0} = A^{(2)} = \frac{2a\mu}{c}\int \Phi_2(\omega, \varkappa)\, \frac{I_{\omega+\varkappa v} \exp\{i[\varkappa\zeta(\omega, \varkappa).z - \omega t]\}}{k^2 - \varepsilon\mu\omega^2/c^2 + \varkappa^2\zeta^2(\omega, \varkappa)} \times kJ_1(k\rho)\, J_1(ka)\, g(k)\, dk\, d\varkappa\, d\omega. \tag{8}$$

In the special case when the current does not vary, and the medium is not a dispersive one, the above replacement means that the field due to the medium at $z \geq 0$ is the field of the reflected current whose magnitude is reduced by the factor Φ_1.

From the boundary conditions we obtain:

$$\zeta = \{1 + (\omega/c\varkappa)^2 [\mu\varepsilon(\omega) - 1]\}^{1/2}, \quad \operatorname{Re}\zeta > 0; \tag{9}$$

$$\Phi_1(\omega, \varkappa) = (\mu - \zeta(\omega, \varkappa))/(\mu + \zeta(\omega, \varkappa));$$
$$\Phi_2(\omega, \varkappa) = 2\mu/(\mu + \zeta(\omega, \varkappa)). \tag{10}$$

In order that Eqs. (6) to (8) be fields that satisfy the foregoing equations, it is also necessary to show that if ζ, Φ_1 and Φ_2 are defined by relations (9) and (10), expressions (7) and (8) satisfy the homogeneous equations in the corresponding regions $z \geq 0$ and $z \leq 0$. To verify that the currents obtained from (7) and (8) vanish in these regions it is sufficient to let $\omega \to \omega - \kappa v$ in the integrands of the expressions for the currents and to deform the path of integration into the lower half-plane of complex κ. In virtue of $\operatorname{Re}\zeta > 0$ and of the form of $\kappa\zeta$, Φ_1 and Φ_2, the only singularities of the integrands will be the singular points ϵ and $1/\epsilon$ (cf., for example, references 3 and 4). We have taken the time-dependent factor in the present case to be the same as in reference 4 $(\exp\{-i\omega t\})$, but the expressions in which we are interested contain $\omega - \kappa v$, so that the poles with respect to κ lie in the upper half-plane of complex κ. Integration over the large semi-circle in the lower half-plane gives zero for certain ranges of values $z \geq 0$ and $z \leq 0$, since $\zeta \to 1$ as $|\kappa| \to \infty$, because $\epsilon\mu \to 1$ as $|\omega| \to \infty$.

---

*The only nonvanishing component A_φ of the four-potential will be denoted throughout simply by A.

3. INTEGRAL EQUATION FOR THE FOURIER COMPONENTS OF THE CURRENT

The change in the current is determined by the flux Φ, which can be obtained from (5) and (7):

$$\Phi = 2\pi aA\Big|_{\substack{\rho=a\\ z=-vt}} = \frac{4\pi a^2}{c}\int \frac{I_{\omega+\varkappa v}}{k^2+\varkappa^2-\omega^2/c^2}\, g(k)\, kJ_1^2(ka)\, dk\, d\varkappa\, d\omega \times \left\{e^{-i(\varkappa v+\omega)t} + \frac{\mu-\zeta(\omega,\varkappa)}{\mu+\zeta(\omega,\varkappa)} e^{-i(\omega-\varkappa v)t}\right\}. \tag{11}$$

For a superconducting ring we can write

$$\Phi(t) = \Phi(-\infty) = LI_\infty / c(1-\beta^2)^{1/2}. \tag{12}$$

On multiplying this equation by $\exp\{i\lambda t\}$ and integrating with respect to t we obtain:

$$\frac{4\pi a^2}{c}\int g(k)\, kJ_1^2(ka)\, dk\, d\varkappa \left\{\frac{I_\lambda}{k^2+\varkappa^2-(\lambda-\varkappa v)^2/c^2} + \frac{\mu-\zeta(\lambda+\varkappa v,\varkappa)}{\mu+\zeta(\lambda+\varkappa v,\varkappa)}\, \frac{I_{\lambda+2\varkappa v}}{k^2+\varkappa^2-(\lambda+\varkappa v)^2/c^2}\right\} = \frac{LI_\infty}{c(1-\beta^2)^{1/2}}\,\delta(\lambda). \tag{13}$$

Here L is the self-inductance of the cirucit

$$L = 4\pi^2 a^2 \int_0^\infty g(k)\, J_1^2(ka)\, dk. \tag{14}$$

If we set $g(k) = \exp\{-k\delta\}$, we obtain from (14) for $\delta \ll a$,

$$L = 4\pi a\{\ln(8a/\delta) - 2\}.$$

We transform Eq. (13) by introducing in the second term of the left hand side the new variables $\kappa v = (\omega-\lambda)/2$, $\lambda + \kappa v = (\omega+\lambda)/2$. We obtain:

$$I_\lambda K(\lambda) + \int K(\lambda,\omega)\, I_\omega d\omega = \frac{LI_\infty}{4\pi a^2(1-\beta^2)^{1/2}}\,\delta(\lambda), \tag{15}$$

where

$$K(\lambda) = \int \frac{kJ_1^2(ka)\, g(k)\, dk\, d\varkappa}{k^2+\varkappa^2-(\lambda-\varkappa v)^2/c^2}, \tag{16}$$

$$K(\lambda,\omega) = \frac{1-\zeta_\lambda}{1+\zeta_\lambda}\,\frac{1}{2v}\int_0^\infty \frac{kJ_1^2(ka)\, g(k)\, dk}{k^2+(\lambda-\omega)^2/4v^2-(\lambda+\omega^2)/4c^2}, \tag{17}$$

with

$$\zeta_\lambda = \left\{1+\beta^2\left(\frac{\lambda+\omega}{\lambda-\omega}\right)^2\left[\mu\varepsilon\left(\frac{\lambda+\omega}{2}\right)-1\right]\right\}^{1/2}. \tag{18}$$

In virtue of the remark made above with respect to the rules for going around the singularities of the integrands, the kernels $K(\lambda)$ and $K(\lambda,\omega)$ are complex; it follows from $I_\lambda = I_\lambda^*$ that

$$K^*(-\lambda) = K(\lambda); \qquad K^*(-\lambda,-\omega) = K(\lambda,\omega). \tag{19}$$

We now evaluate the integrals (16) and (17). The integral (16) with respect to κ can be easily found by taking into account the rules stated above for going around the singularities

$$K(\lambda) = \frac{\pi i}{a(1-\beta^2)^{1/2}}\int_0^\infty \frac{kg(k/a)\, dkJ_1^2(k)}{(\psi^2-k^2)^{1/2}}, \qquad \lambda > 0, \tag{20}$$

where $(\psi^2-k^2)^{1/2} = 1(k^2-\psi^2)^{1/2}$ if $k > \psi$. Here $\psi = \lambda a/c(1-\beta^2)^{1/2}$, while, in the case of negative λ, $K(\lambda)$ can be obtained in accordance with (19). The function $g(k/a)$, which appears in (20), cuts off $k > 1/\gamma \equiv a/\delta$. For $\psi \gg 1/\gamma$ we can set in the integrand of (20) $(\psi^2-k^2)^{1/2} = \psi$. If, in addition, we set $g(k/a) = \exp\{-k\gamma\}$, we obtain for $\gamma \ll 1$

$$K(\lambda) = i/a(1-\beta^2)^{1/2}\psi\gamma. \tag{21}$$

In the other limiting case, $\psi\gamma \ll 1$, we simplify the calculation by setting $g(k/a) = \exp\{-\gamma(k^2-\psi^2)^{1/2}\}$, which corresponds to cutting off $k^2 > \psi^2 + \gamma^{-2} \approx \gamma^{-2}$, and obtain:

$$K(\lambda) = K(0) - \frac{\pi}{2a(1-\beta^2)^{1/2}}\left\{\frac{\lambda}{|\lambda|}\, i\int_0^{2\psi} J_2(x)\, dx - \int_0^{2\psi}\Omega_2(x)\, dx\right\}, \tag{22}$$

$$K(0) = L/4\pi a^2(1-\beta^2)^{1/2},$$

J_2 and Ω_2 are the Bessel and the Lommel-Weber functions of the second order, L is the coefficient of self-inductance.

Further, the integral (17) can be written

$$K(\lambda,\omega) = \frac{1}{2v}\,\frac{1-\zeta_\lambda}{1+\zeta_\lambda}\int_0^\infty \frac{kg(k/a)\, J_1^2(k)\, dk}{k^2+\chi^2}, \tag{23}$$

where

$$\chi = (a/2v)\{(\lambda-\omega)^2 - \beta^2(\lambda+\omega)^2\}^{1/2}. \tag{24}$$

If $\chi \gg 1/\gamma$, we can neglect k^2 compared to χ^2 in the denominator of (23); we then obtain

$$K(\lambda,\omega) = \frac{1}{2v\pi\chi^2\gamma}\,\frac{1-\zeta_\lambda}{1+\zeta_\lambda}. \tag{25}$$

If $\chi \ll 1/\gamma$ we can set $g(k/a) \approx 1$. By writing one of the $J_1(k)$ in the form $J_1(k) = (H_1^{(1)}(k) + H_2^{(2)}(k))/2$, we can write (23) in the form of an integral from $-\infty$ to $+\infty$. The resulting integral can be evaluated by the method of residues, taking into account the rule given above for going around the singularities on the real axis; we then have

$$K(\lambda,\omega) = \frac{1}{2v}\,\frac{1-\zeta_\lambda}{1+\zeta_\lambda}\, I_1(\chi)\, K_1(\chi), \qquad I_1(z) = \frac{1}{i}J_1(iz); \qquad K_1(z) = -\frac{\pi}{2}H_1^{(1)}(iz). \tag{26}$$

4. INVESTIGATION OF THE FIRST APPROXIMATION

If the current is far from the medium or if the medium in general has a small effect on the cur-

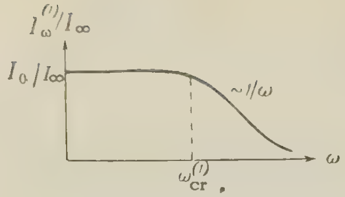

FIG. 2

rent (as is the case, for example, for a dielectric), we can restrict ourselves in solving Eq. (15) to the first approximation obtained by the method of iterations, in which we take for the zero-order approximation the expression for the Fourier components of the time-invariant current, which is equal to the current at infinity $I_\lambda^0 = I_\infty \delta(\lambda)$. The first approximation has the form

$$I_\lambda^{(1)} = - I_\infty K(\lambda, 0) / K(\lambda). \tag{27}$$

On substituting expressions (22) and (26) into (27) we obtain

$$I_\lambda^{(1)} = I_\infty \frac{\zeta_\lambda - 1}{\zeta_\lambda + 1} \frac{a(1-\beta^2)^{1/2}}{2v} I_1(\chi_0) K_1(\chi_0) \Big\{ l - \frac{\pi}{2} \int_0^{2\psi} \Omega_2(x)\, dx$$
$$+ i \frac{\pi}{2} \frac{\lambda}{|\lambda|} \int_0^{2\psi} J_2(x) dx \Big\}^{-1}, \tag{28}$$

$$\chi_0 = (a\lambda / 2v)(1-\beta^2)^{1/2}, \quad \psi = \lambda a / c (1-\beta^2)^{1/2},$$

where l is one-half the linear inductance.

Thus we can introduce two characteristic critical frequencies $\omega_{\mathrm{cr}}^{(1)}$ and $\omega_{\mathrm{cr}}^{(2)}$ which determine the shape of the frequency distribution of the additional currents induced in the ring. For these frequencies we have respectively $\chi_0 = 1$ and $\psi_0 = 1$:

$$\omega_{\mathrm{cr}}^{(1)} = 2v / a (1-\beta^2)^{1/2}; \qquad \omega_{\mathrm{cr}}^{(1)} = (c/a)(1-\beta^2)^{1/2}. \tag{29}$$

In the nonrelativistic limit $\beta \ll 1$ we always have $\omega_{\mathrm{cr}}^{(1)} \ll \omega_{\mathrm{cr}}^{(2)}$, therefore the denominator in (28) is equal to l; if, moreover, $\omega_{\mathrm{cr}}^{(1)}$ is appreciably lower than the characteristic frequencies of the medium, then $\epsilon \approx \epsilon(0)$ and, consequently:

$$I_\omega^{(1)} = I_\infty \beta (\varepsilon(0)\mu - 1) \frac{a}{2cl} \mathrm{I}_1\left(\frac{a|\omega|}{2v}\right) K_1\left(\frac{a|\omega|}{2v}\right). \tag{30}$$

From the asymptotic behavior of the Bessel functions I_1 and K_1 it follows that frequencies lower than $\omega_{\mathrm{cr}}^{(1)}$ are excited in the ring with approximately the same amplitude, and $I_0/I_\infty = (\beta a\ 4cl) \cdot (\epsilon(0)\mu - 1)$ (cf. Fig. 2); the amplitudes of the frequencies $\omega > \omega_{\mathrm{cr}}^{(1)}$ fall off as $1/\omega$.

A frequency distribution of the same form, but with a different numerical factor

$$I_\omega^{(1)} = I_\infty \frac{a}{2vl} I_1\left(\frac{a|\omega|}{2v}\right) K_1\left(\frac{a|\omega|}{2v}\right) \tag{31}$$

can occur under certain conditions also in the case of metals and plasma. If one can assume that in metals the number ν of collisions between electrons and ions considerably exceeds $\omega_{\mathrm{cr}}^{(1)}$, then one can set $\epsilon - 1 = -\omega_0^2/i\nu\omega$; if, moreover, $\omega_{\mathrm{cr}}^{(1)} << \omega_0^2\beta^2/\gamma$, and, consequently, $\beta \gg 2\gamma\lambdabar_0/\omega_0 a$, then in (28) $(\zeta_\lambda - 1)/(\zeta_\lambda + 1) \approx 1$. Consequently, under these assumptions the amplitude of the frequency distribution increases with decreasing velocity and does not decrease as in (30). The condition $\beta \gg 2\gamma\lambdabar_0/\omega_0 a$ in fact means, as can be easily seen, that the skin depth in the medium at a frequency $\omega_{\mathrm{cr}}^{(1)}$ is considerably smaller than the radius of the ring a. If we can assume that the number ν of collisions between electrons and ions in the plasma is considerably smaller than the critical frequency $\omega_{\mathrm{cr}}^{(1)}$, the distribution (31) will hold for most of the excited frequencies provided only the plasma oscillation frequency ω_0 is small in comparison with the critical frequency $\omega_{\mathrm{cr}}^{(1)}$. However, if $\nu \gg \omega_{\mathrm{cr}}^{(1)}$ and $\omega_{\mathrm{cr}}^{(1)} \gg \beta^2 4\pi\sigma$, then for most frequencies the distribution has the form:

$$I_\omega^{(1)} = I_\infty \frac{a\pi}{cl} \frac{i\beta\sigma}{2\omega} \mathrm{I}_1\left(\frac{a|\omega|}{2v}\right) K_1\left(\frac{a|\omega|}{2v}\right); \quad \sigma = \frac{\omega_0^2}{4\pi\nu}. \tag{32}$$

If the conditions $\nu \ll \omega_{\mathrm{cr}}^{(1)}$ and $\omega_{\mathrm{cr}}^{(1)} \gg \omega_0$ are satisfied, we obtain for most frequencies

$$I_\omega^{(1)} = I_\omega \frac{a\omega_0^2}{2vl} \frac{1}{\omega^2} \mathrm{I}_1\left(\frac{a|\omega|}{2v}\right) K_1\left(\frac{a|\omega|}{2v}\right). \tag{33}$$

Thus, for $\nu \gg \omega_{\mathrm{cr}}^{(1)}$ and $\omega_{\mathrm{cr}}^{(1)} \gg \beta^2 4\pi\sigma$ only the frequencies $\omega \ll \beta^2 4\pi\sigma$ are excited with a constant amplitude, while for $\nu \ll \omega_{\mathrm{cr}}^{(1)}$, $\omega_{\mathrm{cr}}^{(1)} \gg \omega_0$ only the frequencies $\omega \ll \omega_0$ are so excited.

With the aid of the foregoing frequency distributions we can find the dependence of the current on the time, or, which is the same thing, on the instantaneous distance $r = -vt$ to the medium. The current and its time derivative are expressed in terms of the integral

$$\int_{-\infty}^{\infty} e^{-i\omega t} d\omega K_1(a|\omega|/2v) \mathrm{I}_1(a|\omega|/2v) = (v/2\pi a^2) M, \tag{34}$$

where M is the coefficient of mutual inductance between the current and its image in the case of a perfectly conducting wall. The limiting expressions for the current defined by (30) and (31) may be obtained by utilizing the limiting values for the coefficient of mutual inductance:

$$\frac{I^{(1)}(t)}{I_\infty} = \begin{cases} \dfrac{\pi}{16 l} \dfrac{a^3}{r^3} \text{ for } r \gg a \text{ and } \dfrac{v}{r} \ll \nu,\ r \gg \dfrac{c^2}{4\pi\sigma v} \text{ or } \dfrac{v}{r} \gg \nu,\ r \gg \dfrac{c}{\omega_0} \\ \dfrac{1}{l} \left\{ \ln \dfrac{4a}{r} - 2 \right\} \text{ for } r \ll a \text{ and } \dfrac{v}{r} \ll \nu,\ r \gg \dfrac{c^2}{4\pi\sigma v} \text{ or } \dfrac{v}{r} \gg \nu,\ r \gg \dfrac{c}{\omega_0}. \end{cases} \tag{35}$$

For $r \ll c^2/4\pi\sigma v$, $v/r \ll \nu$ the current for the distribution (32) can be obtained by integrating (34)

$$\frac{I^{(1)}(t)}{I_\infty} = \frac{\pi\beta\sigma a}{cl}\begin{cases} \dfrac{\pi}{16}\left(\dfrac{a}{r}\right)^2 & \text{for } r \gg a \\ 1 - \dfrac{r}{a}\left(\ln\dfrac{4a}{r} + 1\right) & \text{for } r \ll a. \end{cases} \tag{36}$$

For $v/r \gg \nu$, $r \ll c/\omega_0$ we obtain

$$\frac{I^{(1)}(t)}{I_\infty} = \frac{\omega_0^2 a^2}{4c^2 l}\begin{cases} \pi a/8r & \text{for } r \gg a \\ {}^1/_3 & \text{for } r \ll a. \end{cases} \tag{37}$$

Let us now examine the question as to the manner in which the frequency distribution of the currents in the ring will change as its velocity increases right up to ultrarelativistic values. As $\beta \to 1$ the critical frequency $\omega_{cr}^{(1)}$ increases, while $\omega_{cr}^{(2)}$ decreases. There exists a critical velocity at which these two frequencies become equal, $\beta_{cr} = \sqrt{2} - 1$; since $1/\sqrt{1-\beta^2}$ is not large at this point, the speed β_{cr} is not ultrarelativistic. In the extreme ultrarelativistic case, when not only $\omega_{cr}^{(1)}$ $\omega_{cr}^{(2)}$ but also $\omega_{cr}^{(1)} \gg \gamma\omega_{cr}^{(2)}$, $\gamma = \delta/a$, we can substitute into (27) the value of $K(\lambda)$ from (21):

$$I_\omega = I_\infty \frac{\zeta - 1}{\zeta + 1}\frac{a\delta}{2ic^2}\,\omega\, I_1\left(\frac{a|\omega|(1-\beta^2)^{1/2}}{2c}\right) \times K_1\left(\frac{a|\omega|(1-\beta^2)^{1/2}}{2c}\right) \text{ for } \omega \ll \frac{\omega_{\text{кр}}^{(1)}}{\gamma}, \tag{38}$$

$$I_\omega = I_\infty \frac{\zeta - 1}{\zeta + 1}\frac{2}{i(1-\beta^2)\omega} \text{ for } \omega \gg \frac{\omega_{\text{кр}}^{(1)}}{\gamma}. \tag{39}$$

If $\omega_{cr}^{(1)}/\gamma \ll \omega^{(0)}$, on the order of the characteristic resonance frequencies of the medium, the frequency distribution has the approximate form shown in Fig. 3, since the factor $(\zeta - 1)/(\zeta + 1)$ can be taken to be independent of the frequency, and

$$\frac{I_{\max}}{I_\infty} = \frac{\zeta - 1}{\zeta + 1}\frac{\delta}{c(1-\beta^2)^{1/2}}.$$

As β increases $\omega_{cr}^{(1)}$ also increases, i.e., successively higher harmonics are excited in the ring. Finally, at sufficiently large β the quantity $\omega_{cr}^{(1)}/\gamma$ becomes of order $\omega^{(0)}$; the frequency dependence of the factor $(\zeta - 1)/(\zeta + 1)$ becomes important, for it produces peaks in the frequency distribution at frequencies close to the characteristic frequencies of the medium.

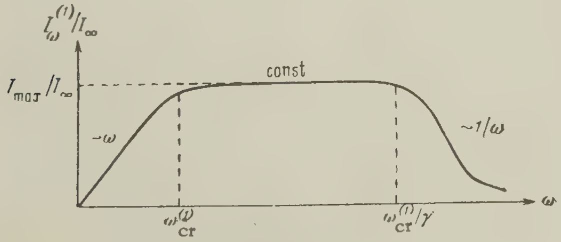

FIG. 3

In the case of plasma or of a metal the characteristic resonance frequency must be set equal to zero, since the induced electric field is a purely rotational one, and the frequency dependence of $(\zeta - 1)/(\zeta + 1)$ is therefore always important. In the following special cases the factor $(\zeta - 1)/(\zeta + 1) = S$ has the following form:

$$S = 1 \quad \text{for } \omega_{cr}^{(1)}/\gamma \ll \nu \text{ and } \omega_{cr}^{(2)}/\gamma \ll 4\pi\sigma;$$

$$S = \pi\sigma i/\omega \quad \text{for } \omega_{cr}^{(1)}/\gamma \ll \nu \text{ and } \omega_{cr}^{(1)}/\gamma \gg 4\pi\sigma;$$

$$S = 1 \quad \text{for } \omega_{cr}^{(1)}/\gamma \gg \nu \text{ and } \omega_{cr}^{(1)}/\gamma \ll \omega_0;$$

$$S = -\omega_0^2/4\omega^2 \quad \text{for } \omega_{cr}^{(1)} \gg \nu\gamma \text{ and } \omega_{cr}^{(1)} \gg \omega_0\gamma.$$

The form of the frequency distribution in these special cases may be easily found from (38) and (39).

From the frequency distributions we can obtain the expression for the current. For a number of limiting cases the analytic expressions for the dependence $I^{(1)}(t)/I_\infty$ of the current on the time are collected in the last column of the table. It is assumed here that $1/(1-\beta^2)^{1/2} \gg 1$, while ϵ is taken to be of the form: $\epsilon = 1 - \omega_0^2/(\omega^2 + i\nu\omega)$, $\sigma = \omega_0^2/4\pi\nu$.

5. THE CASE OF LOW VELOCITIES

In the case of low velocities the problem can be solved in much greater detail. Here we investigate only the case of incidence on a plasma characterized by low losses, i.e., $\epsilon = 1 - \omega_0^2/\omega^2$; $\beta \ll 1$. When these two conditions are satisfied the integral equation for the Fourier components of the current can be solved exactly, since

$$\zeta_\lambda = \{1 - [2\beta\omega_0/(\lambda - \omega)]^2\}^{1/2}; \quad \chi = (a/2v)|\lambda - \omega|$$

and therefore the kernel of the integral equation depends only on the difference $\lambda - \omega$; $K(\lambda, \omega) = K(|\lambda - \omega|)$; moreover, in the case under consideration we may also set $K(\lambda) = K(0) = L/4\pi a^2$. On multiplying (15) by $\exp\{-i\omega t\}$ and integrating with respect to t, we obtain

$$I(t) = I(r) = I_\infty/(1 - M(r)/L); \quad r = -vt, \tag{40}$$

where after integrating with respect to ω (by deforming the path of integration into the upper half-plane of complex ω) we can write for $M(r)$

Dependence of the current on the time

$c/r \ll \nu$	$r \gg c/4\pi\sigma$	$r \gg a_1$*	$(3\pi\delta/16a)(1-\beta^2)(a/r)^4$
,,	,,	$r \ll a_1$	$\delta/r\,(1-\beta^2)^{1/2}$
,,	$r \ll c/4\pi\sigma$	$r \gg a_1$	$(\delta\pi^2\sigma/8c)(1-\beta^2)(a/r)^3$
,,	,,	$r \ll a_1$	$\dfrac{\delta 2\pi\sigma}{c(1-\beta^2)^{1/2}}\left\{\ln\dfrac{4a(1-\beta^2)^{1/2}}{r}-2\right\}$
$c/r \gg \nu$	$r \gg c/\omega_0$	$r \gg a_1$	$(3\pi\sigma/16a)(1-\beta^2)(a/r)^4$
,,	,,	$r \ll a_1$	$\delta/r\,(1-\beta^2)^{1/2}$
,,	$r \ll c/\omega_0$	$r \gg a_1$	$(\delta\pi a\omega^2{}_0/32c^2)(1-\beta^2)(a/r)^2$
,,	,,	$r \ll a_1$	$\delta a\pi\omega_0{}^2/4c^2$

* $a_1 = a(1-\beta^2)^{1/2}$

$$M(r) = 4\pi^2a^2\int_0^\infty \frac{\{1+(\omega_0/kc)^2\}^{1/2}-1}{\{1+(\omega_0/kc)^2\}^{1/2}+1}J_1^2(ka)\,e^{-2kr}\,dk. \quad (41)$$

Thus, the magnetic flux linking the current circuit and produced by the medium has the form

$$\Phi_{cr} = IM/c.$$

Thus, in spite of the fact that the image current in the plasma has a different magnitude for each frequency, the magnetic flux produced by the image currents in the plasma is such as if there exists in the non superconducting plasma an image current I which is numerically equal and oppositely directed to the incident current at a given distance from the plasma (just as in the case of a superconducting wall), but the coefficient of mutual inductance is changed and depends on the frequency of plasma oscillations ω_0.

When $r \gg c/\omega_0$ the quantity M is simply the coefficient of mutual inductance of two circular currents. This coefficient can be expressed in terms of elliptic integrals whose asymptotic values are well known. When $r \ll c/\omega_0$ the coefficient M approaches the constant value

$$M = \frac{\pi a\omega_0^2 a^2}{c^2}\begin{cases}\pi a/8r, & r \gg a,\\ 4/3, & r \ll a.\end{cases} \quad (42)$$

Thus, the current in the ring does not increase indefinitely, but reaches a certain maximum. Therefore the magnetic energy which can be stored in the ring cannot exceed

$$U_{\max} = \Phi^2/2(L-M_{\max}) - \Phi^2/2L \quad (43)$$

or, since $\Phi^2 = \text{const} = L^2I_\infty^2/c^2$,

$$U_{\max} = LI_\infty^2 M_{\max}/2c^2(L-M_{\max}). \quad (44)$$

The last equation also means that the ring will not be reflected from the plasma for all energies of translational motion of the ring. This energy must be less than $U_{\max}$. In the two limiting cases $a \gg c/\omega_0$ and $a \ll c/\omega_0$ the conditions under which reflection occurs can be written in the form

$$mv^2 \leqslant \frac{|I_\infty|^2}{c^2}\,\frac{4\pi a\{\ln(4a\omega_0/c)-2\}\,l}{\ln(2c/\delta\omega_0)}, \quad a \gg \frac{c}{\omega_0}, \quad (45)$$

$$mv^2c^2/I_\infty^2 n \leqslant (16\pi/3)\,a^3r_0; \quad a \ll c/\omega_0; \quad r_0 = e^2/\mu c^2; \quad (46)$$

where m is the mass of the ring, $n = \mu\omega_0^2/4\pi e^2$, μ is the electron mass. If the density of the plasma is so great that $\delta \gg c/\omega_0$, then for any arbitrary values of r the plasma can be considered to be superconducting.

The point at which reflection occurs can be found by equating $U_{\max} = mv^2/2$. The force of repulsion between the ring and the plasma can be obtained both directly from the expression for the fields, and by differentiating V with respect to $r = -vt$

$$F_z = -\frac{I^2}{2c^2}\frac{\partial M}{\partial r} \approx \frac{I_\infty^2}{c^2}\,\frac{\pi^2a^2\omega_0^2}{16c^2}\left(\frac{a}{r}\right)^2 \text{ for } r \ll \frac{c}{\omega_0}; \quad r \gg a, \quad (47)$$

$$F_z = \frac{I_\infty^2}{2c^2}\,\frac{\pi^2a^2\omega_0^2}{c^2} \text{ for } r \ll \frac{c}{\omega_0}; \; r \ll a. \quad (48)$$

The force that stretches the ring can also be found in a similar manner:

$$F_\rho = -\frac{I^2}{2c^2}\frac{\partial M}{\partial a} = \frac{I_\infty^2}{c^2}\,\frac{\pi^2}{4}\,\frac{\omega_0^2a^2}{c^2}\,\frac{a}{r} \text{ for } r \ll \frac{c}{\omega_0}; \; r \gg a. \quad (49)$$

$$F_\rho = \frac{I_\infty^2}{c^2}\,2\pi a^2\frac{\omega_0^2}{c^2} \text{ for } r \ll \frac{c}{\omega_0}; \; r \ll a. \quad (50)$$

6. FORCES AT HIGH VELOCITIES FOR CONSTANT CURRENT

We consider here only the case of plasma with low damping, on the assumption that the current is constant.

The force repelling the ring can be obtained from (7). After integration with respect to κ we obtain

$$F_z = \frac{I_\infty}{c}\, 2\pi a \frac{\partial A^{(1)}}{\partial z}\bigg|_{\substack{z=-vt\\ \rho=a}} = \frac{(2\pi a)^2 I_\infty^2}{c^2(1-\beta^2)} \int_0^\infty \frac{\{1+\beta^2[\varepsilon(ikv/(1-\beta^2)^{1/2})-1]\}^{1/2}-1}{\{1+\beta^2[\varepsilon(ikv/(1-\beta^2)^{1/2})-1]\}^{1/2}+1}\, k \exp\left\{-\frac{2kr}{(1-\beta^2)^{1/2}}\right\} J_1^2(ka)\, dk. \tag{51}$$

When $r = -vt \gg a(1-\beta^2)^{1/2}$, if we restrict ourselves to the first term in the series expansion of a Bessel function, we obtain

$$F_z = \frac{\pi^2 a^4 I_\infty^2}{c^2}(1-\beta^2)\int_0^\infty \frac{\{1+\beta^2[\varepsilon(ikv)-1]\}^{1/2}-1}{\{1+\beta^2(\varepsilon(ikv)-1)\}^{1/2}+1}\, k^3 e^{-2kr}\, dk. \tag{52}$$

In the limiting cases we have

$$F_z = (3\pi^2 I_\infty^2/4c^2)(1-\beta^2)\, a^4/r^4 \quad \text{for } r \gg c/\omega_0, \tag{53}$$

$$F_z = (\pi^2 I_\infty^2/2c^2)\, \omega_0^2 a^2/c^2 \quad \text{for } r \ll c/\omega_0. \tag{54}$$

When $r \ll a\sqrt{1-\beta^2}$ the use of the asymptotic expansion for J_1 leads to the results given in reference 1.

From (7) we obtain the force that stretches the ring:

$$F_\rho = -\frac{2\pi a}{\rho}\frac{I_\infty}{c}\frac{\partial}{\partial\rho}(\rho A^{(1)})$$

$$= \frac{(2\pi a)^2 I_\infty^2}{c^2}(1-\beta^2)^{1/2}\int_0^\infty \frac{\{1+\beta^2(\varepsilon(ikv)-1)\}^{1/2}-1}{\{1+\beta^2(\varepsilon(ikv)-1)\}^{1/2}+1}\, k e^{-2kr}\, dk \tag{55}$$

$$\times J_0(ka(1-\beta^2)^{1/2})\, J_1(ka(1-\beta^2)^{1/2}).$$

In limiting cases we obtain the following expressions

$$F_\rho = \pi^2 a^3 I_\infty^2(1-\beta^2)/4c^2 r^2 \text{ for } r \gg a\sqrt{1-\beta^2} \text{ and } r \gg c/\omega_0, \tag{56}$$

$$F_\rho = 4\pi I_\infty^2/c^2\sqrt{1-\beta^2} \text{ for } r \ll a\sqrt{1-\beta^2} \text{ and } r \gg c/\omega_0. \tag{57}$$

I express my sincere gratitude to V. I. Veksler, M. S. Rabinovich, M. L. Levin, and L. M. Kovrizhnykh for the detailed discussion of the results of this work.

---

[1] V. N. Tsytovich, J. Exptl. Theoret. Phys. (U.S.S.R.) **34**, 1646 (1958).

[2] B. M. Bolotovskii, Usp. Fiz. Nauk **62**, 201 (1957).

[3] L. D. Landau and E. M. Lifshitz, Электродинамика сплошных сред (Electrodynamics of Continuous Media) Moscow, 1957.

[4] N. Bohr, The Passage of Atomic Particles through Matter (Russian translation), IIL, 1950 (note by editor of translation).

Translated by G. Volkoff
301

SOVIET PHYSICS JETP VOLUME 35(8), NUMBER 6 JUNE, 1959

THE SHAPIRO INTEGRAL TRANSFORMATION

CHOU KUANG-CHAO and L. G. ZASTAVENKO

Joint Institute for Nuclear Research

Submitted to JETP editor May 5, 1958

J. Exptl. Theoret. Phys. (U.S.S.R.) 35, 1417-1425 (December, 1958)

We give an integral transformation which is related to the decomposition, into irreducible representations of the proper Lorentz group, of the representation according to which the wave function of a particle with mass M and spin s transforms.

THE problem mentioned in the abstract was stated and solved in 1955 by I. S. Shapiro.[1] Unfortunately, he used a wave-function transformation law which is incorrect for $s > 0$ (the transformation law for the spin under a pure Lorentz transformation[2]), and thus the equations he obtained can be used only for spin zero.

In this paper we solve Shapiro's problem for arbitrary spin using a wave-function transformation law previously obtained;[2] the principles by which the integral transformation is obtained are the same as those used by Shapiro.

In the first two sections we state some known facts which we shall need later.[2,3] In the third and fourth sections we derive the integral transformation.

1. IRREDUCIBLE REPRESENTATIONS OF THE PROPER LORENTZ GROUP

Let

$$k = (k_1 k_2 k_3 k) \tag{1.0}$$

be the 4-momentum of a particle with mass 0, and let

$$k_0 = (00\,kk). \tag{1.0'}$$

Obviously $k = R(n)k_0$, where $R(n)$ is the rotation* which carries the third axis into the direction given by $n = k/k$; if θ and φ are the spherical angle coordinates of n, we may write

$$R(\mathbf{n}) = R_3(\varphi + \pi/2)\,R_1(\theta), \tag{1.1}$$

where $R_3(\alpha)$ is a counterclockwise rotation about the 3-axis through an angle α. Let $k' = Sk$, where S is a transformation of the Lorentz group. We shall denote the relation between $n = k/k$ and $n' = k'/k'$ by

$$\mathbf{n}' = S\mathbf{n}; \tag{1.2}$$

then $n' = S_1 n$ and $n'' = S_2 n'$ implies that $n'' = S_2 S_1 n$. Arbitrary transformation t of the Lorentz group can be written in the form

$$t = rK, \tag{1.3}$$

where $Kn_0 = n_0$ in the sense of (1.2), and r is a pure rotation such that $rn_0 = tn_0$ [again in the sense of (1.2)]. Here the choice of n_0 is arbitrary; (1.3) obviously determines r up to an arbitrary rotation about the n_0 direction. We shall choose n_0 as the unit vector along the third axis; we define r by the condition $r = R_3(\varphi_1)\,R_1(\theta)$, which means that $\varphi_2 = 0$, and then the factorization implied by (1.3) is clearly unique.

Now let $x' = Sx$. It is well known that if $H(x) = x_0 + (\sigma\cdot x)$ and $b(S)$ is the matrix corresponding to S in the 2×2 representation of the Lorentz group, then $H(x') = b(x)H(x)b^*(S)$. If we now choose $x = k_0$ [see Eq. (1.0′)] we see that in the 2×2 representation a K transformation of the type in (1.3) is represented by a matrix of the form

$$K = \begin{pmatrix} k_{11} & k_{12} \\ 0 & k_{22} \end{pmatrix}. \tag{1.4}$$

We now define the transformation $K(S, n)$ by applying (1.3) to the matrix $t = S^{-1}R(n)$ (the definition of $R(n)$ is given in (1.1)):

$$S^{-1}R(\mathbf{n}) = R(S^{-1}\mathbf{n})\,K(S,\,\mathbf{n}) \tag{1.5}$$

[the vector $S^{-1}n$ is defined in (1.2)]. Applying both sides of (1.5) to n_0, we see that in the present case $r = R(S^{-1}n)$.

Further, making use of the uniqueness of the factorization given by (1.3), we find that $K(S, n)$ has the property that

$$K(S_2,\,\mathbf{n})\,K(S_1,\,S_2^{-1}\mathbf{n}) = K(S_2S_1,\,\mathbf{n}), \tag{1.6}$$

which we shall need later.

---

*In what follows we shall always denote by R a pure rotation (or the matrix in the appropriate function space corresponding to such a rotation); L will denote a pure Lorentz transformation.

Consider the association

$$f(\mathbf{n}) \xrightarrow{S} f'(\mathbf{n}) = \alpha(S, \mathbf{n}) f(S^{-1}\mathbf{n}). \tag{1.7}$$

Let us find the properties that $\alpha(S, \mathbf{n})$ must satisfy in order that this association form a representation of the Lorentz group. We have

$$\begin{aligned} f'(\mathbf{n}) \xrightarrow{S_1} f''(\mathbf{n}) &= \alpha(S_1, \mathbf{n}) f'(S_1^{-1}\mathbf{n}) \\ &= \alpha(S_1, \mathbf{n}) \alpha(S, S_1^{-1}\mathbf{n}) f(S^{-1}S_1^{-1}\mathbf{n}). \end{aligned}$$

It is thus necessary that

$$\alpha(S_1, \mathbf{n}) \alpha(S, S_1^{-1}\mathbf{n}) = \alpha(S_1 S, \mathbf{n}). \tag{1.8}$$

It is seen from this that we may choose as $\alpha(S, \mathbf{n})$ any matrix element $[K(S, \mathbf{n})]_{22}$ to any power [see (1.4) to (1.6)]. Thus

$$\alpha = |k_{22}|^a \exp\{i \arg k_{22} \cdot b\}.$$

Now (1.4) implies that if $k' = S^{-1}k$, then $|k_{22}|^2 = |\mathbf{k}|/|\mathbf{k}'|$. Denoting the association $\mathbf{k} \rightarrow \mathbf{n} = \mathbf{k}/|\mathbf{k}|$ by

$$|\mathbf{k}| = k(\mathbf{n}), \tag{1.9}$$

we may write $|k(S, \mathbf{n})_{22}|^2 = k(\mathbf{n})/k(S^{-1}\mathbf{n})$.

Further, let us write*

$$\arg k_{22} = {}^1/_2\, \varphi(S, \mathbf{n}), \tag{1.9a}$$

so that $\alpha(S, \mathbf{n})$ becomes

$$\alpha_{m\rho}(S, \mathbf{n}) = [k(\mathbf{n}) / k(S^{-1}\mathbf{n})]^{1-i\rho/2} e^{im\varphi(S,\mathbf{n})}. \tag{1.10}$$

Equations (1.7) and (1.10) define the complete set of representations of the proper Lorentz group, with ρ taking on all complex values, while m takes on only integral and half-integral values.[3] It can be shown that all these representations are nondecomposable and that all except those for which $i\rho$ is an integer are irreducible; they are all inequivalent, except for pairs one of which has parameters ρ and m, and the other of which has parameters $-\rho$ and $-m$. It is easily shown that when ρ is real, (1.7) gives a unitary representation of the Lorentz group in the sense that for such representations one can define a scalar product

$$(f_1, f_2) \equiv \int f_1^*(\mathbf{n}) f_2(\mathbf{n})\, d\Omega(\mathbf{n}),$$

which remains invariant under (1.7), i.e., which is equal to

$$(f_1', f_2') = \int \left[\frac{k(\mathbf{n})}{k(S^{-1}\mathbf{n})}\right]^2 d\Omega(\mathbf{n})\, f_1^*(S^{-1}\mathbf{n}) f_2(S^{-1}\mathbf{n}).$$

Indeed, we note that

$$[k(\mathbf{n})]^2 d\Omega(\mathbf{n}) = [k(S^{-1}\mathbf{n})]^2 d\Omega(S^{-1}\mathbf{n}).$$

Then writing $S^{-1}\mathbf{n} = \mathbf{m}$, we obtain $(f_1' f_2') = (f_1 f_2)$. These unitary representations form the so-called first class of unitary representations of the Lorentz group.

The Lorentz group also has another set of unitary representations (the second class), but for our purposes only the first will be necessary.

2. THE TRANSFORMATION OF THE SPIN UNDER PROPER LORENTZ TRANSFORMATIONS

Let L_p (or L_p) be a pure Lorentz transformation such that

$$p = L_p p_0, \tag{2.1}$$

where $p = (\mathbf{p}, E)$, and $p_0 = (0, M)$.

Let S be any Lorentz transformation. We shall write the transformation SL_p as a product of a pure Lorentz transformation and a rotation, i.e., $SL_p = LR$. It is easily seen that here $L = L_{sp}$. One can thus consider the formula

$$SL_p = L_{sp} R(S, p) \tag{2.2}$$

to be a definition of the rotation $R(S, p)$.

It is easily shown that

$$\begin{aligned} &R\,(S_2 S_1,\ (S_2 S_1)^{-1} p) \\ &= R(S_2, S_2^{-1} p) R(S_1, (S_2 S_1)^{-1} p). \end{aligned} \tag{2.3}$$

From this one easily finds that the association

$$\Psi_{sM}(\mathbf{p}\sigma) \xrightarrow{S} \Psi'_{sM}(\mathbf{p}\sigma) = R^s(S, S^{-1}p)_{\sigma\sigma'} \Psi_{sM}(S^{-1}\mathbf{p}, \sigma') \tag{2.4}$$

---

*Let us study the angle $\varphi(S, \mathbf{n})$ in more detail.

(a) $S = R$. In this case the definition of $\varphi(s, \mathbf{n})$ in (1.9a) is equivalent to

$$R^{-1}R(\mathbf{n}) = R(R^{-1}\mathbf{n}) R_3(\varphi(R, \mathbf{n})). \tag{1.9b}$$

(b) $S = L_p$ [the definition of L_p is given in (2.1)]. Let the rotation $R(L, \mathbf{n})$ be defined (clearly not uniquely) by

$$L^{-1}\mathbf{n} = R(L, \mathbf{n})\, \mathbf{n}. \tag{1.9c}$$

Then

$$\begin{aligned} L^{-1}R(\mathbf{n}) &= R(L, \mathbf{n}) R^{-1}(L, \mathbf{n}) L^{-1}R(\mathbf{n}) \\ &= R(L, \mathbf{n}) R(\mathbf{n}) \{R^{-1}(\mathbf{n}) R^{-1}(L, \mathbf{n}) L^{-1}R(\mathbf{n})\}. \end{aligned}$$

The transformation in curly brackets does not alter the direction of the 3-axis. If we take advantage of its arbitrariness and choose the rotation $R(L_p, \mathbf{n})$ to be about the axis parallel to $\mathbf{p} \times \mathbf{n}$, the k_{22} matrix element of the transformation in the brackets will be real. (To see this we note that the expression in curly brackets is equal to $R^{-1}(L_{p_0}, \mathbf{n}_0) L_{p_0}^{-1}$. Here $\mathbf{p}_0$ is obtained from $\mathbf{p}$ by the same rotation as leads to $\mathbf{n}_0$, the unit vector in the direction of the 3-axis from $\mathbf{n}$. The proof is completed by a simple calculation involving the matrices of the 2×2 representation.) The angle $\varphi(L, \mathbf{n})$ therefore satisfies the relation

$$R(L_p, \mathbf{n}) R(\mathbf{n}) = R(R(L_p, \mathbf{n})\, \mathbf{n}) R_3(\varphi(L_p, \mathbf{n})). \tag{1.9d}$$

The angle involved in the rotation $R(L_p, \mathbf{n})$ is given in the Appendix.

(where R^s is the matrix which represents the rotation $R(S, S^{-1}p)$ in the $(2s+1)$-dimensional irreducible representation of the three-dimensional rotation group[4]) gives a representation of the Lorentz group. This is the representation according to which the wave function $\Psi_{sM}(\mathbf{p}, \sigma)$ of a particle with mass M and spin s transforms.

3. INTEGRAL TRANSFORMATION

Let us now break up the representation sM defined by (2.4) into irreducible representations ρm [see (1.7) and (1.10)].

For the representation sM we can define the invariant scalar product

$$\sum_\sigma \int \Psi^*(\mathbf{p}, \sigma)\,\Psi(\mathbf{p}, \sigma)\,d^3\mathbf{p}/E_p,$$

so that in decomposing sM we can obtain only unitary representations.* Thus the desired decomposition leads to the integral transformation

$$\Psi_{\mathbf{p}\sigma} = \sum_{m=-s}^{s} \int_0^\infty d\rho \int d\Omega(\mathbf{n})\, Y_{\rho m \mathbf{n}}(\mathbf{p}, \sigma)\, f_{\rho m \mathbf{n}}, \qquad (3.1)$$

$$f_{\rho m \mathbf{n}} = \sum_{\sigma=-s}^{s} \int \frac{d^3\mathbf{p}}{E_p}\, Y'_{\rho m \mathbf{n}}(\mathbf{p}, \sigma)\, \Psi_{\mathbf{p}\sigma}. \qquad (3.1a)$$

The kernels $Y_{\rho m \mathbf{n}}(\mathbf{p}, \sigma)$ and Y' must satisfy the following condition. If $\Psi_{\mathbf{p}\sigma} \rightleftarrows f_{\rho m \mathbf{n}}$ according to (3.1) and (3.1a), and if $\Psi_{\mathbf{p}\sigma} \xrightarrow{S} \Psi'_{\mathbf{p}\sigma}$ according to (2.4) and $f_{\rho m \mathbf{n}} \xrightarrow{S} f'_{\rho m \mathbf{n}}$ according to (1.7), then $\Psi'_{\mathbf{p}\sigma} \rightleftarrows f'_{\rho m \mathbf{n}}$ according to (3.1) and (3.1a), for all S. We may write this as the following condition on $Y_{\rho m \mathbf{n}}(\mathbf{p}, \sigma)$:

$$\begin{aligned} &R^s(S, S^{-1}p)_{\sigma\sigma'} Y_{\rho m S^{-1}\mathbf{n}}(S^{-1}\mathbf{p}, \sigma') \\ &= [k(\mathbf{n})/k(S^{-1}\mathbf{n})]^{-1-i\rho/2} e^{im\varphi(S, \mathbf{n})} Y_{\rho m \mathbf{n}}(\mathbf{p}, \sigma). \end{aligned} \qquad (3.2)$$

The inverse kernel $Y'_{\rho m \mathbf{n}}(\mathbf{p}, \sigma)$ satisfies a similar condition if we write

$$Y'_{\rho m \mathbf{n}}(\mathbf{p}, \sigma) = C_{m\rho} \overline{Y}_{\rho m \mathbf{n}}(\mathbf{p}, \sigma),$$

and if (3.2) is satisfied.

Let us first set $\mathbf{p} = 0$ and $S = R$ in (3.2). Then $R^s(S, S^{-1}p) = R^s(R)$ is simply the matrix corresponding to the rotation R. In this case (3.2) gives

$$R^s(R)_{\sigma\sigma'} Y_{\rho m R^{-1}\mathbf{n}}(0, \sigma') = e^{im\varphi(R, \mathbf{n})} Y_{\rho m \mathbf{n}}(0, \sigma).$$

Comparing this with (1.9b) and recalling that $R_3(\varphi)_{\sigma\sigma'} = e^{-i\sigma\varphi}\delta_{\sigma\sigma'}$, we find that

$$Y_{\rho m \mathbf{n}}(0, \sigma) = R^s(\mathbf{n})_{\sigma m}. \qquad (3.3)$$

Further, let us set $S = L_p$ in (3.2). Then

$$R(S, S^{-1}p)_{\sigma\sigma'} = \delta_{\sigma\sigma'},\quad k(\mathbf{n})/k(S^{-1}\mathbf{n}) = M/(E_p - \mathbf{p}\cdot\mathbf{n}),$$

and we obtain

$$Y_{\rho m \mathbf{n}}(\mathbf{p}, \sigma) = \left(\frac{E_p - \mathbf{p}\cdot\mathbf{n}}{M}\right)^{-1-i\rho/2} e^{-im\varphi(L_p, \mathbf{n})} Y_{\rho m L_p^{-1}\mathbf{n}}(0, \sigma). \qquad (3.4)$$

Noting that in (1.9c) $R(L_p, \mathbf{n})\mathbf{n} = L_p^{-1}\mathbf{n}$, we can rewrite (3.4), using (3.3), in the form

$$Y_{\rho m \mathbf{n}}(\mathbf{p}\sigma) = \left(\frac{E_p - \mathbf{p}\cdot\mathbf{n}}{M}\right)^{-1-i\rho/2} R^s_{\sigma\sigma'}(L_p, \mathbf{n})\, R_{\sigma' m}(\mathbf{n}). \qquad (3.5)$$

Let us now prove that the Y kernel as defined by (3.4) satisfies (3.2). We do this by inserting (3.4) into (3.2). The left side then becomes

$$\begin{aligned} &R(S, S^{-1}p)_{\sigma\sigma'} R_{\sigma' m}(L^{-1}_{S^{-1}p}, S^{-1}\mathbf{n}) \exp\{-im\varphi(L_{S^{-1}p}, S^{-1}\mathbf{n})\} \\ &\quad \times \{k(S^{-1}\mathbf{n})/k(L^{-1}_{S^{-1}p}, S^{-1}\mathbf{n})\}^{1+i\rho/2}, \end{aligned}$$

while the right side becomes

$$\begin{aligned} &\exp\{im\varphi(S, \mathbf{n})\}\, [k(\mathbf{n})/k(S^{-1}\mathbf{n})]^{-1-i\rho/2} [k(\mathbf{n})/k(L_p^{-1}\mathbf{n})]^{1+i\rho/2} \\ &\quad \times \exp\{-im\varphi(L_p, \mathbf{n})\}\, R(L_p^{-1}\mathbf{n})_{\sigma m} \end{aligned}$$

According to (2.2), $SL_{S^{-1}p} = L\ R(S, S^{-1}p)$. Therefore

$$k(L^{-1}_{S^{-1}p} S^{-1}\mathbf{n}) = k[R^{-1}(S, S^{-1}p)\, L_p^{-1}\mathbf{n}] = k(L_p^{-1}\mathbf{n}),$$

since a rotation does not change the magnitude k. Thus the factors k on both sides cancel. Further,

$$\begin{aligned} &R(S, S^{-1}p)_{\sigma\sigma'} R(L^{-1}_{S^{-1}p} S^{-1}\mathbf{n})_{\sigma' m} \\ &= R(S, S^{-1}p)_{\sigma\sigma'} R[R^{-1}(S, S^{-1}p)\, L_p^{-1}\mathbf{n}]_{\sigma' m} = R(L_p^{-1}\mathbf{n})_{\sigma m} \\ &\quad \times \exp\{-im\varphi[R^{-1}(S, S^{-1}p),\ R^{-1}(S, S^{-1}p)\, L_p^{-1}\mathbf{n}]\}. \end{aligned}$$

Thus the rotations on the right and left are also equal; we are left with the angles φ. We use (2.2) to write the last angle obtained in the form

$$\varphi[R^{-1}(S, S^{-1}p),\ L^{-1}_{S^{-1}p} S^{-1}\mathbf{n}].$$

To this we must add $\varphi(L_{S^{-1}p}, S^{-1}\mathbf{n})$; according to (1.8) and (2.2), their sum is

$$\varphi[L_{S^{-1}p} R^{-1}(S, S^{-1}p),\ S^{-1}\mathbf{n}] = \varphi[S^{-1}L_p,\ S^{-1}\mathbf{n}].$$

Taking the angle $\varphi(S, \mathbf{n})$ from the right to the left and adding it here, we obtain $\varphi(L_p, \mathbf{n})$; the same angle remains on the right. This completes the proof.

4. CALCULATION OF $C_{m\rho}$

We have thus arrived at the mutually reciprocal integral equations

$$\begin{aligned} \Psi_{sM}(\mathbf{p}, \sigma) = \sum_m \int d\rho\, d\Omega(\mathbf{n})\, &[(E_p - \mathbf{p}\cdot\mathbf{n})/M]^{-1-i\rho/2} \\ &\times R_{\sigma\sigma'}(L_p, \mathbf{n})\, R_{\sigma' m}(\mathbf{n})\, f_{\rho m}(\mathbf{n}); \end{aligned} \qquad (4.1)$$

---

*In fact, only representations of the first class.[1]

$$f_{\rho m}(\mathbf{n}) = C_{m\rho} \sum_{\sigma} \int \frac{d^3\mathbf{p}}{E_p} [(E_p - \mathbf{p}\mathbf{n})/M]^{-1+i\rho/2} \times \bar{R}_{\sigma\sigma'}(L_{\mathbf{p}}, \mathbf{n}) \bar{R}_{\sigma' m}(\mathbf{n}) \Psi_{sM}(\mathbf{p}\sigma) \quad (4.2)$$

[see Eqs. (3.1) to (3.5)].

To find the still undetermined factor $C_{m\rho}$, let us rewrite (4.1) and (4.2) in the form

$$\delta(\rho-\rho')\delta(\mathbf{n}-\mathbf{n}')\delta_{mm'} = C_{m\rho} \int \frac{d^3\mathbf{p}}{E_p} [(E_p - \mathbf{p}\cdot\mathbf{n})/M]^{-1+i\rho/2} \times [(E_p - \mathbf{p}\cdot\mathbf{n}')/M]^{-1-i\rho'/2} \times \bar{R}_{\sigma\sigma'}(L_p, \mathbf{n}) \bar{R}_{\sigma' m}(\mathbf{n}) R_{\sigma\sigma''}(L_p, \mathbf{n}') R_{\sigma'' m'}(\mathbf{n}'). \quad (4.3)$$

We now multiply both sides of (4.3) by $\bar{R}_{am'}(\mathbf{n}')$, sum over m', integrate over $d\Omega(\mathbf{n}')$, and choose $\mathbf{n} = \mathbf{n}_0$ along the 3-axis. We thus obtain

$$\delta(\rho-\rho')\delta_{ma} = C_{m\rho} \int \frac{d^3\mathbf{p}}{E_p} [(E_p - \mathbf{p}\cdot\mathbf{n}_0)/M]^{-1+i\rho/2} \times [(E_p - \mathbf{p}\cdot\mathbf{n}')/M]^{-1-i\rho'/2} \bar{R}_{\sigma m}(L_p, \mathbf{n}_0) R_{\sigma a}(L_p, \mathbf{n}') d\Omega(\mathbf{n}').$$

In this expression we write $R(L_{\mathbf{p}}, \mathbf{n}') = R(\mathbf{p}/p) \times R(L_{\mathbf{p}_0}, \mathbf{n}'') R^{-1}(\mathbf{p}/p)$. Here $\mathbf{p}_0$ is directed along the 3-axis, and $\mathbf{n}''$ is obtained from $\mathbf{n}'$ by the same transformation which carries $\mathbf{p}$ into $\mathbf{p}_0$. Since $\mathbf{p}\cdot\mathbf{n}' = \mathbf{p}_0\cdot\mathbf{n}''$ and $d\Omega(\mathbf{n}') = d\Omega(\mathbf{n}'')$, we have

$$\delta(\rho-\rho')\delta_{ma} = C_{m\rho} \int \frac{d^3\mathbf{p}}{E_p} [(E_p - \mathbf{p}\cdot\mathbf{n}_0)/M]^{-1+i\rho/2} \times [(E_p - \mathbf{p}_0\cdot\mathbf{n}'')/M]^{-1-i\rho'/2} \times \bar{R}_{\sigma m}(L_p, \mathbf{n}_0) R_{\sigma\alpha}(\mathbf{p}/p) \bar{R}_{\varkappa\beta}(\mathbf{p}/p) R_{\varkappa\beta}(L_{\mathbf{p}_0}\mathbf{n}'') d\Omega(\mathbf{n}'').$$

We shall first perform the integration over the azimuth angles, writing

$$d\Omega(\mathbf{p}) = \sin\theta\, d\theta\, d\varphi, \quad d\Omega(\mathbf{n}'') = \sin\theta''\, d\theta''\, d\varphi''.$$

According to (1.1), $R(\mathbf{p}/p) = R_3(\varphi + \pi/2) R_1(\theta)$. According to Appendix A

$$R(L_{\mathbf{p}}, \mathbf{n}_0) = R_3(\varphi - \pi/2) R_1(\alpha(p, t)) R_3^{-1}(\varphi - \pi/2),$$

$$R(L_{\mathbf{p}_0}\mathbf{n}'') = R_3(\varphi'' + \pi/2) R_1(\alpha(p, t'')) R_3^{-1}(\varphi'' + \pi/2).$$

Here $t = \mathbf{p}\cdot\mathbf{n}/p = \cos\theta$ and $t'' = \mathbf{p}\cdot\mathbf{n}''/p = \cos\theta''$, while the angle $\alpha(p, t)$ is defined [see Eqs. (A.2) to (A.4)]. Since $R_3(\varphi)_{nm} = \delta_{nm} \exp\{-in\varphi\}$,

$$\frac{1}{(2\pi)^2}\delta(\rho-\rho')\delta_{ma} = C_{m\rho} \times \int_0^\infty \frac{p^2dp}{E_p} \int_{-1}^{1} dt \int_{-1}^{1} dt'' [(E_p - pt)/M]^{-1+i\rho/2} \times [(E_p - pt'')/M]^{-1-i\rho'/2} (-1)^{m-\sigma} \sum_{\alpha,\sigma} \bar{u}^s_{\sigma m}(\alpha(p, t)) \times u^s_{\alpha\alpha}(\alpha(p, t'')) u^s_{\sigma\alpha}(\theta) \bar{u}^s_{a\alpha}(\theta) \delta_{am};$$

here the $u^s_{mn}(x)$ are functions defined by Gel'fand and Shapiro.[4] By making use of the properties of these functions,* this equation is easily transformed to the form

$$(1/2\pi)^2\delta(\rho-\rho') = C_{m\rho} \int_0^\infty \frac{p^2dp}{E_p} \int_{-1}^{1} dt \int_{-1}^{1} dt'' [(E_p - pt)/M]^{-1+i\rho/2} \times [(E_p - pt'')/M]^{-1-i\rho'/2} \times \sum_\alpha u^s_{m\alpha}[\alpha(p, t) + \theta] u^s_{\alpha\alpha}(\alpha(p, t'')) \bar{u}^s_{m\alpha}(\theta), \quad (4.4)$$

or

$$(2\pi)^{-2}\delta(\rho-\rho') = C_{m\rho} \int_0^\infty \frac{p^2dp}{E_p} \sum_\alpha F_{\alpha\rho' s}(p) f_{m\alpha\rho s}(p),$$

where

$$F_{\alpha\rho' s}(p) = \int_{-1}^{1} [(E_p - pt'')/M]^{-1-i\rho'/2} u^s_{\alpha\alpha}(\alpha(p, t''))\, dt'';$$

$$f_{m\alpha\rho s}(p) = \int_{-1}^{1} [(E_p - pt)/M]^{-1+i\rho/2} u^s_{m\alpha}[\alpha(pt) + \theta] \bar{u}^s_{m\alpha}(\theta)\, dt.$$

We now calculate $F_{\alpha\rho s}(p)$. We do this by using the power series

$$u^s_{\alpha\alpha}(\alpha) = \sum_q a^q_{s\alpha} x^q,$$

where $x = 1 + \cos\alpha$, and

$$a^q_{s\alpha} = \frac{(-)^{s-q}(s+q)!}{2^q (q-\alpha)!(q+\alpha)!(s-q)!}.$$

The calculation gives

$$F_{\alpha\rho s}(p) = \frac{1}{p}\left\{\sum_q a^q_{s\alpha} 2^{q+1} \frac{q\cos(\lambda\rho/2) + (\rho/2)\sin(\lambda\rho/2)}{q^2 + (\rho/2)^2} + Q_{\alpha\rho s}(p)\right\}. \quad (4.6)$$

Here $\cosh\lambda = E_p/M$, and $Q_{\alpha\rho s}(p)$ can be represented in the form $A(p, \rho)\cos(\lambda\rho/2) + B(p, \rho)\sin(\lambda\rho/2)$, where A and B are functions bounded for all $p > 0$ and approaching zero as $p \to \infty$ as $1/p$ uniformly in ρ.

We now evaluate $f_{m\alpha\rho s}(p)$. To do this we make use of the series

$$u^s_{m\alpha}(\theta) = (1+x)^{|(m+\alpha)/2|}(1-x)^{|(m-\alpha)/2|} \times \sum_0^{n_{\max}}{}' A_n(1+x)^n, \qquad x = \cos\theta.$$

Using (A.5) and (A.6), we find that for $|m \pm \alpha| \neq 0$

$$* \quad u^s_{mn}(\theta) = (-1)^{s-m} i^{n-m} [2^s(s-m)!]^{-1} \times [(s+n)!(s-m)!/(s-n)!(s+m)!]^{1/2} (1-x)^{(m-n)/2} \times (1+x)^{-(m+n)/2} (d/dx)^{s-n} (1-x)^{s-m} (1+x)^{s+m}, \quad x = \cos\theta;$$

$$u^s_{mn}(\theta) = u^s_{nm}(\theta) = u^s_{-n-m}(\theta);$$

$$\sum_\alpha u^s_{m\alpha}(\theta_1) u^s_{\alpha n}(\theta_2) = u^s_{mn}(\theta_1 + \theta_2).$$

$$|f_{m\alpha\rho s}(p)| < \text{const}/p^{1+a}, \tag{4.7}$$

where a is the smaller of $|m \pm \alpha|$. We rewrite the sum in (4.4) in the form

$$\sum_{\alpha} u^{s}_{m\alpha}[\alpha(p,t)+\theta]\,\bar{u}^{s}_{m\alpha}(\theta)\,u^{s}_{\alpha\alpha}(\alpha')$$

$$=\sum_{\alpha} u^{s}_{m\alpha}[\alpha(pt)+\theta]\,\bar{u}^{s}_{m\alpha}(\theta)\,u^{s}_{mm}(\alpha')$$

$$-\sum_{\alpha\mp m} u^{s}_{m\alpha}(\alpha+\theta)\,\bar{u}^{s}_{m\alpha}(\theta)\,[u^{s}_{\alpha\alpha}(\alpha')-u^{s}_{mm}(\alpha')].$$

Because $u_{mm} = u_{-m-m}$, we see that $\alpha = -m$ does not enter into the last sum. Using the summation theorem for the u_{mm} functions, we can write (4.4) in the form

$$\delta(\rho-\rho') = (2\pi)^2 C_{m\rho}\int_0^\infty \frac{p^2dp}{E_p}\Big\{F_{m\rho' s}(p)\,F_{m-\rho s}(p)$$

$$+\sum_{|\alpha|\neq|m|} f_{m\alpha\rho s}(p)\,[F_{\alpha\rho' s}(p)-F_{m\rho' s}(p)]\Big\}. \tag{4.8}$$

It follows from (4.6) and (4.7) that only the product of the principal parts of $F_{m\rho s}$ and $F_{m-\rho s}$ contributes to the δ-function. All the other parts of the integral in (4.8) can only give a finite contribution (which must cancel in the sum). Thus

$$\delta(\rho-\rho') \sim (2\pi)^2 C_{m\rho}\int_0^\infty d\lambda \sum_q \frac{q\cos(\lambda\rho/2)+(\rho/2)\sin(\lambda\rho/2)}{q^2+(\rho/2)^2}$$

$$\times\sum_{q'}\frac{q'\cos(\lambda\rho'/2)+(\rho'/2)\sin(\lambda\rho'/2)}{(q')^2+(\rho'/2)^2}\,2^{q+q'+2}a^{q}_{sm}a^{q'}_{sm}.$$

Since

$$\frac{1}{\pi}\int_0^\infty \cos(\lambda\rho/2)\cos(\lambda\rho'/2)\,d\lambda$$

$$=\frac{1}{\pi}\int_0^\infty \sin(\lambda\rho/2)\sin(\lambda\rho'/2)\,d\lambda = \delta(\rho-\rho')$$

and

$$\int_0^\infty \cos(\lambda\rho/2)\sin(\lambda\rho'/2)\,d\lambda \approx 0,$$

we arrive at

$$\frac{1}{C_{m\rho}} = 16\pi^3\sum_{qq'}\frac{[qq'+(\rho/2)^2]\,a^{q}_{sm}a^{q'}_{sm}2^{q+q'}}{[q^2+(\rho/2)^2]\,[(q')^2+(\rho/2)^2]}.$$

It follows from this that (see Appendix B)

$$C_{m\rho} = \frac{\rho^2+(2m)^2}{(4\pi)^3}. \tag{4.9}$$

5. CONCLUSION

Thus our final result is that if a relation of the form (4.1) exists, the inverse relation is given by (4.2) with $C_{m\rho}$ given by (4.9). In these equations $E_p = (M^2 + p^2)^{1/2}$, the rotation R(n) is defined by (1.1), and $R(L_p, \mathbf{n})$ is defined by (1.9c) and by specifying the direction of its axis perpendicular to both **p** and **n**. By R^{s}_{ab} we denote the matrix elements of the (2s + 1)-dimensional irreducible representation of the three-dimensional rotation group which correspond to the rotation R^4

Equation (4.1) gives the expansion of the wave function $\Psi_{sM}(\mathbf{p}, \sigma)$, transforming like a wave function of a particle with spin s and mass M according to the s, M representation [see (2.4)] in terms of the functions $f_{\rho m}(\mathbf{n})$, transforming according to the irreducible representations of the proper Lorentz group. Equation (4.2) gives these irreducible components of $\Psi_{sM}(\mathbf{p}, \sigma)$ in terms of the function itself.

The authors express their gratitude to Professor M. A. Markov for his interest in the work.

APPENDIX A

Let $\boldsymbol{\alpha}$ be the vector of the rotation $R(L_p, \mathbf{n})$, so that

$$R(L_p,\mathbf{n})\,\mathbf{n} = \cos\boldsymbol{\alpha}\cdot\mathbf{n} + [\boldsymbol{\alpha}\times\mathbf{n}]\sin\alpha/\boldsymbol{\alpha} + \boldsymbol{\alpha}(\boldsymbol{\alpha}\cdot\mathbf{n})(1-\cos\alpha)/\alpha^2.$$

From the conditions

$$L_p^{-1}\mathbf{n} = R(L_p,\mathbf{n})\,\mathbf{n} \quad\text{and}\quad \boldsymbol{\alpha}\sim[\mathbf{p}\times\mathbf{n}], \tag{A.1}$$

which determine $R(L_p, \mathbf{n})$, and from the formula

$$L_p^{-1}\mathbf{n} = [\mathbf{n}M + \mathbf{p}(\mathbf{p}\cdot\mathbf{n})/(E_p+M) - \mathbf{p}]\,[E_p-(\mathbf{p}\cdot\mathbf{n})]^{-1},$$

which is implied by (1.2) and (2.1), we easily arrive at

$$\frac{\boldsymbol{\alpha}}{\alpha}\sin\alpha = \frac{[\mathbf{p}\times\mathbf{n}]}{E_p+M}\left[1+\frac{M}{E_p-(\mathbf{p}\cdot\mathbf{n})}\right]. \tag{A.2}$$

This leads to

$$1+\cos\alpha = \frac{(E_p-\mathbf{p}\cdot\mathbf{n}+M)^2}{(E_p+M)(E_p-\mathbf{p}\cdot\mathbf{n})}, \tag{A.3}$$

$$1-\cos\alpha = \frac{p^2-(\mathbf{p}\cdot\mathbf{n})^2}{(E_p+M)(E_p-\mathbf{p}\cdot\mathbf{n})}. \tag{A.4}$$

It is now easily shown that

$$1+\cos(\alpha+\theta) = (E_p-p)(1+t)/(E-pt), \tag{A.5}$$

$$1-\cos(\alpha+\theta) = (E_p+p)(1-t)/(E-pt), \tag{A.6}$$

where $t = \cos\theta = \mathbf{p}\cdot\mathbf{n}/p$.

APPENDIX B

We shall here prove (4.9). We have

$$\sum_{qq'} a^{q}a^{q'}2^{q+q'}\frac{qq'+(\rho/2)^2}{[q^2+(\rho/2)^2]\,[q'^2+(\rho/2)^2]} = 2\sum_q \frac{q2^{q}a^{q}}{q^2+(\rho/2)^2}\sum_{q'}\frac{2^{q'}a^{q'}}{q+q'}.$$

Comparing the equation $A_q \equiv \sum_{q'} 2^{q'}a^{q'}/(q+q')$

with $u^s_{mm} = \sum_{q'} a_{q'} x^{q'}$, we see that

$$A_q = \frac{1}{2^q} \int_0^2 dx u^s_{mm} x^{q-1}$$

$$= \frac{(-)^{s-m}}{2^{s+q}(s-m)!} \int_0^2 x^{q-m-1} dx \, (d/dx)^{s-m} (2-x)^{s-m} x^{s+m}.$$

When $q > m$, integration by parts shows simply that $A_q = 0$. When $q = m$, we easily obtain

$$A_m = (-)^{s-m} \frac{(s-m)!\,(2m-1)!}{(s+m)!} = \frac{1}{2ma^m_{sm} 2^m}.$$

Thus

$$\sum_{q,q'} = \frac{1}{m^2 + (\rho/2)^2}.$$

[1] I. S. Shapiro, Dissertation, Moscow State University (1955); Dokl. Akad. Nauk SSSR **106**, 647 (1956), Soviet Phys. "Doklady" **1**, 91 (1956).

[2] M. I. Shirokov and Chou Kuang-Chao, J. Exptl. Theoret. Phys. (U.S.S.R.) **34**, 1230 (1958), Soviet Phys. JETP **7**, 851 (1958); Iu. M. Shirokov, J. Exptl. Theoret. Phys. (U.S.S.R.) **34**, 717 (1958), Soviet Phys. JETP **7**, 493 (1958); E. P. Wigner, Revs. Modern Phys. **29**, 255 (1957).

[3] M. A. Naimark, Usp. Mat. Nauk **9**, 19 (1954).

[4] I. M. Gel'fand and Z. Ia. Shapiro, Usp. Mat. Nauk **7**, 3 (1952).

Translated by E. J. Saletan
302

SOVIET PHYSICS JETP VOLUME 35(8), NUMBER 6 JUNE, 1959

A MODEL FOR THE PROCESS OF MULTIPLE PRODUCTION

G. I. KOPYLOV

Joint Institute for Nuclear Research

Submitted to JETP editor June 13, 1958

J. Exptl. Theoret. Phys. (U.S.S.R.) 35, 1426-1434 (December, 1958)

We discuss the idea of constructing a "table of random stars" which could reproduce, in a form suitable for comparison with experiment, theoretical concepts concerning the multiple production of elementary particles. It is shown possible to construct such a table for energies up to 10 Bev.

Most papers on the theory of multiple particle production are devoted to the solution of two problems. The first is the determination of the statistical weights of the various different reactions, and the second is the determination of the momentum distributions. Ordinarily one does not discuss the question of angular correlations or of other correlations between the directions and velocities of the secondary particles. Yet the solution of this question would allow one to reach more definite conclusions on the applicability of the theory to the process of multiple production. Indeed, correlations between the directions of the particles must depend on the nature of the interaction between the particles at the time they are produced. Thus in Fermi's original statistical model of independent secondary particles, the correlations should depend only on restrictions due to the conservation laws, while according to the presently accepted ideas of a resonance interaction between the nucleon and meson, the correlation should be stronger.

A qualitative estimate of the "forward-backward" correlation was already given by Fermi[1] from considerations of angular-momentum conservation. The difficulty in obtaining quantitative results lies in the very complicated calculations necessary. But even if these calculations could be carried out with very simple assumptions, the complication in the form of the interaction matrix (the natural way to proceed with the theory) would present new difficulties. In view of these conditions, an obvious way out would be to establish a model for multiple particle production. But since our ideas as to the mechanism for multiple production are still too cloudy for us to find among large-scale processes one with the appropriate regularities, we may make use of a numerical model. Such a model should be capable of reproducing a large class of physical assumptions on the form of the interaction.

M. I. Podgoretskii and M. Ia. Danysh (in a private communication) have suggested the idea for such a model in the form of a "table of random stars" for the isobaric model. The essence of their proposal is to construct a table of random variables which satisfy the same laws as the momenta of the secondary particles as predicted by the isobaric model. The table of random stars should contain a series of entries each of which represents one case of particle production, i.e., contains the magnitudes and directions of the individual secondary-particle momenta. The statistical analysis of such a table will give the same kind of information on the multiple-production process (statistical weights, momentum distributions, angles, charges, etc.) as will the analysis of actual stars in photographic emulsions or chambers.

The distributions or correlations which one is able to obtain from stars, say, in a hydrogen chamber, can be duplicated on the corresponding table. A shortcoming of the method is the low accuracy obtained from a small table, the large amount of calculation necessary to construct and analyze the table, and the impossibility of obtaining analytic expressions for the results.

It is shown in the present work how this idea can be realized using an electronic computer. It is possible, however, to construct a table containing 100 or 200 lines with some simplifying assumptions for five or six secondary particles by our method without resort to machines.

Our method takes into account energy and momentum conservation in the reaction. It can be generalized to a relatively wide class of concepts concerning the interaction of particles in multiple production. For this reason we are able to answer affirmatively the question of whether it is possible to construct a model for multiple production more accurately than it is possible to test numerically any particular physical model for multiple production.

1. TABLE OF THREE-PARTICLE REACTIONS

Consider the reaction of two particles with total energy E and zero momentum, resulting in the production of three particles with masses m_i, momenta $\mathbf{p}_i$, and total energy e_i (with $i = 1, 2, 3$). According to Fermi's theory, the probability for this reaction is proportional to

$$W(E) = \int d^3\mathbf{p}_1 d^3\mathbf{p}_2 d^3\mathbf{p}_3 \delta\Big(\sum_1^3 e_i - E\Big)\delta\Big(\sum_1^3 \mathbf{p}_i\Big). \quad (1.1)$$

The product of δ-functions represents the momentum distribution density in nine-dimensional momentum space, and the entire problem of constructing a model lies just in achieving such a distribution. But the narrow bands along the intersections of the $\Sigma e_i - E = 0$ and $\Sigma \mathbf{p}_i = 0$ surfaces of the nine-dimensional rectangle have too small a volume for the randomly chosen points with coordinates $\mathbf{p}_i$ to fall sufficiently often into these bands. On the other hand the integral

$$W(E) = 8\pi^2 \int_{D_3} p_1 p_2 (E - e_1 - e_2)\, dp_1 dp_2, \quad (1.2)$$

obtained from (1.1) by simple operations, can be used to achieve the necessary momentum distribution. In this integral the region of integration D_3 (Fig. 1) is bounded by the curves $\cos\theta = \pm 1$ (where θ is the angle between $\mathbf{p}_1$ and $\mathbf{p}_2$). The equations of these curves are

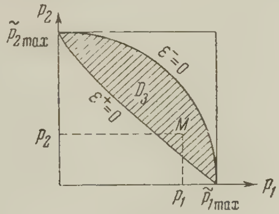

FIG. 1

$$\varepsilon^+ = 0, \ \varepsilon^- = 0, \quad (1.3)$$

where

$$\varepsilon^\pm = e_1 + e_2 + [(p_1 \pm p_2)^2 + m_3^2]^{1/2} - E. \quad (1.4)$$

It follows from (1.2) that the joint probability that the momentum p_1 lies in the interval dp_1 and p_2 lies in the interval dp_2 is distributed with a density (which is thus also the density of points $M(p_1, p_2)$ in D_3) proportional to the function

$$w(p_1, p_2) = p_1 p_2 (E - e_1 - e_2). \quad (1.5)$$

According to (1.5) the points M are not uniformly distributed in D_3. There are two ways of obtaining random variables α distributed in (a, b) with density $f(\alpha)$. These are (a) the rejection method and (b) the "direct" method.[2] The two-dimensional distribution of (1.5) is conveniently obtained by the "rejection method". To do this one must know the maximum of $W(p_1, p_2)$ on D_3. It is easily shown that the values of $p_{1,2}$, which we shall call $\bar{p}_{1,2}$, for which this maximum is attained are the roots of the set of equations

$$p_1^2 / e_1 = p_2^2 / e_2 = E - e_1 - e_2, \quad (1.6)$$

if they lie within D_3. If they do not, then $\bar{p}_{1,2}$ lie on the boundary of D_3 (the curve $\epsilon^- = 0$) and satisfy the set of equations

$$\frac{p_2[E - e_1 - e_2 - (p_1^2/e_1)]}{p_1[E - e_1 - e_2 - (p_2^2/e_2)]} = \frac{p_2 - (E - e_2)(p_1/e_1)}{p_1 - (E - e_1)(p_2/e_2)}, \ \varepsilon^- = 0. \quad (1.7)$$

For high values of the energy E, it is (1.6) which must be solved, while for low ones, it is (1.7).

A pair of numbers p_1, p_2 determines the momenta of all three particles in magnitude and direction. Therefore the procedure for obtaining a single entry in the table of three-particle stars corresponding to Fermi's model is the following.

1. The random variables p_1 and p_2 are picked uniformly in the intervals $(0, \tilde{p}_{1max})$ and $(0, \tilde{p}_{2max})$.* Here

$$\tilde{p}_{1max} = \{[E^2 - (m_1 + m_2 + m_3)^2] \times [E^2 - (m_1 - m_2 - m_3)^2]\}^{1/2} / 2E, \quad (1.8)$$

with a similar expression for $\tilde{p}_{2max}$.

2. One must check that (p_1, p_2) is a point in D_3. The easiest way to do this is to verify that

$$\varepsilon^- < 0, \ \varepsilon^+ > 0. \quad (1.9)$$

If these inequalities are fulfilled, one can always find an angle θ between $\mathbf{p}_1$ and $\mathbf{p}_2$ such that

$$e_1 + e_2 + [(\mathbf{p}_1 + \mathbf{p}_2)^2 + m_3^2]^{1/2} = E. \quad (1.10)$$

If (1.10) is not fulfilled, however, (p_1, p_2) is rejected and a new pair is picked.

3. The random variable β is picked uniformly in the interval $(0, w_{max} \equiv w(\bar{p}_1, \bar{p}_2))$ and the inequality

$$\beta \leqslant w(p_1, p_2); \quad (1.11)$$

is checked. If this inequality is not fulfilled, the (p_1, p_2) pair is rejected.

4. If (1.11) is fulfilled, (1.10) is used to calculate

$$\cos\vartheta = (p_3^2 - p_1^2 - p_2^2) / 2p_1 p_2. \quad (1.12)$$

The momenta of the three particles can now be taken as

---

*The terminology is explained elsewhere.[2,3]

$$\mathbf{p}_1 = \{p_1 \cos\psi,\ -p_1 \sin\psi,\ 0\},$$
$$p_2 = \{p_2 \cos(\vartheta-\psi),\ p_2 \sin(\vartheta-\psi),\ 0\}, \qquad (1.13)$$
$$\mathbf{p}_3 = -\mathbf{p}_1 - \mathbf{p}_2,$$

where ψ is a random angle uniformly distributed in $(0, 2\pi)$.

A table in which each line is calculated from (1.13) will be a table of plane stars. This means that in analyzing an experiment one must reduce all the three-particle stars to a single plane before comparing the experimental and the tabulated statistics. To obtain a table of three-particle stars not restricted to a single plane, what is necessary, obviously, is to allow the end point of the unit normal to the $(\mathbf{p}_1, \mathbf{p}_2, \mathbf{p}_3)$ plane to be uniformly distributed over the unit sphere.

In the next section we give a method for transforming plane stars to stars uniformly distributed in three-space. We also evaluate in this section the efficiency with which our method yields stars.

2. TABLE OF REACTIONS WITH n SECONDARY PARTICLES

General case. Consider the case in which n secondary particles are formed in the interaction, the square of the interaction matrix element $F(\mathbf{p}_1, \ldots, \mathbf{p}_n)$ being a function which remains bounded everywhere. This function F can also depend on the energy E and on the parameters of the initial particles, but in our discussion such dependence is of no import. The momentum part of the expression for the statistical weight is of the form

$$W(E, \mathbf{P}) = \int d^3\mathbf{p}_1 \ldots d^3\mathbf{p}_n F(\mathbf{p}_1, \ldots, \mathbf{p}_n)\, \delta \times \Big(\sum_1^n e_i - E\Big)\, \delta\Big(\sum_1^n \mathbf{p}_i - \mathbf{P}\Big), \qquad (2.1)$$

where $\mathbf{P}$ is the total momentum of the system. The region of integration over the first $(k-1)$ momenta will be denoted by D_k, and the other momenta $\mathbf{p}_k, \ldots, \mathbf{p}_n$ are not restricted in any way except in so far as they are involved in the conservation laws. Let us denote by d_k the region of integration over $\mathbf{p}_k$ for fixed $\mathbf{p}_1, \ldots, \mathbf{p}_{k-1}$ and arbitrary (except for the conservation laws) $\mathbf{p}_{k+1}, \ldots, \mathbf{p}_n$. We shall introduce the following special notation for the energies and momenta of particles $k, \ldots, n$ when the momenta of particles $1, \ldots, k-1$ are fixed:

$$E_k = E - \sum_1^{k-1} e_i, \qquad \mathbf{P}_k = \sum_1^{k-1} \mathbf{p}_i - \mathbf{P}; \qquad (2.2)$$

we also denote the characteristic ("maximum") energy and momentum of particle k in the center-of-mass system of particles $k, \ldots, n$ for fixed values of $\mathbf{p}_1, \ldots, \mathbf{p}_{k-1}$ by

$$E_k^* = (M_k^2 + m_k^2 - \mu_k^2)/2\, M_k (k = 1, \ldots,\ n-1),$$
$$E_n^* = (M_{n-1}^2 - m_{n-1}^2 + m_n^2)/2M_{n-1},$$
$$p_k^* = (E_k^{*2} - m_k^2)^{1/2} \qquad (2.3)$$
$$= \{(M_k^2 - m_k^2 - \mu_k^2) - (2m_k\mu_k)^2\}^{1/2}/2M_k,$$

where M_k is the effective mass of the system of particles $k, \ldots, n$, and μ_k is the mass of the compound particle composed of particles $k+1, \ldots, n$, i.e.,

$$M_k^2 = E_k^2 - P_k^2, \qquad \mu_k = \sum_{k+1}^n m_i. \qquad (2.4)$$

We shall specify $\mathbf{p}_k$ by its spherical coordinates $\mathbf{p}_k = \{p_k, \theta_k, \varphi_k\}$ in a system fixed with respect to the sum of the $\mathbf{p}_1, \ldots, \mathbf{p}_{k-1}$, momenta which have already been picked. We take the polar axis along the $\mathbf{P}_k$ direction, θ_k to be the angle between $\mathbf{P}_k$ and $\mathbf{p}_k$, and calculate φ_k from the vertical plane containing $\mathbf{P}_k$ (Fig. 2). This coordinate system is convenient in that the magnitude of $\mathbf{P}_k + \mathbf{p}_k$ is independent of φ_k; indeed,

$$P_{k+1}^2 = P_k^2 + p_k^2 + 2P_k p_k \cos\vartheta_k. \qquad (2.5)$$

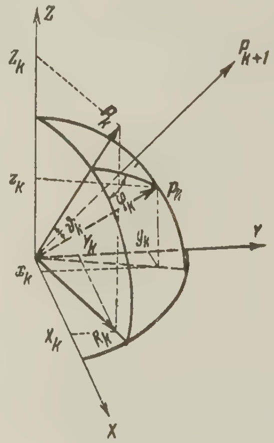

FIG. 2

The Cartesian coordinates of the momentum (see Fig. 2) are given by

$$\mathbf{P}_k = \{X_k,\ Y_k,\ Z_k\}, \qquad R_k = (X_k^2 + Y_k^2)^{1/2}; \qquad (2.6)$$

$$x_k = p_k\left[\frac{X_k}{P_k}\cos\vartheta_k + \left(\frac{Z_k}{P_k}\frac{X_k}{R_k}\cos\varphi_k - \frac{Y_k}{R_k}\sin\varphi_k\right)\sin\vartheta_k\right],$$

$$y_k = p_k\left[\frac{Y_k}{P_k}\cos\vartheta_k + \left(\frac{Z_k}{P_k}\frac{Y_k}{R_k}\cos\varphi_k + \frac{X_k}{R_k}\sin\varphi_k\right)\sin\vartheta_k\right],$$

$$z_k = p_k\left[\frac{Z_k}{P_k}\cos\vartheta_k - \frac{R_k}{P_k}\sin\vartheta_k\cos\varphi_k\right]. \qquad (2.7)$$

Let us now rewrite (2.1). Integrating over $\mathbf{p}_n$

and θ_{n-1}, we eliminate the δ-functions in the integrand, obtaining

$$W(E, \mathbf{P}) = \int d^3\mathbf{p}_1 \ldots d^3\mathbf{p}_{n-2}\, dp_{n-1}\, d\varphi_{n-1}\, p_{n-1} \frac{E_n}{P_{n-1}} \times F(\mathbf{p}_1, \ldots, \mathbf{p}_{n-1}, -\mathbf{P}_{n-1} - \mathbf{p}_{n-1}), \tag{2.8}$$

where $\mathbf{p}_{n-1}$ is the vector whose components are

$$\mathbf{p}_{n-1} = \left\{ p_{n-1}, \cos^{-1} \frac{E_n^2 - m_n^2 - P_{n-1}^2 - p_{n-1}^2}{2P_{n-1}p_{n-1}}, \varphi_{n-1} \right\}, \tag{2.9}$$

and the region D_n of integration is bounded by the surfaces $\cos\theta_{n-1} = \pm 1$, i.e.,

$$\{(P_{n-1} \pm p_{n-1})^2 + m_n^2\}^{1/2} = E_{n-1} - e_{n-1}. \tag{2.10}$$

Now (2.8) can in principle be used to solve the problem of achieving the distribution associated with the model whose interaction is given by F. There are no dependent variables of integration in (2.8), so that the sets of values of $\mathbf{p}_1, \ldots, \mathbf{p}_{n-2}$, p_{n-1}, φ_{n-1} must satisfy certain inequalities rather than equations (as is the case for (2.1)), and this increases greatly the efficiency of drawing. However the amount of calculation necessary to obtain a distribution over $\mathbf{p}_1, \ldots, \mathbf{p}_{n-2}$, p_{n-1}, φ_{n-1} with density $p_{n-1}E_nF/P_{n-1}$ is still extremely large. All further operations should be directed toward decreasing the amount of calculation. An obvious way to do this is to perform as many integrations as possible in (2.8), since this reduces the dimensionality of the region of integration and thus increases the ratio between the volume of this region and the volume of the rectangle under consideration. This goal is not, however, possible to achieve in general with arbitrary forms of F. Since we wish to develop a method suitable for all F, we shall proceed to reduce the amount of calculations in a different way. We write $d^3\mathbf{p}_k$ in the form $p_k^2dp_k \times d\cos\theta_k d\varphi_k$, making use of the spherical coordinate system described above. Then the density of distribution over p_1, $\cos\theta_1$, φ_1; $p_2, \ldots$; $\ldots, \varphi_{n-2}$; p_{n-1}, φ_{n-1} will be of the form

$$\Phi(p_1, \ldots, \varphi_{n-1}) = p_{n-1} \frac{E_n}{P_{n-1}} F \prod_{k=1}^{n-2} p_k^2, \tag{2.11}$$

where the arguments of F are the same as in (2.8). The essential result is that the regions $D_2, \ldots, D_k, \ldots, D_n$ for the solved values $\mathbf{p}_1$; $\mathbf{p}_1, \mathbf{p}_2$; $\ldots$; $\mathbf{p}_1, \mathbf{p}_2, \ldots, \mathbf{p}_{k-1}$; $\ldots$; $\mathbf{p}_1, \ldots, \mathbf{p}_{n-1}$ are independent of $\varphi_1, \ldots, \varphi_{n-1}$. We proceed to prove this assertion.

Let the momenta $\mathbf{p}_1, \ldots, \mathbf{p}_{k-1}$ (where $k \leq n-2$) be fixed. Let us find the region of variation d_k of the momentum $\mathbf{p}_k$. The remaining $k, k+1, \ldots, n$ particles fulfill the relations

$$\sum_k^n e_i = E_k, \qquad \sum_k^n \mathbf{p}_i = -\mathbf{P}_k. \tag{2.12}$$

It is known[4] that if in multiple production one particle has its maximum possible momentum, then all the other secondary particles move as a whole, i.e., as a particle whose mass is equal to the sum of the masses. For particle k this mass is μ_k [see (2.4)]. The conservation laws for two particles with masses m_k and μ_k, total energy E_k and momentum $-\mathbf{P}_k$ can be written in the form

$$(\mathbf{p}_k^2 + m_k^2)^{1/2} + \{(-\mathbf{P}_k - \mathbf{p}_k)^2 + \mu_k^2\}^{1/2} = E_k.$$

This is the equation of the surface which bounds the region d_k of possible positions of the end points of $\mathbf{p}_k$. The location and shape of d_k is most clearly found by a graphical representation of the conservation laws.[5] On going from the center-of-mass system to the laboratory system, the $p_k^* = \text{const}$ sphere is deformed into an ellipsoid of revolution prolate along the direction of relative motion of the two coordinate systems. In the case we are considering the center of the ellipsoid lies at O (whose position vector is $-E_k^*\mathbf{P}_k/M_k$), the major axis (the axis of revolution) is of length $2p_k^*E_k/M_k$ and is directed along $\mathbf{P}_k$, and the minor semiaxis is of length p_k^* (Fig. 3). Here E_k^* and p_k^* are given by (2.3).

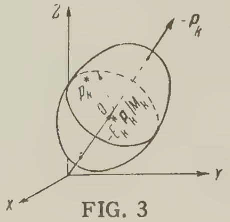

FIG. 3

We can now find the region D_k. Since the energy E_k^* of particle k in the center-of-mass system of particles $k, k+1, \ldots, n$ is no less than its mass m_k, it follows that [see (2.3)]

$$M_k \geqslant \mu_{k-1} \quad (k \leqslant n-1). \tag{2.13}$$

This is not only a necessary condition on $\mathbf{p}_1, \ldots, \mathbf{p}_{k-1}$, but also a sufficient one. That is, when it is fulfilled there always exist $\mathbf{p}_k, \ldots, \mathbf{p}_n$ such that the conservation laws will be fulfilled; for instance, particles $k+1, \ldots, n$ may all be moving in the same direction (in the coordinate system in which $\mathbf{P}_k = 0$), while particle k moves in the opposite direction.

But M_k depends only on the magnitude of $\mathbf{P}_k$, as indicated by (2.4), and this in turn is independent of φ_k [see (2.5)]. Therefore the shape of D_k as given by (2.3) is independent of φ_k (for $k \leq$

$n-1$). For D_n this follows from (2.10).

The fact that the shape of D_k is independent of φ_k for all k from 1 to n makes it possible to decrease the dimensionality of each D_k by a factor of $^2/_3$; thus, for instance, the dimensionality of D_n will be $2(n-1)$ instead of $3(n-1)$. This, in turn, greatly increases the ratio between the volume of D_n and the volume of our rectangle of the same number of dimensions.

Thus we can use the following procedure for obtaining n-particle reactions for an interaction the square of whose matrix element is F. First p_1 and $\cos\theta_1$ are picked from a uniform distribution in $(\tilde{p}_{1\,\mathrm{min}}, \tilde{p}_{1\,\mathrm{max}})$ and $(-1, 1)$; then p_2 and $\cos\theta_2$ are picked from $(\tilde{p}_{2\,\mathrm{min}}, \tilde{p}_{2\,\mathrm{max}})$ and $(-1, 1)$, and (2.13) is checked with $k = 3; \ldots;$ then p_k and $\cos\theta_k$ are picked from[*] $(\tilde{p}_{k\,\mathrm{min}}, \tilde{p}_{k\,\mathrm{max}})$ and $(-1, 1)$, E_{k+1} is calculated from (2.2), and P_{k+1} from (2.5), and (2.13) is verified. If it is not fulfilled, we pick again from p_1, while if it is, we proceed to $k+1$, etc., up to $k = n-1$. For $k = n-1$ only p_{n-1} is picked, within the limits $|E^*_{n-1}P^*_{n-1} \mp p^*_{n-1}E_{n-1}|/M_{n-1}$ (but not between $\tilde{p}_{n-1\,\mathrm{min}}$ and $\tilde{p}_{n-1\,\mathrm{max}}$!), and (2.13) need not be verified. Only now are $\varphi_1, \ldots, \varphi_{n-1}$ picked from $(0, 2\pi)$, value of $\cos\theta_{n-1}$ calculated by (2.9), and the value of $\Phi(p_1, \ldots, \varphi_{n-1})$ calculated by (2.11).

The use of the rejection method to obtain the distribution with density Φ has its peculiarities in the present case. It cannot be used by rote, since if F is everywhere finite, $\Phi_{\mathrm{max}} = \infty$ when $P_{n-1} = 0$. But it is just in the limit $P_{n-1} \to 0$ that the interval of variation of p_{n-1} contracts to a point, so that p_{n-1} is uniquely specified and need not be picked.

After obtaining the distribution with density Φ, the construction of the table is completed by calculating $\mathbf{p}_n = \mathbf{p}_{n-1} - \mathbf{P}_{n-1}$ and writing all the momenta in the cartesian XYZ system using Eqs. (2.6) and (2.7).

Fermi's model $(F \equiv 1)$ allows some simplification of the method of computation. In this case it is possible to carry out the integration over φ_{n-1} and p_{n-1} in (2.8), or more accurately over e_{n-1} between the limits

$$e_{\substack{\mathrm{min}\\ \mathrm{max}}} = (E^*_{n-1}E_{n-1} \mp p^*_{n-1}P_{n-1})/M_{n-1}, \tag{2.14}$$

and to obtain the distribution density[†]

$$\Phi'(\mathbf{p}_1, \ldots, \mathbf{p}_{n-2}) = \frac{4\pi}{3} p^*_{n-1} \frac{3E^*_{n-1}E^*_n E^2_{n-1} - p^{*2}_{n-1}P^2_{n-1}}{M^3_{n-1}} \prod_{i=1}^{n-2} p_i^2. \tag{2.15}$$

The sequence of picking is here the same as in the general case, but ends with the picking of p_{n-2} and $\cos\theta_{n-2}$. Having obtained uniformly distributed points in D_{n-1}, one obtains a nonuniform distribution with density Φ' by the rejection method. In addition, Φ'_{max} can be calculated beforehand; it can be shown, namely, that the maximum value of Φ' is obtained when $P_{n-1} = 0$ and the values of $p_1, \ldots, p_{n-2}$ satisfy the set of equations

$$\frac{p_1^2}{e_1} = \frac{p_2^2}{e_2} = \ldots = \frac{p^2_{n-2}}{e_{n-2}} = \frac{2p^{*2}_{n-1}E^*_{n-1}E^*_nE_{n-1}}{(E^*_{n-1}E^*_n)^2 + p^{*2}_{n-1}(E^{*2}_{n-1} - E^*_{n-1}E^*_n + E^{*2}_n)}. \tag{2.16}$$

These equations are easily solved by an iteration method.

We must still pick the momentum p_{n-1}. Instead, it is better to pick the energy e_{n-1} by the "direct" method, i.e., to solve the equation

$$2e^3_{n-1} - 3E_{n-1}e^2_{n-1} = (2e^3_{\mathrm{min}} - 3E_{n-1}e^2_{\mathrm{min}})(1-\alpha) + (2e^3_{\mathrm{max}} - 3E_{n-1}e^2_{\mathrm{max}})\,\alpha, \tag{2.17}$$

where α is uniformly distributed over $(0, 1)$. Only after this has been done does it make sense to pick $\varphi_1, \ldots, \varphi_{n-1}$.

A characteristic feature of the methods described in Secs. 1 and 2 is the occurrence of unsuccessful pickings, which means that the uniform distributions are obtained by rejection. It is obvious that if there are too many unsuccessful pickings, this method for constructing the table becomes practically useless. It is impossible to evaluate the efficiency of this method in general. A numerical experiment has shown, however, that for meson production by 10-Bev protons, the method is fifty percent efficient (for production of one π meson) and ten percent efficient (for two π mesons). For more mesons, the efficiency is too low for the method to be usable by hand calculation. Nevertheless, it is possible to construct a table for production of 3 or 4 mesons by hand if one integrates Φ' several more times. The use of an electronic computer makes it possible to construct large tables for 5 or 6-particle reactions by our method.

3. THE TABLE OF RANDOM STARS

It is difficult to compare an n-particle table with experiment, since experiment does not observe neutral particles. Such a table must enter as a component part into a table of random stars formed by the collision of two given particles for a given energy E. To form such a table one must consider all forms of reactions which have observable statistical weight. The statistical weight of a reaction determines the average number of entries corresponding to it.

---

[*] For $n = 3$, Eq. (2.15) becomes the same as Block's[6] Eq. (4).

[†] The values of $\tilde{p}_{k\,\mathrm{min}}$ and $\tilde{p}_{k\,\mathrm{max}}$ are calculated by formulas similar to (1.8).

Although in Fermi's model the statistical weights can be calculated and are already known for many reactions, this is not true for a reaction with an arbitrary value of $F(p_1, \ldots, p_n)$; it may turn out to be no less difficult to calculate the statistical weight for such a model than it is to construct the table of random stars. The above method for constructing the table of n-particle reactions, however, can in principle be used to determine the volume W in phase space, the fundamental part of the expression for the statistical weight. Indeed, it is clear that W is equal to the product of the volume of D_n by the average value of Φ as given by (2.11) over this region. But the volume of D_n is equal to the fraction of successful drawings of $p_1, \ldots, p_{n-1}$ in this volume multiplied by the volume of the rectangle of known dimensions circumscribed about D_n. In actuality, the use of this method to calculate the volume in phase space requires a very large number of drawings, because the Φ values are so widely scattered; the smaller the volume of phase space, the greater the number of drawings required.

But if all the statistical weights of the most important reactions which take place at a given energy are known, there is no great difficulty involved in constructing the table of random stars. We arrange all the reactions $N_1, N_2, \ldots, N_j, \ldots$ in an arbitrary order, and with each we associate an interval δ_j on the segment $(0, 1)$, such that the length of δ_j is proportional to the weight of N_j. Then in calculating an entry in the table, one chooses a random point on $(0, 1)$. The index of the δ_j interval in which this point lies gives the reaction N_j which is represented by this entry. One finds (if necessary), again by drawing, which of the momenta in this entry are to belong to charged particles. The momenta of the other particles, since they are not observed, need not be included in the entry.

In a table constructed in this way, (a) the reactions will be randomly shuffled, and (b) the number of entries referring to each reaction will fluctuate in accordance with their statistical weights. These statistical fluctuations will obey the same laws as in the observation of actual stars. On the other hand, one may wish to increase the accuracy of small tables by forbidding such fluctuations.

Using a computer giving stars with $n = 6$, this method can take into account most reactions involving protons with kinetic energies up to 10 Bev. This will give rise to stars with varying numbers of prongs.

The accuracy of the results obtained from a table of random stars depends on essentially the same factors as in the case of real stars. Errors in the determination of the energy and angles of emission of the particles do not occur; one may drop the fluctuations of the frequency of occurrence of the various reactions about the statistical weights; the results will, however, be affected by the error in calculating the statistical weights themselves. If the errors in the weights are of the order of ten percent, it is hardly worth having tables of more than one thousand entries. The allowed margin of error is necessary to obtain nominal distributions and to compare distributions for different energies. The errors in the statistical weights for different E cancel, since they are more or less systematic, and thus comparison of the distributions for different E can be very accurate.

An interesting possibility is that of increasing the accuracy by constructing the table of random stars in the laboratory coordinate system. It is then no longer necessary to transform the actual stars into the center-of-mass system, an operation which can be handled only very roughly for high energies. This simplifies the analysis of the experimental data and increases the accuracy with which the table of random stars can be compared with experiment.

CONCLUSION

The purpose of this paper was to clarify the possibility of constructing a table of random stars. A method for such a construction has been given. It is first of all possible, clearly, to represent Fermi's model and the isobaric model in the form of tables. One may hope that modern computers are entirely able to reproduce reactions with 6 or 7 secondary particles, which means that it should be possible to construct tables of the stars obtained in proton-proton collisions in a 10-Bev accelerator.

The method for constructing the table for these models will give an isotropic angular distribution for the reaction products. In order to explain the actually observed nonisotropic distributions, it is necessary to give the appropriate momentum and angular dependence of the square of the matrix element F.

Our method for constructing the table of random stars is applicable to different forms of F.

The fact that F may be a complicated functions plays no role, since most of the operating time of the computer is spent, in our method, in rejecting the unsuccessfully picked momentum components, rather than performing operations with the successfully picked momenta.

It thus becomes possible to find a phenomenologically satisfactory description of the interaction by testing various hypotheses and comparing the statistical weights so obtained, the distributions, and the correlations with the experimental data. The same kind of an approach can be used to study the decay of unstable particles.

This work was undertaken at the suggestion of M. I. Podgoretskii, and the author takes this opportunity to offer him his sincere gratitude. The author is also grateful to Iu. N. Blagoveshchenskii for many and valuable discussions.

[1] E. Fermi, Progr. Theoret. Phys. (Japan) **5**, 570; Phys. Rev. **92**, 452 (1953); **93**, 1434 (1954).

[2] J. W. Butler, see H. A. Meyer, Symposium on Monte-Carlo Methods (New York, 1955).

[3] Chavchanidze, Shadyri, and Kumsishvili, J. Exptl. Theoret. Phys. (U.S.S.R.) **34**, 912 (1958), Soviet Phys. JETP **7**, 631 (1958).

[4] R. M. Sternheimer, Phys. Rev. **93**, 642 (1954).

[5] J. Blaton, Kgl. Danske Videnskab Selskab, Mat.-fys. Medd. **24**, 20 (1950).

[6] M. M. Block, Phys. Rev. **101**, 796 (1956).

Translated by E. J. Saletan
303

SOVIET PHYSICS JETP VOLUME 35(8), NUMBER 6 JUNE, 1959

RADIATION FROM A CHARGED PARTICLE TRAVERSING A LAYERED MEDIUM

G. M. GARIBIAN

Academy of Sciences, Armenian S.S.R.

Submitted to JETP editor, June 12, 1958; resubmitted August 1, 1958

J. Exptl. Theoret. Phys. (U.S.S.R.) 35, 1435-1439 (December, 1958)

An analysis is made of the transition radiation produced when a charged particle passes through a large number of slabs which are separated by vacuum spaces.

THE transition radiation produced when a charged particle moves from one semi-infinite medium into another has been treated in references 1 and 2. Later, in references 3 and 4, an investigation was made of the radiation field which is produced when a charged particle moves through a slab of material. In the present paper we calculate the transition radiation produced by the passage of a charged particle through an arbitrary number of material layers which are separated by vacuum spaces.

The present work is motivated by the following considerations. Ginzburg and Frank[1] have shown that the intensity of the transition radiation increases logarithmically with increasing particle energy. It is tempting to explore this effect as a means of measuring the energy of highly relativistic particles. Because the effect is so small it is impossible to observe the transition radiation due to a single particle. For this reason it is of interest to investigate the possibility of intensifying the transition radiation by allowing a particle to pass through a large number of material slabs.

1. Suppose that a charged particle with velocity **v** moves along the z axis in the positive direction and traverses m slabs of material, which are perpendicular to the direction of motion of the particle. The slabs are of thickness a and are separated by a distance b; all have the same dielectric constant $\epsilon(\omega)$.

The radiation field in the slabs and in the voids between them will consist of waves which move in the positive (E') and negative (E'') z directions. In the region $z < 0$, however, there will exist only reflected waves; in the region $z > ma + (m-1)b$ there will be only waves which move in the positive z direction. We introduce the notation $\lambda^2 = (\omega^2\epsilon/c^2) - \kappa^2$ and $\lambda_0^2 = (\omega^2/c^2) - \kappa^2$, where it is assumed that the real and imaginary parts of λ and λ_0 are positive.* To compute the radiation fields, E_0'' for $z < 0$ and E_m' for $z > ma + (m-1)b$, we proceed in the following manner.* Writing the continuity conditions for the electric vectors at the boundaries of the $(l+1)$-th slab (cf. references 2 and 4), we obtain four equations by means of which it is possible (eliminating the fields in the slab) to obtain a relation between the tangential Fourier components of the electric fields in the l-th and $(l+1)$-th voids. This relation is of the form:

$$F_{l+1} = MF_l, \tag{1}$$

where

$$F_l = \begin{pmatrix} F_l'' \\ F_l' \end{pmatrix},$$

$$F_l'' = E_{l,t}''(\mathrm{k}) \exp\{-i(\lambda_0 + k_z)(a+b)l\} + \alpha'',$$
$$F_l' = E_{l,t}'(\mathrm{k}) \exp\{i(\lambda_0 - k_z)(a+b)l\} + \alpha',$$

$$\alpha'' = \frac{ei\varkappa}{2\pi^2}\frac{\lambda\lambda_0}{4\varepsilon}\frac{A\exp\{-i\lambda_0 b - ik_z(a+b)\} + B\exp\{-ik_z(a+2b)\}}{(k_1-1)(k_2-1)},$$

$$\alpha' = \frac{-ei\varkappa}{2\pi^2}\frac{\lambda\lambda_0}{4\varepsilon}\frac{C\exp\{i\lambda_0 b - ik_z(a+b)\} + D\exp\{-ik_z(a+2b)\}}{(k_1-1)(k_2-1)},$$

$$\left.\begin{matrix} A \\ B \end{matrix}\right\} = \left(\frac{\varepsilon}{\lambda} + \frac{1}{\lambda_0}\right)\alpha e^{\mp i\lambda a}$$

$$+\left(\frac{\varepsilon}{\lambda} - \frac{1}{\lambda_0}\right)\beta e^{\pm i\lambda a} + \frac{2\varepsilon}{\lambda}\gamma\exp\{\pm ik_z a\},$$

$$\left.\begin{matrix} C \\ D \end{matrix}\right\} = \left(\frac{\varepsilon}{\lambda} - \frac{1}{\lambda_0}\right)\alpha e^{\mp i\lambda a}$$

$$+\left(\frac{\varepsilon}{\lambda} + \frac{1}{\lambda_0}\right)\beta e^{\pm i\lambda a} + \frac{2\varepsilon}{\lambda}\delta\exp\{\pm ik_z a\},$$

$$k_{1,2} = q_{1,2}\exp\{-ik_z(a+b)\}$$

$$= \frac{C_2 + D_1}{2} \pm \left[\left(\frac{C_2 + D_1}{2}\right)^2 - \exp\{-2ik_z(a+b)\}\right]^{1/2},$$

---

*We retain the notation reference 4.

*This method was suggested by I. I. Gol'dman.

and the matrix M is

$$M = \begin{pmatrix} D_1 & C_1 \\ D_2 & C_2 \end{pmatrix},$$

where

$$D_1 = -\frac{\lambda\lambda_0}{4\varepsilon}\exp\{-i\lambda_0 b - ik_z(a+b)\}$$

$$\times\left[\left(\frac{\varepsilon}{\lambda}-\frac{1}{\lambda_0}\right)^2 e^{i\lambda a}-\left(\frac{\varepsilon}{\lambda}+\frac{1}{\lambda_0}\right)^2 e^{-i\lambda a}\right],$$

$$D_2 = \frac{\lambda\lambda_0}{4\varepsilon}\exp\{i\lambda_0 b - ik_z(a+b)\}\left(\frac{\varepsilon^2}{\lambda^2}-\frac{1}{\lambda_0^2}\right)(e^{i\lambda a}-e^{-i\lambda a}),$$

$$C_1 = -\frac{\lambda\lambda_0}{4\varepsilon}\exp\{-i\lambda_0 b - ik_z(a+b)\}$$

$$\times\left(\frac{\varepsilon^2}{\lambda^2}-\frac{1}{\lambda_0^2}\right)(e^{i\lambda a}-e^{-i\lambda a}),$$

$$C_2 = \frac{\lambda\lambda_0}{4\varepsilon}\exp\{i\lambda_0 b - ik_z(a+b)\}$$

$$\times\left[\left(\frac{\varepsilon}{\lambda}+\frac{1}{\lambda_0}\right)^2 e^{i\lambda a}-\left(\frac{\varepsilon}{\lambda}-\frac{1}{\lambda_0}\right)^2 e^{-i\lambda a}\right].$$

The quantities α, β, γ, and δ are given in Eq. (4) of reference 4.

Applying (1) m times we have

$$F_m = M^m F_0, \tag{2}$$

with

$$F_0 = \begin{pmatrix} E''_{0,t}(\mathbf{k}) + \alpha'' \\ \alpha' \end{pmatrix}$$

$$F_m = \begin{pmatrix} \alpha'' \\ E'_{m,t}(\mathbf{k})\exp\{i(\lambda_0 - k_z.(a+b)m\} + \alpha' \end{pmatrix}.$$

In principle the relation in (2) represents a solution of the problem since it yields two equations with two unknowns, $E''_{0,t}(\mathbf{k})$ and $E'_{m,t}(\mathbf{k})$. However, because it is necessary to calculate M^m when this procedure is used the problem remains essentially unsolved. The following method can be used to circumvent the difficulty. We introduce the matrix $S(t)$ defined by the relation

$$S(t) = e^{Mt}, \tag{3}$$

where t is some variable. It is apparent that

$$M^m = (d^m S / dt^m)_{t=0}. \tag{4}$$

It follows from Eq. (3) that S satisfies the differential equation

$$dS / dt = MS. \tag{5}$$

Solving this system of differential equations for the elements of the matrix S and taking account of the fact that $S(0) = 1$, we obtain the following expression:

$$S = \frac{1}{k_1 - k_2}\begin{pmatrix} (D_1 - k_2)e^{k_1 t} + (k_1 - D_1)e^{k_2 t} & C_1(e^{k_1 t} - e^{k_2 t}) \\ D_2(e^{k_1 t} - e^{k_2 t}) & (C_2 - k_2)e^{k_1 t} + (k_1 - C_2)e^{k_2 t} \end{pmatrix}. \tag{6}$$

Using Eqs. (2), (4), and (6) we obtain a system of two equations; the solution yields:

$$\mathrm{E}''_{0,t}(\mathbf{k}) = \frac{ei\varkappa}{2\pi^2 G}\{e^{-i\lambda_0 b}A(q_1^m - q_2^m) \tag{7}$$

$$+ (e^{-i\lambda_0 b}A + e^{-ik_z b}B)[e^{ik_z(a+b)}(q_1^{m-1} - q_2^{m-1})$$

$$+ \ldots + e^{ik_z(a+b)(m-1)}(q_1 - q_2)]\},$$

$$\mathrm{E}'_{m,t}(\mathbf{k}) = -\frac{ei\varkappa}{2\pi^2 G}e^{-i(\lambda_0 - k_z)(a+b)m}\{e^{-ik_z b}D(q_1^m - q_2^m)$$

$$+ (e^{i\lambda_0 b}C + e^{-ik_z b}D) \tag{8}$$

$$\times[e^{-ik_z(a+b)}(q_1^{m-1} - q_2^{m-1}) + \ldots + e^{-ik_z(a+b)(m-1)}(q_1 - q_2)]\},$$

where

$$G = e^{-i\lambda_0 b}\left[\left(\frac{\varepsilon}{\lambda}+\frac{1}{\lambda_0}\right)^2 e^{-i\lambda a}-\left(\frac{\varepsilon}{\lambda}-\frac{1}{\lambda_0}\right)^2 e^{i\lambda a}\right](q_1^m - q_2^m)$$

$$-\frac{4\varepsilon}{\lambda\lambda_0}(q_1^{m-1} - q_2^{m-1}).$$

When m = 1 the last two expressions coincide with the corresponding formulas given in reference 4.

2. It is now necessary to integrate the expressions with respect to $dk_x dk_y = \kappa\, d\kappa\, d\varphi$. The integrals over φ are carried out by means of Bessel functions. We shall be interested in the field at large distances R from the points of entry and exit of the particle in the medium so that the asymptotic expansion for the Bessel functions can be used; the integration over κ is carried out by the method of steepest descent.

We first consider the radiation emitted in the backward direction $(z < 0)$. The expression for $E''_{0\rho}$ is

$$E''_{0\rho}(\mathbf{r}.t) = i\sqrt{\frac{2\pi}{R\sin\theta}}\int E''_{0,t}(\mathbf{k})$$

$$\times(e^{f(\varkappa)R - 3\pi i/4} + e^{\varphi(\varkappa)R + 3\pi i/4})e^{-i\omega t}\sqrt{\varkappa}\,d\varkappa\, dk_z,$$

where

$$f(\varkappa) = i\varkappa\sin\theta + i\lambda_0\cos\theta. \qquad \varphi(\varkappa) = -i\varkappa\sin\theta + i\lambda_0\cos\theta,$$

and $E''_{0,t}(\mathbf{k})$ is determined from Eq. (7).

The saddle point for the function $f(\kappa)$ is $(\omega/c)\sin\theta$. However, because of the presence in

$E''_{0,t}(k)$ of the exponentials in the expressions for q_1 and q_2, which are raised to the m-th power, it can be shown that the line of steepest descent of the integrand is shifted. This does not occur if

$$m(a+b) \ll R. \qquad (9)$$

In the highly relativistic case, in which we shall be interested exclusively, the transition radiation is directed in the backward direction, or in the forward direction, at an angle $\theta_0 \sim \mu/E$, where μ and E are the mass and energy of the particle.

If we now impose the condition

$$a,\ b \ll \lambdabar E^2/\mu^2, \qquad (10)$$

($\lambdabar$ is the wave length divided by 2π), after integration by the method of steepest descent it is possible to set $\theta = 0$ everywhere in λ and λ_0, with the exception of those expressions in which m appears in the exponents. Furthermore, we limit ourselves to those frequencies for which $|q| = 1$; this value encompasses essentially all frequency values if $(\sqrt{\epsilon}+1)^2/(\sqrt{\epsilon}-1)^2 \gg 1$ (when $\epsilon = 1.5$ this ratio is approximately 100). Also, taking $a\sqrt{\epsilon} = b$, we obtain the following expression for the transition radiation emitted in the backward direction:

$$W''_0 = \frac{e^2}{\pi c}\left(\ln\frac{2}{1-\beta} - 1\right)\left(\frac{\sqrt{\varepsilon}-1}{\sqrt{\varepsilon}+1}\right)^2 (\omega_2 - \omega_1)\, 2m, \qquad (11)$$

if $m \ll (\sqrt{\epsilon}+1)^2\,(\sqrt{\epsilon}-1)^2$. Thus, if the conditions given in (10) are satisfied the intensity of the backward transition radiation will, under certain conditions, increase with the number of slabs, provided this number does not exceed the limiting value $(\sqrt{\epsilon}+1)^2/(\sqrt{\epsilon}-1)^2$. As the limiting number of slabs is approached, in order-of-magnitude terms the radiation intensity becomes equal to the radiation intensity for one boundary between a vacuum and an ideal conductor.[1] Any further increase in the number of slabs results in a reduction in the intensity of the transition radiation.

Using an approach similar to that above it can be shown that the intensity of the transition radiation emitted in the forward direction does not increase; the intensity of this component is, in order-of-magnitude terms, equal to the radiation for one slab of material.

3. Consider another case; in place of (10) we have

$$a\mu^2/E^2 \ll \lambdabar \ll b\mu^2/E^2. \qquad (12)$$

Limiting ourselves to frequencies for which $|q| = 1$, we can show that the intensity of the transition radiation, in both the forward and backward directions, is equal to the transition radiation for one slab multiplied by $(2m-1)$. In computing the Poynting-vector flux in this case it is necessary to take account of the fact that the exponentials with $i(\omega/c)b\cos\theta$ give a zero contribution when averaged over the angle θ because of their oscillatory nature. The appearance of the factor $(2m-1)$ is easily understood because in addition to the m slabs we have $(m-1)$ voids, which also act as radiators of transition radiation.

Thus, if the conditions in (12) are satisfied the transition radiation can be increased by a desired factor, where, in accordance with Ref. 4, the radiation in the forward direction is a factor of $(\sqrt{\epsilon}+1)^2/(\sqrt{\epsilon}-1)^2$ larger than in the backward radiation.

Let (λ_1, λ_2) define a wavelength region which satisfies (12); we denote the corresponding frequencies by (ω_1, ω_2). The number of photons emitted in the forward direction in this frequency range is (cf. reference 4):

$$N(\omega_1,\ \omega_2) = \frac{2}{\pi}\frac{e^2}{\hbar c}\left(\ln\frac{2}{1-\beta} - 1\right)\ln\left(\frac{\omega_2}{\omega_1}\right)(2m-1). \qquad (13)$$

It is apparent from this formula that the number of photons is independent of the point of the spectrum at which the frequency range (ω_1, ω_2) is taken. Here, in accordance with reference 4 the relation $|\sqrt{\epsilon}-1| \gg c/\omega a$ must be satisfied. In the optical region this relation is always satisfied. The dangerous frequencies are those which are above the optical region, where $\sqrt{\epsilon} = 1 - 2\pi m e^2/m\omega^2$ (n is the number of electrons per unit volume). Using this expression for $\sqrt{\epsilon}$ we obtain the following condition:

$$(c^2/a)\, m/2\pi n e^2 \ll \lambdabar. \qquad (14)$$

When the values of a and b are fixed, in accordance with Eq. (12), as the particle energy increases photons of higher and higher energy must be used if we wish to measure the particle energy from the intensity of the transition radiation. However, when $E/\mu \gg (ae/c)\sqrt{2\pi n/m}$ [in accordance with Eq. (14)] the radiation in the frequency region given by Eq. (12) cannot be computed from Eq. (13).

Taking $a = 10^{-3}$ cm and $b = 10^{-1}$ cm, we can measure the particle energy up to $E/\mu = 10^3$. When $E/\mu = 10^2$, the number of photons in the wavelength region $(1 \text{ to } 3) \times 10^6$ cm will be 95 if the total number of slabs $m = 10^3$. When $E/\mu = 10^3$ the number of photons in the wavelength region $(1 \text{ to } 3) \times 10^{-8}$ cm is 145 for the same number of slabs. The total length of the stack is 101 cm.

As is well known, the transition radiation is emitted in a narrow cone with opening angle approximately μ/E in the forward direction. Ordinary bremsstrahlung is emitted in the same solid angle. Using the well known expression,[5] for particle energies of $E/\mu = 10^2$ and $E/\mu = 10^3$ we obtain 0.15 bremsstrahlung photons in the frequency region indicated ($Z = 14$, $N = 5 \times 10^{22}$).

It can also be shown that in the one-particle case the coherent radiation produced by virtue of macroscopic radiation, such as that considered by Askar'ian[6] for a particle bunch, is negligibly small.

In the optical region the Cerenkov radiation is emitted at large angles; in regions above the optical region in general there is no Cerenkov radiation (since $\epsilon < 1$).

To carry out the measurements indicated above it would be necessary to be able to make differential intensity measurements of electromagnetic radiation over a wide frequency range.

The author wishes to thank A. Ts. Amatuni and I. I. Gol'dman for valuable discussions.

---

[1] V. L. Ginzburg and I. M. Frank, J. Exptl. Theoret. Phys. (U.S.S.R.) **16**, 15 (1946).

[2] G. M. Garibian, J. Exptl. Theoret. Phys. (U.S.S.R.) **33**, 1403 (1957), Soviet Phys. JETP **6**, 1079 (1958).

[3] V. E. Pafomov, J. Exptl. Theoret. Phys. (U.S.S.R.) **33**, 1074 (1957), Soviet Phys. JETP **6**, 829 (1958).

[4] G. M. Garibian and G. A. Chalikian, J. Exptl. Theoret. Phys. (U.S.S.R.) **35**, 1282 (1958), Soviet Phys. JETP **8**, 894 (1959).

[5] Heitler, Quantum Theory of Radiation (Russ. Transl.) IIL 1956 p. 284. [Oxford, 1953].

[6] G. A. Askar'ian, J. Exptl. Theoret. Phys. (U.S.S.R.) **27**, 761 (1954).

Translated by H. Lashinsky
304

SOVIET PHYSICS JETP VOLUME 35(8), NUMBER 6 JUNE, 1959

PASSAGE OF HIGH-ENERGY MUONS THROUGH MATTER

I. L. ROZENTAL' and V. N. STREL'TSOV

P. N. Lebedev Physics Institute, Academy of Sciences, U.S.S.R.

Submitted to JETP editor June 14, 1958

J. Exptl. Theoret. Phys. (U.S.S.R.) 35, 1440-1446 (December, 1958)

The passage of high-energy muons through thick layers of matter is studied with account of ionization losses, bremsstrahlung, pair production, and "star" production. The energy loss distributions are taken into account for the last three processes. It is shown that taking account of the distribution functions leads to a smaller muon flux at sea level than the calculation on the basis of mean energy losses.

1. The passage of muons through thick layers of matter is related to the characteristics of nuclear interactions of high-energy particles. We are thus able to state that in a nuclear interaction most of the primary energy is carried away by a nucleon.[1,2] The importance of this conclusion increases the interest of the present problem, since the energy spectrum of high-energy muons ($\gtrsim 10^{11}$ ev) can be obtained only by measuring the dependence of muon intensity on depth underground, followed by a calculation based on a specific form of the range-energy relation for muons, which has been calculated in a number of papers. In his fundamental paper George[3] did not use the most accurate cross section obtainable for some of the processes that accompany the passage of muons through matter; moreover, he used mean energy losses instead of basing the calculation on distribution functions. The methods used by Belen'kii[4] and by Mando and Sona,[5] which take only bremsstrahlung into account in addition to ionization losses, are applicable only to not very high energies $< 10^{11}$ ev. In the present work we consider the passage of both low- and high-energy muons through matter, taking account of all known forms of muon interactions and energy-loss fluctuations.

2. It is convenient to divide interactions of relativistic muons into processes that result in continuous energy losses and others that result in infrequent large energy losses. The first type is represented by ionization losses (including Cerenkov radiation), while the second type includes bremsstrahlung, the direct production of electron-positron pairs, and collisions that result in the production of nuclear-interacting particles (which we shall call nuclear processes). In accordance with this division, we shall solve our problem in an approximation that takes into account the distribution of losses in only the second type of processes. Ionization losses will always be assumed equal to their mean value.

Following these preliminary remarks we turn to the equations for energy losses incurred in different processes by fast particles bearing the charge e. Ionization losses, with thickness measured in g/cm^2, are described by (see reference 6)

$$-\frac{dE_i}{dx} = \frac{2\pi NZ}{A}\frac{e^4}{mc^2}\ln\frac{E_1 m^2c^2 Z}{\hbar^2 e^2 N A}, \tag{1}$$

where N is Avogadro's number, m is the electron mass, while Z and A are the charge and atomic weight of the matter, which will be taken as 10 and 20 in our numerical calculations. Strictly speaking, Eq. (1) describes ionization losses subject to the condition that the δ-electron energy is $E_1 \ll E$, where E is the muon energy. However, since E_1 is in the logarithm, which is on the order of 30 or 40 in the energy region of greatest interest for us, we can replace E_1 by E with an error of about 5%. As we shall see, all other cross sections except nuclear losses are taken with the same degree of error. Nuclear losses introduce the principal uncertainty. Equation (1) can conveniently be written as*

$$-dE_i/dx = a + b\ln(E_{\text{Mev}}/1000),$$
$$a = 2.1\ \text{Mev}\cdot\text{cm}^2/\text{g},\quad b = 0.077\ \text{Mev}\cdot\text{cm}^2/\text{g}. \tag{2}$$

Ionization losses depend only slightly on energy and will hereafter be regarded as constant. Since we are interested in the passage of particles with energies above some $E_{\min}$, we average (2) over the energy spectrum, which we assume to be represented by a power law with the exponent $(\gamma + 1)$:

$$\overline{\frac{dE_i}{dx}} = \int_{E_{\min}}^{\infty}\frac{dE_i}{dx}E^{-(\gamma+1)}\,dE \Big/ \int_{E_{\min}}^{\infty}E^{-(\gamma+1)}\,dE. \tag{3}$$

---

*Here and hereafter energies will be expressed in Mev.

When $E > 10^4$ only very slight dependence on γ is exhibited by $\overline{dE_i}/dx$, which can be represented by

$$-\frac{\overline{dE_i}}{dx} = a + b \ln \frac{E_{\min}}{1000}. \tag{4}$$

The effective bremsstrahlung cross section is known to depend on the parameter

$$\delta = 100 \frac{\mu c^2}{E} \frac{E'}{E - E'} Z^{-1/3}, \tag{5}$$

where E' is the energy of the emitted photon and μ is the muon mass (see references 4 and 7, for example). In the limiting cases $\delta \gg 1$ (no screening) and $\delta \ll 1$ (complete screening) the differential cross section $\varphi_r(E, v)$, where $v = E'/E$, is given analytically by

$$\varphi_r^{(1)}(E, v)\, dv = 4\alpha \frac{N}{A} Z^2 r_e^2 \left(\frac{m}{\mu}\right)^2 \times \left\{\left[1 + (1-v)^2 - \frac{2}{3}(1-v)\right] \times \ln\left(\frac{\mu}{m} 183 Z^{-1/3}\right) + \frac{1}{9}(1-v)\right\}\frac{dv}{v} \tag{6}$$

(complete screening) and

$$\varphi_r^{(2)}(E, v)\, dv = \frac{16}{3}\frac{N}{A}\alpha Z^2 r_e^2 \left(\frac{m}{\mu}\right)^2 \left(\frac{3}{4}v + \frac{1-v}{v}\right) \times \left[\ln\left(\frac{12}{5}\frac{1-v}{v}\frac{E}{\mu c^2 Z^{1/3}}\right) - \frac{1}{2}\right] dv \tag{7}$$

(no screening); here

$$\alpha = 1/137, \quad r_e = e^2/mc^2.$$

For our further calculations it will be convenient to introduce the meson radiation unit of length defined by

$$\frac{1}{t_\mu} = 4\alpha \frac{N}{A} Z^2 r_e^2 \left(\frac{m}{\mu}\right)^2 \ln\left(\frac{\mu}{m} 183 Z^{-1/3}\right). \tag{8}$$

In the present case this radiation length is equal to 4.5×10^5 g/cm². These units can be used to write (6) and (7) with good accuracy as follows:

$$\varphi_r^{(1)}(E, v) = 1/v, \tag{9}$$

$$\varphi_r^{(2)}(E, v) = 0.3\left(\frac{3}{4}v + \frac{1-v}{v}\right)\left[\ln\frac{E(1-v)}{v} - 5\right]. \tag{10}$$

We shall now determine the range of applicability of these equations. For this purpose we estimate the average value of the factor $E'/(E - E')$, using the distribution (9), which diverges when the average is taken over the interval $0 < E' < E$, so that (6) and (7) cannot be used for very large energy losses. The average must therefore be taken over the interval $0 < E' < \kappa E$, where κ is close to but not equal to unity. $E'/(E - E')$ exhibits very weak (logarithmic) dependence on κ. Thus when $\kappa = 0.9$ we have $E'/(E - E') \sim 1$ and when $\kappa = 0.99$ we have $E'/(E - E') \sim 3$. We can therefore use (9) when $E \gg \mu c^2 Z^{-1/3} \sim 10^4 Z^{-1/3}$ and (10) when $E \ll 10^4 Z^{-1/3}$. For a rough estimate in the intermediate region $E \sim 10^4 Z^{-1/3}$ we can interpolate the cross section assuming that for $Z = 10$ it is represented by (9) in the entire region $E > 10^4$ and by (10) when $E < 10^4$. From (9) we easily obtain the average energy loss in the region $E > 10^4$:

$$-dE_r/dx = 2.2 \cdot 10^{-6} E \ \text{cm}^2/\text{g}. \tag{11}$$

We shall now consider direct pair production. According to Bhabha[8] the differential cross section $\varphi_p(E, v)$ differs in four energy regions as follows:

$$\varphi_p(E, v)\, dv = \frac{56}{9\pi}(\alpha Z r_e)^2 \frac{N}{A} f(E, v) \frac{dv}{v}, \tag{12}$$

where

$$\begin{aligned} f_1 &= \ln(k_1 E/mc^2)\ln(k_1' m/v\mu), \quad 2mc^2/E < v < 2mc^2/E\alpha Z^{1/3}, \\ f_2 &= \ln(k_2 \alpha Z^{1/3})\ln(k_2' m/\mu v), \quad 2mc^2/E\alpha Z^{1/3} < v < m/\mu, \\ f_3 &= {}^9/_7 (m/\mu v)^2 \ln(k_3 \mu v/\alpha Z^{1/3} m), \quad m/\mu < v < 2mE/\alpha Z^{1/3}\mu^2 c^2, \\ f_4 &= {}^9/_7 (m/\mu v)^2 \ln(k_4 E/\mu c^2), \quad 2mE/\alpha Z^{1/3}\mu^2 c^2 < v < 1, \end{aligned} \tag{13}$$

where all k are of the order of unity but their exact values are unknown. Continuity of the differential cross sections at the boundaries between the intervals is satisfied when $k_1 = 1/2$, $k_1' = 3$, $k_2 = k_3' = 1$, $k_2' = 3$, $k_4 = 2$. In radiation lengths we obtain

$$\varphi_p^{(1)}(E, v)\, dv = -16\left[\ln v^2 + (4.3 + \ln E)\ln v + 4.3 \ln E\right] dv/v, \tag{14}$$

$$\varphi_p^{(2)}(E, v)\, dv = -(280 + 64 \ln v)\, dv/v, \tag{15}$$

$$\varphi_p^{(3)}(E, v)\, dv = (0.0045 + 0.0005 \ln v)\, dv/v^3, \tag{16}$$

$$\varphi_p^{(4)}(E, v)\, dv = 0.0005 \ln(E/50)\, dv/v^3. \tag{17}$$

Equations (14) to (17) apply to the same energy intervals as (13). Multiplying by v and integrating over these intervals, we easily obtain the energy losses corresponding to the functions $\varphi_p^{(1-4)}$. Table I shows these energy losses expressed in terms of 10^{-6} E cm²/g for the different intervals representing four different $dE_p^{(i)}/dx$.

TABLE I

	E			
	$6 \cdot 10^4$	10^5	$6 \cdot 10^5$	10^6
$-dE_p^{(1)}/dx$	0.3	0.2	0.1	—
$-dE_p^{(2)}/dx$	1.7	1.4	1.4	1.4
$-dE_p^{(3)}/dx$	0.8	1.0	1.0	1.0
$-dE_p^{(4)}/dx$	0.1	0.02	—	—
$-\sum_{i=1}^{4} dE_p^{(i)}/dx = -dE_p/dx$	2.9	2.6	2.5	2.4

The direct production of nuclear-interacting particles by muons can be treated consistently as their creation by virtual photons.[3,9] A calculation by the method of Weizsäcker and Williams yields the following cross section for the production of a "star" or electron-nuclear shower with total energy in the interval E', $E' + dE'$:

$$\varphi_n(E, E')\,dE' = \frac{2\alpha}{\pi} N\sigma_\gamma(E')\frac{dE'}{E'}\ln\frac{E}{E'}, \tag{18}$$

where $\sigma_\gamma(E')$ is the total cross section for the production of "stars" and showers by a gamma quantum with energy E'. A somewhat more exact calculation[9] leads to the analogous expression

$$\varphi_n(E, E')\,dE' \approx \frac{2\alpha}{\pi} N \ln\frac{E}{\mu c^2}\,\sigma_\gamma(E')\frac{dE'}{E'} \tag{19}$$

The different forms of the logarithm in (18) and (19) do not represent an essential difference between the two expressions for the following reasons. The first and less important reason is that in reference 9 the entire calculation was performed with accuracy to within a logarithmic factor of the order of unity. The indeterminacy of the cross section $\sigma_\gamma(E')$ is the second and decisive consideration in estimating the accuracy. At sufficiently high energies $(E' > 1000)$ this cross section is usually taken as constant, although this hypothesis is certainly not confirmed by data on $\sigma_\gamma(E')$ at lower energies (see reference 10, for example). Since we do not possess experimental data on the energy-dependence of this cross section we can only compare (18) and (19) with data on the production of showers and "stars" by muons. However the experimental data are not accurate enough to permit a distinction between the two formulas with $\sigma_\gamma(E')$ assumed constant. Following George[3] and Kessler and Maz[11] we assume $\sigma_\gamma(E')$ to have the constant value $d \times 10^{-28}$ cm^2 per nucleon, with the constant d being varied in the numerical computations. Thus by means of (18) and (19) we write the cross section in radiation lengths as follows:

$$\varphi_n(E, v)\,dv = 0.13d\,\frac{\ln(1/v)}{v}\,dv \tag{20}$$

or

$$\varphi_n(E, v)\,dv = 0.13d\,\frac{\ln(E/\mu c^2)}{v}\,dv. \tag{21}$$

It follows that the mean energy loss is*

$$-dE_n/dx = 0.13d\cdot E\,10^{-6}\,\text{cm}^2/\text{g} \tag{22}$$

or

$$-dE_n/dx = 0.13dE\ln(E/\mu c^2)\,10^{-6}\,\text{cm}^2/\text{g}. \tag{23}$$

3. To describe the passage of muons through matter, we shall now set up the kinetic equation. It is convenient to introduce the critical energy ϵ_μ, which represents the ionization losses per radiation length. From (2) and (4) we obtain $\epsilon_\mu = 1.0 \times 10^6$, 1.0×10^6 and 1.2×10^6 for $E_{\min} = 10^4$, 10^5, and 10^6. Using the notation $\epsilon_\mu t_\mu = y$, we easily arrive at an equation to describe the muon spectrum $\pi(E, y)$ by analogy with the kinetic equations of ordinary cascade theory:

$$\frac{\partial\pi(E, y)}{dy} - \frac{\partial\pi(E, y)}{dE} = -\frac{1}{\varepsilon_\mu}\int_0^1\Big[\pi(E, y)\varphi(E, v) - \frac{1}{1-v}\pi\Big(\frac{E}{1-v}, y\Big)\varphi\Big(\frac{E}{1-v}, v\Big)\Big]dv, \tag{24}$$

where $\varphi = \varphi_r + \varphi_p + \varphi_n$.

Assuming that for $y = 0$ the spectrum is represented by the power function

$$\pi(E, 0) = CE^{-(\gamma+1)}, \tag{25}$$

we first solve (24) for small depths, when $y \ll E$. Substituting the solution without the right member, $\pi_0(E, y) = C/(E + y)^{\gamma+1}$, into the right member of (24), we obtain

$$\partial\pi/\partial y - \partial\pi/\partial E = \varphi(E, y); \tag{26}$$

$$\varphi(E, y) = -\frac{1}{\varepsilon_\mu}\int_0^1\Big[\pi_0(E, y)\varphi(E, v) - \frac{1}{1-v}\pi\Big(\frac{E}{1-v}, y\Big)\varphi\Big(\frac{E}{1-v}, v\Big)\Big]dv. \tag{27}$$

We shall seek a solution in the form

$$\pi(E, y) = \pi_0(E, y) + \pi_1(E, y)$$

subject to the initial conditions (25) and $\pi_1(E, 0) = 0$. π_1 satisfies (26) when π is replaced by π_1. The modified equation is easily solved by means of the substitutions $E + y = u$, $E - y = w$. After some simple transformations we obtain

$$\begin{aligned}\pi_1 &= \frac{1}{2}\int_{E-y}^{E+y}\varphi\Big(\frac{E+y+w}{2}, \frac{E+y-w}{2}\Big)dw \\ &= -\frac{1}{2\varepsilon_\mu}\int_0^1\Big\{\frac{2\varphi(E, v)\,y}{(E+y)^{\gamma+1}} - \frac{(1-v)^\gamma 2^{\gamma+1}}{\gamma v}\big[(E+y-yv)^{-\gamma} \\ &\qquad - (E+y)^{-\gamma}\big]\varphi\Big(\frac{E}{1-v}, v\Big)\Big\}dv.\end{aligned} \tag{28}$$

An expansion of $(E + y - yv)^{-\gamma}$ in powers of $yv/(E + y)$ gives

$$\pi_1 = -\frac{y}{\varepsilon_\mu(E+y)^{\gamma+1}}\int_0^1\Big\{\varphi(E, v) - (1-v)^\gamma\varphi\Big(\frac{E}{1-v}, v\Big) \times\Big[1 + \frac{yv(\gamma+1)}{E+y} + \ldots\Big]\Big\}dv. \tag{29}$$

---

*We shall not consider the production of penetrating pairs separately (as was done by George), because the most accurate experiments have shown that this process is only a special case of shower production by muons.[12]

The method used here is valid when the condition $\pi_1 \ll \pi_0$ is satisfied, for which it is sufficient that

$$y \ll \varepsilon_\mu \tag{30}$$

(or $t_\mu \ll 1$). These conditions are both sufficient and necessary, since when $y \gtrsim \epsilon_\mu$ it can be shown that $\pi_1 \gtrsim \pi_0$, which makes the method entirely unsuitable. It follows from (30) that in calculating π_1 we can limit ourselves to the first term in the expansion (29).

4. In this section we obtain a solution for $E > \epsilon_\mu$, for which purpose the expressions for the cross sections φ must be simplified so that they depend only on the ratio v. When $E > \epsilon_\mu$, the cross section for pair production is then approximated with good accuracy (~ 1%). In this approximation we can assume

$$\varphi_p^1 = \varphi_p^{(4)} = 0;$$
$$\varphi_p = \varphi_p^{(2)} \text{ for } 0 < v < m/\mu, \quad \varphi_p = \varphi_p^{(3)} \text{ for } m/\mu < v < 1. \tag{31}$$

When (9) and (18) are used as cross sections of the other processes, (24) becomes

$$\frac{\partial \pi(E, y)}{\partial y} - \frac{\partial \pi(E, y)}{\partial E}$$
$$= -\frac{1}{\varepsilon_\mu}\int_0^1 \left[\pi(E, y) - \frac{1}{1-v}\pi\left(\frac{E}{1-v}, y\right)\right]\varphi(v)\,dv. \tag{32}$$

We shall use Snyder's method[13] to obtain a solution, which will be sought in the form

$$\pi(E, y) = C\exp\{\lambda(\gamma)\,t_\mu\}\,F(E, \gamma). \tag{33}$$

A Mellin transformation in the variable E gives

$$F(E, \gamma) = \varepsilon_\mu^{-(\gamma+1)}\frac{1}{2\pi i}$$
$$\times \int_{-\delta-i\infty}^{\delta+i\infty} \frac{\Gamma(-r)\,\Gamma(\gamma+r+1)}{\Gamma(\gamma+1)} K(\gamma, r)\left(\frac{E}{\varepsilon_\mu}\right)^{-(r+\gamma+1)} dr, \tag{34}$$

where $\delta \gtrsim 0$, Γ is the gamma function, and $K(\gamma, r)$ satisfies the recursion relation

$$K(\gamma, r) = \frac{rK(\gamma, r-1)}{A(\gamma+r) - A(\gamma)},$$
$$A(x) = \int_0^1 [1-(1-v)^x]\,\varphi(v)\,dv, \quad K(\gamma, 0) = 1. \tag{35}$$

When $E/\epsilon_\mu > 1$ we can close the contour with an arc of infinitely large radius and calculate (34) by the method of residues:

$$F(E, \gamma) = E^{-(\gamma+1)}\sum_{n=0}^{\infty} C_{\gamma+n}^n K(\gamma, n)\left(\frac{\varepsilon_\mu}{E}\right)^n(-1)^n. \tag{36}$$

Comparing (36) and (33) with (28) and noting that when $t_\mu \to 0$ and $\epsilon_\mu/E \to 0$ (33) and (28) must coincide, we obtain $\lambda(\gamma) = -A(\gamma)$. It can be shown that our functions φ make (36) converge in the entire region $E > \epsilon_\mu$.

TABLE II

t_μ	$d = 1$			$d = 5$		
	0.3	0.6	1.0	0.3	0.6	1.0
		$\gamma = 2$				
$\varepsilon_\mu/E = 1/2$	1.1	1.2	1.4	1.1	1.25	1.6
$\varepsilon_\mu/E = 1/3$	1.1	1.25	1.5	1.15	1.35	1.7
		$\gamma = 3$				
$\varepsilon_\mu/E = 1/2$	1.2	1.7	2.7	1.4	2.1	4.0
$\varepsilon_\mu/E = 1/3$	1.3	1.9	2.9	1.5	2.2	4.8

5. It is useful to compare the results obtained when meson-intensity fluctuations at different depths are taken into account by means of distribution functions, with the results based on mean energy losses. We find the ratio between the number $N(E, t_\mu)$ of mesons with energies above E at depth t_μ, obtained by means of (33) and (36), and the analogous number $N_S(E, t_\mu)$, computed neglecting distribution functions. We use the fact that

$$N_s(E, t_\mu) = \int_{E_t}^{\infty} F(E, \gamma)\,dE, \tag{37}$$

where E_t is the minimum energy which a muon can expend in passing through the depth t_μ when mean energy losses are used and the final muon energy is E. E_t is obtained from

$$t_\mu = \int_E^{E_t}\left[\varepsilon_\mu + \frac{dE_r}{dt_\mu} + \frac{dE_p}{dt_\mu} + \frac{dE_n}{dt_\mu}\right]^{-1} dE. \tag{38}$$

We finally obtain

$$\frac{N(E, t_\mu)}{N_S(E, t_\mu)} = \frac{\left(\frac{E_t}{E}\right)^\gamma e^{-A(\gamma)t_\mu}\sum_{n=0}^{\infty}(-1)^n C_{\gamma+n}^n K(\gamma, n)(\varepsilon_\mu/E)^n}{\sum_{n=0}^{\infty}(-1)^n \frac{C_{\gamma+n}^n}{\gamma+n} K(\gamma, n)(\varepsilon_\mu/E_t)^n} \tag{39}$$

Numerical values of this ratio for $E = 2\epsilon_\mu$ and $3\epsilon_\mu$ are given in Table II.

Table II shows that N/N_S depends only slightly on ϵ_μ/E and d and that it is greater than unity (see also the general formula (39)). This indicates that a measured intensity at a given depth represents a smaller muon flux than is obtained by means of a calculation neglecting fluctuations.

In conclusion the authors wish to thank G. T. Zatsepin for a discussion of the questions which were touched on in this paper and Z. S. Maksimova for the numerical computations.

---

[1] G. T. Zatsepin, Dissertation, Physics Institute, Academy of Sciences U.S.S.R., Moscow, 1954.

[2] I. L. Grigorov, Dissertation, Physics Institute,

Academy of Sciences U.S.S.R., Moscow, 1954; Usp. Fiz. Nauk **58**, 559 (1956).

[3] E. P. George, Cosmic Ray Physics (Russ. Transl.) Ch. 1, IIL, M., 1954.

[4] S. Z. Belen'kii, **Лавинные процессы в космических лучах** (Cascade Processes in Cosmic Radiation), Gostekhizdat, 1948.

[5] N. Mando and P. Sona, Nuovo cimento **10**, 1275 (1953).

[6] H. Messel and D. Ritson, Phil. Mag. **41**, 1129 (1950).

[7] H. J. Bhabha, Proc. Roy. Soc. (London) **A164**, 257 (1938).

[8] H. J. Bhabha, Proc. Roy. Soc. (London) **A152**, 559 (1935).

[9] H. Kessler and P. Kessler, Nuovo cimento **4**, 601 (1956).

[10] H. A. Bethe and F. de Hoffmann, Mesons and Fields (Russ. Transl.), IIL, M., 1957, Ch. II.

[11] D. Kessler and R. Maz, Nuovo cimento **5**, 1540 (1957).

[12] H. Braddick and B. Leontic, Phil. Mag. **45**, 1287 (1954).

[13] H. Snyder, Phys. Rev. **53**, 960 (1938).

Translated by I. Emin
305

SOVIET PHYSICS JETP VOLUME 35 (8), NUMBER 6 JUNE, 1959

THE STATISTICS OF SPIN AND POLAR EXCITATIONS IN A CRYSTAL

S. V. VONSOVSKII and M. S. SVIRSKII

Institute of Metal Physics, Academy of Sciences, U.S.S.R.

Submitted to JETP editor June 17, 1958

J. Exptl. Theoret. Phys. (U.S.S.R.) 35, 1447-1456 (December, 1958)

The statistics of quasi-particles, the elementary excitations of the spin and electronic system of a crystal, are investigated.

1. Some recent papers[1-3] have asserted, contrary to the general opinion, that spin-waves behave like fermions rather than like bosons. Doubt was also thrown upon the idea that the elementary polar excitations (pairs and holes) in the electronic system of a crystal could behave like bosons.[4] It seems therefore worth while to study once again the statistical properties of spin-waves and polar excitations. In the present paper we point out some defects in the usual treatment of spin and polar excitations in crystals. In particular, these defects give rise to the appearance of fictitious states.[2,5,6] We show that when these defects are removed the spin-waves behave like bosons, and we find the conditions under which polar excitations behave like bosons. We also formulate in this paper a method of second quantization for systems of a finite number of particles described by symmetric wave-functions.

2. The Schrödinger equation with an exchange interaction has the following well-known form:

$$\varepsilon\alpha(f_1,\ldots,f_r)+\sum_{f_1'\ldots f_r'} J_{st}\,[\alpha(f_1',\ldots,f_r')-\alpha(f_1,\ldots,f_r)]=0\,, \quad (1)$$

Here $(f_1, \ldots, f_r)$ are the numbers of the vertices at which r reversed spins are situated. $(f_1', \ldots, f_r')$ is a set of numbers differing from $(f_1, \ldots, f_r)$ by the exchange of two oppositely oriented spins, and J_{st} is the exchange integral for the vertices between which the exchange has occurred. We introduce the operators

$$\varphi_f=\sqrt{N_f}\,\Delta_f^-;\ \varphi_f=\Delta_f^+\sqrt{N_f}\,;$$
$$\psi_f=\sqrt{n_f}\,\delta_f^-;\ \psi_f^+=\delta_f^+\sqrt{n_f}\,; \quad (2)$$

$$\Delta_f^\pm a(\ldots N_f,\ n_f\ldots)=a(\ldots N_f\pm1,\ n_f\ldots);$$
$$\delta_f^\pm a(\ldots N_f,\ n_f\ldots)=a(\ldots N_f,\ n_f\pm1,\ldots), \quad (3)$$

Here N_f is the number of reversed (or right) spins, and n_f is the number of left spins, at the vertex f. Bloch[7] proceeded from Eq. (1) to a second-quantized formalism with the Hamiltonian

$$\mathcal{H}=\frac{1}{2}\sum_{s}\sum_{t} J_{st}\,(\varphi_s\psi_t-\psi_s\varphi_t)\,(\varphi_s^+\psi_t^+-\psi_s^+\varphi_t^+)\,. \quad (4)$$

According to Eq. (3), the operators (2) obey the Bose commutation rules

$$\varphi_f^+\varphi_{f'}-\varphi_{f'}\varphi_f^+=\delta_{ff'}\,,\ \psi_f^+\psi_{f'}-\psi_{f'}\psi_f^+=\delta_{ff'}\,. \quad (5)$$

The operators (2) have the unsatisfactory feature that, according to Eq. (5), they do not place any limit on the occupation numbers of left and right spins at each vertex. Thus they do not obey the Pauli principle. Therefore, instead of Eq. (4), we shall give another representation for the operators $\Delta_f^\pm$ and $\delta_f^\pm$:

$$\Delta_f^- a(\ldots N_f,\ n_f\ldots)=\begin{cases}0 & \text{for}\quad N_f=0\\ a(\ldots 0_f,\ n_f\ldots) & \text{for}\quad N_f=1\end{cases}$$
$$\delta_f^- a(\ldots N_f,\ n_f\ldots)=\begin{cases}0 & \text{for}\quad n_f=0\\ a(\ldots N_f,\ 0_f\ldots) & \text{for}\quad n_f=1\end{cases}$$
$$\Delta_f^+ a(\ldots N_f,\ n_f\ldots)=\begin{cases}a(\ldots 1_f,\ n_f\ldots) & \text{for}\quad N_f=0\\ 0 & \text{for}\quad N_f=1\end{cases}$$
$$\delta_f^+ a(\ldots N_f,\ n_f\ldots)=\begin{cases}a(\ldots N_f,\ 1_f\ldots) & \text{for}\quad n_f=0\\ 0 & \text{for}\quad n_f=1\end{cases} \quad (6)$$

By using Eq. (6) instead of (3), we ensure the fulfilment of the Pauli principle, and yet the deduction of Eq. (4) from (1) is still valid. Equations (2) and (6) imply, instead of Eq. (5), the following commutation rules

$$[\varphi_f^+\varphi_f]_+=[\psi_f^+\psi_f]_+=1\,,$$
$$[\varphi_f^+\varphi_{f'}]_-=[\psi_f^+\psi_{f'}]_-=0 \qquad (f\neq f')\,, \quad (7)$$
$$[\varphi_f\varphi_{f'}]_-=[\varphi_f^+\varphi_{f'}^+]_-=[\psi_f\psi_{f'}]_-=[\psi_f^+\psi_{f'}^+]_-=0\,.$$

The commutation rules for φ_f and ψ_f are therefore different both from the Fermi and the Bose rules. For brevity we call the relations (7) the "plus-minus quantization."

In the homopolar approximation

$$N_f+n_f=1 \quad (8)$$

we need not write the occupation number n_f in the wave-function, because it is uniquely determined by the occupation number N_f. Thus instead of the four operators φ_f, φ_f^+, ψ_f and ψ_f^+, we may introduce two operators c_f and c_f^+, acting only on the numbers N_f. The connection between the old and new operators is given by

$$\psi_f\varphi_f^+ a(\ldots N_f,\ n_f\ldots) = \begin{cases} a(\ldots 1_f,\ 0_f\ldots) & \text{for } N_f = 0,\ n_f = 1 \\ 0 & \text{otherwise} \end{cases} \tag{9}$$

$$\varphi_f\psi_f^+ a(\ldots N_f,\ n_f\ldots) = \begin{cases} a(\ldots 0_f,\ 1_f\ldots) & \text{for } N_f = 1,\ n_f = 0 \\ 0 & \text{otherwise} \end{cases} \tag{10}$$

Consequently, if we introduce a creation operator c_f and an annihilation operator c_f^+ for a right spin at the vertex f, we find

$$c_f = \psi_f\varphi_f^+, \qquad c_f^+ = \varphi_f\psi_f^+. \tag{11}$$

Equation (11), with (2), (6), (7), and (8), implies the following commutation rules*

$$[c_f c_f^+]_+ = 1, \tag{12_1}$$

$$[c_f c_{f'}^+]_- = 0 \qquad (f \neq f'), \qquad [c_f c_{f'}]_- = [c_f^+ c_{f'}^+]_- = 0. \tag{12_2}$$

The Hamiltonian (4) may be expressed in terms of the new operators:

$$\mathscr{H} = \sum_{s \neq t} J_{st}\,(c_s^+ c_s - c_s^+ c_t - N_s N_t). \tag{13}$$

This gives for the linear chain in the nearest-neighbor approximation

$$\mathscr{H} = J\sum_s \sum_{t=s\pm d} (c_s^+ c_s - c_s^+ c_t - N_s N_t), \tag{14}$$

which is identical with the Hamiltonian of Frank.[1] But we differ from Frank in requiring the operators (11) to satisfy not the Fermi commutation rules but the rules (12) of the plus-minus quantization.

To diagonalize (14), we neglect terms of fourth order in the operators[1] c_f, which means that we are neglecting the interaction between spin-waves. We use the Fourier transform

$$c_f = N^{-1/2}\sum_k e^{ikf} c_k, \qquad c_f^+ = N^{-1/2}\sum_k e^{-ikf} c_k^+. \tag{15}$$

Then Eq. (14) gives

$$\mathscr{H} = \sum_k E(k)\, n_k. \tag{16}$$

Here $E(k)$ is the usual energy of a spin-wave with quasi-momentum k, and $n_k = c_k^+ c_k$ is the corresponding occupation number.

To study the statistics of the quasi-particles, we consider the commutation rules for c_k, c_k^+. Equations (12) and (15) imply

$$c_k c_k^+ - c_k^+ c_k = 1 - 2r/N; \tag{17}$$

$$c_k c_{k'}^+ - c_{k'}^+ c_k = -\frac{2}{N}\sum_f e^{i(k'-k)f} N_f \qquad (\text{for } k \neq k'); \tag{18}$$

$$[c_k c_{k'}]_- = [c_k^+ c_{k'}^+]_- = 0. \tag{19}$$

The commutation rules (19) have strictly Bose character, while Eqs. (17) and (18) do not. However, so long as $r/N \ll 1$ (a weakly excited system), Eqs. (17) and (18) approach arbitrarily close to the ordinary Bose relations. In the limit we obtain

$$[c_k c_{k'}^+]_- \approx \delta_{kk'},\ [c_k c_{k'}]_- = [c_k^+ c_{k'}^+]_- = 0. \tag{20}$$

Thus we reach the conclusion that the spin-wave operators obey approximately the ordinary Bose relations, the conditions for these relations to hold being that the number of spin-excitations be small. This condition is satisfied in the region of low temperatures, well below the Curie point.

In spite of the formal similarity of some of our equations to the equations used by Frank[1] and Meyer,[2] our argument differs from theirs in the following respects. Frank introduces the spin-wave creation and annihilation operators c_f and c_f^+, considering them from the beginning as Fermi operators, in view of the fact that N_f can only take the values 0 and 1. He naturally obtains Fermi commutation rules also for the Fourier transformed operators c_k, c_k^+, and deduces from this that spin-waves obey Fermi statistics. Our argument shows that the condition $N_f = 0, 1$ implies that only one (namely the first of the relations (12)) of the commutation rules is of Fermi character. The rest of the commutation rules are of Bose type, as is seen from Eqs. (17) to (19). Also the result of applying these operators twice can be found from Eq. (15):

$$c_k c_k = \frac{1}{N}\sum_f e^{-i2kf} c_f c_f + \frac{1}{N}\sum_{f<f'} e^{-ik(f+f')}[c_f c_{f'}]_+. \tag{21}$$

The first sum on the right side of Eq. (21) vanishes by Eqs. (11) and (9). The second sum would vanish if the last of the relations (12) had Fermi character. But we have seen that this relation has Bose character, and therefore

$$c_k c_k = \frac{2}{N}\sum_{f<f'} e^{-ik(f+f')} c_f c_{f'}. \tag{22}$$

This expression is in general different from zero,* and therefore it is possible for more than one spin-wave to exist in the state with quasi-momentum **k**, as must be the case if they obey Bose statistics. This example illustrates the importance of the departure of part of the relations (12) from the Fermi type. Fermi commutation rules fail to hold for the majority of the relations (12), because the sign functions of Wigner are absent in the operators (2) and (6). The reason for this is that the antisymmetric character of the wave function of a many-electron system was already taken into account in deriving the Schrödinger equation (1). The exchange of left and right spins represented in Eq. (1) is not accompanied by a change in sign of the wave function. Frank introduced the Wigner sign functions into the fermion operators $b_{f\sigma}$ which he used to construct a Hamiltonian in the Heitler-London model. This procedure would not change anything in our work, since the operators occur in the Hamiltonian in such a way that the sign functions cancel each other out. One can see this, for example, by looking at the expression (A6) for the Hamiltonian of the exchange interaction in reference 3. The same remark applies to the work of Meyer,[2] whose Hamiltonian (12) reduces to Frank's Hamiltonian when the external magnetic field is set equal to zero.

---

*Equation (12_2) was also used by Meyer,[2] who wrote p_ν for c_f, and q_ν for c_f^+. Instead of Eq. (12_1) Meyer used $[p_\nu q_\nu]_- = u_\nu = 2p_\nu q_\nu - 1$. But it is easy to verify that $[p_\nu q_\nu]_+ = 1$, which implies Eq. (12_1).

*However, $(c_k)^{N+m} = 0$ for $m > 0$, since it is impossible in the homopolar approximation to have more than N spins in the same direction.

Frank attempted to deduce the Fermi statistics from a direct solution of the Schrödinger equation. We have criticized this work in a paper with Ishmukhametov.[8] Here we only remark that it is unsafe to argue about the statistics of spin-waves on the basis of supplementary conditions in which functions of the type a_{nn}, which ought to vanish by virtue of the Pauli principle, are set equal to nonvanishing quantities. In this connection we may observe that the functions $u_2(R_i, R_i)$, which correspond to the a_{nn}, do vanish in the work of Van Kranendonk.[5]

3. We deduced the Bose statistics for spin-waves from two arguments. First, we showed that more than one spin-wave can exist in a state with a given wave-vector **k**. Second, we showed that when $r/N \ll 1$ the relations (17) to (19) coincide approximately with the usual Bose commutation rules. When we pass from the approximate relations (20) to the exact Bose commutation rules

$$[c_k c_{k'}^+]_- = \delta_{kk'}, \qquad [c_k c_{k'}]_- = [c_k^+ c_{k'}^+]_- = 0 \tag{23}$$

the occupation number n_k becomes unbounded above, although the actual number of spin waves[9] cannot exceed $N/2$. But in the low-temperature region, in which only states with a number of spin-waves small compared to N are measurably excited, the occupation numbers $n_k > N/2$ have no practical effect in calculations of thermodynamic quantities. The contributions from large n_k decrease exponentially. One can verify this by calculating the partition function Z, taking account of the boundedness of the occupation numbers* n_f, as was done in the paper of Tolmachev and Tiablikov.[10] If one uses the operators c_f defined above, one does not need any projection operator P to project the wave function onto the subspace of occupation numbers zero and one. The limitation of the occupation numbers is already included in the definition of the operators c_f. In the zero-order approximation the partition function becomes

$$Z_0 = \sum_{\{n_k\}} \sum_{\{n_f, n_f'\}} S(\ldots n_k \ldots | \ldots n_f \ldots)(a_{\ldots n_f \ldots} a_{\ldots n_f' \ldots}) \times S^*(\ldots n_k \ldots | \ldots n_f' \ldots) \exp\{-\sum_k E(k) n_k / \varkappa T\}, \tag{24}$$

Here T is the temperature, κ is Boltzmann's constant,

$$a_{\ldots n_f \ldots} = \prod_f (c_f)^{n_f} a_0 \tag{25}$$

are a system of orthonormal functions in the space of occupation numbers $n_f = 0$ or 1, a_0 is the vacuum state, and

$$S(\ldots n_f \ldots | \ldots n_k \ldots) = n^{-r/2} (\prod_k n_k!)^{-1/2} \sum_{\mathscr{P}_{f_h}} \prod_k \frac{1}{n_k!} \exp\{-ik(f_{h_1} + \ldots)\}, \tag{26}$$

where $\mathscr{P}_{f_h}$ is a permutation of all the right vertices f_h.

Equations (24) to (26) imply the result (15) of reference 10. This means that at low temperatures, for which $\exp(-E(k)/\kappa T) \ll 1$, the Bloch theory is valid. Compare also the paper of Dyson,[11] where the kinematical interaction, the boundedness of n_f, also produces an exponentially small effect.

So we see that in the low-temperature region it is actually possible to proceed from the approximate Bose relations (20) to the ordinary Bose commutation rules (23).

On the other hand it appears that the requirement that the ordinary Bose commutation rules be strictly valid is not consistent for a system of a finite number of particles, even when the system can be described by a wave-function which is symmetrical with respect to the interchange of particles. The fact is that Eq. (23) can only be satisfied by operators which are represented by infinite matrices. Thus the occupation numbers for particles or quasi-particles in the various states must be unbounded.

---

*The occupation number of right spins, which was denoted by N_f in Sec. 2, is denoted by n_f in Sec. 3. This is to bring the notations into agreement with those of reference 10.

Nevertheless, for a system to obey Bose statistics it is not necessary that the number of particles be unbounded.*

It seems helpful, when second quantizing a system with a finite number N_1 of particles obeying Bose statistics, to use finite-dimensional operators, which satisfy commutation rules different from (23), but keep the occupation numbers bounded. Repeating the usual derivation of the expression for the Hamiltonian of a system which obeys Bose statistics,[15]

$$\mathcal{H} = \sum_p n_p \varepsilon^{(p)} + \frac{1}{2} \sum_{p_1, p_2, p_3, p_4} b^+_{p_1} b^+_{p_2} (p_1, \ p_2 | G | p_3, \ p_4)\, b_{p_4} b_{p_3}, \tag{27}$$

one can verify that the same expression remains valid when one uses the operators

$$b_p = \beta_p \sqrt{n_p}\,, \qquad b_p^+ = \sqrt{n_p}\, \beta_p^+\,, \tag{28}$$

Here β_p and β_p^+ are defined by

$$\beta_p a(\ldots n_p \ldots) = [1 - \delta(n_p - N_1)]\, a(\ldots, n_p + 1, \ldots), \tag{29}$$

$$\beta_d^+ a(\ldots n_p \ldots) = [1 - \delta(n_p)]\, a(\ldots, \ n_p - 1, \ldots) \tag{30}$$

and can be represented by $(N_1 + 1)$-dimensional matrices of the form

$$\beta_p = \begin{vmatrix} 010\ldots0 \\ 001\ldots0 \\ \cdot\ \cdot\ \cdot\ \cdot \\ \cdot\ \cdot\ \cdot\ \cdot \\ 000\ldots1 \\ 000\ldots0 \end{vmatrix} \qquad \beta^+ - \begin{vmatrix} 00\ldots000 \\ 10\ldots000 \\ \cdot\ \cdot\ \cdot\ \cdot\ \cdot \\ \cdot\ \cdot\ \cdot\ \cdot\ \cdot \\ 00\ldots100 \\ 00\ldots010 \end{vmatrix} \tag{31}$$

Equations (28) to (31) imply the following relations between the operators b_p and b_p^+:

$$b_p^+ b_p = n_p\,, \qquad b_p b_p^+ = (n_p + 1)\,[1 - \delta(n_p - N_1)]\,, \tag{32}$$

$$[b_p b_p^+]_- = 1 - (n_p + 1)\, \delta(n_p - N_1), \tag{33$_1$}$$

$$[b_p b_{p'}^+]_- = 0 \qquad (\text{for } p \neq p'), \tag{33$_2$}$$

$$[b_p b_{p'}]_- = [b_p^+ b_{p'}^+]_- = 0\,. \tag{33$_3$}$$

The commutation rules arising from the second quantization of a Bose system of a fixed finite number of particles thus differ from the usual commutation rules by the extra term $(n_p + 1)\,\delta(n_p - N_1)$ on the right side of Eq. (33$_1$). This term makes it impossible for any occupation number to exceed the value $(n_p)_{\max} = N_1$. To prove this, one can calculate the matrix element of the expression

$$n_p b_p - b_p n_p = -[1 - (n_p + 1)\, \delta(n_p - N_1)]\, b_p\,, \tag{34}$$

by using Eq. (33). In the representation in which n_p is diagonal, the matrix element of b_p can differ from zero only when

$$n'_p - n''_p = -[1 - (n'_p + 1)\, \delta(n'_p - N_1)]\,, \tag{35}$$

which implies

$$n''_p = \begin{cases} n'_p + 1 & \text{for } n'_p < N_1 \\ 0 & \text{for } n'_p = N_1 \end{cases}, \tag{36}$$

Thus n_p can actually never exceed N_1.

We now apply the above arguments in the limiting cases $(n_p)_{\max} = \infty$ and $(n_p)_{\max} = 1$. In the first case Eq. (33) reduce to the usual Bose relations, since for any value of n_p the δ-function on the right of Eq. (33$_1$) vanishes when $(n_p)_{\max} = \infty$. In the second case we may use Eq. (32) to transform (33$_1$) into

$$[b_p b_p^+]_+ = 2n_p + 1 - (n_p + 1)\, \delta(n_p - 1) = 1\,, \tag{37}$$

Together with Eq. (33$_2$) and (33$_3$), this gives the plus-minus quantization rules (12), so that the latter may be considered to be a special case of the quantization of a system with bounded occupation numbers. If the index f had referred to a cell in phase-space instead of to a vertex of a lattice, the boundedness of the occupation numbers n_f would have led in general to intermediate statistics.[13] But in the case considered in section (2), after transforming to momentum-space, the occupation numbers n_k were bounded only by the total number of spin-waves which could exist in the given system. This justifies the use of Bose statistics at low temperatures.

4. We now consider the problem of polar excitations. The Hamiltonian for a many-electron system with polar states may be written in the following form, in the notation of second quantization:[16,17]

$$\mathcal{H} = \sum g(f, f')\, a^+_{f\sigma} a_{f'\sigma} + \frac{1}{2} \sum F(f_1, f_2; \ f'_1, \ f'_2)\, a^+_{f_1\sigma_1} a^+_{f_2\sigma_2} a_{f'_2\sigma_2} a_{f'_1\sigma_1} \tag{38}$$

Here all the indices are to be summed. The σ are spin indices. The $a^+_{f\sigma}$ and $a_{f\sigma}$ are Fermi operators which operate on the occupation numbers $n_{f\sigma}$ of states (f, σ) whose wave-functions θ_f form an orthonormal system. The $g(f, f')$ and $F(f_1, f_2; f'_1, f'_2)$ are matrix elements:

$$g(f, f') = \int \theta_f(r) \left[-\frac{\hbar^2}{2m} \nabla^2 + \sum_{f''} u_{f''}(r) \right] \theta_{f'}(r)\, dr, \tag{39}$$

$$F(f_1, f_2; \ f'_1, \ f'_2) = \int \Phi(r, r')\, \theta_{f_1}(r)\, \theta_{f'_1}(r)\, \theta_{f_2}(r')\, \theta_{f'_2}(r')\, dr\, dr' \tag{40}$$

---

*Sommerfeld[12] showed that one can use, instead of the usual Bose-Einstein distribution function, the distribution function of Gentile,[13] putting $(n_p)_{\max} = N_1$. However, in the approximation in which we use the Stirling formula, the improvement so obtained is inconsequential.[14]

Here $u_f(r)$ is the potential energy of an electron in the field of the atomic core at vertex f, while $\Phi(r, r')$ is the potential energy of the Coulomb repulsion between two electrons. Keeping in Eq. (38) those matrix elements which contain not more than two distinct functions θ_f in the integrand, and using the Fermi commutation rules

$$[a_{f\sigma}a^{+}_{f'\sigma'}]_{+} = \delta_{f\sigma,f'\sigma'}, \quad [a_{f\sigma}a_{f'\sigma'}]_{+} = [a^{+}_{f\sigma}a^{+}_{f'\sigma'}]_{+} = 0, \tag{41}$$

we derive from Eq. (38)

$$\begin{aligned} \mathscr{H} &= \sum_{f} g(f, f)\, n_f + \tfrac{1}{2} A \sum_{f} n_f (n_f - 1) \\ &\quad + \tfrac{1}{2} \sum_{f \neq f'} B_{ff'} n_f n_{f'} - \tfrac{1}{2} \sum_{f \neq f'} J_{ff'} \sum_{\sigma} n_{f\sigma} n_{f'\sigma} \\ &\quad + \sum_{f \neq f'} L_{ff'} \sum_{\sigma} a^{+}_{f\sigma} a_{f'\sigma} + \tfrac{1}{2} \sum_{f \neq f'} J_{ff'} \sum_{\sigma_1, \sigma_2} a^{+}_{f\sigma_1} a^{+}_{f\sigma_2} a_{f'\sigma_2} a_{f'\sigma_1} \\ &\quad + \tfrac{1}{2} \sum_{f \neq f'} J_{ff'} \sum_{\sigma_1 \neq \sigma_2} a^{+}_{f\sigma_1} a^{+}_{f'\sigma_2} a_{f\sigma_2} a_{f'\sigma_1}. \end{aligned} \tag{42}$$

Here

$$A = F(f, f; f, f) = \int \Phi(r, r')\, \theta_f^2(r)\, \theta_f^2(r')\, dr\, dr' \tag{43}$$

is the interaction energy between two electrons in the same state θ_f (the self-energy of a pair).

$$B_{ff'} = F(f, f'; f, f') = \int \Phi(r, r')\, \theta_f^2(r)\, \theta_{f'}^2(r')\, dr\, dr' \tag{44}$$

is the energy of Coulomb repulsion of two electrons, one in the state θ_f and the other in the state $\theta_{f'}$.

$$L_{ff'} = g(f, f') + \sum_{f_1} (n_{f_1} - \delta_{ff_1})\, F(f_1, f; f_1, f') \tag{45}$$

is a displacement integral, and

$$\begin{gathered} J_{ff'} = F(f, f'; f', f) = \\ \int \Phi(r, r')\, \theta_f(r)\, \theta_{f'}(r)\, \theta_{f'}(r')\, \theta_f(r')\, dr\, dr' \end{gathered} \tag{46}$$

is an exchange integral. In addition we have used the notation $n_f = \sum_{\sigma} n_{f\sigma}$.

We now define a set of Fermi operators[15]

$$a_{f\sigma} = \alpha_{f\sigma} \nu_{f\sigma}, \quad a^{+}_{f\sigma} = \nu_{f\sigma} \alpha^{+}_{f\sigma}, \tag{47}$$

where $\nu_{f\sigma}$ are the sign functions of Wigner, and the operators $\alpha_{f\sigma}$ and $\alpha^{+}_{f\sigma}$ act according to the rules

$$\alpha_{f\sigma} a(\ldots n_{f\sigma} \ldots) = \begin{cases} a(\ldots, n_{f\sigma} + 1, \ldots) & \text{for } n_{f\sigma} = 0 \\ 0 & \text{for } n_{f\sigma} = 1 \end{cases} \tag{48$_1$}$$

$$\alpha^{+}_{f\sigma} a(\ldots n_{f\sigma} \ldots) = \begin{cases} 0 & \text{for } n_{f\sigma} = 0 \\ a(\ldots, n_{f\sigma} - 1, \ldots) & \text{for } n_{f\sigma} = 1. \end{cases} \tag{48$_2$}$$

It is easy to verify that the sign functions compensate each other in the diagonal terms and in those of the nondiagonal terms (42) which contain the exchange integrals $J_{ff'}$. But in the terms containing $L_{ff'}$ the functions do not compensate. It is convenient to consider two limiting cases: (a) $|L| \gg |J|$ and (b) $|L| \ll |J|$. Here L and J are the values of $L_{ff'}$ and $J_{ff'}$ for nearest neighbors.

In case (a) the nondiagonal terms are dominated by the term $\sum L_{ff'} \sum a^{+}_{f\sigma} a_{f'\sigma}$ which contains a double product of operators $a^{+}_{f\sigma} a_{f'\sigma}$ and describes one-electron transitions. The effect of such transitions upon an electron with left spin will be one of the following: exchange of places between a hole and a left spin, creation of a hole in place of a left spin, creation of a pair in place of a right spin, creation of two single spins in place of a pair and a hole, and finally exchange of places between a pair and a right spin. Analogous processes exist for the transitions of an electron with right spin. We now make a Fourier transformation of the operators $a_{f\sigma}$ and $a^{+}_{f\sigma}$ according to Eq. (15). The resulting operators $a_{k\sigma}$ and $a^{+}_{k\sigma}$ obey Fermi commutation rules of the type of Eq. (41). This shows that the quasi-particles in case (a) obey Fermi statistics.

In case (b) the nondiagonal terms are dominated by the last two sums in Eq. (42), which contain a product of four operators $a_{f\sigma}$ and describe two-electron transitions. Of these sums, the sixth term in Eq. (42) represents an exchange between a pair and a hole, while the last term represents an exchange between a left and a right spin. In this case we are neglecting the processes of creation and annihilation of pairs in one-electron transitions. It is therefore convenient to introduce operators acting upon the occupation numbers of pairs, holes and simple right and left spins. We change slightly the notations used in reference 16 in order to be consistent with Eq. (6). The new operators Φ_f, Ψ_f, φ_f and ψ_f are defined as follows:

$$\begin{gathered} \Phi_f a(\ldots P_f, Q_f, R_f, S_f \ldots) \\ = \delta(1 - P_f)\, a(\ldots P_f - 1, Q_f, R_f, S_f \ldots), \end{gathered} \tag{49}$$

$$\begin{gathered} \Phi^{+}_f a(\ldots P_f, Q_f, R_f, S_f \ldots) \\ = \delta(P_f)\, a(\ldots P_f + 1, Q_f, R_f, S_f \ldots). \end{gathered} \tag{50}$$

Analogously we define Ψ_f, Ψ^{+}_f, ψ_f, ψ^{+}_f, φ_f and φ^{+}_f. Here P_f, Q_f, R_f and S_f take the following values:

$$\begin{array}{ccccl} P_f & Q_f & R_f & S_f & \\ 1 & 0 & 0 & 0 & \text{if the vertex } f \text{ is a pair,} \\ 0 & 1 & 0 & 0 & \text{if the vertex } f \text{ is a hole,} \\ 0 & 0 & 1 & 0 & \text{if the vertex } f \text{ is a right-spin,} \\ 0 & 0 & 0 & 1 & \text{if the vertex } f \text{ is a left-spin.} \end{array} \tag{51}$$

The same argument which led to Eq. (7) now shows that the operators Ψ_f, Φ_f, φ_f and ψ_f satisfy the following relations:

$$\begin{aligned}
&[\Phi_f\Phi_f^+]_+ = [\Psi_f\Psi_f^+]_+ = [\varphi_f\varphi_f^+]_+ = [\psi_f\psi_f^+]_+ = 1,\\
&[\Phi_{f'}\Phi_f^+]_- = [\Psi_{f'}\Psi_f^+]_- = [\varphi_f\varphi_{f'}^+]_- = [\psi_f\psi_{f'}^+]_- = 0 \ (\text{for } f \neq f'),\\
&[\Phi_f\Phi_{f'}]_- = [\Psi_f\Psi_{f'}]_- = [\varphi_f\varphi_{f'}]_- = [\psi_f\psi_{f'}]_- = 0,\\
&[\Phi_f^+\Phi_{f'}^+]_- = [\Psi_f^+\Psi_{f'}^+]_- = [\varphi_f^+\varphi_{f'}^+]_- = [\psi_f^+\psi_{f'}^+]_- = 0.
\end{aligned} \tag{52}$$

We thus find a plus-minus quantization similar to Eq. (7). For the reasons discussed in Sec. 2, the quasi-particles in momentum-space now obey Bose statistics.

The choice between the limiting cases (a) and (b) depends on the ratio between the positive and negative terms in the displacement integral $L_{ff'}$. If these terms are approximately equal then $|L_{ff'}| \ll |J_{ff'}|$. But if terms of one sign predominate in $L_{ff'}$, then $|L_{ff'}| \gg |J_{ff'}|$, for $J_{ff'}$ contains one overlap factor more than $L_{ff'}$. The latter state of affairs will exist, for example, among the terms $g(f, f')$, which are proportional to the effective charge of the atomic core and are negative at least for S-states.

5. We have reached the conclusion that the quasi-particles arising in a many-electron system in a crystal obey Fermi statistics when one-electron transitions are predominant, and obey Bose statistics when two-electron transitions are predominant in the dynamics of the system.* The well-known connection between spin and statistics, according to which particles with half-integer spin obey Fermi statistics and particles with integer spin Bose statistics, is thus preserved. In a single-electron transition in a crystal a half-integer spin moves, while in a two-electron transition an integer spin moves. Our results here confirm the statement of I. M. Lifshitz[4] at the Kiev conference on semiconductors in 1956, concerning the statistics of pairs and holes.*

[1] D. Frank, Z. Physik **146**, 615 (1956).

[2] K. Meyer, Z. Naturforsch. **11a**, 865, (1956).

[3] I. Mannari, Prog. Theor. Phys. **19**, 201 (1958).

[4] M. F. Deigen, I. M. Dykman and K. B. Tolpygo, J. Tekh. Fiz. **27**, 1628 (1957), Sov. Phys. (JTP), **2**, 1513 (1957).

[5] J. Van Kranendonk, Physica, **21**, 749 (1955).

[6] W. Marshall, Proc. Roy. Soc. **A232**, 69 (1955).

[7] F. Bloch, Z. Physik **74**, 295 (1932).

[8] M. S. Svirskii, and B. Kh. Ishmukhametov, **Физика металлов и металловедение** (Physics of Metals and Metal Research) **5**, 548 (1957).

[9] H. A. Bethe and A. Sommerfeld, Elektronentheorie der Metallen (Russ. Transl.) Moscow, 1938, p. 289 [Handb. Physik, B 24/2, 2 Aufl. Berlin, 1933].

[10] V. V. Tolmachev and S. V. Tiablikov, Dokl. Akad. Nauk, SSSR. **108**, 1029 (1956).

[11] F. J. Dyson, Phys. Rev. **102**, 1217 and 1230 (1956).

[12] A. Sommerfeld, Ber. Deutsch. Chem. Ges. **75**, 1988 (1942).

[13] G. Gentile, Nuovo cimento **17**, 493 (1940).

[14] G. Schubert, Z. Naturforsch. **1**, 113 (1946).

[15] V. A. Fok, Z. Physik **75**, 622 and **76**, 852 (1932). P. Gombás, The Many-body Problem in Quantum Mechanics, Moscow, 1958; [Birkhäuser, Basel, 1950.]

[16] S. V. Vonsovskii, Usp. Fiz. Nauk, **48**, 329 (1952).

[17] N. N. Bogoliubov, **Лекції з квантової статистики** (Lectures on Quantum Statistics) Kiev, 1949.

Translated by F. J. Dyson
306

---

*The term "transition" is to be understood to refer to the particular model chosen.

*We take the opportunity to thank I. M. Lifshitz for calling this problem to our attention.

SOVIET PHYSICS JETP VOLUME 35(8), NUMBER 6 JUNE, 1959

ON COORDINATE CONDITIONS IN EINSTEIN'S GRAVITATION THEORY

I. G. FIKHTENGOL' TS

Submitted to JETP editor June 17, 1958

J. Exptl. Theoret. Phys. (U.S.S.R.) **35**, 1457-1465 (December, 1958)

Certain relations connected with the covariance of field equations under transformation of variables are derived. The connection between coordinate conditions and invariance of the field Lagrangian is established. The geometrical and physical properties of the coordinate systems corresponding to the coordinate conditions thus derived are considered.

As is well known, only six of the ten equations in Einstein's theory of gravitation are independent, as a consequence of the conservative character of the Einstein tensor (and mass tensor). Therefore, when obtaining the fundamental field tensor, four additional relations among its components must be stated beside the Einstein gravitation equations and boundary conditions.* Since the choice of these four additional relations fixes the coordinate system in which the gravitational field will be studied, they are usually referred to as the coordinate conditions.

In contradistinction to the covariant character of the Einstein gravitation equations, the aggregate of additional conditions should not be covariant, since a covariant system of equations admits of arbitrary coordinate transformations and therefore determines the quantities sought only within four arbitrary functions. At the same time the covariant character of the Einstein gravitation equations permits one to choose arbitrary coordinate conditions (provided they do not contradict each other or the gravitation equations) and so the question arises: which of the permissible coordinate conditions are preferable when the peculiarities of the given physical problem are taken into account? Closely connected with this is the study of the physical and geometrical properties of the coordinate system chosen; it is scarcely possible to give a consistent physical interpretation of the solution of the field equations without the knowledge of these properties.

The above problems, which have been repeatedly investigated (see, e.g., reference 1), form the subject of the present work (Secs. 3 to 5). At the same time certain general problems connected with the covariance of field equations under transformation of variables are investigated (Secs. 1 and 2).

1. CONSEQUENCES OF COVARIANCE OF FIELD EQUATIONS

We start with the investigation of arbitrary fields whose equations may be written in the Lagrangian formalism

$$\frac{\partial \mathscr{L}}{\partial q_l} - \sum_{k=1}^{n} \frac{\partial}{\partial x_k} \frac{\partial \mathscr{L}}{\partial (\partial q_l / \partial x_k)} = 0 \quad (l = 1, 2, \ldots, m), \qquad (1)$$

where $\mathscr{L} = \mathscr{L}([x_i], [q_j], [\partial q_j/\partial x_i])$ is the field Lagrangian, $[x_i]$ stands for the aggregate of the independent variables $(i = 1, 2 \ldots n)$, and $[q_j]$ stands for the aggregate of the unknown functions $(j = 1, 2 \ldots m)$.

To establish just what consequences follow from covariance of the field equations let us pass in Eq. (1) from the variables $x_k (k = 1, 2 \ldots n)$ and $q_l (l = 1, 2 \ldots m)$ to the new variables x'_k, q'_l defined by

$$x'_k = x'_k([x_i], \varepsilon), \quad q'_l = q'_l([x_i], [q_j], \varepsilon), \qquad (2)$$

where ϵ is some parameter, and

$$(x'_k)_{\varepsilon=0} = x_k, \quad (q'_l)_{\varepsilon=0} = q_l. \qquad (3)$$

It is easy to show, following the methods of references 3 to 5, that if Eq. (1) is covariant under the one-parameter family of transformations defined by Eqs. (2) and (3) then the following is true:

$$\sum_{k=1}^{n} \frac{\partial}{\partial x_k} \left\{ \mathscr{L} \left(\frac{\partial x'_k}{\partial \varepsilon} \right)_{\varepsilon=0} - \sum_{i=1}^{n} \sum_{j=1}^{m} \frac{\partial \mathscr{L}}{\partial (\partial q_j / \partial x_k)} \frac{\partial q_j}{\partial x_i} \left(\frac{\partial x'_i}{\partial \varepsilon} \right)_{\varepsilon=0} + \sum_{j=1}^{m} \frac{\partial \mathscr{L}}{\partial (\partial q_j / \partial x_k)} \left(\frac{\partial q'_j}{\partial \varepsilon} \right)_{\varepsilon=0} - \left(\frac{\partial f_k}{\partial \varepsilon} \right)_{\varepsilon=0} \right\} = 0, \qquad (4)$$

where we understand by $\mathscr{L}$ the untransformed $\mathscr{L}([x_i], [q_j], [\partial q_j/\partial x_i])$ and the functions $f_k = f_k([x_i], [q_j], \epsilon)$ are determined, corresponding to the structure of $\mathscr{L}$ and of the transformation (2), by the equality

---

*It is also necessary to give the equation of state of the masses under study (see, e.g. references 1 and 2).

$$\mathcal{L}^*([x_i],\ [q_j],\ [\partial q_j/\partial x_i],\ \varepsilon) - \mathcal{L}([x_i],\ [q_j],\ [\partial q_j/\partial x_i]) = \sum_{k=1}^{n} \partial f_k([x_i],\ [q_j],\ \varepsilon)/\partial x_k, \tag{5}$$

where

$$\mathcal{L}^*\left([x_i],\ [q_j],\ \left[\frac{\partial q_j}{\partial x_i}\right],\ \varepsilon\right) = \mathcal{L}\left([x_i'],\ [q_j'],\ \left[\frac{\partial q_j'}{\partial x_i'}\right]\right) \frac{D(x_1',\ x_2',\ x_3',\ \ldots,\ x_n')}{D(x_1,\ x_2,\ x_3,\ \ldots,\ x_n)} \tag{6}$$

with x_i', q_j' given by the transformation (2).

The existence of a system of functions f_k which satisfy condition (5) is equivalent to the requirement of covariance of Eq. (1) under the transformation (2). In the special case when the function $\mathcal{L}$ and the transformation (2) are such that the equality $\mathcal{L}^* = \mathcal{L}$ holds, it is possible to put all f_k equal to zero. The function $\mathcal{L}$ is then a relative invariant under the transformation (2) — relative, because the expression for $\mathcal{L}^*$ contains as a factor the Jacobian of the transformation.

We now specify that the field under discussion is a tensor field. Although the results to be established are applied only to the Einstein gravitation equations (in the region outside of masses) to begin with we shall not use the explicit form of the Lagrangian $\mathcal{L}$ but will take $\mathcal{L} = \mathcal{L}([x_\alpha], [g_{\mu\nu}], [\partial g_{\mu\nu}/\partial x_\alpha])$ where $g_{\mu\nu}$ is the fundamental (metric) tensor.* Equations (1) become

$$\frac{\partial \mathcal{L}}{\partial g_{\mu\nu}} - \frac{\partial}{\partial x_\alpha} \frac{\partial \mathcal{L}}{\partial(\partial g_{\mu\nu}/\partial x_\alpha)} = 0. \tag{1$'$}$$

In these equations and in the following greek indices take on the values 0, 1, 2, 3 and repeated indices are to be summed over from 0 to 3.

If Eq. (1′) is covariant under a certain family of coordinate transformations defined by

$$x_\beta' = x_\beta'([x_\alpha],\ \varepsilon), \tag{2$'$}$$

$$(x_\beta')_{\varepsilon=0} = x_\beta, \tag{3$'$}$$

then Eq. (4) becomes

$$\frac{\partial}{\partial x_\alpha}\left\{\mathcal{L}\left(\frac{\partial x_\alpha'}{\partial \varepsilon}\right)_{\varepsilon=0} - \frac{\partial \mathcal{L}}{\partial(\partial g_{\mu\nu}/\partial x_\alpha)} \frac{\partial g_{\mu\nu}}{\partial x_\beta}\left(\frac{\partial x_\beta'}{\partial \varepsilon}\right)_{\varepsilon=0} + \frac{\partial \mathcal{L}}{\partial(\partial g_{\mu\nu}/\partial x_\alpha)}\left(\frac{\partial g_{\mu\nu}'}{\partial \varepsilon}\right)_{\varepsilon=0} - \left(\frac{\partial f_\alpha}{\partial \varepsilon}\right)_{\varepsilon=0}\right\} = 0. \tag{4$'$}$$

The equality (4′) can be substantially simplified due to the fact that the transformation of the dependent variables is, as a consequence of their tensor character, determined entirely by the transformation of the independent variables:

$$g_{\mu\nu}' = \frac{\partial x_\alpha}{\partial x_\mu'} \frac{\partial x_\beta}{\partial x_\nu'} g_{\alpha\beta}. \tag{7}$$

Consequently the derivatives of $g_{\mu\nu}'$ with respect to ϵ can be eliminated from Eq. (4′).

Since

$$\left(\frac{\partial g_{\mu\nu}'}{\partial \varepsilon}\right)_{\varepsilon=0} = -g_{\mu\beta}\frac{\partial}{\partial x_\nu}\left(\frac{\partial x_\beta'}{\partial \varepsilon}\right)_{\varepsilon=0} - g_{\nu\beta}\frac{\partial}{\partial x_\mu}\left(\frac{\partial x_\beta'}{\partial \varepsilon}\right)_{\varepsilon=0},$$

we conclude that if Eq. (1′) is covariant under a certain one-parameter family of transformations defined by Eqs. (2′) and (3′) [and, of course, (7)] then the following relation holds

$$\frac{\partial}{\partial x_\alpha}\left\{\mathcal{L}\left(\frac{\partial x_\alpha'}{\partial \varepsilon}\right)_{\varepsilon=0} - \frac{\partial \mathcal{L}}{\partial(\partial g_{\mu\nu}/\partial x_\alpha)} \frac{\partial g_{\mu\nu}}{\partial x_\beta}\left(\frac{\partial x_\beta'}{\partial \varepsilon}\right)_{\varepsilon=0} - 2\frac{\partial \mathcal{L}}{\partial(\partial g_{\mu\nu}/\partial x_\alpha)} g_{\mu\beta}\frac{\partial}{\partial x_\nu}\left(\frac{\partial x_\beta'}{\partial \varepsilon}\right)_{\varepsilon=0} - \left(\frac{\partial f_\alpha}{\partial \varepsilon}\right)_{\varepsilon=0}\right\} = 0, \tag{8}$$

where f_α is determined from an equation analogous to Eq. (5), corresponding to the structure of $\mathcal{L}$ and of the transformation (2′).

Taking into account the identity

$$\frac{\partial \mathcal{L}}{\partial(\partial g_{\mu\nu}/\partial x_\alpha)} = -g^{\mu\sigma}g^{\nu\tau}\frac{\partial \mathcal{L}}{\partial(\partial g^{\sigma\tau}/\partial x_\alpha)},$$

it is possible to express the relation (8) in a different form, which is more convenient for applications, if the unknown in the field equations is taken to be the contravariant fundamental tensor $g^{\mu\nu}$ rather than the covariant tensor $g_{\mu\nu}$.

2. TENSOR FIELD WITH A LINEARLY-INVARIANT LAGRANGIAN

Using Eq. (8) we now establish just what consequences follow from the assumption that the Lagrangian $\mathcal{L}$ is a relative invariant* under arbitrary linear coordinate transformations. We shall refer to such an $\mathcal{L}$, for brevity, as linearly invariant (omitting the word "relative").

In an n-dimensional space the most general linear coordinate transformation contains $n(n + 1)$ parameters. We are interested in the case of space-time which is four-dimensional and, consequently, the number of parameters is 20.

It is easy to show that the most general linear transformation of the coordinates x_0, x_1, x_2, x_3 can be expressed as a linear combination with constant coefficients of the following twenty simple (one-parameter) linear transformations:

---

*The discussion is analogous for the case $\mathcal{L} = \mathcal{L}([x_\alpha], [A^{(\nu)}_{(\mu)}], [\partial A^{(\nu)}_{(\mu)}/\partial x_\alpha])$ where $A^{(\nu)}_{(\mu)} = A^{\nu_1 \ldots\ \nu_m}_{\mu_1 \ldots\ \mu_l}$ is a tensor of rank $(l + m)$.

*I.e. $\mathcal{L}^* = \mathcal{L}$ where $\mathcal{L}^*$ is determined by an equation of the same type as Eq. (6).

$$\begin{array}{rllll}
1) & x_0' = x_0 + \varepsilon & x_1' = x_1 & x_2' = x_2 & x_3' = x_3, \\
2) & x_0' = x_0 & x_1' = x_1 + \varepsilon & x_2' = x_2 & x_3' = x_3, \\
3) & x_0' = x_0 & x_1' = x_1 & x_2' = x_2 + \varepsilon & x_3' = x_3, \\
4) & x_0' = x_0 & x_1' = x_1 & x_2' = x_2 & x_3' = x_3 + \varepsilon, \\
5) & x_0' = x_0 & x_1' = x_1 - \varepsilon x_2 & x_2' = \varepsilon x_1 + x_2 & x_3' = x_3, \\
6) & x_0' = x_0 & x_1' = x_1 + \varepsilon x_3 & x_2' = x_2 & x_3' = -\varepsilon x_1 + x_3, \\
7) & x_0' = x_0 & x_1' = x_1 & x_2' = x_2 - \varepsilon x_3 & x_3' = \varepsilon x_2 + x_3, \\
8) & x_0' = x_0 - \varepsilon x_1 & x_1' = -\varepsilon x_0 + x_1 & x_2' = x_2 & x_3' = x_3, \\
9) & x_0' = x_0 - \varepsilon x_2 & x_1' = x_1 & x_2' = -\varepsilon x_0 + x_2 & x_3' = x_3, \\
10) & x_0' = x_0 - \varepsilon x_3 & x_1' = x_1 & x_2' = x_2 & x_3' = -\varepsilon x_0 + x_3, \\
11) & x_0' = (1 + \varepsilon) x_0 & x_1' = x_1 & x_2' = x_2 & x_3' = x_3, \\
12) & x_0' = x_0 & x_1' = (1 + \varepsilon) x_1 & x_2' = x_2 & x_3' = x_3, \\
13) & x_0' = x_0 & x_1' = x_1 & x_2' = (1 + \varepsilon) x_2 & x_3' = x_3, \\
14) & x_0' = x_0 & x_1' = x_1 & x_2' = x_2 & x_3' = (1 + \varepsilon) x_3, \\
15) & x_0' = x_0 & x_1' = x_1 + \varepsilon x_2 & x_2' = \varepsilon x_1 + x_2 & x_3' = x_3. \\
16) & x_0' = x_0 & x_1' = x_1 + \varepsilon x_2 & x_2' = x_2 & x_3' = \varepsilon x_1 + x_3, \\
17) & x_0' = x_0 & x_1' = x_1 & x_2' = x_2 + \varepsilon x_3 & x_3' = \varepsilon x_2 + x_3, \\
18) & x_0' = x_0 - \varepsilon x_1 & x_1' = \varepsilon x_0 + x_1 & x_2' = x_2 & x_3' = x_3, \\
19) & x_0' = x_0 - \varepsilon x_2 & x_1' = x_1 & x_2' = \varepsilon x_0 + x_2 & x_3' = x_3, \\
20) & x_0' = x_0 - \varepsilon x_3 & x_1' = x_1 & x_2' = x_2 & x_3' = \varepsilon x_0 + x_3.
\end{array} \qquad (9)$$

We note that the transformations $(9)_1$ to $(9)_{10}$ are special cases of infinitesimal Lorentz transformations, whereas the remaining transformations $(9)_{11}$ to $(9)_{20}$ do not belong to the Lorentz transformations group.

Let us now assume that the Lagrangian $\mathscr{L}$ is linearly invariant. It is then, in particular, a relative invariant under each of the twenty simple transformations (9). Using Eq. (8), we deduce from this fact the following consequences:

From the relative invariance of $\mathscr{L}$ under the translation of the origin of time coordinate x_0 [transformation $(9)_1$] and of the space coordinates x_1, x_2, x_3 [transformations $(9)_2$ to $(9)_4$] it follows that $\mathscr{L}$ is not an explicit function of x_0, x_1, x_2, x_3, i.e., $\mathscr{L} = \mathscr{L}([g_{\mu\nu}], [\partial g_{\mu\nu}/\partial x_\alpha])$.

For a Lagrangian $\mathscr{L}$, which is not an explicit function of x_α, we obtain, after some calculations, the following relations $(10)_k$ corresponding to relative invariance under the transformations $(9)_k$ $(k = 5, 6, \ldots, 20)$ respectively

$$\begin{array}{ll}
5)\ N_1^2 = N_2^1, & 6)\ N_1^3 = N_3^1, \\
7)\ N_2^3 = N_3^2, & 8)\ N_0^1 = -N_1^0, \\
9)\ N_0^2 = -N_2^0, & 10)\ N_0^3 = -N_3^0, \\
11)\ N_0^0 = \mathscr{L}, & 12)\ N_1^1 = \mathscr{L}, \\
13)\ N_2^2 = \mathscr{L}, & 14)\ N_3^3 = \mathscr{L}, \\
15)\ N_1^2 = -N_2^1, & 16)\ N_1^3 = -N_3^1, \\
17)\ N_2^3 = -N_3^2, & 18)\ N_0^1 = N_1^0, \\
19)\ N_0^2 = N_2^0, & 20)\ N_0^3 = N_3^0,
\end{array} \qquad (10)$$

where

$$N_\alpha^\beta = \frac{\partial g_{\mu\nu}}{\partial x_\alpha} \frac{\partial \mathscr{L}}{\partial (\partial g_{\mu\nu} / \partial x_\beta)} + 2 g_{\mu\alpha} \frac{\partial \mathscr{L}}{\partial g_{\mu\beta}} + 2 \frac{\partial g_{\mu\alpha}}{\partial x_\nu} \frac{\partial \mathscr{L}}{\partial (\partial g_{\mu\beta} / \partial x_\nu)}.$$

Collecting the relations (10) we conclude

$$N_\alpha^\beta = \mathscr{L} \delta_{\alpha\beta}.$$

Consequently, the Lagrangian $\mathscr{L}$ is linearly invariant if it is not an explicit function of the variables x_α and if it satisfies the following system of equations:

$$\frac{\partial g_{\mu\nu}}{\partial x_\alpha} \frac{\partial \mathscr{L}}{\partial (\partial g_{\mu\nu} / \partial x_\beta)} + 2 g_{\mu\alpha} \frac{\partial \mathscr{L}}{\partial g_{\mu\beta}} + 2 \frac{\partial g_{\mu\alpha}}{\partial x_\nu} \frac{\partial \mathscr{L}}{\partial (\partial g_{\mu\beta} / \partial x_\nu)} = \mathscr{L} \delta_{\alpha\beta}.$$

We next assume that Eq. (1′) with a linearly invariant Lagrangian is, in addition, covariant under a certain family of nonlinear transformations defined by Eqs. (2′) and (3′). Again starting from the relation (8) we now obtain

$$\frac{\partial \mathscr{L}}{\partial (\partial g_{\mu\nu} / \partial x_\alpha)} g_{\beta\nu} \frac{\partial^2}{\partial x_\alpha \partial x_\mu} \left(\frac{\partial x_\beta'}{\partial \varepsilon} \right)_{\varepsilon=0} = -\frac{1}{2} \frac{\partial}{\partial x_\alpha} \left(\frac{\partial f_\alpha}{\partial \varepsilon} \right)_{\varepsilon=0}, \qquad (11)$$

where the function f_α is determined, as before, by an equation analogous to Eq. (5), corresponding to the structure of $\mathscr{L}$ and of the transformation (2′).

It follows from Eq. (11) that the linearly invariant Lagrangian under discussion will also be a relative invariant under this family of nonlinear transformations if

$$\frac{\partial \mathscr{L}}{\partial(\partial g_{\mu\nu}/\partial x_\alpha)} g_{\beta\nu} \frac{\partial^2}{\partial x_\alpha \partial x_\mu}\left(\frac{\partial x'_\beta}{\partial \varepsilon}\right)_{\varepsilon=0} = 0. \tag{12}$$

In the case of infinitesimal transformations

$$x'_\beta = x_\beta + \varepsilon a^\beta (x_0,\ x_1,\ x_2,\ x_3) \quad (\beta = 0, 1, 2, 3), \tag{13}$$

Equation (12) becomes

$$a^\beta_{\alpha\mu} g_{\beta\nu} \frac{\partial \mathscr{L}}{\partial(\partial g_{\mu\nu}/\partial x_\alpha)} = 0, \tag{14}$$

where we have introduced the abbreviation

$$a^\beta_{\alpha\mu} = \partial^2 a^\beta (x_0, x_1, x_2, x_3)/\partial x_\alpha \partial x_\mu. \tag{15}$$

We note that relation (14) is not only a necessary but also a sufficient condition for the linearly invariant Lagrangian $\mathscr{L}$ to be a relative invariant under the infinitesimal transformation (13).

Relation (14) will be taken as the starting point in the discussion of the problem of coordinate conditions in the Einstein theory of gravitation.

3. RELATION BETWEEN COORDINATE CONDITIONS AND INVARIANCE OF THE FIELD LAGRANGIAN

As is well known, the Einstein gravitation equations, in a region outside of masses, may be expressed in the Lagrangian formalism (1′) with the following Lagrangian:

$$\mathscr{L} = \sqrt{-g}L, \quad \text{where} \quad L = g^{\mu\nu}(\Gamma^\beta_{\mu\alpha}\Gamma^\alpha_{\nu\beta} - \Gamma^\alpha_{\mu\nu}\Gamma^\beta_{\alpha\beta}). \tag{16}$$

In these formulas g stands for the determinant formed from the components of the fundamental tensor $g_{\mu\nu}$ and $\Gamma^\alpha_{\mu\nu}$ stands for the Christoffel symbol of the second kind.

Let us show that the above Lagrangian $\mathscr{L}$ is linearly invariant.

From the general transformation properties of the determinant g (see, e.g., reference 1)

$$\sqrt{-g'}\,\frac{D(x'_0,\ x'_1,\ x'_2,\ x'_3)}{D(x_0,\ x_1,\ x_2,\ x_3)} = \sqrt{-g},$$

we conclude that the requirement $\mathscr{L}^* = \mathscr{L}$, when applied to the present $\mathscr{L}$ [see Eq. (16)], is equivalent to the condition $L' = L$. Consequently the requirement of relative invariance for $\mathscr{L}$ is equivalent in this case to the requirement of (absolute) invariance of L in the usual sense. However, it follows directly from the known transformation properties of the Christoffel symbols that the equality $L' = L$ holds for arbitrary linear transformations of the coordinates. That is, the Lagrangian $\mathscr{L}$ under discussion is indeed linearly invariant.

We now introduce Eq. (16) into Eq. (14). Since in the present case

$$\frac{\partial \mathscr{L}}{\partial(\partial g_{\mu\nu}/\partial x_\alpha)} = \frac{\sqrt{-g}}{2}\{(2g^{\mu\sigma}g^{\nu\tau} - g^{\mu\nu}g^{\sigma\tau})\Gamma^\alpha_{\sigma\tau}$$
$$+ (g^{\mu\nu}g^{\alpha\sigma} - g^{\mu\alpha}g^{\nu\sigma} - g^{\mu\sigma}g^{\nu\alpha})\Gamma^\tau_{\sigma\tau}\},$$

we can write Eq. (14) as

$$a^\beta_{\alpha\beta}g^{\mu\nu}\Gamma^\alpha_{\mu\nu} - a^\alpha_{\mu\nu}(2g^{\mu\beta}\Gamma^\nu_{\alpha\beta} - g^{\mu\nu}\Gamma^\beta_{\alpha\beta}) = 0,$$

which with the help of a simple transformation becomes finally:

$$a^\alpha_{\mu\nu}\partial\mathfrak{G}^{\mu\nu}/\partial x_\alpha - a^\mu_{\alpha\mu}\,\partial\mathfrak{G}^{\alpha\nu}/\partial x_\nu = 0, \tag{17}$$

where, as usual, $\mathfrak{G}^{\mu\nu} = \sqrt{-g}\ g^{\mu\nu}$.

Equation (17), which is a necessary and sufficient condition for invariance of the function* L under the infinitesimal transformation (13), can also be obtained directly from the transformation properties of the function L.

If linear coordinate transformations are considered, Eq. (17) becomes an identity. Thus it does not impose any additional conditions on the fundamental tensor $g_{\mu\nu}$ as is to be expected from the linear invariance of the Lagrangian $\mathscr{L}$. If, however, nonlinear coordinate transformations are also considered besides linear ones and relative invariance of $\mathscr{L}$ under these transformations is demanded, then Eq. (17) gives additional conditions which the tensor $g_{\mu\nu}$ must satisfy. Furthermore, the additional (coordinate) conditions resulting from Eq. (17) represent the necessary and sufficient conditions for the field Lagrangian to be a relative invariant under the given family of nonlinear coordinate transformations. For brevity we shall refer to these families of transformations and to the resultant coordinate conditions as corresponding to each other.

Without stopping to consider the various consequences of the invariance of the field Lagrangian under nonlinear coordinate transformations we pass now to the study of some of the problems related to coordinate conditions and corresponding families of transformations.

4. COORDINATE CONDITIONS PREFERRED FOR A STATIONARY GRAVITATIONAL FIELD

A gravitational field is called stationary in some (not small) region, if a coordinate system exists (the same one for the whole region) for which the components of the fundamental tensor $g_{\mu\nu}$ are independent of the time coordinate x_0. We shall call those coordinate conditions "preferred for a stationary gravitational field" (more accurately, preferred with respect to the stationary property of the gravitational field) whose use yields time independent solutions of the Einstein gravitational equations.

---

*When applied to the function $\mathscr{L}$, invariance in the usual sense is understood.

In order to obtain such coordinate conditions starting from relation (17) we assume that the values of the components of the fundamental tensor $g_{\mu\nu}$ are independent of the time coordinate x_0 and that the field Lagrangian is a relative invariant under arbitrary transformations of the variable x_0. In that case we can put in Eq. (13)

$$a^{\beta}(x_0, x_1, x_2, x_3) = \varphi(x_0, x_1, x_2, x_3)\,\delta_{0\beta} + \psi^{\beta}(x_0, x_1, x_2, x_3), \tag{18}$$

where $\varphi(x_0, x_1, x_2, x_3)$ is an arbitrary (twice differentiable) function and $\psi^{\beta}(x_0, x_1, x_2, x_3)$ is an arbitrary linear function of the coordinates. Taking into account that in the present case [see Eq. (15)]

$$a^{\beta}_{\mu\nu} = \frac{\partial^2 \varphi(x_0, x_1, x_2, x_3)}{\partial x_\mu \partial x_\nu}\,\delta_{0\beta},$$

we deduce from Eq. (17) the following as the necessary and sufficient condition for the field Lagrangian to be a relative invariant under the indicated family of transformations (with the condition $\partial g_{\mu\nu}/\partial x_0 = 0$):

$$\frac{\partial \mathfrak{G}^{\alpha k}}{\partial x_k}\,\frac{\partial^2 \varphi(x_0, x_1, x_2, x_3)}{\partial x_\alpha \partial x_0} = 0,$$

where summation from 1 to 3 over the latin index k is understood. Owing to the arbitrary nature of the function $\varphi(x_0, x_1, x_2, x_3)$, this leads to the following four relations

$$\partial \mathfrak{G}^{\alpha k}/\partial x_k = 0 \quad (\alpha = 0, 1, 2, 3), \tag{19}$$

Relations (19) represent the coordinate conditions preferred for a stationary gravitational field. It also follows from the above that the coordinate conditions (19) and the family of infinitesimal coordinate transformations, defined by Eqs. (13) and (18), correspond to each other when $\partial g_{\mu\nu}/\partial x_0 = 0$.

The following conditions, which are a special case of the coordinate conditions (19),

$$g^{0i} = 0, \quad \partial \mathfrak{G}^{ik}/\partial x_k = 0 \quad (i = 1, 2, 3),$$

were used by Fock[1] to obtain spherically symmetric solutions of the Einstein gravitation equations in the static case.

However one should keep in mind that conditions (19) do not exhaust the class of all possible coordinate conditions preferred for a stationary gravitational field. For instance, the coordinate conditions used by Schwarzchild[6] in obtaining a spherically symmetric solution of Einstein's equations are preferred for a stationary gravitational field and do not coincide with conditions (19).

We will say no more about the difference between the Schwarzchild and Fock solutions; this matter is discussed in the book by Fock.[1]

The well known harmonic coordinate conditions

$$\partial \mathfrak{G}^{\alpha\beta}/\partial x_\beta = 0 \quad (\alpha = 0, 1, 2, 3), \tag{20}$$

widely used by Fock in his work on the astronomical problem of an isolated mass system also belong to the class of coordinate conditions preferred for a stationary gravitational field.

The harmonic coordinate conditions (20) coincide with the conditions (19) under the assumed independence of the components of the fundamental tensor $g_{\mu\nu}$ on the time coordinate x_0; if, however, $\partial g_{\mu\nu}/\partial x_0 \neq 0$ then the conditions (19) and (20) differ substantially. In this connection, it is of interest to find the family of coordinate transformations corresponding to the conditions (20).

5. HARMONIC COORDINATE CONDITIONS

To find the family of coordinate transformations corresponding to harmonic coordinate conditions we put in Eq. (13)

$$a^{\beta}(x_0, x_1, x_2, x_3) = w(x_0, x_1, x_2, x_3)\,x_\beta + \psi^{\beta}(x_0, x_1, x_2, x_3) \tag{21}$$

where $w(x_0, x_1, x_2, x_3)$ is a certain (twice differentiable) function and $\psi^{\beta}(x_0, x_1, x_2, x_3)$ is an arbitrary linear function of the coordinates. In this case [see Eq. (15)]

$$a^{\beta}_{\mu\nu} = w_{\mu\nu} x_\beta + w_\mu \delta_{\nu\beta} + w_\nu \delta_{\mu\beta},$$

where we have used the abbreviations

$$w_\mu = \partial w/\partial x_\mu \quad w_{\mu\nu} = \partial^2 w/\partial x_\mu \partial x_\nu.$$

Consequently, the following is a necessary and sufficient condition [see Eq. (17)] for the field Lagrangian to be a relative invariant under the family of infinitesimal coordinate transformations defined by Eqs. (13) and (21):

$$3w_\mu \partial \mathfrak{G}^{\mu\beta}/\partial x_\beta + x_\mu w_{\mu\nu} \partial \mathfrak{G}^{\nu\beta}/\partial x_\beta - x_\beta w_{\mu\nu} \partial \mathfrak{G}^{\mu\nu}/\partial x_\beta = 0. \tag{22}$$

Now suppose that $w(x_0, x_1, x_2, x_3)$ in Eq. (21) is an arbitrary linear function, then w^μ are some arbitrary constants and $w_{\mu\nu} = 0$. Under these circumstances Eq. (22) provides us directly with the harmonic coordinate conditions of interest.

The harmonic coordinate conditions thus represent the necessary and sufficient conditions for the field Lagrangian to be a relative invariant under the family of all transformations

$$x'_\beta = (1 + \varepsilon\omega)\,x_\beta + \varepsilon\psi^\beta \quad (\beta = 0,\ 1,\ 2,\ 3), \tag{23}$$

where w and ψ^β are some arbitrary linear functions of the coordinates.

If we take into account that the transformations (23) are the infinitesimal analogue of fractional linear coordinate transformations with the same denominator,[1,7] we conclude that in coordinate systems defined by the harmonic coordinate conditions rectilinear and uniform motion in any one of them always corresponds to the same kind of motion in any other. This fundamental property of harmonic coordinate conditions, together with the fact they are preferred for a stationary gravitational field, explains the privileged character of the corresponding coordinate systems in the astronomical problem of an isolated mass system.[1]

We note in conclusion that the harmonic coordinate conditions can be written as follows with the help of the field Lagrangian:

$$g_{\mu\nu}\left(\frac{\partial\mathscr{L}}{\partial\,(\partial g_{\mu\nu}/\partial x_\alpha)} + \frac{\partial\mathscr{L}}{\partial\,(\partial g_{\mu\alpha}/\partial x_\nu)}\right) = 0. \tag{24}$$

---

[1] V. A. Fock, Теория пространства, времени и тяготения (Theory of Space, Time and Gravitation), GTTI, 1955.

[2] L. D. Landau and E. M. Lifshitz, Теория поля (Field Theory), GTTI, 1948 [Engl. Transl. Addison-Wesley, 1951].

[3] E. Noether, Nachr. kgl. Ges. Wiss. Göttinger, 235 (1918).

[4] E. L. Hill, Revs. Modern Phys. **23**, 253 (1951).

[5] R. Courant and D. Hilbert, Methods of Mathematical Physics (Russ. Transl.) **1**, GTTI, 1933).

[6] K. Schwarzchild, Sitzber, preuss. Akad. Wiss. 7, 189 (1916).

[7] H. Weyl, Mathematische Analyse des Raumproblems, Berlin, Springer, 1923.

Translated by A. M. Bincer
307

SOVIET PHYSICS JETP VOLUME 35(8), NUMBER 6 JUNE, 1959

THE STABILITY OF SHOCK WAVES IN MAGNETOHYDRODYNAMICS

S. I. SYROVATSKII

P. N. Lebedev Physics Institute, Academy of Sciences, U.S.S.R.

Submitted to JETP editor June 19, 1958

J. Exptl. Theoret. Phys. (U.S.S.R.) **35**, 1466-1470 (December, 1958)

The interaction between shock waves in a magnetic field and magnetohydrodynamic waves of small amplitude is considered. The condition for stability with respect to spontaneous emission of weak magnetohydrodynamic waves by a shock wave has been obtained. The conditions are found under which the linear equations for a small perturbation do not have a solution. This case is interpreted as the decay of the shock wave.

THE stability of shock waves in magnetic hydrodynamics, so far as we know, has not yet been considered. The usual scheme of investigation of the stability consists in finding the time behavior of arbitrarily small perturbations of the initial flow. Investigations of this type were completed in references 1, 2 for a tangential discontinuity and for a magnetohydrodynamic wave in an incompressible fluid. A similar investigation for shock waves in a compressible medium requires the furnishing of equations of state of the medium and in general is very difficult. However, we can obtain some evidence on the stability of shock waves without having recourse to the general scheme mentioned above. For this purpose we must consider the possibility of spontaneous emission from a shock wave of waves of infinitesimally small amplitudes,[3] and also the interaction of a shock wave with such waves.

In magnetohydrodynamics an arbitrarily small perturbation can be represented in the form of the superposition of waves of four types:[4] fast and slow magneto-acoustical waves, a magnetohydrodynamic wave, and an entropy wave. We shall limit ourselves throughout to a consideration of the interaction of the shock wave with magnetohydrodynamic waves of small amplitude. In such a case, important use is made of the fact that in magnetohydrodynamics a shock wave is two dimensional, that is, in a suitable coordinate system, the vectors of a magnetic field and velocity on both sides of the shock lie in the same plane. Furthermore, there is a system of coordinates in which the discontinuity is at rest, and on each side of which the velocity is directed along the magnetic field intensity. In this case we eliminate from consideration the perpendicular shock wave which is propagated at right angles to the field and also a tangential discontinuity and a rotational discontinuity[5] (the magnetohydrodynamical field in a compressible medium), the investigation of the stability of which is comparatively simple by the usual method. Thus we limit ourselves to the consideration of the so-called oblique shock waves which include as a special case the ordinary shock waves which propagates along the magnetic field.

We assume that the velocity of the medium and the magnetic field intensity are parallel to the plane (x, y) while the shock front coincides with the plane $x = 0$. In the case of an oblique shock, the boundary equations for a perturbation on the surface of the discontinuity $x = 0$ fall into two groups,[2] one of which contains the z components of the perturbations $\mathbf{w}$ and $\mathbf{h}$ of the velocity and magnetic field intensity, while the second does not contain these components. The first group of boundary equations at $x = 0$ has the form

$$\{v_x h_z - H_x w_z\} = 0; \tag{1}$$

$$\{\rho v_x (w_z + v_x \partial\xi/\partial z) - H_x h_z/4\pi\} = 0, \tag{2}$$

where the v_x and H_x are the normal components of the velocity and magnetic field intensity in the unperturbed shock wave, ρ is the density of the medium and $\xi = \xi(x, y, z, t)$ is the displacement of the surface of discontinuity from its position $x = 0$ as a result of the perturbation; the curly brackets denote differences in the values of the quantities contained in them on the two sides of the discontinuity. Equation (1) expresses the continuity of the y component of the electric field, while (2) exhibits the continuity of the flux of the z component of the momentum. The second group of equations contain perturbations of the density, pressure and x and y components of the field and the velocity. Its coupling with the first group is maintained only by the displacement ξ of the surface of discontinuity. However, if the perturbation is itself a plane wave, the wave vector of which lies in the xy plane, then $\partial\xi/\partial z = 0$, and both groups of boundary equations are completely independent. In what follows we shall limit our attention to perturbations of the form

$$e^{i(kx-\omega t)}, \tag{3}$$

which are propagated along the normal to the shock front. Therefore, if only z components of the field and velocity appear on one side of the discontinuity, then, by virtue of the boundary equations, only these components will arise on the other side.

A wave in which the perturbation of the velocity and the intensity of the field are perpendicular to the direction of propagation (x axis) and the unperturbed magnetic field $\mathbf{H}(H_x, H_y, 0)$, is a magnetohydrodynamic wave (of small amplitude)[4,5] and has the properties

$$\omega_0 = \pm kV_A = \pm kH_x/\sqrt{4\pi\rho}\,, \quad w_z = \mp h_z/\sqrt{4\pi\rho}\,, \tag{4}$$

where ω_0 is the frequency of the wave in the system of coordinates in which the medium is at rest, $V_A = H\ /\sqrt{4\pi\rho}$ is the velocity of the wave relative to the liquid, and where it is taken into account that $\mathbf{k} = (k, 0, 0)$. No perturbations of the density, pressure and entropy in a magnetic field exist in a magnetohydrodynamic wave of small amplitude. Thus, magnetohydrodynamic waves of small amplitude which propagate in the plane of the flow and which are polarized perpendicular to this plane can lead to the appearance of waves only of the same type when they interact with the shock wave.

If the medium moves with velocity $\mathbf{v}$, then the coupling of the frequency with the wave vector is evidently defined by the expression

$$\omega = kv_x + \omega_0 = k(v_x \pm V_A). \tag{5}$$

Therefore, on each side of the discontinuity, in general, two waves are possible, one of which is propagated in the direction of the flow,

$$\omega^+ = k^+(v_x + V_A), \quad w_z^+ = -\ h_z^+/\sqrt{4\pi\rho}\,, \tag{6}$$

while the other is propagated against the flow, and for it,

$$\omega^- = k^-(v_x - V_A), \quad w_z^- = h_z^-/\sqrt{4\pi\rho}\,. \tag{7}$$

By virtue of the boundary equations for the perturbation on the surface of discontinuity $x = 0$, the frequencies ω of all arriving and departing waves must be identical, that is,

$$\begin{aligned} k_1^+(v_{1x} + V_{A1}) &= k_1^-(v_{1x} - V_{A1}) \\ &= k_2^+(v_{2x} + V_{A2}) = k_2^-(v_{2x} - V_{A2}). \end{aligned} \tag{8}$$

Here the indices 1 and 2 denote the different sides of the surface of discontinuity, $x < 0$ and $x > 0$, respectively. Without loss of generality, we can assume that $\omega > 0$, while the motion of the medium and the magnetic field intensity are directed toward positive values of x, that is, $v_{1x} > 0$, $v_{2x} > 0$, $H_{1x} = H_{2x} > 0$. Therefore, waves propagating in the positive direction of the x axis correspond to positive k, while waves in the opposite direction correspond to negative k. The choice of the boundary conditions at infinity is determined by the particular arrangement of the problem.

Let us first consider the possibility of spontaneous emission of weak magnetohydrodynamic waves of small amplitude from the shock wave. Since in this case all the waves should be departing from the surface of discontinuity, that is, they should be propagated in the direction of negative x from the side 1 of the discontinuity, and to the direction of positive x with regard to the side 2, then it follows from Eq. (8) that in the region $x < 0$, which corresponds to the incident flow, one or zero departing waves is possible, depending on whether the condition

$$v_{1x} < V_{A1} = H_x/\sqrt{4\pi\rho_1}, \tag{9}$$

is satisfied or not. To the right of the shock front in the region 2, two diverging waves are possible for the condition

$$v_{2x} > V_{A2} = H_x/\sqrt{4\pi\rho_2}, \tag{10}$$

or only one if this equation is not satisfied.

In the case of three emitted waves, two are expressed by the amplitude of the third through relations which follow from the boundary equations (1) and (2)

$$\begin{aligned} (v_{1x} - V_{A1})\,h_{1z}^- &= (v_{2x} + V_{A2})\,h_{2z}^+ + (v_{2x} - V_{A2})\,h_{2z}^-, \\ \sqrt{\rho_1/\rho_2}\,(v_{1x} - V_{A1})\,h_{1z}^- &= -(v_{2x} + V_{A2})\,h_{2z}^+ + (v_{2x} - V_{A2})\,h_{2z}^-. \end{aligned} \tag{11}$$

and the problem of the spontaneous emission from the shock wave of weak magnetohydrodynamic waves thus has a solution that contains one free parameter if conditions (9) and (10) are satisfied. If either of conditions (9) and (10) is not satisfied, the number of diverging waves is less than three. In this case, as can easily be seen from Eq. (11), setting h_{1z}^- and h_{2z}^- separately or simultaneously equal to zero, the boundary equations have only trivial solutions. Thus Eqs. (9) and (10) are necessary and sufficient for the instability of the shock wave relative to emission of magnetohydrodynamic waves of small amplitude.

The equation of continuity of flow $\rho_1 v_{1x} = \rho_2 v_{2x}$, together with the conditions (9) and (10), show that spontaneous emission is possible only for v_{1x}/v_{2x}

$= \rho_2/\rho_1 < \sqrt{\rho_2/\rho_1}$, or $\rho_2/\rho_1 < 1$, that is, only for rarefaction waves. These conditions cannot be simultaneously satisfied in a compression wave, which is consequently stable relative to spontaneous emission of magnetohydrodynamic waves. This result is similar to the well-known result from ordinary hydrodynamics, and testifies to the fact that stationary shock waves are possible in magnetohydrodynamics only as compression waves. True, the proof given above of the instability of rarefaction waves applies only to the case in which the magnetic field intensity satisfies conditions (9) and (10). This is connected with the fact that we have considered as emitted waves only magnetohydrodynamic waves. A general result can be obtained for consideration of all possible waves of small amplitude in magnetic hydrodynamics. However there is no fundamental need of this, since a derivation of the fact that shock waves in magnetic hydrodynamics can only be compressional waves follows from a consideration of the change of entropy in the shock wave.[6]

We now consider the collision between a shock wave and a weak magnetohydrodynamic wave propagated toward it. In addition to the incident wave, there are in general three possible diverging waves, as we have seen: one reflected and two transmitted. However, the presence of three diverging waves is equivalent to satisfying the conditions (9) and (10) and consequently to the instability of the initial shock wave, which in this case is a rarefaction wave. Therefore, of the three departing waves in the stationary discontinuity, only two can be realized: either one is reflected and one is transmitted under the conditions

$$v_{1x} < V_{A1}, \quad v_{2x} \leqslant V_{A2}, \tag{12}$$

or else two are transmitted under the conditions

$$v_{1x} \geqslant V_{A1}, \quad v_{2x} > V_{A2}, \tag{13}$$

while the reflected wave is impossible, since the velocity of the current flow is greater than the velocity of this wave relative to the medium. In both these cases the wave incident on the discontinuity leads to the production of two departing waves whose amplitudes are expressed in terms of the amplitude of the incident wave by means of the boundary conditions.

However, in addition to the cases considered, another possibility is

$$v_{1x} \geqslant V_{A1}, \quad v_{2x} \leqslant V_{A2}. \tag{14}$$

in this case the reflected wave and one of the transmitted ones are impossible, that is, besides the incident wave there is only one departing wave (k_2^+), which is clearly insufficient to satisfy the boundary equations. Actually, in this case, the boundary equations reduce to

$$\begin{gathered} (v_{1x} + V_{A1})\, h_{1z}^{+} = (v_{2x} + V_{A2})\, h_{2z}^{+}, \\ \sqrt{\rho_1/\rho_2}\,(v_{1x} + V_{A1})\, h_{1z}^{+} = (v_{2x} + V_{A2})\, h_{2z}^{+}. \end{gathered} \tag{15}$$

These equations are consistent only if $\rho_1 = \rho_2$, that is, either in the absence of a discontinuity or in a magnetohydrodynamic wave of finite amplitude (a rotational discontinuity), for which the equations of magnetic hydrodynamics reduce to linear equations and, consequently, two such waves do not interact. In the opposite case, the equations are not consistent and have no solution.

Equations (14) do not violate the equation of discontinuity and the equation for the increase of the density at the shock, and actually serve only as conditions for the magnetic field intensity. In particular, it is easy to establish that these conditions can be realized in a parallel shock wave — an ordinary shock wave which is propagated along the field — but are also always satisfied in the fundamental oblique shock wave in which the velocity on one side of the discontinuity and the magnetic field are parallel to the normal, while on the other side they are connected by the relation $\mathbf{v} = \mathbf{H}/\sqrt{4\pi\rho}$ [See reference 4, Eqs. (3.39) and (3.40)].

In our case, the absence of a solution of the linearized system of equations for an infinitesimally small distrubance can only mean that a magnetohydrodynamic wave of infinitesimally small amplitude incident on the shock wave produces a finite change in the original flow, which leads either to disintegration of the shock wave into several new shock waves or to a more general non-stationary flow of the medium.

It is not difficult to demonstrate the possibility of disintegration of a parallel shock wave satisfying conditions (14) into two fundamental oblique shocks. In this case both resultant shock waves move at a constant distance apart, while the direction the magnetic field in the region between them changes from its original direction, re-establishing it after passage of both waves. We can show that the parallel shock under conditions (14) represents two merging fundamental oblique waves, and separates into these waves under the action of a small perturbation. However, such a system of disintegrated shock waves is again unstable relative to a magnetohydrodynamic perturbation oriented perpendicular to the plane of the motion, as a consequence of the instability of the fundamental oblique waves. This means that the disintegration of the initial shock wave into a stationary sequence of shock waves cannot eliminate the instability of the type under consideration. We therefore reach the conclusion that a parallel shock wave satisfying conditions (14) is converted into a certain nonstationary flow under the action of infinitely small perturbations. This nonstationary flow can evidently contain one or several diverging shock waves.

---

[1] S. I. Syrovatskii, J. Exptl. Theoret. Phys. (U.S.S.R.) **24**, 622 (1953).

[2] S. I. Syrovatskii, Труды ИФАН (Trans. Phys. Inst. Acad. Sci.) **8**, 13 (1956).

[3] L. D. Landau and E. M. Lifshitz, **Механика сплошных сред** (Mechanics of Continuous Media), GITTL, Moscow, 1954.

[4] S. I. Syrovatskii, Usp. Fiz. Nauk **62**, 247 (1957).

[5] L. D. Landau and E. M. Lifshitz, **Электродинамика сплошных сред** (Electrodynamics of Continuous Media) GITTL, Moscow, 1956.

[6] S. V. Iordanskii, Dokl. Akad. Nauk SSSR **121**, 610 (1958), Soviet Phys. "Doklady" **3**, 736 (1958).

Translated by R. T. Beyer
308

SOVIET PHYSICS JETP VOLUME 35(8), NUMBER 6 JUNE, 1959

EFFECT OF ELECTRON PARAMAGNETIC RESONANCE ON THE OPTICAL FARADAY EFFECT AT LOW TEMPERATURES

G. V. SKROTSKII, P. S. ZYRIANOV, and T. G. IZIUMOV

Ural' Polytechnic Institute

Submitted to JETP editor June 19, 1958

J. Exptl. Theoret. Phys. (U.S.S.R.) 35, 1471-1474 (December, 1958)

An expression is derived for the angle of rotation of the plane of polarization of light in a sample in a fixed magnetic field to which is applied an rf magnetic field in the region of a paramagnetic resonance. A comparison is made with the experimental data.

1. Daniels and Wesemeyer[1] have reported experimental results concerning the effect of a magnetic resonance on the optical Faraday effect. The measurements were made with a neodymium ethylsulfate single crystal at 1.5°K, using microwave power at 9060 Mcs and the green mercury line at 5461 A. With no microwave power the angle of rotation of the plane of polarization was a linear function of the strength of the fixed magnetic field. When the microwave power was switched on a noticeable reduction in the angle of rotation was observed near resonance. In microwave fields strong enough for saturation no rotation of the plane of polarization could be observed even at very strong fields ($H_0 \sim 1750$ oe).

The relation between the optical Faraday effect and paramagnetic resonance was first noted by Kastler[2] and the quantum-mechanical calculation was carried out by Opechowski.[3] In these papers it is pointed out that the effect of the radio-frequency field is to cause a redistribution in the electron populations in the energy levels which are split by the fixed field (corresponding to different values of the magnetic quantum number). This redistribution leads to a change in the intensity of the Zeeman lines and affects the polarization of the medium.

On the basis of a quantum-mechanical calculation of the magnetic and electric dipole transitions caused by the radio-frequency and optical radiation, Opechowski gives an expression for the polarization tensor which contains a correction for the magnetic dipole transitions. However, it is difficult to compare his results with experiment because of the dipole-transition matrix elements which appear in the expression; also, the population numbers for the initial and final energy levels, between which these transitions take place, are unknown. The analysis in reference 3 does not take account of the magnetic polarization due to the light and this effect is important at low temperatures.

Below we give a simple macroscopic analysis of the effect; this analysis yields an explicit expression for the angle rotation of the plane of polarization of the light near the paramagnetic resonance in a radio-frequency field, h, which is weak compared with the fixed magnetic field $H_0 = H_z$. The constants which appear in the final expressions can be determined from optical, magnetic, and radio-frequency measurements.

2. The effect of a paramagnetic resonance on optical phenomena is due primarily to spin-orbit interactions. The optical effects are characterized by the dielectric permittivity, which is determined by the orbital motion of the electrons in the atom. In the region of a paramagnetic resonance there is a marked change in the spin system. When spin-orbit coupling is taken into account the change in the state of the spin system results in a change in the dielectric permittivity. The latter effect is important in the low-temperature region, where the magnetization of a paramagnet is close to saturation even in a relatively weak magnetic field. The following system of equations[4] can be used for a macroscopic description of these effects:

$$\Delta\mathbf{A} = -\frac{4\pi}{c}\left\{c\,\mathrm{curl}\,\mathbf{M} + \dot{\mathbf{P}} - \frac{1}{4\pi c}\ddot{\mathbf{A}}\right\}; \tag{1}$$

$$\mathbf{P}_\alpha + \omega_\alpha^2\mathbf{P}_\alpha = -(e^2/mc)\,\dot{\mathbf{A}} + (e/mc)\,\dot{\mathbf{P}}\times\mathbf{B}; \tag{2}$$

$$\dot{\mathbf{M}} + \mathbf{M}/\tau = (\chi_0/\tau)\,\mathbf{H} + \gamma\,\mathbf{M}\times\mathbf{B}; \tag{3}$$

$$\mathbf{P} = \sum_\alpha N_\alpha\mathbf{P}_\alpha;\ \ \mathbf{B} = \mathrm{curl}\,\mathbf{A} = \mathbf{H}_0 + \mathbf{H}_i + 4\pi\mathbf{M}, \tag{4}$$

where P and M are the densities of the electric and magnetic moments respectively. The vector potential A is given in the form

$$\mathbf{A} = \mathbf{A}_0 + \mathbf{A}(r, t), \text{ where curl } \mathbf{A}_0 = \mathbf{B}_0 = \mathbf{H}_0 + 4\pi\mathbf{M}_0.$$

As has been shown in reference 4, using this system it is possible to introduce the spin-orbit interaction within the framework of a macroscopic theory. The self-consistent internal field $\mathbf{H}_i$ is due to the spin-spin (source of c curl $\mathbf{M}$) and spin-orbit (source of $\dot{\mathbf{P}}$) interactions. The $\dot{\mathbf{P}}$ term in Eq. (1) describes the polarization current associated with the change of electric dipole moment of the atom due to the rotational electric field. This rotational electric field produces oscillations in the magnetization. Equation (2) describes the change in polarization in the ensemble of atoms which interact with the internal electromagnetic field. Equation (2) contains no damping term; there is no significant change in the final results of the calculation when damping is introduced.

3. If a linearly polarized electromagnetic wave is propagated in the medium in the direction of the fixed magnetizing field H_0, the plane of polarization is rotated. The specific angle of rotation[5]

$$\theta = (\omega / 4c)\,(n_{-}^{2} - n_{+}^{2}) / n \tag{5}$$

is determined by the refractive index $n_{\pm} = ck/\omega$ for waves with right- and left-handed polarization and by the refractive index n if there is no magnetic field $\mathbf{H}_0$.

In order to find $n_{\pm}$ and n we start from Eqs. (1) to (4), taking the solution in the form

$$\mathbf{A} = {}^{1}/_{2}\, \mathbf{r}, \times \mathbf{B}_0 + \sum_{\mathbf{k}\neq 0} \mathbf{A}_{\mathbf{k}} \exp\{-i\omega t + i\mathbf{k}\cdot\mathbf{r}\}; \tag{6}$$

$$\mathbf{P}_{\alpha} = \sum_{\mathbf{k}} \mathbf{P}_{\alpha\mathbf{k}} \exp\{-i\omega t + i\mathbf{k}\cdot\mathbf{r}\}; \tag{7}$$

$$\mathbf{M} = \mathbf{M}_0 + \sum_{\mathbf{k}\neq 0} \mathbf{m}_{\mathbf{k}} \exp\{-i\omega t + i\mathbf{k}\cdot\mathbf{r}\}. \tag{8}$$

Substituting Eq. (7) in Eq. (2), including higher-order terms we have

$$\mathbf{P}_{\alpha k} = i\,\frac{e^2}{mc}\,\frac{\omega}{\omega_{\alpha}^{2} - \omega^{2}}\,\mathbf{A}_{k}. \tag{9}$$

Assuming further that $\mathbf{M} = \mathbf{M}_0 + \mathbf{m}$, in the same approximation we have

$$\operatorname{curl} \mathbf{m}_k = i\,\frac{\gamma}{\omega}\,\mathbf{k}\cdot\mathbf{M}_0(\mathbf{k}\times\mathbf{A}_k). \tag{10}$$

Now, from Eqs. (6) and (1)

$$\left\{\left[k^2 - \frac{\omega^2}{c^2} - \sum_{\alpha}\frac{4\pi N_{\alpha}e^2}{mc^2}\,\frac{\omega^2}{\omega_{\alpha}^{2} - \omega^{2}}\right]^2 - \left(\frac{4\pi\gamma}{\omega}\right)^2 (\mathbf{k}\cdot\mathbf{M})^2 k^2\right\}\mathbf{A}_{\mathbf{k}} = 0. \tag{11}$$

Thus, at optical frequencies the refractive index is

$$n_{\pm}^{2} = (kc/\omega)^2 \equiv n^2\,\{1 \mp (4\pi\gamma/\omega)\,M_{0z}\}, \tag{12}$$

where

$$n = 1 + \sum_{\alpha} (4\pi N_{\alpha} e^2 / m) / (\omega_{\alpha}^{2} - \omega^{2}). \tag{13}$$

Hence, the specific angle of rotation of the plane of polarization

$$\theta = (2\pi\gamma / c)\, n M_{0z} \tag{14}$$

is determined by the dependence of the magnetization component M_{0z} on the fixed magnetizing field H_0 and the amplitude of the radio-frequency field. At saturation, where $M_z = 0$, both values of the index of refraction $n_{\pm} = n$ and $\theta = 0$.

4. If the radio-frequency field h_0 is circularly polarized

$$h_x = h_0 \cos\omega_0 t;\quad h_y = h_0 \sin\omega_0 t, \tag{15}$$

the expression for M_{0z} is found easily, writing Eq. (3) in a coordinate system which rotates about the z-axis at the frequency ω_0.

Under steady-state conditions

$$\boldsymbol{\omega}_0 \times \mathbf{M}_0 = \gamma \mathbf{M} \times \mathbf{H}_0 + (\chi_0 \mathbf{H} - \mathbf{M}_0)/\tau.$$

Solving the last equation for M_z, we have

$$M_{0z} = \chi_0 H_0 \left\{1 - \gamma^2\,\frac{1 - \Delta\omega/\gamma H_0}{\Delta\omega^2 + \tau^{-2} + \gamma^2 h_0^2}\,h_0^2\right\}, \tag{16}$$

where

$$\Delta\omega = \omega_0 + \gamma H_0.$$

Equations (14) and (16) determine the explicit dependence of the angle of rotation of the plane of polarization in a paramagnetic medium as a function of H_0 and h_0.

It follows from Eq. (16) that when $h_0 = 0$ the angle of rotation is proportional to the magnetizing field H_0. If the radio-frequency field is weak $|\gamma|\tau h \ll 1$ the function $\theta(H_0)$ has a valley in the resonance region $\omega_0 = |\gamma| H_0$; the depth of the valley increases with h_0. At stronger radio-frequency fields, where $|\gamma|\tau h < 1$, θ starts to increase rapidly when $|\gamma| H_0 > \omega_0$. For value of H_0 smaller than $\omega/|\gamma|$ there is a change in the sign of the angle, as is apparent from the figure. Because of the approximations made in the derivation Eq. (14), in strong radio-frequency fields we can expect only qualitative agreement with experiment.

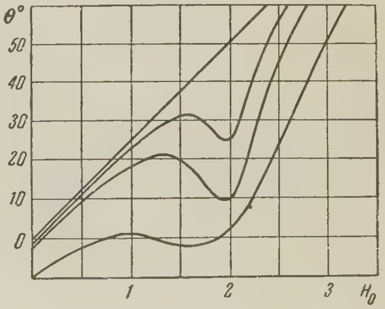

Theoretical dependence of the angle θ on the intensity of the magnetizing field for different values of the radio-frequency field.

[1] J. M. Daniels and H. Wesemeyer, Can. J. Phys. 36, 405 (1958).

[2] A. Kastler, Physica 17, 191 (1951); J. phys. et radium 11, 255 (1950).

[3] W. Opechowski, Revs. Modern Phys. 25, 264 (1953)

[4] P. S. Zyrianov and G. V. Skrotskii, J. Exptl. Theoret. Phys. (U.S.S.R.) 34, 222 (1958), Soviet Phys. JETP 7, 153 (1958).

[5] M. V. Vol'kenshtein, **Молекулярная оптика** (Molecular Optics) GITTL 1951.

Translated by H. Lashinsky
309

SURFACE OSCILLATIONS OF A CHARGED COLUMN IN A LONGITUDINAL MAGNETIC FIELD

CHAO KAI-HUA

Moscow State University

Submitted to JETP editor June 21, 1958

J. Exptl. Theoret. Phys. (U.S.S.R.) 35, 1475-1480 (December, 1958)

An analysis is given of the surface oscillations and stability of a hydrodynamic charged column in an external magnetic field. This analysis represents an extension of the well-known work of Kruskal and Schwarzchild and Tayler on the stability of an uncharged hydrodynamic column. The surface-wave dispersion equation is derived and the features of the oscillation spectrum are investigated. From the experimental point of view these results are of value for investigating the nature of the radiation from a plasma in a magnetic field, an effect which is as yet not fully understood.

1. INTRODUCTION

THE stability of a column (pinch) has been studied by Kruskal and Schwarzchild,[1] who considered a plasma cylinder in which the current flows along the surface. It was shown that a system of this kind is unstable against lateral distortions. A further step in this problem was made by Shafranov[2] and Tayler[3,4] who considered perturbations of other kinds. The analysis was extended to include a more general current distribution over the column cross section and to the case in which there is an arbitrary magnetic field and a conducting wall. It has been shown that there is some improvement in stability in the latter case.

In the work cited above the electric charge of the plasma was not taken into account. However, it is known experimentally, and from the theory of ambipolar diffusion, that a plasma column exhibits a total resultant charge, even though this charge is weak. It is of interest to extend the results of the above work to the case of a charged column since the presence of an external magnetic field leads to peculiar effects: these result from the interaction of the self electric field with the external magnetic field.

There are extensive experimental data on the oscillatory properties of a plasma in an external magnetic field. The frequency of these oscillations covers a wide range (from tens of cycles per second to ultra high frequencies) (cf. for example, reference 5). In certain cases the frequency increases as the external magnetic field is increased. There is a minimum value of the magnetic field at which the field begins to have an effect on the oscillation frequency. Under certain conditions there is a uniformly spaced line spectrum. The number of lines which are observed varies from two to ten. It is difficult to interpret these in terms of "overtones" of a single spectral line. Up to this time this effect has not been explained theoretically.

Without undertaking a complete analysis of these effects, in the present paper we shall examine magnetohydrodynamic surface waves in connection with the above problems.

2. BASIC EQUATIONS

Following Kruskal and Schwarzchild we consider the problem from a magnetohydrodynamic standpoint, assuming infinite conductivity.

The internal region of the plasma is described by the usual system, comprising Maxwell's equations and the hydrodynamic equations:

$$\begin{gathered}\operatorname{div}\mathbf{E}=0,\ \operatorname{div}\mathbf{H}=0,\ \operatorname{curl}\mathbf{E}=-\frac{1}{c}\frac{\partial\mathbf{H}}{\partial t},\\ \operatorname{curl}\mathbf{H}=\frac{4\pi}{c}\mathbf{j}+\frac{1}{c}\frac{\partial\mathbf{E}}{\partial t},\quad \mathbf{E}+\frac{1}{c}[\mathbf{v}\times\mathbf{H}]=\frac{1}{\sigma}\mathbf{j}=0,\\ \frac{\partial\rho}{\partial t}+\operatorname{div}(\rho\mathbf{v})=0,\quad \rho\frac{dv}{dt}=-\operatorname{grad}p+\frac{1}{c}[\mathbf{j}\times\mathbf{H}],\\ \frac{1}{p}\frac{dp}{dt}=\frac{\gamma}{\rho}\frac{d\rho}{dt}\end{gathered}\qquad(1)$$

(γ is the ratio of the specific heats of the plasma).

It is assumed that the electrical conductivity of the external medium is zero and that the pressure is constant. Hence we deal with Maxwell's equations for source-free conditions.

The boundary conditions at the interface are of the form:

$$(\mathbf{n}\cdot\{\mathbf{E}\}) = 4\pi\varepsilon^*, \ (\mathbf{n}\cdot\{\mathbf{H}\}) = 0,$$
$$[\mathbf{n}\times\{\mathbf{E}\}] = \frac{u}{c}\{\mathbf{H}\}, [\mathbf{n}\times\{\mathbf{H}\}] = \frac{4\pi}{c}\mathbf{j}^* - \frac{u}{c}\{\mathbf{E}\}, \tag{2}$$

where n is a unit vector in the direction of the outward normal and $u = \mathbf{n}\cdot\mathbf{v}$; $\{\ldots\}$ denotes the difference in the values of a quantity at the interface. Here and below in all cases we shall include the convection current $\epsilon^*\mathbf{v}$ in the expression for the total current $\mathbf{j}^*$. Also

$$d\mathbf{n}/dt = \mathbf{n}\times[\mathbf{n}\times \operatorname{grad} u], \tag{3}$$

$$\varepsilon^*\overline{\mathbf{E}} + \frac{1}{c}[\mathbf{j}^*\times\overline{\mathbf{H}}] - \mathbf{n}\{p\} = 0, \tag{4}$$

where the bar denotes the average value of a quantity; as in reference 1 this average can be taken simply as half the sum of the values on the two sides of the interface.

3. LINEARIZATION AND SOLUTION OF THE EQUATIONS

We take all quantities in the form

$$q = q_0 + \delta q(r) \exp\{i(m\theta + kz + \omega t)\}, \tag{5}$$

where q_0 is the equilibrium value of a quantity q.

We shall specify the equilibrium state as follows: at the surface of the column there is a charge of uniform density ϵ_0^* which produces a radial electric field $E_0 = 4\pi\epsilon_0^*$. In the equilibrium state there is no current flow. The external magnetic field H_0 is along the z axis. The electric forces are balanced by the pressure difference $\{p\}_0 = E_0^2/8\pi$.

Substituting Eq. (5) in the original equations we obtain a system of linearized equation from which we can obtain an expression for δp in the plasma:

$$\left(1 - \frac{k^2c_H^2}{\omega^2} + \frac{c_H^2}{c_s^2}\right)\left\{\frac{1}{r}\frac{\partial}{\partial r}\left(r\frac{\partial}{\partial r}\right) - \frac{m^2}{r^2}\right\}\delta p$$
$$- \left(1 + \frac{c_H^2}{c^2} - \frac{k^2c_H^2}{\omega^2}\right)\left(k^2 - \frac{\omega^2}{c_s^2}\right)\delta p = 0, \tag{6}$$

where $c_s = (\gamma p_0/\rho_0)^{1/2}$ is the velocity of sound in the plasma, and $c_H = H_0/\sqrt{4\ \rho_0}$ is the velocity of the Alfvén waves. The solution of Eq. (6) is

$$\delta p = \alpha p_0 I_m(\eta r), \tag{7}$$

$$\eta^2 = \frac{(1 + c_H^2/c^2 - k^2c_H^2/\omega^2)\zeta^2}{(1 + c_H^2/c_s^2 - k^2c_H^2/\omega^2)}$$
$$= \frac{(k^2 - \omega^2/c_H^2 - \omega^2/c^2)(k^2 - \omega^2/c_s^2)}{k^2 - \omega^2/c_H^2 - \omega^2/c_s^2} \qquad \zeta^2 = k^2 - \omega^2/c_s^2, \tag{8}$$

I_m is a Bessel function of imaginary argument, and α is the dimensionless amplitude.

From the foregoing it is easy to obtain all the remaining quantities of interest. All of these are expressed in terms of the same amplitude α. The expressions which obtained for the pressure, density, velocity components and field are of the same form as those obtained by Tayler,[4] who did not take displacement current into account; there is one exception: the expression given by Tayler for α^2, which in the present notation is written

$$(k^2 - \omega^2/c_H^2)(k^2 - \omega^2/c_s^2)/(k^2 - \omega^2/c_H^2 - \omega^2/c_s^2),$$

must be replaced by η^2 from (8).

The solutions for the original equations for the region outside the column are given in reference 1. These are characterized by two amplitudes and are proportional to $K'_m(\eta' r)$ or the derivative $K'_m(\eta' r)$, where $\eta'^2 = k^2 - \omega^2/c^2$ (K_m is a Hankel function of imaginary argument).

The boundary conditions yield three independent linear homogeneous relations between the three amplitudes; the existence condition for a non-trivial solution yields the dispersion equation

$$(\omega^2 - c_H^2\zeta^2)\frac{I_m(\eta R)}{\eta R I'_m(\eta R)} = -\left\{\frac{m^2\omega^2\omega_E^2\zeta^2}{c^2\eta^2\eta'^2} + 2\omega\omega_m\frac{\zeta^2}{\eta^2}\right.$$
$$\left. + \frac{c_H^2\zeta^2\eta'^2}{\eta^2}\right\}\frac{K_m(\eta' R)}{\eta' R K'_m(\eta' R)} + \frac{\omega_E^2\zeta^2}{\eta^2}\left(1 + \frac{k^2}{\eta^2}\frac{\eta' R K'_m(\eta' R)}{K_m(\eta' R)}\right), \tag{9}$$

where

$$\omega_E^2 = E_0^2/4\pi R\rho_0, \quad \omega_m = E_0 H_0 m/4\pi c R\rho_0, \tag{10}$$

where R is the radius of the pinch.

Northrup has obtained similar results for plane boundaries.[6]

4. DISCUSSION OF THE DISPERSION EQUATION

We now consider several cases.

(1) The short-wave case:

$$k^2 \gg \omega^2/c^2, \ k^2 \gg \omega^2/c_s^2 \quad (c_s^2 \ll c^2). \tag{11}$$

As will be shown by calculation, the last inequality holds if the following condition is satisfied:

$$c_H^2 \ll c_s^2. \tag{12}$$

Under these conditions we can replace η, η' and ζ by k and Eq. (9) assumes the simpler form:

$$\omega^2 + 2\omega\omega_m I'_m K_m/I_m K'_m + c_H^2 k^2 (I'_m K_m/I_m K'_m - 1)$$
$$- \omega_E^2(1 + kRK'_m/K_m)kRI'_m/I_m = 0. \tag{13}$$

In the last equation the argument of the cylindrical functions is kR in all cases.

The stability condition is

$$\omega_m^2 \left(\frac{I'_m K_m}{I_m K'_m}\right)^2 - c_H^2 k^2 \left(\frac{I'_m K_m}{I_m K'_m} - 1\right) \tag{14}$$
$$+ \omega_E^2 \left(1 + \frac{kRK'_m}{K_m}\right) \frac{kRI'_m}{I_m} \geqslant 0.$$

Except when $m = 0$, the third term is negative while the first two are positive. We neglect the first term in (14) since it is small compared with the third term if $c_H^2 \ll c^2$, as follows directly from (13).

The absolute value of the second term is greater than that of the third only if

$$k \geqslant k_c, \tag{15}$$

where k_c is some critical wave number, which can be determined by setting the left hand part of the inequality in (14) equal to zero; we have

$$F_m(k_c R) = E_0^2 / H_0^2$$

$$F_m(x) = \frac{x^2 (I'_m(x) K_m(x) / I_m(x) K'_m(x) - 1)}{(1 + xK'_m(x) / K_m(x))\, xI'_m(x) / I_m(x)}. \tag{16}$$

With the exception of the case $m = 1$, $F_m(x)$ increases monotonically from 0 to 2 so that stability is possible only when

$$2H_0^2 > E_0^2. \tag{17}$$

When $E_0 = 0$ (uncharged column) the result agrees with Eq. (3.12) given by Tayler[4] for the appropriate conditions (no surface current and no conducting walls). This result also agrees with that obtained by Kislovskii[7] for the case $m = 1$ if we take $\Sigma = 0$, $\mu_1 = \mu_2 = 1$, $H_0 = H_\infty$ in Eq. (15.45) of that reference. These oscillations are nothing more than magnetohydrodynamic waves which propagate in the cylinder.

If there is no external magnetic field ($H_0 = 0$) only the first and last terms remain in Eq. (13). The equation which results coincides with the dispersion relation obtained by A. A. Vlasov for a charged jet. Oscillations of this type are purely electrostatic in origin.

Vlasov has also obtained Eq. (13) without the third term and the factor $2I'_m K_m / I_m K'_m$ in the second term, starting with a completely different model — the inertia motion of a charged jet with an ellipsoidal velocity distribution.* The interesting term in Eq. (13) is the second term; this term, which arises because of the simultaneous presence of E_0 and H_0 can be considered the result of the interaction between the charged column and the external magnetic field.

In the present case the frequency ω_m is the modulation frequency. Actually, the solution of Eq. (13) can be written in the explicit form

$$\omega = \omega_m \Phi_m \pm \{\omega_m^2 \Phi_m^2 + \Omega_m^2\}^{1/2}, \tag{18}$$

where we have used the notation

$$\Phi_m = -I'_m K_m / I_m K'_m,$$

$$\Omega_m^2 = -c_H^2 k^2 (I'_m K_m / I_m K'_m - 1)$$
$$- \omega_E^2 (1 + kRK'_m / K_m)\, kRI'_m / I_m,$$

where $k > k_c$, $\Omega^2 m > 0$, $\Phi_m \approx 1$.

Since $\Omega^2 m \gg \omega_m^2$, we can write

$$\omega \approx \pm \Omega_m + \omega_m \Phi_m. \tag{19}$$

We may recall that when the substitution $m \to -m$ is made ω_m changes sign, whereas Φ_m does not.

A linear combination of the four possible types results in oscillations of the form

$$\cos \Omega_m t \cos (\omega_m \Phi_m t + m\theta). \tag{20}$$

There are modulated oscillations with a modulation frequency $\omega_m \Phi_m$. In the first approximation the factor Φ_m can be taken as unity and we obtain an equally spaced line spectrum, ω_m, with frequencies proportional to E_0 and H_0. Φ_m has some distorting effect on the equal spacing, especially for the first lines in the spectrum.

It is apparent from (19) that

$$\omega^2 \approx \Omega_m^2 \leqslant c_H^2 k^2.$$

In order to satisfy the condition $k^2 \gg \omega^2 / c_s^2$, on which the present calculation is based, the condition given in (12) must be fulfilled.

(2) Long-wave case. For simplicity we assume $k = 0$; thus

$$\eta'^2 = -\frac{\omega^2}{c^2}, \quad \zeta^2 = -\frac{\omega^2}{c_s^2},$$

$$\eta^2 = -\left(\frac{c^2 + c_H^2}{c_s^2 + c_H^2}\right) \frac{\omega^2}{c^2}.$$

The arguments of K_m and K'_m are imaginary.

We now consider Eq. (9). η and η' appear in (9) only in quadratic terms or in the combinations $\eta R I'_m(\eta R)/I_m(\eta R)$, $\eta R K'_m(\eta' R)/K_m(\eta' R)$; it can be shown that $xI'_m(x)/I_m(x)$ is always real for real and imaginary x while $xK'_m(x)/K_m(x)$ is always complex for imaginary x. Whence it is clear that the left side of (9) is always real for real x but the right side is complex. Hence, in general there is no real solution for ω. However, if the following condition is satisfied:

$$|\omega R / c| \gg 1 \tag{21}$$

---

*Reported at the Lomonosov Lectures, Physics Faculty, Moscow State University, October 30, 1957.

it is possible to have a real frequency with a very small imaginary part. When $|x| \ll 1$ we have

$$ixK'_m(ix)/K_m(ix) \approx -m - i\pi x^{2m}/2^{2m-1}[(m-1)!]^2. \tag{22}$$

We assume that ω is so small that $|\eta R| \ll 1$. When $|x| \ll 1$ we have

$$ixI'_m(ix)/I_m(ix) \approx m.$$

Introducing these assumptions it is possible to make a considerable simplification in the dispersion equation (9). If we take

$$\omega = \omega_1 + i\gamma, \quad (\gamma \ll \omega_1), \tag{23}$$

the equation for ω_1 is

$$\beta\omega_1^2 - 2\omega_1\omega_m + m(m-1)\omega_E^2 = 0, \tag{24}$$

where

$$\beta = \frac{c_s^2(c^2 + c_H^2) + c_H^2(c^2 + 2c_H^2 + c_s^2)}{c^2(c_s^2 + c_H^2)}$$

$$\gamma = \frac{m^2\omega_E^2}{\omega_m - \beta\omega_1}\,\frac{\pi(\omega_1 R/2c)^{2m}}{[(m-1)!]^2} \tag{25}$$

We consider Eq. (24) for two cases.

(a) If $c^2 \gg c_H^2$, $\beta \approx 1$,

$$\omega_1 = \omega_m \pm \{\omega_m^2 - m(m-1)\omega_E^2\}^{1/2}$$
$$\approx \omega_m\{1 \pm [(1-m)/m]^{1/2}(c/c_H)\}, \tag{26}$$

and ω_1 is real only when $m = 1$.

(b) If $c^2 \ll c_H^2$, $\beta^2 \approx 2c_H^2/c^2$,

$$\omega_1 = \frac{1}{2}\left(1 \pm \sqrt{(2-m)/m}\right)\frac{E_0 cm}{H_0 R}, \tag{27}$$

and ω_1 is real for $m = 1$ and $m = 2$.

(3) We now estimate the corrections for the quantities computed above. The following numerical values may be taken as typical:

$H_0 \approx 1500$ gausses, pressure $p = 10^{-1}$ to 10^{-5} mm Hg, i.e., the density of neutral particles $n \approx 10^{11}$ to 10^{15} cm^{-3}. Take the mass of the particles as $\mu \approx 2 \times 10^{-24}$ g; then $\rho_0 \approx 10^{-13}$ to 10^{-9} g/cm^3 and $c_H^2 \approx 10^7$ to 10^9 cm/sec, $c_H^2/c^2 = 10^{-6}$ to 10^{-2}.

If we assume that the radius of the column $R \approx 1$ cm, $E_0 \approx 2 \times 10^{-4}$ cgs electrostatic units, $E_0/H_0 \approx 10^{-7}$ and the modulation frequency for case (1) is $\omega_m = 10^2$ to 10^{-2} cps for $m = 1$.

The frequency ω_1 in (26) is ω_m for $m = 1$ while in (27) $\omega_1 \approx 3 \times 10^{-3}$ cps for $m = 1$, $m = 2$.

We wish to thank Professor A. A. Vlasov for suggesting this problem and for guidance and advice in the course of its completion.

---

[1] M. Kruskal and M. Schwarzchild, Proc. Roy. Soc. (London) **A223**, 348 (1954).

[2] V. D. Shafranov, **Атомная энергия** (Atomic Energy) **5**, 38 (1956).

[3] R. J. Tayler, Proc. Phys. Soc. (London) **B70**, 31 (1957).

[4] R. J. Tayler, Proc. Phys. Soc. (London) **B70**, 1049 (1957).

[5] Guthrie and Wakerling, Characteristics of Electrical Discharges in Magnetic Fields, New York, McGraw Hill, 1949.

[6] T. Northrop, Phys. Rev. **103**, 1150 (1956).

[7] A. D. Kislovskii, Dissertation "Theory of Surface Waves in Magnetohydrodynamics," Moscow State Univ., 1958.

Translated by H. Lashinsky
310

SOVIET PHYSICS JETP VOLUME 35 (8), NUMBER 6 JUNE, 1959

FERROMAGNETIC RESONANCE IN A CIRCULARLY POLARIZED MAGNETIC FIELD OF ARBITRARY AMPLITUDE

G. V. SKROTSKII and Iu. I. ALIMOV

Ural' Polytechnic Institute

Submitted to JETP editor, June 23, 1958

J. Exptl. Theoret. Phys. (U.S.S.R.) 35, 1481-1484 (December, 1958)

An analysis is given of the exact solutions of the magnetization equation of motion. The dependence of the magnetization components on the amplitude of the fixed magnetizing field and the amplitude of the radio-frequency field is found. A comparison is made with experimental results.

1. Ferromagnetic resonance is usually observed in a weak periodic radio-frequency field (amplitude h_0). Under these conditions, because of the width of the resonance absorption line the direction of the magnetization vector $\mathbf{M}$ departs so slightly from the direction of the magnetizing field $H_0 = H_Z \gg h_0$ that its projection in this direction may be assumed constant. Even close to resonance the effect is extremely insensitive to the form of the damping terms in the equation of motion and can be satisfactorily described by the Bloch equation

$$\dot{\mathbf{M}} = \gamma\ \mathbf{M}\times\mathbf{H}\ + (\chi_0\mathbf{H} - \mathbf{M})/\tau, \qquad (1)$$

or the Landau-Lifshitz equation, which can be written in the form[1]

$$\dot{\mathbf{m}} = \gamma\ \mathbf{m}\times\mathbf{H}\ + \alpha\ \dot{\mathbf{m}}\times\mathbf{m}\ ,\ \alpha < 0, \qquad (2)$$

where $\mathbf{m} = \mathbf{M}/M_S$; $\mathbf{H} = \mathbf{H}_0 + \mathbf{h}$.

The situation is rather different in strong radio-frequency fields; in these fields the change in M_Z cannot be neglected. In this case the variation of $\mathbf{M}$ becomes very sensitive to the actual form of the damping terms in the equation of motion.

Damon[2] has investigated experimentally effects connected with the change in the z component of the magnetization of a ferromagnet as a function of the field H_0 and the amplitude of the radio-frequency field. Bloembergen and Wang[3] repeated the Damon experiments on ferromagnetic and paramagnetic specimens at various temperatures. It was found in these experiments that at high amplitudes of the radio-frequency field the total magnetization in both paramagnetic and ferromagnetic material does not remain constant. In comparing the experimental results with theory, the authors started with the Bloch equation. It is found that this equation cannot explain a number of the effects which are observed.

Some of the results observed by Bloembergen and Wang have been explained by Suhl[1] on the basis of a number of assumptions concerning the redistribution of energy between spin waves.

Below we give an analysis of the exact solutions of Eqs. (1) and (2) for a circularly polarized radio-frequency field of arbitrary amplitude and of the role of paramagnetic effects in ferromagnets in a strong radio-frequency field.

2. In what follows it will be assumed that the sample is homogeneous and isotropic; the sample will also be assumed to be a sphere with radius less than the skin depth at the frequencies in question. It will also be assumed that the magnetizing field and the radio-frequency field are uniform.

In a coordinate system which rotates about the direction of $\mathbf{H}_0$ at the frequency of the radio-frequency field ω (for the steady-state motion) Eq. (1) assumes the form

$$\tau\ \mathbf{M}_0\times\Delta\boldsymbol{\omega}\ + \chi_0\mathbf{H} - \mathbf{M}_0 = 0, \qquad (3)$$

where $\Delta\omega = \omega + \gamma\mathbf{H}$ solving Eq. (3) for M_{0Z}, we find

$$M_{0z} = \chi_0\left\{H_0 + \gamma\tau^2\frac{\omega h_0^2}{1+\tau^2(\Delta\omega^2+\gamma^2h_0^2)}\right\}, \qquad (4)$$

where $\Delta\omega = \Delta\omega_Z$. When $\Delta\omega = 0$

$$M_{0z} = \chi_0 H_0\,(1+\gamma^2\tau^2h_0^2)^{-1}. \qquad (5)$$

Further, using the relation

$$M_{0x} + iM_{0y} = (\chi' - i\chi'')\,(h_x + ih_y) \qquad (6)$$

and the solution of Eq. (3) for M_{0X} and M_{0y}, we obtain

$$\left.\begin{aligned}\chi' &= \chi_0\left\{1 - \frac{\tau^2\omega\Delta\omega}{1+\tau^2(\Delta\omega^2+\gamma^2h_0^2)}\right\},\\ \chi'' &= \chi_0\,\frac{\tau\omega}{1+\tau^2(\Delta\omega^2+\gamma^2h_0^2)}.\end{aligned}\right. \qquad (7)$$

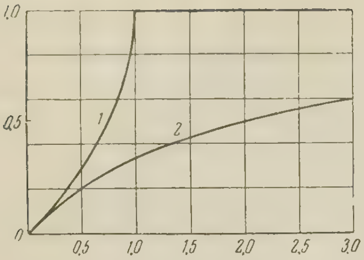

FIG. 1. The quantity $1 - M_z/M_0$ as a function of a^2 for the cases $M_0 = M_s$ (1) and $M_0 = \chi_0 H_0$ (2) with $\Delta\omega = 0$.

In a similar way, starting from Eq. (2), in the rotating coordinate system the steady-state motion is described by

$$[\mathbf{m}_0 \times \Delta\boldsymbol{\omega}] + \alpha(\mathbf{m}_0 \cdot \boldsymbol{\omega})\,\mathbf{m}_0 = \alpha\boldsymbol{\omega}, \tag{8}$$

whence the quantity m_{0z} is found from the following:

$$2m_{0z}^2 = 1 - a^2 - \xi^2 + [(1 - a^2 - \xi^2)^2 + 4\xi^2]^{1/2}, \tag{9}$$

where

$$a = \gamma h_0 / \alpha\omega; \; \xi = \Delta\omega / \alpha\omega.$$

In the weak-field case $a \ll 1$ and $m_{0z} \approx 1$, as is usually assumed in the theory of ferromagnetic resonance. In fields such that $a \le 1$ when $\Delta\omega = 0$

$$M_{0z} / M_s = (1 - a^2)^{1/2}. \tag{10}$$

When $a \ge 1$, the vector m_0 is perpendicular to H_0 and we have total radio-frequency saturation ($M_{0z} = 0$). Computing $M_x + iM_y$ from Eq. (8) and using Eq. (6), we find in this case

$$\chi' = M_s \frac{\gamma}{\alpha\omega} \frac{\xi m_{0z}}{\xi^2 + m_{0z}^2}, \quad \chi'' = M_s \frac{\gamma}{\alpha\omega} \frac{m_{0z}^2}{\xi^2 + m_{0z}^2}, \tag{11}$$

where m_{0z} is determined from Eq. (9).

3. Bloembergen and Wang have investigated the quantity $\eta = 1 - M_{0z}/M_0$ as a function of the amplitude of the radio-frequency field h_0 for $\Delta\omega = 0$, where M_0 is the magnitude of the magnetization vector in the absence of the radio-frequency field ($\chi_0 H_0$ or M_s). In the relatively weak fields which obtain in experiments, η depends linearly on h_0^2, as follows from Eqs. (5) and (10). The slope of the line can be used to determine τ or α.

The dependence of η on h_0^2 for $\Delta\omega = 0$ which follows from Eq. (1) and Eq. (2) is shown in Fig. 1.

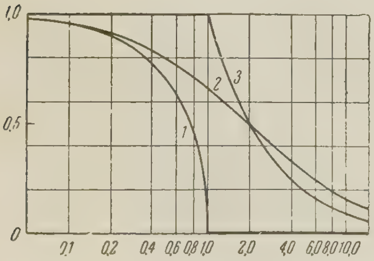

FIG. 2. The quantity $M_z M_0$ (curves 1 and 2) and χ'' (curve 3) as functions of a^2 for $\Delta\omega = 0$; curve 1 is for $M_0 = M_s$ curve 2 is for $M_0 = \chi_0 H_0$.

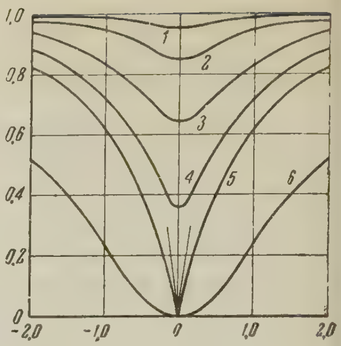

FIG. 3. The dependence of $(M_z/M_s)^2$ on ξ for the following values: 1) $a = 0.2$; 2) $a = 0.4$; 3) $a = 0.6$; 4) $a = 0.8$; 5) $a = 1.0$; 6) $a = 2.0$.

Using the Landau-Lifshitz equations we find $\eta = 1$ when $a \ge 1$.

If the length of the vector **M** remains constant, the ratio M_{0z}/M_0 obeys Eq. (10) for $\Delta\omega = 0$ and vanishes when h_0 equals the half-width of the resonance absorption line $\Delta H = |\alpha| H_0$. On the other hand, if we start from Eq. (1), in accordance with Eq. (5) M_{0z}/M_0 falls off gradually as h_0 increases, finally approaching zero. The quantity M_{0z}/M_0 is shown in Fig. 2 where, with $a \ll 1$, it is assumed that $\sqrt{2}\,\alpha\gamma\tau H_0 = 1$.

Experiments[3] on nickel-zinc and manganese-zinc ferrites at temperatures below the Curie point at $h_0 \le 40$ oersteds have shown the reduction in M_{0z}/M_0 with increasing h_0. Unfortunately, an experiment does not allow us to choose between curve 1 and curve 2 of Fig. 2 since a is less than 0.1. In this case saturation is to be expected at $h_0 \approx 100$ oresteds. Total saturation can occur in relatively weak radio-frequency fields only in ferrites with narrow absorption lines.[4] In paramagnetic materials and ferrites above the Curie point, the dependence of M_{0z}/M_0 is shown by curve 2 of Fig. 2.

In the experiments performed by Damon,[2] carried out on single-crystal nickel ferrites at room temperature, the dependence of M_{0z}/M_0 on field strength H_0 was measured at various amplitudes of the radio-frequency field. The relations obtained are in good agreement with the theory if one starts from Eq. (2). The theoretical dependence of $(M_{0z}/M_s)^2$ on ξ is shown in Fig. 3 for various values of a. When $a \ge 1$ and $\Delta\omega = 0$, M_{0z}/M_s vanishes. It would seem that in the Damon experiments a was not greater than 0.2.

It follows from (4) and (8) that with $\Delta\omega = 0$, $\chi'' = |\gamma|\,\tau M_{0z}$, i.e., the change in χ'' with h_0 is proportional to the change in M_{0z}. The latter situation actually obtains for paramagnetic materials and ferromagnetic materials above the Curie temperature Θ. In ferromagnetic materials with $T < \Theta$, as has been shown in references 2 and 3, the proportionality between χ'' and M_{0z} no longer holds. Up to a certain threshold value of h_0, χ''

remains constant when $\Delta\omega = 0$; then it falls off approximately as a^{-2}.

In accordance with (11), in this case (curve 3, Fig. 2)

$$\chi'' = \gamma M_s / \alpha\omega \text{ for } a < 1 \quad \text{and} \quad \chi'' = \gamma M_s / \alpha\omega a^2 \text{ for } a > 1 \qquad (12)$$

the threshold field is determined by the value $a = 1$, which is larger than that observed experimentally.[1]

4. Equation (2) follows directly from Eq. (1) if we require that the magnitude of the magnetization vector remain constant: $M = M_S$. Equation (1) can be obtained under the assumption that the equilibrium magnetization obeys the Curie law.[5] Hence, it might be supposed that magnetic resonance effects in ferromagnets above the Curie point should obey Eq. (1); this conclusion is found to be in agreement with experiment. On the other hand, at temperature below the Curie temperature, if paramagnetic effects are neglected one would expect the Landau-Lifshitz equations to hold. In cases in which the paramagnetic effects cannot be neglected (for example, at temperatures close to the Curie temperature) one would expect that the ferromagnetic resonance effect would not be satisfactorily described by Eq. (2) or Eq. (1). In this case it would appear that the observed effects can be described by the joint application of Eqs. (1) and (2) if $\mathbf{M} = \mathbf{M}_S + \chi_0\mathbf{H}$.

---

[1] H. Suhl. Proc. I.R.E. **44**, 1270 (1956).

[2] R. W. Damon, Revs. Modern Phys. **25**, 239 (1953).

[3] N. Bloembergen and S. Wang, Phys. Rev. **93**, 72 (1954).

[4] J. F. Dillon Jr., Phys. Rev. **105**, 759 (1957).

[5] G. V. Skrotskii and V. T. Shmatov, J. Exptl. Theoret. Phys. (U.S.S.R.) **34**, 740 (1958), Soviet Phys. JETP **7**, 508 (1958).

Translated by H. Lashinsky
311

SOVIET PHYSICS JETP VOLUME 35(8), NUMBER 6 JUNE, 1959

SPIN STRUCTURE OF THE SCATTERING MATRIX FOR REACTIONS INVOLVING GAMMA RAYS

V. I. RITUS

P. N. Lebedev Physics Institute, Academy of Sciences, U.S.S.R.

Submitted to JETP editor June 23, 1958

J. Exptl. Theoret. Phys. (U.S.S.R.) **35**, 1485-1487 (December, 1958)

The scattering matrix for reactions involving γ rays (such as $\gamma + b \rightarrow a' + b'$ and $\gamma + b \rightarrow \gamma' + b'$) is expanded in terms of spin operators Q_i which are invariant under rotations. A method of constructing the Q_i is given and the number of independent ones is found. If the scattering matrix is invariant under time inversion, the corresponding conditions on the form and number of the Q_i are found. Example are given for the representation of the matrix S by operators Q_i in the case that neither the spin of b, nor the spin of the system $a' + b'$ $(\gamma + b \rightarrow a' + b')$, nor the spins of the particles b, b′ $(\gamma + b \rightarrow \gamma' + b')$ are more than one.

In an earlier paper[1] the author has considered the expansion of the scattering matrix $S(\mathbf{k}', \mathbf{k})$ for the reaction $a + b \rightarrow a' + b'$ in terms of spin operators Q_i which are invariant under rotation and reflection:*

$$S(\mathbf{k}', \mathbf{k}) = \sum_i A_i(\mathbf{k}' \cdot \mathbf{k})\, Q_i(\mathbf{k}', \mathbf{k}, \mathbf{T}) \qquad (1)$$

A method was given for obtaining the independent spin operators and for determining their number. Also considered were the conditions imposed on the form and number of the independent spin operators if the scattering matrix were invariant under time inversion.

In the present paper, these considerations are extended to scattering matrices $S(\mathbf{k}', \mathbf{k})$ for reactions involving γ rays, i.e., reactions like $\gamma + b \rightarrow a' + b'$, $\gamma + b \rightarrow \gamma' + b'$, where the particles b, b′ and the system $a' + b'$ can have any spin and parity.

Using the expansion of the scattering matrix in terms of angle operators L_α,[2] it is not difficult to show that the independent spin operators for the reaction $\gamma + b \rightarrow \gamma' + b'$ will be the operators

$$(\mathbf{k}' \cdot \mathbf{e})\, Q_i^{(\pm)}(\mathbf{k}', \mathbf{k}, \mathbf{T}), \quad i(\mathbf{k}' \cdot \mathbf{s})\, Q_i^{(\mp)}(\mathbf{k}', \mathbf{k}, \mathbf{T}), \qquad (2)$$

where $\mathbf{e}$ is the polarization vector for the incident photon, $\mathbf{s} = \mathbf{k} \times \mathbf{e}$, $Q_i^{(\pm)}$ are the spin operators for the reaction $a + b \rightarrow a' + b'$ which differs from the reaction $\gamma + b \rightarrow a' + b'$ in that the γ-quantum has been replaced by a particle a with spin zero. The operator $Q_i^{(+)}$ corresponds to the case that the inner parity of the system does not change, while $Q_i^{(-)}$ corresponds to the case where the inner parity does change. The upper sign in $Q_i^{(\pm)}$ is to be used in formula (2) when the intrinsic parity of particle b in the reaction $\gamma + b \rightarrow a' + b'$ is the same as the intrinsic parity of the system $a' + b'$, while the lower sign is to be used in the opposite case. From formula (2) and the number of independent spin operators $Q_i^{(\pm)}$ for the reaction $a + b \rightarrow a' + b'$[1] it follows that the number of independent spin invariants for the reaction $\gamma + b \rightarrow a' + b'$ is $(2S' + 1)(2S + 1)$, where S is the spin of particle b and S′ is the spin of the system $a' + b'$. Summing on the possible values of S′, we obtain $(2s'_a + 1)(2s'_b + 1)(2s_b + 1)$ invariants, where s'_a, s'_b, and s_b are the spins of the particles a′, b′, and b. One can similarly show that the independent spin invariants for the reaction $\gamma + b \rightarrow \gamma' + b'$ are given by

$$(\mathbf{e}' \cdot \mathbf{e})\, Q_i^{(\pm)}, \quad (\mathbf{s}' \cdot \mathbf{s})\, Q_i^{(\pm)}, \quad i(\mathbf{s}' \cdot \mathbf{e})\, Q_i^{(\mp)}, \quad -i(\mathbf{e}' \cdot \mathbf{s})\, Q_i^{(\mp)}, \qquad (3)$$

where the $Q_i^{(\pm)}$ are the invariant spin operators for the reaction $a + b \rightarrow a' + b'$, in which a, a′ are particles with spin zero. The signs (±) on the operators $Q_i^{(\pm)}$ mean the same as in the preceding. In formula (3), the upper sign in the operator $Q_i^{(\pm)}$ is to be used if the intrinsic parity of the particles b, b′ in the reaction $\gamma + b \rightarrow \gamma' + b'$ are the same, while the lower sign is to be used in the opposite case. It is clear that the total number of independent spin invariants for the reaction $\gamma + b \rightarrow \gamma' + b'$ is $2(2S' + 1)(2S + 1)$, where S, S′ are the spins of particles b, b′. It should be noted that in reference 3 the number of spin invariants for the photo-production of mesons with spins 0 and 1 and in the scattering of photons from spin $\frac{1}{2}$ particles was found to be, respectively, 4, 14, and 10, while the present considerations lead to 4, 12, and 8. A detailed examination of the last mentioned case shows that the ten invariants mentioned in reference 3 reduce to eight.

---

*The notation used here is the same as in reference 1.

It was shown in reference 1 that if the scattering matrix for elastic scattering of particles with spin is invariant under time inversion, then the form of the invariant spin operators Q_i changes, while the number of independent ones decreases. Similar statements hold for the elastic scattering of photons from particles with spin, $\gamma + b \rightarrow \gamma + b$. The proof is the same as in reference 1. We find that the spin operators enter the scattering matrix in the combinations

$$(\mathbf{e}'\cdot\mathbf{e})\,[Q_i^{(+)}(\mathbf{k}',\ \mathbf{k},\ \mathbf{T}) + Q_i^{(+)+}(\mathbf{k},\ \mathbf{k}',\ \mathbf{T})],$$

$$(\mathbf{s}'\cdot\mathbf{s})\,[Q_i^{(+)}(\mathbf{k}',\ \mathbf{k},\ \mathbf{T}) + Q_i^{(+)+}(\mathbf{k},\ \mathbf{k}',\ \mathbf{T})],$$

$$i\,[(\mathbf{s}'\cdot\mathbf{e})\,Q_i^{(-)}(\mathbf{k}',\ \mathbf{k},\ \mathbf{T}) - (\mathbf{e}'\cdot\mathbf{s})\,Q^{(-)+}(\mathbf{k},\ \mathbf{k}',\ \mathbf{T})],$$

$$-i\,[(\mathbf{e}'\cdot\mathbf{s})\,Q_i^{(-)}(\mathbf{k}',\mathbf{k},\mathbf{T}) - (\mathbf{s}'\cdot\mathbf{e})\ \ Q_i^{(-)+}(\mathbf{k},\ \mathbf{k}',\ \mathbf{T})],$$

i.e., those combinations which are symmetric under hermitian conjugation and simultaneous interchange $\mathbf{k} \rightleftarrows \mathbf{k}'$, $\mathbf{e} \rightleftarrows \mathbf{e}'$. The number of independent spin operators decreases by the number of relations between elements of the scattering matrix for which $j \neq j'$;

$$S^{ii}_{Jj'S\lambda',\,jS\lambda} = S^{ii}_{JjS\lambda,\,jS\lambda'}, \qquad (4)$$

In (4), λ and λ' are numbers characterizing the type of radiation ($\lambda = 1$ for electric and 0 for magnetic radiation), while j, j′ are the moments. There are $2S(2S+1)$ relations (4), where S is the spin of particle b. Hence the number of independent spin invariants for elastic scattering of photons from particles with spin S is $2(2S+1) \times (S+1)$.

As an example, let us write out the matrix $S(\mathbf{k}', \mathbf{k})$ in terms of independent operators Q_i for some reactions like $\gamma + b \rightarrow a' + b'$ and $\gamma + b \rightarrow \gamma' + b'$. If the intrinsic parity of the particle b and of the system $a' + b'$, or of the particles b, b′, are the same, then the reaction will be marked +, while if they are opposite, then the reaction will be marked −. We note that the matrices $S(\mathbf{k}', \mathbf{k})$ of such reactions differ only by the change $\mathbf{e} \rightleftarrows -i\mathbf{s} \equiv -i\mathbf{k} \times \mathbf{e}$ or the change $\mathbf{e}' \rightleftarrows i\mathbf{s}'$.

(1) $\gamma + b \rightarrow a' + b'$.

$S = S' = 0.\ (+).\qquad S(\mathbf{k}',\ \mathbf{k}) = (\mathbf{k}'\cdot\mathbf{e})\,A_1.$

$S = S' = {}^1/_2.\ (-).\qquad S(\mathbf{k}',\mathbf{k}) = i(\mathbf{n}\cdot\mathbf{e})\,A_1 + (\sigma\cdot\mathbf{e})\,A_2$

$+ (\sigma\cdot\mathbf{k}')(\mathbf{k}'\cdot\mathbf{e})\,A_3 + (\sigma\cdot\mathbf{k})(\mathbf{k}'\cdot\mathbf{e})\,A_4.\qquad S = S' = 1.\ (+).$

$$S(\mathbf{k}',\ \mathbf{k}) = (\mathbf{k}'\cdot\mathbf{e})\,A_1 + i\,(\mathbf{S}\cdot[\mathbf{k}'\times\mathbf{e}])\,A_2 + i\,(\mathbf{S}\cdot[\mathbf{k}\times\mathbf{e}])\,A_3$$

$$+ i\,(\mathbf{S}\cdot\mathbf{n})(\mathbf{k}'\cdot\mathbf{e})\,A_4 + [(\mathbf{S}\cdot\mathbf{k}')(\mathbf{S}\cdot\mathbf{e}) + (\mathbf{S}\cdot\mathbf{e})(\mathbf{S}\cdot\mathbf{k}')]\,A_5$$

$$+ [(\mathbf{S}\cdot\mathbf{k})(\mathbf{S}\cdot\mathbf{e}) + (\mathbf{S}\cdot\mathbf{e})(\mathbf{S}\cdot\mathbf{k})]\,A_6 + [(\mathbf{S}\cdot\mathbf{k}')(\mathbf{S}\cdot\mathbf{k}) + (\mathbf{S}\cdot\mathbf{k})(\mathbf{S}\cdot\mathbf{k}')]\,A_7$$

$$+ (\mathbf{S}\cdot\mathbf{k}')^2(\mathbf{k}'\cdot\mathbf{e})\,A_8 + (\mathbf{S}\cdot\mathbf{k})^2(\mathbf{k}'\cdot\mathbf{e})\,A_9.$$

$S = 0,\ S' = 1$ or $S = 1,\ S' = 0.\ (+).$

$$S(\mathbf{k}',\ \mathbf{k}) = i\,(\mathbf{T}\cdot[\mathbf{k}'\times\mathbf{e}])\,A_1 + i\,(\mathbf{T}\cdot[\mathbf{k}\times\mathbf{e}])\,A_2 + i\,(\mathbf{T}\cdot\mathbf{n})(\mathbf{k}'\cdot\mathbf{e})\,A_3.$$

(2) $\gamma + b \rightarrow \gamma' + b'$.

$S = S' = 0.\ (+).\ S(\mathbf{k}',\ \mathbf{k}) = (\mathbf{e}'\cdot\mathbf{e})\,A_1 + (\mathbf{s}'\cdot\mathbf{s})\,A_2.$

$$S = S' = {}^1/_2.\ (+).\ S(\mathbf{k}'\cdot\mathbf{k}) = (\mathbf{e}'\cdot\mathbf{e})\,A_1$$

$$+ (\mathbf{s}'\cdot\mathbf{s})\,A_2 + i\,(\sigma\cdot[\mathbf{e}'\times\mathbf{e}])\,A_3 + i\,(\sigma\cdot[\mathbf{s}'\times\mathbf{s}])\,A_4$$

$$+ i\,(\sigma\cdot\mathbf{k}')(\mathbf{e}'\cdot\mathbf{s})\,A_5 + i\,(\sigma\cdot\mathbf{k})(\mathbf{s}'\cdot\mathbf{e})\,A_6$$

$$+ i\,(\sigma\cdot\mathbf{k}')(\mathbf{s}'\cdot\mathbf{e})\,A_7 + i\,(\sigma\cdot\mathbf{k})(\mathbf{e}'\cdot\mathbf{s})\,A_8,$$

with $A_5 = -A_6$ and $A_7 = -A_8$ for elastic scattering.

$$S = S' = 1.\ (+).\ S(\mathbf{k}',\ \mathbf{k}) = (\mathbf{e}'\cdot\mathbf{e})\,\{A_1 + i\,(\mathbf{S}\cdot\mathbf{n})\,A_2$$

$$+ [(\mathbf{S}\cdot\mathbf{k}')(\mathbf{S}\cdot\mathbf{k}) + (\mathbf{S}\cdot\mathbf{k})(\mathbf{S}\cdot\mathbf{k}')]\,A_3 + (\mathbf{S}\cdot\mathbf{k}')^2A_4 + (\mathbf{S}\cdot\mathbf{k})^2A_5\}$$

$$+ (\mathbf{s}'\cdot\mathbf{s})\,\{A_6 + i\,(\mathbf{S}\cdot\mathbf{n})\,A_7 + [(\mathbf{S}\cdot\mathbf{k}')(\mathbf{S}\cdot\mathbf{k}) + (\mathbf{S}\cdot\mathbf{k})(\mathbf{S}\cdot\mathbf{k}')]\,A_8$$

$$+ (\mathbf{S}\cdot\mathbf{k}')^2A_9 + (\mathbf{S}\cdot\mathbf{k})^2A_{10}\} + i\,(\mathbf{s}'\cdot\mathbf{e})\,[(\mathbf{S}\cdot\mathbf{k}')\,A_{11} + (\mathbf{S}\cdot\mathbf{k})\,A_{12}$$

$$+ i\,(\mathbf{S}\cdot\mathbf{k}')(\mathbf{S}\cdot\mathbf{n})\,A_{13} + i\,(\mathbf{S}\cdot\mathbf{k})(\mathbf{S}\cdot\mathbf{n})\,A_{14}] - i\,(\mathbf{e}'\cdot\mathbf{s})\,[(\mathbf{S}\cdot\mathbf{k}')\,A_{15}$$

$$+ (\mathbf{S}\cdot\mathbf{k})\,A_{16} + i\,(\mathbf{S}\cdot\mathbf{k}')(\mathbf{S}\cdot\mathbf{n})\,A_{17} + i\,(\mathbf{S}\cdot\mathbf{k})(\mathbf{S}\cdot\mathbf{n})\,A_{18}],$$

and for elastic scattering, $A_4 = A_5$, $A_9 = A_{10}$, $A_{11} = A_{16}$, $A_{12} = A_{15}$, $A_{13} = A_{18}$, $A_{14} = A_{17}$.

In these formulas the A_i are functions of $(\mathbf{k}'\cdot\mathbf{k})$ and the energy of the system, while $\mathbf{n} = \mathbf{k}' \times \mathbf{k}$.

---

[1] V. I. Ritus, J. Exptl. Theoret. Phys. (U.S.S.R.) 33, 1264 (1957), Soviet Phys. JETP 6, 972 (1958).

[2] V. I. Ritus, J. Exptl. Theoret. Phys. (U.S.S.R.) 32, 1536 (1957), Soviet Phys. JETP 5, 1249 (1958).

[3] M. Kawaguchi and N. Mugibayashi, Progr. Theoret. Phys. 8, 212 (1952).

Translated by R. Krotkov
312

SOVIET PHYSICS JETP VOLUME 35(8), NUMBER 6 JUNE, 1959

ABSORPTION OF POLARIZED μ^--MESONS BY NUCLEI ANGULAR DISTRIBUTION OF THE NEUTRONS

E. I. DOLINSKII and L. D. BLOKHINTSEV

Moscow State University

Submitted to JETP editor June 24, 1958

J. Exptl. Theoret. Phys. (U.S.S.R.) **35**, 1488-1498 (December, 1958)

The angular distribution of neutrons produced in the absorption of polarized μ^- mesons by nuclei is calculated. Numerical computations are performed for O^{16} and Ca^{40}.

1. INTRODUCTION

THE investigation of the nuclear absorption of μ^- mesons is a possible means to determine the character of the non-electrodynamic interaction of the μ^- mesons with nuclei. The nuclear absorption process of the μ^- mesons goes through an intermediate stage under formation of a mesic atom and continues via the reaction

$$\mu^- + P \rightarrow N + \nu + Q, \qquad (1)$$

in which the proton (P) absorbing the μ^- meson transforms into a neutron (N) and a neutrino (ν). The difficulties involved in the discussion of process (1) in nuclei are not merely of computational nature. The trouble is that, owing to the large amount of released energy ($Q \sim 100$ Mev), the neutrino and the neutron emitted by the nucleus in the capture of the μ^- meson carry rather large angular momenta, and the remaining nucleus can acquire a high excitation energy. One must therefore consider transitions involving comparatively large changes in the angular momentum and highly excited nuclear states, which obviously is a difficult task, because of our insufficient knowledge of the nuclear wave functions.

The nuclei in the nuclear μ^--meson absorption processes were described in most calculations by the nuclear shell model with jj coupling. In this case the ratio of the probabilities for μ^- capture in different nuclei depends on the form of the μ meson-nucleon interaction, so that the Fermi interaction (scalar, vector) can be distinguished from the Gamow-Teller interaction (tensor, axial vector).[1-3]

The experimental ratios of the μ^--capture probabilities for six pairs of nuclei were compared with the computed values of Tolhoek and Luyten[3] in reference 4. In the opinion of the authors, the results point to the possible predominance of the Gamow-Teller interaction. This conclusion is, however, not sufficiently reliable, since the abovementioned calculations have at best semi-quantitative character.

The discovery of parity nonconservation in weak interactions increases the number of effects which may be utilized to decide the question of the type of the μ meson-nucleon interaction. A number of papers[5-9] propose to investigate the asymmetry in the angular distribution of the neutrons from reaction (1) during the absorption of polarized μ^- mesons. In references 5, 9, and 10 it is shown that the nucleus remaining after the μ^- capture is polarized, where the degree of polarization depends on the type of the μ meson-nucleon interaction (the μ^- mesons can be unpolarized). The investigation of the circular polarization and the angular distribution[8] of the γ quanta in the radiative μ^- capture (where, in the second case, the μ^- mesons are assumed to be polarized) also permits the determination of the form of the interaction.

We point out that there are practically no experiments on the absorption of polarized μ^- mesons in μ mesic hydrogen, since the hyperfine structure in the mesic hydrogen atom and the effect of the jumping of the μ^- meson from one proton to another lead to the complete depolarization of the μ^- mesons.[11,12] Furthermore, the probability for absorption of the μ^- mesons in mesic hydrogen is extremely small. It is therefore of greatest interest to investigate theoretically the effects connected with the μ^- capture in complex nuclei. In the present paper we calculate the angular distribution of the neutrons produced according to reaction (1) during the absorption of polarized μ^- mesons by complex nuclei. Preliminary results have been published earlier.[13]

2. ANGULAR DISTRIBUTION OF THE NEUTRONS

The μ^- mesons produced in the decay of π^- mesons are polarized in the direction of their motion. During the slowing down in the medium and the following formation of the mesic atom a depolarization of the μ^- mesons is possible, which can, however, be incomplete.[14] A part of the neutrons produced in process (1) leaves the nucleus immediately after the capture of the μ^- meson, i.e., reaction (1) is a direct process. Under the assumption that, as in other weak interaction processes, parity is not conserved in the μ^- capture, the angular distribution of the neutrons from the direct process has the form

$$1 + P_\mu \alpha \cos\theta, \tag{2}$$

where P_μ is the degree of polarization of the μ^- mesons at the moment of capture, α is asymmetry coefficient depending on the type of the four-fermion interaction of the μ meson-nucleon system and on the degree to which parity is not conserved, and θ is the angle between the direction of polarization of the μ^- meson and the direction of emission of the neutron.

It should be noted that, in addition to the angular distribution (2) of the neutrons emitted by the nucleus in the direct process, there is an isotropic background of neutrons from the decay of the compound nucleus formed in reaction (1). The spectrum of the neutrons of the isotropic background has a maximum at the energy $E_N \sim 1$ to 1.5 Mev, while the maximum for the neutrons of the direct process lies at $E_N \sim 5$ Mev (see Sec. 3). One can thus decrease the background considerably by selecting the neutrons with energies $E_N \gtrsim 3$ Mev. It is to be expected that, for the lighter nuclei, the total number of neutrons consists essentially of neutrons from the direct process.

Assuming parity nonconservation, we can write the Hamiltonian for the four-fermion interaction of the μ mesons with the nucleons in the form

$$H = \sum_k (\overline{\Psi}_N O_k \Psi_P)(\overline{\Psi}_\nu [g_k - g'_k \gamma_5] O\, \Psi_\mu) + \text{herm. conj.}, \tag{3}$$

where $k = s, v, p, t, a$ denotes, respectively the scalar, vector, pseudoscalar, tensor, and axial vector variant, and

$$O_s = 1,\ O_v^\alpha = \gamma_\alpha,\ O_p = \gamma_5,\ O_t^{\alpha\beta} = -i2^{-3/2}(\gamma_\alpha\gamma_\beta - \gamma_\beta\gamma_\alpha),\quad O_a^\alpha = -i\gamma_\alpha\gamma_5, \qquad (\alpha,\ \beta = 1,\ 2,\ 3,\ 4). \tag{4}$$

If $g'_k = -g_k$ we have the theory of the longitudinal neutrino,[15] in which the neutrino produced in process (1) is, with our Hamiltonian (3), polarized in the direction of its motion. If, during the absorption of the μ^- meson, a neutrino is created which is polarized opposite to its direction of motion, then we must change the sign in front of the asymmetry coefficient α.

Since the neutrino carries away most of the energy released in the μ^- capture, while the nucleons in the nucleus acquire only energies of a few Mev, we can treat the nucleons nonrelativistically in the s, v, t, and a variants of the interaction. For the p variant (which vanishes in the nonrelativistic approximation) we use the first approximation for the nucleons (in terms of v/c), in which the small components of the wave function (φ) are expressed in terms of the large ones (ψ) according to the well-known formula $\varphi = [(\sigma\times p)/2Mc]\psi$, where $p = -i\hbar\nabla$. Furthermore, we can neglect terms of order $\lambda\!\!\!^{-}_\nu/a_\mu$ in the p variant ($\lambda\!\!\!^{-}_\nu \sim 2\times10^{-13}$ cm is the de Broglie wavelength of the neutrino, and $a_\mu \sim 2\times10^{-1} Z^{-1}$ cm is the radius of the K orbit of the μ^- mesic atom).

Since the binding energy of the μ^- meson in the K orbit of the mesic atom is much less than its rest energy, we may restrict ourselves to the nonrelativistic approximation of the μ^- meson wave function. The nucleus is described by the shell model with jj coupling. The recoil energy of the nucleus is neglected. For the wave function of the emitted neutron we take the complex potential solution, which takes into account the interaction of the neutron with the remaining nucleus. The potential of the shell model and the potential describing the interaction of the neutron with the nucleus are taken to be spherically symmetric.

With these assumptions the wave functions of the proton in the (n, j, l) subshell, of the neutron, of the μ^- meson, and of the neutrino can be written in the form

$$\psi_P = R_{njl}(r)\,\Omega_{jlj_z}(\mathbf{r}/r), \quad \int_0^\infty R^2_{njl}(r)\,r^2dr = 1, \tag{5}$$

$$\psi_N = \psi_N(\mathbf{r})\,\chi_{s_N}, \quad \Psi_N(\mathbf{r}) = \sum_L i^L(2L+1)\,a_L(r)\,P_L(\mathbf{k}_N\mathbf{r}/k_N r), \tag{6}$$

$$\psi_N(\mathbf{r}) \sim (2\pi)^{-3/2}(e^{i\mathbf{k}_N\mathbf{r}} + (f/r)\,e^{-ik_N r}) \text{ for } r\to\infty,\text{*}$$

$$\psi_\mu = (4\pi)^{-1/2} R_\mu(r)\,\chi_{s_\mu}, \quad \int_0^\infty R^2_\mu(r)\,r^2\,dr = 1, \tag{7}$$

$$\psi_\nu = (2\pi)^{-3/2} u_\nu e^{i\mathbf{k}_\nu\mathbf{r}}. \tag{8}$$

Here n, j, l are the quantum numbers specifying the nuclear subshell in the shell model with jj coupling (n is the number of nodes of $R_{njl}(r)$ plus one, l is the orbital angular momentum, and

---

*This asymptotic form takes account of the creation of the neutron.[16]

$j = l \pm \frac{1}{2}$ is the total momentum of the proton), χ are normalized spinors, u_ν is a normalized Dirac bispinor, and $\Omega_{jlj_z}(\mathbf{r}/r)$ is a spherical spinor.[17] Disregarding the finite dimensions of the nucleus (which is admissible for $Z < 30$), we have

$$R_\mu(r) = 2a_\mu^{-3/2}\exp(-r/a_\mu), \quad a_\mu = \hbar^2/m_\mu e^2 Z.$$

The computational results listed below apply, strictly speaking, only to nuclei with completely filled proton subshells. In this case, according to the Pauli principle, a proton state in the nucleus is described by a wave function in form of a determinant made up of one-particle wave functions of form (5). It is easily shown, however, that the use of wave function (5) directly for the single proton in the calculations, with the subsequent summation over the projections of the total angular momentum j_z and over all proton subshells (n, j, l) in the nucleus, leads to the same result as the calculation using the determinant. If some subshell (n, j, l) in the nucleus is not completely filled, we must, generally speaking, include in the calculations the correlation between the angular momenta of the separate protons in this subshell.* We further note that, if the nuclear spin is different from zero, with the protons contributing to the spin, it is necessary to include the hyperfine structure of the mesic atom in the calculations. Since the latter causes a strong additional depolarization of the μ^- mesons, such cases are not of great interest among the experiments under discussion, and we shall therefore leave them out of our considerations.

With the usual formulas of first order perturbation theory we obtain from Eqs. (3) to (8) for the probability of emission of the neutron from the nucleus with an energy in the interval E_N to $E_N + dE_N$ $(E_N = \hbar^2 k_N^2/2M)$ into the solid angle $d\Omega_N$ under the given angle θ with respect to the direction of polarization of the μ^- meson:†

$$\begin{aligned} dW(E_N, \theta) = \{[((f_{ss} + 2\mathrm{Re}\, f_{sv} + f_{vv}) \\ + 3(f_{tt} + 2\mathrm{Re}\, f_{ta} + f_{aa}))\, A_0(E_N) \\ - 2\mathrm{Re}\,(f_{pt} + f_{pa})\, A_1(E_N) + f_{pp}\, A_2(E_N)] \\ + P_\mu[(-(h_{ss} + 2\mathrm{Re}\, h_{sv} + h_{vv}) + (h_{tt} + 2\mathrm{Re}\, h_{ta} + h_{aa})) \\ \times B_0(E_N) + 2\mathrm{Re}\,(h_{pt} + h_{pa})\, B_1(E_N) - h_{pp}\, B_2(E_N) \\ + 2\mathrm{Im}\,(h_{st} + h_{sa} + h_{vt} + h_{va})\, G_0(E_N) \\ + 2\mathrm{Im}\,(h_{pt} + h_{pa})\, G_1(E_N)]\cos\theta\}\, dE_N\, d\Omega_N/4\pi, \end{aligned} \tag{9}$$

where $A_k(E_N)$, $B_k(E_N)$, and $G_k(E_N)$ $(k = 0, 1, 2)$ are functions of the energy of the emitted neutron depending on the properties of the nucleus under consideration.*

With the help of (9) we can write the angular distribution of the neutrons emitted from the nucleus in the form

$$q(E_N, \theta) = 1 + P_\mu \alpha(E_N)\cos\theta, \tag{10}$$

where

$$\begin{aligned} \alpha(E_N) = \{[(h_{ss} + 2\mathrm{Re}\, h_{sv} + h_{vv}) \\ - (h_{tt} + 2\mathrm{Re}\, h_{ta} + h_{aa})]\, \beta_0(E_N) \\ - 2\mathrm{Re}\,(h_{pt} + h_{pa})\, \beta_1(E_N)\, \gamma_1(E_N) + h_{pp}\, \beta_2(E_N)\, \gamma_2(E_N) \\ + 2\mathrm{Im}\,(h_{st} + h_{sa} + h_{vt} + h_{va})\, \delta_0(E_N) \\ + 2\mathrm{Im}\,(h_{pt} + h_{pa})\, \delta_1(E_N)\}\, \{(f_{ss} + 2\mathrm{Re}\, f_{sv} + f_{vv}) \\ + 3(f_{tt} + 2\mathrm{Re}\, f_{ta} + f_{aa}) - 2\mathrm{Re}\,(f_{pt} + f_{pa})\, \gamma_1(E_N) \\ + f_{pp}\, \gamma_2(E_N)\}^{-1}. \end{aligned} \tag{11}$$

We remember that for μ^- capture in mesic hydrogen[5] (neglecting the fine structure)†

$$\beta_k = 1, \quad \delta_k = 0, \quad \gamma_1 = 0.53\cdot 10^{-1}, \quad \gamma_2 = 0.28\cdot 10^{-2}. \tag{12}$$

Our case is therefore different from that of the mesic hydrogen in that the quantities $\beta_k(E_N)$ and $\gamma_k(E_N)$ are here functions of the neutron energy depending on concrete properties of the nucleus, and also in that additional terms involving $\delta_k(E_N)$ appear. The order of magnitude of the functions $\gamma_k(E_N)$ for the nucleus agrees with the values in formula (12).

In the theory of the longitudinally polarized neutrino $(g_k' = -g_k)$ formula (11) takes the form

$$\begin{aligned} \alpha^{\text{long.}}(E_N) = \{(-|g_s + g_v|^2 + |g_t + g_a|^2)\, \beta_0(E_N) \\ + 2\mathrm{Re}\,[g_p^*(g_t + g_a)]\, \beta_1(E_N)\, \gamma_1(E_N) - |g_p|^2\, \beta_2(E_N)\, \gamma_2(E_N) \\ - 2\mathrm{Im}\,[(g_s^* + g_v^*)(g_t + g_a)]\, \delta_0(E_N) \\ - 2\mathrm{Im}\,[g_p^*(g_t + g_a)]\, \delta_1(E_N)\}\, \{|g_s + g_v|^2 + 3|g_t + g_a|^2 \\ - 2\mathrm{Re}\,[g_p^*(g_t + g_a)]\, \gamma_1(E_N) + |g_p|^2\, \gamma_2(E_N)\}^{-1}. \end{aligned} \tag{13}$$

In the absence of pseudoscalar coupling we obtain from (13)

$$\begin{aligned} \alpha_{svta}^{\text{long.}}(E_N) = \{(-|g_s + g_v|^2 + |g_t + g_a|^2)\, \beta_0(E_N) \\ - 2\mathrm{Im}\,[(g_s^* + g_v^*)(g_t + g_a)]\, \delta_0(E_N)\} \\ \times \{|g_s + g_v|^2 + 3|g_t + g_a|^2\}^{-1}. \end{aligned} \tag{13a}$$

---

*If the incompletely filled nuclear subshell (n, j, l) contains two protons with total spin zero, the formulas below remain valid provided we change $(2j + 1)$ to 2 for this subshell in all formulas of the Appendix.

†The notations used in (9) and in the following formulas of this section are explained in the Appendix at the end of this article.

*Formulas (2) and (3) of reference 13 do not include the terms describing the interference between the Fermi and Gamow-Teller interactions. The interference term missing in (3) is given by formula (A 12) of the Appendix. Furthermore, (2) and (3) should be multiplied by the function $\rho_{njl}(E_N)$, which is also given in the Appendix.

†In reference 5 the tensor and axial vector operators are defined as $O_t^{\alpha\beta} = (1/2)(\gamma_\alpha\gamma_\beta - \gamma_\beta\gamma_\alpha)$ and $O_a^\alpha = \gamma_\alpha\gamma_5$, respectively. Here we use the usual definition [see (4)].

For pure p coupling we have

$$\alpha_p^{\text{long.}}(E_N) = -\beta_2(E_N). \qquad (13b)$$

Integrating over the energy of the emitted neutron E_N, we obtain, instead of (9), (10), (11), and (13), formulas of completely analogous form, in which the functions $A_k(E_N)$, $B_k(E_N)$, $G_k(E_N)$, $\beta_k(E_N)$, $\gamma_k(E_N)$, and $\delta_k(E_N)$ are replaced by the corresponding constants $\widetilde{A}_k$, $\widetilde{B}_k$, $\widetilde{G}_k$, $\widetilde{\beta}_k$, $\widetilde{\gamma}_k$, and $\widetilde{\delta}_k$, which depend, of course, on the properties of the given nucleus.

We note that in the special case of emission of the neutron and the neutrino in opposite directions $(\mathbf{n}_N + \mathbf{n}_\nu = 0)$ the angular distribution of the neutrons has the form (10) with α given by (11) and (13), $\beta_k = 1$, $\delta_k = 0$, and γ_k very close to the γ_k of formula (12).

We add a few remarks concerning the formulas obtained.

1. If it turns out that the interaction of the μ mesons with the nucleons is that of the Gell-Mann — Feynman theory,[18] which assumes the presence of the a and v variants with one common coupling constant, then, according to (13), the asymmetry effect in the angular distribution of the neutrons disappears.

2. The pseudoscalar coupling is multiplied by a factor $\sim 1/20$ in all formulas.

3. The spin-orbit interaction of the emitted neutron with the nucleus has been neglected in the derivation of our formulas. The inclusion of this interaction leads to the expressions given in reference 13. Estimates made for some special cases lead us to assume that the spin-orbit interaction has little effect on the angular distribution of the neutrons. It may, however, become quite important in the computation of the polarization of the neutrons in process (1).

3. NUMERICAL CALCULATIONS FOR O^{16} AND Ca^{40}

The quantities entering into the formulas (9) and (11) were calculated for the μ^- capture in the nuclei O^{16} and Ca^{40}. The calculations were made under the following assumptions.

(A) For the radial proton wave functions in the nucleus we used the wave functions corresponding to a square-well potential. The dependence of the radius of the well R on the mass number A was assumed to have the form $R = r_0 A^{1/3}$. We neglected the dependence of the radial wave function on the quantum number j, so that the binding energies of the protons in the nucleus are completely determined by the values of the quantum numbers n and l. The order in which the proton shells are filled was, hence, taken to be: $1s^2$, $1p^6$, $1d^{10}$, $2s^2$, etc. From the binding energy of the proton in the nucleus, ϵ_p, for a given radius of the potential well, R, we found the well depth U_p with the help of well-known formulas. Then the binding energies of the remaining protons in the nucleus were determined. We note that $G_k(E_N) \equiv 0$ for nuclei with closed proton shells, if we neglect the dependence of the radial wave function of the proton in the nucleus on j. This is easily seen by immediately carrying out the summation over $j = l \pm \frac{1}{2}$ in formula (A4) of the Appendix.

(B) The interaction of the neutron with the nucleus, $V_N(r)$, is described by a complex square well $(V_N(r) = -U_N(1 + i\xi)$ for $0 \leq r < R$, and $V_N(r) = 0$ for $r > R)$ with the same radius R as in the case of the proton.

The use of the complex potential allows us to consider a definite absorption probability for the neutrons in the nucleus. In contrast to the scattering problem where $\xi > 0$, the choice of the asymptotic neutron wave function (6) presupposes in our case that $\xi < 0$.

(C) The coordinate dependence of the μ^--meson wave function in the K orbit is neglected.

The parameters of the proton and neutron potentials and of the proton states in the nucleus are listed in Table I. The values of r_0 and U_N are chosen in agreement with the paper of Feshbach, Porter, and Weisskopf.[19]

TABLE I

Nucleus	$r_0 \cdot 10^{13}$(cm)	U_N (Mev)	U_P (Mev)	Proton energy levels in the nucleus (in Mev)			
				1s	1p	1d	2s
O^{16}	1.45	42	32.3	22.1	12.1*	—	—
Ca^{40}	1.45	42	31.7	25.6	19.3	11.6	8.35*

*The data on the proton binding energy ε_p are taken from Ref. 21.

The calculations were carried out on the "Strela" computer of the Moscow State University. In order to guarantee a sufficient accuracy (~ 5%), we had to include all orbital angular momenta L of the emitted neutron up to L = 3, inclusively, in the case of oxygen, and up to L = 4 for the case of calcium. For the following it is convenient to introduce the dimensionless coupling constants c instead of the coupling constants g_k:

$$\text{for } g_k = c_k (10^{-49} \text{ erg cm}^3)$$

(similarly for g'_k), and to measure the energy

TABLE II

Nucleus	ξ	$\widetilde{W}_0$ (sec^{-1})	$\widetilde{W}_1$ (sec^{-1})	$\widetilde{W}_2$ (sec^{-1})	$\widetilde{\beta}_0$	$\widetilde{\beta}_1$	$\widetilde{\beta}_2$	$\widetilde{\gamma}_1$	$\widetilde{\gamma}_2$	Ratio of the probabilities for μ^- capture in different shells*	Ratio of specific probabilities (per proton) for μ^- capture in different shells
1	2	3	4	5	6	7	8	9	10	11	12
O^{16}	0	$1.62\cdot10^3$	$0.742\cdot10^2$	$0.341\cdot10$	0.034	0.037	0.040	$0.458\cdot10^{-1}$	$0.210\cdot10^{-2}$	1 : 65**	1 : 21.6**
	−0.15	$0.718\cdot10^3$	$0.324\cdot10^2$	$0.146\cdot10$	0.476	0.482	0.489	$0.453\cdot10^{-1}$	$0.203\cdot10^{-2}$	1 : 38**	1 : 12.6**
Ca^{40}	0	$1.33\cdot10^5$	$0.618\cdot10^4$	$2.96\cdot10^2$	0.145	0.146	0.144	$0.415\cdot10^{-1}$	$0.222\cdot10^{-2}$	1 : 7.8 : 290 : 190***	1 : 2.6 : 58 : 190***
	−0.15	$0.327\cdot10^5$	$0.153\cdot10^4$	$0.712\cdot10^2$	0.528	0.528	0.530	$0.418\cdot10^{-1}$	$0.218\cdot10^{-2}$	1 : 11.4 : 148 : 149***	1 : 3.8 : 29.6 : 149***

* These numbers refer to the values of $(\widetilde{W}_{nl})_0$; analogous results are obtained for $(\widetilde{W}_{nl})_{1,2}$.

** $1s : 1p$.

*** $1s : 1p : 1d : 2s$.

E_N in Mev. Formula (9) then yields for the probability of emission of neutrons with energies in the interval E_N to $E_N + dE_N$ as a result of the direct process:

$$dW(E_N) = \{[(\varphi_{ss} + 2\mathrm{Re}\,\varphi_{sv} + \varphi_{vv}) + 3(\varphi_{tt} + 2\mathrm{Re}\,\varphi_{ta} + \varphi_{aa})]W_0(E_N) - 2\mathrm{Re}(\varphi_{pt} + \varphi_{pa})W_1(E_N) + \varphi_{pp}W_2(E_N)\}\,dE_N, \tag{14}$$

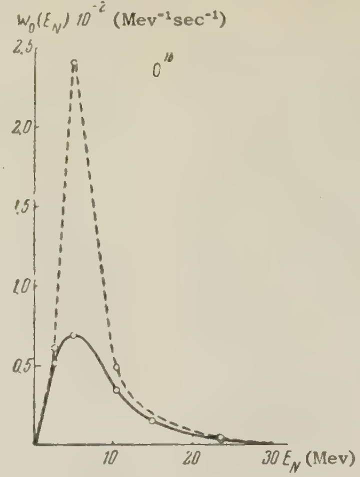

FIG. 1

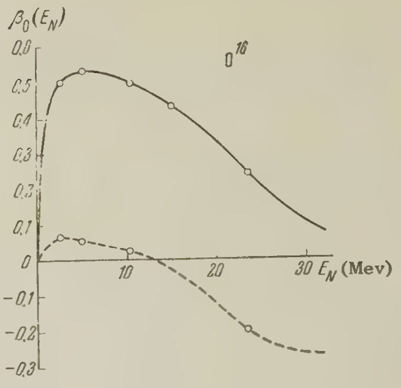

FIG. 2

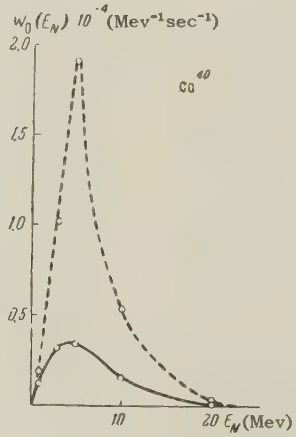

FIG. 3

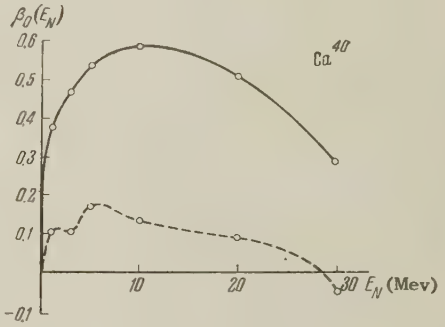

FIG. 4

where $\varphi_{ik} = c_i^* c_k + c_i'^* c_k'$, and the quantities $W_k(E_N)$ are related to the quantities $A_k(E_N)$ in an obvious manner. For the total probability $\widetilde{W} = \int dW(E_N)$ we obtain a completely analogous formula with $W_k(E_N)$ replaced by $\widetilde{W}_k = \int W_k(E_N)\,dE_N$.

The results of the calculations are given in Table II and in Figs. 1 to 4.* The dotted curves in the figures refer to calculations done assuming no absorption of the neutrons in the nucleus $(\xi = 0)$, the solid curves refer to calculations including the absorption effect $(\xi = -0.15)$.

Figure 1 (O^{16}) and Fig. 2 (Ca^{20}) show that the probability of emission of the neutrons on account of the direct process has a clearly expressed maximum at neutron energies of $E_N \sim 5$ Mev. The inclusion of absorption in the nucleus levels out the maximum without changing its position and lowers, of course, the magnitude of the probability.

---

*Figures 1 to 4 show the dependence of the quantities $W_0(E_N)$ and $\beta_0(E_N)$ on the energy E_N. The form of the curves for $W_1(E_N)$ and $W_2(E_N)$ is practically the same as that of the curve for $W_0(E_N)$. The deviation of $\beta_1(E_N)$ and $\beta_2(E_N)$ from $\beta_0(E_N)$ does not exceed a few percent.

In columns 3, 4, and 5 of Table II we list the values of W_0, W_1, and W_2 integrated over the energy of the neutron E_N. Columns 11 and 12 of Table II give the ratios of the μ^--capture probabilities integrated over E_N for the different shells. It follows from these data that, at least for the light nuclei, the μ^- mesons are mainly absorbed by protons belonging to the outer shells of the nucleus. Of the eight protons in O^{16} only the six protons in the outer 1p shell are effective in the μ^- capture, and of the 20 protons in Ca^{20}, only the 12 protons of the two outer shells (1d and 2s). Column 12 shows clearly that our calculations do not support the assumption that the protons in the nucleus absorb the μ^- mesons with approximately equal probabilities (see, e.g., reference 20).

Figures 2 and 4 show the dependence of $\beta_0(E_N)$ on E_N. The effect of the absorption of the neutrons in the nucleus is quite large. It greatly enlarges the value of $\beta_0(E_N)$ while, at the same time, smoothing out its dependence on E_N.* The values of $\widetilde{\beta}_k$ and $\widetilde{\gamma}_k$ are listed in columns 6 to 10 of Table II. The comparison of these data with (12) shows that the difference between our case and the case of μ^- capture in mesic hydrogen is, roughly speaking, that the asymmetry coefficient α_H for mesic hydrogen with neglect of the hyperfine structure is here multiplied by some positive factor smaller than unity. For an absorption corresponding to $\xi = -0.15$, α_H is reduced to about half its value. It is easily shown that $\beta_k(E_N) \sim E_N^{1/2}$ for $E_N \to 0$.

To exhibit the sensitivity of our results to a variation in the parameters, we repeated the calculations for O^{16} with $r_0 = 1.3 \times 10^{-13}$ cm and $U_N = 52$ Mev (in agreement with reference 19, we assumed $r_0 U_N^{1/2} = \text{const}$). The proton parameters were the following: $U_P = 36.6$ Mev, binding energies $\epsilon_P^{1p} = 12.1$ Mev, and $\epsilon_P^{1S} = 24.3$ Mev. Within the limits of error of the calculation, the results agree with the data obtained with our earlier value $r_0 = 1.45 \times 10^{-13}$ Mev (for example, taking $\xi = -0.15$ we get $\widetilde{\beta}_0 = 0.491$, and the ratio of the probabilities of μ^- capture in the 1s and 1p shells is equal to 1:31, etc.).

4. CONCLUSION

The calculations for the absorption of μ^- mesons in oxygen and calcium lead to the following results.

1. The energy spectrum of the neutrons emitted from the nucleus immediately after the μ^- capture has a clearly expressed maximum at neutron energies of $E_N \sim 5$ Mev.

2. The overwhelming majority of the μ^- mesons is absorbed by protons in the outer shells of the nuclei.

3. The angular distribution $q(\theta)$ of the neutrons emitted during the absorption of polarized μ^- mesons by nuclei can, in first approximation, be represented in the form

$$q(\theta) = 1 + P_\mu \widetilde{\beta} \alpha_H \cos\theta,$$

where α_H is the asymmetry coefficient for μ^- meson capture in mesic hydrogen (with neglect of its hyperfine structure), and the factor $\widetilde{\beta}$ $(|\widetilde{\beta}| \leq 1)$ depends on the properties of the nucleus. $\widetilde{\beta} \approx +0.5$ for μ^- capture in O^{16} and Ca^{40}.

4. Since the degree of polarization of the μ^- mesons in the K orbit of the mesic atoms reaches the value $P_\mu \sim 0.15$ to 0.20 (see references 14 and 22), while α_H is enclosed within the limits[5] $-1 \leq \alpha_H \leq +1/3$, one may, for $\widetilde{\beta} \sim 0.5$, expect an asymmetry on the order of 3 to 10% in the angular distribution of the neutrons from the direct process.

Recently there appeared a preliminary account[23] of measurements of the angular distribution of neutrons for the μ^- capture by S, Zn, and Pb. The results are apparently isotropic. It should be noted, however, that the experimental errors of these measurements are comparatively large (2% for S, 3% for Zn, and 10% for Pb). Since the expected asymmetry effect may amount to only a few percent, reliable conclusions can be drawn only from measurements with accuracy of at most a few tenths of a percent.

We express our deep gratitude to I. S. Shapiro for his constant interest in this work and for discussing the results. We owe our sincere gratitude to M. K. Akimov, who did the numerical calculations on the "Strela" computer of the Moscow State University.

APPENDIX

We give a list of the symbols used in the article:

---

*As shown in a number of papers devoted to the calculation of the scattering neutrons from nuclei, the choice of an absorption coefficient corresponding to $\xi = -0.15$ is, for our neutron well parameters and for energies $E_N \sim 5$-15 Mev, quite reasonable.

$$f_{ab} = g_a^* g_b + g_a'^* g_b', \quad h_{ab} = g_a^* g_b' + g_a'^* g_b \quad (a, b = s, v, p, t, a); \tag{A.1}$$

$$A_k(E_N) = C \sum_{njl} [(2j+1)/(2l+1)] (E_\nu^{njl}/2Mc^2)^k A_{njl}(E_N) \rho_{njl}(E_N); \tag{A.2}$$

$$B_k(E_N = C \sum_{njl} [(2j+1)/(2l+1)] (E_\nu^{njl}/2Mc^2)^k B_{njl}(E_N) \rho_{njl}(E_N); \tag{A.3}$$

$$G_k(E_N) = C \sum_{njl} [(2j+1)/(2l+1)] (E_\nu^{njl}/2Mc^2)^k G_{njl}(E_N) \rho_{njl}(E_N); \tag{A.4}$$

$$\beta_k(E_N) = -B_k(E_N)/A_k(E_N), \quad \gamma_k(E_N) = A_k(E_N)/A_0(E_N), \quad \delta_k(E_N) = G_k(E_N)/A_0(E_N); \tag{A.5}$$

$$\widetilde{A}_k = \int A_k(E_N)\, dE_N; \quad \widetilde{B}_k = \int B_k(E_N)\, dE_N, \quad \widetilde{G}_k = \int G_k(E_N)\, dE_N; \tag{A.6}$$

$$\widetilde{\beta}_k = -\widetilde{B}_k/\widetilde{A}_k, \quad \widetilde{\gamma}_k = \widetilde{A}_k/\widetilde{A}_0, \quad \widetilde{\delta}_k = \widetilde{G}_k/\widetilde{A}_0, \quad (k = 0, 1, 2); \tag{A.7}$$

$$A_{njl}(E_N) = \sum_{L\Lambda} (2L+1)(2\Lambda+1)(C_{L0\Lambda0}^{l0})^2 | b_{L\Lambda njl}(E_N) ^2; \tag{A.8}$$

$$\begin{aligned} B_{njl}(E_N) = \operatorname{Re} \sum_{L\Lambda} &[(2L+1)(2L+2)(2L+3)(2\Lambda+1)(2\Lambda+2)(2\Lambda+3)]^{1/2} [C_{L0\Lambda0}^{l0} C_{L+10\Lambda+10}^{l0} W(L+1l1\Lambda;\ \Lambda+1L) \\ &\times b_{L\Lambda njl}(E_N) b_{L+1\Lambda+1njl}^*(E_N) + C_{L+10\Lambda0}^{l0} C_{L0\Lambda+10}^{l0} W[Ll1\Lambda;\ \Lambda+1L+1) b_{L+1\Lambda njl}(E_N) b_{L\Lambda+1njl}^*(E_N)]; \end{aligned} \tag{A.9}$$

$$\begin{aligned} G_{njl}(E_N) = 6(2l+1) W\left(lj1\tfrac{1}{2};\ \tfrac{1}{2}l\right) \operatorname{Im} \sum_{L\Lambda} &[(2L+1)(2L+2)(2L+3)(2\Lambda+1)(2\Lambda+2)(2\Lambda+3)]^{1/2} \\ &\times [C_{L0\Lambda0}^{l0} C_{L+10\Lambda+10}^{l0} X(L\Lambda l;\ L+1\Lambda+1l;\ 111) b_{L\Lambda njl}^*(E_N) b_{L+1\Lambda+1njl}(E_N) \\ &+ C_{L0\Lambda+10}^{l0} C_{L+10\Lambda0}^{l0} X(L\Lambda+1l;\ L+1\Lambda l;\ 111) b_{L+1\Lambda njl}^*(E_N) b_{L\Lambda+1njl}(E_N)]; \end{aligned} \tag{A.10}$$

$$b_{L\Lambda njl}(E_N) = \int_0^\infty R_\mu(r) a_L^*(r) j_\Lambda(k_\nu r) R_{njl}(r) r^2 dr; \tag{A.11}$$

$$C = (2M)^{3/2} \hbar^{-7} c^{-3};$$

$$E_\nu^{njl} = E_{N\,\max}^{njl} - E_N; \quad E_{N\,\max}^{njl} = m_\mu c^2 - \varepsilon_\mu - \varepsilon_P^{njl};$$

$$\rho_{njl}(E_N) = E_N^{1/2} (E_{N\,\max}^{njl} - E_N)^2;$$

$j_\Lambda(x) = (\pi/2x)^{1/2} J_{\Lambda+1/2}(x)$ is the spherical Bessel function; $R_\mu(r)$ is the normalized radial wave function of the μ^- meson for the ground state of the mesic atom; W are the Racah coefficients;[24] the definition of the quantities X is given in reference 25; P_μ is the degree of polarization of the μ^- mesons at the moment of absorption; ϵ_μ is the binding energy of the ground state of the mesic atom; m_μ is the mass of the μ^- meson; ϵ_P^{njl} is the binding energy of the proton in the subshell (n, j, l); M is the mass of the nucleon (we neglect the proton-neutron mass difference).

Leaving out the sum over (n, j, l) in formulas (A.2), (A.3), and (A.4) and substituting these expressions in (9), we obtain a formula describing the absorption of the μ^- meson in a given filled subshell (n, j, l).

We note that $G_{n\,1/2\,0}(E_N) = 0$ for $l = 0$.

$$\begin{aligned} W_{njl}^{svta}(E_N, \theta) = (2^{5/2}/3)(-)^{j-s}(2j+1) \sum_{IL\Lambda I'L'\Lambda' gfh} & i^{L+\Lambda-L'-\Lambda'} (-)^{I+f+h} (2I+1)(2I'+1)(2L+1)(2L'+1)(2\Lambda+1)(2\Lambda'+1) \\ &\times (2g+1)(2f+1)(2h+1) C_{L0\Lambda0}^{l0} C_{L'0\Lambda'0}^{l0} C_{\Lambda0\Lambda'0}^{10} C_{L0h1}^{11} C_{L'0h1}^{11} W\left(I\tfrac{1}{2}\Lambda l;\ Lj\right) X\left(L'\Lambda' l; I'gj; \tfrac{1}{2}1\tfrac{1}{2}\right) \\ &\times X(jI'g;\ If1;\ \Lambda 1 \Lambda') X\left(I1f;\ Lh1;\ \tfrac{1}{2}L'I'\right) \operatorname{Re}\{[h_{st} + h_{sa} + h_{vt} + h_{va}] b_{IL\Lambda njl}^*(E_N) b_{I'L'\Lambda' njl}(E_N)\} \cos\theta. \end{aligned} \tag{A.12}$$

---

[1] J. M. Kennedy, Phys. Rev. **87**, 953 (1952).

[2] A. Rudik, Dokl. Akad. Nauk SSSR **92**, 739 (1953).

[3] H. A. Tolhoek and J. R. Luyten, Nucl. Phys. **3**, 679 (1957).

[4] Sens, Swanson, Telegdi, and Yovanovitch, Phys. Rev. **107**, 1464 (1957).

[5] Shapiro, Dolinskii, and Blokhintsev, Dokl. Akad. Nauk SSSR **116**, 946 (1957), Soviet Phys. "Doklady" **2**, 475 (1957). Nucl. Phys. **4**, 273 (1957).

[6] B. L. Ioffe, J. Exptl. Theoret. Phys. (U.S.S.R.) **33**, 308 (1957), Soviet Phys. JETP **6**, 240 (1958).

[7] H. Uberall, Nuovo cimento **6**, 533 (1957).

[8] Huang, Yang, and Lee, Phys. Rev. **108**, 1340 (1957).

[9] L. Wolfenstein, Nuovo cimento **7**, 706 (1958).

[10] T. Fulton, Nucl. Phys. **6**, 319 (1958).

[11] Ignatenko, Egorov, Khalupa, and Chultem, J. Exptl. Theoret. Phys. (U.S.S.R.) **35**, 894 (1958),

Soviet Phys. JETP **8**, 621 (1959).

[12] S. S. Gershtein, J. Exptl. Theoret. Phys. (U.S.S.R.) **34**, 463 and 993 (1958), Soviet Phys. JETP **7**, 318 and 685 (1958).

[13] E. I. Dolinskii and L. D. Blokhintsev, J. Exptl. Theoret. Phys. (U.S.S.R.) **34**, 759 (1958), Soviet Phys. JETP **3**, 521 (1958).

[14] Garwin, Ledermann, and Weinrich, Phys. Rev. **105**, 1415 (1957).

[15] L. D. Landau, J. Exptl. Theoret. Phys. (U.S.S.R.) **32**, 407 (1957); Soviet Phys. JETP **5**, 337 (1957). T. D. Lee and C. N. Yang, Phys. Rev. **105**, 1671 (1957). A. Salam, Nuovo cimento **5**, 299 (1957).

[16] A. Sommerfeld, Atombau und Spektrallinien, F. Ungar, N. Y., vol. 2.

[17] Berestetskii, Dolginov, and Ter-Martirosian, J. Exptl. Theoret. Phys. (U.S.S.R.) **20**, 527 (1950).

[18] R. P. Feynman and M. Gell-Mann, Phys. Rev. **109**, 193 (1958).

[19] Feshbach, Porter, and Weisskopf. Phys. Rev. **96**, 448 (1954).

[20] J. A. Wheeler, Revs. Mod. Phys. **21**, 133 (1949).

[21] N. Feather, Advances in Physics **2**, 141 (1953).

[22] Egorov, Ignatenko, Khalupa, and Chultem, ОИЯИ, Материалы к IV сессии Ученого Совета, г. Дубна, май 1958. (Joint Inst. for Nucl. Research Report of the IV Session of the Science Council, Dubna, May 1958).

[23] Coffin, Sachs, and Tycko, Bull. Amer. Phys. Soc., Ser II **3**, 52 (1958).

[24] Biedenharn, Blatt, and Rose, Revs. Modern Phys. **24**, 249 (1952).

[25] A. Simon and T. A. Welton, Phys. Rev. **90**, 1036 (1953).

Translated by R. Lipperheide

313

ELECTROMAGNETIC WAVES IN THE REGION OF EXCITON ABSORPTION IN A CRYSTAL

A. S. DAVYDOV and A. F. LUBCHENKO

Moscow State University

Submitted to JETP editor, June 26, 1958

J. Exptl. Theoret. Phys. (U.S.S.R.) 35, 1499-1507 (December, 1958)

A theory is developed for the absorption coefficient and the refractive index in the absorption bands corresponding to exciton excitation in molecular crystals at low temperatures. It is shown that the structure of the absorption band can serve as a means of determining the sign of the effective mass of the exciton. Conditions are found for which the index of refraction equals zero at the short-wave side of the absorption band. Electromagnetic waves at these frequencies are completely reflected from the crystal surface, penetrating it to only a small depth. When the temperature is increased this effect vanishes.

INTRODUCTION

BECAUSE of the recent work of Pekar,[1] Ginzburg,[2] and Agranovich and Rukhadze[3] attention has been directed to the propagation of light in crystals characterized by spatial dispersion. It has been shown in the work cited above that in frequency regions close to the exciton absorption band the index of refraction can have several values for waves of the same frequency, direction of propagation, and polarization. Only the transparent region of the crystal has been studied in references 1 to 3. However, it is of interest to consider propagation of electromagnetic waves in a crystal at frequencies corresponding to absorption bands.

The reduction in the amplitude of an electromagnetic wave as it passes through matter is due to two effects: (a) scattering, (b) conversion of energy in the electromagnetic wave into the energy of motion of the molecules (true absorption). In this paper we shall be interested only in true absorption at crystal temperatures close to zero.

The molecules of a molecular crystal are neutral; hence an optical wave cannot communicate motion to them directly. However, when the molecules are excited there are additional interaction forces between molecules and these shift the equilibrium positions of the molecules. Thus, true absorption is due to coupling between the internal molecular excitations and the molecular oscillations. This coupling leads to a considerable broadening of the absorption band at absolute zero.

Davydov[4] has shown that excitations of two types can be produced in molecular crystals by optical waves: (a) localized excitations that propagate slowly through the crystal and whose polarization is determined by the orientations of the molecules, which are considered as independent absorption center, (b) exciton excitation, i.e., excitations that propagate rapidly in the form of excitation waves in the crystal. These excitations are responsible for the appearance in the absorption spectrum of sharply polarized "crystallographic" absorption bands, the polarization of which is determined by the crystallographic structure.

The absorption bands corresponding to the localized excitation are roughly Gaussian in shape and do not yield any information as to the detailed structure of the crystal. The absorption bands corresponding to exciton excitations, on the other hand, are very sensitive to crystallographic structure. Consequently, an investigation of the structure of exciton absorption bands is one of the methods of studying crystallographic structure, the energy of the exciton states as a function of the propagation vector of the exciton, and the exciton interaction with the lattice vibrations.

An analysis of the structure of the optical absorption band in a molecular crystal has been given by Davydov,[5] using a one-dimensional crystal; Davydov and Rashba have considered a more general case. However, in this work no account was taken of the self-consistency of the problem: the propagation vector of the optical wave which excites the crystal depends on the refractive index and the optical absorption. This self-consistency may be especially important close to an absorption band where, in certain cases, it leads to spatial dispersion. In the present paper we investigate the passage of light through a crystal in the region of the absorption band using a simple model of the molecular crystal; in this model the molecules can execute translational and rotational oscillations about the fixed equilibrium positions.

1. CRYSTAL WAVE FUNCTIONS IN THE PRESENCE OF OPTICAL WAVES

Let G be some region of a molecular crystal with a cubic lattice in each elementary cell of which there is one molecule. All molecules have the same equilibrium orientation. It is further assumed that the region G is a cube with sides $N_i a_i$ $(i = 1, 2, 3)$ where the a_i are the base vectors of the lattice. Then the position of the center of gravity of the molecule is given by the vector $\mathbf{R} = \mathbf{r} + \mathbf{n}$ where $\mathbf{r}$ is the coordinate of the center of region G while $\mathbf{n} = \sum n_i \mathbf{a}_i$, $n = 0, \pm 1, \pm \ldots\ldots \pm N_i/2$ $(i = 1, 2, 3)$. The total number of molecules in region G, $N = N_1 N_2 N_3$ must be large enough to exhibit the basic interaction effects between molecules; at the same time the dimensions of the region must be smaller than the wavelength of the light.

In the absence of interactions between the exciton excitations and the lattice vibrations, the frequency of the exciton excitations can be written in the form

$$\omega_{\mathbf{k}} = \omega_0 + (\tau/2)(\cos \mathbf{k} \cdot \mathbf{a} - 1), \tag{1.1}$$

where $\hbar |\tau|$ is the energy width of the exciton band for excited states. The wave function corresponding to the excitation (1.1) is of the form

$$\psi_{\mathbf{k}} = N^{-1/2} \sum_{\mathbf{n}} e^{i\mathbf{k}\cdot\mathbf{n}} \varphi_{\mathbf{n}}^{f}(\rho_{\mathbf{n}}) \prod_{\mathbf{n}' \neq \mathbf{n}} \varphi_{\mathbf{n}'}(\rho_{\mathbf{n}'}), \tag{1.2}$$

where $\varphi_{\mathbf{n}}^{f}(\rho_{\mathbf{n}})$ and $\varphi_{\mathbf{n}}(\rho_{\mathbf{n}})$ are wave functions which determine the excited and ground states of the molecule at $\mathbf{n}$.

For simplicity we assume that the exciton excitations interact only with two kinds of lattice vibrations: translational and rotational oscillations. The frequencies of these oscillations are given by the relations

$$\nu_p^2 = \nu_{\max}^2 \sin^2(\mathbf{p} \cdot \mathbf{a}/2), \quad \Omega_q = \Omega_0 + \frac{\Delta\Omega}{2}(\cos \mathbf{q} \cdot \mathbf{a} - 1), \tag{1.3}$$

where $|\Delta\Omega|$ is the width of the band of the optical frequency branch. The propagation vectors $\mathbf{k}$, $\mathbf{p}$ and $\mathbf{q}$ run over N discrete values $\sum (2\pi/N_i)\mathbf{b}_i \eta_i$ $(\eta = 0, \pm 1, \pm \ldots\ldots)$ if we take cyclical boundary conditions with periodicity $N_i \mathbf{a}_i$ as boundary conditions. Here the $\mathbf{b}_i$ are the vectors of the reciprocal lattice.

In actual crystals the dependences of ω_k, ν_p, and Ω_q of the propagation vectors can be expressed by more complicated functions than those given in (1.2) and (1.3). It is important, however, that in the limit of infinitely long waves Ω_q and ω_k approach a finite limit while $\nu_p \to 0$. Usually, in molecular crystals the width of the exciton zone exceeds the width of the zones which correspond to lattice vibrations, i.e., the following inequality holds

$$|\tau| > |\Delta\Omega|, \ \nu_{\max}.$$

Further, let H_0 be the Hamiltonian, whose eigenfrequencies

$$E_{\mathbf{kpq}} = \hbar(\omega_{\mathbf{k}} + \nu_{\mathbf{p}} + \Omega_{\mathbf{q}}),$$

and whose eigenfunctions $\Phi_{\mathbf{kpq}} = \psi_{\mathbf{k}}\psi_{\mathbf{p}}\psi_{\mathbf{q}}$ correspond to excitation in the crystal of one exciton, one accoustical phonon and one optical phonon. The ground state of the crystal (at basolute zero) will be a state in which none of these excitations are excited. The energy of this state will be taken as zero energy and the wave function will be denoted by Φ_0.

The operator for the interaction of the excitations with the lattice vibrations is

$$H' = H_1 + H_2,$$

where

$$H_1 = N^{-1/2} \sum_{\mathbf{mn}} V_{\mathbf{nm}}^{(1)} \rho_{\mathbf{n}} \cdot \rho_{\mathbf{m}} \{A_{\mathbf{p}}(e^{i\mathbf{p}\cdot\mathbf{n}} - e^{i\mathbf{p}\cdot\mathbf{m}}) + A_{\mathbf{p}}^{+}(e^{-i\mathbf{p}\cdot\mathbf{n}} - e^{-i\mathbf{p}\cdot\mathbf{m}})\},$$

$$H_2 = N^{-1/2} \sum_{\mathbf{mnq}} V_{\mathbf{nm}}^{(2)} \rho_{\mathbf{n}'} \cdot \rho_{\mathbf{m}} \{A_{\mathbf{q}}(e^{i\mathbf{q}\cdot\mathbf{n}} + e^{i\mathbf{q}\cdot\mathbf{m}}) + A_{\mathbf{q}}^{+}(e^{-i\mathbf{q}\cdot\mathbf{n}} + e^{-i\mathbf{q}\cdot\mathbf{m}})\}.$$

Here $\rho_{\mathbf{n}}$ is the ensemble of internal molecular coordinates for molecule $\mathbf{n}$; $A_{\mathbf{p}}^{+}$ and $A_{\mathbf{q}}^{+}$ are creation operators for the appropriate phonons. When these operate on the function Φ_0 they produce a state with one phonon of the appropriate type. Operators $A_{\mathbf{p}}$ and $A_{\mathbf{q}}$ are annihilation operators for the corresponding phonons.

The operator for the interaction of the electromagnetic wave

$$E = 2E_0 \exp(-\Lambda \cdot \mathbf{R}) \cos(\omega t - \mathbf{Q} \cdot \mathbf{R})$$

with the molecules of the crystal (when the wave length is much larger than the molecular dimension) can be given by the expression*

---

*In computing the exciton excitations, account has already been taken of the dipole-dipole interaction of the molecular electric moments induced by the light wave; hence, in operator (1.4) we introduce the average field rather than the effective field.

$$W = -e\,\mathbf{E}_0 \sum_{\mathbf{n}} \boldsymbol{\rho}_{\mathbf{n}} \sum_{\lambda=+,-} \exp\{(i\lambda\mathbf{Q} - \Lambda)\cdot(\mathbf{r}+\mathbf{n}) - i\lambda\omega t\}. \tag{1.4}$$

In the presence of the light wave, the crystal state is described by the Schrödinger equation

$$(i\hbar\partial/\partial t - H_0 - H_1 - H_2 - W)\,F = 0. \tag{1.5}$$

When the interaction between the excitons and the lattice vibrations is weak, we can use the one-phonon process; hence we seek a solution of (1.5) in the form of a series

$$F = b_0(t)\,\Phi_0 + \sum_{\mathbf{k}\mathbf{p}\mathbf{q}} b_{\mathbf{kpq}}(t)\,\Phi_{\mathbf{kpq}} \exp[-i(\omega_{\mathbf{kpq}} - i\gamma_{\mathbf{kpq}}/2)\,t], \tag{1.6}$$

with initial conditions

$$b(0) = 1, \quad b_{\mathbf{kpq}}(0) = 0. \tag{1.7}$$

The matrix elements of the operator W are of the form

$$(\Phi^*_{\mathbf{k}'}\,|\,W\,|\,\Phi_0) = -N^{-1/2}(\mathbf{E}_0\cdot\mathbf{d}) \sum_{\lambda=+,-} \exp[i(\lambda\mathbf{Q} + i\Lambda)\cdot\mathbf{r} - \lambda\omega t]\,\delta_{\lambda\mathbf{Q},\mathbf{k}'}, \tag{1.8}$$

where $\mathbf{d} = (\varphi^{\mathrm{f}}\,|\,e\boldsymbol{\rho}\,|\,\varphi)$ is the electric dipole moment excited by the optical wave:

$$\delta_{\lambda\mathbf{Q},\mathbf{k}'} = N^{-1} \sum_{\mathbf{n}} e^{-\Lambda\mathbf{n}} \exp[i\,\mathbf{n}\cdot(\lambda\,\mathbf{Q} - \mathbf{k}')].$$

If $N_1\mathbf{a}\Lambda \ll 1$ the matrix elements in (1.8) are different from zero, only when $\mathbf{k}' = \lambda\mathbf{Q}$. If the absorption is not very small the matrix elements (1.8) will be different from zero at several values of $\mathbf{k}'$ close to $\lambda\mathbf{Q}$. From Eqs. (1.6), (1.8), and (1.5) we find as a first approximation (neglecting H_1 and H_2)

$$b = \frac{(\mathbf{E}_0\cdot\mathbf{d})\,N^{1/2}}{\hbar}\,\frac{\exp[i(\omega_{\lambda\mathbf{Q}} - \lambda\omega - i\gamma_{\lambda\mathbf{Q}}/2)] - 1}{\omega_{\lambda\mathbf{Q}} - \lambda\omega - i\gamma_{\lambda\mathbf{Q}}/2}. \tag{1.9}$$

Thus, in the same approximation the wave function for the crystal (when there is an optical wave of frequency ω present, (at large values of t) can be given by the expression

$$F = \Phi_0 + \frac{(\mathbf{E}_0\cdot\mathbf{d})\sqrt{N}}{\hbar} \sum_{\lambda=+,-} \frac{\exp[-i\lambda\omega t + i\lambda\,\mathbf{Q}\cdot\mathbf{r} - \vec{\Lambda}\cdot\mathbf{r}]}{\omega_{\mathbf{Q}} - \lambda\omega - i\gamma_{\lambda\mathbf{Q}}/2}\,\Phi_{\lambda\mathbf{Q}}, \tag{1.10}$$

where $\gamma_{\lambda\mathbf{Q}}$ is a complicated function of frequency, the determination of which requires the solution of Eq. (1.5) in the next approximation, which takes account of the interaction of the excitons with the lattice vibrations.

2. CALCULATION OF THE COEFFICIENTS γ

The matrix elements of the operators that determine the coupling between the excitons and the lattice vibrations can be written in the following form:

$$\begin{aligned}(\Phi^*_{\mathbf{kp}}\,|\,H_1\,|\,\Phi_{\lambda\mathbf{Q}}) &= |\mathbf{d}|^2 V_1 N^{-1/2}\delta_{\lambda\mathbf{Q},\mathbf{k}+\mathbf{p}},\\ (\Phi^*_{\mathbf{kq}}\,|\,H_2\,|\,\Phi_{\lambda\mathbf{Q}}) &= |\mathbf{d}|^2 V_2 N^{-1/2}\delta_{\lambda\mathbf{Q},\mathbf{k}+\mathbf{q}},\end{aligned} \tag{2.1}$$

where

$$V_1 \approx g_1\nu_{\mathbf{p}}^{-1/2}\sin(\mathbf{p}\cdot\mathbf{a}/2)\sin[(2\lambda\mathbf{Q} - \mathbf{p})\cdot\mathbf{a}/2],$$

$$V_2 \approx g_2\Omega_{\mathbf{q}}^{-1/2}\cos(\mathbf{q}\cdot\mathbf{a}/2)\cos[(2\lambda\mathbf{Q} - \mathbf{q})\cdot\mathbf{a}/2].$$

Using Eqs. (2.1) and (1.9), we find $b_{\lambda\mathbf{Q}-\mathbf{q},\mathbf{q}}$ and $b_{\lambda\mathbf{Q}-\mathbf{p},\mathbf{p}}$ from Eq. (1.5); then, multiplying (1.5) by $\Phi^*_{\lambda\mathbf{Q}}$, we have

$$\begin{aligned}\gamma_{\lambda\mathbf{Q}} = \frac{2|\mathbf{d}|^4}{N}\Bigg\{&\sum_{\mathbf{p}}|V_1|^2\,\frac{1 - \exp[-i(\omega_{\mathbf{Q}-\mathbf{p}} - \lambda\omega + \nu_{\mathbf{p}})\,t]}{\omega_{\mathbf{Q}-\mathbf{p}} - \lambda\omega + \nu_{\mathbf{p}}}\\ &+ \sum_{\mathbf{q}}|V_2|^2\,\frac{1 - \exp[-i(\omega_{\mathbf{Q}-\mathbf{q}} - \lambda\omega + \Omega_{\mathbf{q}})\,t]}{\omega_{\mathbf{Q}-\mathbf{q}} - \lambda\omega + \Omega_{\mathbf{q}}}\Bigg\},\end{aligned} \tag{2.2}$$

where λ takes values + or −. It follows directly from Eq. (2.2) that

$$\gamma_{-\mathbf{Q}} = 0. \tag{2.3}$$

Taking account of (2.3), at large values of t, we can write

$$\gamma \equiv \gamma_{\mathbf{Q}} = \gamma_{\mathrm{tr}} + \gamma_{\mathrm{rot}}, \tag{2.4}$$

where

$$\gamma_{\mathrm{tr}} = 2|\mathbf{d}|^4 N^{-1}\sum_{\mathbf{p}}|V_1|^2\,\zeta(\omega_{\mathbf{Q}-\mathbf{p}} + \nu_{\mathbf{p}} - \omega), \tag{2.5}$$

$$\gamma_{\mathrm{rot}} = 2|\mathbf{d}|^4 N^{-1}\sum_{\mathbf{q}}|V_2|^2\,\zeta(\omega_{\mathbf{Q}-\mathbf{q}} + \Omega_{\mathbf{q}} - \omega); \tag{2.6}$$

and $\zeta(x)$ is a singular function defined by the relation

$$\zeta(x) = \lim_{t\to\infty}\frac{1 - \exp(-ixt)}{ix} = \pi\delta(x) + i\,\mathrm{P}\frac{1}{x}.$$

The imaginary part of this function causes a shift in the energy levels of the system and will not be considered in what follows (cf. reference 7, § 16).

In Eq. (2.5) we change the summation to integration and introduce the new variable

$$d\mathbf{p} = d\sigma d\xi(\mathbf{p})/|\operatorname{grad}\xi(\mathbf{p})|, \quad \xi(\mathbf{p}) = \omega_{\mathbf{Q}-\mathbf{p}} + \nu_{\mathbf{p}},$$

where $d\sigma$ is a surface element, and $\xi(\mathbf{p}) = \mathrm{const}$; thus, we can write

$$\gamma_{\mathrm{tr}}(\omega) = \frac{a^3|\mathbf{d}|^4}{4\pi^3}\int_{\xi_1}^{\xi_2} d\sigma d\xi\,\frac{|V_1|^2}{|\operatorname{grad}\xi(\mathbf{p})|}\,\zeta(\xi - \omega)$$

$$= \begin{cases}\dfrac{g_1 a^2|\mathbf{d}|^4}{2\pi^2\sqrt{\nu_{\max}}}\displaystyle\int\frac{\sin^2([2\mathbf{Q} - \mathbf{p}]\cdot\mathbf{a}/2)]\,|\sin(\mathbf{p}\cdot\mathbf{a}/2)|\,d\sigma}{|\tau\sin[(\mathbf{Q} - \mathbf{p})\cdot\mathbf{a}] + \nu_{\max}\cos(\mathbf{p}\cdot\mathbf{a}/2)|}, & \text{if } \xi_1 < \omega < \xi_2,\\ 0 & \text{if } \omega \text{ is outside the interval } \xi_1, \xi_2.\end{cases} \tag{2.7}$$

The quantities ξ_1 and ξ_2 are respectively the smaller and larger of the values $\omega_{\mathbf{Q}}$ and $\omega_{\mathbf{Q}-\pi\mathbf{b}}$

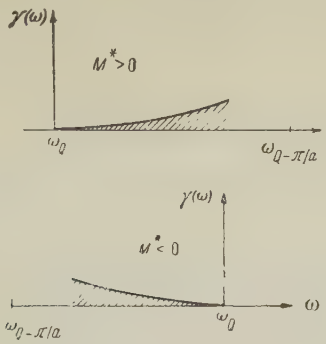

FIG. 1

$+ \nu_{\max}$; the integration in Eq. (2.7) is carried out for all values of **P** which satisfy the condition $\omega = \omega_{\mathbf{Q}-\mathbf{P}} + \nu_{\max}$.

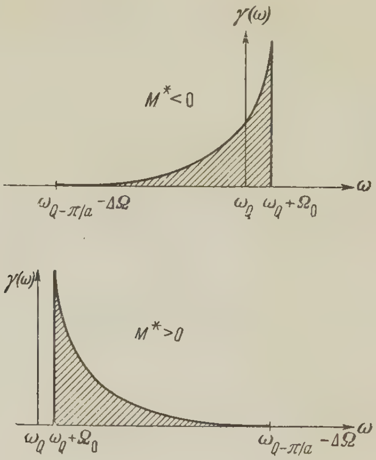

FIG. 2

We now assume that the frequency ω inside the absorption band approaches $\omega_{\mathbf{Q}}$, then $p \rightarrow 0$ and it follows from Eq. (2.7) that $\gamma_{\mathrm{tr}} \rightarrow 0$. In Fig. 1 is shown the dependence of γ_{tr} on ω close to the frequency $\omega_{\mathbf{Q}}$ for positive and negative effective exciton mass. Carrying out a similar transformation of Eq. (2.6), we have

$$\gamma_{\mathrm{rot}}(\omega) = \begin{cases} \dfrac{g^2a^2\,|\mathbf{d}|^4}{2\pi^2} \displaystyle\int \frac{\cos^2[(2\mathbf{Q}-\mathbf{q})\cdot\mathbf{a}/2]\cos^2(\mathbf{q}\mathbf{a}/2)\,d\sigma}{\{\Omega_0 + (\Delta\Omega/2)(\cos\mathbf{q}\cdot\mathbf{a} - 1)\}^{1/2}\,|\,\tau\sin(\mathbf{Q}-\mathbf{q})\cdot\mathbf{a} - \Delta\Omega\sin\mathbf{q}\cdot\mathbf{a}\,|}, & \text{if } \zeta_1 < \omega < \zeta_2 \\ 0, & \text{if } \omega \text{ is outside the interval } \zeta_1, \zeta_2, \end{cases} \tag{2.8}$$

where ζ_1 and ζ_2 are respectively the smaller and larger of the values. $\omega_{\mathbf{Q}} + \Omega_0$ and $\omega_{\mathbf{Q}-\pi b} + \Omega_0 - \Delta\Omega_0$. The integration in Eq. (2.8) is carried out over all values of **q** which satisfy the relation $\omega = \omega_{\mathbf{Q}-\mathbf{q}} + \Omega_{\mathbf{q}}$. In Fig. 2 is shown the dependence of γ_{rot} on frequency for positive and negative effective exciton mass.

If the crystal temperature is not zero, the integrands in Eqs. (2.7) and (2.8) will contain the factors $(\tilde{n}_{\mathbf{p}} + 1)$ and $(\tilde{n}_{\mathbf{q}} + 1)$ respectively where $\tilde{n}_{\mathbf{p}}$ and $\tilde{n}_{\mathbf{q}}$ are the mean numbers of phonons at a given temperature. At high temperatures $(\tilde{n} + 1)$ and γ are proportional to temperature. When the temperature is increased, in addition to the increase in γ, which corresponds to the emission of phonons, there are additional terms which correspond to the absorption of phonons by excitons. Both of these increase γ_{tr} and γ_{rot} and cause considerable expansion of the frequency region in which these quantities are different from zero.

We have considered above the interaction between exciton excitations with two branches of the lattice vibrations. However, a larger number of branches take part in the interaction. Because the different oscillations are independent, each makes an additive contribution to γ; consequently

$$\gamma(\omega) = \sum_i [\gamma_{\mathrm{tr}}^i(\omega) + \gamma_{\mathrm{rot}}^i(\omega)].$$

In Fig. 3 is shown a possible form for the dependence of γ on ω at absolute zero. As the temperature increases the curve $\gamma(\omega)$ expands in both directions about the frequency $\omega_{\mathbf{Q}}$. In computing $\gamma(\omega)$, we consider only the interaction of exciton excitations with lattice vibrations. However, to this value of $\gamma(\omega)$ it is necessary to add the natural width (Γ) of the internal molecular level associated with the finite lifetime of the excited state of the free molecule (radiative and nonradiative transitions). In luminescent crystals $\Gamma \ll \gamma(\omega)$ inside the absorption band so that these corrections need not be introduced.

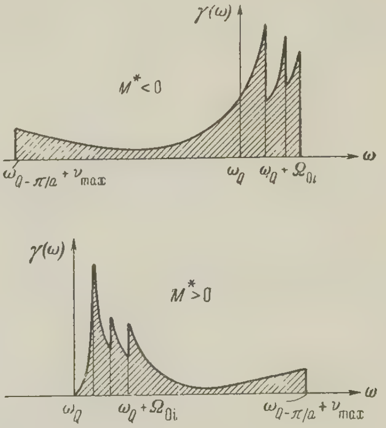

FIG. 3

3. EQUATIONS FOR THE ABSORPTION COEFFICIENT AND THE REFRACTIVE INDEX

To obtain equations for the absorption coefficient and the refractive index for a molecular crystal, we use Eq. (1.10) to compute the average value of the electric moment (per unit volume of the crystal) induced in region G by the light wave

$$\mathbf{P}_{ex} = \frac{\mathbf{d}\,(\mathbf{E}_0\cdot\mathbf{d})2N_0\omega_{\mathbf{Q}}\,[(\omega_{\mathbf{Q}}^2-\omega^2)+i\,(\gamma/2)\,(\omega_{\mathbf{Q}}+\omega)]}{(\omega_{\mathbf{Q}}^2-\omega^2)^2+(\gamma/2)^2\,(\omega_{\mathbf{Q}}+\omega)^2} \times \exp[-\Lambda\cdot\mathbf{r}+i\,(\mathbf{Q}\cdot\mathbf{r}+\omega t)] + \text{compl. conj.} \tag{3.1}$$

where N_0 is the number of molecules per unit volume.

In finding the approximate solution (1.10) of Eq. (1.5), we have taken account only of those states that correspond to a definite internal molecular excitation. The absorption of light, when this state is excited, does not depend on the existence of other molecular levels having some other energy. However, these states introduce an additional term $\{\epsilon_0\}$ in the real part of the dielectric permittivity tensor: $\{\epsilon_0\}$ is relatively insensitive to frequency. For simplicity we shall assume that ϵ_0 is a scalar. Then, the total electric moment produced in the crystal can be written in the form

$$\mathbf{P} = \mathbf{P}_{ex} + \frac{\varepsilon_0 - 1}{4\pi}\,\mathbf{E}, \tag{3.2}$$

where $\mathbf{P}_{ex}$ is defined by Eq. (3.1)

An electromagnetic wave which propagates in the crystal must satisfy the equations

$$\operatorname{curl}\mathbf{E} = -\dot{\mathbf{H}}/c,\quad \operatorname{curl}\mathbf{H} = \dot{\mathbf{D}}/c,\quad \operatorname{div}\mathbf{D} = 0,\quad \operatorname{div}\mathbf{H} = 0,\quad \mathbf{D} = \mathbf{E} + 4\pi\mathbf{P}. \tag{3.3}$$

We seek a plane-wave solution for these equations, assuming that E, H, and P are proportional:

$$e^{-\Lambda r}\exp[i\,(\mathbf{Q}\cdot\mathbf{r} - \omega t)],\quad \mathbf{Q} = \frac{\omega}{c}\,\mu\,\mathbf{s},\quad \Lambda = \frac{\omega}{c}\,\varkappa\,\mathbf{s},$$

where $\mathbf{s}$ is a unit vector in the direction of propagation of the wave. From the above it is easy to obtain the relation

$$\mathbf{E} + 4\pi\mathbf{P} = (\mu + i\varkappa)^2\,[\mathbf{E} - \mathbf{s}\,(\mathbf{s}\cdot\mathbf{E})]. \tag{3.4}$$

We now orient the coordinate system xyz in such a way that the x axis lies along the equilibrium direction of the induced electric moment of each molecule (in our crystal all molecules have the same orientation); thus $\mathbf{d} = \{d, 0, 0\}$.

If the electric field of the light wave is parallel to the x axis, P is collinear with E; then, from Eq. (3.3) it follows that E and D are also collinear and, consequently, that $\mathbf{s}$ is perpendicular to E. Substituting Eq. (3.2) in Eq. (3.4) and separating real and imaginary parts, we have

$$\mu_{xx}^2 - \varkappa_{xx}^2 = \varepsilon_0 + \frac{4\pi\,(e^2/m)\,fN_0\,(\omega_Q - \omega)}{(\omega_Q + \omega)\,[(\omega_Q - \omega)^2 + \gamma^2/4]} \equiv A\,(\omega), \tag{3.5}$$

$$2\mu_{xx}\varkappa_{xx} = \frac{2\pi\,(e^2/m)\,fN_0\gamma}{(\omega_Q + \omega)\,[(\omega_Q - \omega)^2 + \gamma^2/4]} \equiv B\,(\omega), \tag{3.6}$$

where $A(\omega)$ is the real part and $B(\omega)$ the imaginary part of the dielectric permittivity. In obtaining (3.5) and (3.6) we have expressed d^2 in terms of the oscillator strength f, corresponding to the internal molecular transition, using the relation $d^2 = e^2\hbar f/2m\omega_Q$ where m is the mass of the electron. The other two principle elements of the refractive-index tensor and the absorption tensor are

$$\mu_{zz}^2 = \mu_{yy}^2 = \varepsilon_0,\quad \varkappa_{zz} = \varkappa_{yy} = 0.$$

In Eq. (3.5) and (3.6) the frequency ω_Q is a function of the refractive index

$$\omega_Q = \omega_0 + \frac{\tau}{2}\left[\cos\left(\frac{\omega}{c}\,\mu\,\mathbf{s}_1\cdot\mathbf{a}\right) - 1\right], \tag{3.7}$$

where $\mathbf{s}_1$ is a unit vector perpendicular to the x axis; hence, in the region $\omega \approx \omega_0$ the second term in Eq. (3.7) can be of some importance in (3.5) and (3.6). In this frequency region these equations can, in general, lead to the appearance of several values of μ_{xx}^2 at the same frequency.

This situation has already been noted by Pekar, Ginzburg,[2] and Agranovich and Rukhadze.[3] In references 1 to 3, however, absorption was not taken into account, and it was assumed that μ can take on very large values; this tends to overemphasize the role of spatial dispersion. Actually, as has been shown by measurements carried out by Obreimov, Prikhot'ko and their colleagues,[8] at low temperatures, where the absorption bands are relatively narrow, the refractive index for molecular crystals rarely exceeds 10. With $\mu \approx 10$, the ratio $(\omega\mu a/c)^2 \sim 10^{-3}$ so that Eq. (3.7) can be replaced by the approximate expression

$$\omega_Q = \omega_0 - {}^1/_4\tau\,(\omega\mu a/c)^2.$$

In this case

$$A\,(\omega) = \varepsilon_0 + \frac{4\pi\,(e^2/m)\,fN_0\,[\omega_0 - \omega - \tau\,(\mu\omega a/2c)^2]}{(\omega_0 + \omega)\,\{(\omega_0 - \omega - \tau\,[\mu\omega a/2c]^2)^2 + \gamma^2/4\}},$$

$$B\,(\omega) = \frac{2\pi\,(e^2/m)\,fN_0\gamma\,(\omega)}{(\omega_0 + \omega)\,\{(\omega_0 - \omega - \tau\,[\mu\omega a/2c]^2)^2 + \gamma^2/4\}}.$$

Now, assuming that in molecular crystals the majority of absorption bands correspond to excitation of excitons of negative effective mass

$$\tau\,(\mu\omega a/c)^2 < \gamma^2\,(\omega), \tag{3.8}$$

we can make a fairly accurate determination of the absorption coefficient κ and the refractive index μ using the formulas

$$\mu = 2^{-1/2}\left[A_0 + \sqrt{A_0^2 + B_0^2}\right]^{1/2},$$
$$\varkappa = 2^{-1/2}\left[-A_0 + \sqrt{A_0^2 + B_0^2}\right]^{1/2}, \qquad (3.9)$$

where

$$A_0(\omega) = \varepsilon_0 + \frac{4\pi (e^2/m) f N_0 (\omega_0 - \omega)}{(\omega_0 + \omega)\left[(\omega_0 - \omega)^2 + \gamma^2/4\right]}, \qquad (3.5a)$$

$$B_0(\omega) = \frac{2\pi (e^2/m) f N_0 \gamma(\omega)}{(\omega_0 + \omega)\left[(\omega_0 - \omega)^2 + \gamma^2/4\right]}. \qquad (3.6a)$$

The inequality (3.8) is not satisfied at very low temperatures for a small frequency region at the long-wave edge of the absorption band; this region corresponds to excitation of excitons with positive effective mass (cf. Fig. 3). In this region Eq. (3.9) cannot be used; to compute μ and κ it is necessary to take account of the second term of Eq. (3.7). However, when the temperature increases, the value of $\gamma(\omega_0)$ increases rapidly even in bands which correspond to the excitation of excitons with positive effective mass. In this case Eq. (3.8) is satisfied and Eq. (3.9) can be used for all frequencies. True absorption (energy dissipation) occurs only in the frequency region in which $B(\omega)$ is different from zero. As follows from Eqs. (3.5) and (3.6) this region of true absorption coincides with the frequency region in which $\gamma(\omega)$ is different from zero. Frequency regions in which $B(\omega) = 0$ are called transparent regions. If $A_0(\omega) > 0$ in the transparent regions, from Eq. (3.9) we have $\kappa = 0$, $\mu = \sqrt{A_0}$, i.e., the light wave is not attenuated in passage through the material.

If $A_0(\omega) < 0$, from Eq. (3.9) we have $\mu = 0$ and $\kappa = \sqrt{-A_0}$.

It follows from Eq. (3.5a) that when $\gamma(\omega) = 0$ the condition $A(\omega) < 0$ is satisfied for frequencies which satisfy the relation

$$\omega_0 < \omega < \omega_0 + \frac{4\pi e^2 f N_0/m}{\varepsilon_0(\omega + \omega_0)}, \qquad (3.10)$$

where ϵ_0 is the value of the dielectric constant in regions far from the absorption band. If the frequencies are measured in reciprocal centimeters $[\nu]$ the relation is (3.10) can be written in the form

$$[\nu_0] < [\nu] < [\nu_0] + \frac{e^2 f N_0}{2\pi c^2 \varepsilon_0 [\nu_0]\, m}.$$

Taking $N_0 = 4 \times 10^{21}$, $f = 0.2$, $[\nu] = 25{,}000\ \text{cm}^{-1}$ and $\epsilon_0 = 2$, we have

$$e^2 f N_0 / 2\pi c^2 \varepsilon_0 [\nu_0]\, m \approx 73\ \text{cm}^{-1}.$$

In view of the nature of the dependence of γ on ω (Fig. 3), it is easy to show that in the region $\gamma(\omega) = 0$ the condition in (3.2) is satisfied only at very low temperatures and at the high-frequency side of the absorption band, which corresponds to exciton zones with negative effective mass because the frequencies of the limiting rotational oscillations are usually less than 100 cm^{-1} and the true absorption falls off sharply on the high-frequency side. As the temperature is raised, the absorption band expands and it is impossible to satisfy the condition $\gamma = 0$ and (3.10) simultaneously. If the absorption corresponds to the excitation of excitons of positive effective mass the absorption bands have a considerably greater extent on the high-frequency side of ω_0 even at very low temperatures; thus, the condition $\gamma(\omega) = 0$ and (3.12) are not satisfied as a rule.

If (3.10) is satisfied, total reflection obtains at normal incidence of the light on the surface of a thick crystal. In this case, even though there is no true absorption, the light wave is attenuated rapidly inside the crystal. At small crystal thicknesses, when $z\omega\kappa/c < 1$, part of the light wave passes through the crystal. Since the absorption coefficient is usually deduced from the attenuation of light which passes through a layer of material, the effect indicated above [total or partial reflection of light in the frequency regions which satisfy a (3.10)] may introduce considerable distortion into the measurements.

As has been noted above, if the condition $\gamma(\omega) = 0$ and (3.10) are both satisfied, the index of refraction $\mu(\omega) = 0$. Thus, a measurement of the index of refraction on the shortwave side of the absorption band can give evidence as to the existence of the total reflection effect noted above. Such measurements can be used to determine the need for introducing corrections in the measurements of absorption made by the transmission method.*

We may note further that at frequencies for which the dielectric permittivity (3.5) vanishes in the transparency region, the induction D also vanishes identically. In this case, Maxwell's equations (3.3) allow the existence of longitudinal electric waves in the crystal ($H = 0$, $\text{curl}\ E = 0$). The condition $\epsilon = A(\omega) = 0$ can be satisfied at low temperatures on the short-wave side of the absorption band; this is the region of excitation of excitons of negative effective mass.

---

[1] S. I. Pekar, J. Exptl. Theoret. Phys. (U.S.S.R.) **33**, 1022 (1957), Soviet Phys. JETP **6**, 785 (1958).

---

*It should be kept in mind that in determining $\varkappa$ by the transmission method it is necessary to introduce corrections for scattering; these can be significant for narrow absorption bands (at low temperatures).

[2] V. L. Ginzburg, J. Exptl. Theoret. Phys. (U.S.S.R.) **34**, 1593 (1958), Soviet Phys. JETP **7**, 1096 (1958).

[3] V. M. Agranovich and A. A. Rukhadze, J. Exptl. Theoret. Phys. (U.S.S.R.) **35**, 982 (1958), Soviet Phys. JETP 8, 685 (1959).

[4] A. S. Davydov, J. Exptl. Theoret. Phys. (U.S.S.R.) 18, 210 (1948); **Тр. Ин-та физики АН УССР** (Trans. Inst. Phys. Acad. Sci. Ukr. S.S.R.) No. 1, 1951.

[5] A. S. Davydov, **Тр. Ин-та физики АН УССР** (Trans. Inst. Phys. Acad. Sci. Ukr. S.S.R.) No. 3, 1953.

[6] A. S. Davydov and E. I. Rashba, **Укр. физ. журн.** (Ukrainian J. Phys.) **2**, 226 (1957).

[7] W. Heitler, The Quantum Theory of Radiation, Oxford, 1953. (Russ. Transl.)

[8] I. V. Obreimov and A. F. Prikhot'ko **Памяти С. И. Вавилова** (Memorial to S. I. Vavilov) Acad. Sci. Press, 1952 p. 197.

Translated by H. Lashinsky
314

SOVIET PHYSICS JETP VOLUME 35(8), NUMBER 6 JUNE, 1959

CERENKOV RADIATION FROM DIPOLES

V. L. GINZBURG and V. Ia. EIDMAN

P. N. Lebedev Physics Institute, Academy of Sciences, U.S.S.R. and Gor'kii State University

Submitted to JETP editor, June 27, 1958

J. Exptl. Theoret. Phys. (U.S.S.R.) **35**, 1508-1512 (December, 1958)

Cerenkov radiation from electric and magnetic dipoles moving a continuous medium is considered; the radiation from dipoles moving in a channel or slit is also considered.

A particle bunch (packet) which is small compared with the wave length in the medium produce the same Cerenkov radiation as a point charge or point multiple moment corresponding to the entire bunch. Hence the Cerenkov radiation of magnetic and electric dipoles is of interest even though the dipole radiation for individual particles (neutron, electron) is very weak. Moreover, the analyses of the Cerenkov radiation from a magnetic moment given in the literature[1-6] are contradictory. For this reason we present a method of calculation which is somewhat different from that used in reference 2 to 4.

Setting $\operatorname{div} \mathbf{A} = 0$ and expanding the vector potential we obtain the relations (for simplicity it is assumed that the magnetic permeability $\mu = 1$)

$$\Delta \mathbf{A} - \frac{\varepsilon}{c^2}\frac{\partial^2 \mathbf{A}}{\partial t^2} = -\frac{4\pi}{c}\mathbf{j} + \frac{\varepsilon}{c}\frac{\partial}{\partial t}\nabla\varphi, \qquad \Delta\varphi = -\frac{4\pi\rho}{\varepsilon},$$

$$\mathbf{A} = \sum_{\lambda,i}(q_{\lambda i}\mathbf{A}_{\lambda i} + \overset{*}{q}_{\lambda i}\overset{*}{\mathbf{A}}_{\lambda i}), \quad \mathbf{A}_{\lambda i} = c\sqrt{4\pi/\varepsilon}\,\mathbf{e}_{\lambda i}\exp\{i\mathbf{k}_{\lambda}\cdot\mathbf{r}\},$$

$$\mathbf{e}_{\lambda i}\cdot\mathbf{e}_{\lambda j} = \delta_{ij}, \quad \mathbf{k}_{\lambda}\cdot\mathbf{e}_{\lambda i} = 0, \quad i = 1,2;$$

$$\mathscr{H} = \int\frac{\varepsilon E_{\mathrm{tr}}^2 + H^2}{8\pi}dV = \sum_{\lambda,i}{}'(p_{\lambda i}p_{\lambda i}^* + \omega_{\lambda}^2 q_{\lambda i}q_{\lambda i}^*),$$

$$\mathbf{E}_{\mathrm{tr}} = -\frac{1}{c}\frac{\partial\mathbf{A}}{\partial t}, \quad p_{\lambda i} = \frac{dq_{\lambda i}}{dt}, \quad \omega_{\lambda}^2 = \frac{c^2}{\varepsilon}k_{\lambda}^2$$

and the equation

$$\ddot{q}_{\lambda i} + \omega_{\lambda}^2 q_{\lambda i} = \frac{1}{c}\int(\mathbf{j}\cdot\mathbf{A}_{\lambda i})\,dV$$

$$= \sqrt{4\pi/\varepsilon}\,\{e(\mathbf{e}_{\lambda i}\cdot\mathbf{v}) + ic\mathbf{m}\cdot[\mathbf{k}_{\lambda}\times\mathbf{e}_{\lambda i}] \tag{1}$$

$$+ i(\mathbf{e}_{\lambda i}\cdot\mathbf{p})(\mathbf{k}_{\lambda}\cdot\mathbf{v})\}\exp\{i\mathbf{k}_{\lambda}\times\mathbf{v}t\},$$

where

$$\mathbf{j} = \rho\mathbf{v} + c\,\mathrm{curl}\,\mathbf{M} + \frac{\partial\mathbf{P}}{\partial t} \tag{2}$$

$$= e\mathbf{v}\delta(\mathbf{r} - \mathbf{v}t) + c\,\mathrm{curl}([\mathbf{m}\delta(\mathbf{r} - \mathbf{v}t)] + \frac{\partial}{\partial t}[\mathbf{p}\delta(\mathbf{r} - \mathbf{v}t)].$$

Integrating Eq. (1), for example with the initial conditions $q_{\lambda i}(0) = P_{\lambda i}(0) = 0$ we find the energy $\mathscr{H}$. Introducing the density of states $dZ_i(\omega) = (2\pi c)^{-3}\epsilon^{3/2}\omega^2\,d\omega\,d\Omega$, isolating the resonance term in $\mathscr{H}$, which increases in proportion to time, and integrating over the polar angle θ, we obtain an expression for the energy radiated per unit time:

$$\mathscr{H} = \frac{1}{2\pi vc^2}\sum_{i=1,2}\int d\omega\int_0^{2\pi} n^2\omega^3\left\{\mathbf{m}[\mathbf{k}_1\times\mathbf{e}_i] + \frac{1}{n}(\mathbf{e}_i\cdot\mathbf{p})\right\}^2 d\varphi, \tag{3}$$

where $n^2(\omega) = \epsilon(\omega)$ $\cos\theta = c/vn(\omega)$, $\mathbf{k}_1 = \mathbf{k}/k$, θ and φ are the polar and azimuthal angles in a coordinate system in which the z axis is in the direction of the velocity $\mathbf{v}$. In Eq. (3) it is assumed that the charge $e = 0$: if $e \neq 0$, the radiation is equal to the sum of Eq. (3) and the well-known expression for the Cerenkov radiation of a charge. The integration over frequency in Eq. (3) is carried out over the frequency region for which $c/vn(\omega) \leq 1$. At first glance, it may seem that in this calculation no account has been taken of the dispersion in n. However, one is easily convinced that this is not the case and that dispersion has properly been introduced in Eq. (3).

If the magnetic moment (also the electric dipole) is in the direction of $\mathbf{v}$, we obtain from Eq. (3) the standard expression.[1-3] If there is only a magnetic moment $\mathbf{m}_0$ in the system in which the particles (bunch) are at rest, the moments perpendicular to the velocity in Eq. (3) must be taken as $\mathbf{m} = \mathbf{m}_0$ and $\mathbf{p} = \mathbf{v}\times\mathbf{m}/c$. In this case we obtain

$$\mathscr{H} = \frac{m^2}{2vc^2}\int n^2\omega^3\left\{2\left(1 - \frac{1}{n^2}\right)^2 - \left(1 - \frac{v^2}{c^2n^2}\right)\left(1 - \frac{c^2}{v^2n^2}\right)\right\}d\omega. \tag{4}$$

This expression coincides with that given by Frank in reference 2; however, it differs from those given in references 3 and 6. Thus, in reference 3 the following expression appears in place of Eq. (4)

$$\mathscr{H} = \frac{m^2v}{2c^4}\int n^4\omega^3\left(1 - \frac{c^2}{v^2n^2}\right)^2 d\omega. \tag{5}$$

The reason for the discrepancy lies in the fact that in references 3 and 6 use was made of magnetic dipoles formed by magnetic poles. When $\epsilon \neq 1$, such moving "true" magnetic dipoles are not the same as moving current-moments.* More specifically, in place of the moment $(\mathbf{v}\times\mathbf{m})/c$ we have[3] the electric moment $\epsilon(\mathbf{v}\times\mathbf{m})/c$; this is equivalent to taking account of the electrical polarization of the medium due to the dipole itself.[4] It is curious that this case can be realized for bunches; it is necessary (for the frequency being considered) that ϵ, the dielectric permittivity in the bunch itself, be the same as ϵ, that of the surrounding medium (for example, a plasma in a magnetic field).

Using a quantum-mechanical calculation,[1,7-9] starting from the Pauli equation or the Dirac equation (if we do not consider the radiation from the charge) we obtain expressions such as Eq. (4) and similar formulas for a moment parallel to $\mathbf{v}$ (cf. reference 1). In this case, if the spin in the initial state is parallel or anti-parallel to the velocity $\mathbf{v}$, an expression such as Eq. (4) is obtained only in transitions in which there is spin flip since it is only in this case that there are components of the spin operator which are perpendicular to $\mathbf{v}$. Consequently, the Cerenkov radiation of the magnetic moment of the electron or neutron has essentially no quantum-mechanical attributes.

A characteristic feature of Eq. (4) is the fact that the integrand does not vanish at threshold (for $\cos\theta = c/nv = 1$):

$$\mathscr{H} = \frac{m^2}{vc^2}\int n^2\omega^3\left(1-\frac{1}{n^2}\right)^2 d\omega$$

(We may note that Loskutov and Kukanov[9] have obtained precisely the same expression from a quantum-mechanical calculation). This result, however, need not be considered paradoxical since the total energy $\mathscr{H}$ vanishes at threshold and then increases smoothly. Actually, if dispersion is taken into account, as the velocity increases the radiation is observed only at frequencies which correspond to the maximum value of $n(\omega)$. Furthermore, if recoil is taken into account, as is automatically the case in the quantum-mechanical calculation,[1]

$$\cos\theta = \frac{c}{nv} + \frac{\hbar\omega\,(c^2/v^2-1)^{1/2}\,(n^2-1)}{2mc^2n}, \tag{6}$$

where m is the rest mass of the particle or bunch. By virtue of Eq. (6), even if $n = \text{const}$ the radiation starts at one frequency as v increases; in the present case this is the frequency $\omega = 0$. Thus, as v increases there is a gradual expansion of the region of integration and the value of (4) increases.

We may note that an expression such as Eq. (5) can be obtained from a quantum-mechanical calculation. For this purpose, in the Dirac equation for a charged particle we add an appropriate term, proportional to $\gamma_i\gamma_k G_{ik}$; for a particle with non-kinematic magnetic moment, we replace $\gamma_i\gamma_k F_{ik}$ by $\gamma_i\gamma_k H_{ik}$ (here $F_{ik} = \{\mathbf{H}, i\mathbf{E}\}$, $H_{ik} = \{\mathbf{H}, i\mathbf{D}\}$ $\mathbf{D} = \epsilon\mathbf{E}$, $G_{ik} = F_{ik} - H_{ik}$). There is no basis for introducing these changes in the application to an individual particle; when the quantum-mechanical calculation is applied to bunches, however, there is no objection.

In conclusion we consider the Cerenkov radiation due to the motion of dipole moments in voids — channels or slits (for simplicity we assume $\epsilon = 1$ and $\mu = 1$ in the void). In the case of a charged particle it is well known[10,11] that as the radius of the channel or the width of the slit approaches zero the Cerenkov radiation becomes the same as that characteristic of motion in a continuous medium (when $\cos\theta \sim 1$ this occurs when $a/\lambda \ll 1$, where a is the radius of the channel or the width of the slit and $\lambda = \lambda_0/n$ is the wave length in the medium). At first glance it might seem that this result should also apply for dipoles and other multipoles; in general, however, this is not the case.

To compute the effect of a thin channel (slit) on the Cerenkov radiation it is convenient to make use of the reciprocity theorem

$$\int\limits_{(1)} \mathbf{j}_\omega^{(1)}\mathbf{E}_\omega^{(2)}dV = \int\limits_{(2)} \mathbf{j}_\omega^{(2)}\mathbf{E}_\omega^{(1)}dV,$$

---

*If we introduce magnetic poles with density $\rho_m(\mathbf{r})$ the field equation have the form (we take $\rho = 0$, $\mathbf{j} = 0$ and $\mathbf{B} = \mu\mathbf{H}$).

$$\operatorname{curl}\mathbf{H} = \frac{1}{c}\frac{\partial\varepsilon\mathbf{E}}{\partial t}, \qquad \operatorname{div}\varepsilon\mathbf{E} = 0,$$

$$\operatorname{curl}\mathbf{E} = -\frac{1}{c}\frac{\partial\mu\mathbf{H}}{\partial t} - \frac{4\pi}{c}\rho_m\mathbf{v}, \qquad \operatorname{div}\mu\mathbf{H} = 4\pi\rho_m,$$

whence

$$\operatorname{curl}\operatorname{curl}\mathbf{H} + \frac{\varepsilon\mu}{c^2}\frac{\partial^2\mathbf{H}}{\partial t^2} = -\frac{4\pi}{c}\varepsilon\frac{\partial(\rho_m\mathbf{v})}{\partial t},$$

$$\operatorname{curl}\operatorname{curl}\mathbf{E} + \frac{\varepsilon\mu}{c^2}\frac{\partial^2\mathbf{E}}{\partial t^2} = -\frac{4\pi}{c}\operatorname{curl}(\rho_m\mathbf{v}).$$

However, if there are electric charges and currents

$$\operatorname{curl}\operatorname{curl}\mathbf{H} + \frac{\varepsilon\mu}{c^2}\frac{\partial^2\mathbf{H}}{\partial t^2} = \frac{4\pi}{c}\operatorname{curl}(\rho\mathbf{v}),$$

$$\operatorname{curl}\operatorname{curl}\mathbf{E} + \frac{\varepsilon\mu}{c^2}\frac{\partial^2\mathbf{E}}{\partial t^2} = -\frac{4\pi}{c}\mu\frac{\partial(\rho\mathbf{v})}{\partial t}.$$

In other words, the equations for magnetic poles are obtained from the charge equations by making the substitutions

$$\mathbf{E}\to\mathbf{H}, \qquad \mathbf{H}\to-\mathbf{E}, \qquad \rho\to\rho_m, \qquad \mu\to\varepsilon.$$

Thus, when $\mu = 1$ the magnetic moment due to a current is completely equivalent to the "true" magnetic dipole only in vacuum, where $\varepsilon = 1$.

where the $\mathbf{j}_\omega^{(1,2)}$ are the Fourier components of the "transverse" current density in regions 1 and 2; the field $\mathbf{E}_\omega^{(2)}$ is produced by current 2 in region 1 and field $\mathbf{E}_\omega^{(1)}$ is produced by current 1 in region 2. Writing the current in the form $\mathbf{j} = \rho\mathbf{v} + \partial\mathbf{P}/\partial t + c \operatorname{curl} \mathbf{M}$ we have:

$$\int\limits_{(1)} [(\rho\mathbf{v})_\omega^{(1)} \cdot \mathbf{E}^{(2)} + i\omega\mathbf{P}_\omega^{(1)} \cdot \mathbf{E}_\omega^{(2)} - \mu\mathbf{M}_\omega^{(1)} \cdot \mathbf{H}_\omega^{(2)}]\, dV$$
$$= \int\limits_{(2)} [(\rho\mathbf{v})_\omega^{(2)} \cdot \mathbf{E}_\omega^{(1)} + i\omega\mathbf{P}_\omega^{(2)} \cdot \mathbf{E}_\omega^{(1)} - \mu\mathbf{M}_\omega^{(2)} \cdot \mathbf{H}_\omega^{(1)}]\, dV. \qquad (7)$$

For the Cerenkov radiation of a point charge moving along the z axis we have

$$(\rho\mathbf{v})_\omega^{(1)} = \frac{e}{2\pi}\mathbf{v}e^{-i\omega z/v}\,\delta(x)\,\delta(y),$$

and placing an electric dipole $\mathbf{p}^{(2)}$ at point 2, removed from the trajectory, we have

$$\frac{e}{2\pi}\int \mathbf{v}\cdot\mathbf{E}^{(2)}(0,0,z)\,e^{-i\omega z/v}\,dz = i\omega\mathbf{p}^{(2)}\cdot\mathbf{E}\,(2), \qquad (8)$$

where $\mathbf{E}(2) \equiv \mathbf{E}^{(1)}(2)$ is the radiation field at point 2. If the charge moves in a thin channel or narrow slit (i.e., if $a/\lambda \ll 1$) the quantity $\mathbf{v}\cdot\mathbf{E}^{(2)}(0, 0, z)$ remains the same as for a continuous medium since the tangential component of $\mathbf{E}^{(2)}$ is continuous. Hence, as is apparent from Eq. (8) the radiation field $\mathbf{E}$ also remains the same as in a continuous medium. For the radiation of an electric dipole, where $\mathbf{P}^{(1)} = \mathbf{p}\,\delta(z - vt)\,\delta(x)\,\delta(y)$,

$$\int \mathbf{p}\cdot\mathbf{E}^{(2)}(0,0,z)e^{-i\omega z/v}\,dz = \mathbf{p}^{(2)}\cdot\mathbf{E}\ (2). \qquad (9)$$

If the dipole $\mathbf{p}$ is parallel to the axis of the channel or lies in the plane of the slit when $a/\lambda \ll 1$ the radiation field is once again the same as for a continuous medium. For a dipole which is perpendicular to the plane of the slit

$$\mathbf{p}\cdot\mathbf{E}^{(2)}(0,0,z) = \varepsilon(\omega)\,\mathbf{p}\cdot\mathbf{E}_0^{(2)}(0,0,z),$$

where $\mathbf{E}_0^{(2)}$ is the field in the continuous medium produced by dipole 2. If we express the Cerenkov field of dipole 1 (with moment $\mathbf{p}$) in the continuous medium in terms of $\mathbf{E}_0$,

$$\int \mathbf{p}\cdot\mathbf{E}_0^{(2)}e^{-i\omega z/v}\,dz = \mathbf{p}^{(2)}\cdot\mathbf{E}_0\,(2),$$

$$\int \mathbf{p}\cdot\mathbf{E}^{(2)}e^{-i\omega z/v}\,dz = \varepsilon\int \mathbf{p}\cdot\mathbf{E}_0^{(2)}e^{-i\omega z/v}\,dz = \mathbf{p}^{(2)}\cdot\mathbf{E}\ (2).$$

Whence $\mathbf{E} = \epsilon\mathbf{E}_0$. In the case where the dipole is perpendicular to the axis of a thin channel which is in the form of a circular cylinder $\mathbf{E} = \mathbf{E}_0 \cdot 2\epsilon(\epsilon + 1)$. Since the magnetic wave in the field zone is proportional to the electric field the energy radiated in the case of a slit or a channel is increased respectively by a factor of ϵ^2 or $[2\epsilon/(\epsilon+1)]^2$.* A dipole with arbitrary orientation can be analyzed in terms of dipoles that are perpendicular and parallel to the axis of the channel (slit); thus, using the principle of superposition the problem is reduced to one of the foregoing. As is apparent from Eq. (7), the presence of the channel has no effect on the radiation of a magnetic dipole $\mathbf{m}$ when $\mu = 1$. If there are both electric and magnetic dipoles the radiated fields are combined (but obviously not the energy); thus the problem can again be solved.

Obviously a moving current moment and a "true" magnetic moment placed in a void must give the same radiation. This conclusion was verified by Bogdankevich[12] by a direct calculation for different dipoles moving in a circular channel; in particular, in the case of a thin channel it is found, as is to be expected, that the result is the same as the derived result — the field of the electric dipole is increased by a factor of $2\epsilon/(\epsilon+1)$.

In connection with the fact that the Cerenkov radiation of a moving dipole (with $\mu \neq 1$ also a magnetic dipole) depends on the shape of a cavity which can be as narrow as desired, there is some question as to the validity of Eqs. (3) and (4) for the motion of a dipole in a continuous medium. It is clear from the reciprocity theorem that here we are examining the validity of assuming that the field which acts on the dipole $\mathbf{E}_d$ is the average macroscopic field $\mathbf{E}$. If a fixed dipole is introduced into a medium, in general this is not the case (i.e., $\mathbf{E}_d \neq \mathbf{E}$). However, if we consider a particle with charge or a dipole moment which moves along a given trajectory, the average field which acts on a "physically infinitesimally small" portion of the path is precisely the macroscopic field. This same conclusion applies in connection with the original expression (1) for the motion of a particle in a continuous medium; this expression (or the equivalent wave equation) is obtained by averaging the equations of microscopic electrodynamics. Thus, in our opinion the validity of Eqs. (3) and (4) for Cerenkov radiation of point dipoles in a continuous medium should raise no objection.

The authors wish to acknowledge discussions of various pertinent problems with L. S. Bogdankevich, A. V. Gaponov, M. A. Miller, and I. M. Frank.

---

*To compute the radiated energy from Eq. (3) for the case of a channel or slit, we must replace p by the appropriate expression determined from Eq. (9); for example, in the case of a dipole perpendicular to the axis of a circular channel p is replaced by $[2\varepsilon/(\varepsilon + 1)]\mathbf{p}$.

[1] V. L. Ginzburg, J. Exptl. Theoret. Phys. (U.S.S.R.) **10**, 589 (1940).

[2] I. M. Frank, Izv. Akad. Nauk SSSR, Ser. Fiz. **6**, 3 (1942).

[3] I. M. Frank, Сб. памяти С. И. Вавилова (Memorial to S. I. Vavilov) Acad. Sci. Press, 1952, p. 173.

[4] V. L. Ginzburg, Сб. памяти С. И. Вавилова (Memorial to S. I. Vavilov) Acad. Sci. Press, 1952, p. 193.

[5] V. Ia. Eidman, Уч. зап. Горьковск. гос. ун-та (Sci. Reports, Gorkii State University) **30**, 229 (1956).

[6] N. L. Balazs. Phys. Rev. **104**, 1220 (1956).

[7] A. A. Sokolov and Iu. M. Loskutov, J. Exptl. Theoret. Phys. (U.S.S.R.) **32**, 630 (1957), Soviet Phys. JETP **5**, 523 (1957).

[8] M. I. Riazanov, J. Exptl. Theoret. Phys. (U.S.S.R.) **32**, 1244 (1957), Soviet Phys. JETP **5**, 1013 (1957).

[9] Iu. M. Loskutov and A. B. Kukanov, J. Exptl. Theoret. Phys. (U.S.S.R.) **34**, 477 (1958), Soviet Phys. JETP **7**, 328 (1958).

[10] V. L. Ginzburg and I. M. Frank, Dokl. Akad. Nauk SSSR **56**, 699 (1947).

[11] L. S. Bogdankevich and B. M. Bolotovskii, J. Exptl. Theoret. Phys. (U.S.S.R.) **32**, 1421 (1957), Soviet Phys. JETP **5**, 1157 (1957).

[12] L. S. Bogdankevich, J. Tech. Phys. (U.S.S.R.) (in press).

Translated by H. Lashinsky
315

MOTION OF A CHARGED PARTICLE IN AN ANISOTROPIC MEDIUM

G. A. BEGIASHVILI and E. V. GEDALIN

Tbilisi State University

Submitted to JETP editor June 28, 1958

J. Exptl. Theoret. Phys. (U.S.S.R.) 35, 1513-1517 (December, 1958)

Expressions are derived for the electromagnetic field components and the total energy losses are determined for a charged particle moving in an anisotropic gyroelectric and gyromagnetic medium.

1. The energy losses of a charged particle moving in an anisotropic dielectric medium have been considered in a number of papers.[1-3] Sitenko and Kolomenskii[4,5] generalized this work for the case where the medium has optical activity besides the anisotropy (gyroelectric, anisotropic medium). Later Pafomov[6] discussed the Cerenkov radiation in an anisotropic ferrite, using a method which was first applied to the problem of Cerenkov radiation in an anisotropic dielectric by Ginzburg.[1] That paper also contains a discussion of the simplest case of twofold anisotropy (anisotropic ϵ and μ). In the present paper we determine the components of the electromagnetic field and the energy losses of a charged particle moving in a medium with twofold anisotropy (anisotropic ϵ and μ), using the Fourier method;[5] moreover, the medium is assumed to be gyrotropic with respect to its electric and magnetic[7] properties.

This problem may be of interest for the use of anisotropic ferrodielectrics to generate microradiowaves.

2. The electromagnetic field arising in the medium during the motion of the point charge q with velocity **v** is determined by the Maxwell equations:

$$\operatorname{curl} \mathbf{E} = -\frac{1}{c}\frac{\partial \mathbf{B}}{\partial t}, \quad \operatorname{curl} \mathbf{H} = \frac{1}{c}\frac{\partial \mathbf{D}}{\partial t} + \frac{4\pi}{c} q\mathbf{v}\,\delta(\mathbf{r} - \mathbf{v}t);$$
$$\operatorname{div} \mathbf{B} = 0, \quad \operatorname{div} \mathbf{D} = 4\pi q \delta(\mathbf{r} - \mathbf{v}t). \tag{1}$$

We shall find a solution to this system of equations by the Fourier method in writing

$$\mathbf{E}(\mathbf{r},t) = \iint \mathbf{E}(\mathbf{k},\omega)\, e^{i\mathbf{k}\cdot\mathbf{r} - i\omega t} dk\, d\omega, \tag{2}$$

etc. Using the relation between the Fourier components

$$D_i(\mathbf{k},\omega) = \varepsilon_{ik}(\omega) E_k(\mathbf{k},\omega), \qquad \varepsilon_{ik} = \varepsilon^*_{ki},$$
$$B_i(\mathbf{k},\omega) = \mu_{ik}(\omega) H_k(\mathbf{k},\omega), \qquad \mu_{ik} = \mu^*_{ki}, \tag{3}$$

we obtain the following equation for the Fourier components of the electric field intensity:

$$T_{ik}E_k = -i\frac{q}{2\pi^2}\,\frac{v_i}{\omega^2}\,\delta\left(\frac{n}{c}\varkappa_j v_j - 1\right), \tag{4}$$

where

$$T_{ik} = n^2 \varepsilon_{iab}\,\varepsilon_{klm}\varkappa_a\varkappa_m\mu^{-1}_{bl} + \varepsilon_{ik},$$
$$n^2 = k^2c^2/\omega^2, \quad \varkappa_i = k_i/k,$$

and ϵ_{ikl} is the completely antisymmetric unit tensor of third rank.

The solution of Eq. (4) can be written in the form

$$E_i = -i\frac{q}{2\pi^2\omega^2}\,T^{-1}_{ik}v_k\,\delta\left(\frac{n}{c}v_j\varkappa_j - 1\right), \tag{5}$$

We obtain for the total energy loss per unit length due to the remote collisions the expression

$$-\frac{d\mathcal{E}}{dl} = i\frac{q^2}{2\pi^2 v}\int\limits_{-\infty}^{\infty}\int\limits_{0}^{k_m}\int\limits_{4\pi} T^{-1}_{ik}v_i v_k \delta\left(\frac{n}{c}v_j\varkappa_j - 1\right)\frac{d\omega}{\omega^2}k^2 dk\, do, \tag{6}$$

where k_m is the maximal value of k, which is of order 1/b, where b is the minimum parameter of remote collisions.

3. We apply (6) to the motion of a point charge in an optically-active uniaxial crystal, for which the tensors for the dielectric constant ϵ_{ik} and the magnetic permeability μ_{ik} have the form

$$\varepsilon_{ik} = \begin{pmatrix} \varepsilon_1, & -i\varepsilon_2, & 0 \\ i\varepsilon_2, & \varepsilon_1, & 0 \\ 0, & 0, & \varepsilon_3 \end{pmatrix}; \quad \mu_{ik} = \begin{pmatrix} \mu_1, & -i\mu_2, & 0 \\ i\mu_2, & \mu_1, & 0 \\ 0, & 0, & \mu_3 \end{pmatrix} \tag{7}$$

For the tensor μ^{-1}_{ik} (the reciprocal of the magnetic permeability tensor μ_{ik}) we obtain*

$$\mu^{-1}_{ik} = \begin{pmatrix} a, & -ib, & 0 \\ ib, & a, & 0 \\ 0, & 0, & g \end{pmatrix};$$
$$a = \mu_1/(\mu_1^2 - \mu_2^2), \quad b = \mu_2/(\mu_2^2 - \mu_1^2), \quad g = 1/\mu_3. \tag{8}$$

---

*We assume here that (a) we can choose a coordinate system in which ε_{ik} and μ_{ik} have the form (7), which is, of course, the case for the simplest media,[6] and (b) the reciprocal tensor μ^{-1}_{ik} exists for all frequencies.

In this case the tensor T_{ik} has the form

$$T_{ik} = \begin{pmatrix} -n^2(\varkappa_3^2 a + \varkappa_2^2 g) + \varepsilon_1, & n^2(\varkappa_1\varkappa_2 g + ib\varkappa_3^2) - i\varepsilon_2, & n^2(\varkappa_1\varkappa_3 a - ib\varkappa_2\varkappa_3) \\ n^2(\varkappa_1\varkappa_2 g - ib\varkappa_3^2) + i\varepsilon_2, & -n^2(\varkappa_3^2 a + g\varkappa_1^2) + \varepsilon_1, & n^2(\varkappa_2\varkappa_3 a + ib\varkappa_1\varkappa_3) \\ n^2(\varkappa_1\varkappa_3 a + ib\varkappa_2\varkappa_3), & n^2(\varkappa_2\varkappa_3 a - ib\varkappa_1\varkappa_3), & -n^2 a(1 - \varkappa_3^2) + \varepsilon_3 \end{pmatrix}. \tag{9}$$

To find the reciprocal tensor we have to divide the minors corresponding to the elements T_{ik} by the determinant of this tensor:

$$T = \Phi(\vartheta)[n^2 - n_1^2][n^2 - n_2^2], \tag{10}$$

$$\Phi(\vartheta) = \varepsilon_1 ag \sin^4\vartheta + \varepsilon_1 a^2 \cos^2\vartheta \sin^2\vartheta + \varepsilon_3 a^2 \cos^4\vartheta \tag{11}$$
$$+ \varepsilon_3 ag \cos^2\vartheta \sin^2\vartheta - \varepsilon_3 b^2 \cos^4\vartheta - \varepsilon_1 b^2 \cos^2\vartheta \sin^2\vartheta,$$

$$n_{1,2}^2 = \{(a\varepsilon_1^2 + g\varepsilon_1\varepsilon_3 - a\varepsilon_2^2)\sin^2\vartheta + 2(a\varepsilon_1 - b\varepsilon_2)\varepsilon_3\cos^2\vartheta \tag{12}$$
$$\pm [(\varepsilon_1^2 a - \varepsilon_2^2 a - \varepsilon_1\varepsilon_3 g)^2 \sin^4\vartheta + 4a(a - g)\varepsilon_2^2\varepsilon_3^2\cos^4\vartheta$$
$$+ 4b^2\varepsilon_1\varepsilon_3(\varepsilon_2^2 - \varepsilon_1^2 + \varepsilon_1\varepsilon_3)\cos^4\vartheta + 4g\varepsilon_1\varepsilon_3(a\varepsilon_2\varepsilon_3 - b\varepsilon_1\varepsilon_3)\cos^2\vartheta$$
$$+ 4ab\varepsilon_2\varepsilon_3(\varepsilon_2^2 - \varepsilon_1^2)]^{1/2}\} / 2\Phi(\vartheta).$$

$n_{1,2}$ are the refraction indices for the ordinary and extraordinary waves, and ϑ is the angle between the optical axis of the crystal and the direction of propagation of the waves **k**.

4. We apply formula (6) to the first, simplest case: a charge moving along the optical axis. In this case we have

$$-\frac{d\mathcal{E}}{dz} = i\frac{q^2 v}{\pi c^3}\int_{-\infty}^{\infty}\int_0^{n_m}\int_0^{\pi}\{n^4[(a^2 - ag - b^2)\cos^2\vartheta$$
$$+ ag]\cos^2\vartheta + n^2[(\varepsilon_1 g - 2a\varepsilon_1 + 2\varepsilon_2 b)\cos^2\vartheta - \varepsilon_1 g] + \varepsilon_1^2 - \varepsilon_2^2\}$$
$$\times \frac{\delta(n\beta\cos\vartheta - 1)\sin\vartheta\, d\vartheta\, n^2 dn\,\omega\, d\omega}{\Phi(\vartheta)[n^2 - n_1^2(\vartheta)][n^2 - n_2^2(\vartheta)]}, \tag{13}$$

where we have introduced the variable $n = kc/\omega$ instead of k.

As in reference 5, we choose a coordinate system in which the z axis is directed along the optical axis of the crystal. The particle moves along the z axis. In integrating over the angles we take account of the δ function, where the integration over n is, of course, restricted to the region from $1/\beta$ to $n_m = k_m c/\omega$. The integration yields

$$-\frac{d\mathcal{E}}{dz} = -\frac{q^2}{c^2\pi}\operatorname{Re} i\int_0^{\infty}\{(ag - \varepsilon_1\beta^2 g)n_1^2 + (a^2 - ag - b^2)/\beta^2$$
$$+ (\varepsilon_1 g - 2a\varepsilon_1 + 2b\varepsilon_2) + (\varepsilon_1^2 - \varepsilon_2^2)\beta^2\}\{\varepsilon_1 ag\beta^2(n_1^2 - n_2^2)\}^{-1}$$
$$\times \ln\{n_m^2\beta^2 - n_1^2\beta^2)/(1 - n_1^2\beta^2)\}\,\omega\, d\omega$$
$$-\frac{q^2}{c^2\pi}\operatorname{Re} i\int_0^{\infty}\{(ag - \varepsilon_1\beta^2 g)n_2^2 + (a^2 - ag - b^2)/\beta^2 \tag{14}$$
$$+ (\varepsilon_1 g - 2a\varepsilon_1 + 2b\varepsilon_2) + (\varepsilon_1^2 - \varepsilon_2^2)\beta^2\}\{\varepsilon_1 ag\beta^2(n_2^2 - n_1^2)\}^{-1}$$
$$\times \ln\{(n_m^2\beta^2 - n_2^2\beta^2)/(1 - n_2^2\beta^2)\}\,\omega\, d\omega,$$

where

$$n_{1,2}^2 = \{(ag - a^2)\varepsilon_1$$
$$+ ag(\varepsilon_1 - \varepsilon_3) + b^2\varepsilon_1 + (\varepsilon_1^2 a - \varepsilon_2^2 a + \varepsilon_1\varepsilon_3 g)\beta^2$$
$$\pm [(\varepsilon_1^2 a - \varepsilon_2^2 a - \varepsilon_1\varepsilon_3 g)^2\beta^4 \tag{15}$$
$$- 2a\varepsilon_1(\varepsilon_3 g - \varepsilon_1 a)^2\beta^2 + 2a^2\varepsilon_2^2(\varepsilon_1 a + \varepsilon_3 g)\beta^2$$
$$+ 2b^2\varepsilon_1(a\varepsilon_1^2 - a\varepsilon_2^2 + g\varepsilon_1\varepsilon_3)\beta^2 - 8abg\varepsilon_1\varepsilon_2\varepsilon_3\beta^2 + (g\varepsilon_3 - \varepsilon_1)^2 a^2$$
$$+ b^2\varepsilon_1(b^2\varepsilon_1 - 2a^2\varepsilon_1 + 2ag\varepsilon_3)]^{1/2}\}/2\varepsilon_1 ag\beta^2$$

are the values of the refraction indices in the directions of maximal radiation determined from the equations

$$\cos\vartheta_{1,2} = 1/\beta^2 n_{1,2}^2(\vartheta_{1,2}).$$

The right hand side of (14) is different from zero only in two cases: (a) when the argument of the logarithm is negative, and (b) if the expression under the integral sign has poles, i.e., for frequencies such that ϵ_1, ϵ_2, and ϵ_3 are simultaneously zero. Thus we obtain

$$-\frac{d\mathcal{E}}{dz} = -\frac{q^2}{c^2}\int\{(ag - \varepsilon_1\beta^2 g)n_1^2 + (a^2 - ag - b^2)\beta^{-2}$$
$$+ \varepsilon_1 g - 2a\varepsilon_1 + 2b\varepsilon_2$$
$$+ (\varepsilon_1^2 - \varepsilon_2^2)\beta^2\}\{\varepsilon_1 ag(n_1^2 - n_2^2)\beta^2\}^{-1}\omega\, d\omega - \frac{q^2}{c^2}\int\{(ag - \varepsilon_1\beta^2 g)n_2^2$$
$$+ (a^2 - ag - b^2)\beta^{-2} + \varepsilon_1 g - 2a\varepsilon_1 + 2b\varepsilon_2 \tag{16}$$
$$+ (\varepsilon_1^2 - \varepsilon_2^2)\beta^2\}\{\varepsilon_1 ag(n_2^2 - n_1^2)\beta^2\}^{-1}\omega\, d\omega$$
$$+ \frac{q^2}{v^2}\sum_i \frac{\omega_i}{|d\varepsilon_1/d\omega|_i}\left(\frac{ag\nu_1^2 + \beta^{-2}(a^2 - ag - b^2)}{ag(\nu_1^2 - \nu_2^2)}\right)_i \ln\frac{n_m^2\beta^2 - \nu_1^2\beta^2}{1 - \nu_1^2\beta^2}$$
$$+ \frac{q^2}{v^2}\sum_i \frac{\omega_i}{|d\varepsilon_1/d\omega|_i}\left(\frac{ag\nu_2^2 + \beta^{-2}(a^2 - ag - b^2)}{ag(\nu_2^2 - \nu_1^2)}\right)_i \ln\frac{n_m^2\beta^2 - \nu_2^2\beta^2}{1 - \nu_2^2\beta^2},$$

where

$$\nu_{1,2}^2 = [\{(ag - a^2) + ag(1 - \varepsilon_3/\varepsilon_1) + b^2$$
$$\pm [a^2(g\varepsilon_3/\varepsilon_1 - 1)^2 + b^2(b^2 - 2a^2 - 2ag\varepsilon_3/\varepsilon_1)]^{1/2}\}/2ag\beta^2]_{\omega = \omega_i}.$$

The integration in the first two terms of (16) goes over the frequency regions determined by the inequalities

$$n_m^2\beta^2 > n_1^2\beta^2 > 1\,, \quad n_m^2\beta^2 > n_2^2\beta^2 > 1 \tag{17}$$

respectively. We note that (16) goes over into the corresponding expression of the paper of Sitenko and Kolomenskii[5] for $a = g = 1$ and $b = 0$. In this case the third term, which comes from the magnetic anisotropy, vanishes.

In the case of an anisotropic magneto-active ferrite we obtain ($\epsilon_2 = 0$, $\epsilon_1 = \epsilon_3 = 1$):

$$d\mathcal{E}/dz = (q/c)^2 \int (1/\beta^2 - 1/a)\, \omega d\omega\,. \tag{18}$$

If $\mu_2 = 0$ (anisotropic ferrite), formula (18) goes over into the corresponding formula of the paper of Pafomov.[6]

5. In order to determine the character of the losses (16) we have to compute the energy flux through the cylindrical surface surrounding the trajectory of the charge. For this purpose we must determine the fields **E** and **H** arising in the medium during the motion of the charge, after which we make use of the Poynting theorem in the usual manner.

We omit these rather cumbersome calculations and remark only that, under the assumption that ϵ_1, ϵ_2, and ϵ_3 do not have any common roots, the losses on account of the Cerenkov radiation are represented by the first two terms in formula (16).

6. We now consider the second case: a charge moving perpendicular to the optical axis of the crystal. We choose the directions of the axes as in reference 5; the z axis is directed along the optical axis of the crystal. The particle moves along the y axis. We then obtain

$$-\frac{d\mathcal{E}}{dy} = i\frac{q^2}{2\pi^2c^2}\int_{-\infty}^{\infty}\int_{0}^{2\pi}\int_{1/\beta}^{n_m}\frac{En^2 - F}{An^4 + Bn^2 + C}\, n\,dn\,d\varphi\,\omega\,d\omega\,, \tag{19}$$

where

$$A = \beta^2\{(ag - a^2 + b^2)(\varepsilon_1 - \varepsilon_3)\sin^4\varphi$$
$$+ [(a^2 - ag - b^2)\varepsilon_1 + ag(\varepsilon_3 - \varepsilon_1)]\sin^2\varphi + ag\varepsilon_1\};$$
$$B = [(a\varepsilon_1^2 + g\varepsilon_1\varepsilon_3 - a\varepsilon_2^2) + 2b\varepsilon_2\varepsilon_3 - 2a\varepsilon_1\varepsilon_3]\beta^2\sin^2\varphi$$
$$- [(a^2 - ag + b^2)\varepsilon_1$$
$$+ ag(\varepsilon_3 - \varepsilon_1)]\sin^2\varphi - 2(ag - a^2 + b^2)(\varepsilon_1 - \varepsilon_3)\sin^4\varphi;$$
$$C = \beta^2(\varepsilon_1^2\varepsilon_3 - \varepsilon_2^2\varepsilon_3)$$
$$- [(a\varepsilon_1^2 + g\varepsilon_1\varepsilon_3 - a\varepsilon_2^2) + 2b\varepsilon_2\varepsilon_3 - 2a\varepsilon_1\varepsilon_3]\sin^2\varphi$$
$$+ \beta^{-2}(ag - a^2 + b^2)(\varepsilon_1 - \varepsilon_3)\sin^4\varphi;$$
$$E = (ag - a\varepsilon_1\beta^2)\cos^2\varphi + (a^2 - b^2)\sin^2\varphi - \beta^2\varepsilon_3\sin^2\varphi;$$
$$F = (ag - a^2 + b^2)\sin^2\varphi$$
$$- \beta^2(\varepsilon_1 + \varepsilon_3)a\sin^2\varphi + \beta^2\varepsilon_1\varepsilon_3 - \beta^2\varepsilon_3 g;$$

φ is the angle between the x axis and the projection of **k** on the zx plane.

From (19) we obtain for the energy losses the expression

$$-\frac{d\mathcal{E}}{dy} = \frac{q^2}{2\pi^2c^2}\operatorname{Re} i\int_0^{2\pi}\int_0^{\infty}\frac{En_1^2 - F}{n_1^2 - n_2^2}\ln\frac{n_m^2\beta^2 - n_1^2\beta^2}{1 - n_1^2\beta^2}\,d\varphi\,\omega\,d\omega$$
$$+ \frac{q^2}{2\pi^2c^2}\operatorname{Re} i\int_0^{2\pi}\int_0^{\infty}\frac{En_2^2 - F}{n_2^2 - n_1^2}\ln\frac{n_m^2\beta^2 - n_2^2\beta^2}{1 - n_2^2\beta^2}\,d\varphi\,\omega\,d\omega\,, \tag{20}$$

where

$$n_{1,2}^2 = (-B \pm \sqrt{B^2 - AC})/2A.$$

The conic surfaces corresponding to the ordinary and extraordinary waves are complicated (dependence on φ). The field intensities on the different generatrices of these surfaces are not the same. The integration in (20) can in principle be carried out to the very end if ϵ_{ik} and ϵ_{ik} are given as functions of the frequency.

In the special case $a = g = 1$, $b = 0$ formula (20) goes over into formula (26) of reference 5.

The authors express their sincere gratitude to G. R. Khutsishvili for valuable advice and comments.

---

[1] V. L. Ginzburg, J. Exptl. Theoret. Phys. (U.S.S.R.) **10**, 601, 608 (1940).

[2] M. I. Kaganov, J. Exptl. Theoret. Phys. (U.S.S.R.) **23**, 507 (1953).

[3] A. A. Kolomenskii, Doklady Akad. Nauk SSSR **86**, 1097 (1952).

[4] A. A. Kolomenskii, J. Exptl. Theoret. Phys. (U.S.S.R.) **24**, 167 (1953).

[5] A. G. Sitenko and A. A. Kolomenskii, J. Exptl. Theoret. Phys. (U.S.S.R.) **30**, 511 (1956), Soviet Phys. JETP **3**, 410 (1956).

[6] V. E. Pafomov, J. Exptl. Theoret. Phys. (U.S.S.R.) **30**, 761 (1956), Soviet Phys. JETP **3**, 597 (1956).

[7] P. S. Epstein, Revs. Modern Phys. **28**, 3 (1956).

Translated by R. Lipperheide
316

SOVIET PHYSICS JETP VOLUME 35(8), NUMBER 6 JUNE, 1959

A NEW METHOD IN STATISTICAL PERTURBATION THEORY

CHEN CHUN-SIAN

Moscow State University

Submitted to JETP editor July 7, 1958

J. Exptl. Theoret. Phys. (U.S.S.R.) 35, 1518-1521 (December, 1958)

A new variant of the statistical perturbation theory is presented, which consists in the setting up of a model of a dynamical system whose Hamiltonian contains the inverse temperature in parametric form. It is shown that for this dynamical system the perturbation theory is equivalent to the ordinary statistical perturbation theory and is much more convenient for practical calculation.

ACCORDING to the principles of statistical physics, the thermodynamic properties of systems in thermal equilibrium can be determined by the sum of states. In quantum statistics the latter is usually represented as (in the case of a grand canonical ensemble)

$$\Xi = \mathrm{Sp}\,(e^{-\beta H+\alpha N}), \tag{1}$$

where $\beta = 1/\Theta$; Θ is the temperature in energy units; $\alpha = \beta\mu$; μ is the chemical potential.

Taking into account the formal similarity between the statistical operator of a canonical ensemble and the operator describing the time sequence of a dynamical system, a number of authors have developed several variants of the statistical perturbation theory in analogy with the corresponding formalism in contemporary quantum field theory.[1] The fact that only slight practical results have been obtained in this direction is connected in large measure with new difficulties of calculation. Thus, for example, instead of the averaging of the quantum amplitudes over a real vacuum, we deal here with an averaging over the canonical ensemble of free particles; inasmuch as we have the quantity $i\beta$ in place of the time variable t, integration always extends from zero to some finite value. It must be noted that in the researches of Bogoliubov, Zubarev, and Tserkovnikov[2,3] the statistical perturbation theory supplemented by the method of canonical transformations is successfully applied to the exact calculation of thermodynamic functions of some model problems in the theory of superfluidity and superconductivity. We now consider a new version of statistical perturbation theory, which consists in the setting up of a model dynamical system, the determination of the ground-state energy of which makes it possible to compute the change in the thermodynamic potential of the system upon inclusion of the interaction for a given temperature β.

Keeping in mind the description with the aid of the grand canonical ensemble, we represent the Hamiltonian of the system under consideration as

$$H = H_0 + V,\ H_0 = \sum_{ks}(E(k) - \mu)\, a_{ks}^{+} a_{ks} + \sum_{q} \omega(q) b_q^{+} b_q, \tag{2}$$

where a_{ks}^{+}, a_{ks}, b_q^{+}, b_q are the Fermi and Bose amplitudes; $E(k)$ and $\omega(q)$ are the eigen energies of the fermions and bosons with quantum numbers k, s, and q, respectively; μ is the chemical potential, determined from the condition of the equality of the average number of fermions with the actual number of fermions in the system; V is the Hermitian form of a_{ks}^{+}, a_{ks} and b_q^{+}, b_q.

We introduce these statistical sum Ξ and the thermodynamic potential

$$\Psi = -\beta^{-1}\ln\Xi = -\beta^{-1}\ln\,[\mathrm{Sp}\, e^{-\beta H}].$$

We then have the very well-known relations (reference 1, see also reference 4):

$$\begin{gathered} \Xi/\Xi_0 = \langle\!\langle \mathfrak{S} \rangle\!\rangle = \exp \langle\!\langle \mathfrak{S} \rangle\!\rangle_{\text{coup}}, \\ \Psi = \Psi_0 - \beta^{-1} \langle\!\langle \mathfrak{S} \rangle\!\rangle_{\text{coup}}, \end{gathered} \tag{3}$$

where

$$\Psi_0 = -\beta^{-1}\ln\Xi_0 = -\beta^{-1}\ln\,[\mathrm{Sp}\, e^{-\beta H_0}],$$

$$\mathfrak{S} = e^{\beta H_0} e^{-\beta H},\ \langle\!\langle A \rangle\!\rangle = \Xi_0^{-1}\,\mathrm{Sp}\,[e^{-\beta H_0} A].$$

the index "coup" means that in each term of the expansion all the intermediate states are coupled together by the matrix elements of V.

To obtain an explicit form of the expansion of $\mathfrak{S}$ in V, we assume a new much simpler method in place of the ordinary formalism of time sequence according to the temperature variable, since the finite limit of integration brings about an appreciable complication.

We introduce the Laplace transform of the statistical operator[1]

$$e^{-\beta H} = \frac{1}{2\pi i}\int_{\Gamma} e^{-\beta z}\frac{1}{z-H}\,dz;$$

$(z-H)^{-1} = (z-H_0)^{-1} + (z-H_0)^{-1}R(z)(z-H_0)^{-1}$, $R(z) = V + V(z-H_0)^{-1}V + \ldots$ [the contour Γ proceeds downward, parallel to the imaginary axis, to the left of all singularities of the function $(z-H)^{-1}$].

It is known[5] that the matrix element $R(z)$ and the function $(z-H)^{-1}$ are analytic as functions of the complex variable z if we make a cut along the real axis beginning at some point up to $+\infty$. For a finite volume of the system, the singularities are densely-located poles.

We can then write (3) in the form

$$\Psi = \Psi_0 - (\beta\Xi_0)^{-1}\frac{1}{2\pi i}\int_{\Gamma} e^{-\beta z}\,\mathrm{Sp}\,[(z-H_0)^{-2}R(z)_{\text{coup}}]\,dz$$

$$= \Psi_0 - \beta^{-1}\frac{1}{2\pi i}\int_{-\infty}^{\infty} d\varepsilon \int_{\Gamma} d\zeta\,\frac{e^{-\zeta\beta}}{\zeta^2} \ll \delta(\varepsilon - H_0)R(\zeta+\varepsilon)_{\text{coup}} \gg .$$

making use of the invariance of the trace relative to a cyclic permutation of the cofactors, it is easy to establish that

$$\frac{1}{2\pi i}\int_{\Gamma} d\zeta\,\zeta^{-2}e^{-\zeta\beta} \ll \delta(\varepsilon - H_0)R(\zeta+\varepsilon)_{\text{coup}} \gg$$

$$= -\beta \ll \delta(\varepsilon - H_0)R(\varepsilon)_{\text{coup}} \gg .$$

In this case all terms containing $(\epsilon - E'_p)^{-2}$ (where E'_p is the energy of any intermediate state) cancel each other. Thus, we are led to the very useful expression of statistical permutation theory first obtained by Bloch.[1]

$$\Psi = \Psi_0 + \int_{-\infty}^{\infty} d\varepsilon \ll \delta(\varepsilon - H_0)R(\varepsilon)_{\text{coup}} \gg . \qquad (4)$$

The basic idea of the present paper consists of the fact that the second term in (4) can be replaced by the change in energy of the ground state of any model of the dynamic system upon inclusion of the interaction. In the Hamiltonian of this model system (we shall call it the statistical model Hamiltonian), β entered as a numerical parameter.

Let us prove the fundamental theorem, following the scheme of Bloch.[1] Let A be the product of the Fermi and Bose amplitudes; then we have the equality

$$\ll A \gg = \langle \Phi_F | A | \Phi_F \rangle \equiv \langle A \rangle, \qquad (5)$$

where $|\Phi_F\rangle$ is the vacuum state of the new Fermi and Bose amplitudes determined by the relations

$$a^+_{ks} = (1-f_k)^{1/2}c^+_{ks} + f_k^{1/2}b_{ks}, \quad a_{ks} = (1-f_k)^{1/2}c_{ks} + f_k^{1/2}b^+_{ks}.$$
$$c_{ks}|\Phi_F\rangle = b_{ks}|\Phi_F\rangle = 0.$$
$$(6)$$
$$b_q = (1+h_q)^{1/2}\eta_{q0} + h_q^{1/2}\eta^+_{q1}, \quad b^+_q = (1+h_q)^{1/2}\eta^+_{q0} + h_q^{1/2}\eta_{q1},$$
$$\eta_{q0}|\Phi_F\rangle = \eta_{q1}|\Phi_F\rangle = 0,$$

where f_k and h_q upon determination are equal to the mean occupation number of the fermion state k, s and the boson state q

$$f_k \equiv \ll a^+_{ks}a_{ks} \gg = (1 + e^{\beta(E(k)-\mu)})^{-1},$$
$$(7)$$
$$h_q \equiv \ll b^+_q b_q \gg = (e^{\beta\omega(q)} - 1)^{-1}.$$

We now prove the theorem by induction. First we note that $\ll A \gg$ differs from zero only when A consists of the aggregate of pairs of creation and annihilation operators of the boson or the fermion relative to one and the same individual state. Since $\exp(-\beta H_0)$ has been factored, it then suffices to exhibit this theorem for any given state k. If all the pairs in A refer to different states, then the theorem is identical with the determination of f_k and h_q, since

$$f_k \equiv \ll a^+_{ks}a_{ks} \gg = \langle a^+_{ks}a_{ks} \rangle,$$
$$(8)$$
$$h_q \equiv \ll b^+_q b_q \gg = \langle b^+_q b_q \rangle.$$

In the case of the presence of several pairs with the same index, the problem reduces to the proof of the following two assertions:

(a) If $\ll Aa^+_{ps}a_{ps}B \gg = \langle Aa^+_{ps}a_{ps}B \rangle$ and $\ll AB \gg = \langle AB \rangle$, then $\ll Aa_{ps}a^+_{ps}B \gg = \langle Aa_{ps}a^+_{ps}B \rangle$.

This assertion is the consequence of the commutation relation for a_{ps} and a^+_{ps}, while A and B are the products of the operators a^+_{ks}, a_{ks}, b^+_q, b_q. For the case of bosons we have: if $\ll AB \gg = \langle AB \rangle$ and $\ll Ab^+_q b_q \gg = \langle Ab^+_q b_q \rangle$, then

$$\ll Ab_q b^+_q B \gg = \langle Ab_q b^+_q B \rangle.$$

(b) If in A there are n pairs of Fermi amplitudes with the index k, or m pairs of boson amplitudes with index q, we have the equalities

$$\ll a^{+n}_{ks}a^n_{ks} \gg = \langle a^{+n}_{ks}a^n_{ks} \rangle, \quad \ll b^{+m}_q b^m_q \gg = \langle b^{+m}_q b^m_q \rangle.$$

In the case of fermions, the equality is trivial since the mean value of the null operator appears on both sides. In the Bose case, writing out both sides,

$$\ll b^{+m}_q b^m_q \gg = \ll (b^+_q b_q - m + 1)(b^+_q b_q - m + 2)\ldots b^+_q b_q \gg$$
$$= m!h^m_q \langle b^{+m}_q b^m_q \rangle = h^m_q \langle \eta^m_{q1}\ \eta^{+m}_{q1} \rangle = m!h^m_q.$$

(a) and (b) contain the complete proof of the theorem.

We now consider the model dynamical system with the Hamiltonian

$$H^{\mathrm{st}} = H_0^{\mathrm{st}} + V; \qquad H_0^{\mathrm{st}} = \sum_{ks} (E(k) - \mu)\,(c_{ks}^{+} c_{ks} - b_{ks}^{+} b_{ks})$$

$$+ \sum_{q} \omega(q)\,(\eta_{q0}^{+} \eta_{q0} - \eta_{q1}^{+} \eta_{q1}) \,. \tag{9}$$

The change in the ground state energy of this system will be

$$\Delta E^{\mathrm{st}} = \int_{-\infty}^{\infty} \left\langle \delta(\varepsilon - H_0^{\mathrm{st}}) \left[V + V \frac{1}{\varepsilon - H_0^{\mathrm{st}}} V + \ldots \right]_{\mathrm{coup}} \right\rangle d\varepsilon \,. \tag{10}$$

Applying our theorem to the expression under the integral, it is not difficult to note the identities (10) and the second term (4). Choice of H_0^{st} guarantees the averaging over the present dynamical vacuum and the correct energy gaps. Thus we obtain

$$\Psi = \Psi_0 + \Delta E^{\mathrm{st}} \,, \tag{11}$$

i.e., the correction to the thermodynamical potential at a given temperature is equal to the change in the ground state energy for the dynamical system with the Hamiltonian H^{st}. This assertion completes the program outlined above.

We now proceed to a discussion of the results.

1. The physical idea which underlies the foregoing formal transformations is that the statistical average over the canonical ensemble is considered as a quantum mechanical averaging over the state $|\Phi_F\rangle$, in which the individual states are filled with the probability corresponding to their weights in the ensemble. The ordinary formalism of perturbation theory is built up relative to $|\Phi_F\rangle$. Consequently, $|\Phi_F\rangle$ is the analogue of the vacuum state of the free system at temperatures different from zero. For fermions, it is a Fermi sphere with a diffuse edge, while for bosons it is a "smeared" Bose-condensate. (The states below the condensate are filled with the probability h_k). The appearance of quasi-particles b, c, η on $|\Phi_F\rangle$ corresponds to a departure from statistical equilibrium. At zero temperature, they go over into a real perturbation: the electron-hole on the Fermi sphere and the boson on the condensate (the boson $\eta_{k_1}^{+}$, $\bar{\eta}_{k_1}$ does not appear at absolute zero).

2. The new formulation possesses a great advantage for practical calculations since, for the treatment of the statistical model of the Hamiltonian, we can without complication call upon the entire methodology developed for the investigation of other dynamic systems: in particular, perturbation theory and the Green's-function method of modern quantum field theory, and also the method of canonical transformations in its many versions. In particular, for consideration of phase transitions of second order and Bose-Fermi systems, we can formulate the principles of compensations of the various diagrams of Bogoliubov[6] at temperatures differing from absolute zero.

In conclusion the author expresses his gratitude to Academician N. N. Bogoliubov, V. V. Tolmachev, S. V. Tiablikov and also to V. A. Moskalenko, Chao K'ei-hua and Chou Hsi-shin for their interest in the work and for a number of valuable suggestions.

---

[1] T. Matsubara, Progr. Theoret. Phys. **14**, 351 (1955); S. Bloch and C. Dominicis, Preprint.

[2] Bogoliubov, Zubarev, and Tserkovnikov, Dokl. Akad. Nauk SSSR **117**, 788 (1957); Soviet Phys. "Doklady" **2**, 535 (1957).

[3] D. N. Zubarev and Iu. A. Tserkovnikov, Dokl. Akad. Nauk SSSR **120**, 991 (1958), Soviet Phys. "Doklady" **3**, 603 (1958).

[4] J. Hubbard, Proc. Roy. Soc. (London) **A240**, 539 (1957); C. Bloch, Preprint.

[5] N. M. Hugenholtz, Physics **23**, 481 (1957).

[6] N. N. Bogoliubov, J. Exptl. Theoret. Phys. (U.S.S.R.) **34**, 58 (1958); Soviet Phys. JETP **7**, 41 (1958).

Translated by R. T. Beyer
317

SOVIET PHYSICS JETP VOLUME 35(8), NUMBER 6 JUNE, 1959

ASYMPTOTIC THEORY OF A ONE-DIMENSIONAL FOUR-FERMION INTERACTION

A. A. ANSEL' M

Leningrad Physico-Technical Institute, Academy of Sciences, U.S.S.R.

Submitted to JETP editor July 9, 1958

J. Exptl. Theoret. Phys. (U.S.S.R.) 35, 1522-1531 (December, 1958)

We study a fermion field interacting with itself, in a world with one space and one time dimension. Asymptotic expressions are obtained for the vertex part and Green's function by summing an infinite series of graphs. The theory is free of divergences, and there is no charge-renormalization. It turns out that the single-limit technique gives the correct form of the leading term in the asymptotic expansion of the exact solution, but the double-limit technique gives an incorrect result. The theory is compared with the exact solution of Thirring.

1. INTRODUCTION

LANDAU, Abrikosov, and Khalatnikov[1] solved the equations of quantum electrodynamics in the asymptotic region $p^2 \gg m^2$, where p is the momentum 4-vector of a particle and m is its mass. They obtained the following relation between the bare charge e_0 and the renormalized charge e_c:

$$e_c^2 = e_0^2 / [1 + (e_0^2/3\pi)L], \tag{1}$$

where $L = \ln(\Lambda^2/m^2)$ and Λ is the cut-off momentum. If we pass to the limit $L \to \infty$ in Eq. (1), then, no matter how e_0 varies with L, e_c tends to zero and consequently the interaction disappears. This happens provided only that $e_0^2 > 0$, that is to say, if e_0 is real. Also, the renormalized photon Green's function $d_c(\xi)$, $\xi = \ln(p^2/m^2)$, is given by

$$d_c(\xi) = [1 - (e_c^2/3\pi)\xi]^{-1} \tag{2}$$

and has a pole at $p^2 = m^2 \exp(3\pi \cdot 137)$. This contradicts the well-known theorem of Lehmann.[2] The appearance of the plus-sign in the denominator of Eq. (1) produces these unpleasant effects, and is a reflection of the fact, proved by Lehmann, that the renormalization constant Z_3^{-1} (in this case equal to $1 + (e_0^2/3\pi)L$) must exceed unity.*

The relation (1) between the bare and renormalized charge was obtained on the assumption of weak coupling, $e_0^2 \ll 1$. The double-limit technique proves the correctness of Eq. (1) for any value of e_0^2, if we pass to the limit of a point interaction in a suitable way.[7] The question then arises, whether the final result depends on the method by which one passes to the limit. In the present paper we consider a simple model of a one-dimensional four-fermion interaction. This example shows that the double-limit technique can give a completely different result from the single-limit technique. The application of the double-limit technique to this problem leads to a violation of the Pauli principle in the cut-off theory before passing to the limit.

Thirring[8] has recently obtained an exact solution to the problem of a one-dimensional four-fermion interaction. It is interesting to compare his result with the results of methods which have been developed in the study of other types of field theory. We shall find that the single-limit technique leads to the correct expression for the leading term in the expansion of the vertex part in a series of the form*

$$\alpha_0(\xi) = f_0[g_0(L - \xi)] + g_0^2 f_2[g_0(L - \xi)] + g_0^4 f_4[g_0(L - \xi)] + \ldots, \tag{3}$$

but the two-limit technique gives an incorrect result. We leave open the question, whether this fact is a consequence of the violation of the Pauli principle in the cut-off theory, or whether it indicates a general deficiency of the two-limit technique.

The study of this example is interesting for another reason. We have here a completely different relation between renormalized and bare charge

---

*Abrikosov, Galanin, and Khalatnikov[3] obtained a result similar to Eq. (1) for pseudoscalar meson theory. If we give up the requirement that e_0^2 be positive, so that the Hamiltonian becomes non-Hermitian, we are forced to introduce an indefinite metric. This problem has been studied in detail for the example of the Lee model[4] by Källèn and Pauli[5] and by Heisenberg.[6]

*Terms of the form $g_0 f_1[g_0(L - \xi)]$, $g_0^3 f_3[g_0(L - \xi)$, etc. are absent. This can be seen from a detailed study of the graphs, or from the exact solution of Thirring.[8]

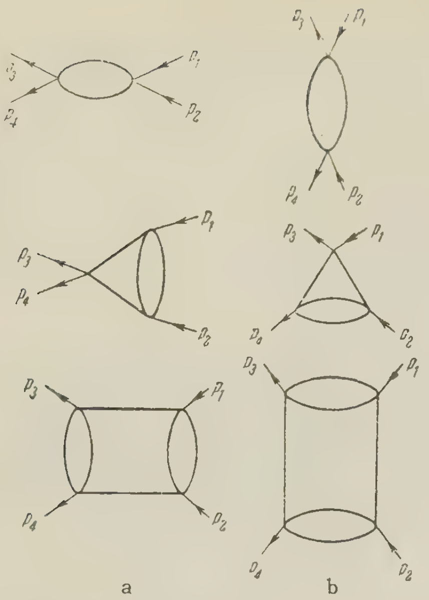

a b

FIG. 1

from that which arises in the interaction of a fermion with a boson field. Examination of the structure of the graphs shows that the insertion of an additional vertex produces one extra factor g_0 and two fermion Green's functions. This means that the quantity which is invariant under renormalization is now $g_0\alpha_0(\xi)\,\beta_0^2(\xi)$, where α_0 is the vertex part and β_0 is the Green's function. The series for the vertex part has the form of Eq. (3), where the leading term contains the product of L with the first power of g_0. The renormalized charge in this theory is presumably determined by the behavior of the vertex part, since the leading terms in the expansion of β_0 have the form $(g_0^2 L)^n$. Therefore the relation between renormalized and bare charge must have the form

$$g_c = g_0/(1 \pm a g_0 L) \tag{4}$$

where g_0 is positive, and a is a positive number of the order of unity.

If the sign is plus in the denominator of Eq. (4), we meet with the same difficulties as before, but if the sign is minus the renormalized charge can be different from zero. Equation (4) is obtained from the double-limit technique, but only after throwing away a certain number of divergent graphs, which in the single-limit technique are cancelled by diagrams which are retained in Eq. (4). In fact, thanks to this cancellation, the theory does not contain any real divergences. Thus Eq. (4) is incorrect, and the problem of a zero charge does not arise. The correct form of the series (3) is

$$\alpha_0(\xi') = f_0(g_0\xi') + g_0^2 f_2(g_0\xi') + g_0^4 f_4(g_0\xi') + \dots \tag{3'}$$

Here $\xi' = \ln(p_{\text{in}}^2/p_{\text{out}}^2)$, and p_{in} and p_{out} are the momenta of the incoming and outgoing particles in the vertex part.

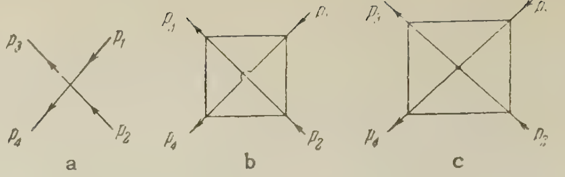

a b c

FIG. 2

All these results are confirmed by the calculation of Thirring.[8]

2. EXPRESSION FOR THE INTERACTION ENERGY

We consider a fermion field $\psi_\alpha(x)$, depending on one space and one time coordinate $x = (x_1, x_0)$. The operator $\psi_\alpha(x)$ satisfies a Dirac equation, in which there are two anticommuting matrices γ_μ ($\mu = 1, 4$), representable with two rows and columns.* For definiteness we shall write

$$\gamma_1 = \sigma_x,\quad \gamma_4 = \sigma_z,\quad \gamma_5 = i\gamma_1\gamma_4 = \sigma_y \tag{5}$$

where σ are the Pauli matrices.

Instead of the usual five types of four-fermion interaction we now have three, scalar, pseudoscalar and vector. The most general form of the Hamiltonian is

$$\begin{aligned} H &= c_S(\bar\psi\psi) + c_P(\bar\psi\sigma_y\psi)(\bar\psi\sigma_y\psi) + c_V(\bar\psi\sigma_\mu\psi)(\bar\psi\sigma_\mu\psi) \\ &= (g_0/4)\,Q_{\alpha\beta\gamma\delta}\bar\psi_\alpha\bar\psi_\beta\psi_\gamma\psi_\delta. \end{aligned} \tag{6}$$

$$\bar\psi = \psi^*\gamma_4 = \psi^*\sigma_z,\quad \mu = (x, z).$$

Since the operators ψ_γ, ψ_δ, $\bar\psi_\alpha$, $\bar\psi_\beta$ in Eq. (6) anticommute, we must have

$$Q_{\alpha\beta\gamma\delta} = -Q_{\beta\alpha\gamma\delta} = -Q_{\alpha\beta\delta\gamma}. \tag{7}$$

Therefore

$$-c_S = c_P = c_V \equiv g_0/4, \tag{8}$$

which shows that in the one-dimensional case there exists only the single antisymmetric interaction: $(-S + P + V)$.

3. DETERMINATION OF THE VERTEX PART IN THE CASE WHEN ALL EXTERNAL MOMENTA ARE OF THE SAME ORDER

The vertex part $\Gamma(p_4\xi_4, p_3\xi_3, p_2\xi_2, p_1\xi_1)$ is the sum of all diagrams with two incoming and two outgoing lines (Figs. 1 and 2). We divide the graphs into two classes. The first class contains graphs in which some pair of external lines can be separated from the remaining pair by a cut crossing two lines (Fig. 1). The second class contains graphs in which such a cut is impossible (Fig. 2). Graphs of the second class can be considered as units out of which graphs of the first class are constructed by joining together the outgoing lines from one graph with the ingoing graph of another. Figure 1 shows graphs of the first class in which one unit consists of the simplest graph of the second class, a single point (Fig. 2a). Each point can in general be replaced by any graph of the second class. To find out which terms in the expansion (3) of the vertex part contain contributions from a given graph, it is sufficient to study the units from which the graph is composed. For example all graphs whose units are points give contributions* $[g_0(L-\xi)]^n$. If one unit is an "unsealed envelope" (Fig. 2b), the contribution is of order $g_0^2[g_0(L-\xi)]^n$, and so on. To determine the leading term of the series (3) in the approximation $g_0 \ll 1$, we need to sum the graphs of the first class whose units are points, which are those illustrated in Fig. 1.

---

*Although the field is quantized with Fermi statistics, it does not posses spin. The spin operator is connected with rotations in three dimensions and therefore cannot exist in this example. The two values of the index α in the operator ψ_α correspond to the two signs of the particle energy.

We denote by $f(p_4\xi_4, p_3\xi_3, p_2\xi_2, p_1\xi_1)$ the sum of those diagrams in which the incoming momenta (p_1, p_2) can be separated from the outgoing momenta (p_3, p_4) as described above (for example, the "lying bricks" in Fig. 1a). We denote by $\varphi(p_4\xi_4, p_3\xi_3, p_2\xi_2, p_1\xi_1)$ the sum of all graphs in which (p_1, p_3) can be separated from (p_2, p_4) (for example the "standing bricks" in Fig. 1b). In this approximation the vertex part becomes

$$\Gamma(p_4\xi_4, p_3\xi_3, p_2\xi_2, p_1\xi_1) = Q_{\xi_4\xi_3\xi_2\xi_1} + f(p_4\xi_4, p_3\xi_3, p_2\xi_2, p_1\xi_1)$$
$$+ \varphi(p_4\xi_4, p_3\xi_3, p_2\xi_2, p_1\xi_1) - \varphi(p_4\xi_4, p_3\xi_3, p_1\xi_1, p_2\xi_2). \quad (9)$$

If all the momenta p_4, p_3, p_2, p_1 are of the same order $(\sim p)$, then because of the logarithmic structure of the theory Γ must have the form:

$$\Gamma(p_4\xi_4, p_3\xi_3, p_2\xi_2, p_1\xi_1) = Q_{\xi_4\xi_3\xi_2\xi_1}\alpha(\xi),$$
$$f(p_4\xi_4, p_3\xi_3, p_2\xi_2, p_1\xi_1) = Q_{\xi_4\xi_3\xi_2\xi_1} f(\xi),$$
$$\varphi(p_4\xi_4, p_3\xi_3, p_2\xi_2, p_1\xi_1) - \varphi(p_4\xi_4, p_3\xi_3, p_1\xi_1, p_2\xi_2)$$
$$= Q_{\xi_4\xi_3\xi_2\xi_1}\varphi(\xi), \quad (10)$$
$$\alpha(\xi) = 1 + f(\xi) + \varphi(\xi), \ \xi = \ln(p^2/m^2).$$

Using the method by which Diatlov, Sudakov, and Ter-Martirosian[9] determined the meson-meson scattering amplitude, it is easy to write down integral equations for the functions f, φ, and α. No new difficulties of principle arise. We therefore omit the algebra and state the result

$$f(\xi) = -\frac{g_0}{2\pi}\int_\xi^L \alpha^2(z)\,\beta^2(z)\,dz, \quad \varphi(\xi) = \frac{g_0}{2\pi}\int_\xi^L \alpha^2(z)\,\beta^2(z)\,dz, \quad (11)$$

where $(\beta/i\hat{p})$ is the fermion Green's function. The meaning of these equations is that both the functions f and φ are composed of two vertex parts joined by two lines. The numerical coefficients in front of the integrals are most easily determined by first-order perturbation theory. Equation (11) implies

$$\alpha(\xi) = 1, \quad (12)$$

and if also $\beta = 1$, then

$$f(\xi) = -\frac{g_0}{2\pi}(L-\xi), \ \varphi(\xi) = \frac{g_0}{2\pi}(L-\xi). \quad (13)$$

The result of this analysis is that each "lying brick" cancels in the asymptotic region against a similar "standing brick." Consequently, the vertex part is unchanged by the interaction, and the "bricks" themselves are equal to their lowest-order perturbation-theory approximations.

4. DETERMINATION OF THE GREEN'S FUNCTION

The main result of the preceding section, that $\alpha(\xi) = 1$, did not depend on the form of the fermion Green's function. This fact arose from the special cancellation of graphs which we discussed; otherwise we might have expected that $\alpha(\xi)$ would contain terms proportional to $[g_0(L-\xi)]^n$. The Green's function might have been assumed to be free, since the corrections to it are at least of order $g_0^2(L-\xi)$. In that case the connection between renormalized and bare charge would have had the form of Eq. (4). However, it turned out that the vertex part is not renormalized by the interaction, and we must now determine the Green's function. We shall show that in the asymptotic region the expression for the Green's function also coincides with its lowest-order approximation, independently of the value of the vertex part. Thus the whole theory becomes free of divergences, and there is no renormalization of charge. There remains the question of the higher approximations to Γ, for example the contributions from graphs of the type shown in Fig. (2b) and (2c). We shall see later, from the exact solution of Thirring,[8] that these diagrams also contain no divergent parts, and consequently do not give rise to charge renormalization.

We shall derive the Dyson-Schwinger equation for this problem:

$$G^{-1}(p) = G_0^{-1}(p) - \Sigma^*(p). \quad (14)$$

---

*It is convenient to divide the vertex part by a factor $(2\pi)^2 g_0/i$. Then a single point gives simply the contribution $Q_{\xi_4\xi_3\xi_2\xi_1}$.

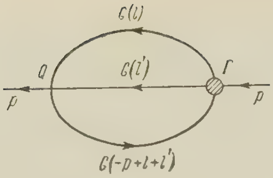

FIG. 3

It is easy to write down an expression for the self-energy operator Σ^*, by considering the graph illustrated in Fig. 3. We find

$$G^{-1}_{\xi\xi'}(p) = (i\hat{p} + m)_{\xi\xi'} - (g_0^2/2)\int Q_{\xi\eta\alpha\gamma}\, G_{\alpha\beta}(l)\, G_{\gamma\delta}(l') \quad (15)$$

$$\times\Gamma(l\beta,\, l'\delta,\, p\xi',\, -p + l + l'\varepsilon)\, G_{\varepsilon\eta}(-p + l + l')\, \frac{d^3 l}{(2\pi)^2}\, \frac{d^2 l'}{(2\pi)^2}.$$

In the region $p^2 \gg m^2$, we can write

$$G(p) = \beta(\xi)/i\hat{p},\ \ \xi = \ln(p^2/m^2),$$

$$\Gamma(p_4\xi_4,\, p_3\xi_3,\, p_2\xi_2,\, p_1\xi_1) = Q_{\xi_4\xi_3\xi_2\xi_1}\,\alpha(\xi,\, \eta,\, \zeta). \quad (16)$$

Here ξ, η, and ζ are the logarithms of the three independent momenta on which Γ depends. The integral (15) is formally linearly divergent. After integrating over the angles, only a logarithmic divergence remains. We may therefore make the replacement

$$G(-p + l + l') \to -i\beta\, \frac{1}{\hat{l} + \hat{l}'}\, \hat{p}\, \frac{1}{\hat{l} + \hat{l}' - \hat{p}}. \quad (17)$$

After this we have on the right of Eq. (15) an integral of the form

$$\int \frac{l_\mu l'_\lambda (l + l')_\sigma (l + l' - p)_\rho\, d^2l\, d^2l'}{l^2 l'^2 (l + l')^2 (l + l' - p)^2} = A\delta_{\mu\lambda}\delta_{\sigma\rho} + B(\delta_{\mu\sigma}\delta_{\lambda\rho} + \delta_{\mu\rho}\delta_{\lambda\sigma}), \quad (18)$$

where A and B are some invariant quantities. This integral is multiplied by the following combination of matrices:

$$Q_{\xi\eta\alpha\gamma}(\gamma_\mu)_{\alpha\beta}(\gamma_\lambda)_{\gamma\delta}\, Q_{\beta\delta\xi'\varepsilon}(\gamma_\sigma\hat{p}\gamma_\rho)_{\varepsilon\eta}. \quad (19)$$

A simple calculation shows that the product of (18) and (19) is equal to zero. Therefore in the asymptotic region

$$\beta = 1,\ \ G(p) = G_0(p) = 1/i\hat{p}. \quad (20)$$

If the spinor combination in front of the integral had not been zero, then with a free vertex part we would have obtained the following expression for β:

$$\beta = [1 + ag_0^2(L - \xi)]^{-1/4}, \quad (20)$$

Here a is a number of the order of unity (which happens to be zero). The relation between bare and renormalized charge would have had the form of Eq. (1).

5. CALCULATION OF THE VERTEX PART WHEN THE EXTERNAL MOMENTA HAVE DIFFERENT ORDERS OF MAGNITUDE

To compare our theory with the result of Thirring, it is useful to calculate the vertex part for the case in which the incident momenta (p_1, p_2) and the outgoing momenta (p_3, p_4) are of different orders of magnitude. Following the method of Diatlov et al.,[9] we assume that in the asymptotic region the "lying brick" depends on the logarithms of three momenta:

$$f(p_4\xi_4,\, p_3\xi_3,\, p_2\xi_2,\, p_1\xi_1) = f(\xi,\, \eta,\, \zeta;\, \xi_4,\, \xi_3,\, \xi_2,\, \xi_1),$$

$$\xi = \ln\frac{p_{\text{out}}^2}{m^2},\ \ \eta = \ln\frac{(p_1 + p_2)^2}{m^2} = \ln\frac{(p_3 + p_4)^2}{m^2},\ \ \zeta = \ln\frac{p_{\text{in}}^3}{m^2} \quad (21)$$

$$p_{\text{out}}^2 = \max\{p_3^2,\, p_4^2\},\quad p_{\text{in}}^2 = \max\{p_1^2,\, p_2^2\}.$$

In the most general case

$$\xi > \zeta > \eta,\ p_{\text{out}}^2 \gg p_{\text{in}}^2 \gg (p_1 + p_2)^2. \quad (22)$$

In the same way the "standing brick" gives

$$\varphi(p_4\xi_4,\, p_3\xi_3,\, p_2\xi_2,\, p_1\xi_1) = \varphi(\xi',\, \eta',\, \zeta';\, \xi_4,\, \xi_3,\, \xi_2,\, \xi_1), \quad (23)$$

$$\xi' = \ln\frac{p_{\text{I}}^2}{m^2},\ \ \eta' = \ln\frac{(p_4 - p_2)^2}{m^2} = \ln\frac{(p_3 - p_1)^2}{m^2},\ \ \zeta' = \ln\frac{p_{\text{II}}^2}{m^2},$$

$$p_{\text{I}}^2 = \max\{p_4^2,\, p_2^2\},\quad p_{\text{II}}^2 = \max\{p_3^2,\, p_1^2\}.$$

The condition (22) is the most general case for f, but is a special case for φ. When Eq. (22) holds,

$$\xi' = \eta' = \zeta' = \xi. \quad (24)$$

We calculate the vertex part assuming these conditions to be satisfied. We find

$$\Gamma(p_4\xi_4,\, p_3\xi_3,\, p_2\xi_2,\, p_1\xi_1) = Q_{\xi_4\xi_3\xi_2\xi_1}\,\alpha(\xi,\, \eta,\, \zeta),$$

$$f(p_4\xi_4,\, p_3\xi_3,\, p_2\xi_2,\, p_1\xi_1) = Q_{\xi_4\xi_3\xi_2\xi_1}\, f(\xi,\, \eta,\, \zeta),$$

$$\varphi(p_4\xi_4,\, p_3\xi_3,\, p_2\xi_2,\, p_1\xi_1) - \varphi(p_4\xi_4,\, p_3\xi_3,\, p_1\xi_1,\, p_2\xi_2) \quad (25)$$

$$= Q_{\xi_4\xi_3\xi_2\xi_1}\,\varphi(\xi),$$

$$\alpha(\xi,\, \eta,\, \zeta) = 1 + f(\xi,\, \eta,\, \zeta) + \varphi(\xi).$$

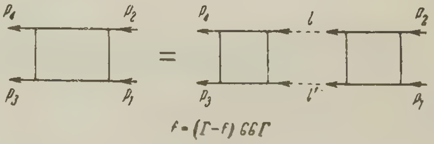

FIG. 4

An examination of Fig. 4 leads to the following integral equation:

$$\begin{aligned} &f(p_4\xi_4, p_3\xi_3, p_2\xi_2, p_1\xi_1) \\ &= (ig_0/2)\int [Q_{\xi_4\xi_3\alpha\gamma} + \varphi(p_4\xi_4, p_3\xi_3, l\alpha, l'\gamma) \\ &\quad - \varphi(p_4\xi_4, p_3\xi_3, l'\gamma, l\alpha)] \qquad (26) \\ &\times G_{\alpha\beta}(l)\, G_{\gamma\delta}(l')\, \Gamma(l\beta, l'\delta, p_2\xi_2, p_1\xi_1)\, d^2l/(2\pi)^2, \\ &\quad l' = p_1 + p_2 - l. \end{aligned}$$

This equation is derived by dividing the "lying brick" in such a way that on the left side there is only a point and "standing bricks". A similar equation can be written down for the "standing brick," but it is not essential for what follows. We eliminate the spinor indices from Eq. (26), transform the integration to euclidean space, and change to logarithmic variables, with the result

$$\begin{aligned} f(\xi, \eta, \zeta) &= -(g_0/2\pi)\int_{\eta}^{\zeta} [1 + \varphi(\xi)][1 + f(z, \eta, \zeta) + \varphi(\zeta)]\, dz \\ &\quad - (g_0/2\pi)\int_{\zeta}^{\xi} [1 + \varphi(\xi)][1 + f(z, \eta, \zeta) + \varphi(z)]\, dz \qquad (27) \\ &\quad - (g_0/2\pi)\int_{\xi}^{L} [1 + \varphi(z)][1 + f(z, \eta, \zeta) + \varphi(z)]\, dz. \end{aligned}$$

We have set $\beta = 1$ in accordance with the results of section 3. When $\eta = \zeta$, we obtain an equation for the function $f(\xi, \eta) = f(\xi, \eta, \eta)$. We use Eq. (13) for φ. It is convenient to change to the new variables

$$\begin{aligned} x = 1 + (g_0/2\pi)(L - \xi),\ y = 1 + (g_0/2\pi)(L - \eta), \\ t = 1 + (g_0/2\pi)(L - z), \end{aligned} \qquad (28)$$

in terms of which the integral equation becomes

$$f(x, y) = \frac{1}{6}x^3 - \frac{1}{2}xy^2 + \frac{1}{3} + x\int_{y}^{x} f(t, y)\, dt + \int_{x}^{1} tf(t, y)\, dt. \qquad (29)$$

Differentiating Eq. (29) twice with respect to x, we find

$$d^2f(x, y)/dx^2 = x + f(x, y), \qquad (30)$$

which has the solution

$$f(x, y) = C_1(y)\, e^{x} + C_2(y)\, e^{-x} - x. \qquad (31)$$

The initial condition

$$(df(x, y)/dx)_{x=y} = 0, \qquad (32)$$

gives

$$C_2(y) = C_1(y)\, e^{2y} - e^{y}. \qquad (33)$$

Substituting Eq. (33) back into Eq. (29), we find $C_1(y) = e^{-y}$. Thus our final result is

$$\begin{aligned} &f(x, y) = e^{x-y} - x,\ f(\xi, \eta) \\ &= \exp\{(g_0/2\pi)(\eta - \xi)\} - 1 - (g_0/2\pi)(L - \xi). \end{aligned} \qquad (34)$$

When $\xi = \eta$, this expression reduces to Eq. (13). The vertex part then becomes

$$\alpha(\xi, \eta) = \exp\{(g_0/2\pi)(\eta - \xi)\} = (p_{\text{in}}/p_{\text{out}})^{g_0/\pi}. \qquad (35)$$

Equation (12) shows that this expression is valid not only when $p_{\text{in}}^2 \gg p_{\text{out}}^2$, but also when $p_{\text{in}}^2 \approx p_{\text{out}}^2$. It is easy to prove that it is valid in general for any values of p_{in}^2 and p_{out}^2. For this purpose one uses not Eq. (26), but the analogous equation obtained by cutting the "lying brick" in such a way that only a point and a "standing brick" is left on the right side.

6. THE DOUBLE-LIMIT TECHNIQUE

In this section we shall derive an expression for the vertex part, using a special version of the double-limit technique, which was recently used[10] for proving the vanishing of the charge in a real three-dimensional theory with a four-fermion interaction.

Consider any vertex at which the operator

$$H = (g_0/4)(\bar{\psi}_\alpha (O_j)_{\alpha\gamma}\psi_\gamma)(\bar{\psi}_\beta (O_j)_{\beta\delta}\psi_\delta)$$

annihilates two particles with momenta p_1p_2 and creates a pair of particles with momenta p_3p_4. Obviously, the particle p_1 may be annihilated either by ψ_γ or by ψ_δ, and the particle p_3 may be created either by $\bar{\psi}_\alpha$ or by $\bar{\psi}_\beta$, and so on. In a local theory, the result of adding together these four possibilities is only to make the contribution of a simple vertex diagram equal to $g_0O_j \times O_j$ instead of $(g_0/4)O_j \times O_j$. This simple result is connected with the indentity of the particles, since the operator ψ_δ can be paired either with $\bar{\psi}_\alpha$ or with $\bar{\psi}_\beta$, etc. ($Q_{\alpha\beta\gamma\delta} = -Q_{\alpha\beta\delta\gamma} = \ldots\ldots$).

In a cut-off theory, we have to destroy the identity of particles, and distinguish cases in which p_1 and p_3 are annihilated and created in the same pair or in different pairs. Likewise also for p_2 and p_4. To represent these two possibilities, we draw the vertex either in the way shown in Fig. 5a or as in Fig. 5b. We cut off the divergent integrals over momentum variables which follow along the fermion lines at the momentum Λ, while the integrals over momenta which cross from line to line are cut off at the momentum λ.

We suppose that the limiting process is carried out with $\lambda/\Lambda \ll 1$. It has been shown[10] that in this case, of all the graphs which contribute to the vertex part, only those illustrated in Fig. 6 remain.

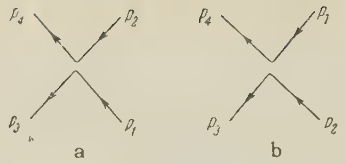

FIG. 5

Also the Green's function can be considered to be free ($\beta = 1$). The graphs of Fig. 6 are easily summed, using Eq. (11), and we thus obtain

$$\alpha(\xi) = \frac{1}{1-(g_0/4\pi)(L-\xi)}, \quad g_c = \frac{g_0}{1-(g_0/4\pi)L}, \quad L = \ln\frac{\Lambda^2}{m^2}. \tag{36}$$

If $g_0 < 0$, the renormalized charge g_c tends to zero, no matter how g_0 varies with Λ and λ. Thus the double-limit technique leads to a zero charge in a theory completely free from divergences. The whole picture can be seen with unusual clarity from this example.

By using a special form of limiting process with $\Lambda \to \infty$, $\lambda \to \infty$, $\lambda/\Lambda \to 0$, we have thrown away a set of graphs (a part of the "standing brick") which in the local theory cancel against the remaining graphs. In this way we artificially introduced divergences into a non-divergent theory.

From these results we cannot decide the question, whether the double-limit technique is generally useless, or whether the trouble could be avoided by introducing the cut-off in such a way as not to violate general principles such as the Pauli principle, gauge invariance, etc. At least one can say that the double-limit technique might lead to incorrect results also in the three-dimensional case,[10] where one is dealing with a field interacting with itself or with several fields interacting in an antisymmetric combination (A – V, S + P – T, 2(S – P) – (A + V)).

7. CONCLUSIONS

Thirring[8] considered the problem of a field with the interaction Hamiltonian given by Eqs. (6) and (8), but instead of studying the asymptotic region $p^2 \gg m^2$ he omitted the mass term from the equations from the beginning. He obtained an exact solution of the problem in the Schrödinger representation, without using the condition $g_0 \ll 1$. He obtained an expression for the matrix element of a Schrödinger operator between the physical vacuum and a physical three-particle state:

$$\langle 3|\psi_1(x)|0\rangle = \frac{\exp\{-i(p_b - p_c + k_m)x\}}{L^{3/2}(p_c - p_b)} \cdot \frac{1}{\sqrt{1+\lambda^2}}\left(\frac{p_b}{|p_c|}\right)^{(\arctan\lambda)/\pi} \tag{37}$$

Here p_b, p_c and k_m are the momenta of the particles in the state $\langle 3|$, L is the normalization volume, and λ is the coupling constant (g_0 in our notations). The matrix element (37) has a similar meaning to the vertex part which we studied earlier. The fact that $\psi_1(x)$ is a Schrödinger operator is unimportant, since it can easily be transformed into a Heisenberg operator $\psi_1(x) = e^{-iHt}\psi_1(x)e^{iHt}$, the only effect being to multiply the matrix element by a factor e^{-iE_3t} where E_3 is the energy of the three-particle state. The quantity $(1+\lambda^2)^{-1/2} \times (p_b/|p_c|)^{(\arctan\lambda)/\pi}$, which tends to unity as $\lambda \to 0$, can be expanded in a series of the form (3′):

$$\frac{1}{\sqrt{1+\lambda^2}}\left(\frac{p_b}{|p_c|}\right)^{(\arctan\lambda)/\pi} = e^{\lambda\xi'/2\pi} - \lambda^2 e^{\lambda\xi'/2\pi}\left[\frac{1}{2} + \frac{1}{6\pi}(\lambda\xi')\right] + \lambda^4 e^{\lambda\xi'/2\pi}\left[\frac{3}{8} + \frac{11}{60\pi}(\lambda\xi') + \frac{1}{72\pi^2}(\lambda\xi')^2\right] + \cdots, \quad \xi' = \ln(p_l^2/p_c^2). \tag{38}$$

The first term of this series coincides with Eq. (35). The general structure of the expression confirms the correctness of our assumption that the higher approximations to the vertex part do not contain divergences and consequently do not lead to any charge renormalization.

It is a very curious fact, that the double-limit technique leads to an incorrect result for the renormalized vertex part when the charge has one sign, and leads to a zero charge when the charge has the other sign. One may suppose that this is all the result of using a cut-off which destroys the symmetry between identical particles. An example of a similar kind* is provided by electrodynamics with all vacuum-polarization effects omitted. In this case all the divergences cancel by virtue of Ward's identity $Z_1 = Z_2$. In this case also, if one uses a cut-off which is not gauge invariant, one can obtain a renormalized charge equal to zero.

After this work was finished, we received a preprint of a paper by M. E. Maier and D. V. Shirkov, in which the method of the renormalization group led to a result similar to Eq. (35). This is not surprising, because the single-limit method is essentially identical with ordinary renormaization.

In conclusion I express my thanks to K. A. Ter-

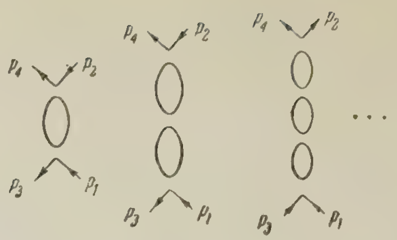

FIG. 6

---

*This example was suggested by I. Ia. Pomeranchuk.

Martirosian, at whose suggestion this work was done, for his constant guidance and help. I also thank I. Ia. Pomeranchuk and A. D. Galanin for criticism.

---

[1] Landau, Abrikosov and Khalatnikov, Dokl. Akad. Nauk SSSR, **95**, 497, 773, and 1177 (1954).

[2] H. Lehmann, Nuovo cimento **11**, 342 (1954).

[3] Abrikosov, Galanin, and Khalatnikov, Dokl. Akad. Nauk SSSR, **97**, 793 (1954).

[4] T. D. Lee, Phys. Rev. **95**, 1329 (1954).

[5] G. Källèn and W. Pauli, Kgl. Danske Videnskab. Selskab, Mat.-Fys. Medd., **30**, No. 7 (1955).

[6] W. Heisenberg, Nucl. Phys., **4**, 532 (1957).

[7] A. A. Abrikosov and I. M. Khalatnikov, Dokl. Akad. Nauk SSSR, **103**, 993 (1955); I. Ia. Pomeranchuk, Dokl. Akad. Nauk SSSR, **103**, 1005; **104**, 51, and **105**, 461 (1955).

[8] W. Thirring, Ann. of Phys., **3**, 91 (1958).

[9] Diatlov, Sudakov, and Ter-Martirosian, J. Exptl. Theoret. Phys. (U.S.S.R.), **32**, 767 (1957), Soviet Phys. JETP **5**, 631 (1957); see also Pomeranchuk, Sudakov, and Ter-Martirosian, Phys. Rev. **103**, 784 (1956).

[10] Abrikosov, Galanin, Gorkov, Landau, Pomeranchuk and Ter-Martirosian, Phys. Rev. **111**, 321 (1958).

Translated by F. J. Dyson
318

SOVIET PHYSICS JETP VOLUME 35(8), NUMBER 6 JUNE, 1959

BOSE EXCITATIONS IN IONIC CRYSTALS

M. Sh. GITERMAN, P. S. ZYRIANOV, and G. G. TALUTS

Ural' State University

Submitted to JETP editor July 9, 1958

J. Exptl. Theoret. Phys. (U.S.S.R.) 35, 1532-1537 (December, 1958)

A study is made of second-quantized elementary Bose excitations of a system of electrons (excitons) interacting with polarization vibrations of a crystal. In the case of weak coupling the interaction leads to a decrease of exciton energy and an increase of effective exciton mass. These effects are estimated quantitatively.

THE interaction between an exciton and lattice oscillations has been considered in a number of papers as a single-particle problem. Exciton energy and the dependence of exciton-phonon interaction on the internal state of the exciton have been investigated for strong coupling by Pekar and Dykman[1] using the methods of polaron theory and by Moskalenko[2] using Bogoliubov's[3] theory of adiabatic perturbations. Ipatova[4] used the method of Lee, Low, and Pines[5] for intermediate coupling and Dykman[6] used the method of traces for weak coupling. In reference 7 Moskalenko regarded the interaction as a small perturbation. Haken[8] has applied the Feynman variational method to the exciton problem.

In the present paper excitons are regarded as elementary excitations in a many-electron system interacting with a lattice. The Hamiltonian of the system is composed of three parts representing electrons, phonons and their interaction:

$$H = H_{\rm el} + H_{\rm ph} + H_{\rm int}. \tag{1}$$

We shall investigate the energy spectrum of weakly excited state of the system assuming that each lattice site holds a single electron, which may exist in either the ground state $(\lambda = 0)$ or an excited state $(\lambda = 1)$:

$$n_{f0} + n_{f1} = 1; \quad n_{f\lambda} = a^+_{f\lambda} a_{f\lambda}, \tag{2}$$

where f is the index of a lattice site and $a^+_{f\lambda}$ and $a_{f\lambda}$ are electron creation and destruction operators. The condition for weak excitations is

$$\bar{n}_{f1} \ll \bar{n}_{f0}. \tag{3}$$

In distinction from a real model of ionic crystals such as those of alkali halides we here disregard the two kinds of sites as well as spin closure of the electron states. The present scheme can also be applied to a more real model[9] although such a complication is not required for the investigation of excitons. Indeed, the excited state may represent either an excitation at halide sides f (Dexter's exciton[10]) or electron transfers to neighboring alkali sites g (the usual exciton model). In the latter case there are no valence electrons in the ground state at sites g, which therefore need not be considered explicitly. The homopolar condition (2) will then apply to a pair of neighboring f and g sites. We shall not consider spin closure, which is important for the analysis of singlet and triplet exciton states. We also assume that all electron spins are parallel and that excitations are not accompanied by spin flips. The spin subscript will now be dropped.

The Hamiltonian of a many-electron system subject to the homopolar condition (2) is given by

$$\begin{aligned} H_{\rm el} &= \sum L(f\lambda f\lambda')\, a^+_{f\lambda} a_{f\lambda'} \\ &+ \sum F(f_1\lambda_1 f_2\lambda_2 f_1\lambda_1' f_2\lambda_2')\, a^+_{f_1\lambda_1} a^+_{f_2\lambda_2} a_{f_2\lambda_2'} a_{f_1\lambda_1'} \qquad (4) \\ &+ \frac{1}{2} \sum F(f_1\lambda_1 f_2\lambda_2 f_2\lambda_2' f_1\lambda_1')\, a^+_{f_1\lambda_1} a^+_{f_2\lambda_2} a_{f_1\lambda_1'} a_{f_2\lambda_2'}, \end{aligned}$$

where L and F are additive and binary matrix elements, respectively, with summation over all subscripts. This Hamiltonian is diagonalized by neglecting all terms in which more than two operators have the subscript $\lambda = 1$ [weak excitation condition (3)]. After introducing the operators $b_f = a^+_{f0} a_{f1}$, $b^+_f = a^+_{f1} a_{f0}$, which in approximation (3) obey the commutation relations of Bose statistics, making a linear substitution for operators b_f, b^+_f and passing to k-space:

$$b_f = N^{-1/2} \sum_k b_k e^{-i\mathbf{k}\cdot\mathbf{f}}; \quad b^+_f = N^{-1/2} \sum_k b^+_k e^{i\mathbf{k}\cdot\mathbf{f}}$$

(N is the number of lattice sites in the fundamental crystal region) we obtain[11]

$$H_{\mathrm{el}} = \sum_k v_k b_k^+ b_k + \frac{1}{2}\sum_k u_k b_k b_{-k} + \frac{1}{2}\sum_k u_k^* b_k^+ b_{-k}^+. \tag{5}$$

The energy of elementary excitation (excitons in atomic semiconductors) is then given by $v'_k = \sqrt{v_k^2 - u_k^2}$, where v_k and u_k are certain combinations of Coulomb and exchange integrals. We have analyzed the energy spectrum of these excitations[12] for comparison with single-particle theories, and have found that for a simple cubic lattice with the constant a when k is small v_k and u_k are given by

$$\begin{gathered} v_k = E_1 - E_0 + d - (R - I) - 6|Q| + \hbar^2k^2/2M, \\ u_k = -6|Q| + |Q|k^2a^2. \end{gathered} \tag{6}$$

This expression contains the width $E_1 - E_0$ of the forbidden crystal energy band, the Coulomb interaction R and the exchange interaction I between an electron and a hole, the exciton transfer integral Q, the effective exciton mass M and, finally, the quantity d, which is proportional to one-half the sum of the valence and conduction band widths:

$$\begin{gathered} R = \int \theta_0^*(\mathbf{r}_1)\,\theta_1^*(\mathbf{r}_2)\,\Phi(\mathbf{r}_1\bullet\mathbf{r}_2)\,\theta_0(\mathbf{r}_1)\,\theta_1(\mathbf{r}_2)\,d\mathbf{r}_1 d\mathbf{r}_2, \\ I = \int \theta_1^*(\mathbf{r}_1)\,\theta_0^*(\mathbf{r}_2)\,\Phi(\mathbf{r}_1\bullet\mathbf{r}_2)\,\theta_0(\mathbf{r}_1)\,\theta_1(\mathbf{r}_2)\,d\mathbf{r}_1 d\mathbf{r}_2, \\ Q = \int \theta_1^*(\mathbf{r}_1)\,\theta_0^*(\mathbf{r}_2 - \mathbf{a})\,\Phi(\mathbf{r}_1\bullet\mathbf{r}_2)\,\theta_0(\mathbf{r}_1)\,\theta_1(\mathbf{r}_2 - \mathbf{a})\,d\mathbf{r}_1 d\mathbf{r}_2, \\ M^{-1} = (m_{\mathrm{el}} + m_{\mathrm{h}})^{-1} + 2|Q|a^2\hbar^{-2}. \end{gathered} \tag{7}$$

Here $\Phi(r_1r_2)$ is the interelectron interaction energy and θ_λ are the single-particle basis functions that are used for the transition to the second quantized representation.

The phonon energy operator in terms of the Bose creation and destruction operators ξ_K^+ and ξ_K, respectively, of a phonon with frequency ω_K is given by

$$H_{\mathrm{ph}} = \sum_\varkappa \hbar\omega_\varkappa \xi_\varkappa^+ \xi_\varkappa. \tag{8}$$

Finally, the term in (1) which describes the electron-phonon interaction becomes after second quantization

$$H_{\mathrm{int}} = \sum_{f\lambda\lambda'\varkappa} K(f\lambda f\lambda'\varkappa)\, a_{f\lambda}^+ a_{f\lambda'}(\xi_\varkappa + \xi_{-\varkappa}^+), \tag{9}$$

where

$$K(f\lambda f\lambda'\varkappa) = \int \theta_{f\lambda}^*(\mathbf{r})\, A_\varkappa e^{i\varkappa\cdot\mathbf{r}}\, \theta_{f\lambda'}(\mathbf{r})\, d\mathbf{r};$$

$$A_\varkappa = |\varkappa|^{-1}(2\pi e^2\hbar\omega_\varkappa c_\varkappa/\Omega)^{1/2}.$$

Here Ω is the volume of the fundamental crystal region, $c_K = 1/n^2 - 1/\epsilon(\omega_K)$, and n^2 and ϵ are the square of the refractive index and the dielectric constant of the crystal. For a specific calculation this interaction is given the usual form of an interaction between electrons and longitudinal optical lattice vibrations (in the approximation of a dielectric continuum). We shall hereinafter be interested only in the interaction between the lattice and an assumed small number of excited electrons; we shall therefore use the interaction law (9), which is usually employed for the "excess" electrons in the crystal. Any other form of interaction would only change the coefficient K but would not affect the scheme of the calculation. Introducing into (9) the Bose operators b_f and b_f^+ that were defined above and making use of their Fourier components and of (2), we obtain

$$\begin{aligned} H_{\mathrm{int}} &= \sum_{f\lambda\lambda'\varkappa} K(f\lambda f\lambda'\varkappa)\, a_{f\lambda}^+ a_{f\lambda'}(\xi_\varkappa + \xi_{-\varkappa}^+) \\ &= \sum_{f,\varkappa} \{K(f0f0\varkappa)(a_{f0}^+ a_{f0} + a_{f1}^+ a_{f1}) \\ &\quad + [K(f1f1\varkappa) - K(f0f0\varkappa)]\, a_{f1}^+ a_{f1} + K(f1f0\varkappa)\, a_{f1}^+ a_{f0} \\ &\quad + K(f0f1\varkappa)\, a_{f0}^+ a_{f1}\}(\xi_\varkappa + \xi_{-\varkappa}^+) \\ &= \sum_{k,\varkappa} [W(\varkappa)\, b_k^+ b_{k-\varkappa} + \sqrt{N} K_{01} b_{-\varkappa} + \sqrt{N} K_{10} b_\varkappa^+](\xi_\varkappa + \xi_{-\varkappa}^+), \end{aligned} \tag{10}$$

where

$$\begin{gathered} W(\varkappa) = K(f1f1\varkappa) - K(f0f0\varkappa) = A_\varkappa J_0(\varkappa), \\ K_{01} = K_{10}^* = K(f0f1\varkappa) = A_\varkappa J_1(\varkappa), \\ J_0(\varkappa) = \int e^{i\varkappa\cdot\mathbf{r}}(|\theta_1(\mathbf{r})|^2 - |\theta_0(\mathbf{r})|^2)\, d\mathbf{r}, \\ J_1(\varkappa) = \int e^{i\varkappa\cdot\mathbf{r}}\theta_0^*(\mathbf{r})\,\theta_1(\mathbf{r})\, d\mathbf{r}. \end{gathered} \tag{11}$$

Thus, by means of (5), (8), and (10) the complete Hamiltonian of the system can be put into the form

$$H = H_0 + H_1, \tag{12}$$

$$H_0 = \sum_k v_k b_k^+ b_k + \frac{1}{2}\sum_k u_k b_k b_{-k} + \frac{1}{2}\sum_k u_k^* b_k^+ b_{-k}^+ + \sum_\varkappa \hbar\omega_\varkappa \xi_\varkappa^+ \xi_\varkappa,$$

$$\begin{aligned} H_1 = \sum_{k,\varkappa} W(\varkappa)\, b_k^+ b_{k-\varkappa}(\xi_\varkappa + \xi_{-\varkappa}^+) &+ \sqrt{N}\sum_\varkappa K_{10}(\varkappa)\, b_\varkappa^+(\xi_\varkappa + \xi_{-\varkappa}^+) \\ &+ \sqrt{N}\sum_\varkappa K_{01}(\varkappa)\, b_{-\varkappa}(\xi_\varkappa + \xi_{-\varkappa}^+). \end{aligned}$$

We shall consider weak exciton-phonon coupling so that H_1 is regarded as a perturbation. Before employing perturbation theory it is convenient to renormalize the exciton vacuum in H_0, diagonalizing H_0 in the Bose amplitudes b_k by means of a linear transformation.[13] Following this transformation the Hamiltonian of the system becomes

$$\begin{aligned} H = H_0 + H_1, \quad H_0 &= \sum_k v'_k \beta_k^+ \beta_k + \sum_\varkappa \hbar\omega_\varkappa \xi_\varkappa^+ \xi_\varkappa, \\ H_1 &= \sum_{k\varkappa} [W'(k,\varkappa)\, \beta_k^+ \beta_{k-\varkappa}(\xi_\varkappa + \xi_{-\varkappa}^+) \\ &\quad + W''(k,\varkappa)\, \beta_k^+ \beta_{-k+\varkappa}^+(\xi_\varkappa + \xi_{-\varkappa}^+) \\ &\quad + K'_{01}(k,\varkappa)\, \beta_\varkappa^+(\xi_\varkappa + \xi_{-\varkappa}^+) + \text{compl. conj}], \end{aligned} \tag{13}$$

where

$$v'_k = \sqrt{v_k^2 - u_k^2}, \tag{14}$$

$$W'(k, \varkappa) = W(\varkappa)(1 + A_k A_{k-\varkappa})/[(1 - A_k^2)(1 - A_{k-\varkappa}^2)]^{1/2},$$

$$W''(k, \varkappa) = W(\varkappa) A_{k-\varkappa}/[(1 - A_k^2)(1 - A_{k-\varkappa}^2]^{1/2},$$

$$K'_{10}(k, \varkappa) = (K_{10}(\varkappa) + K_{01}(\varkappa) A_k)/[(1 - A_\varkappa^2)(1 - A_{k-\varkappa}^2)]^{1/2},$$

$$A_k = (\sqrt{v_k^2 - u_k^2} - v_k)/u_k.$$

In the first-order perturbation nonvanishing corrections to eigenvalues of the energy are given only by the first term in H_1 while the remaining terms give only second-order corrections due to virtual processes.

We now proceed to use perturbation theory in the form of a canonical transformation to obtain corrections of exciton energy resulting from the exciton's interaction with the phonon field. The canonical transformation of the Hamiltonian (13) is given by

$$\mathscr{H} = e^{-S} H e^{S} = H_0 + H_1$$

$$+ [H_0 + H_1, S] + {}^1/_2 [[H_0 S] S] + \cdots .$$

The generating function S is taken in the form

$$S = \sum_{k,\varkappa} \eta(k, \varkappa) \beta_k^+ \beta_{k-\varkappa} \xi_\varkappa - \sum_{k,\varkappa} \eta^*(k - \varkappa, -\varkappa) \beta_k^+ \beta_{k-\varkappa} \xi_{-\varkappa}^+ ,$$

and the coefficients $\eta(k, \kappa)$ are obtained from the condition $H_1 + [H_0 S] = 0$. The first-order perturbation gives

$$\mathscr{H} = \sum_k v''_k \beta_k^+ \beta_k + \sum_\varkappa \hbar \omega'_\varkappa \xi_\varkappa^+ \xi_\varkappa , \tag{15}$$

where

$$v''_k = v'_k - \sum_\varkappa |W'(k, \varkappa)|^2 / (v'_{k+\varkappa} - v'_k + \hbar\omega_\varkappa),$$

$$\omega'_\varkappa = \omega_\varkappa + \frac{1}{\hbar} \sum_k \frac{2\,|W'(k, \varkappa)|^2 (v_k - v_{k-\varkappa})}{(v'_k - v'_{k-\varkappa})^2 - \hbar^2 \omega_\varkappa^2} \overline{b_k^+ b_k} . \tag{16}$$

Here ω'_κ is the renormalized frequency of "free" phonons. If the expressions given above contain divergent denominators the canonical transformation method must be used in the form which Bogoliubov proposed in his papers on the theory of superconductivity.

For the purpose of simplifying the succeeding calculations we shall make the reasonable assumption that the exciton transfer integral is considerably smaller than the width of the energy gap in the crystal:

$$|Q| \ll E_1 - E_0. \tag{17}$$

Then from (14) and (6)

$$W'(k, \varkappa)$$

$$\approx W(\varkappa) \left\{ 1 + \frac{9\,|Q|^2}{2(E_1 - E_0)^2} \left[1 - \left(\frac{a^2}{6} + \frac{\hbar^2}{2(E_1 - E_0)(m_{\text{el}} + m_{\text{h}})} \right) \right. \right.$$

$$\left. \left. \times (k^2 + (k - \varkappa)^2) \right] \right\} \approx W(\varkappa).$$

By a series expansion of the denominators in the coefficients v''_k of Eq. (15) in terms of exciton momenta, by integrating instead of summing over phonon momenta, and by using (6), (7), (9), and (11), we obtain from (16) the following expressions for the variation of the energy gap width and of the effective exciton mass:

$$\Delta E' = \Delta E - \frac{e^2 \hbar}{4\pi^2} \int \frac{|J_0(\varkappa)|^2 \omega_\varkappa c_\varkappa}{\varkappa^2 (\hbar\omega_\varkappa + \hbar^2 \varkappa^2 / 2M)} d\varkappa ,$$

$$M^* = M \left[1 + \frac{e^2 \hbar^3}{2\pi^2 M k^2} \int \frac{|J_0(\varkappa)|^2 (k\varkappa)^2 \omega_\varkappa c_\varkappa}{\varkappa^2 (\hbar\omega_\varkappa + \hbar^2 \varkappa^2 / 2M)^3} d\varkappa \right] . \tag{18}$$

Thus the exciton-phonon interaction lowers the energy level of the exciton and increases its effective mass. This result agrees qualitatively with the results of Dykman[6] and Moskalenko[7] for weak exciton-phonon coupling. The shift of the exciton energy level that results from interelectron and electron-phonon interactions may be essential for an examination of certain effects. For example, the character of the field dependence of energy shifts in electric and magnetic fields is changed; specifically linear terms with respect to the field appear.[14] For an electron interacting with the phonon field we must set $\theta_0(r) = 0$ in (11) and pass to the wavelength limit. This gives the energy reduction $\alpha\hbar\omega$ that is known from polaron theory[15] with the dimensionless coupling constant $\alpha = e^2 c (m/2\omega\hbar^3)^{1/2}$.

For numerical estimates it is necessary to adopt a definite form of the second-quantization basis functions $\theta_\lambda(r)$, compute $J_0(\kappa)$ from (11) and calculate the integrals in (18). When expanding the wave function of the system in second-quantization basis functions we use an incomplete set of functions, stopping after the first two terms ($\lambda = 0$ and $\lambda = 1$); the selected functions $\theta_0(r)$ and $\theta_1(r)$ must therefore represent as adequately as possible the real electron states in the crystal. We have performed a calculation for the Cu_2O crystal, where the coupling between excitons and the lattice is apparently weak. We used the Zhilich function[16] $\theta_0(r) = A \exp\{-1.03\, r/a_B\}$ and the Slater function[17] $\theta_1(r) = B \exp\{-0.743\, r/a_B\}$ with values of ω_κ and c_κ for the wavelength limit. The exciton energy level is reduced by 0.027 ev while its effective mass is increased by 0.4%. No quantitative accuracy can be claimed because of the crude model used and the tentative character of the wave functions. However it should be interesting to develop our many-electron method further by using a specific model and also by considering the behavior of the system in an external field.

In conclusion we wish to thank S. V. Vonsovskii for discussions of the results.

---

[1] S. I. Pekar and I. M. Dykman, Тр. ИФАН УССР (Trans. Inst. Phys., Acad. Sci. Ukr. S.S.R.) **3**, 92 (1952).

[2] V. A. Moskalenko, Уч. зап. Кишинев.cxx универс. (Sci. Reports, Kishinev. Univ.) **17**, 103 (1955).

[3] N. N. Bogoliubov, Укр. математ. журнал (Ukr. Math. J.) **2**, 3 (1950).

[4] I. P. Ipatova, J. Tech. Phys. (U.S.S.R.) **26**, 2786 (1956), Soviet Phys. "Tech. Phys." **1**, 2692 (1957).

[5] Lee, Low, and Pines, Phys. Rev. **90**, 297 (1953).

[6] I. M. Dykman, J. Tech. Phys. (U.S.S.R.) **27**, 1731 (1957), Soviet Phys. "Tech. Phys." **2**, 1609 (1957).

[7] V. A. Moskalenko, J. Exptl. Theoret. Phys. (U.S.S.R.) **30**, 959 (1956), Soviet Phys. JETP **3**, 801 (1956).

[8] H. Haken, Z. Physik **147**, 323 (1957).

[9] M. Sh. Giterman, Физика металлов и металловедение (Physics of Metals and Metal Research) **5**, 364 (1957); **6**, 930 (1958).

[10] D. L. Dexter, Phys. Rev. **83**, 435 (1951); **108**, 707 (1957).

[11] V. S. Galishev and S. V. Vonsovskii, Физика металлов и металловедение (Physics of Metals and Metal Research) **3**, 385 (1956).

[12] G. G. Taluts and M. Sh. Giterman, Физика металлов и металловедение (Physics of Metals and Metal Research) (in press).

[13] N. N. Bogoliubov, Лекцii з квантовоi статистики (Lectures on Quantum Statistics) (in Ukrainian), Kiev, 1949.

[14] G. G. Taluts and M. Sh. Giterman, Физика металлов и металловедение (Physics of Metals and Metal Research) (in press).

[15] C. R. Allcock, Adv. in Phys. **5**, 412, 1956).

[16] A. G. Zhilich, Вестник ЛГУ (Bulletin, Leningrad State University) **4**, 31 (1957).

[17] J. C. Slater, Phys. Rev. **36**, 57 (1930).

Translated by I. Emin
319

SOVIET PHYSICS JETP VOLUME 35(8), NUMBER 6 JUNE, 1959

RADIO EMISSION FROM AN ATOMIC EXPLOSION

A. S. KOMPANEETS

Institute for Chemical Physics, Academy of Sciences, U.S.S.R.

Submitted to JETP editor July 15, 1958

J. Exptl. Theoret. Phys. (U.S.S.R.) 35, 1538-1544 (December, 1958)

It is shown that in an atomic explosion, which is accompanied by asymmetric emission of γ quanta, radio waves are emitted due to the presence of a current in the ionized air. The duration of the oscillation in each half-wave is of the order of $10\,\mu$ sec. For a given asymmetry in emission of the γ rays, the amplitude of the oscillations depends weakly on the total number of quanta.

IT is known that atomic bomb blasts are accompanied by characteristic radio signals which are recorded at distances of thousands and tens of thousands of kilometers. In propagating over such large distances the radio pulse spectrum becomes much more complex than the spectrum of the initially emitted pulse.[1] Only the latter spectrum will be studied in the present paper. This is the spectrum which one can record at a distance of say one hundred kilometers from the point of the explosion. In other words, we shall try to determine the effective radiator.

G. M. Gandel'man and L. P. Feoktistov (private communication) have described how an electric field develops in the air under the action of the γ quanta. The quanta give rise to Compton electrons which move preferentially forward, i.e., away from the point of the blast. But since the flux of quanta decreases approximately exponentially with distance from the blast origin, the numbers of negative charges which are transferred to points at different distances from the origin are different. This nonuniformity of the charge density results in the appearance of an electric field.

In moving along their paths, the Compton electrons produce a large number of secondary electrons, thus making the air conducting and producing a current which tends to annul the field. If the γ quanta are emitted asymmetrically, the current radiates an electromagnetic pulse. But the duration of the pulse due to the electronic current can be of the order of one or a few microseconds, which can give radiowaves in the meter wave length band. The longer wave length oscillations are of great interest.

The cause of these oscillations has been given by O. I. Leipunskii (private communication). The electrons attach themselves not to positive ions but mainly to neutral O_2 molecules. The air acquires an ionic conductivity and a current in it lasts much longer than it does during the stage where the conduction is electronic. At the moment when ionic conduction is established there is still an electric field in the air. O. I. Leipunskii showed that the magnitude of this field is practically independent of the initial ionization at the given space point: if the ionization is greater, the initial space charge density is greater, but then so is the electronic conductivity of the air which causes the dissipation of this space charge. This same result is obtained in more rigorous form in the present paper.

But if the field is independent of the initial ionization, the initial asymmetry in emission of the quanta has no effect on it. Thus the field is purely radial and symmetric. An asymmetry arises because of the ionic conduction of the air which is, of course, greater on the side toward which more quanta were emitted. As the later computations show, the asymmetric ionic current gives a pulse of reasonable order of magnitude and the expected duration.

1. THE INITIAL FIELD

Let the number of γ quanta emerging from the blast origin per unit solid angle per unit time in a given direction be $N_0/4\pi$. (The total number of emitted quanta will then be $\overline{N}_0$, where the average is taken over all solid angle.) We denote the mean free path of the quanta by λ, and the number of secondary electrons per Compton electron by ν. Then the number of free electrons which appear at distance r from the blast origin per unit time per unit volume is

$$J = \dot{N}_0 \nu e^{-r/\lambda} / 4\pi\lambda r^2. \qquad (1)$$

We shall not treat effects related to multiple scattering of quanta since they are of secondary importance.

If γ is the probability per unit time of attachment of an electron to a molecule and n_e is the volume concentration of secondary electrons, then n_e satisfies the differential equation

$$\partial n_e / \partial t + \gamma n_e = J. \tag{2}$$

which has the integral

$$n_e = e^{-\gamma t} \int_0^t J(t') \exp(\gamma t')\, dt'. \tag{3}$$

The space charge density ρ is determined by the law of conservation of charge, which in the present case gives the equation

$$\partial \rho / \partial t = -\operatorname{div} \sigma_e \mathbf{E} + \dot{\rho}_0, \tag{4}$$

where $\mathbf{E}$ is the electric field, σ_e is the electronic conductivity of the air, which is considerably greater than its ionic conductivity so long as there are free electrons present, and $\dot{\rho}_0$ is the rate of increase of the space charge density resulting from displacement of the Compton electrons through the air.

We use l to denote the average radial component of the free path of the Compton electrons. Obviously, $l \ll \lambda$. $\dot{\rho}_0$ is given by the difference between the numbers of electrons leaving a given point and coming toward it, or

$$\dot{\rho}_0 = e[J(r) - J(r+l)] / \nu.$$

For points not too close to the origin, this gives

$$\dot{\rho}_0 = Jle / \lambda\nu. \tag{5}$$

The Poisson equation gives

$$\operatorname{div} \mathbf{E} = 4\pi\rho. \tag{6}$$

Substituting in Eq. (4), we find

$$\operatorname{div}\left(\frac{1}{4\pi} \frac{\partial \mathbf{E}}{\partial t} + \sigma_e \mathbf{E}\right) = \dot{\rho}_0. \tag{7}$$

We note that the diffusion current has been omitted since it is much smaller than the conduction current in the cases we are considering.

As already stated, σ_e and $\dot{\rho}_0$ depend on the angle. Nevertheless we shall show that at the instant of time in which we are interested the field has only a radial component. Thus the divergence operator on the right side of (6) actually contains only derivatives with respect to r:

$$\frac{1}{r^2} \frac{\partial}{\partial r} r^2 \left(\frac{1}{4\pi} \frac{\partial E_r}{\partial t} + \sigma_e E_r\right) = \dot{\rho}_0. \tag{8}$$

We impose the boundary condition $E_r(\infty, t) = 0$ on E_r. Integrating Eq. (8) subject to this condition, and using Eqs. (5) and (1), we get

$$\partial E_r / \partial t + 4\pi\sigma_e E_r = -(\dot{N}_0 el / \lambda r^2) \exp(-r/\lambda). \tag{9}$$

Then

$$E_r = -(el / r^2\lambda)\, e^{-r/\lambda} \int_0^t \exp\left\{-4\pi \int_{t'}^t \sigma_e(t'')\, dt''\right\} \dot{N}_0(t')\, dt'. \tag{10}$$

As already stated, σ_e is the electronic conductivity of the air. Denoting the electron mobility by the symbol ω_e, we get [cf. Eq. (3)]:

$$\sigma_e = e\omega_e n_e = \frac{e\omega_e \nu}{4\pi r^2 \lambda} e^{-r/\lambda} \int_0^t \dot{N}_0(t''') \exp\{\gamma(t''' - t)\}\, dt'''. \tag{11}$$

A double integral of σ_e with respect to the time appears in the expression for E_r. This can be reduced to a single integral, giving

$$4\pi \int_{t'}^t \sigma_e dt'' = \frac{e\omega_e \nu}{r^2\lambda} e^{-r/\lambda} \frac{1}{\gamma} \left[\int_0^t \dot{N}_0(t'')(1 - \exp\{\gamma(t'' - t)\})\, dt'' - \int_0^{t'} \dot{N}_0(t'')(1 - \exp\{\gamma(t'' - t')\})\, dt''\right]. \tag{12}$$

To find E_r we must assign the time dependence of $\dot{N}_0$. We can say the following about the shape of this time dependence. Initially, while the chain reaction is still developing, $\dot{N}_0(t)$ increases very rapidly. After reaching a maximum, $\dot{N}_0(t)$ decreases, but at a rate much slower than its rate of rise.

We may assume the dependence

$$\dot{N}_0(t) = A \exp\{-\beta t\}. \tag{13}$$

As we shall see from the later calculations the field E_r is extremely insensitive to the value of β so long as the inequality

$$\beta < \gamma \tag{14}$$

is satisfied. $1/\gamma$, the time for attachment of an electron to a molecule, is approximately 4×10^{-7} sec (cf. reference 2), while $1/\beta$ is larger than this, which is the basis for the inequality (14).

We substitute the time dependence (13) in formula (12) and carry out the integration, giving

$$\begin{aligned} E_r = \frac{el}{\lambda r^2} e^{-r/\lambda} & \\ \times \exp\left\{-\frac{e\omega_e \nu \exp(-r/\lambda)}{r^2\lambda\gamma}\left[\frac{A}{\beta} - \frac{A\gamma \exp(-\beta t)}{\beta(\gamma - \beta)} + \frac{A \exp(-\gamma t)}{\gamma - \beta}\right]\right\} & \\ \times \int_0^t A e^{-\beta t'}\, dt' \exp & \\ \times \left\{\frac{e\omega_e \nu \exp(-r/\lambda)}{r^2\lambda\gamma}\left[\frac{A}{\beta} - \frac{A\gamma \exp(-\beta t')}{\beta(\gamma - \beta)} + \frac{A \exp(-\gamma t)}{\gamma - \beta}\right]\right\}. & \end{aligned} \tag{15}$$

The exponential in this equation contains the quantity

$$e\omega_e A\nu \exp(-r/\lambda)/\lambda r^2\beta(\gamma-\beta)$$

in its argument. Setting A/β equal to the total number of quanta, which is say 10^{22}, the number ν of secondary electrons per γ quantum $\sim 3\times 10^4$, $r \sim \lambda \sim 3\times 10^4$ cm, $\omega_e \sim 2.5\times 10^6$ cgs units, we find that the order of magnitude of the expression in the exponent is 4×10^3, i.e., it is very large. Consequently the main contribution to the integral (15) comes from large values of t', when the function $\exp(-\beta t')$ is smallest, since it appears with a negative sign in the integral. (This is also the reason why the stage of increase in number of quanta is unimportant). This statement is valid if the inequality (14) is satisfied, i.e., if the exponential $\exp(-\gamma t')$ is smaller than $\exp(-\beta t')$. Then the exponential $\exp(-\gamma t')$ has no effect on the value of the integral and drops out of the final expression for E_r, if t is not too small. The result of the integration is

$$E_r = E = (\gamma-\beta)\, l/\omega_e\nu. \tag{16}$$

A similar result was obtained by O. I. Leipunskii.

Thus the total number of γ quanta and their angular distribution actually are not affected by the magnitude of the residual field, so long as A/β is sufficiently large. But this is practically always the case.

E denotes the radial field. It does not go to zero at the origin. Consequently the charge density has a singularity at the origin:

$$\rho = \frac{1}{4\pi r^2}\frac{\partial}{\partial r} r^2 E = \frac{E}{2\pi r}.$$

But this singularity does not contribute anything to the total charge, since ρ is multiplied by $r^2\,dr$ when we integrate over the volume. The appearance of such a singularity is entirely reasonable physically, since $J(r,t)$ has a singularity at the origin. A numerical calculation gives a value for E of order of magnitude 2 v/cm.

2. ELECTROMAGNETIC OSCILLATIONS

The time of development of the initial field is of order of magnitude $1/\beta$, which may be assumed to be about one microsecond. The period of the electromagnetic oscillations is approximately ten times as large. Thus the whole process can be divided into two stages: the first stage is the development of the field considered in the preceding section, and the second is the damping of the oscillations produced by the field.

In the second stage, the conductivity of the air is ionic. Consequently the damping of the oscillations is much less than it would be for the case of electronic conductivity.

The number of ions decreases continually as a result of recombination. The recombination process must be taken into account along with the ionic conductivity, because the recombination coefficient is related to the ion mobility by the formula (cf. reference 2)

$$b \approx 4\pi e(\omega_+ + \omega_-) = 4\pi e\omega. \tag{17}$$

This formula is in satisfactory agreement with experiment for air at normal density.

We shall now find the expression for the ionic conductivity of the air as a function of coordinates and time. For the density of ions of one sign we have $dn/dt = -bn^2$, so that

$$n = 1/(bt + 1/n_0). \tag{18}$$

Here n_0 is the initial number of ions per cc. Considering that there is only a slight angular dependence of the emission of quanta, we write

$$n = 1/[bt + (1+\xi\cos\vartheta)/\bar{n}_0].$$

Limiting ourselves to terms of first order in ξ, we get the following expression for the electrical conductivity:

$$\sigma = ne\omega = \frac{e\omega}{bt + 1/\bar{n}_0} - \frac{e\omega\xi\cos\vartheta}{\bar{n}_0(bt + 1/\bar{n}_0)^2} \equiv \sigma_0 + \sigma_1\cos\vartheta. \tag{19}$$

In this formula, $\bar{n}_0$ is defined by the equation

$$\bar{n}_0 = (A\nu/4\pi\beta\lambda^3)\,\mu(r/\lambda), \tag{20}$$

where

$$\mu(x) = x^{-2}e^{-x}. \tag{21}$$

Thus at the initial instant the field is radially symmetric and is given by Eq. (16), while the electric field depends on angle. Consequently the current will have a corresponding asymmetry.

The electrical conductivity leads to a falloff of the initial field with time. Keeping only the term with σ_0, we have

$$\partial E_{0r}/\partial t + 4\pi\sigma_0 E_{0r} = 0, \tag{22}$$

where the index 0 on E_{0r} is a reminder that in this approximation the field is assumed to be centrally symmetric. Integrating (22) we find, by making use of (18):

$$E_{0r} = E\exp\left\{-\int_0^t 4\pi\sigma_0\,dt'\right\} = E\exp\left\{-\frac{4\pi e\omega}{b}\ln(b + 1/\bar{n}_0)\Big|_0^t\right\}. \tag{23}$$

If we took Eq. (17) literally, we should replace the coefficient of the logarithm by unity. We shall however set

$$4\pi e\omega / b \equiv \alpha, \tag{24}$$

where α can be determined from experimental data. Thus

$$E_{0r} = E\,(bt\bar{n}_0 + 1)^{-\alpha}. \tag{25}$$

The effect of recombination is to give a power law for the damping instead of an exponential law which one would get if the ion concentration were constant in time. The quantity $\sigma_1 \cos\vartheta$, which was assumed to be small, will be multiplied by E_{0r}, which gives an inhomogeneous term in Maxwell's equations and gives rise to an asymmetric current. The assumption that the asymmetry is small was of course made only for computational reasons. If we assumed arbitrarily large asymmetry, we would have to perform numerical integration of the Maxwell equations with respect to three independent variables (radius, angle, and time), which is immeasurably more difficult than the (also numerical) determination of quantities which depend only on the radius and the time.

We shall write the Maxwell equations in the form

$$\operatorname{curl} \mathbf{H} = \frac{1}{c}\frac{\partial \mathbf{E}}{\partial t} + \frac{4\pi\sigma}{c}\mathbf{E}, \tag{26}$$

$$\operatorname{curl} \mathbf{E} = -\frac{1}{c}\frac{\partial \mathbf{H}}{\partial t}, \tag{27}$$

$$\operatorname{div} \mathbf{H} = 0. \tag{28}$$

As usual for conducting media, we need not write the equation for $\operatorname{div} \mathbf{E}$, since it follows from (26).

We look for a solution of the system (26) to (28) in the form

$$E_r = E_{0r} + E_1 \cos\vartheta, \quad E_\vartheta = E_2 \sin\vartheta, \quad E_\varphi = 0;$$

$$H_r = H_\vartheta = 0, \quad H_\varphi = H \sin\vartheta.$$

When this form is substituted in the Maxwell equations, the angular dependence separates off, and we get a system of equations for E_1, E_2, and H.

We introduce the following dimensionless variables:

$$x = r/\lambda, \quad y = ct/\lambda, \quad H = \xi E H', \quad E_1 = \xi E E_1,$$

$$E_2 = \xi E E_2, \quad m = (e\omega\nu/\alpha\lambda^2 c)\,A/\beta.$$

Then the final system of equations which is to be integrated numerically has the form*

$$\frac{2H'}{x} = \frac{\partial E_1'}{\partial y} + \frac{m\alpha\mu(x)\,E_1'}{m\mu(x)\,y+1} + \frac{m\alpha\mu(x)}{(m\mu(x)\,y+1)^{2+\alpha}}; \tag{29}$$

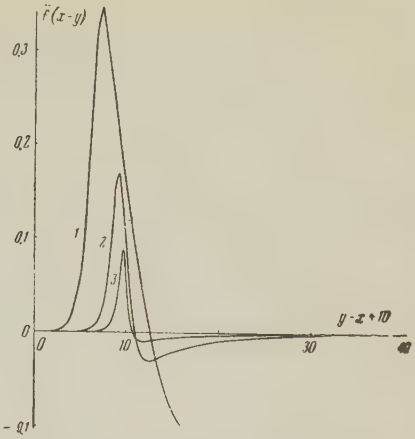

*Values of parameters: 1) α = 4, m = 200; 2) α = 1, m = 10; 3) α = 1, m = 1.

$$-\frac{1}{x}\frac{\partial}{\partial x}\left(xH'\right) = \frac{\partial E_2'}{\partial y} + \frac{m\alpha\mu(x)\,E_2'}{m\mu(x)\,y+1}, \tag{30}$$

$$\frac{1}{x}\left(\frac{\partial}{\partial x}(xE_2') + E_1'\right) = -\frac{\partial H'}{\partial y}, \tag{31}$$

where $\mu(x)$ is given by (21).

The initial condition on H', E_1' and E_2' is that all three are zero for $t = 0$.

From symmetry considerations, the electric field at $r = 0$ must be along the line from which the angle ϑ is measured. This gives

$$E_1'(0, t) + E_2'(0, t) = 0. \tag{32}$$

The magnetic field at the origin must be equal to zero:

$$H'(0, t) = 0. \tag{33}$$

We now consider the question of radiation of electromagnetic waves. At a large distance from the point of the blast, where the function $\mu(x)$ may be assumed to be equal to zero, we can make the substitution

$$\zeta = \frac{1}{x}\frac{\partial}{\partial x}(x^2 H') \tag{34}$$

and reduce the system (29) to (31) to the wave equation

$$\partial^2\zeta/\partial x^2 - \partial^2\zeta/\partial y^2 = 0, \tag{35}$$

whose solution we write as $\zeta = \dddot{f}(x-y)$. The field is given in terms of the function f by the formulas

$$\begin{aligned} H' &= x^{-1}\ddot{f}(x-y) - x^{-2}\dot{f}(x-y), \\ E_2' &= x^{-1}\ddot{f}(x-y) - x^{-2}\dot{f}(x-y) + x^{-3}f(x-y). \end{aligned} \tag{36}$$

Thus the function f determines the effective radiating dipole. It is determined by integrating the system numerically along the characteristic $x = y$ out to the region where $\mu(x) = 0$. The results of the integration are given in the figure for three cases. The ordinate is the function $\ddot{f}(x-y)$ and the abscissa is the quantity $y - x + 10$. As we see, the signal amplitude depends approximately logarithmically on the value of m, i.e., on the total number of quanta. The signal duration has approximately the same dependence. The latter result seems very natural, since the wave length is comparable with the dimensions of the ionized region, which depend logarithmically on the number of quanta.

---

*If the asymmetry of the emission of quanta is quadrupole, with the shape $\xi(3\cos^2\vartheta - 1)/2$, there will be a coefficient of 3 before the E_1' in (31).

In conclusion, I express my gratitude to O. I. Leipunskii who pointed out the role of the ionic conductivity of the air in the production of the radio signal and stimulated the present work by numerous discussions. The analysis of the equations and the necessary computations for the present problem were done by A. A. Miliutin, S. L. Kamenomostskaia, and V. I. Kozhevnikov, to whom I express my deep indebtedness. I thank A. A. Dorodnitsyn and M. V. Keldysh for providing the computing machines.

---

[1] Ia. L. Al'pert, Usp. Fiz. Nauk **60**, 369 (1956).

[2] A. von Engel and M. Steenbeck, Elektrische Gasentladungen, vol. 1, Berlin: Springer, 1932.

Translated by M. Hamermesh
320

SOVIET PHYSICS JETP VOLUME 35(8), NUMBER 6 JUNE, 1959

THE LIMITS OF APPLICABILITY OF THE QUASI-CLASSICAL EQUATION OF STATE OF MATTER

D. A. KIRZHNITS

P. N. Lebedev Physics Institute, Academy of Sciences, U.S.S.R.

Submitted to JETP editor July 17, 1958

J. Exptl. Theoret. Phys. (U.S.S.R.) 35, 1545-1557 (December, 1958)

Quantum corrections have been found for the equation of state obtained with the aid of the Thomas-Fermi model. It is shown that, at all temperatures and densities, the lowest order quantum and exchange corrections to the pressure are negative, their ratio not exceeding $1/3$; it equals $2/9$ in the degenerate electron gas region and $1/3$ in the high-temperature region. The boundary of the region of temperatures and densities is found for which the relative contribution of the quantum correction to the pressure is small and application to the Thomas-Fermi model is feasible.

1. INTRODUCTION

THE problem of the equation of state of matter, i.e., the relation between the pressure, density and temperature, is of importance for many problems in physics and related sciences. In the derivation of this equation for condensed media, wide use is made of the Thomas-Fermi method (for brevity T-F), along with other methods. In a large number of papers setting forth the application of this method (see, for example, references 1 to 3), quantitative results are obtained relating to a wide range of densities and temperatures.

Although the T-F method is known to be approximate, the necessary analysis of the applicability of these results has not been carried out. In the literature there are only qualitative considerations of the non-applicability of the method for small compressions (in the region of low temperatures) and on the improvement of its applicability with increase in temperature. However, the quantitative problems of the limits of the regions of density and temperature in which the method is applicable with a given accuracy, and on the size of the corrections to the quasi-classical equations of state, remain essentially unresolved. The present research represents an attempt at a solution of this problem.

It should be observed that the ordinary method of applying the T-F method for the derivation of the equation of state is connected with second-order approximations. In the first place, use is made of a simplified model,[4] in which we consider isolated spherical cells that contain a motionless nucleus (of charge Z) and Z electrons. The radius of the cell corresponds to the given density; at the boundaries of the cell, the derivative of the potential is equal to zero. In this model no account is taken of many factors: pecularities connected with the crystalline structure, vibrations of the nuclei, collective interaction of the particles, etc. An analysis of these factors enters into the framework of the present research* and in what follows we shall make use of the model thus considered.

In the second place, an exact quantum mechanical solution of the problem, within the framework of this model, is replaced by an approximate consideration according to T-F method, which is the quasi-classical approximation to the Hartree-Fock method. Like the latter, the T-F method also disregards the effects of strong correlation between the particles; these effects were estimated for low temperatures in reference 5, where their contribution to the pressure is shown to be small and to be decreasing with increase in the latter.

The quantum effects that reflect the inaccuracy of the quasi-classical approximation play a much more important role; the following account is devoted to their investigation. For an uncompressed atom these effects were considered quantum mechanically in references 6 to 8.

The quantity

$$q = \hbar^2 / l^2 p_0^2, \tag{1.1}$$

where l is a characteristic length and p_0 is the characteristic momentum, appears as a parameter that defines the role of the quantum correction.

---

*It can be assumed that in the really important part of the region where the Thomas-Fermi method is itself applicable, the role of these factors is not large and they can be considered independently of quantum effects (about the latter, see below).

We use non-dimensional variables throughout the work. As the pressure $\mathscr{P}$, the numerical density of the electrons ρ, and the temperature T we use

$$\mathscr{P} = PZ^{10/3}e^2/a_0^4, \quad \rho = \nu n Z^2/a_0^3, \quad kT = \vartheta Z^{4/3}e^2/a_0, \tag{1.2}$$

where a_0 is the Bohr radius and $n = 3a_0^3/4\pi Z R^3$ is the mean density.

It is convenient to choose the potential Φ and the distance from the nucleus r in the form

$$\xi = (\mu - \Phi)/kT, \qquad x = r/R, \tag{1.3}$$

where μ is the chemical potential and R is the radius of the cell.

We proceed to estimate the parameter q. We consider two regions: I — the region of degeneracy of the electron gas $(n/\vartheta^{3/2} \gg 1)$ and II — the region of high temperatures $(n/\vartheta^{3/2} \ll 1)$. For p_0 we have (M is the mass of the electron)

$$p_0 \sim \hbar\rho^{1/3} \sim (\hbar/a_0)Z^{2/3}n^{1/3}, \qquad \mathrm{I}$$

$$p_0 \sim \sqrt{MkT} \sim (\hbar/a_0)Z^{2/3}\vartheta^{1/2}. \qquad \mathrm{II}$$

An estimate of l is more complicated; it is given by (see Sec. 3):

$$l \sim a_0 Z^{-1/3} n^{-1/6} \quad \mathrm{I} \qquad l \sim a_0 Z^{-1/3}(\vartheta/n)^{1/2} \quad \mathrm{II}$$

As a result we obtain

$$\begin{aligned} q &\sim Z^{-2/3}n^{-1/3} \quad \mathrm{I} \\ q &\sim Z^{-2/3}n/\vartheta^2 \quad \mathrm{II} \end{aligned} \tag{1.4}$$

It then follows that the quantum corrections: (a) decrease with increasing nuclear charge Z (see references 6 and 7), (b) fall off with increasing temperature for a fixed density, and (c) at a fixed temperature, increase with increasing density in II and decrease in region I, and thus have a maximum at $n \sim \vartheta^{3/2}$. These rules are demonstrated in Fig. 3, which is drawn from the results of Sec. 7 (the dashed curve corresponds to $n \sim \vartheta^{3/2}$).

We now proceed to the problem of exchange effects, which is closely related to the foregoing. Ordinarily, exchange effects are either generally disregarded (T-F model) or are considered exactly within the framework of the classical (Thomas-Fermi-Dirac) model (see reference 3, for example). Such a manner of calculation of the exchange is, strictly speaking, inconsistent, since the quantum effects, which are not considered in this case, are commensurable with the exchange effects (reference 6). It would be more valid to limit the exchange correction to the lowest order since higher order corrections lie beyond the limits of accuracy of the model.

As the corresponding parameter of the expansion we have the quantity (see Sec. 5)

$$2MA(p_0, r)/p_0^2 \sim e^2\hbar^2\rho/p_0^2. \tag{1.5}$$

It is easy to see that this parameter is identical to q, so that the quantum and exchange corrections differ only by a numerical factor.

To conclude this section we consider the peculiarities of the Hartree-Fock approximation at temperatures differing from zero, wherein the state of the system is a mixture of pure states. In this case the concepts of the single particle approximation and the approximation in which the density matrix is multiplicative do not, strictly speaking, coincide. The multiplicative approximation usually employed (it is used in the present research) corresponds to the fact that the force field is unique for all the pure states mentioned above; self-consistency is thus produced over the entire mixed state as a whole. Self-consistency within the framework of each of the pure states separately is the more accurate (and is compatible with the single-particle description). In this case, however, the multiplicative character is destroyed and the solution of the problem is made more complicated, to say the least. The corresponding effects must be considered on a par with the usual correlations (the latter are responsible for the inapplicability of the single-particle approach).

The following notation is used in this paper: $\tilde{a}$ denotes that the quantity $a(\mathbf{r})$ is referred to the surface of the system (in particular at the point $r = R$).

2. EXPRESSION FOR THE PRESSURE IN THE HARTREE APPROXIMATION

We begin with the expression for the force acting on the system. The total momentum of the latter can be written in the form

$$G_i = \mathrm{Sp}\,(\hat{\rho}\,\hat{p}_i), \tag{2.1}$$

where $\hat{\rho}$ is the density matrix operator,[7] $\hat{\mathbf{p}} = -i\hbar\nabla$ is the momentum of the particle; the spur is taken over all variables except the spin. Differentiating (2.1) with respect to the time and taking into account

$$i\hbar\, d\hat{\rho}/dt = [\hat{H}, \hat{\rho}],$$

we get the following expression for the force:

$$dG_i/dt = -(i/\hbar)\,\mathrm{Sp}\,\{[\hat{H}, \hat{\rho}]\,\hat{p}_i\}. \tag{2.2}$$

Here,

$$\hat{H} = \hat{p}^2/2M + \Phi(\mathbf{r}) \tag{2.3}$$

is the single particle Hamiltonian; $\Phi = U + B$, where U is the potential of the external field, $B(\mathbf{r}) = e^2 \int d\mathbf{r}' \rho(\mathbf{r}')/|\mathbf{r} - \mathbf{r}'|$ is the self-consistent potential of the electrons, ρ is the numerical particle density.

We compute the spur in (2.1) and (2.2) with the aid of the plane waves

$$\psi_{\mathbf{p}s}(\mathbf{r}, \sigma) = (2\pi\hbar)^{-3/2} \exp(i\mathbf{p}\cdot\mathbf{r}/\hbar)\delta_{s\sigma}.$$

We then have for the arbitrary (but diagonal in the spin variables*) operator O

$$\operatorname{Sp}\hat{O} = \sum_{s\sigma}\int d\mathbf{r}\int d\mathbf{p}\,\bar{\psi}_{\mathbf{p}s}\,\hat{O}\psi_{\mathbf{p}s} = 2(2\pi\hbar)^{-3}\int d\mathbf{r}\int d\mathbf{p}\,\langle\hat{O}\rangle_{\mathbf{p}}, \tag{2.4}$$

where

$$\langle\hat{O}\rangle_{\mathbf{p}} \equiv \exp(-i\mathbf{p}\cdot\mathbf{r}/\hbar)\hat{O}\exp(i\mathbf{p}\cdot\mathbf{r}/\hbar).$$

In this notation the distribution function over the coordinates and the momentum takes the simple form[9]

$$f(\mathbf{r}, \mathbf{p}) = (2\pi\hbar)^{-3}\langle\hat{\rho}\rangle_{\mathbf{p}}.$$

In this case the density is connected to f by the relation

$$\rho(\mathbf{r}) = 2\int f(\mathbf{r}, \mathbf{p})\,d\mathbf{p}. \tag{2.5}$$

From (2.2) to (2.4) we have the following expression for the spatial density of the force

$$-\frac{2i}{\hbar}\int d\mathbf{p}\Big\{-\frac{i\hbar}{M}\mathbf{p}\cdot\nabla f - \frac{\hbar^2}{2M}\Delta f$$

$$- [f(\mathbf{r}, \mathbf{p} - i\hbar\nabla) - f(\mathbf{r}, \mathbf{p})]\,\Phi(\mathbf{r})\Big\}p_i, \tag{2.6}$$

where the gradient in the latter term operates on Φ. Expanding this term in a series in $\hbar$ and integrating by parts, we establish the fact that it reduces to the expression $-\nabla_i\Phi\rho$. In the subsequent integration over $\mathbf{r}$, the term $-\nabla_i\beta\rho$ drops out (the internal forces) and we obtain the relation

$$dG_i/dt = -\int \rho\nabla_i U\,d\mathbf{r} - \int \sigma_{ik}\,dS_k. \tag{2.7}$$

Here the first term is the exchange force, σ_{ik} is the strain tensor

$$\sigma_{ik} = (2/M)\int d\mathbf{p}\,p_i p_k f(\mathbf{r}, \mathbf{p}) - (i\hbar/M)\int d\mathbf{p}\,p_i\nabla_k f(\mathbf{r}, \mathbf{p}). \tag{2.8}$$

Integration over the second term of (2.7) is carried out over the surface of the system; denoting the direction of the corresponding normal by $\mathbf{n}$ we obtain the desired expression for the pressure ($\mathscr{P} = n_i n_k \sigma_{ik}$)

$$\mathscr{P} = (2/M)\int d\mathbf{p}\,(\mathbf{n}\cdot\mathbf{p})^2\tilde{f} - (i\hbar/M)\int d\mathbf{p}\,(\mathbf{n}\cdot\mathbf{p})(\mathbf{n}\cdot\nabla\tilde{f}). \tag{2.9}$$

We recall that the tilde denotes evaluation at a point on the surface.

3. THE EQUATION OF STATE IN T-F MODEL

In the quasi-classical approximation which corresponds to the T-F model, we can discard the second term in (2.9), which vanishes with $\hbar$, and set

$$f(\mathbf{r}, \mathbf{p}) = F(E) \equiv (2\pi\hbar)^{-3}[\exp\{(E - \mu)/kT\} + 1]^{-1}, \tag{3.1}$$

where

$$E(\mathbf{r}, \mathbf{p}) \equiv p^2/2M + \Phi(\mathbf{r}).$$

Then (2.9) gives the well-known equation[2] (nondimensional variables are used; see Introduction):

$$P = (2\sqrt{2}/3\pi^2)\,\vartheta^{5/2} I_{3/2}(\tilde{\xi}), \tag{3.2}$$

where*

$$I_n(x) = \int_0^\infty y^n dy/(\exp(y - x) + 1),$$

while

$$I_n'(x) = nI_{n-1}(x). \tag{3.3}$$

To find the limiting value of ξ, we must solve the equation for the potential. We connect the latter with density by the Poisson equation

$$\Delta_x\xi(x) = \gamma\nu(x),\quad \gamma = (36\pi)^{1/2} n^{1/2}(\tilde{\xi}) \tag{3.4}$$

The corresponding boundary conditions are

$$x\xi|_0 = \gamma/3\quad \xi'|_1 = 0.$$

The first of these corresponds to $\Phi \to -Ze^2/r$ for $r \to 0$.

In the T-F model, substitution of (3.1) in (2.5) gives the following expression for the density:

$$\nu = (\sqrt{2}/\pi^2)\,\vartheta^{3/2} n^{-1} I_{1/2}(\xi), \tag{3.5}$$

whence

$$\Delta_x\xi = \alpha I_{1/2}(\xi),\quad \alpha = (\sqrt{2}/\pi)(6/\pi)^{2/3}\vartheta^{1/2} n^{-2/3}. \tag{3.6}$$

It is now expedient to transform to the integral equation

$$\xi(x) = \tilde{\xi} + \alpha\int_x^1 I_{1/2}[\xi(t)]\,(t/x - 1)\,t\,dt \tag{3.7}$$

with the normalization condition

$$\int_0^1 I_{1/2}(\xi)\,t^2\,dt = \beta,\quad \beta = \gamma/3\alpha = (\pi^2/3\sqrt{2})\,n\vartheta^{-3/2}. \tag{3.8}$$

---

*States are considered in which the same occupation numbers apply to all levels that refer to the same energy.

*These functions were investigated and tabulated in reference 10.

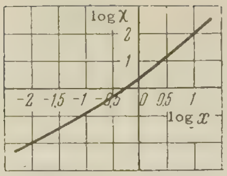

FIG. 1

The solution of the problem in the approximation under consideration is thus determined by two parameters β and α. The first of these is identical with the degeneracy parameter of a homogeneous electron gas, the second, as is evident from (3.7), is the parameter of the homogeneity of the distribution, determining the departure of $\xi(x)$ from the constant $\tilde{\xi}$.

Equation (3.7) is usually solved numerically. We limit ourselves to its analytic solution in the region in which the distribution is close to uniform. We use the iteration method, assuming α to be a small quantity. Substituting the resulting solution in (3.8), we can find the desired value of $\tilde{\xi}$. Simple calculations give*

$$\tilde{\xi} = \xi^0 - \alpha I_{1/2}/10 + \ldots,$$
$$P = (2\sqrt{2}/3\pi^2)\,\vartheta^{5/2}[I_{3/2} - (3\alpha/20)I^2_{1/2} + \cdots]. \tag{3.9}$$

Here the functions I have the argument ξ^0, which is determined by the relation

$$I_{1/2}(\xi^0) = 3\beta. \tag{3.10}$$

If we can neglect corrections due to inhomogeneity, we have the following equation of state

$$P = \vartheta^{5/2}\chi(n/\vartheta^{3/2}), \tag{3.11}$$

where the function $\chi(x)$ is determined parametrically:

$$\chi = (2\sqrt{2}/3\pi^2)\,I_{3/2}(\xi^0), \qquad x = (\sqrt{2}/\pi^2)\,I_{1/2}(\xi^0).$$

Its form is shown in Fig. 1.

In the region where the electron gas is degenerate ($\beta \gg 1$ and, in accord with (3.10), $\xi^0 \to \infty$), we have $I_{1/2} = {}^2/_3\,\xi^{3/2}$, $I_{3/2} = {}^2/_5\,\xi^{5/2}$, from which we find the well-known equation[11]

$$P = {}^1/_5\,(3\pi^2)^{2/3} n^{5/3}. \tag{3.11'}$$

In the opposite limiting case of high temperatures ($\beta \ll 1$, $\xi^0 \to -\infty$)

$$I_{1/2} = (\sqrt{\pi}/2)e^{\xi}, \quad I_{3/2} = {}^3/_2 I_{1/2}$$

then the usual Clapeyron equation holds:

$$P = n\vartheta. \tag{3.11''}$$

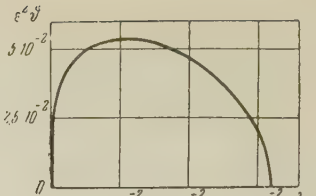

FIG. 2

The relative error in the pressure connected with neglect of non-uniformity is determined by (3.9)

$$\delta P/P = an^{4/3}/P, \quad a = (2\pi/5)(3/4\pi)^{2/3}. \tag{3.12}$$

We now find the boundaries of the region outside of which $\delta P/P$ is less than a given quantity ϵ, while within it it is greater than ϵ. Introducing the notation $\epsilon^3 n = \sigma$, $\epsilon^2\vartheta = \tau$, we have

$$a\sigma^{4/3}/\tau^{5/2}\chi(\sigma/\tau^{3/2}) = 1. \tag{3.13}$$

for $\beta \gg 1$, this gives $\sigma = (2\pi^3)^{-1}$, for $\beta \ll 1$, $\tau = a\sigma^{1/3}$. The curve corresponding to (3.13) is shown in Fig. 2. With its help we can, for example, establish that use of Eq. (3.11′) in the degenerate case gives the correct order of magnitude of the quantities (within the framework of the T-F model), i.e., $\epsilon \sim 1$, at pressures

$$\mathcal{P} > 6\cdot 10^5 Z^{10/3} \text{ atmos.}$$

In conclusion, we find the expression for the length parameter l (see Introduction). It will be the greater of the quantities

$$\xi/\nabla\xi, \quad (\xi/\Delta\xi)^{1/2}.$$

We can limit ourselves to these two quantities if we consider only the quantum correction of lowest order (see below). Estimating by Eqs. (3.7) and (3.8), we obtain

$$l \sim (\xi^0\vartheta/n^{1/3})^{1/2} R.$$

In the degenerate case $\xi^0 \sim n^{2/3}\vartheta$, at high temperatures $\xi^0 \sim 1$ (with logarithmic accuracy). We then easily obtain the estimates given in the Introduction.

4. QUANTUM CORRECTIONS TO THE PRESSURE

We now proceed to find the corrections to the equations of state necessitated by the inaccuracy of the quasi-classical approximation. For this purpose we expand (2.9) in powers of $\hbar$, limiting ourselves to terms of second order; quantum corrections of lowest order will be taken into account.

Besides consideration of the second term of (2.9), it is necessary to introduce a more accurate expression for the distribution function. We begin with the density matrix operator in the form[7]

---

*It follows from (3.9) that the actual parameter of the expansion is not α but $\alpha I'_{1/2}$ (the quantities $I^2_{1/2}/I'_{1/2}$, $I_{3/2}$ are of the order of unity).

$$(2\pi\hbar)^{-3}\hat{\rho} = F(\hat{H}) \equiv (2\pi\hbar)^{-3}\left[\exp\left(\frac{\hat{H}-\mu}{kT}\right)+1\right]^{-1}, \tag{4.1}$$

where $\hat{H}$ is the Hamiltonian of (2.3). If we neglect the non-commutability of its components, we immediately return to (3.1). To obtain quantum corrections to the distribution functions, we must take into consideration the first commutators of the operators $\hat{p}^2/2M$ and Φ. A simple calculation gives:[7]

$$\begin{aligned} f(\mathbf{r},\ \mathbf{p}) = F(E) &- (i\hbar\mathbf{p}\nabla\Phi/2M + \hbar^2\Delta\Phi/4M)\,F''(E) \\ &- (\hbar^2/6M)\,[(\nabla\Phi)^2 \\ &+ (\mathbf{p}\nabla)^2\Phi/M]F'''(E) - (\hbar^2(\mathbf{p}\nabla\Phi)^2/8M^2)\,F^{\mathrm{IV}}(E) + \cdots \end{aligned} \tag{4.2}$$

Substituting this expression in (2.9) and considering that $\partial\Phi/\partial r = 0$ on the surface of the spherical cell, we have

$$\mathcal{P} = \frac{1}{3\pi^2 M\hbar^3}\int F(\widetilde{E})\,p^4 dp$$

$$+\frac{2\widetilde{\Phi}''}{15\pi^2 M^2\hbar}\int\left\{5F''(\widetilde{E}) + \frac{p^2}{M}F'''(\widetilde{E})\right\}p^4 dp.$$

It is easy to prove that the last integral on the right side vanishes identically.

Thus, in the approximation under consideration, the pressure is connected with the potential on the boundary by the same relation (3.2) as in the T-F model. This value of the potential will, however, differ from the corresponding quasi-classical value.

In what follows, the subscript zero denotes any quantity that refers to the T-F approximation. Setting $\xi = \xi_0 + \xi_1$, expanding (3.2) in ξ_1, and also taking (3.3) into account, we get the following expression for the relative quantum correction to the pressure

$$\delta_1 P/P_0 = (3I_{1/2}(\widetilde{\xi}_0)/2I_{3/2}(\widetilde{\xi}_0))\,\xi_1. \tag{4.3}$$

To find $\widetilde{\xi}_1$, we must solve the T-F equation with quantum corrections. Substituting (4.2) in (2.5), we obtain

$$\delta\nu = \frac{\sqrt{2}}{24\pi^2}(4\pi/3)^{2/3}Z^{-2/3}\vartheta^{1/2}n^{-1/3}\{I'''_{1/2}(\xi)(\nabla_x\xi)^2 + 2I''_{1/2}(\xi)\Delta_x\xi\}.$$

for the quantum correction to the density.

Substituting this expression in (3.4), expanding in ξ_1, and taking (3.6) into account,

$$\begin{aligned} &\Delta\xi_1 - \alpha I'_{1/2}(\xi_0)\,\xi_1 \\ &= \frac{\sqrt{2}\,Z^{-2/3}}{6\pi\vartheta^{1/2}}\left\{I'''_{1/2}(\xi_0)(\nabla\xi_0)^2 + 2\alpha I''_{1/2}(\xi_0)\,I_{1/2}(\xi_0)\right\}. \end{aligned} \tag{4.4}$$

A simple substitution can be suggested to simplify (4.4). Setting

$$\xi_1 = \frac{\sqrt{2}Z^{-2/3}}{6\pi\vartheta^{1/2}}(I'_{1/2}(\xi_0) + u_1),$$

we obtain

$$\Delta u_1 - \alpha I'_{1/2}(\xi_0)\,u_1 = \alpha\,[(I'_{1/2}(\xi_0))^2 + I_{1/2}(\xi_0)I''_{1/2}(\xi_0)] \tag{4.5}$$

with the boundary conditions

$$xu_1|_0 = 0, \quad u'_1|_1 = 0.$$

In this case, the quantum correction to the pressure becomes

$$\delta_1 P/P_0 = \frac{\sqrt{2}}{4\pi}\,\frac{Z^{-2/3}}{\vartheta^{1/2}}\,\frac{I_{1/2}(\widetilde{\xi}_0)}{I_{3/2}(\widetilde{\xi}_0)}\{I'_{1/2}(\widetilde{\xi}_0) + \widetilde{u}_1\}. \tag{4.6}$$

5. EXCHANGE CORRECTIONS TO THE EQUATION OF STATE

Account of exchange effects is brought about by replacing the Hamiltonian (2.3) by the expression[7]

$$\hat{H} = \hat{p}^2/2M + \Phi(\mathbf{r}) - \hat{A}, \tag{5.1}$$

where

$$\hat{A} = 4\pi e^2\hbar^2\int d\mathbf{p}'\cdot p'^{-2}\hat{\rho}(\mathbf{r},\ \mathbf{p}' + \hat{\mathbf{p}}). \tag{5.2}$$

Corresponding to this, there appears in (2.6) the additional term

$$2\int d\mathbf{p}\,\{\nabla f(\partial A/\partial\mathbf{p}) - \nabla A(\partial f/\partial\mathbf{p})\}, \tag{5.3}$$

where $A(\mathbf{r}, \mathbf{p}) \equiv \langle\hat{A}\rangle_{\mathbf{p}}$. We consider only quasi-classical exchange effects [therefore (5.3) amounts to the ordinary Poisson bracket]: mixed exchange-quantum corrections are quantities of a higher border of smallness.

In the following, exchange effects are considered as small (see Introduction), so that we can replace f in (5.3) by the expression (3.1). Simple calculations give the following expression for the contribution of (5.3) to the strain tensor:

$$-\int d\mathbf{p}\,(f\partial A/\partial p_k - A\partial f/\partial p_k)p_i$$

and to the pressure

$$\delta'\mathcal{P} = -\frac{1}{3}\int d\mathbf{p}\widetilde{A}(\mathbf{r},\ \mathbf{p})\widetilde{f}(\mathbf{r},\ \mathbf{p}). \tag{5.4}$$

Furthermore, substitution in (3.1) of the expression $p^2/2M + \Phi - A$ for $E(\mathbf{r}, \mathbf{p})$ changes the distribution function by an amount

$$\delta f(\mathbf{r},\ \mathbf{p}) = -2MA\partial f/\partial(p^2) = -A\partial f/\partial\Phi. \tag{5.5}$$

A change in pressure is also associated with this circumstance: substituting (5.5) in (2.9), we have

$$\delta''\mathcal{P} = \frac{4}{3}\int d\mathbf{p}\widetilde{A}\widetilde{f}. \tag{5.6}$$

Adding (5.4) and (5.5), we have (see Appendix I)

$$\frac{(\delta' P + \delta'' P)}{P_0} = \frac{3Z^{-2/3}}{\sqrt{2}\,\pi\vartheta^{1/2}I_{3/2}(\widetilde{\xi}_0)}\int_{-\infty}^{\widetilde{\xi}_0}(I'_{1/2}(\xi))^2 d\xi. \tag{5.7}$$

Finally, exchange effects change the value of $\tilde{\xi}$ in Eq. (3.2). Denoting $\xi = \xi_0 + \xi_2$, we have

$$\delta''' P / P_0 = (3 I_{1/2}(\tilde{\xi}_0) / 2 I_{3/2}(\tilde{\xi}_0)) \tilde{\xi}_2. \qquad (5.8)$$

To find $\tilde{\xi}_2$ we solve the T-F equation with the exchange correction. Starting out from (2.5) and (5.5), we have for the exchange correction to the density

$$\delta\rho = -\frac{\partial}{\partial\Phi}\int d\mathbf{p} A f,$$

or (see Appendix I)

$$\delta\nu = \frac{2Z^{-2/3}\nu}{\pi^3 n}[I'_{1/2}(\xi)]^2. \qquad (5.9)$$

With the help of (3.4) we get

$$\Delta u_2 - \alpha I'_{1/2}(\xi_0) u_2 = 6\alpha [I'_{1/2}(\xi_0)]^2, \qquad (5.10)$$

where

$$\xi_2 = \frac{1}{3\sqrt{2\pi}} \frac{Z^{-2/3}}{\vartheta^{1/2}} u_2.$$

The boundary conditions for μ_1 and μ_2 are identical.

The total exchange correction to the pressure then has the form

$$\frac{\delta_2 P}{P_0} = \frac{\sqrt{2}}{4\pi} \frac{Z^{-2/3}}{\vartheta^{1/2} I_{3/2}(\tilde{\xi}_0)} \left\{ 6 \int_{-\infty}^{\tilde{\xi}_0} [I'_{1/2}(\xi)]^2 d\xi + I_{1/2}(\tilde{\xi}_0) \tilde{u}_2 \right\}. \qquad (5.11)$$

6. RELATION BETWEEN THE QUANTUM AND EXCHANGE CORRECTIONS

Equations (4.5), (4.6) for the quantum corrections and (5.10), (5.11) for the exchange corrections have an identical structure and can be written in the same fashion. Indeed,

$$\frac{\delta_i P}{P_0} = \frac{Z^{-2/3}}{2\sqrt{2}\pi\vartheta^{1/2} I_{3/2}(\tilde{\xi}_0)} \left\{ \int_{-\infty}^{\tilde{\xi}_0} \Psi_i(\xi) d\xi + I_{1/2}(\tilde{\xi}_0) \tilde{u}_i \right\}, \qquad (6.1)$$

$$\Delta u_i - \alpha I'_{1/2}(\xi_0) u_i = \alpha \Psi_i(\xi_0); \quad x u_i|_0 = 0, \quad u'_i|_1 = 0, \qquad (6.2)$$

where i = 1, 2 (index 1 corresponds to the quantum, index 2 to the exchange corrections), while the functions Ψ_i have the form

$$\Psi_1 = I_{1/2} I''_{1/2} + (I'_{1/2})^2, \Psi_2 = 6 (I'_{1/2})^2. \qquad (6.3)$$

Their ratio

$$\eta(\xi_0) = \Psi_1 / \Psi_2 = {}^1/_6 (1 + I_{1/2} I''_{1/2} / (I'_{1/2})^2) \qquad (6.4)$$

is a slowly-varying monotonic function.

In the region of degeneracy, where $\tilde{\xi}_0 \to \infty$, η is constant* and is equal to $2/9$. The same is also characteristic of the ratio of the quantum and exchange corrections:

$$\delta_1 P / \delta_2 P = 2/9. \qquad (6.5)$$

In the opposite limiting case $\xi_0 \to -\infty$, $\eta = 1/3$ and

$$\delta_1 P / \delta_2 P = 1/3. \qquad (6.6)$$

It must be kept in mind that the condition $\xi_0 \to -\infty$ cannot be satisfied throughout the entire volume of the atom, since the electron gas is always degenerate close to the nucleus ($\xi_0 \sim Ze^2/rT \to \infty$). Therefore, the ratio (6.6) holds only for sufficiently large $-\tilde{\xi}_0$, where the region just mentioned plays a small role.

Going on to a consideration of the general case, we expand $\eta(\xi_0)$ in a series about the point $\tilde{\xi}_0$. Taking into consideration the boundary conditions in Eq. (3.5), we find

$$\eta(\xi_0) = \eta(\tilde{\xi}_0)(1 + C(x-1)^2 + \cdots),$$

where

$$C = \alpha I_{1/2}(\tilde{\xi}_0) \eta'(\tilde{\xi}_0) / 2\eta(\tilde{\xi}_0).$$

If C is small in comparison with unity, η can be considered constant, equal to $\eta(\tilde{\xi}_0)$. In this case, in accord with (6.2),

$$\tilde{u}_1 / \tilde{u}_2 = \eta(\tilde{\xi}_0). \qquad (6.7)$$

To find the regions in which C is small, we return to Eq. (3.8). Keeping in mind the monotonic character of the functions $I_{1/2}(\xi_0)$ and $\xi_0(x)$, we have

$$n / \vartheta^{3/2} > (\sqrt{2}/\pi^2) I_{1/2}(\tilde{\xi}_0).$$

Hence

$$|C| = \frac{2\sqrt{2}}{\pi}(3/4\pi)^{2/3} \vartheta^{1/2} n^{-2/3} |I_{1/2}\eta'/\eta| < 0.66 |I_{1/2}^{2/3}\eta'/\eta| n^{-1/3}.$$

The function $|I_{1/2}^{2/3}\eta'/\eta|$ has a maximum equal to 1.2×10^{-3}, whence

$$n > 3 \cdot 10^{-10} |C|^{-3}.$$

Even for C = 0.02, this condition reduces to $\eta > 3 \times 10^{-5}$, which corresponds to densities greater than $5 \times 10^{-4} Z^2$ g/cm³; in this way, virtually the entire region subject to this consideration is used up. Therefore, the ratio (6.7) is valid practically everywhere. Taking this into account, we have, furthermore,

---

*ξ_0 is itself an increasing function inside the atom. Therefore, if the gas is degenerate on the boundary of the cell, it is clearly degenerate inside the atom, too.

$$\frac{\delta_1 P}{P_0} - \eta(\tilde{\xi}_0)\frac{\delta_2 P}{P_0} = \frac{Z^{-2/3}}{2\sqrt{2}\pi\vartheta^{1/2} I_{3/2}(\tilde{\xi}_0)} \int\limits_{-\infty}^{\tilde{\xi}_0} [\eta(\xi) - \eta(\tilde{\xi}_0)]\,\Psi_2(\xi)\,d\xi. \tag{6.8}$$

$\eta(\xi)$ is a monotonically decreasing function; therefore, the right hand side of (6.8) is always positive.

At the same time we can show that $\delta_1 P$ and $\delta_2 P$ are negative quantities. With this purpose we make the substitution

$$x^{-1} v_i(x) = u_i(x) + I_{1/2}^{-1}(\tilde{\xi}_0) \int\limits_{-\infty}^{\tilde{\xi}_0} \Psi_i(\xi)\,d\xi.$$

in (6.1), (6.2). Then

$$\frac{\delta_i P}{P_0} = \frac{Z^{-2/3}\,\tilde{I}_{1/2}}{2\sqrt{2}\pi\vartheta^{1/2}\,\tilde{I}_{3/2}}\,\tilde{v}_i,$$

$$\ddot{v}_i - \alpha I'_{1/2} v_i = \alpha x\Big[\Psi_i(\xi_0) + (I'_{1/2}(\xi_0)/I_{1/2}(\tilde{\xi}_0)) \int\limits_{-\infty}^{\tilde{\xi}_0} \Psi_i d\xi\Big],$$

$$v_i|_0 = 0; \quad v'_i|_1 = v_i|_1.$$

It is shown in Appendix II that an equation of this type (under the condition that its right hand side is positive) has a solution which is a non-positive function.

It then follows that the quantum and exchange corrections to the pressure always decrease the latter:

$$\delta_1 P < 0, \quad \delta_2 P < 0. \tag{6.9}$$

In conjunction with what was said above on the sign of the right hand side of (6.8), this yields

$$0 < \delta_1 P/\delta_2 P < \eta(\tilde{\xi}_0). \tag{6.10}$$

In this case the departure of $\delta_1 P/\delta_2 P$ from $\eta(\tilde{\xi}_0)$ takes place only in the region in which the degeneracy parameter $\beta \sim 1$.

Thus, the ratio of the quantum correction of the lowest order to the corresponding exchange correction does not exceed one third.

7. QUANTUM AND EXCHANGE CORRECTIONS IN THE REGION OF HOMOGENEITY

We now proceed to search for the explicit expressions for the quantum and exchange corrections in the region in which the distribution is close to uniform (as in Sec. 3, this corresponds to smallness of the parameter $\alpha I'_{1/2}$). Putting (6.1) and (6.2) in integral form, we have

$$u_i(x) = \tilde{u}_i + \alpha \int\limits_x^1 \{\Psi_i + I'_{1/2} u_i(t)\}(t/x - 1)\,t\,dt \tag{7.1}$$

with the condition

$$\int\limits_0^1 (\Psi_i + I'_{1/2} u_i)\,t^2 dt = 0. \tag{7.2}$$

Using the same method as in Sec. 3, we find as the zero approximation

$$\tilde{u}_i = -\Psi_i / I'_{1/2}. \tag{7.3}$$

substitution of this expression (6.1) gives

$$\frac{\delta_i P}{P_0} = -\frac{Z^{-2/3}}{2\sqrt{2}\pi\vartheta^{1/2}}\,\frac{I_{1/2}^2}{I_{3/2}\,I'_{1/2}}\,\frac{d}{d\xi_0}\Big\{\int\limits_{-\infty}^{\xi^0} \Psi_i\,d\xi / I_{1/2}\Big\}. \tag{7.4}$$

We rewrite (7.4) in the form

$$-Z^{2/3}\,\delta_i P/P_0 \equiv \vartheta^{1/2}\,\Xi_i. \tag{7.5}$$

The functions Ξ, Ψ, I etc. in (7.3), (7.4) and in the formulas below refer to the argument ξ^0 which is determined by Eq. (3.10).

In the region of degeneracy we have for the quantum correction

$$-Z^{2/3}\,\frac{\delta_1 P}{P_0} = \frac{5}{18\pi(3\pi^2)^{1/3}}\,n^{-1/3}, \tag{7.6}$$

for $\xi_0 \to -\infty$,

$$-Z^{2/3}\,\delta_1 P/P_0 = (\pi/6)\,n\vartheta^{-2}. \tag{7.7}$$

The corresponding exchange corrections can easily be found by recalculation* (see Sec. 6). We now proceed to find the boundaries of the region outside of which the quantity $-Z^{2/3}\delta_i P/P_0$ is less than a given value δ_i while inside, it is greater than that value. In this way a region is defined in which the T-F model is applicable with a given accuracy $\delta Z^{-2/3}$.

Combining (7.5) and (3.10), we have

$$\delta_i^3 n = (\sqrt{2}/\pi^2)\,I_{1/2}\Xi_i^3, \quad \delta_i^2\vartheta = \Xi_i^2, \tag{7.8}$$

While for large $n/\vartheta^{3/2}$ we have $\delta_i^3 n = (3\pi^5)^{-1}(5/18)^3$, and in the opposite case, $\delta_i^2\vartheta = (\pi\delta_i^3 n/6)^{1/2}$. The corresponding curves are plotted in Figs. 3, 4.†

Further, it is necessary to find the limits of applicability of these results. With this purpose, let us find the further terms of the expansion of $\tilde{u}_i$ and $\delta_i P/P_0$ in series in α. In this case, the structures of Eqs. (7.1), (7.2), and (6.1) are such

---

*Calculation by Eq. (7.5) shows that the minimum ratio $\delta_1 P/\delta_2 P$ is equal to 1/5 (and corresponds to $\xi^0 = 6$). We note that the temperature correction (7.6) is proportional to θ^2 for $\delta_1 P/P_0$ and to $\vartheta^2 \ln \vartheta$ for $\delta_2 P/P_0$. This pecularity of exchange effects, to which our attention was drawn by A. S. Kompaneets, is connected with the long-range character of the Coulomb forces. See also Figs. 3 and 4.

†These curves can be also used to find the values of $\delta_i P/P_0$. For this purpose, the curves must be plotted with the coordinates (n, ϑ) for different values of δ.

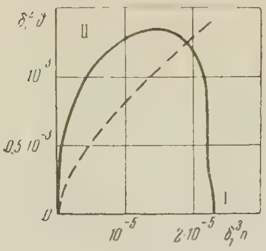

FIG. 3

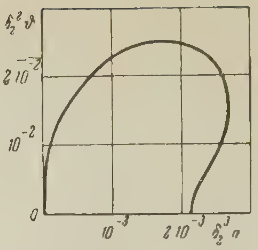

FIG. 4

that the term that is linear in α drops out of $\tilde{u}_i$ and $\delta_i P$. Therefore, the term linear in α in $\delta_i P/P_0$ is connected with the expansion of P_0. Account of inhomogeneity thus leads to the appearance in (7.4) of a factor

$$1 + (3\alpha / 20)\, I_{1/2}^2 / I_{3/2},$$

and everything said in Sec. 3 on the limits of applicability of the homogenous approximation remains in force relative to $\delta_i P/P_0$.

Thus, the functions (7.8) can be used only when the corresponding curves lie inside the region of homogeneity, i.e., when they envelop the curve (3.1) (with a given value of ϵ). This takes place for sufficiently small δ_i. Thus the corrections for inhomogeneity do not change the order of magnitude of the quantities entering into (7.4) and (7.8) ($\epsilon \sim 1$) for $\delta_1 < 0.1$ and $\delta_2 < 0.5$, that is, for

$$|\delta_1 P| / P_0 < 0.1\, Z^{-2/3}, \quad |\delta_2 P| / P_0 < 0.5\, Z^{-2/3}. \tag{7.9}$$

Thus, in the region of degeneracy, the T-F model is valid with accuracy $\delta_1 = 0.01$ at pressures

$$\mathscr{P} > 10^6 Z^{10/3} \text{ atmos.}$$

If we are interested only in the region in which the degeneracy parameter $\beta \lesssim 1$, the conditions (7.9) can be somewhat modified.

For less stringent requirements on the accuracy (larger $\delta_i P/P_0$) or larger Z, the curves under consideration lie outside the region of homogeneity. An analytic solution in this case is not possible; numerical results will be published when they are obtained. We shall abandon at this point a comparison of the results with experiment.

In conclusion, I take this opportunity to thank V. L. Ginzburg, E. L. Feinberg and E. S. Fradkin for discussions and L. V. Pariiskaia for the numerical calculations.

APPENDIX I

The integral

$$\int d\mathbf{p}\, Af = 4\pi e^2 \hbar^2 \int \frac{d\mathbf{p}\, d\mathbf{p}'}{|\mathbf{p} - \mathbf{p}'|^2} f(\mathbf{r}, \mathbf{p}) f(\mathbf{r}, \mathbf{p}')$$

reduces after integration over the angles to the form

$$\frac{e^2 M^2 (kT)^2}{2\pi^3 \hbar^4} \varkappa(\xi),$$

where

$$\varkappa(\xi) = \int_0^\infty \frac{dx}{\exp(x - \xi) + 1} \int_0^\infty \frac{dy}{\exp(y - \xi) + 1} \ln \left| \frac{\sqrt{x} + \sqrt{y}}{\sqrt{x} - \sqrt{y}} \right|.$$

Making the substitution $x \rightarrow x + \xi$, $y \rightarrow y + \xi$, we have

$$\varkappa'(\xi) = \left[\int_\xi^\infty \frac{dx}{(\exp x + 1)\sqrt{x + \xi}} \right]^2 = (I_{-1/2}(\xi))^2.$$

making use of Eq. (3.3) we obtain, finally,

$$\varkappa(\xi) = 4 \int_{-\infty}^{\xi} (I'_{1/2}(x))^2 dx.$$

APPENDIX II

We shall show that the equation

$$y'' - A(x)\, y = B(x) \tag{a}$$

with B(x) a quantity of constant sign and with boundary conditions given at both ends of the interval of integration that are invariable relative to the substitution $y \rightarrow -y$, has a sign-constant solution y(x), the sign of which is opposite to the sign of B.

We limit ourselves to boundary conditions of the simplest form. If they are

$$y(0) = 0, \quad y(1) = 0 \text{ or } y(0) = 0, \quad y'(1) = 0,$$

then in place of (a) we can consider the functional

$$\int_0^1 \{(y')^2/2 + Ay^2/2 + By\}\, dx, \tag{b}$$

the minimum of which is realized by the solution of Eq. (a) [we are discussing the minimum, since the coefficient in the first term of (b) is positive].

Inasmuch as the first two terms of (b) and the boundary conditions do not change in the substitution $y \rightarrow -y$, while the latter term changes sign, the extremal of y(x) belongs to the class of constant-sign functions so that $By < 0$. Actually, if the function y is constant in sign and $By > 0$, or if y changes sign inside the interval of integration, then it clearly does not achieve the minimum of (b), since the function $-|y(x)|$ (for $B > 0$) or

$|y(x)|$ (for $B < 0$) reduces to the much lower value of the functional.

In the presence of a more complicated boundary condition

$$y(0) = 0, \quad y'(1) = y(1)$$

it is necessary to make the functional more complicated, adding to the integrand the quantity $-(d/dx)(y^2/2)$ [in the opposite case, (a) and (b) will not be equivalent to each other]. The parity of this quantity relative to y is conserved by virtue of the previous discussion.

---

[1] Feynman, Metropolis and Teller, Phys. Rev. **75**, 1561 (1949).

[2] R. Latter, Phys. Rev. **99**, 1854 (1955); J. Chem. Phys. **24**, 280 (1956).

[3] K. Cowan and J. Ashkin, Phys. Rev. **105**, 144 (1957).

[4] P. Gambos, Die statistische Theorie des Atoms und ihre Anwendungen, Springer-Wien, 1949 (Russian translation, IIL, Moscow, 1951).

[5] D. A. Kirzhnits, J. Exptl. Theoret. Phys. (U.S.S.R.) **35**, 1198 (1958); Soviet Phys. JETP **8**, 835 (1959).

[6] A. S. Kompaneets and E. S. Pavlovskii, J. Exptl. Theoret. Phys. (U.S.S.R.) **31**, 427 (1956); Soviet Phys. JETP **4**, 328 (1957).

[7] D. A. Kirzhnits, J. Exptl. Theoret. Phys. (U.S.S.R.) **32**, 115 (1957); Soviet Phys. JETP **5**, 64 (1957); Dissertation, Physics Institute, Academy of Sciences, USSR, Moscow, 1956.

[8] S. Golden, Phys. Rev. **105**, 604 (1957).

[9] L. D. Landau and E. M. Lifshitz, Статистическая физика (Statistical Physics) GITTL, 1951.

[10] J. McDougall and E. Stoner, Phil. Trans. Roy. Soc. (London) **237**, 67 (1938); Beer, Chase and Choquard, Helv. Phys. Acta. **28**, 529 (1955).

[11] N. March, Proc. Phys. Soc. (London) **A68**, 726 (1955).

Translated by R. T. Beyer
321

SOVIET PHYSICS JETP VOLUME 35(8), NUMBER 6 JUNE, 1959

ON THE THEORY OF SUPERCONDUCTING ALLOYS

I. THE ELECTRODYNAMICS OF ALLOYS AT ABSOLUTE ZERO

A. A. ABRIKOSOV and L. P. GOR'KOV

Institute for Physics Problems, Academy of Sciences, U.S.S.R.

Submitted to JETP editor July 16, 1958

J. Exptl. Theoret. Phys. (U.S.S.R.) **35**, 1558-1571 (December, 1958)

In this paper we give the theory of superconductors containing impurities at the absolute zero. The dependence of the penetration depth on the impurity concentration is considered for small atomic concentrations. We have obtained the electrodynamic equations in an alternating field for superconductors with a mean free path which is smaller than the correlation length.

It is well known that Bardeen, Cooper, and Schrieffer[1] succeeded in formulating the electrodynamics of superconductors with the aid of their theory of superconductivity. They obtained equations connecting the current with the vector potential which replaced the old equations of the phenomenological theory of H. and F. London. Of most interest was the non-local character of the connection between the current and the field for the majority of pure superconductors.

The non-local character is put into the very basis of the theory which is based on the physical idea of Cooper's[2] about the formation of bound singlet pairs of electrons near the Fermi surface under the action of the phonon interaction. The dimensions of such a pair causes the existence of a correlation between electrons at distances of the order $\xi_0 \sim 10^{-4}$, which becomes apparent in the form of a non-local connection between the field and the current, if the penetration depth of the field is less than ξ_0. The majority of pure superconductors belong to that class.

The creation of a theory of superconductivity made it possible to consider a whole series of phenomena. With its aid they could construct the thermodynamics and electrodynamics of superconductors[1] and, in particular, determine the behavior of superconductors in a high-frequency field.[3] A very interesting problem is that of "alloys," i.e., of superconductors with impurity atoms of other elements or other lattice defects. In the normal state these defects cause the so-called residual resistance.

At very small concentrations the role of impurities is small. Increasing the concentration, however, leads to a decrease of the spatial correlation of the electrons in the superconductor. For a sufficiently concentrated alloy the role of the correlation parameter goes over from ξ_0 to the electron mean free path. Thanks to this, it is natural to expect the appearance of a local connection between the current and the vector potential for such concentrations where the mean free path becomes less than the penetration depth. The difference with the Londons' theory will lie in a change in the constant of proportionality of $\mathbf{j}$ to $\mathbf{A}$. Below we shall consider this problem, assuming, however, that the atomic impurity concentration is small.

The problem of the penetration of a weak electromagnetic field into a medium is solved if we know the Green function of the field in the medium

$$D_{ik}(x-x') \doteq \frac{4\pi i}{c}\langle T(A_i(x)A_k(x'))\rangle. \tag{1}$$

The function D_{ik} is directly connected with experimentally observed quantities. Let $D_{ik}(\mathbf{k}, \omega_0)$ be the Fourier transform of $D_{ik}(\mathbf{x}-\mathbf{x}')$:

$$D_{ik}(x-x') = \frac{4\pi}{(2\pi)^4}\int \exp\{i\mathbf{k}\cdot(\mathbf{x}-\mathbf{x}')$$

$$- i\omega_0(t-t')\} D_{ik}(\mathbf{k}, \omega_0) d^3\mathbf{k}\, d\omega_0.$$

In view of the symmetry of the tensor D_{ik} we have

$$D_{ik}(\mathbf{k}, \omega_0) = D_1(\mathbf{k}^2, \omega_0)(\delta_{ik} - k_i k_k / k^2) + D_2(\mathbf{k}^2, \omega_0) k_i k_k / k^2.$$

The function D_2 which determines the longitudinal part of D_{ik} is connected with the gauge of the vector potential and is arbitrary. The physical quantities depend only on the transverse part, i.e., on D_1.

With the aid of the general theory of the anomalous skin effect we can arrive at the following formula for the surface impedance in the case of diffuse scattering at the surface*

$$Z = \frac{4\pi^2 i\omega_0}{c^2} \Big/ \int\limits_0^\infty \ln\left[\mathbf{k}^2 D_1(\mathbf{k}^2, \omega_0)\right] d\,|\,\mathbf{k}\,|. \qquad (2)$$

We recall that the penetration depth of the field is

$$\delta = \operatorname{Re}\left[\frac{c^2}{4\pi\omega_0}\, iZ\right]. \qquad (3)$$

Usually, instead of finding the function D_{ik} one finds the connection between the current and the vector potential

$$j_i = -Q_{ik}(\mathbf{k}, \omega_0)\, A_k(\mathbf{k}, \omega_0). \qquad (4)$$

To find the connection between the tensors D_{ik} and Q_{ik}. It is sufficient to substitute (4) into the Maxwell equation and to write down with its aid an equation for D_{ik}. This gives

$$(D^{-1})_{ik} = (\mathbf{k}^2\delta_{ik} - k_i k_k) + \frac{4\pi}{c} Q_{ik}. \qquad (5)$$

The first term corresponds to the "zero" value of the tensor D_{ik}, obtained by neglecting the interaction of the field with the electrons. In Eqs. (2) to (5) we have implied $\omega_0 > 0$.

From Eq. (5) it is clear that the tensor Q_{ik} must be symmetric. Also, since the current is conserved $(k_i j_i = 0)$ it follows from Eq. (4) that it must be transverse.† Equation (5) determines thus only the transverse part of D_{ik} and its longitudinal part remains arbitrary, as it should be.

We evaluate below the function $D_{ik}(\mathbf{k}, \omega_0)$ for a superconductor with impurities, using the techniques of the quantum field theory‡ (see reference 4, which in contradistinction to other methods[1,5] makes it possible to state the problem very clearly). We assume that we have already taken into account the interaction of the electrons with the impurities and consider their interaction with the electromagnetic field. The Hamiltonian of this interaction is

$$H_1' = \frac{e^2}{mc^2}\,\psi^+(x)\,\psi(x)\,\mathbf{A}^2(x) + \frac{ie\mathbf{A}(x)}{2mc}\,(\nabla_{\mathbf{x}} - \nabla_{\mathbf{x}'})_{x\to x'}\,\psi^+(x')\,\psi(x). \qquad (6)$$

Dyson's equation for the function D will be of the form

$$D^{-1} = D^{-1}_{(0)} +$$ 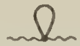 $$+$$ 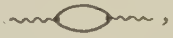 , (7)

where a solid line corresponds to an electron and a wavy one to a photon. More complicated diagrams with internal photon lines can be neglected in the non-relativistic approximation.

Comparing Eqs. (7) and (5) we see that, apart from a factor $4\pi/c$ the term added to $D_{(0)}$ corresponds to the tensor Q_{ik}. The first term of this addition gives simply $(Ne^2/mc)\,\delta_{ik}$ in Q_{ik}. The second diagram is more complicated. For the following it is convenient to separate, as is usually done, one of the photon vertices, for instance p_i, from the remaining part which, apart from a coefficient, can be considered as the result of including the photon vertex p_k in the electron line. To find the coefficient is not difficult (the factor 2 comes from taking the trace over the spin). In this way we get

$$Q_{ik}(\mathbf{k}, \omega_0) = \frac{Ne^2}{mc}\,\delta_{ik} - \frac{2ie^2}{m^2c}\int p_i \Pi_k(p_+, p_-)\,\frac{d^4p}{(2\pi)^4}, \qquad (8)$$

where $p_\pm = (\mathbf{p} \pm \mathbf{k}/2,\ \omega \pm \omega_0/2)$.

As far as the interaction of the electrons with the impurities is concerned, the corresponding term in the Hamiltonian is of the form

$$H_2' = \sum_a H_a, \qquad H_a = u(\mathbf{x} - \mathbf{x}_a)\,\psi^+(x)\,\psi(x), \qquad (9)$$

where $u(\mathbf{x} - \mathbf{x}_a)$ is the interaction potential with an impurity atom at the point $\mathbf{x}_a$. We shall assume that the impurity atoms are randomly distributed in the metal and that their distance apart is large compared to the lattice period. We assume, of course, that the impurity concentration is so small that the interaction between the electrons is not changed. We shall denote the impurity vertex in the Feynman diagrams by a cross. It corresponds to a factor

$$u(\mathbf{q})\,e^{i\mathbf{q}\cdot\mathbf{x}_a}\,\delta(\omega_1 - \omega_2), \qquad (10)$$

where $u(\mathbf{q})$ is the Fourier component of the potential $u(\mathbf{x})$ and $\mathbf{q}$ is the momentum transferred.

For the sake of clarity we first give the calculations for the application to a normal metal with a residual resistance (Sec. 1). We then consider superconducting alloys (Sec. 2). All calculations refer only to the absolute zero.

---

*The correspondence of this equation with the usual expression is easily established using Eqs. (4) and (5).

†The method of finding the tensor Q_{ik} usually employed in various problems of the theory of superconductivity (see references 1 and 3) leads to an expression which is not purely transverse. One can, however, show by means of a more rigorous calculation based on the equations of reference 4 that to get the correct result for the given problem it is sufficient to retain only the transverse part of the tensor Q_{ik} obtained by the usual method, or to use a vector potential satisfying the condition div $\mathbf{A} = 0$.

‡We must emphasize that the method used here is suitable only at $T = 0$. In the case where $T \neq 0$ there will occur, instead of simple time-ordered products, more complicated combinations which make this method practically innapplicable to the problem under consideration.

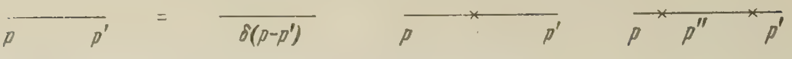

FIG. 1

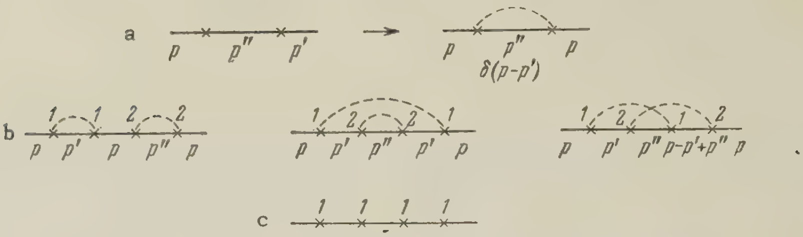

FIG. 2

1. RESIDUAL RESISTANCE OF A NORMAL METAL

We introduce the Green function of a system of fermions

$$G_{\alpha\beta}(x, x') = -i\langle T(\psi_\alpha(x)\ \psi_\beta^+(x'))\rangle. \tag{11}$$

For a pure metal we have:*

$$G_{0\alpha\beta}(x-x') = \delta_{\alpha\beta}(2\pi)^{-4}\int G_0(p)\,e^{ip(x-x')}d^4p, \qquad G_0(p) = (\omega - \xi + i\delta\,\mathrm{sign}\,\omega)^{-1}, \tag{12}$$

where $\xi = v(|\mathbf{p}| - p_0)$, $v = p_0/m$, $\delta \to +0$. When impurities are present the Green function (11) is not the same as expression (12). We shall write it in the form

$$G_{\alpha\beta}(x, x') = \delta_{\alpha\beta}(2\pi)^{-7}\int G(\mathbf{p}, \mathbf{p}', \omega) \times \exp\{i\mathbf{p}\cdot\mathbf{x} - i\mathbf{p}'\cdot\mathbf{x}' - i\omega(t-t')\}\,d^3\mathbf{p}\,d^3\mathbf{p}'\,d\omega. \tag{13}$$

The function $G(\mathbf{p}, \mathbf{p}', \omega)$ is expressed as a sum of the diagrams given in Fig. 1 according to the well-known rules of field theory. Each line corresponds to $G_0(\mathbf{p})$.

Summing over the diagrams gives an integral equation for $G(\mathbf{p}, \mathbf{p}', \omega)$:

$$G(\mathbf{p}, \mathbf{p}', \omega) = \delta(\mathbf{p}-\mathbf{p}')\,G_0(p) + (2\pi)^{-3}\int G_0(p)\sum_a u(\mathbf{p}-\mathbf{p}'')\,e^{i(\mathbf{p}-\mathbf{p}'')\mathbf{x}_a}\,G(\mathbf{p}'', \mathbf{p}', \omega)\,d^3\mathbf{p}'' \tag{14}$$

We are not interested in the exact solution of (14), since the impurity atoms are randomly distributed over the metal. We must average all expressions over the positions of all impurity atoms. It is then essential that by virtue of our assumption about the smallness of the atomic concentration the average distance apart of the impurity atoms is much larger than the atomic distances in the metallic lattice, so that the averaging can take place over volumes with dimensions large compared to the interatomic distances. After such an averaging, the Green function $G(\mathbf{p}, \mathbf{p}', \omega)$ is clearly of the form

$$\overline{G(\mathbf{p}, \mathbf{p}', \omega)} = G(\mathbf{p}, \omega)\,\delta(\mathbf{p}-\mathbf{p}'). \tag{15}$$

The absolute magnitude of the momenta $\mathbf{p}$, $\mathbf{p}'$ which are of interest to us are of the order of magnitude of the momentum p_0 at the Fermi surface which in turn is of the order of the inverse of the interatomic distances. This fact makes it at once easy to carry out the averaging.

We shall perform the calculation in the Born approximation, i.e., we shall assume that $p_0^3\int u(\mathbf{x})\,d^3\mathbf{x} \ll E_{ph}$. Once can show that the final results expressed in terms of the collision time will also be correct in the general case.

The simplest diagram for G contains only one cross. The value obtained by averaging over the position of the impurity atom is a constant $\overline{u(\mathbf{q})\,e^{i(\mathbf{q}\cdot\mathbf{x}_\alpha)}} = u(0)$, which can be included in the ground state energy and which in the following we assume to be equal to zero. The next diagram, as far as complexity is concerned, contains two crosses referring to one atom (Fig. 2a). The average value of these diagrams (without external G_0) is equal to

$$\frac{1}{V}\int |u(\mathbf{p}-\mathbf{p}')|^2\,G_0(p')\,\frac{d^3\mathbf{p}'}{(2\pi)^3}, \tag{16}$$

where V is the volume of the system. In the following we shall be interested in values of $|\mathbf{p}|$ which in absolute magnitude are close to p_0. The integral in Eq. (16) can be split into two parts: an integral over values of $|\mathbf{p}'|$ far from the Fermi surface and one over values near the Fermi surface (the limits of the second integral over $|\mathbf{p}'|$ can be taken symmetric with respect to $|\mathbf{p}'| = p_0$). The integral over the far region gives a real constant which together with $u(0)$ is a renormalization of the chemical potential and need not be considered. One may assume that in the second integral $u(\mathbf{p}-\mathbf{p}')$ is a slowly-varying function. Substituting Eq. (12) for $G_0(\mathbf{p})$ and summing over the impurity atoms (which simply means multiplying by the number of atoms) we get the essential contribution to the G-function:

---

*Here and henceforth we use units with ħ = 1.

$$i \operatorname{sign} \omega / 2\tau,$$

where

$$\frac{1}{\tau} = n \frac{p_0 m}{(2\pi)^2} \int |u(\theta)|^2 d\Omega \qquad (17)$$

is the time between collisions, n the number of impurity atoms per unit volume. From this it is clear that the region near the Fermi surface plays the leading role in the integrals.

From this point of view not all diagrams are equivalent. Let us compare, for instance, the three diagrams of Fig. 2b. (Dotted lines connect crosses referring to one atom.) We see easily that in the first two expressions the integration over $\mathbf{p}'$ and $\mathbf{p}''$ can be performed over arbitrary angles between the momenta near the Fermi surface. On the other hand, in the third integral the requirement that all arguments of the G-functions are near the Fermi surface leads to a limitation of the angles. As a result the contribution from such a graph turns out to be less by a factor $(vp_0G)^{-1}$ as compared to the others. Since in the following we need values of ω and $\xi \sim 1/\tau$ where τ is the time between collisions, the smallness of the "intersecting" graphs can be estimated to be $(p_0 l)^{-1}$ where $l = v\tau$ is the mean free path.

One can easily show that a small contribution is also given by diagrams containing more than two crosses from one impurity atom. Let us, for instance, compare the total contribution (from all impurity atoms) of diagrams of the kind of the first one of Fig. 2b with diagrams of the type 2c. The first ones give a quantity of the order of magnitude

$$\frac{1}{\tau^2} G_0 \sim \frac{1}{\tau}.$$

The second ones give, as far as order of magnitude is concerned

$$\frac{1}{\tau} \frac{u^2(\mathbf{q}) p_0^4}{v^2} \sim \frac{1}{\tau} \left[\frac{\int u dV p_0^3}{E_{\mathrm{ph}}} \right]^2 \ll \frac{1}{\tau}.$$

It is thus clear that we need consider only diagrams containing up to two crosses on one impurity atom.

Summing all essential diagrams (i.e., only "pair" diagrams and those which do not contain "intersections" like the third diagram of Fig. 2b) we get the following expression for the G-function:

$$G(p) = G_0(p) + nG_0(p) \int |u(\mathbf{p} - \mathbf{p}')|^2 G(p') \frac{d^3\mathbf{p}'}{(2\pi)^3} G(p). \qquad (18)$$

If we do not wish to use the Born approximation, it is necessary to take into account diagrams with many crosses at one impurity atom. One can show that all changes which this entails are taken into account by replacing the Born amplitude $u(\theta)$ by the total scattering amplitude. This remains true also for all calculations in the following. We can therefore imply in all formulae by $u(\theta)$ the total scattering amplitude.

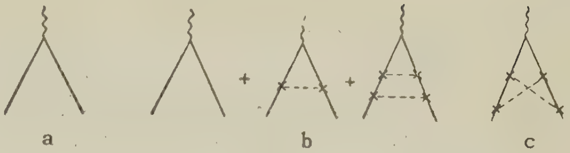

FIG. 3

The solution of Eq. (18) is

$$G(p) = \frac{1}{\omega - \xi - \bar{G}(\omega)},$$

where $\bar{G}(\omega)$ satisfies the equation

$$\bar{G}(\omega) = n \int |u(\mathbf{p} - \mathbf{p}')|^2 \frac{1}{\omega - \xi - \bar{G}(\omega)} \frac{d^3\mathbf{p}'}{(2\pi)^3}$$

Assuming $\bar{G}(\omega)$ to be purely imaginary $(\bar{G}(\omega) = -i\beta)$ and applying to the integral on the right hand side the same approach as was applied to (16) we find

$$\beta = \operatorname{sign} \beta / 2\tau,$$

where τ is determined by Eq. (17). Comparing G which is obtained in this manner with the case of small amounts of impurities $(G \rightarrow G_0)$ we find that $\beta = \operatorname{sign} \omega / 2\tau$ or

$$G = (\omega - \xi + i \operatorname{sign} \omega / 2\tau)^{-1}. \qquad (19)$$

Going over to the x-representation we see easily that the whole change in G as compared to G_0 is obtained by multiplying the latter by an exponential screening factor

$$G = G_0 e^{-|\mathbf{x} - \mathbf{x}'|/2l}, \qquad (20)$$

where $l = v\tau$.

We now proceed to evaluate Q_{ik}. Putting the photon vertex into the electron Green function $G(\mathbf{p}, \mathbf{p}', \omega)$ we get:

$$\Pi(p_+, p_-) \qquad (21)$$
$$= (2\pi)^{-3} \int G\left(\mathbf{p}_+, \mathbf{p}'_+, \omega + \frac{\omega_0}{2}\right) \mathbf{p}' G\left(\mathbf{p}'_-, \mathbf{p}_-, \omega - \frac{\omega_0}{2}\right) d^3\mathbf{p}'.$$

The function $G(\mathbf{p}, \mathbf{p}', \omega)$ entering here corresponds to the sum of the diagrams in Fig. 1 and is described by Eq. (14). To average over the positions of the impurity atoms we must take into account that the average of two Green functions is not equal to the product of the two average values.

For a pure metal expression (21) corresponds to the diagram of Fig. 3a. After averaging over the positions of the impurity atoms, it turns out that apart from the simple diagrams corresponding to the transition from the zeroth Green functions $G_0(p)$ to the function $G(p)$ of (19) the essential diagrams for the quantity (21) are those of Fig. 3b. The large contribution from these corrections is connected with the fact that the photon momentum occurring in the vertex $|\mathbf{k}| \ll p_0$. Diagrams of another kind, for instance the graph of Fig. 3c, are far smaller since one of the integrations in them is over a region of momenta far from the Fermi surface. The averaging of the quantity (21) is thus performed by the summation of the "ladder" diagrams of Fig. 3b.

The integral equation for $\Pi(p_+, p_-)$ is

$$\Pi(p_+, p_-) = G(p_+)G(p_-)\left[\mathbf{p} + \frac{n}{(2\pi)^3}\int |u(\mathbf{p}-\mathbf{p}')|^2 \Pi(p'_+, p'_-)\,d^3\mathbf{p}'\right]. \quad (22)$$

There are two limiting cases possible:

(a) The skin effect is anomalous, $(kv) \gg \tau$; it is easy to verify that the integral on the right hand side of (22) will be negligibly small in that case $(\sim 1/kv\tau)$.

(b) The skin effect is normal, $(kv) \ll 1/\tau$; this case is just of the greatest interest to us. In Eq. (22) we can then assume $\mathbf{p}_+ = \mathbf{p}_-$.

The vector obtained from the integral on the right hand side of (22) will clearly be parallel to $\mathbf{p}$. We introduce the notation

$$\mathbf{p}\Lambda(\omega, \omega_0) = \frac{n}{(2\pi)^3}\int |u(\mathbf{p}-\mathbf{p}')|^2 \Pi(p'_+, p'_-)\,d^3\mathbf{p}'. \quad (23)$$

Since $|\mathbf{p}| \approx p_0$, we can assume $\Lambda(\omega, \omega_0)$ to be independent of $|\mathbf{p}|$. We multiply (22) by $n(2\pi)^{-3} \times |u(\mathbf{1}-\mathbf{p})|^2$ and integrate over $d^3\mathbf{p}$:

$$\mathbf{1}\Lambda(\omega, \omega_0) = \frac{n}{(2\pi)^3}\int |u(\mathbf{1}-\mathbf{p})|^2 \mathbf{p} G(p_+)G(p_-)\left[1 + \Lambda(\omega, \omega_0)\right] d^3\mathbf{p}. \quad (24)$$

Replacing $G(p)$ by Eq. (19) we find easily that $\Lambda(\omega, \omega_0)$ is only different from zero if $|\omega| < \omega_0/2$, since in the opposite case both poles in (24) for the integration over ξ according to (20) lie in the same half-plane. In that integral Λ does not depend on ω. Integrating over ξ and using the relation

$$\cos\theta = \cos\theta'\cos\theta'' + \sin\theta'\sin\theta''\cos(\varphi' - \varphi''), \quad (25)$$

we get

$$\Lambda(\omega, \omega_0) = \begin{cases} \dfrac{i}{\tau_1}\dfrac{1}{\omega_0 + i/\tau_{tr}} & \omega^2 < \omega_0^2/4, \\ 0, & \omega^2 > \omega_0^2/4, \end{cases} \quad (26)$$

where

$$\frac{1}{\tau_1} = \frac{1}{\tau} - \frac{1}{\tau_{tr}}; \quad \frac{1}{\tau_{tr}} = \frac{nmp_0}{(2\pi)^2}\int |u(\theta)|^2 (1 - \cos\theta)\,d\Omega. \quad (27)$$

After substituting (26) into (22) and (7) and integrating, assuming that $\omega_0\tau \ll 1$, we find

$$Q_{ik} = -\frac{4\pi i\omega_0\sigma}{c^2}\delta_{ik}. \quad (28)$$

The "transport" collision time enters into the conductivity $\sigma = Ne^2\tau_{tr}/m$, as should be the case.

2. SUPERCONDUCTING ALLOYS

The method given above will now be applied to a study of a superconductor with impurities. The main difference as compared to what was given above lies in the fact that a superconductor is described by three Green functions:

$$\begin{aligned} \delta_{\alpha\beta}G(x, x') &= -i\langle T(\psi_\alpha(x)\psi_\beta^+(x'))\rangle; \\ \hat{I}_{\alpha\beta}F^+(x, x') &= \langle T(\psi_\alpha^+(x)\psi_\beta^+(x'))\rangle; \\ -\hat{I}_{\alpha\beta}F(x, x') &= \langle T(\psi_\alpha(x)\psi_\beta(x'))\rangle, \end{aligned} \quad (29)$$

where $\hat{I}_{\alpha\beta} = -\hat{I}_{\beta\alpha}$, $\hat{I}^2 = -E$. These functions were introduced in reference 4 for a pure superconductor and are equal to

$$\begin{aligned} G(x - x') &= (2\pi)^{-4}\int G(p)e^{ip(x-x')}d^4p, \\ F^+(x - x') &= (2\pi)^{-4}\int F^+(p)e^{ip(x-x')}d^4p, \\ F(x - x') &= F^+(x - x'), \end{aligned}$$

where

$$G_0(p) = \frac{\omega + \xi}{\omega^2 - \xi^2 - \Delta^2 + i\delta}; \quad F_0^+(p) = \frac{i\Delta}{\omega^2 - \xi^2 - \Delta^2 + i\delta} \quad (\delta \to +0). \quad (30)$$

The occurrence of three Green functions makes it necessary to change the diagram technique.* The functions G, F^+, and F can be represented by the lines with arrows given in Fig. 4a. If vertices are included in an electron line it is necessary to put an arrow next to the vertex. If the interaction Hamiltonian includes products $\psi_\alpha^+(y')\psi_\alpha(y)$ (this always occurs in our problem) the arrows around the vertex must be aimed in the same direction. There are then two possibilities: both arrows can be directed towards the left or towards the right. From Fig. 4c it is clear what will be the result of including vertices $\psi^+\psi$ in the functions G, F^+, and F. The result can be written in the form

$$\begin{aligned} G(x, x') &\to G(x, y')G(y, x') + F(x, y)F^+(y', x'); \\ F^+(x, x') &\to F^+(x, y')G(y, x') + G(y, x)F^+(y', x'); \\ F(x, x') &\to G(x, y')F(y, x') + F(x, y)G(x', y'). \end{aligned} \quad (31)$$

---

*The technique with three Green functions was worked out by S. T. Beliaev[6] in an application to the Bose gas.

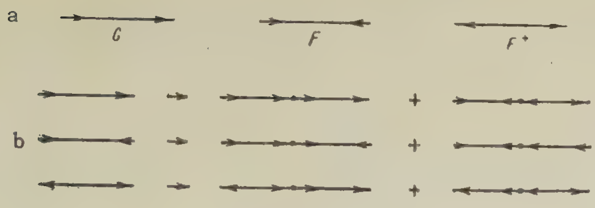

FIG. 4

The inclusion of vertices leads in this way to the appearance of F and F^+ lines in the diagrams for G and similarly to G lines in the diagrams for F and F^+. The equations for G, F^+, and F are therefore more complicated than Eq. (14), obtained by summing the diagrams of Fig. 1 with one G-function.

The derivation of these equations and their solution are given in the Appendix. It turns out that the averaging over the positions of the impurity atoms of the functions $G(p)$ and $F^+(p) = F(p)$ can be obtained from the expressions (30) for a pure superconductor by the substitution

$$\omega;\ \Delta \to \omega\eta;\quad \Delta\eta, \tag{32}$$

where

$$\eta = \begin{cases} 1 + i/2\tau\sqrt{\omega^2 - \Delta^2}; & \omega^2 > \Delta^2, \\ 1 + 1/2\tau\sqrt{\Delta^2 - \omega^2}; & \omega^2 < \Delta^2; \end{cases}$$

τ is the collision time for the metal in its normal state. One can easily verify that, as in Eq. (18) of Sec. 1, these equations signify in coordinate space a multiplication of the function $G_0(x)$ and $F_0^+(x)$ by $e^{-|\mathbf{x}|/2l}$

We now turn to the determination of the function Q_{ik}. This time we have two diagrams corresponding to the simple loop for a normal metal. They are given in Fig. 5. This means that instead of a product of two G's we have now the combination $GG - FF^+$ (the sign is due to the fact that the operator $\nabla_{\mathbf{y}} - \nabla_{\mathbf{y}'}$ occurs in the electromagnetic interaction, which changes sign if the direction of the arrows at the vertex is changed). For the following it will again be convenient for us, taking the two loops of Fig. 5 together, and taking one of the photon vertices p_i separately, to consider the remaining factor as the result of including the photon vertex p_k in the function G. After this Q_{ik} will be of the form (8) and the problem lies in evaluating the vector Π.

To average Π over the impurities we note at once that since superconductivity changes the Green functions only near the Fermi surface we need again only sum over ladder graphs of the type given in Fig. 3b. Owing to the modified diagram technique, we must consider, as can easily be seen from Fig. 6, not one, but four different vectors $\Pi^{(i)}$ $(i = 1, \ldots, 4)$ which occur as a result of including photon vertices in G, F^+, $G^{(-)}$, and F (where $G^{(-)}$ denotes G with the arguments interchanged). The first of these quantities enters directly into the integral (8) for Q_{ik}.

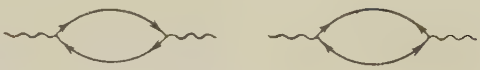

FIG. 5

We obtain easily for the $\Pi^{(i)}$ a set of four integral equations. The first one of them is obtained with the aid of Fig. 6 and has the form:

$$\Pi^{(1)}(p_+, p_-) = \mathbf{p}\,[G(p_+)\,G(p_-) - F(p_+)\,F(p_-)] \tag{33}$$
$$+ G(p_+)\,G(p_-)\,\Lambda^{(1)} + F(p_+)\,G(p_-)\,\Lambda^{(2)}$$
$$+ F(p_+)\,F(p_-)\,\Lambda^{(3)} + G(p_+)\,F(p_-)\,\Lambda^{(4)}.$$

The quantities $\Lambda^{(i)}$ $(\omega, \omega_0, \mathbf{k}, \mathbf{p})$ are the integrals (23) of the $\Pi^{(i)}(p_+, p_-)$. The remaining equations are obtained in a similar way. We shall not write them down since, as was pointed out above, we only need $\Pi^{(1)}(p_+, p_-)$.

As was already noted, for high impurity concentrations the role of the correlation length is assumed here not by $\xi_0 = v/\Delta$ but by the mean free path l. As the impurity concentration increases this length decreases. We shall consider here the case where l is much less than the penetration depth. It is then natural to expect a local connection between the current and the vector potential. The case considered is characterized by the condition $kl \ll 1$, which leads to a considerably simplified equation.

Indeed, neglecting $\mathbf{k}$, we obtain $\mathbf{p}_+ = \mathbf{p}_-$. It is easy to check that in that case $\Lambda^{(i)}(\omega, \omega_0, \mathbf{k}, \mathbf{p}) \approx \mathbf{p}\Lambda^{(i)}(\omega, \omega_0)$ and

$$\Lambda^{(3)}(\omega, \omega_0) = -\Lambda^{(1)}(\omega, \omega_0); \quad \Lambda^{(2)}(\omega, \omega_0) = \Lambda^{(4)}(\omega, \omega_0). \tag{34}$$

The set of equations for $\Lambda^{(1,2)}$ takes the form

$$\mathbf{p}\Lambda^{(1)}(\omega, \omega_0) = \frac{n}{(2\pi)^3}\int |u(\mathbf{p} - \mathbf{p}')|^2\,\mathbf{p}'\,\{[G(p'_+)\,G(p'_-)$$
$$- F(p'_+)\,F(p'_-)] \times [1 + \Lambda^{(1)}(\omega, \omega_0)]$$
$$+ [F(p'_+)\,G(p'_-) + G(p'_+)\,F(p'_-)]\,\Lambda^{(2)}(\omega, \omega_0)\}\,d^3\mathbf{p}; \tag{35}$$
$$\mathbf{p}\Lambda^{(2)}(\omega, \omega_0) = \frac{n}{(2\pi)^3}\int |u(\mathbf{p} - \mathbf{p}')|^2\,\mathbf{p}'\,\{[F(p'_+)\,G(p'_-)$$
$$- G(-p'_+)\,F(p'_-)]\ [1 + \Lambda^{(1)}(\omega, \omega_0)]$$
$$+ [G(-p'_+)\,G(p'_-) + F(p'_+)\,F(p'_-)]\,\Lambda^{(2)}(\omega, \omega_0)\}\,d^3\mathbf{p}.$$

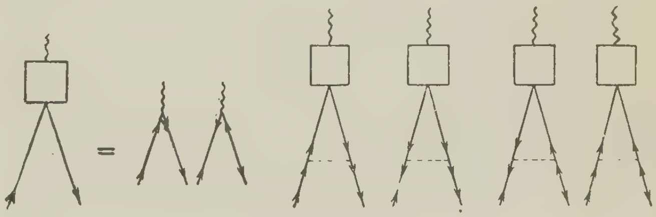

FIG. 6

Substituting into (35) the expressions (30) and (32) for the functions G and F, integrating over ξ, and using the relation (25) we arrive at the following expressions for the quantities of interest to us:

$$\Lambda^{(1)}(\omega, \omega_0) = \frac{i}{2\tau_1} \frac{1 - (\omega_+\omega_- + \Delta^2) / \sqrt{\omega_+^2 - \Delta^2}\sqrt{\omega_-^2 - \Delta^2}}{\sqrt{\omega_+^2 - \Delta^2} + \sqrt{\omega_-^2 - \Delta^2} + i/\tau_{tr}};$$

$$\Lambda^{(2)}(\omega, \omega_0) = \frac{\Delta}{2\tau_1} \frac{2\omega}{\sqrt{\omega_+^2 - \Delta^2}\sqrt{\omega_-^2 - \Delta^2}\left[\sqrt{\omega_+^2 - \Delta^2} + \sqrt{\omega_-^2 - \Delta^2} + i/\tau_{tr}\right]}. \tag{36}$$

Substituting (34) and (36) into (33) we find $\Pi^{(1)}(p_+, p_-)$ and substituting this into Eq. (8) we get an expression for Q:

$$Q_{ik}(\omega_0) = \delta_{ik}\left\{\frac{Ne^2}{mc} - \frac{ie^2N}{2\pi mc}\int d\xi \int_C d\omega[((\omega_+\omega_- + \Delta^2)\eta_+\eta_- + \xi^2)\right.$$

$$\times (1 + \Lambda^{(1)}(\omega, \omega_0)) + 2i\Delta\omega\Lambda^{(2)}(\omega, \omega_0)] \tag{37}$$

$$\times \frac{1}{[\xi^2 - (\omega_+^2 - \Delta^2)\eta_+^2][\xi^2 - (\omega_-^2 - \Delta^2)\eta_-^2]}.$$

The contour around the singular points in the integral over ω is given in Fig. 7a for the case $\omega_0 < 2\Delta$ and in Fig. 7c for the case $\omega_0 > 2\Delta$. Before performing the integration (37) we note that the integral of the first term in (33) diverges. One must therefore observe the well-known caution in the problem of the order of integration over ω and ξ. A closer inspection shows that one must first integrate by parts.

We first find the penetration depth of a static magnetic field into a superconductor. The latter is connected with Q_{ik} by the relation

$$\delta = \sqrt{\frac{c}{4\pi Q(0)}}; \quad \text{if } Q_{ik} = \delta_{ik}Q). \tag{38}$$

The contour C in Fig. 7a can in the case $\omega_0 = 0$ conveniently be deformed so that the integration over ω is performed along the imaginary axis (this is possible because of the decrease of the expression under the integral sign as $\omega \to \infty$):

$$Q_{ik}(0) = \delta_{ik}Q(0) = \frac{Ne^2}{mc}\delta_{ik}\left\{1\right.$$

$$+ \frac{1}{2\pi}\iint_{-\infty}^{\infty} d\xi\, d\omega \frac{1 + \dfrac{\Delta^2}{2\tau_1(\omega^2 + \Delta^2)\left(\sqrt{\omega^2 + \Delta^2} + 1/2\tau_{tr}\right)}}{\xi^2 + (\sqrt{\omega^2 + \Delta^2} + 1/2\tau_{tr})^2}$$

$$\left. - \frac{1}{\pi}\iint_{-\infty}^{\infty} \frac{d\xi\, d\omega\, \omega^2\left(1 + \dfrac{1}{2\tau\sqrt{\omega^2 + \Delta^2}}\right)^2}{[\xi^2 + (\sqrt{\omega^2 + \Delta^2} + 1/2\tau_{tr})^2]^2}\right\}.$$

Integrating by parts over ω in the first term of the first integral makes it possible formally to cancel the diverging terms in that expression. In the remaining double integral one can change the order of integration. The integral over ξ is at once performed:

$$Q(0) = \frac{Ne^2}{mc}\left\{1 - \frac{\Delta^2}{4\tau_{tr}}\int_{-\infty}^{\infty} \frac{d\omega}{(\omega^2 + \Delta^2)^{3/2}(\sqrt{\omega^2 + \Delta^2} + 1/2\tau_{tr})}\right\}.$$

After that we integrate over ω and find

$$Q(0) = \frac{Ne^2}{mc}\tau_{tr}\Delta\begin{cases}\pi - \dfrac{4\tau_{tr}\Delta}{\sqrt{1 - (2\tau_{tr}\Delta)^2}}\cosh^{-1}\dfrac{1}{2\tau_{tr}\Delta}; & 2\tau_{tr}\Delta < 1,\\ \pi - \dfrac{4\tau_{tr}\Delta}{\sqrt{(2\tau_{tr}\Delta)^2 - 1}}\arccos\dfrac{1}{2\tau_{tr}\Delta}; & 2\tau_{tr}\Delta > 1.\end{cases} \tag{39}$$

Substituting this into Eq. (38) we can from this obtain the penetration depth. If $\tau_{tr}\Delta \ll 1$ it is (in the usual units) of the form

$$\delta = \frac{c}{2\pi}\sqrt{\hbar/\sigma\Delta}, \tag{40}$$

where $\sigma = Ne^2\tau_{tr}/m$ is the conductivity of the metal in the normal state. In the case $\tau_{tr}\Delta \gg 1$ the expression for the penetration depth goes over into the usual London formula:

$$\delta = \sqrt{mc^2/4\pi Ne^2}.$$

It is well known[1] that pure superconductors fall into two classes: in one we have $\delta > v/\Delta$ for all temperatures; they can be called London superconductors. In that case there is no limit whatever for the quantity $\tau_{tr}\Delta$. For the other superconductors, which can be called Pippard superconductors, we have $\delta < v/\Delta$ at $T = 0$. In that case from the condition $l \ll \delta$ follows always that $\tau_{tr}\Delta \ll 1$. The Pippard superconductors are thus described by Eq. (40) for $l \ll \delta$. In the case when the mean free path $l \gg \delta$ the theory developed in reference 1 is clearly correct for Pippard superconductors,

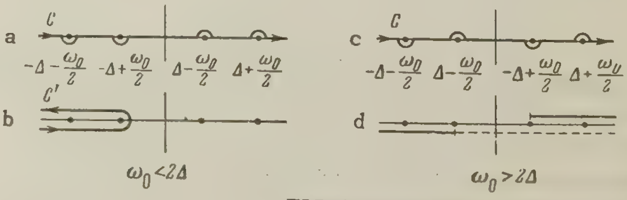
a
C
$-\Delta-\frac{\omega_0}{2}$
$-\Delta+\frac{\omega_0}{2}$
$\Delta-\frac{\omega_0}{2}$
$\Delta+\frac{\omega_0}{2}$
b
C'
$\omega_0<2\Delta$
c
C
$-\Delta-\frac{\omega_0}{2}$
$\Delta-\frac{\omega_0}{2}$
$-\Delta+\frac{\omega_0}{2}$
$\Delta+\frac{\omega_0}{2}$
d
$\omega_0>2\Delta$

FIG. 7

independent of the relation between l and v/Δ. From this theory we obtain

$$Q(k, 0) = \frac{3\pi^2}{4mc} \frac{Ne^2\Delta}{vk}. \qquad (41)$$

Comparison of (40) and (41) shows that Eq. (40) must be used, if

$$\delta / l_{tr} \gg 3\pi / 4. \qquad (42)$$

We now proceed to the case of an alternating field. It is of interest to follow the transition from a superconductor to a normal metal as the frequency ω_0 increases from zero to $\omega_0 \gg \Delta$. We consider only the case $\tau_{tr}\Delta \ll 1$. We subtract from the expression under the integral sign its value at $\omega_0 = 0$. The remainder can then be integrated first over ξ. In the case when $\omega_0 < 2\Delta$ we go over to the contour C′ (Fig. 7b) for the integration over ω. We get

$$Q(\omega_0) = \frac{Ne^2}{mc} \left\{ \int\limits_{\Delta+\omega_0/2}^{\infty} d\omega \left[1 - \frac{\omega_+\omega_- + \Delta^2}{\sqrt{\omega_+^2 - \Delta^2}\sqrt{\omega_-^2 - \Delta^2}} \right] \right.$$

$$\times \frac{\sqrt{\omega_+^2 - \Delta^2} + \sqrt{\omega_-^2 - \Delta^2}}{\left(\sqrt{\omega_+^2 - \Delta^2} + \sqrt{\omega_-^2 - \Delta^2}\right)^2 + 1/\tau_{tr}^2}$$

$$\left. + \tau_{tr} \int\limits_{\Delta-\omega_0/2}^{\Delta+\omega_0/2} \frac{\omega_+\omega_- + \Delta^2}{\sqrt{\omega_+^2 - \Delta^2}\sqrt{\omega_-^2 - \Delta^2}} \right\}.$$

The contribution from the first integral is of the order $(\tau\Delta)^2$ and we can neglect it. The second integral leads to a complete elliptic integral.[7] The final expression has the following form for the case $\omega_0 < 2\Delta$

$$Q(\omega_0) = \frac{2\sigma\Delta}{c} E\left(\frac{\omega_0}{2\Delta}\right). \qquad (43)$$

In particular, we get for $\omega_0 \ll 2\Delta$

$$Q(\omega_0) = \frac{\pi\sigma\Delta}{c}\left[1 - \left(\frac{\omega_0}{4\Delta}\right)^2\right]. \qquad (44)$$

In the case $\omega_0 > 2\Delta$ it is convenient to complete the integral to go from $-\infty$ to $+\infty$ in the lower half-plane (Fig. 7c). This part can then be discarded, since there are no poles in the expression under the integral sign. This makes it possible to simplify the expressions considerably. As a result, Q can be expressed as the sum of elliptic integrals, if $\tau\Delta \ll 1$:

$$Q(\omega_0) = \frac{\sigma}{c}\left\{\omega_0 E(\varkappa) - \frac{\omega_0^2 - (2\Delta)^2}{\omega_0} K(\varkappa) \right.$$
$$\left. - i\left[\omega_0 E(\varkappa_1) - \frac{(2\Delta)^2}{\omega_0} K(\varkappa_1)\right]\right\}, \qquad (45)$$

where $\kappa = 2\Delta/\omega_0$; $\kappa_1 = \sqrt{1-\kappa^2}$.

In particular if $\omega_0 \gg 2\Delta$

$$Q(\omega_0) = -\frac{\sigma\omega_0}{c}\left\{i\left[1 - \frac{2\Delta^2}{\omega_0^2}\left(\ln\frac{2\omega_0}{\Delta} + \frac{1}{2}\right)\right] - \frac{\pi\Delta^2}{\omega_0^2}\right\}. \qquad (46)$$

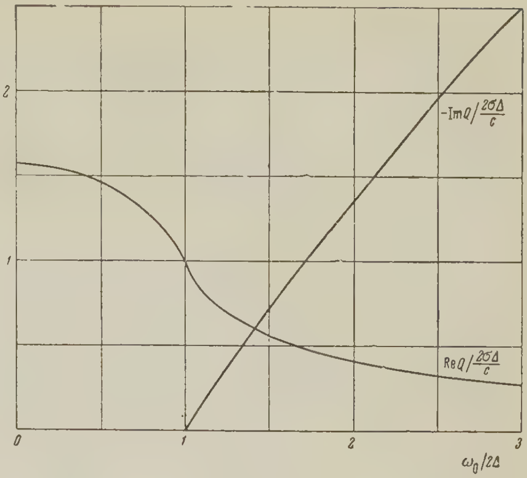

FIG. 8

From Eq. (46) it is clear that if $\omega_0 \gg \Delta$ the superconducting properties disappear; the usual formula for the normal skin effect turns up. It is of interest that the imaginary part of the current corresponding to absorption occurs only for $\omega_0 > 2\Delta$; the connection of this threshold energy and the binding energy of the pairs is evident. Near the threshold $|\omega_0 - 2\Delta| \ll \Delta$ we have:

$$Q = \frac{\sigma}{c}\left[2\Delta + \left(\Delta - \frac{\omega_0}{2}\right)\left(\ln\frac{16\Delta}{2\Delta - \omega_0} - 1\right)\right]; \quad \omega_0 < 2\Delta, \qquad (47)$$
$$Q = \frac{\sigma}{c}\left[2\Delta - \left(\frac{\omega_0}{2} - \Delta\right)\left(\ln\frac{16\Delta}{\omega_0 - 2\Delta} - 1 + i\pi\right)\right]; \quad \omega_0 > 2\Delta.$$

In Fig. 8 we have given the complete curves of the dependence of the real and imaginary parts of Q on ω_0. Along the ordinate axis are put $\mathrm{Re}\left[Q\middle/\frac{2\Delta\sigma}{c}\right]$ and $-\mathrm{Im}\left[Q\middle/\frac{2\sigma\Delta}{c}\right]$ in their dependence on $\omega_0/2\Delta$. The impedance of a bulk specimen with a plane surface is obtained with the aid of Eq. (4) and is of the form

$$Z = -\frac{i\omega_0}{c}\sqrt{\frac{4\pi}{cQ(\omega_0)}}; \qquad (48)$$

If Q is complex the radical means the analytical continuation of that quantity which is positive for real Q.

The Eqs. (39), (40), and (43) to (48) describe completely the behavior of alloys in a constant or alternating weak electromagnetic field at $T = 0$. Apart from alloys, these expressions can also be applied to films of a pure substance with a thickness less than the penetration depth. Such films are as a rule polycrystalline and the dimensions of the crystallites are not more than the film thickness. The presence of boundaries between the crystallites will lead to a break-up of the correlation. The local character of the connection in the case $\delta \gg l$ makes it possible to apply the results obtained above to films without any changes. It may then turn out to be convenient to use the complex dielectric susceptibility which is connected with Q through the relation

$$\varepsilon = -4\pi c Q/\omega^2 \tag{49}$$

In conclusion the authors use this opportunity to express their gratitude to Academician L. D. Landau for his constant attention and valuable remarks.

APPENDIX

In the case of the superconducting alloy the equations replacing (14) are easily found by drawing the corresponding diagrams. They are of the form

$$G(\mathbf{p}, \mathbf{p}', \omega) = G_0(p)\,\delta(\mathbf{p}-\mathbf{p}')$$
$$+ \frac{1}{(2\pi)^3}\Big\{G_0(p)\int u(\mathbf{p}-\mathbf{p}'')\sum_a e^{i(\mathbf{p}-\mathbf{p}'')\mathbf{x}_a}\,G(\mathbf{p}'', \mathbf{p}', \omega)\,d^3\mathbf{p}''$$
$$+ F_0(p)\int u(\mathbf{p}-\mathbf{p}'')\sum_a e^{i(\mathbf{p}-\mathbf{p}'')\mathbf{x}_a}\,F^+(\mathbf{p}'', \mathbf{p}', \omega)\,d^3\mathbf{p}''\Big\};$$

$$F^+(\mathbf{p}, \mathbf{p}', \omega) = F_0^+(p)\,\delta(\mathbf{p}-\mathbf{p}') \tag{A.1}$$
$$+ \frac{1}{(2\pi)^3}\Big\{F_0(p)\int u(\mathbf{p}-\mathbf{p}'')\sum_a e^{i(\mathbf{p}-\mathbf{p}'')\mathbf{x}_a}\,G(\mathbf{p}'', \mathbf{p}', \omega)\,d^3\mathbf{p}''$$
$$+ G_0(-p)\int u(\mathbf{p}-\mathbf{p}'')\sum_a e^{i(\mathbf{p}-\mathbf{p}'')\mathbf{x}_a}\,F^+(\mathbf{p}'', \mathbf{p}', \omega)\,d^3\mathbf{p}''\Big\}$$

In principle it is necessary to consider also the equations for the function $-I_{\alpha\beta}F(x, x') = \langle T(\psi_\alpha(x)\psi_\beta(x'))\rangle$.

For a pure superconductor $F(x, x') = F^+(x, x')$. This property will be true also for alloys after Eq. (A.1) is averaged over the positions of the impurity atoms.

The averaging is performed exactly as in Sec. 1. Using the equations[4] that are satisfied by the functions $G_0(p)$ and $F_0(p)$, this set can be put into a very simple form:

$$(\omega - \xi - \overline{G_\omega})\,G(p) + (i\Delta - \overline{F_\omega^+})\,F^+(p) = 1,$$
$$(\omega + \xi - \overline{G_\omega})\,F^+(p) - (i\Delta - \overline{F_\omega^+})\,G(p) = 0.$$

The solution of this set is

$$G(p) = \frac{\omega - \overline{G_\omega} + \xi}{(\omega - \overline{G_\omega})^2 + (i\Delta - \overline{F_\omega^+})^2 - \xi^2};$$
$$F^+(p) = \frac{i\Delta - \overline{F_\omega^+}}{(\omega - \overline{G_\omega})^2 + (i\Delta - \overline{F_\omega^+})^2 - \xi^2}. \tag{A.2}$$

Remembering the definition of $\overline{G}_\omega$ we see that as before $\overline{G}_\omega$ contains a constant term which means a renormalization of the chemical potential and which arises from the integration far from the Fermi surface:

$$\delta\mu = \frac{n}{(2\pi)^3}\int \frac{|u(\mathbf{p}-\mathbf{p}')|^2\,\xi\,d\xi}{(\omega - G_\omega)^2 + (i\Delta - F_\omega^+)^2 - \xi^2}.$$

After subtracting this term, the remaining part of $\overline{G}_\omega$ is apart from a coefficient determined by the same integral as $\overline{F_\omega^+}$, as is clear from (A.2). In this way

$$\overline{G_\omega}/\omega = \overline{F_\omega^+}/\Delta.$$

After this it is easy to find that the solution of the set (A.2) gives Eqs. (30) and (32).

---

[1] Bardeen, Cooper, and Schrieffer, Phys. Rev. 108, 1175 (1957).

[2] L. N. Cooper, Phys. Rev. 104, 1189 (1956).

[3] Abrikosov, Gor'kov, and Khalatnikov, J. Exptl. Theoret. Phys. (U.S.S.R.) 35, 265 (1958), Soviet Phys. JETP 8, 182 (1959); D. C. Mattis and J. Bardeen, Phys. Rev. 111, 412 (1958).

[4] L. P. Gor'kov, J. Exptl. Theoret. Phys. (U.S.S.R.) 34, 735 (1958), Soviet Phys. JETP 7, 505 (1958).

[5] N. N. Bogoliubov, J. Exptl. Theoret. Phys. (U.S.S.R.) 34, 58, 73 (1958), Soviet Phys. JETP 7, 41, 51 (1958); V. V. Tolmachev and S. V. Tiablikov, J. Exptl. Theoret. Phys. (U.S.S.R.) 34, 66 (1958), Soviet Phys. JETP 7, 46 (1958).

[6] S. T. Beliaev, J. Exptl. Theoret. Phys. (U.S.S.R.) 34, 417 (1958), Soviet Phys. JETP 7, 289 (1958).

[7] E. Jahnke and F. Emde, Tables of Functions, Dover, New York, 1945.

Translated by D. ter Haar
322

Letters to the Editor

WAVE SOLUTIONS OF NONLINEAR GENERALIZATIONS OF RELATIVISTIC EQUATIONS

D. F. KURDGELAIDZE

Moscow State University

Submitted to JETP editor July 8, 1958

J. Exptl. Theoret. Phys. (U.S.S.R.) 35, 1572-1573 (December, 1958)

ACCORDING to the general idea of the nonlinear unified field theory, the entire set of elementary particles is constructed from one fundamental spinor field. Since, however, the spinor equation is taken to be nonlinear, the fields obtained for the other particles are also nonlinear.

The relativistically-invariant equation for the elementary particles can, in the linear theory, be written in the well-known general form[1]

$$(\Gamma_\mu \partial / \partial x_\mu + k_0)\psi = 0, \qquad (1)$$

where Γ_μ is a matrix; in particular, if $\Gamma_\mu = \gamma_\mu$, we have the Dirac equation, if $\Gamma_\mu = \beta_\mu$, the Duffin-Kemmer equation, etc.

As was shown in reference 1, there exists a nondegenerate invariant form $y \equiv (\psi^* T \psi)$ (T is a matrix) for all finite-dimensional representations of the full Lorentz group. Hence, if we change k_0 in (1) to $C(y) = k_0 + f(y)$, we again obtain a relativistically invariant equation

$$(\Gamma_\mu \partial / \partial x_\mu + C(y))\psi = 0, \qquad (2)$$

which is now nonlinear.

We arrive at an equation of this form, if, for example, all particles are "merged" into one field obeying the nonlinear generalization of the Dirac equation in conformity with group theory:

$$(\gamma_\mu \partial / \partial x_\mu + A(y))\psi = 0. \qquad (3)$$

As in the linear theory, Eq. (3) is an irreducible representation $D_{1/2}$ in the space of the basis vectors $\{\psi_k\}$. By forming the product $D_{1/2} \times D_{1/2}$ from two spinor equations of form (3), we obtain then the irreducible representations $D_0 + D_1$ in the space of the basis vectors $\{\psi_i \psi_k\} \equiv \{\psi_{ik}\}$. We write the resulting equation in the general form

$$(\beta_\mu \partial / \partial x_\mu + B(y))\psi = 0. \qquad (4)$$

In reference 2 we determined the exact wave solutions of Eq. (3). The method developed there may, however, also be applied to the general equation (2). Indeed, if we require a solution in the form

$$\psi_\alpha = u_\alpha(\varepsilon, \alpha_1 \ldots \alpha_i, k_\mu)\varphi(\sigma), \quad \sigma = k_\mu x_\mu, \quad u^*_\alpha u_\alpha = 1,$$
$$k_\mu = (k_n, i\omega), \quad \omega = \varepsilon E, \quad \varepsilon = \pm 1, \quad c = \hbar = 1, \qquad (5)$$

where $\epsilon, \alpha_1, \ldots, \alpha_i$ are parameters specifying the state of the particles, Eq. (2) takes the form

$$(\Gamma_\mu k_\mu d\varphi / d\sigma + C(\rho)\varphi)u(\varepsilon, \alpha_1, \ldots \alpha_i, k_\mu) = 0, \quad \rho = \varphi^*\varphi, \qquad (6)$$

We further add the conjugate equation

$$\bar{u}(\varepsilon, \alpha_1 \ldots \alpha_i, k_\mu)(\Gamma_\mu k_\mu d\varphi^* / d\sigma - \bar{C}(\rho)\varphi^*) = 0. \qquad (7)$$

If we now subject the functions $\varphi(\sigma)$ and $\varphi^*(\sigma)$ to the system of equations (2.4) of reference 2, we obtain for the amplitude

$$(i\Gamma_\mu k_\mu + \lambda)u = 0, \quad \bar{u}(i\Gamma_\mu k_\mu + \lambda) = 0. \qquad (8)$$

$\varphi(\sigma)$ and $\varphi^*(\sigma)$ were determined in reference 2. The solutions of (8) can be taken from the linear theory. In particular, in the case of equation (4), where $\Gamma_\mu = \beta_\mu$, we have $\bar{\psi} = \psi^* \eta_4$, $\eta_4 = 2\beta_4^2 - 1$, $\bar{C}(y) = C^*(y)$, with the solutions of equation (8) known from reference 3.

On the other hand, if $C(y)$ has a form such that the four-dimensional current is conserved,

$$\frac{\partial}{\partial x_\mu}(\bar{\psi}\Gamma_\mu\psi) = (\bar{u}\Gamma_\mu k_\mu u)\frac{d}{d\sigma}(\varphi^*\varphi) = 0, \qquad (9)$$

then $\varphi^*\varphi = \text{const}$, or $(\bar{u}\Gamma_\mu k_\mu u) = -\lambda(\bar{u}u) = 0$.

The unique complex solution $\varphi(\sigma)$ $\varphi^*(\sigma)$ is given by (2.13) of reference 2. The real solution $\varphi^* = \varphi \neq \text{const}$ leads to $(\bar{u}\Gamma_\mu k_\mu u) = -\lambda(\bar{u}u) = 0$. These solutions were found in reference 2 with $\Gamma_\mu = \gamma_\mu$ and the normalization $u^*u = 1$.

We further note that, since the equation for $\varphi(\sigma)$ with given $C(y)$ has identical form for all $\Gamma_\mu = \gamma_\mu$, β_μ, etc., the quadratic equation resulting from it also has the same form for all fields (just as the relativistic wave equation in the linear theory).

I regard it as my obligation to express my deep gratitude to D. D. Ivanenko and G. A. Sokolik for a discussion of this paper.

---

[1] I. M. Gel'fand and A. M. Iaglom, J. Exptl. Theoret. Phys. (U.S.S.R.) 18, 703 (1948).

[2] D. F. Kurdgelaidze, J. Exptl. Theoret. Phys. (U.S.S.R.) 32, 1156 (1957); Soviet Phys. JETP 5, 941 (1957).

[3] F. Booth and A. Wilson, Proc. Roy. Soc. A175, 483 (1940).

Translated by R. Lipperheide
323

NONLINEAR INTERACTION OF RADIO WAVES PROPAGATING IN A PLASMA

V. L. GINZBURG

P. N. Lebedev Physics Institute, Academy of Sciences, U.S.S.R.

Submitted to JETP editor, August 23, 1958

J. Exptl. Theoret. Phys. (U.S.S.R.) 35, 1573-1575 (December, 1958)

WHEN high-power radio waves propagate in a plasma, in particular, in the earth's ionosphere, several nonlinear effects are observed: cross-modulation (the Luxemburg effect) and the interaction of unmodulated radio waves with their "self-effect" (cf. for example reference 1, §64 and references 2 and 3. In the work cited above consideration has been given only to the nonlinearity associated with the dependence of the effective number of collisions ν_{eff} on the field strength $\mathbf{E}_1$ of a strong radio wave, say 1. In the simplest case, in which radio wave 1 is unmodulated, $\mathbf{E}_1 = \mathbf{E}_0 \cos(\omega t - \mathbf{k}\cdot\mathbf{r}) = \mathbf{E}_0 \cos\varphi$; the condition $\omega^2 \gg \nu_{\text{eff}}^2$ is satisfied and we can neglect the constant magnetic field. In this case the nonlinear effect is simply related to the change in electron velocity. The velocity associated with the forced oscillations is $\mathbf{v}_1 = (e/m\omega)\,\mathrm{E}_0 \sin\varphi$ and the change in the absolute magnitude of the velocity is $\Delta v \approx e^2 E_0^2 \sin^2\varphi/2m^2\omega^2 v_0$ where $v_0 \sim \sqrt{\kappa T/m}$ is the velocity associated with the thermal motion (e and m are the charge and mass of the electron and it is assumed that $\Delta v \ll v = v_0 + \Delta v$).

The corresponding change in electrical conductivity is

$$\Delta\sigma/\sigma = \Delta\nu_{\text{eff}}/\nu_{\text{eff}} = \Delta v/v_0 = e^2 E_0^2 \sin^2\varphi / 2m^2 v_0^2 \omega^2, \quad (1)$$

since $\sigma = e^2 N\nu_{\text{eff}}/m\omega^2$, where N is the electron concentration. For simplicity, it is assumed that the basic role is played by collisions of electrons with molecules, so that ν_{eff} is proportional to the velocity v. When the electron velocity distribution, modulation etc. are taken into account the picture becomes more complicated. These effects, however, will not be important in what follows, since we wish to point out the existence of a nonlinear effect of another kind.

In a non-uniform isotropic plasma (also in a uniform magneto-plasma), in contrast with an isotropic uniform plasma, the electron concentration depends on the field associated with the radio wave. In the absence of transverse charges, when $\operatorname{div} \epsilon'\mathbf{E} = 0$, in an isotropic non-uniform medium we have

$$\operatorname{div}\mathbf{E} = 4\pi\bar{\rho} = -\mathbf{E}\cdot\nabla\varepsilon'/\varepsilon',$$

where $\epsilon' = \epsilon - i4\pi\sigma/\omega$ is the complex dielectric permittivity. If the ion motion is neglected in the plasma, we have $\bar{\rho} = e\Delta N$ where ΔN is the change in electron concentration. Thus wave 1 produces a change

$$\begin{aligned}\Delta\varepsilon' &= -4\pi e^2\,\Delta N / m\omega(\omega - i\nu_{\text{eff}}) \\ &= e\mathbf{E}\cdot\nabla\varepsilon' / m\varepsilon'\omega(\omega - i\nu_{\text{eff}}),\end{aligned} \quad (2)$$

since

$$\varepsilon' = 1 - 4\pi e^2 N / m\omega(\omega - i\nu_{\text{eff}}).$$

In a magneto-plasma, which for simplicity we also consider uniform and nonabsorbing, for $\operatorname{div}\mathbf{D} = \partial(\epsilon_{ik}E_k)/\partial x_i = 0$ generally speaking $\operatorname{div}\mathbf{E} = 4\pi e\Delta N \neq 0$. We consider a plane wave in a magneto-active medium, having in mind elliptical polarization of the general form

$$\mathbf{E}_1 = \mathbf{E}_{0a}\cos\varphi + \mathbf{E}_{0b}\sin\varphi,$$

obviously

$$\frac{\Delta N}{N} = -\frac{\omega n/c}{4\pi eN}\{E_{0a}\cos\theta_a \sin\varphi + E_{0b}\cos\theta_b\cos\varphi\}, \quad (3)$$

where $\varphi = \omega t - \mathbf{k}\cdot\mathbf{r}$, $n = ck/\omega$ is the refractive index for the given wave, which is assumed to be normal (ordinary and extraordinary components) and θ_a and θ_b are the angles between $\mathbf{E}_{0a}$, $\mathbf{E}_{0b}$ and $\mathbf{k}$. All these quantities can be found from the general formulas (cf. reference 1, §§62 and 75). The change in electron concentration ΔN is proportional to the change in the complex permittivity tensor for the magneto-active plasma ϵ'_{ik}. If the external magnetic field is strong and we neglect unusual directions of propagation (for example, along the pole) $\cos\theta_a$ and $\cos\theta_b$, can be quantities of order unity. In such cases the effect given by (3) is larger than the effect given by (2) if the wavelength $\lambdabar = cn/\omega$ is smaller than the characteristic distance L, the distance in which there is a significant change in the properties of the medium.

It is clear from (1) and (3) that the relation between the present nonlinear effect and the one usually considered is characterized by the parameter

$$\xi = m^2 v^2 \omega^3 n / 2\pi c e^3 N E_0. \quad (4)$$

with $n \sim 1$, $v \sim 10^7$ ($T \sim 300°K$), $\xi \sim 10^{-23}\omega^3/NE_0$. It is apparent that with $N \sim 10^5$ and $\omega \sim$

10^7 ($\lambda = 2\pi c/\omega \sim 180$ m), $\xi \sim 1$ for a field $E_0 \sim 1/300$ v/m.

It is important to note that the usual effect (1) is a quadratic effect and leads to the appearance of combination frequencies $\omega' \pm 2\omega$ (ω' is the frequency of the field of a weak radiowave which propagates in a medium which is perturbed by a strong wave at frequency ω). On the other hand, the effects in (2) and (3) are linear* with respect to field 1 and the combination frequencies are $\omega' \pm \omega$.

It should be noted that effects (2) and (3) are, by their nature, the same as occur in the scattering of transverse (radio) waves on plasma waves in an isotropic medium (cf. references 4 and 5).†

The concrete role played by the effect described in (2) and (3) on the propagation of radio waves in the ionosphere of the earth and the solar corona require special investigation.

---

*Obviously we are considering here the nonlinear dependence of the tensor ε'_{ik} on the field. In this case the field equations are clearly nonlinear.

†We note that the existence, of plasma oscillations excited by various perturbations in the ionosphere can be verified experimentally by observing on earth radio waves in which combination frequencies are produced as a result of scattering in the ionosphere.

[1] Al'pert, Ginzburg, and Feinberg, Распространение радиоволн (Propagation of Radio Waves) Gostekhizdat, Moscow, 1953.

[2] I. M. Vilenskii, J. Exptl. Theoret. Phys. (U.S.S.R.) 22, 544 (1952); 26, 42 (1954).

[3] A. V. Gurevich, Радиотехника и электроника (Radio Engineering and Electronics) 1, 704 (1956); Радиофизика (Изв. Вузов) (Radio Physics, Bull. of the Colleges) 1, 4-5 (1958).

[4] Akhiezer, Prokhoda and Sitenko, J. Exptl. Theoret. Phys. (U.S.S.R.) 33, 750 (1957), Soviet Phys. JETP 6, 576 (1958).

[5] V. L. Ginzburg and V. V. Zhelezniakov, Астрономич. журн. (Astronom. J.) 35, 694 (1958).

Translated by H. Lashinsky
324

ELECTRON-POSITRON PAIRS FROM THE DECAY $\pi^0 \rightarrow e^- + e^+ + \gamma$

Iu. A. BUDAGOV, S. VIKTOR, V. P. DZHELEPOV, P. F. ERMOLOV, and V. I. MOSKALEV

Joint Institute for Nuclear Research

Submitted to JETP editor August 26, 1958

J. Exptl. Theoret. Phys. (U.S.S.R.) 35, 1575-1577 (December, 1958)

FOURTEEN events of charge-exchange scattering of π^- mesons on hydrogen with the subsequent decay of the π^0 meson into a photon and a Dalitz electron-positron pair[2] were observed in a diffusion chamber filled with hydrogen at 25 atmos and placed in the 150 Mev π^--meson beam of the synchrocyclotron of the Joint Institute for Nuclear Research.[1] The sensitive volume of the chamber measured 380 mm in diameter. A constant magnetic field of 9000 Oe intensity was used. The 14 events mentioned were found in the scanning of 45,000 stereophotographs and were identified by π^--meson track endings in hydrogen accompanied by electron-positron pairs. Photographs of two such events are shown in Fig. 1. It is estimated that other processes giving rise to similar pairs (internal conversion of photons in the reaction $\pi + p \rightarrow n + \gamma$, pair creation by a photon near the decay point of $\pi^0 \rightarrow 2\gamma$, etc) are negligible under our experimental conditions.

The number of conventional π^0-meson decays (into two photons) must be known in order to determine the relative probability for the decay process $\pi^0 \rightarrow e^- + e^+ + \gamma$. Direct counting of the number of charge exchange events is extremely difficult in a diffusion chamber, owing to the existence of local insensitive regions and to edge effects. However the number of π^0 mesons can be determined from data on the cross sections for charge-exchange and elastic π^--p scattering,[3] whose ratio is 1.8 at energies ~150 Mev. Since we observed 600 events of elastic π^--p scattering it follows that the number of π^0 mesons was 1080. Consequently the ratio of the probabilities for the

Pair No.	E^- (Mev)	E^+ (Mev)	$E=E^-+E^+$ (Mev)	α° (lab. frame)	θ° (lab. frame)
1	—	—	—	2.5	118
2	>134	70	>204	16	50
3	19	41	60	36	95
4	106	>24	>130	7	91
5	20	111	131	8	145
6	27	6	33	22	117
7	89	67	156	6	50
8	>14	>96	>110	>5	100
9	—	—	—	2	110
10	>58	103	>161	53	140
11	36	>134	>170	3	99
12	10	24	34	38	86
13	166	20	186	28	65
14	22	27	49	46	118.5

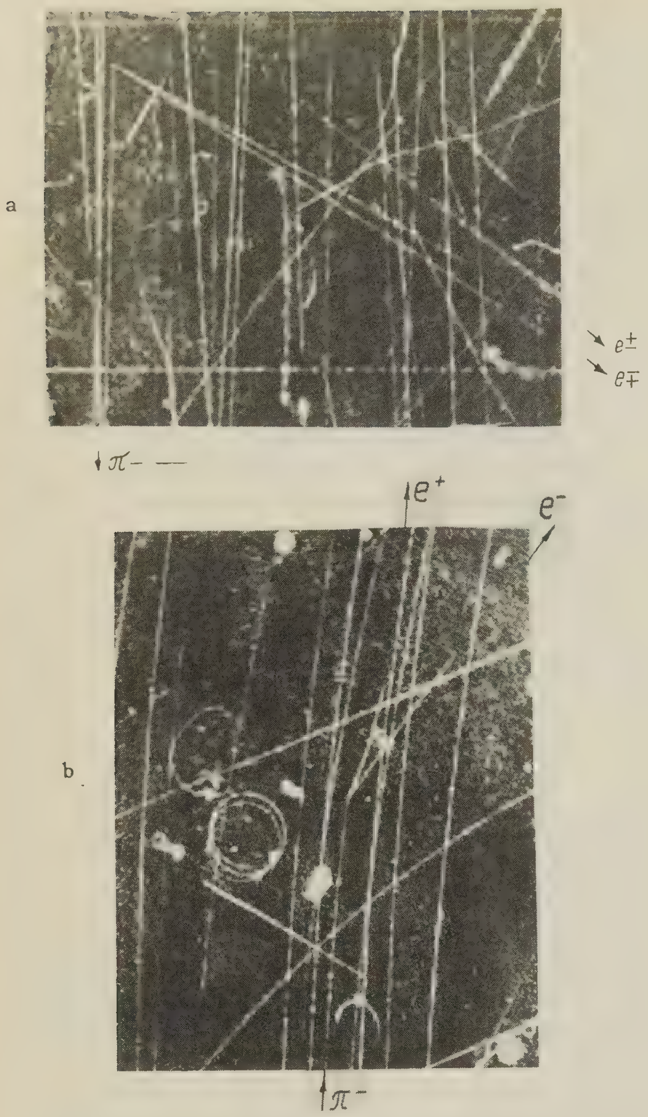

FIG. 1. Photographs of $\pi^- + p \to \pi^0 + n$ followed by the decay $\pi^0 \to e^- + e^+ + \gamma$, as seen in the diffusion chamber: a) pair No. 1, b) pair No. 2.

decays $\pi^0 \to e^- + e^+ + \gamma$ and $\pi^0 \to 2\gamma$ is $2\rho_0 = 0.0130 \pm 0.0024$ and the coefficient of internal conversion for this reaction is $\rho_0 = 0.0065 \pm 0.0012$, the indicated error being the probable statistical error. This value for ρ_0 is in good agreement with theoretical calculations[2,4] as well as with experimental data.[5-8]*

The results of the analysis of the electron-positron pairs are given in the table. The electron energy E^- and the positron energy E^+ were determined to an accuracy of 10 to 15% or better from the radii of curvature of the tracks. Only lower limits for these energies are given in the case of very short tracks. The No. 1 and No. 9 pairs were found in film exposed without a magnetic field. A comparison of E^- and E^+ fails to show any tendency for the energy to be divided equally between the members of a pair, which tendency appeared in the experiments of Sargent et al[8] and also especially in those of Anand.[6] The total energy $E = E^- + E^+$ lies in the interval 17 to 270 Mev for all pairs, corresponding to the energy spectrum of γ rays from the decay of π^0 mesons obtained as a product of the charge-exchange process.

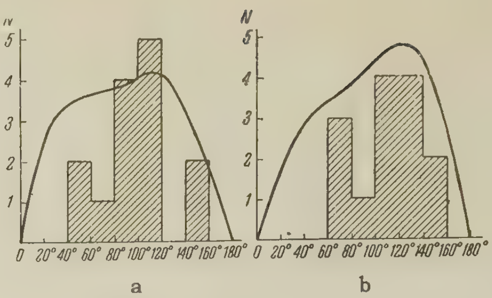

FIG. 2. a) θ(lab. frame), b) $\theta(\pi^- - p$ c.m. frame).

The last columns of the table give the correlation angle α (laboratory frame) between the electron and the positron of a pair, and the angle θ (laboratory frame) between the direction of motion of the center-of-mass of the pair and incident π^- meson. The accuracy of measurement of the angles α is ±1° or better, of the angles $\theta - \pm 2°$ or better. The overall form of the angular distribution of the pairs in the angle α is in agreement with the dependence $P(\alpha)d\alpha \approx \text{const}\, d\alpha/\alpha$ obtained by Dalitz.[2] The angular distribution of the pairs relative to the direction of the incident π^- mesons is characterized by a preferential emission of pairs into the back hemisphere, analogous to the distribution found by Schein et al.[10] In view of the fact that the electrons and positrons from the decay $\pi^0 \to e^- + e^+ + \gamma$ are well correlated, the angular distribution of the pairs should coincide to a high degree of accuracy with the angular distribution of photons from the $\pi^0 \to 2\gamma$ decay. Figure 2 is a histogram of the angular distribution of pairs relative to the direction of the π^- meson obtained in our experiment: a — in the laboratory frame, and b — in the π^--p center-of-mass frame. There is no contradiction with the solid curves which represent, on an arbitrary scale, the angular distribution $(d\sigma/d\Omega) \sin\theta$ of photons from the decay of π^0 mesons obtained from the reaction $\pi^- + p \to \pi^0 + n$ with 150-Mev π^- mesons.[11]

In conclusion we note that in none of the seven pairs whose total energy was measured accurately do the kinematics satisfy the requirements for the $\pi^0 \to e^- + e^+$ decay; nor have we found any cases of $\pi^0 \to e^- + e^+ + e^- + e^+$ in the scanned photographs.

We are continuing this work and the final results and analysis will be reported later.

The authors are grateful to L. I. Krasnoslobodtseva for help in the scanning of photographs.

---

*The internal conversion coefficients of reference 8 were obtained by using the value P = 0.94 ± 0.20 for the Panofsky ratio. If one accepts the value[9] P = 1.15 – 1.9 then the internal conversion coefficients derived from the data of reference 8 are in disagreement with other experiments and with theory.

---

[1] Budagov, Viktor, Dzhelepov, Ermolov, and Moskalev, Report at Conference on Cloud Chambers, Diffusion Chambers, and Bubble Chambers, Joint Inst. for Nucl. Research, November, 1957.

[2] R. H. Dalitz, Proc. Phys. Soc. **A64**, 667 (1951).

[3] L. M. Barkov and B. A. Nikolskii, Usp. Fiz. Nauk **61**, 341 (1957).

[4] N. M. Kroll and W. Wada, Phys. Rev. **98**, 1355 (1955).

[5] Daniel, Davies, Mulvey, and Perkins, Phil. Mag. **43**, 753 (1952).

[6] B. M. Anand, Proc. Roy. Soc. **220A**, 183 (1953).

[7] Lindenfeld, Sachs, and Steinberger, Phys. Rev. **89**, 531 (1953).

[8] Sargent, Cornelius, Rinehart, Lederman, and Rogers, Phys. Rev. **98**, 1349 (1955).

[9] Fischer, March, and Marshall, Phys. Rev. **109**, 533 (1958).

[10] Schein, Fainberg, Haskin, and Glasser, Phys. Rev. **91**, 973 (1953).

[11] Ashkin, Blaser, Feiner, and Stern, Phys. Rev. **101**, 1149 (1956).

Translated by A. M. Bincer
325

---

*MEASUREMENT OF THE POLARIZATION OF INTERNAL CONVERSION ELECTRONS**

V. A. LIUBIMOV and M. E. VISHNEVSKII

Submitted to JETP editor October 10, 1958

J. Exptl. Theoret. Phys. (U.S.S.R.) **35**, 1577-1579 (December, 1958)

As a consequence of parity nonconservation in β decay, the daughter nucleus is polarized along the direction of emission of the β electron. Consequently, the conversion electrons resulting from the internal conversion process following β decay will have definite polarization related to the direction of emission of the β electron.

Formulas for this polarization were obtained by Berestetskii and Rudik[2] and by Geshkenbein.[3] It follows from these formulas that the polarization of conversion electrons depends on the same combination of coupling constants and matrix elements as the angular distribution of electrons from β decay of oriented nuclei.

We report here on the results of measurement of the polarization of internal conversion electrons following the β decay of $\text{Hg}^{203}\left(? \xrightarrow{\beta} 3/2\,+ \xrightarrow{e_K} 1/2\,+\right)$. The β electrons were registered by counters 1 and 2. The conversion electrons, emitted at an angle of 90° with respect to the β electrons, were registered by counters 3 and 4 after passing through a system of magnetic lenses and undergoing scattering through an angle of 125° from a scatterer. The axis of counters 3 and 4 was at an angle of $\pi/2$ with respect to the axis of counters 1 and 2. Amplitude discrimination and the tuning of the spectrometer to the energy of the conversion electrons were used to distinguish the conversion electrons from the β electrons. Counters 3 and 4 were wired in coincidence with counters 1 and 2. The setup was such that β-e_K coincidences were registered separately in counters 1 and 3, 1 and 4, 2 and 3, and 2 and 4.

If the conversion electrons are transversely polarized parallel (or antiparallel) to the direction of emission of the β electrons, then one should observe, in the single scattering by a heavy element thin scatterer, azimuthal asymmetry in the direction of counters 3 and 4, which, in the absence of asymmetries in the apparatus, equals $N_{13}/N_{14} = N_{24}/N_{23} = \alpha < 1$ (or > 1). Here N_{ik} stands for the number of coincidences in counters i and k after subtraction of the background due to accidental coincidences.

The azimuthal asymmetry of the conversion electrons scattered by gold (0.4 mg/cm^2) was found to be

$$\alpha_{\text{Au}} = \sqrt{\frac{N_{13}}{N_{14}}\frac{N_{24}}{N_{23}}} = 1.11 \pm 0.04.$$

The asymmetry inherent in the apparatus was found by using aluminum as a scatterer, which should yield practically no azimuthal asymmetry due to the electron polarization: $\alpha_{\text{Al}} = 0.97 \pm 0.03$. Thus, correcting for apparatus asymmetry, we find

$$\alpha = \alpha_{\text{Au}}/\alpha_{\text{Al}} = 1.15 \pm 0.05.$$

Taking into account the finite thickness of the scatterer yields $\alpha_{corr} = 1.21 \pm 0.07$. Consequently, conversion electrons resulting after the β decay of Hg^{203} are polarized antiparallel to the direction of emission of the β-electrons.

The spin and parity of the ground state of Hg^{203} are unknown. Since, however, the value ln (ft) = 6.4 is not large it is to be expected that the spin of the ground state of Hg^{203} will not differ by more than unity from the spin of the excited state of Tl^{203}, the daughter nucleus in the β decay.

If one assumes that the β-interaction coupling constants satisfy the relations $C_S = -C'_S$, $C_T = -C'_T$, $C_V = C'_V$, $C_A = C'_A$, as established in the experiments on the polarization of β-electrons,[4] then the value of α to be expected for a spin assignment of $5/2^{\pm}$, $3/2^{\pm}$, $1/2^{\pm}$ for the ground state of Hg^{203} is $\alpha_{5/2} = 0.87$, $\alpha_{3/2} = 0.95$ to 1.15, $\alpha_{1/2} = 1.25$ for electrons of average energy ~ 100 kev.

The results of the measurement indicate with a large probability that the ground state of Hg^{203} has spin $1/2$, and disagree with the spin $5/2$ assignment. Consequently, the absence of a direct β transition from Hg^{203} to the ground state of Tl^{203} with spin $1/2^{+}$ cannot be explained as spin forbidden.

In conclusion we express our gratitude to Academician A. I. Alikhanov for his interest in this work.

---

*This work was reported at the International Conference on High Energy Physics in Geneva, June-July 1958.[1]

---

[1] V. A. Lyubimov and M. E. Vishnevsky, Proc. of the 1958 Ann. Int. Conf. on High Energy Physics, CERN, p. 248.

[2] V. B. Berestetskii and A. P. Rudik, J. Exptl. Theoret. Phys. (U.S.S.R.) **35**, 159 (1958), Soviet Phys. JETP **8**, 111 (1959).

[3] B. V. Geshkenbein, J. Exptl. Theoret. Phys. (U.S.S.R.) **35**, 1235 (1958), Soviet Phys. JETP **8**, 865 (1959).

[4] Alikhanov, Eliseev, and Liubimov, J. Exptl. Theoret. Phys. (U.S.S.R.) **34**, 1045 (1958), Soviet Phys. JETP **7**, 723 (1958).

Translated by A. M. Bincer
326

ANTIFERROMAGNETISM OF THE GAMMA PHASE OF IRON

E. I. KONDORSKII and V. L. SEDOV

Moscow State University

J. Exptl. Theoret. Phys. (U.S.S.R.) **35**, 1579 (December, 1958)

It is known that the magnetic susceptibility of the α phase (volume-centered cubic lattice) of iron obeys the Curie-Weiss law, $\kappa(T-\Theta) = C$, at temperatures above the Curie point (770°C). It is also known that the susceptibility of the γ phase (face-centered cubic lattice) of iron also obeys the Curie-Weiss law in the temperature range (910 to 1400°C) in which this phase is stable, but with different values of the parameters C and Θ. It is therefore interesting to determine whether the γ phase of iron is ferromagnetic or antiferromagnetic at low temperatures, if a $\gamma \rightarrow \alpha$ transition is effected by introducing alloying additives and suitable heat treatment.

We investigated the temperature dependence of the magnetic susceptibility of austenitic steel in the temperature interval from 109 to 11.3°K. The investigated specimen contained 18% Cr and 9% Ni. The specific susceptibility κ was measured by a procedure previously described by the authors.[1]

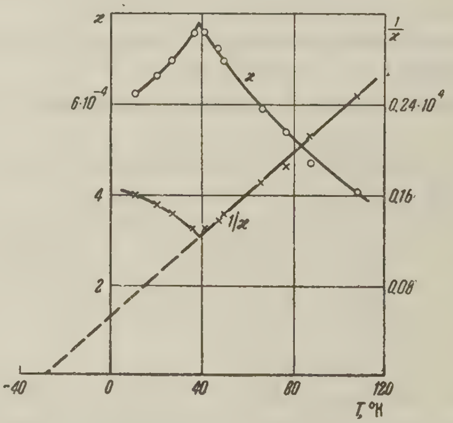

The measurement results are shown in the diagram. As can be seen from the plot, there is a clearly pronounced antiferromagnetic transformation near 40°K. The value of the paramagnetic Curie point Θ_p is (28 ± 3)°K. The results obtained give grounds for assuming that in a face-centered lattice of iron the exchange interactions would lead to antiferromagnetism at low temperatures, the same as in the neighboring elements manganese[2,3] and chrome.[4]

---

[1] E. I. Kondorskii and V. L. Sedov, J. Exptl. Theoret. Phys. (U.S.S.R.) **35**, 845 (1958), Soviet Phys. JETP **8**, 586 (1959).

[2] T. R. McGuire and C. J. Kreissman, Phys. Rev. **85**, 452 (1952).

[3] C. G. Shull and M. K. Wilkinson, Bull. Am. Phys. Soc. 27, No. 1, 24 (1952).

[4] C. G. Shull and M. K. Wilkinson, Revs. Modern Phys. 25, 100 (1953).

Translated by J. G. Adashko
327

ON THE PROBLEM OF TESTING THE INVARIANCE OF AN INTERACTION UNDER TIME REVERSAL

L. I. LAPIDUS

Joint Institute for Nuclear Research

Submitted to JETP editor Sepatember 5, 1958

J. Exptl. Theoret. Phys. (U.S.S.R.) 35, 1580-1581 (December, 1958)

THE discovery of the noninvariance of the weak interactions under space inversion and charge conjugation has greatly increased interest in a more detailed study of the symmetry properties of the strong interactions. In the present note we point out the possibility of a direct experimental test of the invariance of various interactions under time reversal, based on the relations between polarization phenomena in inverse reactions.[1-5] Until recently such tests were based on the ratio of the cross-sections of inverse reactions averaged over the spins,[6] and for the weak interactions on a number of consequences arising from the reality (or purely imaginary nature) of the interaction constants. Very recently it has been proposed[7,8] that the symmetry of strong interactions under time reversal be studied by examining the equality of the polarization and asymmetry in elastic scattering.[9,10] On the basis of the results of references 1 to 5, analogous tests can be carried out with various nuclear reactions. For example, the polarization of the neutron in the reaction $d + d \rightarrow n + He^3$, with the deuterons unpolarized, agrees, within the usual factor appearing in the balance relations, with the asymmetry in the cross-section of the inverse reaction $n + He^3 \rightarrow d + d$ with polarized neutrons. An examination of the relation between the polarization and the asymmetry, and of more complicated relations, would be a test of the invariance of the interaction under time reversal, since it is known that parity is very precisely conserved in the strong interactions of ordinary particles.[11] For this same purpose one can also use the reaction $p + T \rightleftarrows n + He^3$. And in general, by looking at a table of nuclear reactions, one can pick out many other reactions that can be used for this purpose.

For the reactions involving γ-ray quanta we can look at the photodisintegration of the deuteron and the radiative capture of a neutron by a proton:

$$n + p \rightleftarrows d + \gamma. \qquad (1)$$

Here, in addition to the relations that hold, for example, between the polarization of the neutron from the photodisintegration of the deuteron and the asymmetry in the cross-section for radiative capture of polarized neutrons by protons, one can make a comparison of the polarization of the photons from the radiative capture and the asymmetry of the photodisintegration cross section with polarized γ radiation.

For studying the time reversibility of processes of pion production we can take the reaction

$$p + p \leftrightarrows d + \pi^+, \qquad (2)$$

which has been studied in detail in reference 1. Recent experiments[12,13] can be regarded as the first stage of such a test. The results of Neganov and Parfenov show that the relations between the unpolarized cross-sections are satisfied to within 10 to 15 percent, which agrees with the estimates of Henley and Jacobsohn,[6] which were based on different experimental data.

For the study of the symmetry of interactions involving strange particles we can consider the reaction

$$K^- + d \rightleftarrows \Sigma^- + p, \qquad (3)$$

which Lee once proposed for the determination of the spins of the particles,[14] and also a number of similar reactions.[15] The polarization of the Σ^-, which one can hope to detect from the asymmetry of its decay, must agree with the asymmetry of the K^- in the reaction $\Sigma^- + p \rightarrow d + K^-$ with the Σ^- polarized (for example, by the process that produces it). The study of the polarization phenomena in the reaction (3) can also help to settle the question as to whether there is a connection between the small asymmetry in the decay of the Σ^- from the reaction $\pi + N \rightarrow \Sigma^- + K$ and threshold effects.

---

[1] L. I. Lapidus, J. Exptl. Theoret. Phys. (U.S.S.R.) 33, 204 (1957), Soviet Phys. JETP 6, 160 (1958).

[2] A. I. Baz', J. Exptl. Theoret. Phys. (U.S.S.R.) 32, 628 (1957), Soviet Phys. JETP 5, 521 (1957).

[3] L. I. Lapidus, J. Exptl. Theoret. Phys. (U.S.S.R.) 34, 922 (1958), Soviet Phys. JETP 7, 638 (1958).

[4] M. I. Shirokov, J. Exptl. Theoret. Phys. (U.S.S.R.) 33, 975 (1957), Soviet Phys. JETP 6, 748 (1958).

[5] Bilen'kii, Lapidus, Puzikov, and Ryndin, J. Exptl. Theoret. Phys. (U.S.S.R.) 35, 959 (1958), Soviet Phys. JETP 8, 669 (1959).

[6] E. M. Henley and B. A. Jacobsohn, Phys. Rev. 108, 502 (1957).

[7] F. Mandl, Proc. Phys. Soc. 71, 686 (1958).

[8] R. J. N. Phillips, Nuovo cimento 8, 265 (1958).

[9] L. Wolfenstein and J. Ashkin, Phys. Rev. 85, 947 (1952).

[10] R. H. Dalitz, Proc. Phys. Soc. A65, 175 (1952).

[11] D. H. Wilkinson, Phys. Rev. 109, 1603 (1958).

[12] B. S. Neganov and L. B. Parfenov, J. Exptl. Theoret. Phys. (U.S.S.R.) 34, 767 (1958), Soviet Phys. JETP 7, 528 (1958).

[13] Akimov, Savchenko, and Soroko, J. Exptl. Theoret. Phys. (U.S.S.R.) 35, 89 (1958), Soviet Phys. JETP 8, 64 (1959).

[14] T. D. Lee, Phys. Rev. 99, 337 (1955).

[15] L. I. Lapidus, J. Exptl. Theoret. Phys. (U.S.S.R.) 31, 342 (1956), Soviet Phys. JETP 4, 447 (1957).

Translated by W. H. Furry
328

THE UNIVERSAL FERMI INTERACTION AND THE CAPTURE OF MUONS IN HYDROGEN

CHOU KUANG-CHAO and V. MAEVSKII

Joint Institute for Nuclear Research

Submitted to JETP editor September 13, 1958

J. Exptl. Theoret. Phys. (U.S.S.R.) 35, 1581-1582 (December, 1958)

THE theory of the universal Fermi interaction with (V-A) coupling proposed by Marshak and Sudarshan[1] and by Feynman and Gell-Mann[2] is supported by all existing experimental evidence on β decay. To explain the equality of the Fermi β-decay constant and the constant for the μ decay, Feynman and Gell-Mann have put forward the hypothesis of a conserved vector current in the weak interactions. This hypothesis leads to the appearance of an anomalous magnetic-moment effect in the β decay ("β magnetism"). Calculations of the effect have been made by Gell-Mann and others[3-5] and have apparently already received experimental confirmation in β decay.[6]

The latest experimental data show that the probability of the β decay or (μ, ν) decay of hyperons is apparently considerably smaller than that given by the universal (V-A) theory.[7] But even if these data are confirmed and we are forced to abandon the universal interaction including the hyperons, nevertheless the universal interaction between (p, n), (e, ν), and (μ, ν) will remain an extremely probable hypothesis.

Since it already seems that the β decay and the decay of the μ meson can be explained within the framework of the (V-A) theory, it is of particular interest to examine the process of μ capture and test the idea of the universal (V-A) interaction in this case.

In the present note we present expressions for the probability of the capture, the angular distribution, and the polarization of the emerging neutrons in the case of capture of polarized μ^- mesons by protons, based on the assumption of the universal (V-A) coupling with conserved vector current as proposed by Gell-Mann and Feynman.

The capture probability and the angular distribution are (in units $\hbar = c = 1$):

$$w = (2\pi)^{-2} (\pi a_\mu^3)^{-1} 2^{-1} G^2 I \, [1 + \alpha P \, (\mathbf{n} \cdot \mathbf{s})] \, p^2 \, d\Omega,$$

$$I = 1 + 3\lambda^2 + \beta (1 + \lambda^2) + \beta\mu (2\lambda + \beta\mu / 2),$$

$$I\alpha = 1 - \lambda^2 + \beta (1 + \lambda^2) - \beta\mu (2\lambda + \beta\mu / 2).$$

The total probability for capture is

$$\tau^{-1} = 2^{-1} G^2 \pi^{-2} a_\mu^{-3} p^2 I.$$

The polarization $\langle \sigma_n \rangle$ of the neutrons is given by the formula

$$I \, [1 + \alpha P (\mathbf{n} \cdot \mathbf{s})] \langle \sigma_n \rangle = [a + b \, (\mathbf{n} \cdot \mathbf{s})] \, \mathbf{n} + c\mathbf{s},$$

$$a = -2 \, [\lambda (\lambda + 1) + \beta\lambda + \beta\mu (\lambda + \beta\mu / 4)],$$

$$b = -\beta P \, [\lambda (\lambda + 1) - \mu (1 + \lambda + \beta\mu / 2)],$$

$$c = 2P (\lambda - 1) \, [\lambda + \beta (\lambda + \mu) / 2].$$

Here we have used the notations: $p\mathbf{n}$ is the momentum of the neutron, and $P\mathbf{s}$ is the polarization of the μ meson ($\mathbf{n}$ and $\mathbf{s}$ are unit vectors); $\lambda = -C_A/C_V$, $\beta = p/M$; $G \equiv 2^{1/2} C_V$ is the universal coupling constant; M is the nucleon mass; $\mu = \mu_p - \mu_n$ is the difference of the magnetic moments of the proton and neutron; $a_\mu = (m_\mu e^2)^{-1}$ is the radius of the mesonic K orbit in hydrogen.

Terms of the order $(v/c)^2$ have been neglected in the calculation (v is the speed of the neutron). In addition it has been assumed that in the pseudovector coupling the higher moments do not give an additional renormalization. A numerical computation (taking $G = (1.01 \pm 0.01) \times 10^{-5} M^{-2}$, $\mu = 4.7$, $\lambda = 1.24$, $\beta = 0.1$) shows that the effect of the anomalous magnetic moment increases the total probability of capture by ≈17 percent, and the angular correlation coefficient by a factor of about 2.4; the polarization of the neutrons is changed only slightly as compared with the results of the ordinary theory. At present calculations are being carried out on the capture of mesons by nuclei according to the Feynman — Gell-Mann theory. It can be expected that in this case also the correction introduced by the anomalous magnetic moment will be large.

---

[1] E. C. G. Sudarshan and R. E. Marshak, Phys. Rev. **109**, 1860 (1958).

[2] R. P. Feynman and M. Gell-Mann, Phys. Rev. **109**, 193 (1958).

[3] M. Gell-Mann, Test of the Nature of the Vector Interaction in β Decay (preprint).

[4] J. Bernstein and R. Lewis, The Vector Interaction in β Decay (preprint).

[5] Weinberg, Marshak, Okubo, Sudarshan, and Teutsch, Phys. Rev. Letters **1**, 25 (1958).

[6] Boehm, Soergel, and Stech, Phys. Rev. Letters **1**, 77 (1958).

[7] F. Eisler, R. Plano, et al., Leptonic Decay Modes of the Hyperons (preprint).

Translated by W. H. Furry
329

ON THE SPECTRUM OF THE ELECTRON-PHOTON COMPONENT OF EXTENSIVE AIR SHOWERS

I. A. IVANOVSKAIA and I. V. RAKOBOLSKAIA

P. N. Lebedev Physics Institute, Academy of Sciences, U.S.S.R.

Submitted to JETP editor June 27, 1958

J. Exptl. Theoret. Phys. (U.S.S.R.) 35, 1583-1584 (December, 1958)

An experiment was carried out in 1958 in Moscow in an attempt to explain the discrepancies observed in our earlier experiments.[1,2]

In these experiments we studied the electron-photon component of extensive atmospheric showers (EAS), and in particular the fraction of high-energy electrons and photons near the shower axis. A cloud chamber with lead plates was used for that purpose.[3] The energy of electrons and photons was determined from the number of particles in the cascade showers produced by them in the lead plates.

The energy spectra obtained for the region $< 10^9$ ev in references 1 and 2 were different. In addition, the fraction of high-energy electrons and photons $\rho\,(\geq 10^9)/\rho\,(>0)$ at 0 to 3 m from the shower axis amounted to $(1.85 \mp 0.25)\,\%$ according to reference 1 and to $\geq 10\%$ according to reference 2. Several reasons for the discrepancy were indicated:[1] (a) difference in shower sizes, (b) different transition effects in the roof above the apparatus, and (c) large errors in the axis location by means of the hodoscope in reference 1.

An additional experiment was carried out at sea level to study the problem, using the same cloud chamber. The selection method[4] made it possible to record EAS, the axes of which fell in 70% of the cases at a distance 0 to 3 m from the chamber. The mean shower size was $\sim 3 \times 10^4$ particles. Such showers were studied in reference 1 with best statistics. A total of 385 showers were recorded during 400 hours of operation.

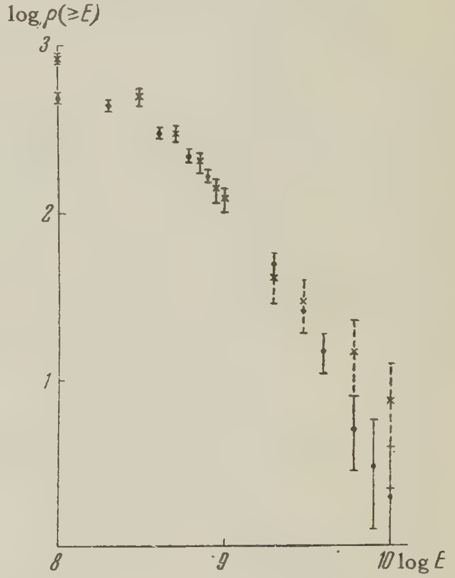

Integral energy spectra of the electron-photon component. The ordinate represents log $\rho\,(\geq \mathrm{E})$, where $\rho(\geq \mathrm{E})$ is proportional to the density of electrons and photons per 1 m² in one shower. The abscissa represents log E, where E is the energy in ev, ×) data of reference 1 in the range 0 to 3 m, ●) data of the present experiment for all distances (70% of the showers in the range 0 to 3 m). The spectra are normalized at $\mathrm{E} = 10^9$ ev.

As the result of the measurements we obtained the integral energy spectrum of the electron-photon component shown in the figure. The spectrum obtained in reference 1 for distances 0 to 3 m is included for a comparison. It can be seen that the spectra are different below 10^9 ev.

The fraction of high-energy electrons and photons was defined, as in the earlier experiments, as the ratio of the density of electrons and photons with $\mathrm{E} \geq 10^9$ measured in the cloud chamber, to the density of electrons with $E > 0$ obtained by means of the hodoscope. It was found that $\rho\ (\geq 10^9)/\rho\ (> 0) = (12 \mp 3)\%$ at distances 0 to 3 m from the shower axis.

It seems to us, after a careful study of the data of references 1 and 2, and of the newly-obtained results, that the reasons for the discrepancy between the results of the present work and those of reference 1 are the following:

(1) At distances 0 to 3 m, the axes of the showers recorded in the later experiment and in reference 1 were differently distributed with respect to the distance from the cloud chamber. This fact can play a substantial role, since the main contribution to the fraction of high-energy electrons and photons at these distances is due to showers the axis of which fell less than one meter from the chamber.

(2) In reference 1, showers were recorded at < 1 m from the chamber, which could cause a large fluctuation of the fraction of high-energy particles since the distribution of the latter is different from Poissonian.

(3) In view of the small number of counters in the hodoscope,[1] the distance from the cloud chamber was not measured accurately enough, and a certain amount of showers from larger distances could have been ascribed to the 0 to 3 m region.

A detailed analysis of the above hypotheses will be presented later.

The hypothesis that the fraction of high-energy electrons and photons depends strongly on the shower size has not been confirmed. Calculations show that the transition effect in the roof above the apparatus was almost equal in both experiments and, consequently, cannot explain the discrepancy of the results.

From the comparison, we can conclude that the discrepancy between the theory and the experiment with respect to the fraction of high-energy electrons and photons in EAS is apparently smaller than that reported in reference 1.

In conclusion, the authors wish to thank G. T. Zatsepin, S. I. Nikol'skii, and O. I. Dovzehnko for a discussion of the results.

---

[1] Ivanovskaia, Kulikov, Rokobol'skaia, and Sarycheva, J. Exptl. Theoret. Phys. (U.S.S.R.) **33**, 358 (1957), Soviet Phys. JETP **6**, 276 (1958).

[2] Danilova, Dovzhenko, Nikol'skii, and Rakobol'skaia, J. Exptl. Theoret. Phys. (U.S.S.R.) **34**, 541 (1958), Soviet Phys. JETP **7**, 374 (1958).

[3] I. A. Ivanovskaia and A. G. Novikov, J. Tech. Phys. (U.S.S.R.) **26**, 209 (1956), Soviet Phys. "Tech. Phys." **1**, 206 (1956).

[4] Dovzhenko, Nikol'skii, and Rakobol'skaia, J. Exptl. Theoret. Phys. (U.S.S.R.) **36**, 17 (1959), Soviet Phys. JETP **9** (in press).

Translated by H. Kasha
330

AUTHOR INDEX TO VOLUME 35 (8)

References with L are Letters to the Editor

Abrikosov, A. A. and I. E. Dzialoshinskii. Spin Waves in a Ferromagnetic Metal — 535.
— and L. P. Gor'kov. On the Theory of Superconducting Alloys. I. The Electrodynamics of Alloys at Absolute Zero — 1090.
— L. P. Gor'kov, and I. M. Khalatnikov. A Superconductor in a High Frequency Field — 182.
Adamovich, M. I. An Investigation of the Final States in the Photoproduction of Negative π Mesons on Deuterium — 29.
— G. V. Kuz'micheva, V. G. Larionova, and S. P. Kharlamov. Photoproduction of Negative Pions from Deuterium near the Threshold — 21.
Adel'son-Velskii, G. M. (see Gol'din, L. L.) — 127.
Agranovich, V. M. and A. A. Rukhadze. Energy Losses of an Electron in a Medium with Spatial Dispersion — 819.
— and A. A. Rukhadze. On the Propagation of Electromagnetic Waves in a Medium with Appreciable Spatial Dispersion — 685.
— and V. S. Stavinskii. On the Theory of the "Second Moment" in the Nuclear Model of Lane, Thomas, and Wigner — 896L.
Akhiezer, A. I. and A. G. Sitenko. Theory of Excitation of Hydromagnetic Waves — 82.
— V. G. Bar'iakhtar, and S. V. Peletminskii. Coupled Magnetoelastic Waves in Ferromagnetic Media and Ferroacoustic Resonance — 157.
— G. Ia. Liubarskii, and R. V. Polovin. The Stability of Shock Waves in Magnetohydrodynamics — 507.
Akimov, Iu. K., O. V. Savchenko, and L. M. Soroko. Investigation of the $p + p \rightarrow d + \pi^+$ Reaction with a Polarized Proton Beam — 64.
Aksenov, S. I. Nuclear Magnetic Resonance Shift in Molybdenum — 207L.
Akulov, N. S. and A. V. Cheremushkina. On the Hall Effect at the Curie Point — 357L.
Aleksandrov, Iu. A., V. N. Andreev, and I. I. Bondarenko. On the Question of Antigravitation — 911L.
Alekseeva, K. I. and N. L. Grigorov. Inelastic Interaction between Cosmic Ray Protons of Kinetic Energy above 7 Bev — 416.
Alekseevskii, N. E. and Iu. P. Gaidukov. Anisotropy of the Electrical Resistance of a Gold Monocrystal in a Magnetic Field at 4.2°K — 383L.
— The Influence of Plastic Deformation on the Anomalous Behavior of the Resistance of Gold at Low Temperatures — 558L.
Alikhanov, A. I., G. P. Eliseev, and V. A. Liubimov. Polarization of RaE Electrons and Time-Reversal Invariance — 740L.
Alimarin, I. P. (see Malysheva T. V.) — 772.
Alkhazov, D. G., A. P. Grinberg, G. M. Gusinskii, K. I. Erokhina, and I. Kh. Lemberg. Coulomb Excitation of Aluminum — 736L.
— Coulomb Excitation of High-Energy Nuclear Levels in Even Isotopes of Tungsten — 926.
— Lifetime of the First Excited State of Mg^{24} — 737L.
Alimov, Iu. I. (see Skrotski, G. V.) — 1035.
Al'tshuler, A. A. and K. A. Valiev. On the Theory of Longitudinal Relaxation of Paramagnetic Salt Solutions — 661.
Andreev, V. N. (see Aleksandrov, Iu. A.) — 911L.
Andreev, V. V. and V. I. Gerasimenko. On the Theory of Paramagnetic Resonance and Paramagnetic Relaxation in Metals — 846.
Andriankin, E. I. Propagation of a Non-Self-Similar Thermal Wave — 295.
Ankudinov, V. A. (see Fogel', Ia. M.) — 601.
Ansel'm, A. A. Asymptotic Theory of a One-Dimensional Four-Fermion Interaction —1065.
Asanov, R. A. Beta Decay of a Spin-$3/2$ Particle — 552L.
Avalov, R. G. (see Biakov, V. M.) — 826.
Azbel', M. Ia., V. I. Gerasimenko, and I. M. Lifshitz. On the Theory of Paramagnetic Resonance of Metals — 480.
Babaian, Kh. P., N. A. Marutian, K. A. Matevosian, and M. G. Sarinian. Energy Dependence of the Angular Correlation of Positrons from $\pi \rightarrow \mu \rightarrow e$ Decay — 387.
Badalian, G. V. A Study of Fast Deuterons at 3200 m above Sea Level — 209L.
Bannik, B. P. and S. A. Buniatov. Hyperfragments from σ_K Stars — 913L.
Barabanenkov, Iu. N. Hydrodynamic Analysis of the Compression of a Rarified Plasma in an Axially-Symmetric Magnetic Field — 893L.
Barshenkov, V. S. (see Blokhintsev, D. I.) — 215L.
Bar'iakhtar, V. G. and M. I. Kaganov. Cerenkov Radiation in the Passage of a Charged Particle through a Ferrite — 532.
— (see Akhiezer, A. I.) — 157.
Barmin, V. V., V. P. Kanavets, B. V. Morozov, and I. I. Pershin. Energy Dependence of the Asymmetry Coefficient in $\pi^+ \rightarrow \mu^+ \rightarrow e^+$ Decays for the Low Energy Part of the Positron Spectrum — 374L.
Bashkirov, Sh. Sh. and K. A. Valiev. Polarization of Nuclear Moments and Nuclear-Resonance Line Widths in Crystals — 471.
— (see Valiev, K. A.) — 208L.
Baz', A. N. and L. B. Okun', On the Λ-Hyperon Creation Cross Section near the Σ-Hyperon Creation Threhold — 526.
Bazhanov, E. B., Iu. M. Volkov, and L. A. Kul'chitskii. Investigation of 15 to 65-Mev Protons Produced in the Photodisintegration of Aluminum and Nickel — 224.
Bedritskii, A. I. The Scattering of Spin-2 Particles by a Coulomb Field — 892L.
Begiashvili, G. A. and E. V. Gedalin. Motion of a Charged Particle in an Anisotropic Medium — 1059.

Beliaev, V. B. and B. N. Zakhar'ev. Depolarization of μ^- Mesons in Hydrogen, Deuterium, and Tritium — 699.

Belousov, A. S., S. V. Rusakov, and E. I. Tamm. Photoproduction of Slow π^0 Mesons on Complex Nuclei — 247.

Belovitskii, G. E. Inelastic Scattering of 300-Mev Positive and Negative π Mesons by Photographic Emulsion Nuclei — 581.

Berestetskii, V. B. Nuclear Orientation in Radiative K Capture — 371L.

— and A. P. Rudik. The Polarization of the Internal-Conversion Electrons Emitted after β-Decay — 111.

Berezhnoi, Iu. A. (see Sitenko, A. G.) — 899L.

Biakov, V. M. and R. G. Avalov. The Acceleration of Cosmic Rays in a Fluctuating Magnetic Field — 826.

Bilen'kii, S. M. and R. M. Ryndin. Method for Determining Hyperon Polarization in the Reaction $\pi + p \rightarrow Y + K$. — 574L.

— L. I. Lapidus, L. D. Puzikov, and R. M. Ryndin. On Finding the Matrix of the $a + a' \rightarrow b + b'$ Reaction — 669.

Birzgal, A. P. (see Gol'din, L. L.) — 127.

Blinov, G. A., M. F. Lomanov, Ia. Ia. Shalamov, V. A. Shebanov, and V. A. Shchegolev. Interaction of 80 to 300 Mev π^+ Mesons with Light Nuclei — 609.

Blokhintsev, D. I. On a Possible Limit on the Applicability of Quantum Electrodynamics — 174.

— V. S. Barashenkov, and V. G. Grishin. Diffraction Scattering of Fast Particles — 215L.

Blokhintsev, L. D. (see Dolinskii, E. I.) — 1040.

Bondarenko, V. V. (see Kvartskhava, I. F.) — 634.

Bondarenko, I. I. (see Aleksandrov, Iu. A.) — 911L.

Borisova, N. I. (see Kurchatov, B. V.) — 40.

Borovik-Romanov, A. S. and N. M. Kreines. Transition from the Antiferromagnetic into the Ferromagnetic State in $CoSO_4$ — 734L.

Brandt, N. B. and V. A. Venttsel. Effect of Uniform Compression on the Oscillation of the Magnetic Susceptibility of Bismuth at Low Temperatures — 757.

Buchel'nikova, I. A. Cross Sections for the Capture of Slow Electrons by O_2 and H_2O Molecules and Molecules of Halogen Compounds — 783.

Budagov, Iu. A., S. Victor, V. P. Dzhelepov, P. F. Ermolov, and V. I. Moskalev. Electron-Positron Pairs from the Decay $\pi^0 \rightarrow e^- + e^+ + \gamma$ — 1101L.

Buimistrov, V. M. On the Precision of Quantum Mechanical Mean Values Computed by the Variational Method — 812.

Buniatov, S. A. (see Bannik, B. P.) — 913L.

Burgov, N. A. and Iu. V. Terekhov. Types of Interaction in Beta Decay of Na^{24} — 651.

Cerenkov, P. A. (see Denisov, F. P.) — 376L.

Chalikian, G. A. (see Garibian, G. M.) — 894L.

Chao Kai-hua. Surface Oscillations of a Charged Column in a Longitudinal Magnetic Field — 1031.

Charakhch'ian, A. N. and T. N. Charakhch'ian. Measurement of Cosmic-Ray Intensity in the Stratosphere at Various Altitudes and Latitudes — 761.

Charakhch'ian, T. N. (see Charakhch'ian, A. N.) — 761.

Chavchanidze, V. V. and M. E. Perel'man. A Contribution to Neutrino Theory — 204L.

Cheishvili, O. D. (see Khutsishvili, G. R.) — 859.

— (see Vashakidze, I. Sh.) — 741L.

Chechernikov, V. I. and Iu. D. Volkov. Temperature Dependence of the Paramagnetic Susceptibility of Nickel-Zinc Ferrites — 606.

Chen Ch'un-Hsien. A New Method In Statistical Perturbation Theory — 1062.

Cheremushkina, A. V. (see Akulov, N. S.) — 357L.

Chernov, G. M. (see Estulin, I. V.) — 51.

Chirkov, A. K. and A. A. Kokin. Paramagnetic Resonance of Free Radicals in Weak Fields — 36.

Chistiakov, L. V. (see Kurchatov, B. V.) — 40.

Chou Kuang-Chao. Selection Rules in Reactions Involving Polarized Particles — 543L.

— and V. Maevskii. The Universal Fermi Interaction and the Capture of Muons in Hydrogen — 1106L.

— and L. G. Zastavenko. The Shapiro Integral Transformation — 990.

Chubinskii, O. V. (see Gustova, L. V.) — 957.

Chubinskii, O. V. (see Gustov, L. V.) — 920L.

Chultem, D. (see Ignatenko, A. E.) — 621.

Chultem, D. (see Ignatenko, A. E.) — 792.

Csikai, J. and A. Szalay. The Effect of Neutrino Recoil in the β-Decay of He^6 — 749.

Danysh, M. Ia. (see Gramenitskii, I. M.) — 381L.

Davydov, A. S. and G. F. Filippov. Magnetic Transitions between Collective Excited States of Even-Even Nuclei — 488.

— Rotational States of Nonaxial Nuclei — 303.

— and A. F. Lubchenko. Electromagnetic Waves in the Region of Exciton Absorption in a Crystal — 1048.

Davydov, B. I. Phonomenological Equations of Statistical Dynamics of an Incompressible Turbulent Liquid — 364L.

Degtiarev, I. F. (see Kirenskii, L. V.) — 403.

Deigen, M. F. (see Vinetskii, V. L.) — 198L.

Demirkhanov, R. A., T. I. Gutkin, and V. V. Dorokhov. Nuclear Binding Energies in the Region of the 82 Proton and 126 Neutron Magic Numbers — 639.

Denisenko, G. F. (see Perfilov, N. A.) — 438.

Denisov, F. P. and P. A. Cerenkov. Ranges of Na^{24} Recoil Nuclei and the Mechanism of Certain Photonuclear Reactions — 376L.

— (see Volkova, L. V.) — 372L.

Diatlov, I. T. Photoproduction of Electron and μ-Meson Pairs on Nucleons — 108

Didenko, A. N. Interaction between a Charged Current-Conducting Jet Moving in a Circle and a Ferrite — 455.

Ding Da-Tsao (see Wang, Kan Chang) — 625.

Dmitrenko, I. M., B. I. Verkin, and B. G. Lazarev. Magnetic Properties of Metals at Low Temperatures. IV. Influence of Homogeneous Compression on the De Haas-Van Alphen Effect in Zinc Crystals — 229.

— (see Verkin, B. I.) — 200L.

Dmitriev, V. A. Transition Effect for Electrons in Walls of an Ionization Chamber — 382L.

Dobrynin, Iu. P. (see Sosnovskii, A. N.) — 739L.

Dolginov, A. Z. Polarization Correlation of Beta Particles and Gamma Quanta in Allowed Decay of Oriented Nuclei — 123.

— and I. N. Toptygin. Clebsch-Gordan Expansion for Infinite-Dimensional Representations of the Lorentz Group — 550L.

Dolinskii, E. I. On a Method for Determining the Parity

of Strange Particles — 902L.
— and L. D. Blokhintsev. Absorption of μ Mesons by Nuclei; Angular Distribution of the Neutrons — 1040.
Dorfman, Ia. G. Diamagnetism and Interatomic Bonds in Molecules and Non-Metallic Crystals — 368L.
Dorokhov, V. V. (see Demirkhanov, R. A.) — 639.
Dremin, I. M. Investigation of K_{e3}-Decay with the Emission of a Gamma Photon — 355L.
Dubrovskii, L. N. (see Ding Da-Tsao) — 625.
Dukel'skii, V. M. and V. M. Sokolov. Negative Ions of Iron, Cobalt, and Nickel — 569L.
Dul'kova, L. S., I. B. Sokolova, and M. G. Shafranova. Elastic Scattering of 300-Mev Pions by Deuterons — 217.
Dushin, N. V. Production of Two π Mesons in Collisions between π Mesons or γ Quanta with Nucleons or Deuterons — 278.
Dzhelepov, V. P. (see Budagov, Iu. A.) — 1101L.
— (see Fliagin, V. B.) — 592.
Dzhrbashian, V. A. Angular Correlation of Circularly Polarized Gamma Quanta on the μ Mesonic Atom — 212L.
Dzialoshinskii, I. E. (see Abrikosov, A. A.) — 535.
Efimov, V. N. Scattering of Slow Neutrons by Deuterons — 98.
Egorov, Iu. S. (see Sergeev, A. G.) — 242.
Egorov, L. B. (see Ignatenko, A. E.) — 621.
Egorov, L. B. (see Ignatenko, A. E.) — 792.
Eidman, V. Ia. (see Ginzburg, V. L.) — 1055.
Eliseev, G. P. (see Alikhanov, A. I.) — 740L.
Ermolov, P. F. (see Budagov, Iu. A.) — 1101L.
Erokhina, K. I. (see Alkhazov, D. G.) — 736L.
— (see Alkhazov, D. G.) — 926.
— (see Alkhazov, D. G.) — 737L.
Estulin, I. V., G. M. Chernov, and Z. V. Pastukhova. The Decay Scheme of Mo^{99} — 51.
— (see Kalinkin, L. F.) — 410.
Fadeev, L. D. Dispersion Relations in Non-Relativistic Scattering Theory — 299.
Fain, V. M. (see Ginzburg, V. L.) — 567L.
Fedorov, F. I. Projection Operators in the Theory of Elementary Particles — 339.
Fedorov, G. V. (see Volkenshtein, N. V.) — 61.
Fenyes, I. Analogy between the Mechanical and Thermodynamical Equations of Motion and the Onsager Reciprocity Relation — 725L.
Feoktistov, V. A. (see Nelipa, N. F.) — 167.
Fesenko, A. I. (see Ivanov, Iu, M.) — 905L.
Fikhtengol'ts, I. G. Coordinate Conditions in Einstein's Gravitation Theory — 1018.
Filimonov, Iu. I. and B. V. Pshenichnikov. Lower Excited States of Th^{231} — 378L.
— (see Golenetskii, S. V.) — 917L.
Filimonov, V. A. (see Liul'ka, V. A.) — 717.
Filippov, G. F. (see Davydov, A. S.) — 488.
Filippov, G. F. (see Davydov, A. S.) — 303.
Fliagin, V. B., V. P. Dzhelepov, V. S. Kiselev, and K. O. Oganesian. The $n + p \rightarrow \pi^0 + d$ Reaction for Neutrons of 600-Mev Effective Energy and the Charge-Independence Hypothesis — 592.
— (see Kiselev, V. S.) — 564L.
Fogel' Ia. M., V. A. Ankudinov, and D. V. Pilipenko. Electron Capture and Loss in Collisions of Fast Carbon and Oxygen Atoms with Gas Molecules — 601.
— , R. V. Mitin, V. F. Kozlov, and N. D. Romashenko. On the Applicability of Massey's Adiabatic Hypothesis to Double Charge Exchange — 390.
Fomin, P. I. Radiation Corrections to Bremsstrahlung — 491.
Friedlander, E. and E. Ruckenstein. The Nature of the Particles that Carry away most of the Energy in Nuclear Collisions at Moderate Energies — 75.
Funshtein, B. L. (see Zherebtsova, K. I.) — 947.
Gadzhiev, S. A. (see Mukhtarov, A. I.) — 895L.
Gaidukov, Iu. P. (see Alekseevskii, N. E.) — 383L.
— (see Alekseevskii, N. E.) — 558L.
Galoshina, E. V. (see Volkenshtein, N. V.) — 916L.
Garber, R. I., V. S. Kogan, and L. M. Poliakov. Growth and Dissolution of Pores in Crystals — 953.
Garibian, G. M. Radiation from a Charged Particle Traversing a Layered Medium — 1003.
— and G. A. Chalikian. The Radiation from a Charged Particle Passing through a Plate — 894L.
Garif'ianov, N. S. Paramagnetic Relaxation in Potassium Sulphate and Ammonium Iron Sulphate — 426.
— Second Relaxation in a Spin System in Certain Compounds of Elements of the Iron Group — 366L.
— and M. A. Starikov. Electronic Paramagnetic Resonance in Alloys of Alkali Metals — 553L.
Gedalin, E. V. (see Begiashvili, G. A.) — 1059.
Geilikman, B. T. On Axially Asymmetric Nuclei — 690.
Gerasimenko, V. I. (see Andreev, V. V.) — 846.
— (see Azbel', M. Ia.) — 480.
Gershtein, S. S. (see Zel'dovich, Ia. B.) — 451.
— (see Zel'dovich, Ia. B.) — 570.
Geshkenbein, B. V. Polarization of Internal Conversion Electrons Following Beta Decay — 865.
Gindin, I. A., B. G. Lazarev, Ia. D. Starodubov, and V. I. Khotkevich. Low Temperature Polymorphism in Metals — 556L.
Gintsburg, M. A. Exchange Effects in Ferromagnetic Resonance — 730L.
Ginzburg, V. L. Nonlinear Interaction of Radio Waves Propagating in a Plasma — 1100L.
— and V. Ia. Eidman. Cerenkov Radiation from Dipoles — 1055.
— and V. M. Fain. Radiation of a Multilevel System Moving in a Medium with a Velocity Greater than the Velocity of Light — 567L.
Giterman, M. Sh., P. S. Zyrianov, and G. G. Taluts. Bose Excitations in Ionic Crystals — 1072.
Gladun, A. D. (see Tager, A. S.) — 560L.
Glasko, V. B., F. Leriust, Ia. P. Terletskii, and S. F. Shushurin. An Investigation of Particle-Like Solutions of a Nonlinear Scalar Field Equation — 312.
Glotova, G. I., V. L. Granovskii, and V. I. Savoskin. Comparison of the Decay Rates of Plasma in Hydrogen and Deuterium — 965.
Gofman, U. (see Kondorskii, E. I.) — 380L.
Gol'din, L. L., G. M. Adel'son-Velskii, A. P. Birzgal, A. D. Piliia, and K. A. Ter-Martirosian. Alpha Decay of Nonspherical Nuclei — 127.
Golenetskii, S. V., L. I. Rusinov, and Iu. I. Filimonov. Alpha Decay of Isomeric Bi^{210} — 917L.

Gol'fand, Iu. A. On the Theory of the Weak Interactions I. — 118.
— On the Theory of the Weak Interactions II.— 504.
Golitsyn, G. S. Undimensional Motion in Magnetohydrodynamics — 538.
— and K. P. Staniukovich. Some Remarks on the Structure of Shock Waves — 575L.
Gor'kov, L. P. (see Abrikosov, A. A.) — 1090.
— (see Abrikosov, A. A.) — 182.
Gornyi, N. B. Discrete Energy Losses of Electrons in Solids and Yield of Secondary Electrons — 193L.
Gramenitskii, I. M., M. Ia. Danysh, V. B. Liubimov, M. I. Podgoretskii, and D. Tuvdendorzh. On the Problem of Angular Correlation of Secondary Particles Produced in High-Energy Nuclear Collisions — 381L.
Granovskii, V. L., K. P. Riumina, V. I. Savoskin, and G. G. Timofeeva. Observations of the Pinch Effect at Decreasing Currents — 33.
— (see Glotova, G. I.) — 965.
Grashin, A. F. Energy Dependence of Multiple-Production Reaction Cross Sections Near Threshold — 499.
— (see Lomanov, M. F.) — 615.
Grazhdankina, N. P. and D. I. Gurfel'. X-ray Diffraction Study of the Thermal Expansion of Antiferromagnetic MnTe — 631.
Grechishkin, V. S. Investigation of Relaxation Process in a Series of Fluorine Compounds of Carbon — 253.
Gribov, V. N. The Spectral Representation of the Two-Meson Green's Function — 287.
Grigorov, N. L., A. V. Podgurskaia, A. I. Saval'eva, and L. M. Poperekova. Interaction of Cosmic Ray Particles with Various Nuclei — 1.
— (see Alekseeva, K. I.) — 416.
Grinberg, A. P. (see Alkhazov, D. G.) — 736L.
— (see Alkhazov, D. G.) — 926.
— (see Alkhazov, D. G.) — 737L.
Grishin, V. G. Diffraction Scattering of 6.15-Bev Protons by Protons — 345.
— (see Blokhintsev, D. I.) — 215L.
Gurevich, A. V. The Temperature of Plasma Electrons in a Variable Electric Field — 271.
Gurevich, V. L. Oscillations in the Conductivity of Metallic Films in Magnetic Fields — 464.
Gurfel', D. I. (see Grazhdankina, N. P.) — 631
Gurzhi, R. N. Mutual Electron Correlations in Metal Optics — 673.
Guseva, V. V., G. T. Zatsepin, and G. B. Khristiansen. On the Zenith Angle Distribution of High-Energy Extensive Air Showers — 577.
Gusinskii, G. M. (see Alkhazov, D. G.) — 736L.
— (see Alkhazov, D. G.) — 926.
— (see Alkhazov, D. G.) — 737L.
Gustova, L. V. and O. V. Chubinskii. Hard Gamma Radiation of As^{76}. Decay Scheme of As^{76} — 957.
—, L. P. Timofeeva, and O. V. Chubinskii. The Hard Radiation of Ag^{110} — 920L.
Gutkin, T. I. (see Demirkhanov, R. A.) — 639.
Iakovlev, Iu. P. (see Ostroumov, V. N.) — 949.
Iakovlev, L. G. Wave-Front Velocity in Electrodynamics Containing Higher Derivatives — 542L.
Iakovlev, V. I. (see Murzina, E. A.) — 906L.
Iakovleva, I.V. Depolarization of π^+ Mesons in Metals — 676.
Ignatenko, A. E., L. B. Egorov, B. Khalupa, and D. Chultem. Investigation of the Depolarization of Negative Muons in Liquid Hydrogen — 621.
— Measurement of the Polarization of Negative μ Mesons in Carbon, Oxygen, Magnesium, Sulphur, Zinc, Cadmium, and Lead Mesic Atoms — 792.
Ioffe, B. L. (see Vaks, V. G.) — 151.
Iogansen, L. V. and M. S. Rabinovich. Coherent Electron Radiation in a Synchrotron. I. — 708.
Isaev, P. S. (see Zlatev, I.) — 213L.
Ivanchik, I. I. Angular Distribution for the Diffraction Scattering of Deuterons — 733L.
Ivanenko, I. P. On the Cascade Theory of Showers — 94.
— and B. E. Samosudov. Cascade Curves for Copper — 884.
— (see Volkanskaia, T. G.) — 202L.
Iu. M. Ivanov and A. I. Fesenko. μ^+-Meson Depolarization in Nuclear Emulsions with Different Gelatin Content — 905L.
Ivanovskaia, I. A. and I. V. Rakobol'skaia. On the Spectrum of the Electron-Photon Component of Extensive Air Showers — 1107.
Ivanter, I. G. Possibility of Determining the Interaction Constants from Experiments on $K_{\mu 3}$ Decays — 79.
Iziumov, T. G. (see Skrotskii, G. V.) — 1028.
Iziumov, Iu. A. Interaction between Outer and Inner Electrodes in Ferromagnetic Transition — 804.
Jacobi, G. A. (see Kolesnikov, N. N.) — 265.
Kaganov, M. I. and V. G. Peschanskii. Galvano-Magnetic Effects in Metals with Nearly Equal Numbers of Electrons and Holes — 734L.
— and V. M. Tsukernik. Effect of Thermoelectric Forces on the Skin Effect in a Metal — 327.
— (see Bar'iakhtar, V. G.) — 532.
Kaganskii, M. G. (see Kaminskii, D. L.) — 646.
Kaipov, D. K., V. N. Shakhvorostov, and Iu. G. Kosiak. Production of Pions in Condensed Media by Cosmic Rays in the Stratosphere — 573L.
Kaitmazov, S. D. and A. M. Prokhorov. Paramagnetic Resonance of the Free Radicals Obtained by Freezing a Plasma of H_2S — 381L.
Kalashnikova, V. I. (see Lebedev, V. I.) — 370L.
Kalinkin, L. F., A. S. Melioranskii, and I. V. Estulin. Gamma Radiation from Radiative Capture of Thermal Neutrons by Mo^{95}, Ag^{107}, Te^{123}, and Cs^{133} Nuclei — 410.
Kaminskii, D. L. and M. G. Kaganskii. Positron Spectrum of $Eu^{152,154}$ — 646.
Kanavets, V. P. (see Barmin, V. V.) — 374L.
Kaner, E. A. On Some Peculiarities of Cyclotron Resonance in Metals with Non-Convex Fermi Surfaces — 671.
Karpov, M. V. (see Kel'man, V. M.) — 779.
Kazarinov, Iu. M. and Iu. N. Simonov. Neutron-Proton Collisions at 586-Mev Neutron Energy — 56.
Kazarov, R. E. and R. B. Liudvigov. On the Penetrating Component in Extensive Air Showers — 915L.
Kel'man, V. M., V. A. Koliunov, and M. V. Karpov. Application of Magnetic Slits for Forming Circular Charged-Particle Trajectories — 779.
—, R. Ia. Metskhvarishvili, B. K. Preobrazhenskii, V. A. Romanov, and V. V. Tuchkevich. Investigation of Con-

version Electron Spectra of Neutron-Deficient Isotopes of Lutecium — 914L.

Khachatrian, B. V. (see Ter-Mikaelian, M. L.) — 898L.

Khalatnikov, I. M. (see Abrikosov, A. A.) — 182.

Khalupa, B. (see Ignatenko, A. E.) — 621.

— (see Ignatenko, A. E.) — 792.

Kharlamov, S. P. (see Adamovich, M. I.) — 21.

Kheifets, S. A. (see Orlov, Iu. F.) — 354L.

Khokhlov, Iu. K. Moment of Inertia of Nonspherical Nuclei — 165.

Khotkevich, V. I. (see Gindin, I. A.) — 556L.

Khrimian, G. V. Investigation of Nuclear Disintegration Produced by the Charged Component of Cosmic Radiation — 752.

Khristiansen, G. B. (see Guseva, V. V.) — 577.

— (see Kulikov, G. V.) — 441.

Khutsishvili, G. R. On the Overhauser Effect in Nonmetals II — 720.

— and O. D. Cheishvili. Double Elastic Scattering of Deuterons in a Magnetic Field — 859.

— (see Matinian, S. G.) — 377L.

Khvashchevskii, S. (see Koval'skii, N. G.) — 656.

Kirakosian, Z. A. (see Kocharian, N. M.) — 933.

Kirenskii, L. V. and I. F. Degtiarev. On the Thermal Stability of the Domain Structure in Silicon-Iron Crystals — 403.

— and V. V. Veter. Change in Width of Boundary Layer in Ferromagnets by Means of the Magneto-Optical Kerr Effect — 568L.

Kirilov-Ugriumov, V. G., L. P. Kotenko, E. P. Kuznetsov, and F. M. Sergeev. Elastic Scattering of 5 to 22 Mev Positive Pions by Carbon — 907L.

Kirzhnits, D. A. Correlation Energy of an Inhomogeneous Electron Gas — 835.

— The Limits of Applicability of the Quasi-Classical Equation of State of Matter — 1081.

Kiselev, V. S., K. O. Oganesian, R. A. Poze, and V. B. Fliagin. New Measurements of the Neutron Spectrum in the Bombardment of Be by 680-Mev Protons — 564L.

— (see Fliagin, V. B.) — 592.

Kladnitskaia, E. N. (see Wang, Kan-Chang) — 625.

Kligman, F. I. On the Distribution of Nucleon Density in Nuclei — 255.

Klimontovich, Iu. L. On a Possible Statistical Description of Systems of Particles Interacting with the Field — 891L.

— and S. V. Temko. Kinetic Equations for a System of Particles Interacting with Lattice Vibrations — 799.

Kocharian, N. M., G. S. Saakian, and Z. A. Kirakosian. Energy Spectra and Nuclear Interactions of Cosmic-Ray Particles — 933.

Kogan, A. V., V. D. Kul'kov, L. P. Nikitin, N. M. Reinov, I. A. Sokolov, and M. F. Stel'makh. Measurement of β-γ Correlation from Oriented Nuclei — 903L.

Kogan, V. S. (see Garber, R. I.) — 953.

Kokin, A. A. (see Chirkov, A. K.) — 36.

Kol'chinskaia, T. I. (see Sergeev, A. G.) — 242.

Koliunov, V. A. (see Kel'man, V. M.) — 779.

Kolesnikov, N. N. and G. A. Jacobi. Short Range Interaction between the Electron and Other Particles — 265.

Kolganova, E. D. (see Vaisenberg, A. O.) — 448.

Komar, A. A. The Scattering of Spin $^3/_2$ Particles by a Coulomb Field — 559L.

Komarov, V. V., V. G. Neudachin, A. M. Popova, and I. B. Teplov. On the Mechanism of Stripping in Reactions Involving the Capture of Two Nucleons — 679.

Komel'kov, V. S. Selfconstricting Discharges in Deuterium at High Rates of Current Growth — 10.

Kompaneets, A. S. Radio Emission from an Atomic Explosion — 1076.

Kondorskii, E. I. and V. L. Sedov. Change of Saturation Magnetization and of Electrical Resistance of Iron-Nickel under Hydrostatic Compression at Low Temperatures — 586.

— and V. L. Sedov. Antiferromagnetism of the Gamma Phase of Iron — 1104L.

—, V. E. Rode, and U. Gofman. The Saturation Magnetization of Nickel-Copper Alloys at Low Temperatures — 380L.

Kontorovich, V. M. On the Interaction between Small Disturbances and Discontinuities in Magnetohydrodynamics and on the Stability of Shock Waves — 851.

Kopaleishvili, T. I. and V. I. Mamasakhlisov. The Inelastic Scattering of Deuterons by Mg^{24} — 711.

Kopvillem, U. Kh. Spin-Spin Paramagnetic Relaxation Time in the Absence of a Static Magnetic Field for $Co(NH_4)_2 \cdot 6H_2O$ at Helium Temperatures — 349L.

Kopylov, G. I. A Model for the Process of Multiple Production — 996.

Kosevich, A. M. Influence of Deformations on Oscillation Effects in Metals at Low Temperatures — 171

— The De Haas-Van Alphen Effect in Pulsed Magnetic Fields — 512.

Kosiak, Iu. G. (see Kaipov, D. K.) — 573L.

Kotenko, L. P. (see Kirilov-Ugriumov, V. G.) — 907L.

Kovalev, V. P. and V. S. Stavinskii. Computing the Spectra of Fission Neutrons — 545.

Koval'skii, N. G., I. M. Podgornyi, and S. Khvashchevskii. Energy of the X-Rays Emitted by Intense Pulsed Discharges in Hydrogen — 656.

Kovrizhnykh, L. M. (see Veksler, V. I.) — 781.

Kozlov, V. F. (see Fogel', Ia. M.) — 390.

Krasil'nikov, D. D. Increase of the Barometric Effect with the Energy of Extensive Air Showers — 203L.

Kreines, N. M. Magnetic Anisotropy of Single-Crystal $CuSO_4$ in the Antiferromagnetic State — 972.

— (see Borovik-Romanov, A. S.) — 734L.

Kucher, T. I. Hole Bands in NaCl — 732L.

Kulikov, G. V. and G. B. Khristiansen. On the Size Spectrum of Extensive Air Showers — 441.

Kul'kov, V. D. (see Kogan, A. V.) — 903L.

Kul'chitskii, L. A. (see Bazhanov, E. B.) — 224.

Kumekin, Iu. P., M. G. Meshcheriakov, S. B. Nurushev, and G. D. Stoletov. Triple Scattering of 660-Mev Protons I. Measurement of the Depolarization Parameter D(90°) — 977.

Kurbatov, L. V. (see Skrotskii, G. V.) — 148.

Kurchatov, B. V., V. N. Mekhedov, L. V. Chistiakov, M. Ia. Kuznetsova, N. I. Borisova, and V. G. Solov'ev. Secondary Nuclear Reactions Induced in Bismuth and Lead by High-Energy Proton Bombardment — 40.

Kurdgelaidze, D. F. Wave Solutions of Nonlinear Generalizations of Relativistic Equations — 1099.

Kutikov, I. E. (see Sosnovskii, A. N.) — 739L.

Kutuzov, V. A. Paramagnetic Absorption in Parallel

Fields at 9.3×10^9 cps. in the Salts $Fe(NH_4)(SO_4)_2 \cdot 12H_2O$ and $Fe(NO_3)_3 \cdot 9H_2O$ — 910L.
Kuz'micheva, G. V. (see Adamovich, M. I.) — 21.
Kuznetsov, E. P. (see Kirilov-Ugriumov, V. G.) — 907L.
Kuznetsov, V. V. and V. N. Mekhedov. Tritium Production in Metals by 120 to 660-Mev Protons — 406.
Kuznetsova, M. Ia. (see Kurchatov, B. V.) — 40.
Kvartskhava, I. F., V. V. Bondarenko, R. D. Meladze, and K. V. Suladze. Electric Explosion of Spiral Wires in Vacuum — 634.
Landau, L. D. On the Theory of the Fermi Liquid — 70.
Lapidus, L. I. On the Problem of Testing the Invariance of an Interaction under Time Inversion — 1105L.
— (see Biln'kii, S. M.) — 669.
Larionova, V. G. (Adamovich, M. I.) — 21.
E. Larish and I. Shekhtman. Production of Two Temperatures in an Ionized Gas in a Magnetic Field — 355L.
— Propagation of Detonation Waves in the Presence of a Magnetic Field — 139.
Latyshev, G. D. (see Sergeev, A. G.) — 242.
Lazarev, B. G. (see Dmitrenko, I. M.) — 229.
— (see Gindin, I. A.) — 556L.
Lebedev, A. I. Level Widths of π-Mesonic Atoms — 729L.
Lebedev, V. I. and Kalshnikova, V. I. Average Number of Neutrons Emitted in the Fission of Th^{229} by Thermal Neutrons — 370L.
Lemberg, I. Kh. (see Alkhazov, D. G.) — 736L.
— (see Alkhazov, D. G.) — 926.
— (see Alkhazov, D. G.) — 737L.
Leriust, F. (see Glasko, V. B.) — 312.
Lifshitz, I. M. and V. G. Peschanskii. Galvanomagnetic Characteristics of Metals with Open Fermi Surfaces. I. — 875.
— and D. G. Sanikidze. Pomeranchuk Effect and Diagram of State for He^3-He^4 Solutions — 713.
— and V. V. Slezov. Kinetics of Diffusive Decomposition of Supersaturated Solid Solutions — 331.
— (see Azbel', M. Ia.) — 480.
Liubarskii, G. Ia. and R. V. Polovin. Simple Magnetoacoustic Waves — 351L.
— The Splitting of a Small Discontinuity in Magnetohydrodynamics — 901L.
— (see Akhiezer, A. I.) — 507.
— Polovin, R. V. — 351L.
Liubimov, V. A. and M. E. Vishnevskii. Measurement of the Polarization of Internal Conversion Electrons — 1103L.
— (see Alikhanov, A. I.) — 740L.
Liubimov, V. B. (see Gramenitskii, I. M.) — 381L.
Liudvigov, R. B. (see Kazarov, R. E.) — 915L.
Liul'ka, V. A. and V. A. Filimonov. Binding Energy of Light Hypernuclei According to Meson Theory — 717.
Lomanov, M. F., A. G. Mehkovskii, Ia. Ia. Shalamov, V. A. Shebanov, and A. F. Grashin — 615.
— (see Blinov, G. A.) — 609.
Lubchenko, A. F. (see Davydov, A. S.) — 1048.
Luk'ianov, A. V., Iu. V. Orlov, and V. V. Turotsev. Optical Model for the Interaction of Neutrons of Intermediate Energy with Nuclei — 521.
Maevskii, V. (see Chou, Kuang-Chao) — 1106L.
Makarova, T. P. (see Zherebtsova, K. I.) — 947.
Maksimenko, V. M. Statistical Interpretation of Experimental Data on Multiple Production of Particles at 1 to 20 Bev — 909L.
Maksiutenko, B. P. Relative Yields of Delayed Neutrons in Fission of U^{238}, U^{235} and Th^{232} by Fast Neutrons — 565L.
Malakhov, I. Ia. (see Sorokin, P. V.) — 969.
Malysheva, T. V. and I. P. Alimarin. A Radiochemical Study of the (p, pxn), (p, 4pxn) and (p, 5pxn) Reactions — 772.
Mamasakhlisov, V. I. (see Kopaleishvili, T. I.) — 711.
Marutian, N. A. (see Babaian, Kh. P.) — 387.
Matevosian, K. A. (see Babaian, Kh. P.) — 387
Matinian, S. G. Nonlocal Effects in Weak Interactions of Fermions — 548L.
— and G. R. Khutsishvili. Isotopic Invariance in Anti-Hyperon Processes — 377L.
Matveev, A. N. On the Electron Capture Mechanism and the Current Limit in Betatrons — 259.
Mekhedov, V. N. (see Kurchatov, B. V.) — 40.
— (see Kuznetsov, V. V.) — 406.
Meladze, R. D. (see Kvartskhava, I. F.) — 634.
Melioranskii, A. S. (see Kalinkin, L. F.) — 410.
Meshcheriakov, V. A. The π-Mesonic Atom and Corrections to the Dispersion Relations — 200L.
Meshcheriakov, M. G. (see Kumekin, Iu. P.) — 977.
Meshkovskii, A. G., Ia. Ia. Shalamov, and V. A. Shebanov. Energy Spectrum and Angular Distributions of π^+ Mesons Produced in Proton-Proton Collisions at 660 to 670 Mev — 46.
— (see Lomanov, M. F.) — 615.
Metskhvarishvili, R. Ia. (see Kel'man, V. M.) — 914L.
Mikhul, E. K. The Statistical Weights of K^+ and K^- Mesons Produced in Pion-Nucleon Collisions — 205L.
Milekhin, G. A. Hydrodynamic Theory of Multiple Production of Particles in Collisions between Fast Nucleons and Nuclei — 829.
— On the Hydrodynamic Theory of Multiple Production of Particles — 682.
Miller, M. A. Reflection of Electrons from a High-Frequency Potential Barrier — 206L.
— Several Possibilities Associated with the Separation of Charged Particles in an Inhomogeneous High-Frequency Electromagnetic Field — 561L.
Minervina, Z. V. (see Vaisenberg, A. O.) — 448.
Mitin, R. V. (see Fogel', Ia. M.) — 390.
Morozov, B. V. (see Barmin, V. V.) — 374L.
Moskalev, V. I. (see Bugdanov, Iu. A.) — 1101L.
Mukhin, A. I., E. B. Ozerov, and B. Pontecorvo. Energy Dependence of μ^+-e^+ Decay Asymmetry — 237.
Mukhtarov, A. I. and Gadzhiev, S. A. Radiative Decay of π^+ Mesons and Effects of Parity Nonconservation — 895L.
Murzina, E. A., S. I. Nikol'skii, and V. I. Iakovlev. Observation of Nuclear-Active Particles of Cosmic Radiation with Energy $\geq 10^{13}$ ev — 906L.
Nelipa, N. F. Elastic Scattering of Photons on Excited Nucleons — 460.
— and V. A. Feoktistov. On the Polarization of Recoil Nucleons in the Photoproduction of Pions — 167.
Nemilov, Iu. A., A. N. Pisarevskii, and L. D. Soshin. Study of γ-Rays from As^{78} Decay — 555L.
— The First Excited State of Tb^{159} — 554L.
— (see Zherebtsova, K. I.) — 947.
Nesterov, V. G. and G. N. Smirenkin. Fission Cross

Section of Pu^{240} by Fast Neutrons — 367L.
Neudachin, V. G. Exchange Effects in Stripping Reactions — 815.
— (see Komarov, V. V.) — 679.
Nikishov, A. I. and I. L. Rozental'. Determination of the Energy of Fast Particles from the Angular Distribution of their Reaction Products — 115.
Nikitin, L. P. (see Kogan, A. V.) — 903L.
Nikol'skii, S. I. and A. A. Pomanskii. Investigation of Extensive Cosmic Ray Showers under Dense Substances — 430.
— (see Murzina, E. A.) — 906L.
Novozhilov, Iu. V. On the Scattering of "Dressed" Particles in Quantum Field Theory — 515.
Nurushev, S. B. (see Kumekin, Iu. P.) — 977.
Obreimov, I. V. and V. I. Startsev. Work of Formation of an Elastic Twin in Calcite — 743.
Obukhov, A. I. Determination of the Momentum and Excitation Energy Acquired by a Heavy Nucleus in the Interaction with a Fast Nucleon — 727L.
Oganesian, K. O. (see Fliagin, V. B.) — 592.
— (see Kiselev, V. S.) — 564L.
Okonov, E. O. On the Possible Existence of the Ξ^0 Hyperon — 863.
Okun', L. B. (see Baz', A. N.) — 526.
Orlov, Iu. F. On the Mechanism of the Damping of Free Oscillations in a Cyclic Accelerator — 362L.
— and S. A. Kheifets. Depolarization of Electrons Due to Radiation in a Magnetic Field — 354L.
Orov, Iu. V. (see Luk'ianov, A. V.) — 521.
Ostroumov, V. N. and Iu. P. Iakovlev. Multi-Charged Particles Emitted in Disintegration of Carbon Nuclei by 660-Mev Protons — 949.
Ozerov, E. B. (see Mukhin, A. I.) — 237.
Pargamanik, L. E. and V. V. Ul'ianov. Momenta with Semi-Transparent Nuclei — 177.
Pastukhova, Z. V. (see Estulin, I. V.) — 51.
Pekar, S. I. The Energy of Excitons for Very Small Quasi-Momenta — 360L.
Peletminiskii, S. V. (see Akhiezer, A. I.) — 157.
Perel', V. I. Wave Functions of Many-Electron Systems — 476.
Perel'man, M. E. On the Theory of Composite π^0 Mesons — 350L.
— (see Chavchanidze, V. V.) — 204L.
Perfilov, N. A. and G. F. Denisenko. Triple Disintegrations of Uranium Nuclei — 438.
Pershin, I. I. (see Barmin, V. V.) — 374L.
Peschanskii, V. G. (see Kaganov, M. I.) — 734L.
— (see Lifshitz, I. M.) — 875.
Peshkov, V. P. Observation of the Lambda Transition in Helium in the Presence of a Thermal Current through the Phase Boundary — 943.s
Pesotskaia, E. A. (see Vaisenberg, A. O.) — 448.
Petrzhak, K. A. (see Vasil'ev, I. A.) — 795.
Piliia, A. D. (see Gol'din, L. L.) — 127.
Pilipenko, D. V. (see Fogel', Ia. M.) — 601.
Pisarevskii, A. N. (see Nemilov, Iu. A.) — 555L.
— (see Nemilov, Iu. A.) — 554L.
Pitaevskii, L. P. Calculation of the Phonon Part of the Mutual Friction Force in Superfluid Helium — 888.
— Phenomenological Theory of Superfluidity near the λ Point — 282.
Podgoretskii, M. I. (see Gramenitskii, I. M.) — 381L.
Podgornyi, I. M. (see Koval'skii, N. G.) — 656.
Podgurskaia, A. V. (see Grigorov, N. L.) — 1.
Podlubnyi, L. P. On the Multiple Interaction in Quantum Field Theory — 728L.
Poliakov. L. M. (see Garber, R. I.) — 953.
Polovin, R. V. and G. Ia. Liubarskii. Impossibility of Refraction Shock Waves in Magnetohydrodynamics — 351L.
— (see Akhiezer, A. I.) — 507.
— (see Liubarskii, G. Ia.) — 351L.
— (see Liubarskii, G. Ia.) — 901L.
Pomanskii, L. A. (see Nikol'skii, S. I.) — 430.
Pomeranchuk, I. Ia. Isotopic Effect in the Residual Electrical Resistance of Metals — 693.
— On the Stability of a Fermi Liquid — 361L.
Pontecorvo, B. M. (see Mukhin, A. I.) — 237.
Poperekova, L. M. (see Grigorov, N. L.) — 1.
Popov, Iu. M. Cross Sections of Possible Nonradiative Recombination in Semiconductors — 348L.
Popov, V. S. On the Behavior of a Particle of Arbitrary Spin in an External Magnetic Field — 687.
Popova, A. M. (see Komarov, V. V.) — 679.
Poze, R. A. (see Kiselev, V. S.) — 564L.
Preobrazhenskii, B. K. (see Kel'man, V. M.) — 914L.
Prokhorov, A. M. (see Kaitmazov, S. D.) — 381L.
Prokof'ev, Iu. A. (see Sosnovskii, A. N.) — 739L.
Pshenichnikov, B. V. (see Filimonov, Iu. I.) — 378L.
Puzikov, L. D. (see Bilen'kii, S. M.) — 669.
Rabin, N. V. (see Vaisenberg, A. O.) — 448.
Rabinovich, M. S. (see Iogansen, L. V.) — 708.
Raizer, Iu. P. (see Zel'dovich, Ia. B.) — 980.
Rakobol'skaia, I. V. (see Ivanovskaia, I. A.) — 1107L.
Reinov, N. M. (see Kogan, A. V.) — 903L.
Remennyi, A. S. (see Sergeev, A. G.) — 242.
Riazanov, G. V. Quantum-Mechanical Probabilities as Sums over Paths — 85.
Ristau, O. (see Shoffa, G.) — 445.
Ritus, V. I. Spin Structure of the Scattering Matrix for Reactions Involving Gamma Rays — 1038.
Riumina, K. P. (see Granovskii, V. L.) — 33.
Rode, V. E. (see Kondorskii, E. I.) — 380L.
Romanov, V. A. (see Kel'man, V. M.) — 914L.
Romashko, N. D. (see Fogel', Ia. M.) — 390.
Rozental', I. L. and V. N. Strel'tsov. Passage of High-Energy Muons through Matter — 1007.
— (see Nikishov, A. I.) — 115.
Ruckenstein, E. (see Friedlander, E.) — 75.
Ruckpaul, K. (see Shoffa, G.) — 445.
Rudik, A. P. (see Berestetskii, V. B.) — 111.
Rukhadze, A. A. On the Problem of Two-Nucleon Interaction in the Tamm-Dancoff Method — 352L.
— (see Agranovich, V. M.) — 819.
— (see Agranovich, V. M.) — 685.
Rusakov, S. V. (see Belousov, A. S.) — 247.
Rusinov, L. I. (see Golenetskii, S. V.) — 917L.
Ryndin, R. M. (see Bilen'kii, S. M.) — 574L.
— (see Bilen'kii, S. M.) — 669.
Saakian, G. S. (see Kacharian, N. M.) — 933.
Samosudov, V. E. (see Ivanenko, I. P.) — 884.
Sanikadze, D. G. Contribution to the Theory of the

Pomeranchuk Effect in He^3 — 192L.
— (see Lifshitz, I. M.) — 713.
San'ko, L. A., Zh. S. Takibaev, and Ts. I. Shakhova. Investigation of the Angular Distribution of Secondary Particles in Showers Produced by High-Energy Nucleons — 396.
Sarinian, M. G. (see Babaian, Kh. P.) — 387.
Savchenko, O. V. (see Akimov, Iu. K.) — 64.
Savel'eva, A. I. (see Grigorov, N. L.) — 1.
Savoskin, V. I. (see Glotova, G. I.) — 965.
— (see Granovskii, V. L.) — 33.
Sedov, V. L. (see Kondorskii, E. I.) — 586.
— (see Kondorskii, E. I.) — 1104L.
Semenenko, E. E. (see Sudovtsov, A. M.) — 211L.
Serebrennikov, Iu. I. The Possibility of Estimating the Mean Lifetime of Alpha Particles within Nuclei — 547L.
Sergeev, A. G., V. D. Vorob'ev, A. S. Remennyi, T. I. Kol'chinskaia, G. D. Latyshev, and Iu. S. Egorov. Effect of Finite Nuclear Size on the Relative Internal Conversion Coefficients in L Subshells — 242.
Sergeev, F. M. (see Kirilov-Ugriumov, V. G.) — 907L.
Shabanskii, V. P. Nonequilibrium Processes in Impurity Semiconductors — 101.
Shafranova, M. G. (see Dul'kova, L. S.) — 217.
Shakhova, Ts. I. (see San'ko, L. A.) — 396.
Shakhvorostov, V. N. (see Kaipov, D. K.) — 573L.
Shalamov, Ia. Ia. (see Blinov, G. A.) — 609.
— (see Lomanov, M. F.) — 615.
— (see Meshkovskii, A. G.) — 46.
Shal'nikov, A. I. A Method for the Observation of Helium II Films — 386L.
Shamov, V. P. Fission of Silver by High-Energy Protons — 219.
Shchegolev, V. A. (see Blinov, G. A.) — 609.
Shebanov, V. A. (see Blinor, G. A.) — 609.
— (see Lomanov, M. F.) — 615.
— (see Meshkovskii, A. G.) — 46.
Shekhter, V. M. Hyperon Beta Decay — 316.
Shekhtman, I. (see Larish, E.) — 139.
— (see Larish, E.) — 355L.
Shirokov, Iu. M. Relativistic Theory of Polarization Effects — 703.
Shishkin, L. A. Sound Absorption in Ferromagnetic Dielectrics in a Magnetic Field at Low Temperatures — 197L.
Shkoda-Ul'ianov, V. A. On the Possibility of Applying the Belen'kii-Tamm Equilibrium Spectrum to the Determination of (γ, n) Reactions — 726L.
Shoffa, G., O. Ristau, and K. Ruckpaul. Anomaly in the Magnetic Anisitropy of $K_3Fe(CN)_6$ Single Crystals at Low Temperatures — 445.
Shushurin, S. F. (see Glaski, V. B.) — 312.
Silin, V. P. On the Theory of the Optical Properties of Conductors in the Case of Oblique Incidence of the Radiation — 700.
— The Oscillations of a Degenerate Electron Fluid — 870.
Simonov, Iu. N. (see Kazarinvo, Iu. M.) — 56.
Sitenko, A. G. and Iu. A. Berezhnoi. Diffraction Breakup of Light Nuclei — 899L.
— (see Akhiezer, A. I.) — 82.
Skobov, V. G. Decay of a Photon into two Photons in a Homogeneous Magnetic Field — 919L.
Skripov, V. P. Heat of Mixing of Light and Heavy Water — 903L.
Skrotskii, G. V. Equations of Motion for a System Consisting of Two Types of Interacting Spins — 550L.
— and Iu. I. Alimov. Ferromagnetic Resonance in a Circulatory Polarized Magnetic Field of Arbitrary Amplitude — 1035.
— and L. V. Kurbatov. Theory of the Anisotropy of the Width of Ferromagnetic Resonance Absorption Line — 148.
—, P. S. Zyrianov, and T. G. Iziumov. Effect of Electron Paramagnetic Resonance on the Optical Faraday Effect at Low Temperatures — 1028.
Slezov, V. V. (see Lifshitz, I. M.) — 331.
Smirenkin, G. N. (see Nesterov, V. G.) — 367L.
Smirnitskii, V. M. (see Vaisenberg, A. O.) — 448.
Sokolov, I. A. (see Kogan, A. V.) — 903L.
Sokolov, V. M. (see Dukel'skii, V. M.) — 569L.
Sokolova, I. B. (see Dul'kova, L. S.) — 217.
Solov'ev, M. I. (see Wang, Kan-Chang) — 625
Solov'ev, V. G. Nucleonic Interaction which Produces a Superfluid State of the Nucleus — 572L.
— (see Kurchatov, B. V.) — 40.
Sorokin, P. V., A. K. Val'ter, I. Ia. Malkhov, and A. Ia. Taranov. Polarization of Protons Elastically Scattered from Si^{28} Nuclei — 969.
Soroko, L. M. Proton-Proton Scattering in the $^1D_2$ State at 616 Mev — 190L.
— (see Akimov, Iu. K.) — 64.
Soshin, L. D. (see Nemilov, Iu. A.) — 555L.
— (see Nemilov, Iu. A.) — 554L.
Sosnovskii, A. N., P. E. Spivak, Iu. A. Prokof'ev, I. E. Kutikov, and Iu. P. Dobrynin. Measurement of the Half-Life of the Neutron — 739L.
Spivak, P. E. (see Sosnovskii, A. N.) — 739L.
Staniukovich, K. P. Shock Waves in a Conducting Ultra-relativistic Gas — 359L.
— Stationary Relativistic Motions of a Gas in a Conducting Medium — 529.
— (see Golitsyn, G. S.) — 575L.
Starikov, M. A. (see Garif'ianov, N. A.) — 553L.
Starodubov, Ia. D. (see Gindin, I. A.) — 556L.
Startsev, V. I. (see Obreimov, I. V.) — 743.
Stavinskii, V. S. (see Agranovich, V. M.) — 896L.
— (see Kovalev, V. P.) — 545.
Stel'makh, M. F. (see Kogan, A. V.) — 903L.
Stepanov, K. N. Low Frequency Oscillations of a Plasma in a Magnetic Field — 808.
— On the Damping of Electromagnetic Waves in a Plasma Situated in a Magnetic Field — 195L.
Stoletov, G. D. (see Kimekin, Iu. P.) — 977.
Strel'tsov, V. N. (see Rozental', I. L.) — 1007.
Sudovtsov, A. M. and E. E. Semenenko. On the Influence of Domain Structure on the Electrical Resistivity of Iron at Low Temperatures — 211L.
Suladze, K. V. (see Kvartskhava, I. F.) — 634.
Svirskii, M. S. (see Vonsovskii, S. V.) — 1012.
Syrovatskii, S. I. The Stability of Shock Waves in Magnetohydrodynamics — 1024.
Szalay, A. (see Csikai, J.) — 749.
Tager, A. S. and Gladun, A. D. Use of Cyclotron Resonance in Semiconductors for the Amplification and Generation of

Microwaves — 560L.
Takibaev, Zh. S. An Estimate of the Energy of Shower-Producing Particles with Allowance for their Energy Spectrum — 191L.
— (see San'ko, L. A.) — 396.
Taluts, G. G. (see Giterman, M. Sh.) — 1072.
Tamm, E. I. (see Belousov, A. S.) — 247.
Taranov, A. Ia. (see Sorokin, P. V.) — 969.
Tavger, B. A. Splitting of Atomic Terms with Integer Total Angular Momentum in a Magnetic Crystal — 322.
Temko, S. V. (see Klimontovich, Iu. L.) — 799.
Teplov, I. B. (see Komarov, V. V.) — 679.
Ter-Martirosian, K. A. (see Gol'din, L. L.) — 127.
Ter-Mikaelian, M. L. and B. V. Khachatrian. On the Limits of Applicability of the Impact Parameter Method — 898L.
Terekhov, Iu. V. (see Burgov, N. A.) — 651.
Terletskii, Ia. P. (see Glasko, V. B.) — 312.
Timofeev, G. A. (see Vokonskaia, T. G.) — 202L.
Timofeeva, G. G. (see Granovskii, V. P.) 33.
Timofeeva, L. P. (see Gustova, L. V.) — 920L.
Toptygin, I. N. (see Dolginov, A. Z.) — 550L.
Tsukernik, V. M. (see Kaganov, M. I.) — 327.
Tsytovich, V. N. Interaction between a Medium and a Ring Current Incident to it — 983.
Tuchkevich, V. V. (see Kel'man, V. M.) — 914L.
Turchinskaia, M. I. (see Volkenshtein, N. V.) — 916L.
Turovtsev, V. V. (see Luk'ianov, A. V.) — 521.
Tuvdendorzh, D. (see Gramenitskii, I. M.) — 381L.
Ul'ianov, V. V. (see Pargamanik, L. E.) — 177.
Urbakh, V. Iu. A Nonlinear Theory of Vector Fields — 143.
Vaisenberg, A. I., V. M. Smirnitskii, E. D. Kolganova, Z. V. Minervina, E. A. Pesotskaia, and N. V. Rabin. Angular Correlation for Low-Energy Positrons Emitted in π^+-μ^+-e^- Decay — 448.
Vaks, V. G. and B. L. Ioffe. On the $\pi \rightarrow e + \nu + \gamma$ Decay — 151.
Valiev, K. A. and Sh. Sh. Bashkirov. Stimulated R. F. Amplifier Working on Hyperfine Levels of Paramagnetic Atoms — 208L.
— (see Al'tshuler, S. A.) — 661.
— (see Bashkirov, Sh. Sh.) — 471.
Val'ter, A. K. (see Sorokin, P. V.) — 969.
Varfolomeev, A. T. Absorption of Slow π^- Mesons by Nuclei — 373L.
Vashakidze, I. Sh. and O. D. Cheirshvili. A Note on d-d Reactions — 741L.
Vasil'ev, I. A. and K. A. Petrzhak. Radiochemical Study of the Photofission of Th^{232} — 795.
Veksler, V. I. and L. M. Kovrizhnykh. Cyclic Acceleration of Particles in High Frequency Fields — 781.
Venttsel', V. A. (see Brandt, N. B.) — 757.
Verkin, B. I. and I. M. Dmitrenko. Effect of Uniaxial Elastic Deformations on the Magnetic Properties of Zinc Crystals at Low Temperatures — 200L.
— (see Dmitrenko, I. M.) — 229.
Veter, V. V. (see Kirenskii, L. V.) — 568L.
Victor, S. (see Budagov, Iu. A.) — 1101L.
Vinetskii, V. L. and M. F. Deigen. Influence of Acoustic Vibrations on the Parameters of the Bands of Impurity Absorption in Crystals — 198L.
Vishnevskii, M. E. (see Liubimov, V. A.) — 1103L.
Vladimirskii, V. V. Optical Methods of Observing the Ionization along Fast Particle Tracks — 384L.
Volkenshtein, N. V., G. V. Fedorov, and S. V. Vonsovskii. Hall Effect in Pure Nickel at Helium Temperatures — 61.
—, M. I. Turchinskaia, and E. V. Galoshina. Peculiarities of Magnetization of the Disordered Ni_3Mn Alloy at Low Temperatures — 916L.
Volkonskaia, T. G., I. P. Ivanenko, and G. A. Timofeev. Electron-Photon Cascades in Lead — 202L.
Volkov, Iu. D. (see Chchernikov, V. I.) — 606.
Volkov, Iu. M. (see Bazhanov, E. B.) — 224.
Volkova, L. V. and F. P. Denisov. Recoil Range of Na^{24} and the Mechanism of $Al^{27}(p, 3pn)$ and $P^{31}(p, 5p3n)$ for 660-Mev Protons — 372L.
Volkovyskii, R. Iu. Circular Polarization of Internal γ-Bremsstrahlung in β-Decay and Time — 562L.
Vonsovskii, S. V. and M. S. Svirskii. The Statistics of Spin and Polar Excitations in a Crystal — 1012.
— (see Volkenshtein, N. V.) — 61.
Vorob'ev, Iu. A. Range of Nitrogen and Beryllium Ions in Air — 912L.
Vorob'ev, V. D. (see Sergeev, A. G.) — 242.
Wang, Kan-Chang, Wang Tso-Tsiang, Ding Da-Tsao, L. N. Dubrovskii, E. N. Kladnitskaia, and M. I. Solov'ev. An Investigation of the Interaction between 250-270 Mev π^+ Meson and Carbon Nuclei with the Aid of a Propane Bubble Chamber — 625.
Wang, Tso-Tsiang, (see Kan-Chang, Wang) — 625.
Weiner, R. Nuclear Isomerism and Atomic Spectra — 196L.
Zaikin, D. A. On the Deviation of the Equilibrium Shape of Atomic Nuclei from Axial Symmetry — 365L.
Zakhar'ev, B. N. (see Beliaev, V. B.) — 699.
Zastavenko, L. G. On the Question of the Uniqueness of Phase Analysis — 544L.
— (see Chou, Kuang-Chao) — 990.
Zatsepin, G. T. (see Guseva, V. V.) — 577.
Zel'dovich, Ia. B. and S. S. Gershtein. Formation of Hydrogen Mesic Molecules — 451.
— and Raizer, Iu. P. Physical Phenomena that Occur when Bodies Compressed by Strong Shock Waves Expand in Vacuo — 980.
Zel'tser, G. I. Fock's Cyclic Symmetry Condition and Young's Patterns — 738L.
Zlatev, I. and P. S. Isaev. Bremsstrahlung and Pair Production from Protons with Allowance for Form Factor — 213L.
Zherebtsova, K. I., T. P. Makarova, Iu. A. Nemilov, and B. L. Funshtein. Ratio of Isomeric and Ground State Yields of Zn^{69} Produced in Various Nuclear Reactions — 947.
Zhirnov, V. A. A Contribution to the Theory of Domain Walls in Ferroelectrics — 822.
Zyrianov, P. S. Generalized Self-Consistent Field Equations — 309.
— (see Giterman, M. Sh.) — 1072.
— (see Skrotskii, G. V.) — 1028.

Analytic Subject Index to Volume 35 (8)

References with L are Letters to the Editor. Items are listed under the following categories:

Acoustics
Astrophysics
Atomic and Molecular Beams
Atomic Mass and Abundance
Atomic Structure and Spectra
Biographical Material
Chemical Effects and Properties
Cosmic Radiation
Dielectrics and Dielectric Properties
Diffraction
Diffusion
Elasticity and Plasticity
Electrical Conductivity and Resistance
Electrical Discharges
Elementary Particle Interactions
Field Theory
Films, Properties
Fluid Dynamics
Gamma Rays
Gases
Geophysics
Helium, Liquid
Imperfections in Solids
Ions and Electrons, Mobility
Liquids
Magnetic Properties
Magnetic Resonance
Mathematical Methods
Methods and Instruments
Methods and Instruments
Microwaves
Miscellaneous
Molecular Aggregates
Molecular Structure and Spectra
Neutrino
Nuclear Fission
Nuclear Moments and Spin
Nuclear Photoeffects
Nuclear Reactions, General
Nuclear Reactions Induced by α Particles and He^3
Nuclear Reactions Induced by Deuterons and Tritons
Nuclear Reactions Induced by Mesons
Nuclear Reactions Induced by Neutrons
Nuclear Reactions Induced by Protons
Nuclear Spectra
Nuclear Structure Theory
Optical Properties
Quantum Mechanics
Radioactivity
Range and Energy Loss of Particles
Relativity and Gravitation
Scattering of Deuterons
Semiconductors
Spectra, General
Statistical Mechanics and Thermodynamics
Superconductivity
Thermal Properties
X-Rays

Absorption of Radiation (see Radiation)
Acoustics
  Coupled Magnetoelastic Waves in Ferromagnetic Media and Ferroacoustic Resonance. A. I. Akhiezer, V. G. Bar'iakhtar, and S. V. Peletminskii — 157.
Afterglow (see Electrical Discharges)
Alloys (see Crystalline State)
Annihilation (see Electrons and Positrons)
Antiferroelectric Phenomena (see Dielectrics and Dielectric Properties)
Antiferromagnetism (see Magnetic Properties)
Arcs (see Electric Discharges)
Astrophysics
  Impossibility of Rarefaction Shock Waves in Magnetohydrodynamics. R. V. Polovin and G. Ia. Liubarskii — 351L.
  Nonlinear Interaction of Radio Waves Propagating in a Plasma. V. L. Ginzburg — 1100L.
Atomic and Molecular Beams
  On the Applicability of Massey's Adiabatic Hypothesis to Double Charge Exchange. Ia. M. Fogel, R. V. Mitin, V. F. Kozlov, and N. D. Romashko — 390.
  Stimulated R. F. Amplifier Working on Hyperfine Levels of Paramagnetic Atoms. K. A. Valiev and Sh. Sh. Bashkirov — 208L.
Atomic Mass and Abundance
  Nuclear Binding Energies in the Region of the 82 Proton and 126 Neutron Magic Numbers. R. A. Demirkhanov, T. I. Gutkin, and V. V. Dorokhov — 639.
Atomic Structure and Spectra
  Effect of Electron Paramagnetic Resonance on the Optical Faraday Effect at Low Temperatures. G. V. Skrotskii, P. S. Zyrianov, and T. G. Iziumov — 1028.
  Electron Capture and Loss in Collisions of Fast Carbon and Oxygen Atoms with Gas Molecules. Ia. M. Fogel', V. A. Ankudinov, and D. V. Pilipenko — 601.
  Hard Gamma Radiation from As^{76}. Decay Schedule of As^{76}. L. V. Gustova and O. V. Chubinskii — 957.
  Negative Ions of Iron, Cobalt, and Nickel. V. M. Dukel'skii and V. M. Sokolov — 569L.
  Nuclear Isomerism and Atomic Spectra. R. Weiner — 196L.
  On the Theory of Longitudinal Relaxation of Paramagnetic Salt Solutions. S. A. Al'tshuler and K. A. Valiev — 661.
  Paramagnetic Resonance of Free Radicals in Weak Fields. A. K. Chirkov and A. A. Kokin — 36.
  Wave Functions of Many-Electron Systems. V. I. Perel' — 476.

Auger Effect (see Atomic Structure and Spectra)
Barkhausen Effect (see Magnetic Properties)
Biographical Material
  Academician Vladimir Aleksandrovich Fock — 923.
Boson Theory (see Radiation)
Broadening of Spectral Lines (see Atomic Structure and Spectra; Spectra, General)
Capture Cross Sections (see Electrons and Positrons; Nuclear Reactions, General; Radiation)
Cerenkov Effect (see Radiation)
Chemical Effects and Properties
  Cross Sections for the Capture of Slow Electrons by O_2 and H_2O Molecules and Molecules of Halogen Compounds. I. S. Buchel'nikova — 783.
  Investigation of Relaxation Processes in a Series of Fluorine Compounds of Carbon. V. S. Grechishkin — 253.
Chemiluminescence (see Luminescence)
Cold Emission (see Electrical Properties)
Compton Effect (see Radiation)
Conductivity, Electrical (see Electrical Conductivity and Resistance)
Cosmic Radiation
  A Study of Fast Deuterons at 3200 m above Sea Level. G. V. Badalian — 209L.
  An Estimate of the Energy of Shower-Producing Particles with Allowance for their Energy Spectrum. Zh. S. Takibaev — 191L.
  Cascade Curves for Copper. I. P. Ivanenko and B. E. Samosudov — 884.
  Energy Spectra and Nuclear Interactions of Cosmic-Ray Particles. N. M. Kocharian, G. S. Saakian, and Z. A. Kirakosian — 933.
  Increase of the Barometric Effect with the Energy of Extensive Air Showers. D. D. Krasil'nikov — 203L.
  Inelastic Interaction between Cosmic Ray Protons of Kinetic Energy above 7 Bev and Carbon and Hydrogen Nuclei. K. I. Alekseeva and N. L. Grigorov — 416.
  Influence of Multiple Scattering on the Development of High-Energy Electron-Photon Cascades in Lead. T. G. Volkonskaia, I. P. Ivanenko, and G. A. Timofeev — 202L.
  Interaction of Cosmic Ray Particles with Various Nuclei. N. L. Grigorov, A. V. Podgurskaia, A. I. Savel'eva, and L. M. Poperekova — 1.
  Investigation of Extensive Cosmic Ray Showers under Dense Substances. S. I. Nikol'skii and A. A. Pomanskii — 430.
  Investigation of Nuclear Disintegration Produced by the Charged Component of Cosmic Radiation. G. V. Khrimian — 752.
  Investigation of the Angular Distribution of Secondary Particles in Showers Produced by High-Energy Nucleons. L. A. San'ko, Zh. S. Takibaev, and Ts. I. Shakhova — 396.
  Measurement of Cosmic-Ray Intensity in the Stratosphere at Various Altitudes and Latitudes. A. N. Charakhch'ian and T. N. Charakhch'ian — 761.
  Observation of Nuclear-Active Particles of Cosmic Radiation with Energy $\geq 10^{13}$ ev. E. A. Murzina, S. I. Nikol'skii, and V. I. Iakovlev — 906L.
  On the Cascade Theory of Showers. I. P. Ivanenko — 94.
  On the Penetrating Component in Extensive Air Showers. R. E. Kazarov and R. B. Liudvigov — 915L.
  On the Possible Existence of the Ξ^0-Hyperon. E. O. Okonov — 863.
  On the Problem of Angular Correlation of Secondary Particles Produced in High-Energy Nuclear Collisions. I. M. Gramenitskii, M. Ia. Danysh, V. B. Liubimov, M. I. Podgoretskii, and D. Tuvdendorzh — 381L.
  On the Size Spectrum of Extensive Air Showers. G. V. Kulikov and G. B. Khristiansen — 441.
  On the Spectrum of the Electron-Photon Component of Extensive Air Showers. I. A. Ivanovskaia and I. V. Rakobol'skaia — 1107L.
  On the Zenith Angle Distribution of High-Energy Extensive Air Showers. V. V. Guseva, G. T. Zatsepin, and G. B. Khristiansen — 577.
  Passage of High Energy Muons through Matter. I. L. Rozental' and V. N. Strel'tsov — 1007.
  Production of Pions in Condensed Media by Cosmic Rays in the Stratosphere. D. K. Kaipov, V. N. Shakhorostov, and Iu. G. Kosiak — 573L.
  The Acceleration of Cosmic Rays in a Fluctuating Magnetic Field. V. M. Biakov and R. G. Avalov — 826.
  Transition Effect for Electrons in Walls of an Ionization Chamber. V. A. Dmitriev — 382L.
Cosmology (see Relativity and Gravitation)
Critical Potentials (see Atomic Structure and Spectra)
Cross Section (see Electrons and Positrons; Nuclear Reactions, General; Scattering, General)
Crystal Counters (see Methods and Instruments)
Crystalline State (see also Electrical Properties; Magnetic Properties; Semiconductors, etc.)
  A Contribution to the Theory of Domain Walls in Ferroelectrics. V. A. Zhirnov — 822.
  Anisotropy of the Electrical Resistance of a Gold Monocrystal in a Magnetic Field at 4.2°K. N. E. Alekseevskii and Iu. P. Gaidukov — 383L.
  Anomaly in the Magnetic Anisotropy of $K_3Fe(CN)_6$ Single Crystals at Low Temperatures. G. Shoffa, O. Ristan, and K. Ruckpaul — 445.
  Bose Excitations in Ionic Crystals. M. Sh. Giterman, P. S. Zyrianov, and G. G. Taluts — 1072.
  Change of Saturation Magnetization and of Electrical Resistance of Iron-Nickel under Hydrostatic Compression at Low Temperatures. E. I. Kondorskii and V. L. Sedov — 586.
  Effect of Uniform Compression on the Oscillation of the Magnetic Susceptibility of Bismuth at Low Temperatures. N. V. Brandt and V. A. Venttsel — 757.
  Electromagnetic Waves in the Region of Exciton Absorption in a Crystal. A. S. Davydov and A. F. Lubchenko — 1048
  Galvanomagnetic Characteristics of Metals with Open Fermi Surfaces. I. I. M. Lifshitz and V. G. Peschanskii — 875.
  Growth and Dissolution of Pores in Crystals. R. I. Garber, V. S. Kogan, and L. M. Poliakov — 953.
  Hole Bands in NaCl. T. I. Kucher — 732L.
  Influence of Acoustic Vibrations on the Parameters of the Bands of Impurity Absorption in Crystals. V. L. Vinetskii and M. F. Deigen — 198L.
  Interaction between Outer and Inner Electrons in Ferromagnetic Transition Metals. Iu. A. Iziumov — 804.
  Isotopic Effect in the Residual Electrical Resistance of

Metals. I. Ia. Pomeranchuk — 693.
  Kinetic Equations for a System of Particles Interacting with Lattice Vibrations. Iu. L. Klimontovich and S. V. Temko — 799.
  Kinetics of Diffusive Decomposition of Supersaturated Solid Solutions. I. M. Lifshitz and V. V. Slezov — 331.
  Low Temperature Polymorphism of Metals. I. A. Gindin, B. G. Lazarev, Ia. D. Starodubov, and V. I. Khotkevich — 556L.
  On the Theory of Paramagnetic Resonance and Paramagnetic Relaxation in Metals. V. V. Andreev and V. I. Gerasimenko — 846.
  Peculiarities of Magnetization of the Disordered Ni_3Mn Alloy at Low Temperatures. N. V. Volkenshtein, M. I. Turchinskaia, and E. V. Galoshina — 916L.
  Splitting of Atomic Terms with Integer Total Angular Momentum in a Magnetic Crystal. B. A. Tavger — 322.
  Temperature Dependence of the Paramagnetic Susceptibility of Nickel-Zinc Ferrites. V. I. Chechernikov and Iu. D. Volkov — 606.
  The Statistics of Spin and Polar Excitations in a Crystal. S. V. Vonsovskii and M. S. Svirskii — 1012.
  Work of Formation of an Elastic Twin in Calcite. I. V. Obreimov and V. I. Startsev — 743.
  X-ray Diffraction Study of the Thermal Expansion of Antiferromagnetic MnTe. N. P. Grazhdankina and D. I. Furfel' — 631.
Diamagnetism (see Magnetic Properties)
Dielectrics and Dielectric Properties
  Cross Sections for the Capture of Slow Electrons by O_2 and H_2O Molecules and Molecules of Halogen Compounds. I. S. Buchel'nikova — 783.
  Electromagnetic Waves in the Region of Exciton Absorption in a Crystal. A. S. Davydov and A. F. Lubchenko — 1048.
  Energy Losses of an Electron in a Medium of Spatial Dispersion. V. M. Agranovich and A. A. Rukhadze — 819.
  Influence of Acoustic Vibrations on the Parameters of the Bands of Impurity Absorption in Crystals. V. L. Vinetskii and M. F. Deigen — 198L.
  Motion of a Charged Particle in an Anisotropic Medium. G. A. Begiashvili and E. V. Gedalin — 1059.
  On the Propagation of Electromagnetic Waves in a Medium with Appreciable Spatial Dispersion. V. M. Agranovich and A. A. Rukhadze — 685.
  The Energy of Excitons for Very Small Quasi-Momenta. S. I. Pekar — 360L.
Diffraction
  Angular Distribution for the Diffraction Scattering of Deuterons. I. I. Ivanchik — 733L.
Diffusion
  Kinetics of Diffusive Decomposition of Supersaturated Solid Solutions. I. M. Lifshitz and V. V. Slezov — 331.
Elasticity and Plasticity
  Work of Formation of an Elastic Twin in Calcite. I. V. Obreimov and V. I. Startsev — 743.
Electrical Breakdown (see Dielectrics and Dielectric Properties; Electrical Discharges)
Electrical Conductivity and Resistance
  Anisotropy of the Electrical Resistance of a Gold Monocrystal in a Magnetic Field at 4.2°K. N. E. Alekseevskii and Iu. P. Gaidukov — 383L.
  Change of Saturation Magnetization and of Electrical Resistance of Iron-Nickel under Hydrostatic Compression at Low Temperatures. E. I. Kondorskii and V. L. Sedov — 586.
  Effect of Thermoelectric Forces on the Skin Effect in a Metal. M. I. Kaganov and V. M. Tsukernik — 327.
  Electric Explosion of Spiral Wires in Vacuum. I. F. Kvartskhava, V. V. Bondarenko, R. D. Meladze, and K. V. Suladze — 634.
  Galvano-Magnetic Effects in Metals with Nearly Equal Numbers of Electrons and Holes. M. I. Kaganov and V. G. Peschanskii — 734L.
  Influence of Deformations on Oscillation Effects in Metals at Low Temperatures. A. M. Kosevich — 171.
  Isotopic Effect in the Residual Electrical Resistance of Metals. I. Ia. Pomeranchuk — 693.
  On the Influence of Domain Structure on the Electrical Resistivity of Iron at Low Temperatures. A. M. Sudovtsov and E. E. Semenenko — 211L.
  Oscillations in the Conductivity of Metallic Films in Magnetic Fields. V. L. Gurevich — 464.
  Peculiarities of Magnetization of the Disordered Ni_3Mn Alloy at Low Temperatures. N. V. Volkenshtein, M. I. Turchinskaia, and E. V. Galoshina — 916L.
  Radio Emission from an Atomic Explosion. A. S. Kompaneets — 1076.
  The influence of Plastic Deformation on the Anomalous Behavior of the Resistance of Gold at Low Temperatures. N. E. Alekseevskii and Iu. P. Gaidukov — 558L.
Electrical Discharges
  Electric Explosion of Spiral Wires in Vacuum. I. F. Kvartskhava, V. V. Bondarenko, R. D. Meladze, and K. V. Suladze — 634.
  Energy of the X-Rays Emitted by Intense Pulsed Discharges in Hydrogen. N. G. Koval'skii, I. M. Podgornyi, and S. Khvashchevskii — 656.
  Hydrodynamic Analysis of the Compression of a Rarefied Plasma in an Axially-Symmetric Magnetic Field. Iu. N. Barabanenkov — 893L.
  Low-Frequency Oscillations of a Plasma in a Magnetic Field. K. N. Stepanov — 808.
  Observations of the Pinch Effect at Decreasing Currents. V. L. Granovskii, K. P. Riumina, V. I. Savoskin, and G. G. Timofeeva — 33.
  Paramagnetic Resonance of the Free Radicals Obtained by Freezing a Plasma of H_2S. S. D. Kaitmazov and A. M. Prokhorov — 381L.
  Production of Two Temperatures in an Ionized Gas in a Magnetic Field. E. Larish and I. Shekhtman — 355L.
  Selfconstricting Discharges in Deuterium at High Rates of Current Growth. V. S. Komel'kov — 10.
  Several Possibilities Associated with the Separation of Charged Particles in an Inhomogeneous High-Frequency Electromagnetic Field. M. A. Miller — 561L.
  Surface Oscillations of a Charged Column in a Longitudinal Magnetic Field. Chao Kai-hua. 1031.
  The Temperature of Plasma Electrons in a Variable Electric Field. A. V. Gurevich — 271.

Electrical Properties (see also Dielectrics and Dielectric Properties; Electrical Conductivity and Resistance; Semiconductors; Superconductivity)
  A Contribution to the Theory of Domain Walls in Ferroelectrics. V. A. Zhirnov — 822.
  Comparison of the Decay Rates of Plasma in Hydrogen and Deuterium. G. I. Glotova, V. L. Granovskii, and V. I. Savoskin — 965.
  Correlation Energy of an Inhomogeneous Electron Gas. D. A. Kirzhnits — 835.
  Effect of Thermoelectric Forces on the Skin Effect in a Metal. M. I. Kaganov and V. M. Tsukernik — 327.
  Galvanomagnetic Characteristics of Metals with Open Fermi Surfaces. I. I. M. Lifshitz and V. G. Peschanskii — 875.
  Galvano-Magnetic Effects in Metals with Nearly Equal Numbers of Electrons and Holes. M. I. Kaganov and V. G. Peschanskii — 734L.
  Kinetic Equations for a System of Particles Interacting with Lattice Vibrations. Iu. L. Klimontovich and S. V. Temko — 799.
Electrodynamics (see Electromagnetic Theory and Electrodynamics)
Electromagnetic Theory and Electrodynamics (see also Microwaves)
  A Nonlinear Theory of Vector Fields. V. Iu. Urbakh — 143.
  Application of Magnetic Slits for Forming Circular Charged-Particle Trajectories. V. M. Kel'man, V. A. Koliunov, and M. V. Karpov — 779.
  Bremsstrahlung and Pair Production from Protons with Allowance for Form Factor. I. Zlatev and P. S. Isaev — 213L.
  Cerenkov Radiation from Dipoles. V. L. Ginzburg and V. Ia. Eidman — 1055.
  Cerenkov Radiation in the Passage of a Charged Particle Through a Ferrite. V. G. Bar'iakhtar and M. I. Kaganov — 532.
  Coherent Electron Radiation in a Synchroton. I. L. V. Iogansen and M. S. Rabinovich — 708.
  Coupled Magnetoelastic Waves in Ferromagnetic Media and Ferroacoustic Resonance. A. I. Akhiezer, V. G. Bar'iakhtar, and S. V. Peletminskii — 157.
  Cyclic Acceleration of Particles in High-Frequency Fields. V. I. Veksler and L. M. Kovrizhnykh — 781.
  Effect of Thermoelectric Forces on the Skin Effect in a Metal. M. I. Kaganov and V. M. Tsukernik — 327.
  Electromagnetic Waves in the Region of Exciton Absorption in a Crystal. A. S. Davydov and A. F. Lubchenko — 1048.
  Energy Losses of an Electron in a Medium with Spatial Dispersion. V. M. Agranovich and A. A. Rukhadze — 819.
  Energy of the X-Rays Emitted by Intense Pulsed Discharges in Hydrogen. N. G. Koval'skii, I. M. Podgornyi, and S. Khvashchevskii — 656.
  Hydrodynamic Analysis of the Compression of a Rarefied Plasma in an Axially-Symmetric Magnetic Field. Iu. N. Barabanenkov — 893L.
  Interaction between a Charged Current-Conducting Jet Moving in a Circle and a Ferrite. A. N. Didenko — 455.
  Interaction between a Medium and a Ring Current Incident to It. V. N. Tsytovich — 983.
  Low-Frequency Oscillations of a Plasma in a Magnetic Field. K. N. Stepanov — 808.
  Motion of a Charged Particle in an Anisotropic Medium. G. A. Begiashvili and E. V. Gedalin — 1059.
  Nonlinear Interaction of Radio Waves Propagating in a Plasma. V. L. Ginzburg — 1100L.
  Observations of the Pinch Effect at Decreasing Currents. V. L. Granovskii, K. P. Riumina, V. I. Savoskin, and G. G. Timofeeva — 33.
  On the Damping of Electromagnetic Waves in a Plasma Situated in a Magnetic Field. K. N. Stepanov — 195L.
  On the Theory of the Optical Properties of Conductors in the Case of Oblique Incidence of the Radiation. V. P. Silin — 700.
  Oscillations in the Conductivity of Metallic Films in Magnetic Fields. V. L. Gurevich — 464.
  Production of Two Temperatures in an Ionized Gas in a Magnetic Field. E. Larish and I. Shekhtman — 355L.
  Radiation from a Charged Particle Traversing a Layered Medium. G. M. Garibian — 1003.
  Radiation of a Multilevel System Moving in a Medium wit a Velocity Greater than the Velocity of Light. V. L. Ginzburg and V. M. Fain — 567L.
  Radio Emission from an Atomic Explosion. A. S. Kompaneets — 1076
  Reflection of Electrons from a High-Frequency Potential Barrier. M. A. Miller — 206L.
  Surface Oscillations of a Charged Column in a Longitudinal Magnetic Field. Chao Kai-hua — 1031
  The Radiation from a Charged Particle Passing through Plate. G. M. Garibian and G. A. Chalikian — 894L.
  The Temperature of Plasma Electrons in a Variable Electrical Field. A. V. Gurevich — 271.
  Theory of Excitation of Hydromagnetic Waves. A. I. Akhiezer and A. G. Sitenko — 82.
  Wave-Front Velocity in Electrodynamics Containing High Derivatives. L. G. Iakovlev — 542L.
Electron Diffraction (see Scattering of Electrons and Positrons)
Electron-Optical Effects (see Optical Properties)
Electron Optics (see Methods and Instruments)
Electrons and Positrons (see also Electromagnetic Theory and Electrodynamics; Elementary Particle Interactions, Scattering of Electrons and Positrons)
  Bremsstrahlung and Pair Production from Protons with Allowance for Form Factor. I. Zlatev and P. S. Isaev — 213L.
  Correlation Energy of an Inhomogeneous Electron Gas. D. A. Kirzhnits — 835.
  Depolarization of Electrons Due to Radiation in a Magneti Field. Iu. F. Orlov and S. A. Kheifets — 354L.
  Electron-positron Pairs from the Decay $\pi^0 \to e^- + e^+ + \gamma$ Iu. A. Budagov, S. Victor, V. P. Dzhelepov, P. F. Ermolov, and V. I. Moskalev — 1101L.
  Energy Dependence of the Asymmetry Coefficient in $\pi^+ \to \mu^+ \to e^+$ Decays for the Low Energy Part of the Positron Spectrum. V. V. Barmin, V. P. Kanavets, B. V. Morozov, and I. I. Pershin — 374L.
  Hyperon Beta Decay. V. M. Shekhter — 316.
  Influence of Multiple Scattering on the Development of

  - High-Energy Electron-Photon Cascades in Lead. T. G. Volkonskaia, I. P. Ivanenko, and G. A. Timofeev — 202L.
  - Kinetic Equations for a System of Particles Interacting with Lattice Vibrations. Iu. L. Klimontovich and S. V. Temko — 799.
  - Measurement of the Polarization of Internal Conversion Electrons. V. A. Liubimov and M. E. Vishnevskii — 1103L.
  - Nuclear Orientation in Radiative K Capture. V. B. Berestetskii — 371L.
  - On Some Peculiarities of Cyclotron Resonance in Metals with Non-Convex Fermi Surfaces. E. A. Kaner — 671.
  - On the Cascade Theory of Showers. I. P. Ivanenko — 94.
  - Polarization of RaE Electrons and Time-Reversal Invariance. A. I. Alikhanov, G. P. Eliseev, and V. A. Liubimov — 740L.
  - Positron Spectrum of $Eu^{152,154}$. D. L. Kaminskii and M. G. Kaganskii — 646.
  - Short Range Interaction between the Electron and Other Particles. N. N. Kolesnikov and G. A. Jacobi — 265.
  - The Decay Scheme of Mo^{99}. I. V. Estulin, G. M. Chernov, and Z. V. Pastukhova — 51.
  - The Temperature of Plasma Electrons in a Variable Electric Field. A. V. Gurevich — 271.
  - Transition Effect for Electrons in Walls of an Ionization Chamber. V. A. Dmitriev — 382L.
  - Types of Interaction in Beta Decay. The Decay of Na^{24}. N. A. Burgov and Iu. V. Terekhov — 651.
- Electrons, Scattering of (see Scattering of Electrons and Positrons)
- Electrons, Secondary (see Electrical Properties)
- Electrostriction (see Dielectrics and Dielectric Properties)
- Elementary Particle Interactions
  - A Contribution to Neutrino Theory. V. V. Chavchanidze and M. E. Perel'man — 204L.
  - A Model for the Process of Multiple Production. G. I. Kopylov — 996.
  - Angular Correlation of Circularly Polarized Gamma Quanta on the μ-Mesonic Atom. V. A. Dzhrbashian — 212L.
  - Asymptotic Theory of a One-Dimensional Four-Fermion Interaction. A. A. Ansel'm — 1065.
  - Beta Decay of a Spin-$3/2$ Particle. R. A. Asanov — 552L.
  - Depolarization of Electrons Due to Radiation in a Magnetic Field. Iu. F. Orlov and S. A. Kheifets — 354L.
  - Determination of the Energy of Fast Particles from the Angular Distribution of their Reaction Products. A. I. Nikishov and I. L. Rozental' — 115.
  - Elastic Scattering of Photons on Excited Nucleons. N. F. Nelipa — 460.
  - Electron-Positron Pairs from the Decay $\pi^0 \to e^- + e^+ + \gamma$. Iu. A. Budagov, S. Victor, V. P. Dzhelepov, P. F. Ermolov, and V. I. Moskalev — 1101L.
  - Energy Dependence of the Asymmetry Coefficient in $\pi^+ \to \mu^+ \to e^+$ Decays for the Low Energy Part of the Positron Spectrum. V. V. Barmin, V. P. Kanavets, B. V. Morozov, and I. I. Pershin — 374L.
  - Formation of Hydrogen Mesic Molecules. Ia. B. Zel'dovich and S. S. Gershtein — 451.
  - Hyperfragments from σ_K-Stars. B. P. Bannik and S. A. Buniatov — 913L.
  - Hyperon Beta Decay. V. M. Shekhter — 316.
  - Inelastic Interaction between Cosmic Ray Protons of Kinetic Energy above 7 Bev and Carbon and Hydrogen Nuclei. K. I. Alekseeva and N. L. Grigorov — 416.
  - Influence of Multiple Scattering on the Development of High-Energy Electron-Photon Cascades in Lead. T. G. Volkonskaia, I. P. Ivananko, and G. A. Timofeev — 202L.
  - Interaction of Cosmic Ray Particles with Various Nuclei. N. L. Grigorov, A. V. Podgurskaia, A. I. Savel'eva, and L. M. Poperekova — 1.
  - Interaction of 80 to 300 Mev π^+ Mesons with Light Nuclei. G. A. Blinov, M. F. Lomanov, Ia. Ia. Shalamov, V. A. Shebanov, and V. A. Shchegolev — 609.
  - Investigation of K_{e3}-Decay with the Emission of a Gamma Photon. I. M. Dremin — 355L.
  - Measurement of β-γ Correlation from Oriented Nuclei. A. V. Kogan, V. D. Kul'kov, L. P. Nikitin, N. M. Reinov, I. A. Sokolov, and M. F. Stel'makh — 903L.
  - Measurement of the Polarization of Internal Conversion Electrons. V. A. Liubimov and M. E. Vishnevskii — 1103L.
  - Measurement of the Polarization of Negative μ Mesons in Carbon, Oxygen, Magnesium, Sulphur, Zinc, Cadmium, and Lead Mesic Atoms. A. E. Ignatenko, L. B. Egorov, B. Khalupa, and D. Chultem — 792.
  - Measurement of the Total Charged μ-Meson Production Cross Section in Neutron-Proton Collisions at 586-Mev Neutron Energy. Iu. M. Kazarinov and Iu. N. Simonov — 56.
  - Method for Determining Hyperon Polarization in the Reaction $\pi + p \to Y + K$. S. M. Bilen'kii and R. M. Ryndin — 574 L.
  - μ^+-Meson Depolarization in Nuclear Emulsions with Different Gelatin Content. Iu. M. Ivanov and A. I. Fesenko — 905L.
  - Nonlocal Effects in Weak Interactions of Fermions. S. G. Matinian — 548L.
  - Nuclear Orientation in Radiative K Capture. V. B. Berestetskii — 371L.
  - On a Method for Determining the Parity of Strange Particles. E. I. Dolinskii — 902L.
  - On a Possible Limit on the Applicability of Quantum Electrodynamics. D. I. Blokhintsev — 174.
  - On the Cascade Theory of Showers. I. P. Ivanenko — 94.
  - On the Multiple Interaction in Quantum Field Theory. L. I. Podlubnyi — 728L.
  - On the Possible Existence of the Ξ^0-Hyperon. E. O. Okonov — 863.
  - On the Problem of Angular Correlation of Secondary Particles Produced in High-Energy Nuclear Collisions. I. M. Gramenitskii, M. Ia. Danysh, V. B. Liubimov, M. I. Podgoretskii, and D. Tuvdendorzh — 381L.
  - On the Problem of Testing the Invariance of an Interaction under Time Inversion. L. I. Lapidus — 1105L.
  - On the Scattering of "Dressed" Particles in Quantum Field Theory. Iu. V. Novozhilov — 515.
  - On the Theory of the Weak Interactions. I. Iu. A. Gol'fand — 118.
  - On the Theory of the Weak Interactions. II. Iu. A. Gol'fand — 504.

- Polarization Correlation of Beta Particles and Gamma Quanta in Allowed Decay of Oriented Nuclei. A. Z. Dolginov — 123.
- Polarization of RaE Electrons and Time-Reversal Invariance. A. I. Alikhanov, G. P. Eliseev, and V. A. Liubimov — 740L.
- Production of Pions in Condensed Media by Cosmic Rays in the Stratosphere. D. K. Kaipov, V. N. Shakhorostov, and Iu. G. Kosiak — 573L.
- Production of Two π Mesons in Collisions between π Mesons or γ Quanta with Nucleons or Deuterons. N. V. Dushin — 278.
- Radiative Decay of π^+-Mesons and Effects of Parity Nonconservation. A. I. Mukhtarov and S. A. Gadzhiev — 895L.
- Selection Rules in Reactions Involving Polarized Particles. Chou Kuang-Chao — 543L.
- The Effect of Neutrino Recoil in the Beta Decay of He^6. J. Csikai and A. Szalay — 749.
- The π-Mesonic Atom and Corrections to the Dispersion Relations. V. A. Meshcheriakov — 200L.
- The Polarization of the Internal-Conversion Electrons Emitted after Beta Decay. V. B. Berestetskii and A. P. Rudik — 111.
- The Scattering of Spin-$\frac{3}{2}$ Particles by a Coulomb Field. A. A. Komar — 559L.
- The Spectral Representation of the Two-Meson Green's Function. V. N. Gribov — 287.
- The Universal Fermi Interaction and the Capture of the μ Meson by the Proton. Ia. B. Zel'dovich and S. S. Gershtein — 570.
- The Universal Fermi Interaction and the Capture of Muons in Hydrogen. Chou Kuang-Chao and V. Maevskii 1106L.
- Transition Effect for Electrons in Walls of an Ionization Chamber. V. A. Dmitriev — 382L.
- Types of Interaction in Beta Decay. The Decay of Na^{24}. N. A. Burgov and Iu. V. Terekhov — 651.

Elements (see Atomic Mass and Abundance)
Energy Loss of Particles (see Range and Energy Loss)
Energy States of Atoms (see Atomic Structure and Spectra)
Energy States of Nucleus (see Nuclear Reactions; Nuclear Spectra; Nuclear Structure)
Evaporation (see Liquids)
Excitation of Atoms (see Atomic Structure and Spectra)
Excitation of Nucleus (see Nuclear Reactions; Nuclear Spectra; Nuclear Structure)
Faraday Effect (see Optical Properties)
Ferroelectric Phenomena (see Dielectrics and Dielectric Properties)
Field Emission (see Electrical Properties)
Field Theory
- A Contribution to Neutrino Theory. V. V. Chavchanidze and M. E. Perel'man — 204L.
- A Nonlinear Theory of Vector Fields. V. Iu. Urbakh — 143.
- An Investigation of Particle-Like Solutions of a Nonlinear Scalar Field Equation. V. B. Glasko, F. Leriust, Ia. P. Terletskii, and S. F. Shushurin — 312.
- Asymptotic Theory of an One-Dimensional Four-Fermion Interaction. A. A. Ansel'm — 1065.
- Bremsstrahlung and Pair Production from Protons with Allowance for Form Factor. I. Zlatev and P. S. Isaev — 213L.
- Circular Polarization of Internal γ-Bremsstrahlung in β-Decay and Time Reversal Invariance. R. Iu. Volkovyskii — 562L.
- Depolarization of Electrons Due to Radiation in a Magnetic Field. Iu. F. Orlov and S. A. Kheifets — 354L.
- Hyperon Beta Decay. V. M. Shekhter — 316.
- Investigation of K_{e3}-Decay with the Emission of a Gamma Photon. I. M. Dremin — 355L.
- Isotopic Invariance in Anti-Hyperon Processes. S. G. Matinian and G. R. Khutsishvili — 377L.
- Nuclear Orientation in Radiative K Capture. V. B. Berestetskii — 371L.
- On the Multiple Interaction in Quantum Field Theory. L. I. Podlubnyi — 728L.
- On the $\pi \rightarrow e + \nu + \gamma$ Decay. V. G. Vaks and B. L. Ioffe — 151.
- On the Scattering of "Dressed" Particles in Quantum Field Theory. Iu. V. Novozhilov — 515.
- On the Theory of Composite π^0 Mesons. M. E. Perel'man — 350L.
- On the Theory of the Weak Interactions. I. Iu. A. Gol'fand — 118.
- On the Theory of the Weak Interactions. II. Iu. A. Gol'fand — 504.
- Projection Operators in the Theory of Elementary Particles. F. I. Fedorov — 339.
- The Spectral Representation of the Two-Meson Green's Function. V. N. Gribov — 287.
- The Universal Fermi Interaction and the Capture of the μ Meson by the Proton. Ia. B. Zel'dovich and S. S. Gershtein — 570.
- Wave Solutions of Nonlinear Generalizations of Relativistic Equations. D. F. Kurdgelaidze — 1099L.

Films, Properties
- A Method for the Observation of Helium II Films. A. I. Shal'nikov — 386L.
- Effect of Thermoelectric Forces on the Skin Effect in a Metal. M. I. Kaganov and V. M. Tsukernik — 327.

Fine Structure (see Atomic Structure and Spectra)
Fission of Nucleus (see Nuclear Fission)
Fluid Dynamics
- Impossibility of Rarefaction Shock Waves in Magnetohydrodynamics. R. V. Polovin and G. Ia. Liubarskii — 351L.
- Observation of the Lambda Transition in Helium in the Presence of a Thermal Current through the Phase Boundary. V. P. Peshkov — 943.
- On the Interaction between Small Disturbances and Discontinuities in Magnetohydrodynamics and on the Stability of Shock Waves. V. M. Kontorovich — 851.
- Phenomenological Equations of Statistical Dynamics of an Incompressible Turbulent Liquid. B. I. Davydov — 364L.
- Physical Phenomena that Occur when Bodies Compressed by Strong Shock Waves Expand in Vacuo. Ia. B. Zel'dovich and Iu. P. Raizer — 980.
- Propagation of Detonation Waves in the Presence of a Magnetic Field. E. Larish and I. Shekhtman — 139.
- Shock Waves in a Conducting Ultrarelativistic Gas. K. P. Staniukovich — 359L.

Simple Magnetoacoustic Waves. G. Ia. Liubarskii and R. V. Polovin — 351L.
Some Remarks on the Structure of Shock Waves. G. S. Golitsyn and K. P. Staniukovich — 575L.
Surface Oscillations of a Charged Column in a Longitudinal Magnetic Field. Chao Kai-Hua — 1031.
The Oscillations of a Degenerate Electron Fluid. V. P. Silin — 870.
The Splitting of a Small Discontinuity in Magnetohydrodynamics. G. Ia. Liubarskii and R. V. Polovin — 901L.
The Stability of Shock Waves in Magnetohydrodynamics. A. I. Akhiezer, G. Ia. Liubarskii, and R. V. Polovin — 507.
The Stability of Shock Waves in Magnetohydrodynamics. S. I. Syrovatskii — 1024.
Unidimensional Motion in Magnetohydrodynamics. G. S. Golitsyn — 538.
Galvanomagnetic Effect (see Magnetic Properties)
Gamma Rays
Alpha Decay of Isomeric Bi^{210}. S. V. Golenetskii, L. I. Rusinov, and Iu. I. Filimonov — 917L.
Bremsstrahlung from π Mesons Interaction with Nuclei. M. F. Lomanov, A. G. Meshkovskii, Ia. Ia. Shalamov, V. A. Shebanov, and A. F. Grashin — 615.
Coulomb Excitation of Aluminum. D. G. Alkhazov, A. P. Grinberg, G. M. Gusinskii, K. I. Erokhina, and I. Kh. Lemberg — 736L.
Coulomb Excitation of High-Energy Nuclear Levels in Even Isotopes of Tungsten. D. G. Alkhazov, A. P. Grinberg, G. M. Gusinskii, K. I. Erokhina, and I. Kh. Lemberg — 926
Effect of Finite Nuclear Size on the Relative Internal Conversion Coefficients in L Subshells. A. G. Sergeev, V. D. Vorob'ev, A. S. Remennyi, T. I. Kol'chinskaia, G. D. Latyshev, and Iu. S. Egorov — 242.
Elastic Scattering of Photons on Excited Nucleons. N. F. Nelipa — 460.
Gamma Radiation from Radiative Capture of Thermal Neutrons by Mo^{95}, Ag^{107}, Te^{123}, and Cs^{133} Nuclei. L. F. Kalinkin, A. S. Melioranskii, and I. V. Estulin — 410.
Hard Gamma Radiation from As^{76}. Decay Schedule of As^{76}. L. V. Gustova and O. V. Chubinskii — 957.
Investigation of Conversion Electron Spectra of Neutron-Deficient Isotopes of Lutecium. V. M. Kel'man, R. Ia. Metskhvarishvili, B. K. Preobrazhenskii, V. A. Romanov, and V. V. Tuchkevich — 914L.
Investigation of 15 to 65-Mev Protons Produced in the Photodisintegration of Aluminum and Niclel. E. B. Bazhanov, Iu. M. Volkov, and L. A. Kul'chitskii — 224.
Lifetime of the First Excited State of Mg^{24}. D. G. Alkhazov, A. P. Grinber, G. M. Gusinskii, K. I. Erokhina, and I. Kh. Lemberg — 737L.
Magnetic Transitions between Collective Excited States of Even-Even Nuclei. A. S. Davydov and G. F. Fillipov — 488.
Measurement of β-γ Correlation from Oriented Nuclei. A. V. Kogan, V. D. Kul'kov, L. P. Nikitin, N. M. Reinov, I. A. Sokolov, and M. F. Stel'makh — 903L.
Photoproduction of Electron and μ-Meson Pairs on Nucleons. I. T. Diatlov — 108.
Photoproduction of Slow π^0 Mesons on Complex Nuclei. A. S. Belousov, S. V. Rusakov, and E. I. Tamm — 247.
Study of Gamma Rays from As^{78} Decay. Iu. A. Nemilov, A. N. Pisarevskii, and L. D. Soshin — 555L.
The Decay Scheme of Mo^{99}. I. V. Estulin, G. M. Chernov, and Z. V. Pastukhova — 51.
The First Excited State of Tb^{159}. Iu. A. Nemilov, A. N. Pisarevskii, and L. D. Soshin — 554L.
The Hard γ Radiation of Ag^{110}. L. V. Gustova, L. P. Timofeeva, and O. V. Chubinskii — 920L.
Gases
Comparison of the Decay Rates of Plasma in Hydrogen and Deuterium. G. I. Glotova, V. L. Granovskii, and V. I. Savoskin — 965.
Propagation of a Non-Self-Similar Thermal Wave. E. I. Andriankin — 295.
Selfconstricting Discharges in Deuterium at High Rates of Current Growth. V. S. Komel'kov — 10.
Stationary Relativistic Motions of a Gas in a Conducting Medium. K. P. Staniukovich — 529.
Unidimensional Motion in Magnetohydrodynamics. G. S. Golitsyn — 538.
Geophysics
Nonlinear Interaction of Radio Waves Propagating in a Plasma. V. L. Ginzburg — 1100L.
Gravitation (see Relativity and Gravitation)
Gyromagnetization (see Magnetic Properties)
Hall Effect (see Electrical Conductivity and Resistance; Semiconductors)
Helium, Liquid
A Method for the Observation of Helium II Films. A. I. Shal'nikov — 386L.
Calculation of the Phonon Part of the Mutual Friction Force in Superfluid Helium. L. P. Pitaevskii — 888.
Contribution to the Theory of the Pomeranchuk Effect in He^3. D. G. Sanikidze — 192L.
Observation of the Lambda Transition in Helium in the Presence of a Thermal Current through the Phase Boundary. V. P. Peshkov — 943.
Phenomenological Theory of Superfluidity near the Lambda Point. L. P. Pitaevskii — 282.
Pomeranchuk Effect and Diagram of State for He^3-He^4 Solutions. I. M. Lifshitz and D. G. Sanikidze — 713.
High Voltage Tubes and Machines (see Methods and Instruments)
Hyperfine Structure (see Atomic Structure and Spectra; Nuclear Moments and Spin)
Hyperons (see Mesons and Hyperons)
Imperfections in Solids
Influence of Acoustic Vibrations on the Parameters of the Bands of Impurity Absorption in Crystals. V. L. Vinetskii and M. F. Deigen — 198L.
Inelastic Scattering (see Nuclear Reactions; Scattering)
Instruments (see Methods and Instruments)
Internal Conversion (see Nuclear Spectra)
Ionization (see also Electrical Discharges; Range and Energy Loss of Particles)
Electron Capture and Loss in Collisions of Fast Carbon and Oxygen Atoms with Gas Molecules. Ia. M. Fogel', V. A. Ankudinov, and D. V. Pilipenko — 601.
Nonlinear Interaction of Radio Waves Propagating in a Plasma. V. L. Ginzburg — 1100L.
On the Applicability of Massey's Adiabatic Hypothesis

to Double Charge Exchange. Ia. M. Fogel', R. V. Mitin, V. F. Kozlov, and N. D. Romashko — 390.
Optical Methods of Observing the Ionization along Fast Particle Tracks. V. V. Vladimirskii — 384L.
Production of Two Temperatures in an Ionized Gas in a Magnetic Field. E. Larish and I. Shekhtman — 355L.
Ionization Potentials of Atoms (see Atomic Structure and Spectra)
Ions (see also Electrical Discharges)
Comparison of the Decay Rates of Plasma in Hydrogen and Deuterium. G. I. Glotova, V. L. Granovskii, and V. I. Savoskin — 965.
Cross Sections for the Capture of Slow Electrons by O_2 and H_2O Molecules and Molecules of Halogen Compounds. I. S. Buchel'nikova — 783.
Electron Capture and Loss in Collisions of Fast Carbon and Oxygen Atoms with Gas Molecules. Ia. M. Fogel', V. A. Ankudinov, and D. V. Pilipenko — 601.
Negative Ions of Iron, Cobalt, and Nickel. V. M. Dukel'skii and V. M. Sokolov — 569L.
On the Theory of Longitudinal Relaxation of Paramagnetic Salt Solutions. S. A. Al'tshuler and K. A. Valiev — 661.
Optical Methods of Observing the Ionization along Fast Particle Tracks. V. V. Vladimirskii — 384L.
Several Possibilities Associated with the Separation of Charged Particles in an Inhomogeneous High-Frequency Electromagnetic Field. M. A. Miller — 561L.
Stimulated R. F. Amplifier Working on Hyperfine Levels of Paramagnetic Atoms. K. A. Valiev and Sh. Sh. Bashkirov — 208L.
The Temperature of Plasma Electrons in a Variable Electric Field. A. V. Gurevich — 271.
Ions and Electrons, Mobility
A Method for the Observation of Helium II Films. A. I. Shal'nikov — 386L.
Production of Two Temperatures in an Ionized Gas in a Magnetic Field. E. Larish and I. Shekhtman — 355L.
Isobars (see Atomic Mass and Abundance)
Isomers, Nuclear (see Nuclear Spectra)
Isotopes (see Atomic Mass and Abundance; Radioactivity)
Kerr Effect (see Optical Properties)
Liquid Helium (see Helium, Liquid)
Liquids
Observation of the Lambda Transition in Helium in the Presence of a Thermal Current through the Phase Boundary. V. P. Peshkov — 943.
On the Stability of a Fermi Liquid. I. Ia. Pomeranchuk — 361L.
On the Theory of the Fermi Liquid. L. D. Landau — 70.
Magnetic Fields (see Electromagnetic Theory and Electrodynamics)
Magnetic Properties
Anisotropy of the Electrical Resistance of a Gold Monocrystal in a Magnetic Field at 4.2°K. N. E. Alekseevskii and Iu. P. Gaidukov — 383L.
Anomaly in the Magnetic Anisotropy of $K_3Fe(CN)_6$ Single Crystals at Low Temperatures. G. Shoffa, O. Ristan, and K. Ruckpaul — 445.
Antiferromagnetism of the Gamma Phase of Iron. E. I. Kondorskii and V. L. Sedov — 1104L.
Cerenkov Radiation in the Passage of a Charged Particle Through a Ferrite. V. G. Bar'iakhtar and M. I. Kaganov — 532.
Change in Width of Boundary Layer in Ferromagnets by Means of the Magneto-Optical Kerr Effect. L. V. Kirenskii and V. V. Vetter — 568L.
Change of Saturation Magnetization and of Electrical Resistance of Iron-Nickel under Hydrostatic Compression at Low Temperatures. E. I. Kondorskii and V. L. Sedov — 586.
Coupled Magnetoelastic Waves in Ferromagnetic Media and Ferroacoustic Resonance. A. I. Akhiezer, V. G. Bar'iakhtar, and S. V. Peletminskii — 157.
Diamagnetism and Interatomic Bonds in Molecules and Non-Metallic Crystals. Ia. G. Dorfman — 368L.
Effect of Uniaxial Elastic Deformations on the Magnetic Properties of Zinc Crystals at Low Temperatures. B. I. Verkin and I. M. Dmitrenko — 200L.
Effect of Uniform Compression on the Oscillation of the Magnetic Susceptibility of Bismuth at Low Temperatures. N. V. Brandt and V. A. Venttsel — 757.
Equations of Motion for a System Consisting of Two Types of Interacting Spins. G. V. Skrotskii — 550L.
Galvano-Magnetic Effects in Metals with Nearly Equal Numbers of Electrons and Holes. M. I. Kaganov and V. G. Peschanskii — 734L.
Hall Effect in Pure Nickel at Helium Temperatures. N. V. Volkenshtein, G. V. Fedorov, and S. V. Vonsovskii — 61.
Impossibility of Rarefaction Shock Waves in Magnetohydrodynamics. R. V. Polovin and G. Ia. Liubarskii — 351L.
Interaction between Outer and Inner Electrons in Ferromagnetic Transition Metals. Iu. A. Iziumov — 804.
Magnetic Anisotropy of Single-Crystal $CuSO_4$ in the Antiferromagnetic State. N. M. Kreines — 972.
Magnetic Properties of Metals at Low Temperatures. IV. Influence of Homogeneous Compression on the de Haas-van Alphen Effect in Zinc Crystals. I. M. Dmitrenko, B. I. Verkin, and B. G. Lazarev — 229.
Motion of a Charged Particle in an Anisotropic Medium. G. A. Begiashvili and E. V. Gedalin — 1059.
On the Hall Effect at the Curie Point. N. S. Akulov and A. V. Cheremushkina — 357L.
On the Influence of Domain Structure on the Electrical Resistivity of Iron at Low Temperatures. A. M. Sudovtsov and E. E. Semenko — 211L.
On the Theory of Longitudinal Relaxation of Paramagnetic Salt Solutions. S. A. Al'tshuler and K. A. Valiev — 661.
On the Thermal Stability of the Domain Structure in Silicon-Iron Crystals. L. V. Kirenskii and I. F. Degtiarev — 403.
Paramagnetic Resonance of Free Radicals in Weak Fields. A. K. Chirkov and A. A. Kokin — 36.
Peculiarities of Magnetization of the Disordered Ni_3Mn Alloy at Low Temperatures. N. V. Volkenshtein, M. I. Turchinskaia, and E. V. Galoshina — 916L.
Second Relaxation in a Spin System in Certain Compounds of Elements of the Iron Group. N. S. Garif'ianov — 366L.
Simple Magnetoacoustic Waves. G. Ia. Liubarskii and R. V. Polovin — 351L.
Some Remarks on the Structure of Shock Waves. G. S.

Golitsyn and K. P. Staniukovich — 575L.
Spin-Spin Paramagnetic Relaxation Time in the Absence of a Static Magnetic Field for $Co(NH_4)_2(SO_4)_2 \cdot 6H_2O$ at Helium Temperatures. U. Kh. Kopvillem — 349L.
Spin Waves in a Ferromagnetic Metal. A. A. Abrikosov and I. E. Dzialoshinskii — 535.
Splitting of Atomic Terms with Integer Total Angular Momentum in a Magnetic Crystal. B. A. Tavger — 322.
Temperature Dependence of the Paramagnetic Susceptibility of Nickel-Zinc Ferrites. V. I. Chechernikov and Iu. D. Volkov — 606.
The de Haas-van Alphen Effect in Pulsed Magnetic Fields. A. M. Kosevich — 512.
The Influence of Plastic Deformation on the Anomalous Behavior of the Resistance of Gold at Low Temperatures. N. E. Alekseevskii and Iu. P. Gaidukov — 558L.
The Saturation Magnetization of Nickel-Copper Alloys at Low Temperatures. E. I. Kondorskii, V. E. Rode, and U. Gofman — 380L.
The Stability of Shock Waves in Magnetohydrodynamics. A. I. Akhiezer, G. Ia. Liubarskii, and R. V. Polovin — 507.
The Stability of Shock Waves in Magnetohydrodynamics. S. I. Syrovatskii — 1024.
Transition from the Antiferromagnetic into the Ferromagnetic State in $CoSO_4$. A. S. Borovik-Romanov and N. M. Kreines — 734L.
X-ray Diffraction Study of the Thermal Expansion of Antiferromagnetic MnTe. N. P. Grzhdankina and D. I. Gurfel' — 631.

Magnetic Resonance
Coupled Magnetoelastic Waves in Ferromagnetic Media and Ferroacoustic Resonance. A. I. Akhiezer, V. G. Bar'iakhtar, and S. V. Peletminskii — 157.
Effect of Electron Paramagnetic Resonance on the Optical Faraday Effect at Low Temperatures. G. V. Skrotskii, P. S. Zyrianov, and T. G. Iziumov — 1028.
Electronic Paramagnetic Resonance in Alloys of Alkali Metals. N. S. Garif'ianov and M. A. Starikov — 553L.
Exchange Effects in Ferromagnetic Resonance. M. A. Gintsburg — 730L.
Ferromagnetic Resonance in a Circulatory Polarized Magnetic Field of Arbitrary Amplitude. G. V. Skrotskii and Iu. I. Alimov — 1035.
Investigation of Relaxation Processes in a Series of Fluorine Compounds of Carbon. V. S. Grechishkin — 253.
Nuclear Magnetic Resonance Shift in Molybdenum. S. I. Aksenov — 207L.
On the Overhauser Effect in Nonmetals. II. G. R. Khutsishvili — 720.
On the Theory of Longitudinal Relaxation of Paramagnetic Salt Solutions. S. A. Al'tshuler and K. A. Valiev — 661.
On the Theory of Paramagnetic Resonance and Paramagnetic Relaxation in Metals. V. V. Andreev and V. I. Gerasimenko — 846.
On the Theory of Paramagnetic Resonance of Metals. M. Ia. Azbel', V. I. Gerasimenko, and I. M. Lifshitz — 480.
Paramagnetic Absorption in Parallel Fields at 9.3×10^9 cps in the Salts $Fe(NH_4)(SO_4)_2 \cdot 12H_2O$ and $Fe(NO_3)_3 \cdot 9H_2O$. V. A. Kutuzov — 910L.
Paramagnetic Relaxation in Potassium Sulfate and Ammonium Iron Sulfate. N. S. Garif'ianov — 426.
Paramagnetic Resonance of Free Radicals in Weak Fields. A. K. Chirkov and A. A. Kokin — 36.
Paramagnetic Resonance of the Free Radicals Obtained by Freezing a Plasma of H_2S. S. D. Kaitmazov and A. M. Prokhorov — 381L.
Polarization of Nuclear Moments and Nuclear-Resonance Line Widths in Crystals of Cu^{++} Ion Salts. Sh. Sh. Bashkirov and K. A. Valiev — 471.
Second Relaxation in a Spin System in Certain Compounds of Elements of the Iron Group. N. S. Garif'ianov — 366L.
Sound Absorption in Ferromagnetic Dielectrics in a Magnetic Field at Low Temperatures. L. A. Shishkin — 197L.
Spin-Spin Paramagnetic Relaxation Time in the Absence of a Static Magnetic Field for $Co(NH_4)_2(SO_4)_2 \cdot 6H_2O$ at Helium Temperatures. U. Kh. Kopvillem — 349L.
Theory of the Anisotropy of the Width of Ferromagnetic Resonance Absorption Line. G. V. Skrotskii and L. V. Kurbatov — 148.
Use of Cyclotron Resonance in Semiconductors for the Amplification and Generation of Microwaves. A. S. Tager and A. D. Gladun — 560L.

Magneto-Optical Effects (see Optical Properties)

Magnetoresistance (see Electrical Conductivity and Resistance; Semiconductors)

Magnetostriction (see Magnetic Properties)

Mathematical Methods
A Model for the Process of Multiple Production. G. I. Kopylov — 996.
A New Method in Statistical Perturbation Theory. Ch'en Ch'un Hsien — 1062.
Alpha Decay of Nonspherical Nuclei. L. L. Gol'din, G. M. Adel'son-Velskii, A. P. Birzgal, A. D. Piliia, and K. A. Ter-Martirosian — 127.
Asymptotic Theory of a One-Dimensional Four-Fermion Interaction. A. A. Ansel'm — 1065.
Clebsch-Gordan Expansion for Infinite-Dimensional Representations of the Lorentz Group. A. Z. Dolginov and I. N. Toptygin — 550L.
Correlation Energy of an Inhomogeneous Electron Gas. D. A. Kirzhnits — 835.
Determination of the Energy of Fast Particles from the Angular Distribution of their Reaction Products. A. I. Nikishov and I. L. Rozental' — 115.
Dispersion Relations in Non-Relativistic Scattering Theory. L. D. Faddeev — 299.
Fock's Cyclic Symmetry Condition and Young's Pattern. G. I. Zel'tser — 738L.
Generalized Self-Consistent Field Equations. P. S. Zyrianov — 309.
On Some Peculiarities of Cyclotron Resonance in Metals with Non-Convex Fermi Surfaces. E. A. Kaner — 671.
On the Behavior of a Particle of Arbitrary Spin in an External Magnetic Field. V. S. Popov — 687.
On the Precision of Quantum Mechanical Mean Values Computed by the Variational Method. V. M. Buimistrov — 812.
Projection Operators in the Theory of Elementary Par-

  - ticles. F. I. Fedorov — 339.
  - Quantum-Mechanical Probabilities as Sums over Paths. G. V. Riazanov — 85.
  - Relativistic Theory of Polarization Effects. Iu. M. Shirokov — 703.
  - Scattering of Slow Neutrons by Deuterons. V. N. Efimov — 98.
  - Splitting of Atomic Terms with Integer Total Angular Momentum in a Magnetic Crystal. B. A. Tavger — 322.
  - The Shapiro Integral Transformation. Chou Kuang-Chao and L. G. Zastavenko — 990.
  - The Spectral Representation of the Two-Meson Green's Function. V. N. Gribov — 287.
  - Wave Functions of Many-Electron Systems. V. I. Perel' — 476.
- Measurements (see Methods and Instruments)
- Mechanics, Quantum (see Quantum Mechanics)
- Mechanics, Quantum — Atomic Structure and Spectra (see Atomic Structure and Spectra)
- Mechanics, Quantum — of Solid Bodies (see Crystalline State)
- Mechanics, Statistical (see Statistical Mechanics and Thermodynamics)
- Meson Field Theory (see Field Theory)
- Mesons and Hyperons (see also Cosmic Radiation; Elementary Particle Interactions; Nuclear Reactions Induced by Mesons; Scattering of Mesons)
  - Absorption of μ^- Mesons by Nuclei; Angular Distribution of the Neutrons. E. I. Dolinskii and L. D. Blokhintsev — 1040.
  - Absorption of Slow π^- Mesons by Nuclei. A. T. Varfolomeev — 373L.
  - An Investigation of the Final States in the Photoproduction of Negative π Mesons on Deuterium. M. I. Adamovich — 29.
  - An Investigation of the Interaction between 250—270 Mev π^+ Meson and Carbon Nuclei with the Aid of a Propane Bubble Chamber. Wang Kan-Chang, Wang Tso-Tsiang, Ding Da-Tsao, L. N. Dubrovskii, E. N. Kladnitskaia, and M. I. Solov'ev — 625.
  - Angular Correlation for Low-Energy Positrons Emitted in $\pi^+ \rightarrow \mu^+ - e^-$ Decay. A. O. Vaisenberg, V. A. Smirnitskii, E. D. Kolganova, Z. V. Minervina, E. A. Pesotskaia, and N. V. Rabin — 448.
  - Beta Decay of a Spin-$3/2$ Particle. R. A. Asanov — 552L.
  - Binding Energy of Light Hypernuclei According to Meson Theory. V. A. Liul'ka and V. A. Filimonov — 717.
  - Bremsstrahlung from π Mesons Interacting with Nuclei. M. F. Lomanov, A. G. Meshkovskii, Ia. Ia. Shalamov, V. A. Shebanov, and A. F. Grashin — 615.
  - Depolarization of μ^- Mesons in Hydrogen, Deuterium and Tritium. V. B. Beliaev and B. N. Zakhar'ev — 699.
  - Depolarization of μ^+ Mesons in Metals. I. V. Iakovleva — 676.
  - Diffraction Scattering of Fast Particles. D. I. Blokhintsev, V. S. Barashenkov, and V. G. Grishin — 215L.
  - Elastic Scattering of 5 to 22-Mev Positive Pions by Carbon. V. G. Kirillov-Ugriumov, L. P. Kotenko, E. P. Kuznetsov, and F. M. Sergeev — 907L.
  - Elastic Scattering of 300-Mev Pions by Deuterons. L. S. Dul'kova, I. B. Sokolova, and M. G. Shafranova — 217.
  - Electron-Positron Pairs from the Decay $\pi^0 \rightarrow e^- + e^+ + \gamma$. Iu. A. Budagov, S. Victor, V. P. Dzhelepov, P. F. Ermolov, and V. I. Moskalev — 1101L.
  - Energy Dependence of μ^+-e^+ Decay Asymmetry. A. I. Mukhin, E. B. Ozerov, and B. Pontecorvo — 237.
  - Energy Dependence of the Angular Correlation of Positrons from $\pi^+ \rightarrow \mu^+ \rightarrow e^+$ Decay. Kh. P. Babaian, N. A. Marutian, K. A. Matevosian, and M. G. Sarinian — 387.
  - Energy Dependence of the Asymmetry Coefficient in $\pi^+ \rightarrow \mu^+ \rightarrow e^+$ Decays for the Low Energy Part of the Positron Spectrum. V. V. Barmin, V. P. Kanavets, B. V. Morozov, and I. I. Pershin — 374L.
  - Energy Spectrum and Angular Distributions of π^+ Mesons Produced in Proton-Proton Collisions at 660—670 Mev. A. G. Meshkovskii, Ia. Ia. Shalamov, and V. A. Shebanov — 46.
  - Formation of Hydrogen Mesic Molecules. Ia. B. Zel'dovich and S. S. Gershtein — 451.
  - Hydrodynamic Theory of Multiple Production of Particles in Collisions between Fast Nucleons and Nuclei. G. A. Milekhin — 829.
  - Hyperfragments from σ_K-Stars. B. P. Bannik and S. A. Buniatov — 913L.
  - Hyperon Beta Decay. V. M. Shekhter — 316.
  - Inelastic Scattering of 300-Mev Positive and Negative π Mesons by Photographic Emulsion Nuclei. G. E. Belovitskii — 581.
  - Interaction of 80 to 300-Mev π^+ Mesons with Light Nuclei. G. A. Blinov, M. F. Lomanov, Ia. Ia. Shalamov, V. A. Shebanov, and V. A. Shchegolev — 609.
  - Investigation of the Angular Distribution of Secondary Particles in Showers Produced by High-Energy Nucleons. L. A. San'ko, Zh. S. Takibaev, and Ts. I. Shakhova — 396.
  - Investigation of the Depolarization of Negative Muons in Liquid Hydrogen. A. E. Ignatenko, L. B. Egorov, B. Khalupa, and D. Chultem — 621.
  - Investigation of the $p + p \rightarrow d + \pi^+$ Reaction with a Polarized Proton Beam. Iu. K. Akimov, O. V. Savchenko, and L. M. Soroko — 64.
  - Isotopic Invariance in Anti-Hyperon Processes. S. G. Matinian and G. R. Khutsishvili — 377L.
  - Level Widths of π-Mesonic Atoms. A. I. Lebedev — 729L.
  - Measurement of the Polarization of Negative μ Mesons in Carbon, Oxygen, Magnesium, Sulphur, Zinc, Cadmium, and Lead Mesic Atoms. A. E. Ignatenko, L. B. Egorov, B. Khalupa, and D. Chultem — 792.
  - Measurement of the Total Charged π Meson Production Cross Section in Neutron-Proton Collisions at 586-Mev Neutron Energy. Iu. M. Kazarinov and Iu. N. Simonov — 56.
  - Method for Determining Hyperon Polarization in the Reaction $\pi + p \rightarrow Y + K$. S. M. Bilen'kii and R. M. Ryndin — 574L.
  - μ^+-Meson Depolarization in Nuclear Emulsions with Different Gelatin Content. Iu. M. Ivanov and A. I. Fesenko — 905L.
  - Nonlocal Effects in Weak Interactions of Fermions. S. G. Matinian — 548L.
  - On a Method for Determining the Parity of Strange Par-

ticles. E. I. Dolinskii — 902L.
On the Λ-Hyperon Creation Cross Section Near the Σ-Hyperon Creation Threshold. A. N. Baz' and L. B. Okun' — 526.
On the Hydrodynamic Theory of Multiple Production of Particles. G. A. Milekhin — 682.
On the $\pi \rightarrow e + \nu + \gamma$ Decay. V. G. Vaks and B. L. Ioffe — 151.
On the Possible Existence of the Ξ^0-Hyperon. E. O. Okonov — 863.
On the Problem of Angular Correlation of Secondary Particles Produced in High-Energy Nuclear Collisions. I. M. Gramenikskii, M. Ia. Danysh, V. B. Liubimov, M. I. Podgoretskii, and D. Tuvdendorzh — 381L.
On the Problem of Testing the Invariance of an Interaction under Time Inversion. L. I. Lapidus — 1105L.
On the Problem of Two-Nucleon Interaction in the Tamm-Dancoff Method. A. A. Rukhadze — 352L.
On the Theory of Composite π^0 Mesons. M. E. Perel'man — 350L.
Photoproduction of Negative Pions from Deuterium near the Threshold. M. I. Adamovich, G. V. Kuz'micheva, V. G. Larionova, and S. P. Kharlamov — 21.
Photoproduction of Slow π^0 Mesons on Complex Nuclei. A. S. Belousov, S. V. Rusakov, and E. I. Tamm — 247.
Possibility of Determining the Interaction Constants from Experiments on $K_{\mu 3}$ Decays. I. G. Ivanter — 79.
Production of Pions in Condensed Media by Cosmic Rays in the Stratosphere. D. K. Kaipov, V. N. Shakhorostov, and Iu. G. Kosiak — 573L.
Production of Two π Mesons in Collisions between π Mesons or γ Quanta with Nucleons or Deuterons. N. V. Dushin — 278.
Proton-Proton Scattering in the $^1D_2$ State at 616 Mev. L. M. Soroko — 190L.
Radiation from a Charged Particle Traversing a Layered Medium. G. M. Garibian — 1003.
Radiative Decay of π^+ Mesons and Effects of Parity Nonconservation. A. I. Mukhtarov and S. A. Gadzhiev — 895L.
Statistical Interpretation of Experimental Data on Multiple Production of Particles at 1 to 20 Bev — 909L.
The $n + p \rightarrow \pi^0 + d$ Reaction for Neutrons of 600-Mev Effective Energy and the Charge-Independence Hypothesis. V. B. Fliagin, V. P. Dzhelepov, V. S. Kiselev, and K. O. Oganesian — 592.
The π-Mesonic Atom and Corrections to the Dispersion Relations. V. A. Meshcheriakov — 200L.
The Statistical Weights of K^+ and K^- Mesons Produced in Pion-Nucleon Collisions. E. K. Mikhul — 205L.
The Universal Fermi Interaction and the Capture of the μ Meson by the Proton. Ia. B. Zel'dovich and S. S. Gershtein — 570.
Transition Effect for Electrons in Walls of an Ionization Chamber. V. A. Dmitriev — 382L.
Metals (see Crystalline State)
Metastable Atoms (see Atomic Structure and Spectra)
Methods and Instruments
A Method for the Observation of Helium II Films. A. I. Shal'nikov — 386L.
Application of Magnetic Slits for Forming Circular Charged-Particle Trajectories. V. M. Kel'man, V. A. Koliunov, and M. V. Karpov — 779.
Coupled Magnetoelastic Waves in Ferromagnetic Media and Ferroacoustic Resonance. A. I. Akhiezer, V. G. Bar'iakhtar, and S. V. Peletminskii — 157.
Cyclic Acceleration of Particles in High-Frequency Fields. V. I. Veksler and L. M. Kovrizhnykh — 781.
Energy of the X-Rays Emitted by Intense Pulsed Discharges in Hydrogen. N. G. Koval'skii, I. M. Podgornyi, and S. Khvashchevskii — 656.
Gamma Radiation from Radiative Capture of Thermal Neutrons by Mo^{95}, Ag^{107}, Te^{123}, and Cs^{133} Nuclei. L. F. Kalinkin, A. S. Melioranskii, and I. V. Estulin — 410.
Low Temperature Polymorphism of Metals. I. A. Gindin, B. G. Lazarev, Ia. D. Starodubov, and V. I. Khotkevich — 556L.
On the Electron Capture Mechanism and the Current Limit in Betatrons. A. N. Matveev — 259.
On the Mechanism of the Damping of Free Oscillations in a Cyclic Accelerator. Iu. F. Orlov — 362L.
On the Possibility of Applying the Belen'kii-Tamm Equilibrium Spectrum to the Determination of (γ, n) Reactions. V. A. Shkoda-Ul'ianov — 726L.
On the Thermal Stability of the Domain Structure in Silicon-Iron Crystals. L. V. Kirenskii and I. F. Degtiarev — 403.
Several Possibilities Associated with the Separation of Charged Particles in an Inhomogeneous High-Frequency Electromagnetic Field. M. A. Miller — 561L.
Microwaves
Coherent Electron Radiation in a Synchrotron I. L. V. Iogansen and M. S. Rabinovich — 708
Coupled Magnetoelastic Waves in Ferromagnetic Media and Ferroacoustic Resonance. A. I. Akhiezer, V. G. Bar'iakhtar, and S. V. Peletminskii — 157.
Cyclic Acceleration of Particles in High-Frequency Fields. V. I. Veksler and L. M. Kovrizhnykh — 781.
Effect of Electron Paramagnetic Resonance on the Optical Faraday Effect at Low Temperatures. G. V. Skrotskii, P. S. Zyrianov, and T. G. Iziumov — 1028.
Reflection of Electrons from a High-Frequency Potential Barrier. M. A. Miller — 206L.
Several Possibilities Associated with the Separation of Charged Particles in an Inhomogeneous High-Frequency Electromagnetic Field. M. A. Miller — 561L.
Stimulated R. F. Amplifier Working on Hyperfine Levels of Paramagnetic Atoms. K. A. Valiev and Sh. Sh. Bashkirov — 208L.
Miscellaneous
Decay of a Photon into Two Photons in a Homogeneous Magnetic Field. V. G. Skobov — 919L.
On the Question of Antigravitation. Iu. A. Aleksandrov, V. A. Andreev, and I. I. Bondarenko — 911L.
Radio Emission from an Atomic Explosion. A. S. Kompaneets — 1076.
Molecular Aggregates
Cross Sections for the Capture of Slow Electrons by O_2 and H_2O Molecules and Molecules of Halogen Compounds. I. S. Buchel'nikova — 783.
Molecular Structure and Spectra
Diamagnetism and Interatomic Bonds in Molecules and Nonmetallic Crystals. Ia. G. Dorfman — 368L.

Moments, Nuclear (see Nuclear Moments and Spin)

Neutrino

  Angular Correlation for Low-Energy Positrons Emitted in $\pi^+ \rightarrow \mu^+ \rightarrow e^-$ Decay. A. O. Vaisenberg, V. A. Smirnitskii, E. D. Kolganova, Z. V. Minervina, E. A. Pesotskaia, and N. V. Rabin — 448.

  Energy Dependence of μ^+-e^+ Decay Asymmetry. A. I. Mukhin, E. B. Ozerov, and B. Pontecorvo — 237.

  Energy Dependence of the Angular Correlation of Positrons from $\pi \rightarrow \mu \rightarrow e$ Decay. Kh. P. Babaian, N. A. Marutian, K. A. Matevosian, and M. G. Sarinian — 387.

  Nonlocal Effects in Weak Interactions of Fermions. S. G. Matinian — 548L.

  On the $\pi \rightarrow e + \nu + \gamma$ Decay. V. G. Vaks and B. L. Ioffe — 151.

  The Effect of Neutrino Recoil in the Beta Decay of He^6. J. Csikai and A. Szalay — 749.

  Types of Interaction in Beta Decay. The Decay of Na^{24}. N. A. Burgov and Iu. V. Terekhov — 651.

Neutrons (see Elementary Particle Interaction)

Nuclear Fission

  Average Number of Neutrons Emitted in the Fission of Th^{229} by Thermal Neutrons. V. I. Lebedev and V. I. Kalashnikova — 370L.

  Computing the Spectra of Fission Neutrons. V. P. Kovalev and V. S. Stavinskii — 545.

  Determination of the Momentum and Excitation Energy Acquired by a Heavy Nucleus in the Interaction with a Fast Nucleon. A. I. Obukhov — 727L.

  Fission Cross Section of Pu^{240} by Fast Neutrons. V. G. Nesterov and G. N. Smirenkin — 367L.

  Fission of Silver by High-Energy Protons. V. P. Shamov — 219.

  Radiochemical Study of the Photofission of Th^{232}. I. A. Vasil'ev and K. A. Petrzhak — 795.

  Relative Yields of Delayed Neutrons in Fission of U^{238}, U^{235} and Th^{232} by Fast Neutrons. B. P. Maksiutenko — 565L.

  Triple Disintegrations of Uranium Nuclei. N. A. Perfilov and G. F. Denisenko — 438.

Nuclear Moments and Spin

  Investigation of Relaxation Processes in a Series of Fluorine Compounds of Carbon. V. S. Grechishkin — 253.

  Moment of Inertia of Nonspherical Nuclei. Iu. K. Khokhlov — 165.

  On the Distribution of Nucleon Density in Nuclei. F. I. Kligman — 255.

  Rotational States of Nonaxial Nuclei. A. S. Davydov and G. F. Filippov — 303.

  The Decay Scheme of Mo^{99}. I. V. Estulin, G. M. Chernon, and Z. V. Pashtukhova — 51.

Nuclear Photoeffects

  An Investigation of the Final States in the Photoproduction of Negative π Mesons on Deuterium. M. I. Adamovich — 29.

  Investigation of 15 to 65-Mev Protons Produced in the Photodisintegration of Aluminum and Nickel. E. B. Bazhanov, Iu. M. Volkov, and L. A. Kul'chitskii — 224.

  On the Possibility of Applying the Belen'kii-Tamm Equilibrium Spectrum to the Determination of (γ, n) Reactions. V. A. Shkoda-Ul'ianov — 726L.

  Photoproduction of Negative Pions from Deuterium near the Threshold. M. I. Adamovich, V. G. Kuz'micheva, V. G. Larionova, and S. P. Kharlamov — 21.

  Production of Two π Mesons in Collisions between π Mesons or γ Quanta with Nucleons or Deuterons. N. V. Dushin — 278.

  Ranges of Na^{24} Recoil Nuclei and the Mechanism of Certain Photonuclear Reactions. F. P. Denisov and P. A. Cerenkov — 376L.

  Spin Structure of the Scattering Matrix for Reactions Involving Gamma Rays. V. I. Ritus — 1038.

Nuclear Reactions, General

  A Note on d-d Reactions. I. Sh. Vashakidze and O. D. Cheishvili — 741L.

  A Radiochemical Study of the (p,pxn), (p,4pxn), and (p,5pxn) Reactions. T. V. Malysheva and I. P. Alimarin — 772.

  An Investigation of the Interaction between 250 — 270 Mev π^+ Meson and Carbon Nuclei with the Aid of a Propane Bubble Chamber. Wang Kan-Change, Wang Tso-Tsiang, Ding Da-Tsaŏ, L. N. Dubrovskii, E. N. Kladnitskaia, and M. I. Solov'ev — 625.

  Angular Distribution for the Diffraction Scattering of Deuterons. I. I. Ivanchik — 733L.

  Coulomb Excitation of Aluminum. D. G. Alkhazov, A. P. Grinberg, G. M. Gusinskii, K. I. Erokhina, and I. Kh. Lemberg — 736L.

  Determination of the Momentum and Excitation Energy Acquired by a Heavy Nucleus in the Interaction with a Fast Nucleon. A. I. Obukhov — 727L.

  Diffraction Breakup of Light Nuclei. A. G. Sitenko and Iu. A. Bereshnoi — 899L.

  Energy Dependence of Multiple-Production Reaction Cross Sections Near Threshold. A. F. Grashin — 499.

  Fission of Silver by High-Energy Protons. V. P. Shamov — 219.

  Hydrodynamic Theory of Multiple Production of Particles in Collisions between Fast Nucleons and Nuclei. G. A. Milekhin — 829.

  Hyperfragments from σ_K-Stars. B. P. Bannik and S. A. Buniatov — 913L.

  Inelastic Scattering of 300-Mev Positive and Negative π Mesons by Photographic Emulsion Nuclei. G. E. Belovitskii — 581.

  Lifetime of the First Excited State of Mg^{24}. D. G. Alkhazov, A. P. Grinberg, G. M. Gusinskii, K. I. Erokhina, and I. Kh. Lemberg — 737L.

  On the Hydrodynamic Theory of Multiple Production of Particles. G. A. Milekhin — 682.

  On the Mechanism of Stripping in Reactions Involving the Capture of Two Nucleons. V. V. Komarov, V. G. Neudachin, A. M. Popova, and I. B. Teplov — 679.

  On the Theory of the Interaction of Fast Neutrons of Various Angular Momenta with Semi-Transparent Nuclei. L. E. Pargamanik and V. V. Ul'ianov — 177.

  Optical Model for the Interaction of Neutrons of Intermediate Energy with Nuclei. A. V. Luk'ianov, Iu. V. Orlov, and V. V. Turovtsev — 521.

  Photoproduction of Electron and π-Meson Pairs on Nucleons. I. T. Diatlov — 108.

  Radio Emission from an Atomic Explosion. A. S. Kompaneets — 1076.

Selection Rules in Reactions Involving Polarized Particles. Chou Kuang-Chao — 543L.

Spin Structure of the Scattering Matrix for Reactions Involving Gamma Rays. V. I. Ritus — 1038.

The Nature of the Particles That Carry Away Most of the Energy in Nuclear Collisions at Moderate Energies. E. Friedlander and E. Ruckenstein — 75.

The Possibility of Estimating the Mean Lifetime of Alpha Particles within Nuclei. Iu. I. Serebrennikov — — 547L.

The Universal Fermi Interaction and the Capture of the μ Meson by the Proton. Ia. B. Zel'dovich and S. S. Gershtein — 570.

Nuclear Reactions Induced by α Particles and He^3

Coulomb Excitation of High-Energy Nuclear Levels in Even Isotopes of Tungsten. D. G. Alkhazov, A. P. Grinberg, G. M. Gusinskii, K. E. Erokhina, and I. Kh. Lemberg — 926.

On the Mechanism of Stripping in Reactions Involving the Capture of Two Nucleons. V. V. Komarov, V. G. Neudachin, A. M. Popova, and I. B. Teplov — 679.

Nuclear Reactions Induced by Deuterons and Tritons

A Note on d-d Reactions. I. Sh. Vashakidze and O. D. Cheishvili — 741L.

Angular Distribution for the Diffraction Scattering of Deuterons. I. I. Ivanchik — 733L.

Diffraction Breakup of Light Nuclei. A. G. Sitenko and Iu. A. Berezhnoi — 899L.

Exchange Effects in Stripping Reactions. V. G. Neudachin — 815.

On the Mechanism of Stripping in Reactions Involving the Capture of Two Nucleons. V. V. Komarov, V. G. Neudachin, A. M. Popova, and I. B. Teplov — 679.

Ratio of Isomeric and Ground State Yields of Zn^{69} Produced in Various Nuclear Reactions. K. I. Zherebtsova, T. P. Makarova, Iu. A. Nemilov, and B. L. Funshtein — 947.

Nuclear Reactions Induced by Mesons

Absorption of μ^- Mesons by Nuclei; Angular Distribution of the Neutrons. E. I. Dolinskii and L. D. Blokhintsev — 1040.

Absorption of Slow μ^- Mesons by Nuclei. A. T. Varfolomeev — 373L.

An Investigation of the Interaction between 250 — 270 Mev π^+ Meson and Carbon Nuclei with the Aid of a Propane Bubble Chamber. Wang Kan-Chang, Wang Tso-Tsiang, Ding Da-Tsao, L. N. Dubrovskii, En. N. Kladnitskaia, and M. I. Solov'ev — 625.

Bremsstrahlung from π Mesons Interacting with Nuclei. M. F. Lomanov, A. G. Meshkovskii, Ia. Ia. Shalamov, V. A. Shebanov, and A. F. Grashin — 615.

Diffraction Breakup of Light Nuclei. A. G. Sitenko and Iu. A. Berezhnoi — 899L.

Formation of Hydrogen Mesic Molecules. Ia. B. Zel'dovich and S. S. Gershtein — 451.

Inelastic Scattering of 300-Mev Positive and Negative π Mesons by Photographic Emulsion Nuclei. G. E. Belovitskii — 581.

Interaction of 80 to 300-Mev π^+ Mesons with Light Nuclei. G. A. Blinov, M. F. Lomanov, Ia. Ia. Shalamov, V. A. Shebanov, and V. A. Shchegolev — 609.

Isotopic Invariance in Anti-Hypeson Processes. S. G. Matinian and G. R. Khutsishvili — 377L.

On the Polarization of Recoil Nucleons in the Photoproduction of Pions. N. F. Nelipa and V. A. Feoktistov — 167.

Production of Two π Mesons in Collisions between π Mesons or γ Quanta with Nucleons or Deuterons. N. V. Dushin — 278.

Statistical Interpretation of Experimental Data on Multiple Production of Particles at 1 to 20 Bev. V. M. Maksimenko — 909L.

Nuclear Reactions Induced by Neutrons

Average Number of Neutrons Emitted in the Fission of Th^{229} by Thermal Neutrons. V. I. Lebedev and V. I. Kalashnikova — 370L.

Investigation of the Angular Distribution of Secondary Particles in Showers Produced by High-Energy Nucleons. L. A. San'ko, Zh. S. Takibaev, and Ts. I. Shakhova — 396.

Measurement of the Total Charged π-Meson Production Cross Section in Neutron-Proton Collisions at 586-Mev Neutron Energy. Iu. M. Kazarinov and Iu. N. Simonov — 56.

On the Mechanism of Stripping in Reactions Involving the Capture of Two Nucleons. V. V. Komarov, V. G. Neudachin, A. M. Popova, and I. B. Teplov — 679.

On the Theory of the Interaction of Fast Neutrons of Various Angular Momenta with Semi-Transparent Nuclei. L. E. Pargamanik and V. V. Ul'ianov — 177.

Optical Model for the Interaction of Neutrons of Intermediate Energy with Nuclei. A. V. Luk'ianov, Iu. V. Orlov, and V. V. Turovtsev — 521.

Ratio of Isomeric and Ground State Yields of Zn^{69} Produced in Various Nuclear Reactions. K. I. Zherebtsova, T. P. Makarova, Iu. A. Nemilov, and B. L. Funshtein — 947.

Relative Yields of Delayed Neutrons In Fission of U^{238}, U^{235}, and Th^{232} by Fast Neutrons. B. P. Maksiutenko — 565L.

Study of γ Rays from As^{78} Decay. Iu. A. Nemilov, A. N. Pisarevskii, and L. D. Soshin — 555L.

The $n + p \to \pi^0 + d$ Reaction for Neutrons of 600-Mev Effective Energy and the Charge-Independence Hypothesis. V. B. Fliagin, V. P. Dzhelepov, V. S. Kiselev, and K. O. Oganesian — 592.

Nuclear Reactions Induced by Protons

Determination of the Momentum and Excitation Energy Acquired by a Heavy Nucleus in the Interaction with a Fast Nucleon. A. I. Obukhov — 727L.

Energy Spectrum and Angular Distributions of π^+ Mesons Produced in Proton-Proton Collisions at 660 — 670 Mev. A. G. Meshkovskii, Ia. Ia. Shalamov, and V. A. Shevanov — 46.

Exchange Effects in Stripping Reactions. V. G. Neudachin — 815.

Fission of Silver by High-Energy Protons. V. P. Shamov — 219.

Investigation of the Angular Distribution of Secondary Particles in Showers Produced by High-Energy Nucleons. L. A. San'ko, Zh. S. Takibaev, and Ts. I. Shakova — 396.

Multi-Charged Particles Emitted in Disintegration of Carbon Nuclei by 660-Mev Protons. V. N. Ostroumov

and Iu. P. Iakovlev — 949.
New Measurements of the Neutron Spectrum in the Bombardment of Be by 680-Mev Protons. V. S. Kiselev, K. O. Oganesian, R. A. Poze, and V. B. Fliagin — 564L.
On the Mechanism of Stripping in Reactions Involving the Capture of Two Nucleons. V. V. Komarov, V. G. Neudachin, A. M. Popova, and I. B. Teplov — 679.
On the Problem of Angular Correlation of Secondary Particles Produced in High-Energy Nuclear Collisions. I. M. Gramenitskii, M. Ia. Danysh, V. B. Liubimov, M. I. Podgoretskii, and D. Tuvdendorzh — 381L.
Recoil Range of Na^{24} and the Mechanism of Al^{27}(p, 3pn) and P^{31}(p, 5p3n) for 660-Mev Protons. L. V. Volkova and F. P. Denisov — 372L.
Secondary Nuclear Reactions Induced in Bismuth and Lead by High-Energy Proton Bombardment. B. V. Kurchatov, V. N. Mekhedov, L. V. Chistiakov, M. Ia. Kuznetsova, N. I. Borisova, and V. G. Solov'ev — 40.
Statistical Interpretation of Experimental Data on Multiple Production of Particles at 1 to 20 Bev. V. M. Maksimenko — 909L.
Triple Disintegrations of Uranium Nuclei. N. A. Perfilov and G. F. Denisenko — 438.
Tritium Production in Metals by 120 and 660-Mev Protons. V. V. Kuznetsov and V. N. Mekhedov — 406.

Nuclear Scattering (see Scattering)

Nuclear Spectra
Alpha Decay of Isomeric Bi^{210}. S. V. Golenetskii, L. I. Rusinov, and Iu. I. Filimonov — 917L.
Alpha Decay of Nonspherical Nuclei. L. L. Gol'din, G. M. Adel'son-Velskii, A. P. Birzgal, A. D. Piliia, and K. A. Ter-Martirosian — 127.
Coulomb Excitation of Aluminum. D. G. Alkhazov, A. P. Grinberg, G. M. Gusinskii, K. I. Erokhina, and I. Kh. Lemberg — 736L.
Coulomb Excitation of High-Energy Nuclear Levels in Even Isotopes of Tungsten. D. G. Alkhazov, A. P. Grinberg, G. M. Gusinskii, K. E. Erokhina, and I. Kh. Lemberg — 926.
Effect of Finite Nuclear Size on the Relative Internal Conversion Coefficients in L Subshells. A. G. Sergeev, V. D. Vorob'ev, A. S. Remennyi, T. I. Kol'chinskaia, G. D. Latyshev, and Iu. S. Egorov — 242.
Gamma Radiation from Radiative Capture of Thermal Neutrons by Mo^{95}, Ag^{107}, Te^{123}, and Cs^{133} Nuclei. L. F. Kalinkin, A. S. Melioranskii, and I. V. Estulin — 410.
Hard Gamma Radiation from As^{76}. Decay Schedule of As^{76}. L. V. Gustova and O. V. Chubinskii — 957.
Investigation of Conversion Electron Spectra of Neutron-Deficient Isotopes of Lutecium. V. M. Kel'man, R. Ia. Metskhvarishvili, B. K. Preobrazhenskii, V. A. Romanov, and V. V. Tuchkevich — 914L.
Lifetime of the First Excited State of Mg^{24}. D. G. Alkhazov, A. P. Grinberg, G. M. Gusinskii, K. I. Erokhina, and I. Kh. Lemberg — 737L.
Lower Excited States of Th^{231}. Iu. I. Filimonov and B. V. Pshenichnikov — 378L.
Magnetic Transitions between Collective Excited States of Even-Even Nuclei. A. S. Davydov and G. F. Filippov — 488.
Polarization of Protons Elastically Scattered from Si^{28} Nuclei. P. V. Sorokin, A. K. Val'ter, I. Ia. Malakhov, and A. Ia. Taranov — 969.
Positron Spectrum of Eu^{152,154}. D. L. Kaminskii and M. G. Kaganskii — 646.
Rotational States of Nonaxial Nuclei. A. S. Davydov and G. F. Filippov — 303.
Study of γ Rays from As^{78} Decay. Iu. A. Nemilov, A. N. Pisarevskii, and L. D. Soshin — 555L.
The Decay Scheme of Mo^{99}. I. V. Estulin, G. M. Chernov, and Z. V. Pastukhova — 51.
The First Excited State of Tb^{159}. Iu. A. Nemilov, A. N. Pisarevskii, and L. D. Soshin — 554L.
The Hard Gamma Radiation of Ag^{110}. L. V. Gustova, L. P. Timofeeva, and O. V. Chubinskii — 920L.

Nuclear Structure Theory
A Note on d-d Reactions. I. Sh. Vashakidze and O. D. Chishvili — 741L.
Alpha Decay of Nonspherical Nuclei. L. L. Gol'din, G. M. Adel'son -Velskii, A. P. Birzgal, A. D. Pilia, and K. A. Ter-Martirosian — 127.
Coulomb Excitation of Aluminum. D. G. Alkhazov, A. P. Grinberg, G. M. Gusinskii, K. I. Erokhina, and I. Kh. Lemberg — 736L.
Coulomb Excitation of High-Energy Nuclear Levels in Even Isotopes of Tungsten. D. G. Alkhazov, A. P. Grinberg, G. M. Gusinskii, K. E. Erokhina, and I. Kh. Lemberg — 926.
Gamma Radiation from Radiative Capture of Thermal Neutrons by Mo^{95}, Ag^{107}, Te^{123}, and Cs^{133} Nuclei. L. F. Kalinkin, A. S. Melioranskii, and I. V. Estulin — 410.
Lifetime of the First Excited State of Mg^{24}. D. G. Alkhazov, A. P. Grinberg, G. M. Gusinskii, K. I. Erokhina, and I. Kh. Lemberg — 737L.
Magnetic Transitions between Collective Excited States of Even-Even Nuclei. A. S. Davydov and G. F. Filipov — 488.
Moment of Inertia of Nonspherical Nuclei. Iu. K. Khokhlov — 165.
Mutual Electron Correlations in Metal Optics. R. N. Gurzhi — 673.
Nuclear Binding Energies in the Region of the 82 Proton and 126 Neutron Magic Numbers. R. A. Demirkhanov, T. I. Gutkin, and V. V. Dorokhov — 639.
Nucleonic Interaction which Produces a Superfluid State of the Nucleus. V. G. Solov'ev — 572L.
On Axially Asymmetric Nuclei. B. T. Geilikman — 690.
On the Deviation of the Equilibrium Shape of Atomic Nuclei from Axial Symmetry — 365L.
On the Distribution of Nucleon Density in Nuclei. F. I. Kligman — 255.
On the Problem of Two-Nucleon Interaction in the Tamm-Dancoff Method. A. A. Rukhadze — 352L.
On the Theory of the "Second Moment" in the Nuclear Model of Lane, Thomas, and Wigner. V. M. Agranovich and V. S. Stavinskii — 896L.
Ratio of Isomeric and Ground State Yields of Zn^{69} Produced in Various Nuclear Reactions. K. I. Zherebtsova, T. P. Makarova, Iu. A. Nemilov, and B. L. Funshtein — 947.
Rotational States of Nonaxial Nuclei. A. S. Davydov and G. F. Filippov — 303.

  Scattering of Slow Neutrons by Deuterons. V. N. Efimov — 98.
  The Decay Scheme of Mo^{99}. I. V. Estulin, G. M. Chernov, and Z. V. Pastukhova — 51
  The Inelastic Scattering of Deuterons by Mg^{24}. T. I. Kopaleishvili, and V. I. Mamakakhlisov — 711.
  The Possibility of Estimating the Mean Lifetime of Alpha Particles within Nuclei. Iu. I. Serebrennikov — 574L.
Optical Instruments (see Methods and Instruments)
Optical Properties
  Effect of Electron Paramagnetic Resonance on the Optical Faraday Effect at Low Temperatures. G. V. Skrotskii, P. S. Zyrianov, and T. G. Iziumov — 1028.
  Electromagnetic Waves in the Region of Exciton Absorption in a Crystal. A. S. Davydov and A. F. Lubchenko — 1048.
  Energy Losses of an Electron in a Medium with Spatial Dispersion. V. M. Agranovich and A. A. Rukhadze — 819.
  Motion of a Charged Particle in a Anisotropic Medium. G. A. Begiashvili and E. V. Gedalin — 1059.
  Observation of the Lambda Transition in Helium in the Presence of a Thermal Current through the Phase Boundary. V. P. Peshkov — 943.
  On the Propagation of Electromagnetic Waves in a Medium with Appreciable Spatial Dispersion. V. M. Agranovich and A. A. Rukhadze — 685.
  On the Theory of the Optical Properties of Conductors in the Case of Oblique Incidence of the Radiation. V. P. Silin — 700.
Pair Production (see Electrons and Positrons)
Phosphors and Phosphorescence (see Luminescence; Semiconductors)
Photoconductivity (see Electrical Conductivity and Resistance)
Photodisintegration (see Nuclear Photoeffects)
Photoelectric Effect (see Electrical Properties)
Photography and Photographic Emulsions (see Methods and Instruments; Optical Properties)
Photometry (see Methods and Instruments; Optical Properties)
Photons (see Radiation)
Photovoltaic Effect (see Electrical Properties; Semiconductors)
Piezoelectric Effect (see Dielectrics and Dielectric Properties)
Polarization, Electrical (see Dielectrics and Dielectric Properties)
Positrons (see Electrons and Positrons)
Probability (see Mathematical Methods)
Protons (see Elementary Particle Interactions)
Quantum Electrodynamics (see also Field Theory)
  Bremsstrahlung and Pair Production from Protons with Allowance for Form Factor. I. Zlatev and P. S. Isaev — 213L.
  Cerenkov Radiation from Dipoles. V. L. Ginzburg and V. Ia. Eidman — 1055.
  Depolarization of Electrons Due to Radiation in a Magnetic Field. Iu. F. Orlov and S. A. Kheifets — 354L.
  Nuclear Orientation in Radiative K Capture. V. B. Berestetskii — 371L.
  On a Possible Limit on the Applicability of Quantum Electrodynamics. D. I. Blokhintsev — 174.
  On the Multiple Interaction in Quantum Field Theory. L. I. Podlubnyi — 728L.
  Radiation Corrections to Bremsstrahlung. P. I. Fomin — 491.
Quantum Mechanics
  Alpha Decay of Nonspherical Nuclei. L. L. Gol'din, G. M. Adel-son-Velskii, A. P. Birzgal, A. D. Piliia, and K. A. Ter-Martirosian — 127.
  Circular Polarization of Internal γ Bremsstrahlung in β Decay and Time Reversal Invariance. R. Iu. Volkovyskii — 562L.
  Dispersion Relations in Nonrelativistic Scattering Theory. L. D. Faddeev — 299.
  Formation of Hydrogen Mesic Molecules. Ia. B. Zel'dovich and S. S. Gershtein — 451.
  Generalized Self-Consistent Field Equations. P. S. Zyrianov — 309.
  Hole Bands in NaCl. T. I. Kucher — 732L.
  Hydrodynamic Theory of Multiple Production of Particles in Collisions between Fast Nucleons and Nuclei. G. A. Milekhin — 829.
  On Finding the Matrix of the $a + a' \to b + b'$ Reaction. S. M. Bilen'kii, L. I. Lapidus, L. D. Puzikov, and R. M. Ryndin — 669.
  On the Behavior of a Particle of Arbitrary Spin in an External Magnetic Field. V. S. Popov — 687.
  On the Problem of Two-Nucleon Interaction in the Tamm-Dancoff Method. A. A. Rukhadze — 352L.
  On the Theory of the Interaction of Fast Neutrons of Various Angular Momenta with Semi-Transparent Nuclei. L. E. Pargamanik and V. V. Ul'ianov — 177.
  On the Theory of the "Second Moment" in the Nuclear Model of Lane, Thomas, and Wigner. V. M. Agranovich and V. S. Stavinskii — 896L.
  Phenomenological Theory of Superfluidity near the Lambda Point. L. P. Pitaevskii — 282.
  Polarization of Internal Conversion Electrons following Beta Decay. B. V. Geshkenbein — 865.
  Quantum-Mechanical Probabilities as Sums over Paths. G. V. Riazanov — 85.
  Radiation of a Multilevel System Moving in a Medium with a Velocity Greater than the Velocity of Light. V. L. Ginzburg and V. M. Fain — 567L.
  Relativistic Theory of Polarization Effects. Iu. M. Shirokov — 703.
  Selection Rules in Reactions Involving Polarized Particles. Chou Kuang Chao — 543L.
  Short Range Interaction between the Electron and Other Particles. N. N. Kolesnikov and G. A. Jacobi — 265.
  Splitting of Atomic Terms with Integer Total Angular Momentum in a Magnetic Crystal. B. A. Tavger — 322.
  The π-Mesonic Atom and Corrections to the Dispersion Relations. V. A. Meshcheriakov — 200L.
  The Shapiro Integral Transformation. Chou Kuang-Chao and L. G. Zastavenko — 990.
  The Statistics of Spin and Polar Excitations in a Crystal. S. V. Vonsovskii and M. S. Svirskii — 1012.
  Wave Functions of Many-Electron Systems. V. I. Perel' — 476.

Wave Solutions of Nonlinear Generalizations of Relativistic Equations. D. F. Kurdgelaidze — 1099L.
Quenching of Radiation (see Radiation)
Radar (see Methods and Instruments; Radiation)
Radiation (see also Range and Energy Loss of Particles)
Cerenkov Radiation in the Passage of a Charged Particle Through a Ferrite. V. G. Bar'iakhtar and M. I. Kaganov — 532.
Circular Polarization of Internal γ Bremsstrahlung in β Decay and Time Reversal Invariance. R. Iu. Volkovyskii — 562L.
Coherent Electron Radiation in a Synchrotron. I. L. V. Iogansen and M. S. Rabinovich — 708.
Depolarization of Electrons Due to Radiation in a Magnetic Field. Iu. F. Orlov and S. A. Kheifets — 354L.
Interaction between a Charged Current-Conducting Jet Moving in a Circle and a Ferrite. A. N. Didenko — 455.
On a Possible Statistical Description of Systems of Particles Interacting with the Field. Iu. L. Klimontovich —891L.
On the Limit of Applicability of the Impact-Parameter Method. M. L. Ter-Mikaelian and B. V. Khachatrian — 898L.
On the $\pi \rightarrow e + \nu + \gamma$ Decay. V. G. Vaks and B. L. Ioffe — 151.
Radiation Corrections to Bremsstrahlung. P. I. Fomin — 491.
Radiation of a Multilevel System Moving in a Medium with a Velocity Greater than the Velocity of Light. V. L. Ginzburg and V. M. Fain — 567L.
Stimulated R. F. Amplifier Working on Hyperfine Levels of Paramagnetic Atoms. K. A. Valiev and Sh. Sh. Bashkirov — 208L.
The First Excited State of Tb^{159}. Iu. A. Nemilov, A. N. Pisarevskii, and L. D. Sochin — 554L.
The Radiation from a Charged Particle Passing through a Plate. G. M. Garibian and G. A. Chalikian — 894L.
Use of Cyclotron Resonance in Semiconductors for the Amplification and Generation of Microwaves. A. S. Tager and A. D. Gladun — 560L.
Radioactivity
Alpha Decay of Isomeric Bi^{210}. S. V. Golenetskii, L. I. Rusinov, and Iu. I. Filimonov — 917L.
Alpha Decay of Nonspherical Nuclei. L. L. Gol'din, G. M. Adel'son-Velskii, A. P. Birzgal, A. D. Piliia, and K. A. Ter-Martirosian — 127.
Cerenkov Radiation from Dipoles. V. L. Ginzburg and V. Ia. Eidman — 1055.
Circular Polarization of Internal γ Bremsstrahlung in β Decay and Time Reversal Invariance. R. Iu. Volkovyskii — 562L.
Gamma Radiation from Radiative Capture of Thermal Neutrons by Mo^{95}, Ag^{107}, Te^{123}, and Cs^{133} Nuclei. L. F. Kalinkin, A. S. Melioranskii, and I. V. Estulin — 410.
Hard Gamma Radiation from As^{76}. Decay Schedule of As^{76}. L. V. Gustova and O. V. Chubinskii — 957.
Investigation of Conversion Electron Spectra of Neutron-Deficient Isotopes of Lutecium. V. M. Kel'man, R. Ia. Metskhvarishvili, B. K. Preobrazhenskii, V. A. Romanov, and V. V. Tuchkevich — 914L.
Measurement of β-γ Correlation from Oriented Nuclei. A. V. Kogan, V. D. Kul'kov, L. P. Nikitin, N. M. Reinov, I. A. Sokolov, and M. F. Stel'makh — 903L.
Measurement of the Half-Life of the Neutron. A. N. Sosnovskii, P. E. Spivak, Iu. A. Prokof'ev, I. E. Kutikov, and Iu. P. Dobrynin — 739L.
On the $\pi \rightarrow e + \nu + \gamma$ Decay. V. G. Vaks and B. L. Ioffe — 151.
Polarization of Internal Conversion Electrons following Beta Decay. B. V. Geshkenbein — 865.
Radiation from a Charged Particle Traversing a Layered Medium. G. M. Garibian — 1003.
Relative Yields of Delayed Neutrons in Fission of U^{238}, U^{235}, and Th^{232} by Fast Neutrons. B. P. Maksiutenko — 565L.
Secondary Nuclear Reactions Induced in Bismuth and Lead by High-Energy Proton Bombardment. B. V. Kurchatov, V. N. Mekhedov, L. V. Chistiakov, M. Ia. Kuznetsova, N. I. Borisova, and V. G. Solov'ev — 40.
Study of Gamma Rays from As^{78} Decay. Iu. A. Nemilov, A. N. Pisarevskii, and L. D. Soshin — 555L.
The Decay Scheme of Mo^{99}. I. V. Estulin, G. M. Chernov and Z. V. Pastukhova — 51.
The Hard Gamma Radiation of Ag^{110}. L. V. Gustova, L. P. Timofeeva, and O. V. Chubinskii — 920L.
The Polarization of the Internal-Conversion Electrons Emitted after Beta Decay. V. B. Berestetskii and A. P. Rudik — 111.
Range and Energy Loss of Particles
Energy Losses of an Electron in a Medium with Spatial Dispersion. V. M. Agranovich and A. A. Rukhadze — 819.
Multi-Charged Particles Emitted in Disintegration of Carbon Nuclei by 660-Mev Protons. V. N. Ostroumov and Iu. P. Iakovlev — 949.
Range of Nitrogen and Beryllium Ions in Air. Iu. A. Vorob'ev — 912L.
Rectifiers (see Electrical Conductivity and Resistance; Semiconductors)
Relativity and Gravitation
A Nonlinear Theory of Vector Fields. V. Iu. Urbakh — 143.
Clebsch-Gordan Expansion for Infinite-Dimensional Representations of the Lorentz Group. A. Z. Dolginov and I. N. Toptygin — 550L.
Coordinate Conditions in Einstein's Gravitation Theory. I. G. Fikhtengol'ts — 1018.
Stationary Relativistic Motions of a Gas in a Conducting Medium. K. P. Staniukovich — 529.
Resistance, Electrical (see Electrical Conductivity and Resistance)
Resonance Radiation (see Radiation)
Scattering, General (see also Elementary Particle Interactions; Nuclear Reactions; Range and Energy Loss of Particles)
Diffraction Scattering of Fast Particles. D. I. Blokhintsev, V. S. Barashenkov, and V. G. Grishin — 215L.
Dispersion Relations in Nonrelativistic Scattering Theory. L. D. Faddeev — 299.
Double Elastic Scattering of Deuterons in a Magnetic Field. G. R. Khutsishvili and O. D. Cheishvili — 859.
Elastic Scattering of Photons on Excited Nucleons.

N. F. Nelipa — 460.
  On the Problem of Two-Nucleon Interaction in the Tamm-Dancoff Method. A. A. Rukhadze — 352L.
  On the Question of the Uniqueness of Phase Analysis. L. G. Zastavenko — 544L.
  On the Scattering of "Dressed" Particles in Quantum Field Theory. Iu. V. Novozhilov — 515.
  On the Theory of the Fermi Liquid. L. D. Landau — 70.
  On the Theory of the Interaction of Fast Neutrons of Various Angular Momenta with Semi-Transparent Nuclei. L. E. Pargamanik and V. V. Ul'ianov — 177.
  Optical Model for the Interaction of Neutrons of Intermediate Energy with Nuclei. A. V. Luk'ianov, Iu. V. Orlov, and V. V. Turovtsev — 521.
  Spin Structure of the Scattering Matrix for Reactions Involving Gamma Rays. V. I. Ritus — 1038.
  The π-Mesonic Atom and Corrections to the Dispersion Relations. V. A. Meshcheriakov — 200L.
  The Scattering of Spin-$^3/_2$ Particles by a Coulomb Field. A. A. Komar — 559L.
  The Scattering of Spin 2 Particles by a Coulomb Field. A. I. Bedritskii — 892L.
Scattering of Deuterons
  Angular Distribution for the Diffraction Scattering of Deuterons. I. I. Ivanchik — 733L.
  Double Elastic Scattering of Deuterons in a Magnetic Field. G. R. Khutsishvili and O. D. Cheishvili — 859.
  The Inelastic Scattering of Deuterons by Mg^{24}. T. I. Kopaleishvili and V. I. Mamashakhlisov — 711.
Scattering of Electrons and Positrons (see also Electrons and Positrons)
  Bremsstrahlung and Pair Production from Protons with Allowance for Form Factor. I. Zlatev and P. S. Isaev — 213L.
  Isotopic Effect in the Residual Electrical Resistance in Metals. I. Ia. Pomeranchuk — 693.
  On the Distribution of Nucleon Density in Nuclei. F. I. Kligman — 255.
Scattering of Mesons (see also Nuclear Reactions Induced by Mesons)
  An Investigation of the Interaction between 250 — 270 Mev π^+ Meson and Carbon Nuclei with the Aid of a Propane Bubble Chamber. Wang Kan-Chang, Wang Tso-Tsiang, Ding Da-Tsao, L. N. Dubrovskii, E. N. Kladnitskaia, and M. I. Solov'ev — 625.
  Diffraction Scattering of Fast Particles. D. I. Blokhintsev, V. S. Barashenkov, and V. G. Grishin — 215L.
  Elastic Scattering of 5 to 22 Mev Positive Pions by Carbon. V. G. Kirillov-Ugriumov, L. P. Kotenko, E. P. Kuznetsov, and F. M. Sergeev — 907L.
  Elastic Scattering of 300-Mev Pions by Deuterons. L. S. Dul'kova, I. B. Sokolova, and M. G. Shafranova — 217.
  Inelastic Scattering of 300-Mev Positive and Negative π Mesons by Photographic Emulsion Nuclei. G. E. Belovitskii — 581.
  Interaction of 80 to 300 Mev π^+ Mesons with Light Nuclei. G. A. Blinov, M. F. Lomanov, Ia. Ia. Shalamov, V. A. Shebanov, and V. A. Shchegolev — 609.
  The π-Mesonic Atom and Corrections to the Dispersion Relations. V. A. Meshcheriakov — 200L.
Scattering of Neutrons (see also Nuclear Reactions Induced by Neutrons)
  New Measurements of the Neutron Spectrum in the Bombardment of Be by 680-Mev Protons. V. S. Kiselev, K. O. Oganesian, R. A. Poze, and V. B. Fliagin — 564L.
  On the Theory of the Interaction of Fast Neutrons of Various Angular Momenta with Semi-Transparent Nuclei. L. E. Pargamanik and V. V. Ul'ianov — 177.
  Optical Model for the Interaction of Neutrons of Intermediate Energy with Nuclei. A. V. Luk'ianov, Iu. V. Orlov, and V. V. Turovtsev — 521.
  Scattering of Slow Neutrons by Deuterons. V. N. Efimov — 98.
Scattering of Protons (see also Nuclear Reactions Induced by Protons)
  Diffraction Scattering of 6.15-Bev Protons by Protons. V. G. Grishin — 345.
  Investigation of the $p + p \rightarrow d + \pi^+$ Reaction with a Polarized Proton Beam. Iu. K. Akimov, O. V. Savchenko, and L. M. Soroko — 64.
  Multi-Charged Particles Emitted in Disintegration of Carbon Nuclei by 660-Mev Protons. V. N. Ostroumov and Iu. P. Iakovlev — 949.
  Polarization of Protons Elastically Scattered from Si^{28} Nuclei. P. V. Sorokin, A. K. Val'ter, I. Ia. Malakhov, and A. Ia. Taranov — 969.
  Proton-Proton Scattering in the $^1D_2$ State at 616 Mev. L. M. Soroko —190L.
  The π-Mesonic Atom and Corrections to the Dispersion Relations. V. A. Meshcheriakov — 200L.
  Triple Scattering of 660-Mev Protons I. Measurement of the Depolarization Parameter D(90°). Iu. P. Kumekin, M. G. Meshcheriakov, S. B. Nurushev, and G. D. Stoletov — 977.
Scattering of Radiation (see Radiation)
Scintillation Counters (see Methods and Instruments)
Secondary Emission (see Electrical Properties)
Semiconductors
  Cross Sections of Possible Nonradiative Recombination in Semiconductors. Iu. M. Popov — 348L.
  Discrete Energy Losses of Electrons in Solids and Yield of Secondary Electrons. N. B. Gornyi — 193L.
  Effect of Thermoelectric Forces on the Skin Effect in a Metal. M. I. Kaganov and V. M. Tsukernik — 327.
  Nonequilibrium Processes in Impurity Semiconductors. V. P. Shabanskii — 101.
  Use of Cyclotron Resonance in Semiconductors for the Amplification and Generation of Microwaves. A. S. Tager and A. D. Gladun — 560L.
Solid State (see Crystalline State)
Solutions (see Liquids)
Sound (see Acoustics)
Spallation (see Nuclear Reactions)
Spark Discharge (see Electrical Discharges)
Spectra, Atomic (see Atomic Structure and Spectra)
Spectra, General
  Hard Gamma Radiation from As^{76}. Decay Schedule of As^{76}. L. V. Gustova and O. V. Chubinskii — 957.
  On the Theory of Longitudinal Relaxation of Paramagnetic Salt Solutions. S. A. Al'tshuler and K. A. Valiev — 661.
  Splitting of Atomic Terms with Integer Total Angular Momentum in a Magnetic Crystal. B. A. Tavger — 322.
Spectra, Nuclear (see Nuclear Spectra)

Spectroscopy Technique (see Methods and Instruments)
Spinor Fields (see Field Theory)
Stark Effect (see Atomic Structure and Spectra)
Statistical Mechanics and Thermodynamics
  A New Method in Statistical Perturbation Theory. Ch'en Ch'un Hsien — 1062.
  Analogy between the Mechanical and Thermodynamical Equations of Motion and the Onsager Reciprocity Relation. I. Fenyes — 725L.
  Generalized Self-Consistent Field Equations. P. S. Zyrianov — 309.
  Influence of Deformations on Oscillation Effects in Metals at Low Temperatures. A. M. Kosevich — 171.
  Nonequilibrium Processes in Impurity Semiconductors. V. P. Shabanskii — 101.
  Observation of the Lambda Transition in Helium in the Presence of a Thermal Current through the Phase Boundary. V. P. Peshkov — 943.
  On a Possible Statistical Description of Systems of Particles Interacting with the Field. Iu. L. Klimontovich — 891L.
  On the Stability of a Fermi Liquid. I. Ia. Pomeranchuk — 361L.
  On the Theory of the Fermi Liquid. L. D. Landau — 70.
  Phenomenological Theory of Superfluidity near the Lambda Point. L. P. Pitaevskii — 282.
  The Limits of Applicability of the Quasi-Classical Equation of State of Matter. D. A. Kirzhnits — 1081.
  The Oscillations of a Degenerate Electron Fluid. V. P. Silin — 870.
  The Statistics of Spin and Polar Excitations in a Crystal. S. V. Vonsovskii and M. S. Svirskii — 1012.
Statistical Methods (see Mathematical Methods)
Superconductivity
  A Superconductor in a High Frequency Field. A. A. Abrikosov, L. P. Gor'kov, and I. M. Khalatnikov — 182.
  On the Theory of Superconducting Alloys. I. The Electrodynamics of Alloys at Absolute Zero. A. A. Abrikosov and L. P. Gor'kov — 1090.
Thermal Properties
  Change of Saturation Magnetization and of Electrical Resistance of Iron-Nickel under Hydrostatic Compression at Low Temperatures. E. I. Kondorskii and V. L. Sedov — 586.
  Effect of Thermoelectric Forces on the Skin Effect in a Metal. M. I. Kaganov and V. M. Tsukernik — 327.
  Heat of Mixing of Light and Heavy Water. V. P. Skripov — 903L.
  Low Temperature Polymorphism of Metals. I. A. Gindin, B. G. Lazarev, Ia. D. Starodubov, and V. I. Khotkevich — 556L.
  Observation of the Lambda Transition in Helium in the Presence of a Thermal Current through the Phase Boundary. V. P. Peshkov — 943.
  On the Thermal Stability of the Domain Structure in Silicon-Iron Crystals. L. V. Kirenskii and I. F. Degtiarev — 403.
  Paramagnetic Resonance of the Free Radicals Obtained by Freezing a Plasma of H_2S. S. D. Katimazov and A. M. Prokhorov — 381L.
  Propagation of a Non-Self-Similar Thermal Wave. E. I. Andriankin — 295.
  Some Remarks on the Structure of Shock Waves. G. S. Golitsyn and K. P. Staniukovich — 575L.
Thermionic Emissions (see Electrical Properties)
Thermodynamics (see Statistical Mechanics and Thermodynamics)
Thermoelectric Effect (see Electrical Properties; Semiconductors)
Total Cross Sections (see Electrons and Positrons; Nuclear Reactions)
Uncertainty Principle (see Quantum Mechanics)
Vacuum Tubes (see Methods and Instruments)
Viscosity (see Liquids)
Wave Mechanics (see Quantum Mechanics)
Work Function (see Electrical Properties)
X-Rays
  Electric Explosion of Spiral Wires in Vacuum. I. F. Kvartskhava, V. V. Bondarenko, R. D. Meladze, and K. V. Suladze — 634.
  Energy of the X-Rays Emitted by Intense Pulsed Discharges in Hydrogen. N. G. Koval'skii, I. M. Podgornyi, and S. Khvashchevskii — 656.

ERRATA TO VOLUME 7

Page	Reads	Should Read
533, title	Nuclear magnetic moments of Sr^{87} and Mg^{95}	Nuclear magnetic moments of Sr^{87}
645 Eq. (1)	$\ldots + \varkappa \sqrt{j_0 (j_0 + 1)}$	$\ldots - \varkappa \sqrt{j_0 (j_0 + 1)}$
647 Eq. (11)	$(L+1) \lvert B_L^- \rvert^2 - L \lvert B_L^+ \rvert^2$	$L(L+1) [\lvert B_L^- \rvert^2 - \lvert B_L^+ \rvert^2]$
894 Eq. (12)	$\varepsilon_{11} = 1 - \sum \frac{\cdots}{\sqrt{\pi / \mu}}$	$\varepsilon_{11} = 1 - \sum \frac{\cdots}{\sqrt{\pi}\, \mu}$
897 Eq. (45)	$\sqrt{\pi / 2}$	$\sqrt{\pi / 8}$
979 Table II, heading	$\lvert E_\gamma > 50$ **Mev** $\lvert E_\gamma > 50$ **Mev**	$\lvert E_\gamma < 50$ **Mev** $\lvert E_\gamma > 50$ **Mev**
1023 Figure caption		a) $\omega < \omega_H$, b) $\omega > \omega_H$
1123 Eq. (2)	$\Gamma = \mu_2 / \mu_1$	$\Gamma = \mu_2 / \mu_1, \ \mu_\perp = (\mu_1^2 - \mu_2^2) / \mu_1$

ERRATA TO VOLUME 8

Page	Reads	Should Read
375 Figure caption	a) positrons of energy up to 0.4 ϵ, b) positrons of energy up to 0.3 ϵ.	a) positrons of energy up to 0.3 ϵ, b) positrons of energy up to 0.4 ϵ.
816 Beginning of Eq. (8)	$I_2^5 = (4\pi)^2 \ldots$	$I_2^2 = (4\pi)^5 \ldots$